Profilage de l'ubiquitylation des protéines dans les cellules résistantes au bortézomib : rôle des enzymes de ubiquitylation

Maria Gonzalez Santamarta

Université Fédérale
Toulouse Midi-Pyrénées

THÈSE

En vue de l'obtention du
DOCTORAT DE L'UNIVERSITÉ DE TOULOUSE

Délivré par l'Université Toulouse 3 - Paul Sabatier

Présentée et soutenue par

María GONZALEZ SANTAMARTA

Le 18 février 2022

Profilage de l'ubiquitylation des protéines dans les cellules résistantes au bortézomib : rôle des enzymes de ubiquitylation

---

Ecole doctorale : **BSB - Biologie, Santé, Biotechnologies**

Spécialité : **CANCEROLOGIE**

Unité de recherche :
LCC - Laboratoire de Chimie de Coordination

Thèse dirigée par
Manuel RODRIGUEZ et Dimitris XIRODIMAS

Jury

M. Guillaume BOSSIS, Rapporteur
M. Nicolas BIDERE, Rapporteur
M. Daniel TAILLANDIER, Rapporteur
Mme Karine Reybier, Examinatrice
M. Manuel. S. RODRIGUEZ., Directeur de thèse

ACKNOWLEDGEMENTS

This project has received funding from the European Union's Horizon 2020 research and innovation programme under the Marie Skłodowska-Curie grant agreement No 765445, and an extension awarded by the ARC foundation for cancer research.

First of all, I would like to thank my supervisor Dr, Manuel Rodriguez for giving me the opportunity to do the PhD in his lab.

I would like to thank Rune Matthiesen and his collaborators for their marvellous work in the Mass Spectrometry Analysis.

I wish to express my deepest gratitude to all the people from Rosa Barrio´s Lab at CICbioGUNE (Bilbao) for their assistance and help in the completion of this project.

And last but not least, I would like to thank all the members of the UbiCARE team, especially Clémence Coutelle-Rebut.

TABLE OF CONTENTS

1. Abbreviations.

ABC: ATP-binding cassette
ABCB1: Multi-drug resistance, MDR1 or P-glycoprotein
AKT: Protein Kinase B
ALS: Autophagy-Lysosome System
AQUA: Absolute Quantification
ASCT: Autologous Stem Cell Transplant
ATF6: Transcription factor 6
ATG: Autophagy related genes/proteins
ATM: Ataxia Telangiectasia mutated
AUTACs: Autophagy-targeting chimera
BCL2: B-cell Lymphoma 2
BCR: B-cell receptor
BiP/Grp 78: Immunoglobulin heavy chain binding protein, also referred as 78-kDa glucose-regulated protein
BS3: bis(sulfosuccinimidyl)suberate
BTK: Bruton's tyrosine kinase
BTZ/Velcade: Bortezomib
CART: Chimeric Antigen Receptor T cell therapy
CDK4: Cyclin-dependent kinase 4
CDK6: Cyclin-dependent kinase 6
CDKN1B: Cyclin-dependent Kinase inhibitor 1B
CDKN2A: Cyclin-dependent Kinase inhibitor 2A
CDR: Complementary Determining Region
CFZ/Kypolis: Carfilzomib
CI: Combination Index
CK2: Serine/Threonine-selective protein kinase 2
CMA: Chaperone-Mediated Autophagy
CP: Core Particle
CQ: Cloroquine
CRPC: Castration-Resistant Prostate Cancer
DDR: DNA Damage Response
DMP: Dimethyl pimelimidate dihydrochloride
dsAb: single domain Antibody
DSB: Double Strand Breaks
DUBs: Deubiquitylating enzymes
E1: Ubiquitin-activating enzyme
E2: Ubiquitin-conjugating enzyme
E3: Ubiquitin ligase
ECM: Extracellular Matrix
ER: Endoplasmic Reticulum
ERAD:ER-associated-degradation
MHC: Major Histocompatibility Complex
ESI: Electrospray Ionization
FACS: Fluorescence-activated single cell sorting:
FBXO10: F-box protein 10
FDA: Food and Drug Administration

FISH: Fluorescence in situ hybridization
FT: Flow Through
GC: Germinal Center
GO: Gene Ontology
GSK3B: Glycogen Synthase Kinase 3 B
H3K36: Histone 3 lysine 36
HDAC6: Histone deacetylase 6
HDT: High Dose Therapy
HECT: Homologous to E6-associated protein C-terminus
HPLC: High-Performance Liquid Chromatography
HTT: Huntingtin protein
IF: Immunolfuorescence
IGH: Immunoglobulin heavy chain
IGHV: Heavy Chain Variable Region Genes
IP: Immunoprecipitation
IRF4: Interferon Regulatory Factor 4
iTRAQ : isobaric tags for relative and absolute quantification
IXZ/Ninlano: Ixazomib
JAMM: JAB1/MPN/MOV34 proteases /metalloenzymes
KEAP1: Kelch-like ECH-Associated Protein 1
LC: Liquid-separation Chromatography
LIR: LC3 Interacting Region
LUBAC: Linear Ubiquitination Assembly Complex
MALDI: Matrix Assisted-Laser
MARCKS: Membrane protein myristoylated alanine-rich C-kinase substrate
MCL: Mantle Cell Lymphoma
MDM2: Human homology of mouse double-minute 2
MINDY: Motif interacting with Ubiquitin novel DUB family
MIPI: Mantle cell international prognostic index
miRNA: micro RNA
MJD: Machado-Josephin disease proteases
MM: Multiple myeloma
MRM: Multiple Reaction Monitoring
MRZ: Marizomib
MS: Mass Spectrometry
mTOR: Mammalian target of rapamycin
mTORC1: mTOR-Raptor complex
mTORC2: mTOR-Rictor complex
MYC: v-Myc Myelocytomatosis viral oncogene homolog
NAC: N-acetylcysteine
NBR1: New Autophagy Receptor
NEED8: Neural precursor cell expressed developmentally down-regulated protein 8
NEMO: NF-kappa-B essential modulator
NF-KB: Nuclear factor kappa-B (light-chain enhancer of activated B-cells)
NHL: Non-Hodgkin's Lymphoma
NK: Natural killer
NP: Nanobodies-Precipitations

NRF2: Nuclear factor NF-E2 p45-related factor
NSD2: Multiple myeloma SET domain-containing protein type III (MMSET)
OPTN: Optineurin
OPZ: Oprozomib
OR: Overall Response
OS: Overall Survival
OTUs: Ovarian Tumour domain proteases
p97/VCP: Ubiquitin binding ER-associated degradation protein
PAX5: Transcription factor Paired box 5
PDGFA: Platelet derived growth factor subunit A
PE: Phosphatidylethanolamine
PFS: Progression-Free Survival
PI: Proteasome inhibitor
PI3K: Phosphoinositide-3 Kinase
PI3P: class III phosphatidylinositol 3-kinase [PI(3)KC3)] complex
PQC: Protein Quality Control
PRDM1/BLIMP: PR domain zinc finger protein 1
PRDM1/BLIMP-1: PR domain zinc finger protein 1
PROTACs: Proteolysis-targeting chimeric molecules
Pru: Pleckstrin-like receptor for Ubiquitin
PTMs: Posttranslational Modifications
R/R: Relapse/Refractory
RB1: Retinoblastoma 1
RBR: RING-Between-RING
R-CHOP: Rituximab- Cyclophosphamide, Doxorubicin, Vincristine, and Prednisone treatment
R-HCVAD/MA: Rituximab-based Hyper-fractionated cyclophosphamide, Vincristine, Doxorubicin, and Dexamethasone alternating with high-dose Methotrexate and Cytarabine treatment
RING: Really Interesting New Gene
RM: Rituximab Maintenance
ROS: Reactive oxygen species
RPs: Regulatory capping Particles
RT: Room temperature
SCF: E3 ligase SKp1-Cul-F box protein
SILAC: Stable Isotope Labelling
SLRs: Sequestosome-1-like receptors
SOX11: Sex-Determining Region Y-Box 11
SQSTM1/P62: Autophagy receptor sequestrosome 1
STAT3: Activator of transcription 3
SUMO: Small Ubiquitin-like Modifier
TG2: Transglutaminase 2
TMT: Tandem Mass Tagging
TOF : Time Of Flight
TP53: Tumour Suppressor P53
TRIM: Tripartite Motif-containing enzymes
TUBEs: Tandem Ub-binding Domains
Ub: Ubiquitin

UBA: Ubiquitin-Associated Domains
UbcH10: Ubiquitin-conjugating enzyme H10
UBD: Ubiquitin Binding Domains
UbLs: Ubiquitin-like Proteins
UCH: Ub-sp C-terminal hydrolases
UIM: Ub-interacting motif
ULK1: nc-51 like autophagy activating kinase 1, also called ATG1
UPR: Unfolded Protein Response
UPS: Ubiquitin Proteasome System
USPs: Ub-specific proteases
VR-CAP: Versus Rituximab, Cyclophosphamide, Doxorubicin, Vincristine treatment
VTP: Verteporfin
WB: Western Blotting
WHO: World Health Organization
XBP1 : Inositol-requiring enzyme 1 (IRE1)-X box binding protein 1
XPO1: Exportin 1
ZUFSP: Zinc finger with UFM1-specific peptidase domain protein

2. List of Tables.

3. List of Figures.

4. Summary.

Disruption of proteostasis is often the cause or consequence of pathologies, including haematological malignancies like Mantle Cell lymphoma (MCL). MCL is an aggressive non-Hodgkin lymphoma, with a poor rate of survival and frequent relapses after Bortezomib (BTZ) treatment. The two major intracellular degradation pathways, the Ubiquitin-proteasome (UPS) and autophagy-lysosome (ALS) systems, rely on Ubiquitin (Ub) to drive protein degradation acting as a single coordinated network. Using Ub traps (TUBEs) associated to mass spectrometry (MS) to compare the Ub proteome of the BTZ-resistant MCL cell line (ZBR) and its parental BTZ-sensitive counterpart (Z138), the hosting lab found Ub playing a major role in BTZ response/resistance and unveiled a molecular switch from UPS to ALS, describing proteaphagy as a hallmark of resistance. K63 Ub chains and other enzymes were also detected enriched in ZBR in this analysis.

We hypothesized that this enrichment could predispose them to activate autophagy and signaling events implicated in MCL cell survival and BTZ resistance, being focused on the identification of mechanism and proteins directly involved. To explore this hypothesis, we used several experimental strategies including the isolation and identification of the Ub proteome, and the used of combinatorial chemical treatments.

TRIM24, which is known to regulate the activity of the tumor suppressor p53, was found more enriched in ZBR cells at basal levels. TRIM24 stability is compromised differently after inhibition of the proteasome (BTZ) or autophagy using Bafilomycin A (BafA), in Z138 and ZBR cells suggesting a possible role in UPS-ALS crosstalk. We have used dTRIM24, a validated Proteolysis Targeting Chimeric (PROTAC) to target TRIM24 in our MCL model. Our results show that a combined dTRIM24/ZBR treatment reduces proteasome levels and promotes cooperative apoptotic effects in the ZBR cell line. Interestingly, a dTRIM24 treatment enhanced the formation of K48 and K63 chains and the Ub-associated fraction of p62 and proteasome subunits in ZBR cells.

UBR proteins (UBR2, UBR4 and UBR5 found enriched in ZBR) are involved in the regulation of the N-end rule pathway, related to the ZZ domain of the autophagy receptor p62/SQSTM1 under proteotoxic stress conditions. Verteporfin (VTP), one of the most effective p62 inhibitors, strongly induces apoptosis in ZBR cells. However, since VTP also induces ROS (oxygen-containing reactive species), we used an inhibitor of the p62 ZZ domain (XRK3F2) to further explore the role of p62 and its impact on UBR enzymes. We found that XRK3F2 differently affects the stability of UBR enzymes in ZBR compared to Z138 cells. However, the viability of Z138 and ZBR cells was similar, suggesting that changes in protein levels of UBR enzymes are not associated to BTZ resistance and that VTP is a better treatment to enhance apoptosis in ZBR cells.

To better understand the response to VTP in BTZ-resistant cells, we collaborated with *Hybrigenics* to characterise K48 and K63 Ub chain specific nanobodies (now commercialised by Nanotag). After setting conditions for nanobodies-precipitations (NP), the Ub proteome from ZBR and Z138 MCL cells treated or not with VTP was analysed by MS. Results confirmed an enrichment of K63 Ub chains in ZBR and provided a list of protein candidates playing a

role in BTZ resistance, also validating TRIM24 ZBR enrichment, as well as other crucial cellular factors regulating protein synthesis and metabolism.

In sum, our results indicate that Ub chain remodeling mediated by Ub enzymes, such as TRIM24, could contribute to regulating survival of BTZ-resistant MCL cells. Further experiments are required to validate the role of the identified factors highly enriched in ZBR to better understand their role in cell viability and response to this proteasome inhibitor. Altogether, this work should contribute to the identification of potential biomarkers to improve diagnosis, prognosis, and new treatments for BTZ-resistant patients.

5. Résumé.

L'altération de la protéostase peut être la cause ou conséquence de pathologies comme le lymphome à cellules du manteau (MCL), lymphome non-hodgkinien agressif avec un faible taux de survie et des rechutes après un traitement par l'inhibiteur de protéasome Bortezomib (BTZ).

Les voies Ubiquitine-protéasome (UPS) et autophagie-lysosome (ALS) reposent sur l'Ubiquitine (Ub) pour la dégradation intracellulaire des protéines au sein d'un seul réseau protéolytique coordonné. A l'aide de pièges à Ub (TUBEs) associés à la spectrométrie de masse (MS) pour comparer le protéome de l'Ub de la lignée cellulaire MCL résistante au BTZ (ZBR) et de son homologue parental (Z138), notre équipe a découvert que l'Ub joue un rôle dans la réponse au BTZ et dévoilé un passage moléculaire de l'UPS à l'ALS, décrivant la protéaphagie comme une caractéristique de la résistance au BTZ. On observe également un enrichissement des chaînes d'Ub K63 dans la lignée ZBR.

Notre hypothèse est que cet enrichissement pourrait la prédisposer à activer l'autophagie et les événements de signalisation liés à la résistance au BTZ, le but étant d'identifier le mécanisme et protéines impliqués. A cette fin, nous avons identifié le protéome d'Ub associé aux chaînes d'Ub K63 et K48 des cellules Z138/ZBR. Des traitements chimiques combinatoires permettent en outre de bloquer les enzymes E3 enrichies dans ZBR (TRIM24, UBR2, UBR4 et UBR5) et le récepteur d'autophagie p62.

TRIM24 est plus enrichi dans les cellules ZBR aux niveaux basaux. Sa stabilité est compromise différemment dans les cellules Z138 et ZBR après inhibition du protéasome ou de l'autophagie en utilisant la Bafilomycine A (BafA), suggérant qu'elle joue un rôle dans la diaphonie UPS-ALS. Nous avons utilisé dTRIM24, une chimère validée ciblant la protéolyse (PROTAC) pour cibler TRIM24 dans nos modèles. Un traitement dTRIM24/ZBR réduit le protéasome et favorise les effets apoptotiques coopératifs dans les cellules ZBR. Leur traitement par dTRIM24 favorise la formation des chaînes K48 et K63 et la fraction associée à l'Ub de p62 et des sous-unités du protéasome.

Les protéines UBR participent à la régulation de la voie de la règle N-end, qui cible le protéome Arg pour la dégradation via le domaine ZZ du récepteur d'autophagie p62/SQSTM1 en situation de stress protéotoxique. La vertéporfine (VTP) induit fortement l'apoptose des cellules ZBR, seule ou en combinaison avec le BTZ. Comme la VTP induit des espèces ROS, nous avons utilisé un inhibiteur du domaine ZZ de la p62 (XRK3F2) pour explorer le rôle de la p62 sur les enzymes UBR. Nous avons constaté que XRK3F2 a un impact différent sur la stabilité des enzymes UBR dans les cellules ZBR et Z138. La viabilité des cellules Z138 et ZBR est similaire lors d'un traitement individuel ou combiné au BTZ, ce qui suggère que les changements dans les niveaux de protéines des enzymes UBR ne sont pas associés à la résistance au BTZ et que la VTP est un meilleur traitement pour augmenter l'apoptose dans les cellules ZBR.

Pour mieux comprendre la réponse à la VTP dans les cellules résistantes au BTZ, nous avons caractérisé les *nanobodies* spécifiques des chaînes K48 et K63 avec *Hybrigenics* (outils commercialisés par Nanotag). Après avoir établi les conditions pour les nanobodies-

précipitations (NP), le protéome d'Ub des cellules ZBR et Z138 traitées ou non avec la VTP a été analysé par MS. Les résultats confirment l'enrichissement des chaînes K63 dans ZBR, fournissant une liste de protéines candidates jouant un rôle dans la résistance au BTZ.

Nos résultats indiquent que le remodelage de la chaîne d'Ub par des enzymes d'Ub pourrait contribuer à réguler la résistance des cellules MCL au BTZ. D'autres expériences sont nécessaires pour valider le rôle des facteurs identifiés et comprendre leur rôle dans la viabilité cellulaire et la réponse au BTZ. Ce travail devrait contribuer à l'identification de biomarqueurs potentiels pour le diagnostic et traitement des patients résistants au BTZ.

6. Preamble.

Protein homeostasis, or proteostasis, contributes to maintaining a protein equilibrium that is compatible with the regulation of cell functions and viability. Proteostasis also allows the cell to adapt and respond to different stress situations and environmental stimuli. When this equilibrium is disrupted, different pathologies appear including cancer types and neurodegenerative diseases (Gonzalez-Santamarta et al., 2020; Olivier Coux et al., 2020).

This protein equilibrium is controlled by the complex action of many post-translational modifications (PTM) such as phosphorylation, acetylation, and ubiquitylation, that control the localization, degradation, function, and the interaction between proteins regulating almost all cellular processes. Almost all proteins undergo PTMs at least once in their lifetime, highlighting their importance in modulating protein activity. Ubiquitylation dramatically affects the structure of modified proteins due to its capacity to form multiple chain topologies. In this way, ubiquitylation regulates the function of multiple crucial cellular factors. Enzymes implicated in the regulation of protein ubiquitylation [ligases or deubiquitylases (DUBs)] have been associated with multiple pathologies and are potential biomarkers and drug targets (Komander and Rape, 2012; Mattern et al., 2019).

Two major intracellular proteolytic pathways use Ub to recruit proteins to be targeted for degradation: The Ubiquitin proteasome system (UPS) and the Autophagy lysosome system (ALS). Both systems degrade misfolded or damaged proteins, avoiding their accumulation and consequent toxicity inside the cells. Initially, both systems were believed to act separately. However recent evidences suggest a single network in which they act in an orchestrated manner. Although both systems degrade ubiquitylated proteins in some instances, it is believed that a different Ub chain architecture is sufficient to distinguish targets that are degraded by these two pathways. Ub is much more than a signal to target proteolysis since it also regulates signal transduction pathways, protein trafficking and localization, among other functions. Nevertheless, the understanding of the regulation of protein activity by ubiquitylation is still at its early stages. At present, the technical limitations are a major bottleneck to explore complex Ub chain-types (Ji and Kwon, 2017; Kocaturk and Gozuacik, 2018; Nam et al., 2017; Quinet et al., 2020).

To explore some of these open questions, we have contributed to the development of new tools and technology to understand the functions exclusively associated with specific Ub chain types (K63 and K48). We have used Mantle Cell Lymphoma (MLC) as our main disease model. MCL is a very aggressive and heterogeneous haematological disease, with a poor rate of patient survival and a high percentage of relapses in patients treated with Bortezomib (BTZ), a proteasome inhibitor (PI) approved for its treatment by the Food and Drug Administration (FDA).

MCL is characterized by a high genetic instability. Therefore, it accumulates genomic alterations while progressing, like defects in the cellular stress response, cell differentiation, apoptosis, autophagy, or mutations in the drug target. Studies have also highlighted the importance and influence of microenvironmental factors and epigenetics in the expression of critical genes. Multiple molecular mechanisms have been proposed to be at the origin of the resistant phenotype for native and acquired BTZ resistance (Gonzalez-Santamarta et al.,

2020). Despite all efforts made to recover BTZ sensitivity in different disease models, there is a lack of consensus in the scientific community.

Data generated by our group suggest a dysregulation between the UPS and the ALS, in BTZ-resistant MCL cells (Grégoire Quinet et al, 2021). In fact, when using autophagy inhibitors, accumulated proteasome subunits can be visualized inside the autophagosomes vacuoles, coherent with an elevated basal proteophagy (the degradation of the proteasome through the ALS). The elimination of proteasomes could be an important mechanism that contributes to regulate BTZ resistance in MCL cells. Different Ub chain types were also observed in BTZ-resistant cells, together with an enrichment of Ub enzymes.

Since ubiquitylation may be at the “centre” of the UPS/ALS crosstalk, it would be of crucial importance to discover if there are different Ub-driven mechanisms contributing to the development of BTZ resistance. This knowledge would open opportunities to develop new treatments to recover BTZ sensitiveness, and ultimately improving the expected patient’s response and survival rate.

7. Mantle Cell Lymphoma (MCL).

Mantle Cell lymphoma (MCL) is a generally aggressive, and incurable type of B-cell non-Hodgkin's lymphoma (NHL). MCL is characterized by a translocation (11;14)(q13;q32), and a consequently constitutive overexpression of Cyclin D1.1 (Maddocks, 2018). Fluorescent in situ hybridization (FISH) reveals translocation t(11; 14) in almost all MCL cell lines (Ladha et al., 2019), and immunohistochemistry preferentially shows positivity for cyclin D1 (Figure1 B) (Motokura, 2019; Pérez-Galán et al., 2011). Cyclin D1–negative cases having typical morphology have been described but often show overexpression of cyclin D2 or D3 (Pérez-Galán et al., 2011).

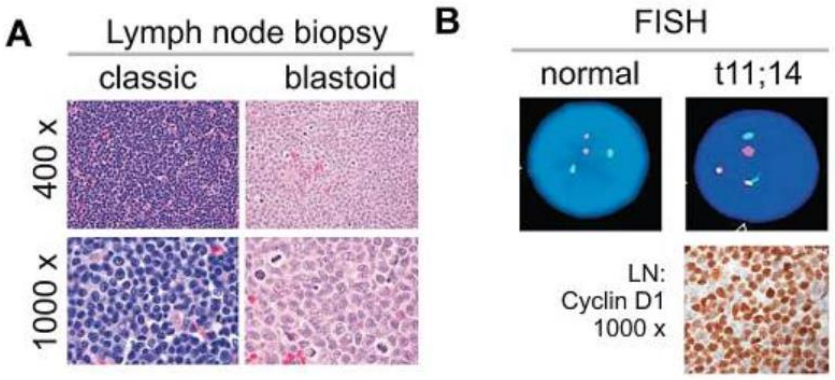

Figure 1: Mantle Cell Lymphoma characterization: Panel A; The pathologic subclassification (morphology and immunophenotyping) of 2 main subsets: classic and blastoid. Panel B; Fluorescence in situ hybridization (FISH) cytogenetics showing translocation t(11;14)(q13;q32) and immunohistochemistry for cyclin D1 overexpression detection (Pérez-Galán et al., 2011).

This haematological malignancy is a heterogeneous disease, with different and variable presentations, commonly classic and blastoid (Dreyling et al., 2018) (Figure 1 A), clinical and biologic risk factors and treatment approaches. This heterogenicity makes it very difficult to characterize, monitor the progression and the clinical response. Despite an improvement in understanding the biology and the continuous development of therapeutic strategies, favourable long-term outcomes of patients have not been achieved, and relapses are frequent even after intensive chemotherapy, contributing to a median survival of 5-7 years (Ladha et al., 2019; Maddocks, 2018; Motokura, 2019).

MCL clinically manifests as a generalized lymphadenopathy (abnormal lymph nodes; monomorphic small to medium sized lymphoid cells with irregular nuclei) (Veloza et al., 2019). Additional clinical features usually involve extra nodal sites, commonly observed in the peripheral blood, spleen, gastrointestinal tract, and central nervous system - the latest only seen in less than 5% of patients (Edwin and Kahl, 2018; Veloza et al., 2019).

MCL comprises of 2.5–6% of all NHLs (Ladha et al., 2019), and is composed of small-to-medium-sized cleaved lymphoid cells, which are proliferating in the nodules. The median age at disease presentation is 60 years with a male predilection (male-to-female ratio ≥2:1)

(Edwin and Kahl, 2018; Veloza et al., 2019). When diagnosed, extranodal involvement is common, then considering the disease to be in an advanced stage (Motokura, 2019).

These tumours are prone to the acquisition of other abnormalities like in cell cycle control, survival pathways and in DNA damage responses, leading to an aggressive behaviour during its progression. Because of this genetic instability, the clinical behaviour can usually correlate with the genetic background (Klener, 2019).

Compared to other NHLs, MCL exhibits shorter durations of treatments response, although the rapidity of the progression of the disease makes the initial treatment of patients at diagnosis (Maddocks, 2018). MCL treatment has evolved during the last years, and patients have different options depending on age, performance status, aggressiveness of the phenotype and possibility of bone marrow transplant (also known as autologous stem cell transplant or hematopoietic stem cell transplant, ASCT). As patients with MCL tend to be elderly with comorbidities, most of them are not eligible for intensive therapies or ASCT (Ladha et al., 2019).

Treatment choice has evolved from combination chemotherapy, to combination of targeted therapy, epigenetic modulation therapy, and immunotherapy. In a short period of time, the FDA (Food and Drug Administration) has approved 4 drugs for treating MCL: lenalidomide, an immunomodulatory agent; Bortezomib/Velcade (BTZ), a proteasome inhibitor; and Ibrutinib and acalabrutinib, both Bruton kinase (BTK) inhibitors (Ladha et al., 2019).

7.1 Mantle Cell Lymphoma Classification.

In the 1970s, investigators observed a histologically distinctive subtype of NHL, which resembled centrocytes of reactive germinal center (GC) because of its medium differentiation phenotype (Lennert et al., 1975). This subtype originates from mantle zones of secondary follicles and expresses B cell markers. At that time, it was characterized into nodular or classical, diffuse also called non-nodal, and blastoid mantle zone subtypes. However, MCL usually has a nodular or diffuse morphology with only 20% of the cases showing blastoid morphology. This blastic characterization, but also peripheral blood involvement at diagnosis, were preferentially seen as bad prognostic indicators (Ladha et al., 2019).

Histologically, MCL can be divided into classical, blastoid, and pleomorphic morphologies (blastoid subtype with larger cells) (Dreyling et al., 2018). MCL can also undergo a histological transformation from classical to blastoid morphology, a process called blastoid transformation (Klener, 2019).

In 2016, The World Health Organization (WHO) Classification of Tumours of Haematopoietic and Lymphoid Tissues (Swerdlow et al., 2016) updated the MCL subclassification, recognizing two molecular pathways of development, depending on different clinical presentations; classical or nodal MCL (80-90%) and leukemic nonmodal MCL (10-20 %) (Figure 2) (Edwin and Kahl, 2018; Klener, 2019; Pérez-Galán et al., 2011). The classical MCL involves lymph

nodes and extra nodal sites, while the non-nodal MCL subtype involves the peripheral blood, bone marrow and spleen (Edwin and Kahl, 2018).

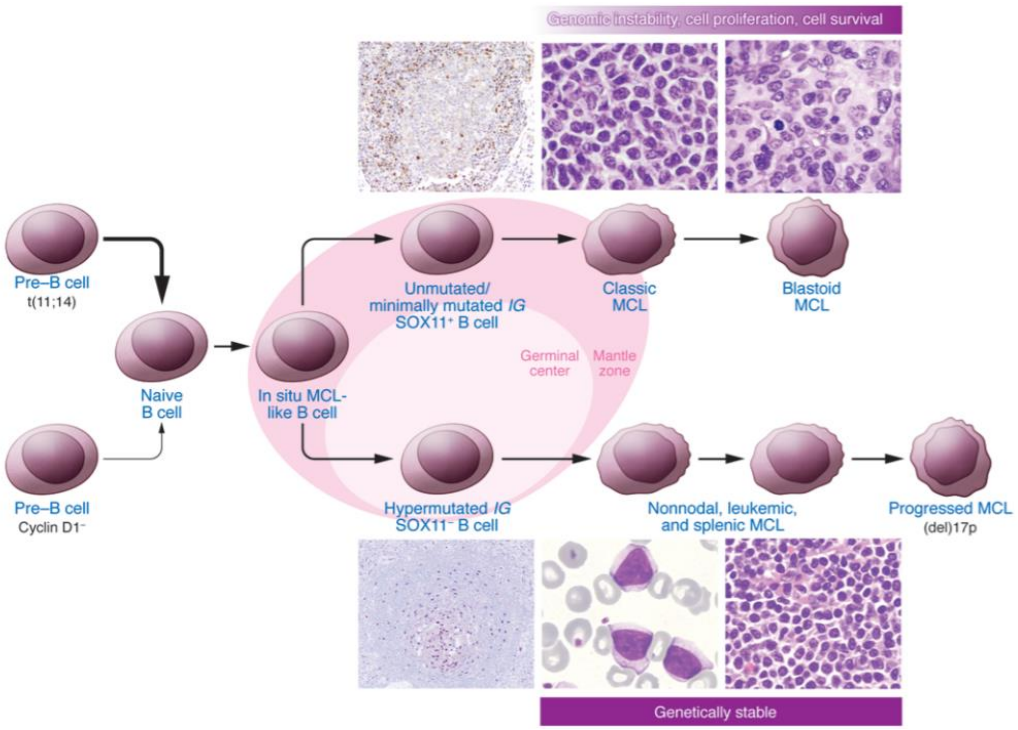

Figure 2: Model/Scheme representation of two different molecular subtypes of MCL (classic and non-nodal MCL). The naive B cell carrying the t (11;14) translocation and Cyclin D1 overexpression, colonizes the mantle zone of the lymphoid follicle and generates an in situ MCL lesion. Most MCLs evolve from these cells or cells in the marginal zone with no or limited IGHV somatic mutations, SOX11 expression: They are usually genetically unstable and can undergo a blastoid transformation. Alternatively, some naïve B cells can enter the germinal centre and undergo IGHV somatic hypermutations. These cells are genetically stable and do not express SOX11. The tumours derived from these cells tend to spread to the peripheral blood and spleen more than to lymph nodes (Jares et al., 2012).

Classical MCL is composed of mature B cells that do not enter into the GC, have no or minimal mutations in immunoglobulin heavy chain variable region genes (IGHV), and express transcription factor Sex-Determining Region Y-Box 11 (SOX11) (Klener, 2019).

In contrast, and less commonly, leukemic non-nodal MCL develops from the Germinal Center (GC) experienced memory B-cells (Klener, 2019), carrying IGHV somatic hypermutations, and lack of, or minimal, SOX11 expression. This type of MCL behaves in a more indolent manner, without genetic instability. However, secondary genetic abnormalities, such as mutations of the tumour suppressor P53 (TP53, “the guardian of the genome”), can result in a more aggressive behaviour and a poor disease outcome (Maddocks, 2018; Pérez-Galán et al., 2011).

7.2 Mantle Cell Lymphoma molecular pathogenesis.

At the centre of MCL biology, we can find Cyclin-D1 aberrant expression, cell cycle control, and DNA damage pathways dysregulation, but also signalling pathways that enhance tumour proliferation and evaded apoptosis contributing to MCL pathogenesis. These include the PI3K/AKT/mammalian target of the rapamycin (mTOR) pathway, the nuclear factor kappa-light-chain-enhancer of activated B cells (NF-kB), the BCL-2 proteins family of apoptosis regulators, and the Wnt signalling pathway (Pérez-Galán et al., 2011).

The t(11;14)(q13;q32) translocation is the most common genomic hallmark of MCL, placing the cell cycle regulator cyclin D1 (Figure 1, B) under control of the immunoglobulin heavy chain (IGH), leading to a constitutive D1 overexpression (Edwin and Kahl, 2018). Aberrant expression of cyclin D1 is not believed to be the initial event of the pathogenesis but it certainly contributes to tumour proliferation and poor clinical outcome. However, additional secondary genomic alterations associated with high proliferative behaviour involving several oncogenic pathways are needed for a complete transformation and aggressive behaviour in MCL (Figure 3) (Beà and Amador, 2017).

Cyclin D1 gene, CCND1, consists of 5 exons which can be spliced into cyclin D1a and D1b isoforms. Cyclin D1a contains mRNA destabilizing elements that limit its half-life. Cyclin D1a short transcripts (due to genomic deletions and point mutations) without those destabilizing elements leading to long-lived cyclin D1a mRNA and protein expression, are found in high proliferative tumours and are related to patient's short survival. Cyclin-dependent kinase 4 (CDK4) or 6 (CDK6) are also often overexpressed in MCL. They have been proved to promote tumorigenesis by forming a complex with CyclinD1a to promote cell-cycle entry inside the cells (Pérez-Galán et al., 2011).

Additional events can enhance the oncogenic potential of nuclear cyclin D like inhibition of nuclear export through a mutation in the glycogen synthase kinase 3 β (GSK3β), and the constitutive ubiquitylation in the cytosol to promote the degradation by the proteasome due to mutations in the E3 ligase SKp1-Cul1-F box protein (SCF; FBX4-αB Crystallin) (Pérez-Galán et al., 2011). Moreover, cyclin D1 protein overexpression can be further promoted by overactivation of the PI3K pathway (Klener, 2019).

IGHV can display either a germline configuration (Ig-unmutated), as found in naive B cells, or somatic mutations (Ig-mutated) indicating a response to antigen. However, the prognostic role of the IGHV mutation in MCL has not been confirmed and remains to be determined (Li et al., 2019; Pérez-Galán et al., 2011).

Besides Cyclin D1 overexpression, SOX11 has been described as a diagnostic maker that is equally expressed in D1-positive and D1-negative MCL phenotype. SOX11 regulates cell migration, invasion, growth, and angiogenesis, and was identified to be generally overexpressed in MCL as compared to other NHLs, but absent in non-nodal leukemic MCL. As this subset of patients present a more indolent behaviour of the disease, its ability to play a pathogenic role in tumorigenesis and aggressiveness of the disease must be highlighted (Beà and Amador, 2017).

In MCL, SOX11 overexpression contributes to tumour development by altering the terminal B-cell differentiation program, preventing MCL cells from entering into germinal center reactions. Different methylated regions in the SOX11 promotor of nodal MCL cells have been identified, explaining the aberrant expression of SOX1 (Klener, 2019).

The overexpression of SOX11 causes B-cell development alterations by prolonging PAX5 (The transcription factor Paired box 5), a key player in restricting the differentiation of lymphoid progenitors toward the B-cell lineage, and consequently Blimp1 transcription factor inactivation. Simultaneously, SOX11 represses the BCL6 transcription factor (involved in T cell differentiation), blocking the entrance of the cells into the GC. Moreover, SOX11 promotes angiogenesis via the activation of the PDGFA (platelet derived growth factor subunit A) pathway facilitating tumour growth. On the contrary, SOX11-negative non-nodal MCL tumours have low levels of PDGFA, and consequently low angiogenesis, contributing to the indolent behaviour (Beà and Amador, 2017; Hsi, 2014).

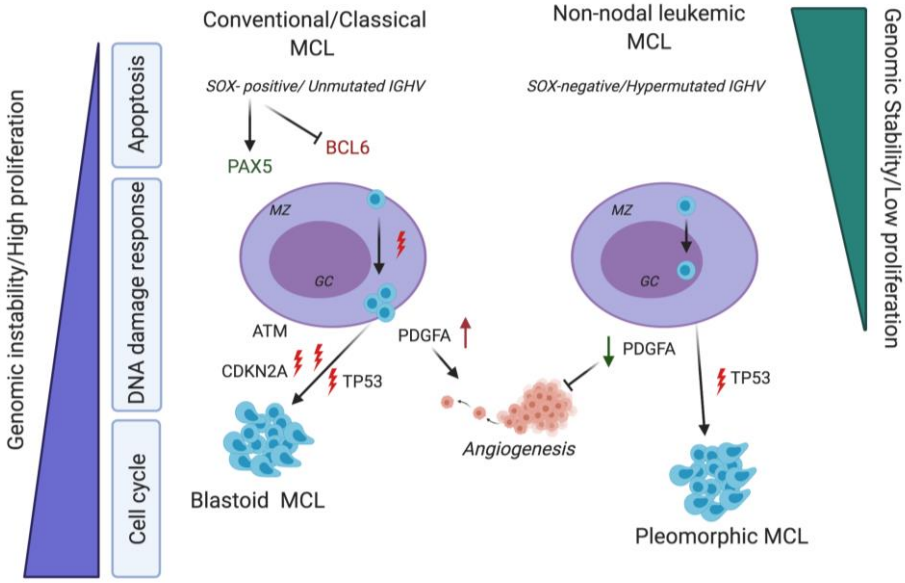

Figure 3: Model of genetic lesions that cooperate with cyclin D1 overexpression and t(11;14) translocation in different subsets of MCL. Left: classical/conventional or SOX11-positive MCL. Right: non-nodal leukemic SOX11-negative MCL. In classical MCL, SOX11 overexpression causes B-cell development alterations by prolonging PAX5 expression and repression of BCL6 transcription, blocking the entrance of the cells into the GC, and PDGFA pathway activation leading to angiogenesis. On the contrary, SOX11-negative non-nodal MCL tumours have low levels of PDGFA, and consequently low angiogenesis, responsible of the indolent behaviour.
Created with BioRender.com.

Cyclin D1 overexpression alone is insufficient for the malignant transformation of lymphocytes. Additional molecular aberrations leading to the dysregulation of different signalling pathways have been proved to drive MCL pathogenesis (Figure 3). MCL is one of

the B-cell malignancies with the highest degree of genomic instability, genetic lesions, and many secondary chromosomal alterations in regions that contain genes involved in cell-cycle regulation, DNA damage response, genotoxic stress pathways, epigenetic regulation, and key survival cell signalling (Klener, 2019). Nevertheless, at the time of diagnosis, 80% of patients had genetic lesions apart from translocation t(11;14); deletion of TP53, ataxia-telangiectasia mutated (ATM), cyclin-dependent kinase inhibitor 2A (CDKN2A), cyclin-dependent kinase inhibitor 1B (CDKN1B), and retinoblastoma 1 (RB1), or even amplifications of B-cell lymphoma 2 (BCL2), V-Myc myelocytomatosis viral oncogene homolog (MYC), CDK2, CDK4, and human homolog of mouse double-minute 2 (MDM2) (Klener, 2019).

7.3 Genotoxic stress pathways.

The ataxia-telangiectasia mutated (ATM) gene, encoding a tumour suppressor involved in DNA damage response, is one of the most frequently deleted or mutated gene in MCL (40–50%). Although ATM deletions have never been correlated with bad outcome in MCL, ATM aberrations can increase genetic instability and chromosomal imbalances (Camacho et al., 2002; Klener, 2019).

TP53 is another interesting tumour suppressor gene involved in this disease and known to play an important role in DNA damage responses and genotoxic stress pathways. The important role of p53 to maintain genome integrity is illustrated by the loss of p53 function in most human tumours and the high rate of tumour development in p53 knockout mice. p53 is a transcription factor that binds to specific sequences in the upstream region of many genes whose protein products regulate cell cycle progression and apoptosis. Under normal conditions, p53 acts in a way that cells do not proliferate upon damaged DNA. Consequently, the loss of this protective function allows the uncontrolled growth of cells containing oncogenic mutations (Desterro et al., 2000).

As already mentioned, TP53 mutations have been detected in blastoid or leukemic non-nodal MCL cases (14-31%) and are associated with a bad prognosis. Interestingly, TP53 mutation has been associated with worse outcome than TP53 deletion (Klener, 2019). At the same time, the overexpression of negative regulators, like MDM2 and MDM4, and serine/threonine kinase PIM1 (a protein that stabilizes MDM2) has been described in MCL, altering TP53 levels (Pérez-Galán et al., 2011).

Additionally, deletions in CDKN2A, which encodes two different tumour suppressors–p16INK4A (an inhibitor of CDK), and structurally unrelated p14ARF–also lead to p53 stabilization in MCL (Klener, 2019).

7.4 Key pro-survival and apoptotic cell signalling pathways.

The B-cell Receptor (BCR) pathway plays a central role in survival and proliferation. BCR signalling leads to the activation of different intracellular complexes that trigger key downstream effector molecules to promote aberrant activation of different pathways in the MCL cell biology mechanism. These molecules include the Bruton's tyrosine kinase (BTK), the

phosphoinositide-3 kinase (PI3K), the protein kinase B (AKT), the mammalian target of rapamycin (mTOR), and the nuclear factor kappa B (NFκB) (Klener, 2019). Additionally, the Wnt signalling pathway, which is critical to cell repair and maintenance of stem cell functions and therefore cell survival, has been detected to be dysregulated in MCL.

In MCL, PI3K is activated through BCR and CD19, as well as by oncogenic lesions like overexpression of microRNA (miRNA) miR-17–92 which suppresses expression of PTEN and PHLPP2 phosphatases, key negative regulators of the PI3K–AKT–mTOR pathway (Klener, 2019). mTOR, a serine-threonine kinase downstream of the AKT signalling pathway, forms the complexes mTORC1 (mTOR-Raptor) and mTORC2 (mTOR-Rictor), which have distinct substrates and activation mechanisms. In addition, the phosphorylation of the ribosomal protein 4E-BP1, a TORC1 substrate, has been proved to be a key step in the oncogenic pathway downstream of the AKT/mTOR axis, resulting in an increased translation of proteins like cyclin D1, c-MYC, and MCL-1. Interestingly, rapamycin, an allosteric inhibitor of the mTORC1 complex, does not induce apoptosis in MCL, but promotes cell cycle arrest believed to be mediated by an increase in the Cyclin-D1 proteolysis degradation (Pérez-Galán et al., 2011).

The NF-κB family of transcription factors is involved with the activation of transcription of genes involved in survival, proliferation, and apoptosis. The NF-κB signalling pathways are classified into canonical and non-canonical. The canonical pathway prompts inflammatory responses, immune regulation, and cell proliferation, while the non-canonical leads to B cell maturation and lymphoid organogenesis (Balaji et al., 2018). The canonical pathway is activated through phosphorylation and the consequent degradation of pI-κBα, a negative regulator. Constitutive activation of the canonical pathway has been reported in MCL cell lines, and gene expression profiling showed frequent high expression of NF-κB target genes, such as antiapoptotic proteins BCL-2, BCL-XL, XIAP, and cFLIP (Pérez-Galán et al., 2011).

BCR engagement and TNF signalling in the lymphoma microenvironment may contribute as well to NF-κB activation, as NF-κB signalling can also drive the transcription of the TNF family member BAFF/BLyS, a potent B-cell survival factor, activating a positive feedback loop that contributes to tumour cell survival (Pérez-Galán et al., 2011).

Wnt signalling can be activated through 2 different mechanisms: β-catenin (canonical pathway), and c-Jun N-terminal kinase activation (alternative pathway, or non-canonical). The canonical pathway is more affected in cancer, and it has been detected as overactivated in MCL. WNT3 and WNT10a are indeed consistently overexpressed in MCL cell lines and patient biopsies, leading to a constitutive activation of the Wnt canonical pathway (Gelebart et al., 2008). Furthermore, the serine-threonine-selective kinase 2 (CK2), which is constitutively phosphorylated in MCL, phosphorylates β-catenin impeding its proteasomal degradation, resulting in an increase in its transcriptional activity (Gelebart et al., 2008; Pérez-Galán et al., 2011).

In addition, BCL-2 a regulator of apoptosis, has been detected to be deregulated in almost all MCL cell lines with frequent high-level of BCL2 copy number gains. At the same time, high MCL1 (pro-survival member of Bcl-2 family proteins) expression is common in more aggressive tumours. The molecular mechanisms driving this overexpression are complex,

and usually related to BCL-2 gains and BCL2 mRNA overexpression as a consequence of aberrant activation of pro-survival pathways, like NF-κB signalling, or as a result of loss of its negative regulators like loss of miRNA miR-15/16, due to frequent 13q deletions. Moreover, the dysregulation of PTMs can increase the stability of BCL2 proteins, such as deficiency of FBXO10 [F-box protein 10, Substrate-recognition component of the SCF (SKP1-CUL1-F-box protein)-type E3 Ub ligase complex] leading to a decreased degradation and turnover (Klener, 2019).

7.5 Epigenetic regulation.

Different studies have highlighted the important contribution of microenvironmental and epigenetics to genomic stability in MCL by altering the expression of critical genes. Epigenetic regulation involves acetylation and methylation to regulate the access of transcription factors to DNA. The acetylation of histones leads to an open chromatin conformation that facilitates the access of transcription factors to DNA. In contrast, the methylation of gene promoters can silence gene expression. Both acetylation and methylation can be altered in tumours and can contribute to disease pathogenesis. In MCL different genes has been identified to be silenced by hypermethylation, but also some of them upregulated by hypomethylation, like NOTCH1, CDK5, and HDAC1 (Pérez-Galán et al., 2011).

Nevertheless, the most recent example of epigenetic MCL contribution, relate NSD2 mutations (alias multiple myeloma SET domain-containing protein type III (MMSET)) coding for a histone methyltransferase specific for methylation of histone 3 lysine 36 (H3K36). In MCL, NSD2 mutations have been correlated with shorter survival and blastoid transformation (Klener, 2019). The inhibition of NSD2 sensitizes cancer cells to PI3K inhibitors and DNA-damaging agents, thus emerging as a new relevant druggable target in MCL and other cancers with recurrent gene mutations. Other epigenetic modifiers commonly mutated in MCL include MLL2, MLL3, and SMARCA4. For example, loss-of-function mutations of MLL2, an H3K4 methyltransferase, have been described in different B-cell lymphomas, and mutations in SMARCA4 have been associated with poor response in MCL (Klener, 2019).

7.6 Mantle Cell Lymphoma: prognosis factors, front line treatments and management.

New MCL patients are diagnosed based on clinically manifest symptoms. However, other medical checks-ups can involve a detection of lymphocytosis during routine blood cell collections, and polymerase chain reaction (PCR) to detect tumour cells in the peripheral blood and/or bone marrow (Motokura, 2019).

Mantle cell international prognostic index (MIPI), ki-67 proliferation index, and TP53 mutations are the preferred prognostic biomarkers (Ladha et al., 2019). MIPI was elaborated with data from 455 patients with advanced stage MCL. It considers age, Eastern Cooperative Oncology Group performance status, lactate dehydrogenase levels, and white blood cell

count (Hoster et al., 2008; Motokura, 2019). The MIPI score divides patients into low, intermediate and high-risk groups - the low risk group having a 5-year overall survival (OS), intermediate risk group a median of 51 months and high-risk group 29 months (Ladha et al., 2019).

Later in time, the MIPI index was modified with the incorporation of the Ki-67 proliferation index, a growth fraction marker (Motokura, 2019). The Ki-67 proliferation index is a biomarker independent of MIPI which helps to predict survival of patients receiving high dose immunochemotherapy and ASCT. In general, a high proliferative index evaluated by Ki67 immunohistochemical staining associates with poor outcomes in patients (Ladha et al., 2019).

These markers rely on tissue biopsy, however not all patients are necessarily subject to lymph node biopsy. Many patients with sufficient numbers of circulating MCL cells can be safely diagnosed based on flow cytometry and confirmation of t(11;14) translocation by locus-specific FISH (Klener, 2019).

In general, low-risk patients benefit from a standard immunochemotherapy regimen, or even are candidates for a diverse chemo-free regimen, and patients carrying high levels of adverse prognostic factors (high-risk MIPI and Ki-67, TP53 mutations and blastoid morphology) do not benefit from intensified immunochemotherapy regimen and ASCT (Klener, 2019).

MCL therapy is stratified by age (younger versus elderly) but also, by the patient capability to undergo high-dose therapy (HDT) with ASCT. High dose immunochemotherapy is recommended for young fit patients, which is usually combined with AST, nevertheless rarely performed for elderly patients. If the risk among patients with MCL is low based on MIPI, the expectant management, or “watch and wait” strategy, is an option, particularly for elderly patients having an indolent phenotype (Edwin and Kahl, 2018). It has been proved that individuals of this group can be safely watched, initially without any compromise to their long-term outcome. (Rule, 2019). Nevertheless, chemotherapy-free regimens are preferred for elderly patients due to their less severe hematologic toxicity (Motokura, 2019).

Patients with aggressive B-cell lymphomas were commonly treated with anti-CD20 antibody drug immunochemotherapy, rituximab, cyclophosphamide, doxorubicin, vincristine, and prednisone (R-CHOP), without any long-term improvement. As an alternative, intensive immunochemotherapy regimens, such as rituximab-based hyper fractionated cyclophosphamide, vincristine, doxorubicin, and dexamethasone alternating with high-dose methotrexate and cytarabine (R-HCVAD/ MA) have significantly improved the outcomes of younger patients (median OS of 11-13 years) (Motokura, 2019).

For young patients, the current standard treatment involves a consolidation in responders with HDT-ASCT, even if the benefit of HDT-ASCT is uncertain for patients with TP53 aberrations. All patients should be treated with rituximab maintenance (RM), usually every 2–3 months for 2–3 years, and relapses in the low-risk MIPI group of patients are rare. Elderly patients are usually treated with an R-CHOP-like regimen or R-bendamustine, with or without cytarabine. However, BTZ, in combination with cyclophosphamide, doxorubicin, and

prednisone (so-called VR-CAP), was the only immunochemotherapy regimen that was associated with prolonged OS (Motokura, 2019).

BTZ (Bortezomib/Valcade), a proteasome inhibitor, has shown efficacy as monotherapy, in relapsed MCL patients. When combined in frontline setting, bortezomib has shown an overall response (OR) of 81% to 91%. BTZ shows better results than vincristine in the standard R-CHOP regimen (VR-CAP) in young patients. In fact, the analysis showed a clear relationship between higher dose and longer OS (Ladha et al., 2019).

In addition, Bortezomib maintenance therapy – after Bortezomib R-CHOP induction – not only showed that it was well tolerated but also improved response and survival (Ladha et al., 2019). However in elderly patients, bortezomib-based therapy is associated with a high incidence of painful peripheral neuropathy and herpes zoster, which requires dose adjustment and antiviral prophylaxis (Motokura, 2019).

Despite this initial stratification, different therapy options can be observed in the different group of patients, and different clinical trials are being tested. There is no standard frontline therapy for MCL, and quite frequently treatment leads to the development of resistance. Treating these patients is still a challenge for the scientific and clinical community and developing a personalized and precise therapeutic strategy is the direction to ultimately find a curative option.

Challenges in MCL treatment include a heterogeneous pathophysiology, high progression and recurrence, shorter disease-free interval, advanced patient age, and the achievement of long-term remission avoiding toxicities (Ladha et al., 2019). Understanding the molecular mechanism that controls or contributes to the development of resistance in MCL cells, is a major issue to address by fundamental biology in order to provide knowledge for clinical purposes and combinational treatment choices (Maddocks, 2018).

In the last decades, different innovative therapies and treatments have been introduced to MCL clinical practice to improve the landscape of MCL patients. Due to the different molecular pathways implicated in the phenotype development, different molecular targets have been proposed (Klener, 2019).

8. Proteasome inhibitor resistant mechanism.

Proteasome inhibitors (PI) have been developed for clinical purposes to treat human diseases in which the Ubiquitin (Ub) proteolytic pathway is involved. They have also become powerful research tools in probing the structure and function of the proteasome and Ub pathway. Most of them act as pseudo-substrates that become linked covalently to the active site of the different proteasome subunits, resulting in catalytic inactivation (Roeten et al., 2018).

The FDA approved the use of Bortezomib (referred as BTZ) in 2003, then carfilzomib (CFZ, Kyprolis) in 2012, and ixazomib (IXZ, Ninlaro) in 2015. These PIs have changed the

management of hematologic malignancies like multiple myeloma (MM) and MCL, improving patient outcomes. PIs exploit the dependence on the Ub proteasome pathway, a feature characteristic of cells with a high protein turnover and immunoglobulin production (Roeten et al., 2018). BTZ was first approved for treating refractory relapse MCL, but due to clinical tolerance and side effects it is included now as a first line treatment for MM and MCL (Nunes and Annunziata, 2017).

Proteasome inhibitors lead to cell death by affecting different pathways. One of them is the NF-κB pathway, a pro-survival signalling pathway for many cell types. IκBα is an endogenous negative regulator of the NF-κB transcription factor, that is usually degraded by the proteasome. However, when the proteasome is inhibited, IκBα remains intact, preventing the transcription of many genes. Inhibition of the NF-κB pathway was initially thought to be the principal mechanism of PI anti-cancer activity. However, the use of PS-1145, a IκB kinase inhibitor, did not promote the same cellular toxicity, suggesting that other mechanisms may be involved. Amongst those, we can find the induction of apoptosis through the c-Jun NH2-terminal kinase (JNK) and p53. Additionally, PIs can prevent the degradation of pro-apoptotic family proteins, like Bim, Bid and Bik, promoting its accumulation to trigger caspase activation, and increasing levels of BH3-only protein NOXA (BCL2 family member) resulting in the same outcome (Nunes and Annunziata, 2017).

BTZ is a peptide boronic acid that reversibly inhibits primarily the chymotrypsin-like activity of the proteasome. It is the first proteasome inhibitor approved by the FDA and was initially used in clinical trials of relapsed MCL. BTZ, as other PIs, was initially hypothesized to acts as an anticancer agent through the inhibition of the NF-κB signalling. However, in MM and MCL, BTZ is thought to induce apoptosis through the up-regulation of the BH3-only protein NOXA, induced by cellular stress response, triggered by the accumulation of polyubiquitylated proteins that induce endoplasmic reticulum stress and the generation of reactive oxygen species (ROS). NOXA is transcriptionally induced by a decreased ubiquitylation of histone H2A that facilitates access to the NOXA gene (PMAIP1) promoter, and the binding of ATF3 and ATF4 transcription factors, triggering BAK- and BAX-dependent mitochondrial apoptosis, and a transcriptional response involving the NRF2 transcription factor, amplifying the oxidative stress response (Pérez-Galán et al., 2011).

BTZ has been used for decades as a treatment of MM and MCL. It is however often associated with neuropathy and acquired resistance. As a consequence, second generation PIs have been developed to overcome these aspects, such as marizomib (MRZ), carfilzomib (CFZ), ixazomib (IXZ) and oprozomib (OPZ) (Roeten et al., 2018). MRZ, unlike BTZ, targets all the catalytic sites of the proteasome in a reversible manner, reducing off-target effects and toxicities in patients. However, preclinical adaptation to these new agents has been already displayed despite major efforts, highlighting the need for alternative strategies to overcome PI resistance (Yong et al., 2018).

Resistance to proteasome inhibitors has been observed in various cancer types including haematological, pancreatic or breast cancer (Roeten et al., 2018). The full understanding of the mechanisms underlying PI resistance in cancer is a prerequisite to design new strategies to recover sensitivity to these agents.

8.1 Relapse/refractory MCL.

Relapse/refractory (R/R) MCL is an incurable disease with a median OS of 1–2 years. Due to our increasing knowledge of the biology of MCL, several innovative agents have been designed, tested, and approved for therapy, dramatically changing the treatment landscape for those patients. However, despite these recent scientific improvements, relapses after treatment are still frequent and molecular mechanisms associated are poorly understood (Klener, 2019). Apart from BTZ, additional treatments for relapse/refractory MCL include lenalidomide, ibrutinib, and Chimeric Antigen Receptor T cell therapy (CART therapy under development), among others.

Lenalidomide is an emerging new player in the treatment of lymphoma, approved for the treatment of patients with R/R MCL by the Food and Drug Administration in 2013 (Maddocks, 2018). It is an immunomodulatory agent with an antitumor activity, an oral derivative of thalidomide that stimulates T-cells causing natural killer (NK)–cell expansion and cytotoxicity, but also induction of apoptosis through the downregulation of cyclin D1 (Edwin and Kahl, 2018). Despite poor results initially observed when combined with BTZ, a clinical benefit was observed when using lenalidomide and rituximab as front-line treatment in some patients. However, toxicity was displayed, maybe due to inadequate doses, and incidence of infections make this treatment difficult to apply in older patients (Ladha et al., 2019).

Ibrutinib is a covalent inhibitor of BTK (commonly overexpressed in MCL), which is important for signalling via B-cell receptors. Ibrutinib binds covalently and with high affinity to the active site of BTK, inhibiting the B-cell receptor signalling leading to downstream impairment of cell growth, proliferation, survival, adhesion, and migration. Patients with R/R MCL have the best OS rate when using this strategy. However, common side effects include bleeding, diarrhoea, rash, and atrial fibrillation (Motokura, 2019).

CART therapy offers an innovative intervention for MCL patients, improving response and duration of R/R MCL. It involves removing endogenous T cells, to genetically reprogram them so they can attack and target the CD19 protein on B cells. Introducing engineered T cells can display an immune reaction in the host patient. Therefore, investigators are modifying various parts of CART therapy to improve its feasibility and efficiency (Ladha et al., 2019). As CART treatment is offering a good response level at its initial steps of development, it may offer in no time the potential of a curative approach in selective patients outside of the limited role of AST (Gauthier and Maloney, 2020; Maddocks, 2018).

8.2 Molecular mechanisms associated with bortezomib resistance.

Cancer cells sometimes fail to respond to a specific chemotherapeutic regimen because of the presence of inherently resistant cells, harbouring pre-existing random mutations, (intrinsic resistance), but also because cancer cells can acquire drug resistance through a continuous exposure to the treatment (acquired resistance). Chemotherapeutic resistance is a multifactorial process in which different mechanisms have been described so far, depending on the cancer cell type and tumour. However, it is unclear for researchers

whether it is a selective process or an adaptative one. Most probably is that due to cancer cells heterogeneity, tumour cells with the same genetic background transiently acquire a resistant phenotype in a non-genetic manner (Valletti et al., 2019).

Since the approval of BTZ as a treatment of R/R MCL, numerous phenomena have been described to explain innate or acquired resistance observed in more than half of patients (Diefenbach and O'Connor, 2010). It is known that the development of resistance to BTZ in MCL is an adaptive process, which takes place gradually and includes metabolic changes and/or deregulated (re)activation of adaptive processes like plasmocytic differentiation, autophagy, or improper activation of intracellular signalling pathways such as PI3K/AKT/mTOR axis or NF-κB, among others (Gonzalez-Santamarta et al., 2020).

In the last decade, different molecular mechanisms involved in BTZ resistance (innate and acquired) have been proposed (Figure 4) learning from MCL and MM. In order to present the complex landscape displayed in BTZ inherent/acquired resistance, different mechanisms will be discussed in the following sections, including defects in the initiation/regulation of cellular stress pathways, cell differentiation, apoptosis, autophagy, mutations and alterations in the expression of the drug target (Robak et al., 2018).

8.3 Inherent resistance.

PSMB5 mutations have been proved to lower the PI binding capacity to the 20S proteasome, the PI target (Franke et al., 2012; Soriano et al., 2016). Those mutations have been mainly found in tumours after receiving a heavy PI-based therapy, suggesting that these mutations appear later during the process of clonal selection. Four PSMB5 mutations were detected in a single MM patient having received a prolonged BTZ-based treatment (Barrio et al., 2018). However, Soriano and colleagues challenge this hypothesis as they showed that proteasome activity is dispensable in BTZ-resistant MM cell lines (Soriano et al., 2016), indicating that other mechanisms may be required for a complete resistant phenotype in those cells.

Dysregulation in the apoptosis signalling pathway is a common mechanism of drug resistance found in different haematological malignancies. This pathway is controlled by the BCL-2 family members, composed by pro-survival proteins (BCL-2, BCL-XL, MCL-1, BCLW and BFL1/A) and proapoptotic factors represented by multidomain (BAX, BAK and BOK) and BH3-only (BIM, PUMA, NOXA, BAD, BID, BMF, BIK and HRK) proteins. Upon the activation of cytotoxic or stress signals, the BH3-only proteins interact with their pro-survival counterparts, leading to the release and oligomerization of BAX and BAK, permeabilization of the mitochondrial outer membrane, cytosolic release of apoptogenic factors, and ultimately the activation of the caspase family of proteases promoting cell death (Valentin et al., 2018). In MCL cells, BTZ can promote an accumulation of MCL-1, blocking the pro-apoptotic signalling of NOXA, thus delaying the onset of cell death. In fact, blocking NOXA expression or inhibiting MCL-1 has been efficiently used to modulate the response to BTZ in MCL (Pérez-Galán et al., 2007).

Constitutive NF-κB activity is often present in MCL (Yang et al., 2008). High NF-κB activity was found in BTZ refractory tumour cells, and the lack of response to BTZ has been linked to a proteasome-independent degradation of the intrinsic NF-κB inhibitor, IκBα (Yang et al., 2008). The NF-κB pathway also regulates CK2, a multifaceted serine/threonine kinase involved in several signalling cascades. CK2 modulates the IκBα protein turnover, p53 function, AKT activation, and has a role in the control of endoplasmic reticulum (ER) stress and unfolded protein response (UPR). CK2 is overexpressed in many blood tumours, and inhibition of CK2, has been proved to downregulate NF-κB, and activate transcription 3 (STAT3). Additionally, in combination with BTZ, CK2 inhibition enhances the proteotoxic effect, suggesting that CK2 levels may be involved in MCL resistance to BTZ (Manni et al., 2012).

As already mentioned in the previous sections, the BCR pathway is another pathway that regulates cell survival and proliferation of MCL cells (Chattopadhyay et al., 2018). It includes a heterodimer of CD79A/B molecules, and a key co-receptor CD19. The upregulation of those molecules has been proposed to promote BTZ resistance in MCL cells, as the use of dasatinib (a kinase inhibitor) has been proved to reduce the level of phosphorylated BCR kinases like LYN, promoting synergistic activity in combination to BTZ (Kim et al., 2015).

In MCL, the redox status is a crucial mediator of BTZ efficacy, as PIs lead to the generation of large amounts of reactive oxygen species (ROS) (Pérez-Galán et al., 2006). The nuclear factor NF-E2 p45-related factor 2 (NRF2) was identified as a key regulator of this response. Under physiological conditions, it is sequestrated by Kelch-like ECH-Associated Protein 1 (KEAP1) in the cytosol. When KEAP1 is oxidized by ROS, NRF2 is released to the nucleus where it initiates the transcription of genes involved in the adaptive oxidative stress response. Resistant tumours show a minimal change in the expression of NRF2 target genes as well as genes related to protein ubiquitylation or proteasome components, in contrast to BTZ-sensitive MCL. Accordingly, a high expression of NRF2 target genes has been correlated with poor sensitivity to proteasome inhibition (Weniger et al., 2011). In Addition, a recent study highlighted the capacity of ROS to regulate cell sensitivity to BTZ. Authors showed that O2- was involved in the sensitization of MCL to BTZ, while H2O2 impaired apoptosis (Luanpitpong et al., 2018).

8.4 Acquired resistance.

PI-acquired BTZ resistance has been linked to different factors that appear to be interconnected, showing in some cases cross-resistant profiles between different PIs. Those encompass the upregulation of 20S proteasome subunits including β5c, the downregulation of 19S proteasome subunits, the overexpression of efflux pumps, adaptive metabolic changes, the modulation of the unfolded protein response, and the alteration of the autophagy degradation pathway.

In MM, Franke and colleagues suggested that the upregulation of the β5c subunit appears as a consequence of PSMB5 mutations, and due to prolonged exposure to BTZ (Franke et al., 2012). However, when comparing BTZ-adapted MCL cell lines with their parental counterparts, a reduced expression of 19S proteasome subunits was detected in the BTZ-

resistant phenotype. Interestingly, when autophagy was blocked with inhibitors such as bafilomycin A (BafA) or chloroquine (CQ), the level of those proteasome subunits was increased, suggesting an autophagy-mediated degradation in MCL BTZ-resistant cells. Supporting this hypothesis, Quinet et al showed that a constitutive activated proteaphagy contributes to developing resistance to BTZ in MCL cells. In Quinet's model, it is hypothesized that BTZ-resistant cells bypass proteasome inhibition relying on autophagy, through the degradation of proteasomes (Grégoire Quinet et al, 2021).

ABC (ATP-binding cassette) transporters such as ABCB1 (multi-drug resistance, MDR1 or P-glycoprotein, P-gp) mediate drug resistance by alterations of the absorption and elimination of those. Thus, high ABCB1 expression has been correlated with bad prognosis, resistance and aggressiveness in MM (Abraham et al., 2010). High overexpression of the ABCB1 protein limits the cytotoxicity capacity of BTZ/CFZ proteasome-inhibiting activity. However, resistance to BTZ/CFZ has been proved to be independent from proteasome activity but dependant on energy metabolism, redox homeostasis, protein folding and degradation. Authors also confirmed the upregulation of the heat-shock proteins HSP70 and HSP90, apart from ABCB1 in CFZ-resistant cells (Abraham et al., 2010; Besse et al., 2018). In line with this data, the deregulated expression of several cytosolic HSP70 family members has been associated with BTZ acquired and innate resistance in MCL (Weinkauf et al., 2009) and MM (Davenport et al., 2007).

NRF2 seems to be another node for BTZ- and CFZ-resistance in MM, but also in inherent MCL BTZ resistance, as different clinical data show NRF2 upregulation in relapsed patients (Riz et al., 2016). This protein is involved in redox homeostasis by inducing antioxidant and detoxification genes and by modulating energy metabolism (Hayes and Dinkova-Kostova, 2014).

In the last decade, numerous studies have indicated, that components of the BM stroma, extracellular matrix (ECM), cytokines, chemokines and growth factors, are involved in BTZ resistance in MM cells (Podar et al., 2009). The membrane protein myristoylated alanine-rich C-kinase substrate (MARCKS) plays an important role in cell adhesion, spreading, invasion, and is crucial for metastasis (Finlayson and Freeman, 2009). MARCKS is overexpressed in MM cell lines and involved in the cross-resistance to the farnesyltransferase inhibitor R115777, and BTZ (Yang et al., 2015). In line with these, the insulin-like growth factor IGF-1, that is produced by plasma cells and present in the BM microenvironment, has been proposed to promote proliferation and drug resistance in MM cells through the activation of the MAPK and PI3K/AKT-signalling pathways (Podar et al., 2009).

Cells that synthesize large amount of proteins usually exhibit an expanded ER network, that promotes UPR activation in conditions of ER stress, when coping with unfolded or misfolded proteins like in the case of MM and MCL cells (Vincenz et al., 2013). The ER stress upregulates three UPR signalling branches: transcription factor 6 (ATF6), protein kinase R (PKR)-like ER kinase (PERK)-ATF4 and inositol-requiring enzyme 1 (IRE1)-X box binding protein 1 (XBP1), which suppress global translation and promote protein folding and degradation. ATF6 translocates into the nucleus and activates the XBP1 promoter. At the same time, IRE1 oligomerizes and auto-phosphorylates, resulting in the activation of its endonuclease activity, that cleaves XBP1 mRNA into an active XBP1s form. XBP1s acts as

transcription factor and activates genes encoding protein folding and chaperones. A low "IRE1-XBP1" phenotype has been found in MM cells resistant to BTZ, suppressing ER stress response (Mimura et al., 2012).

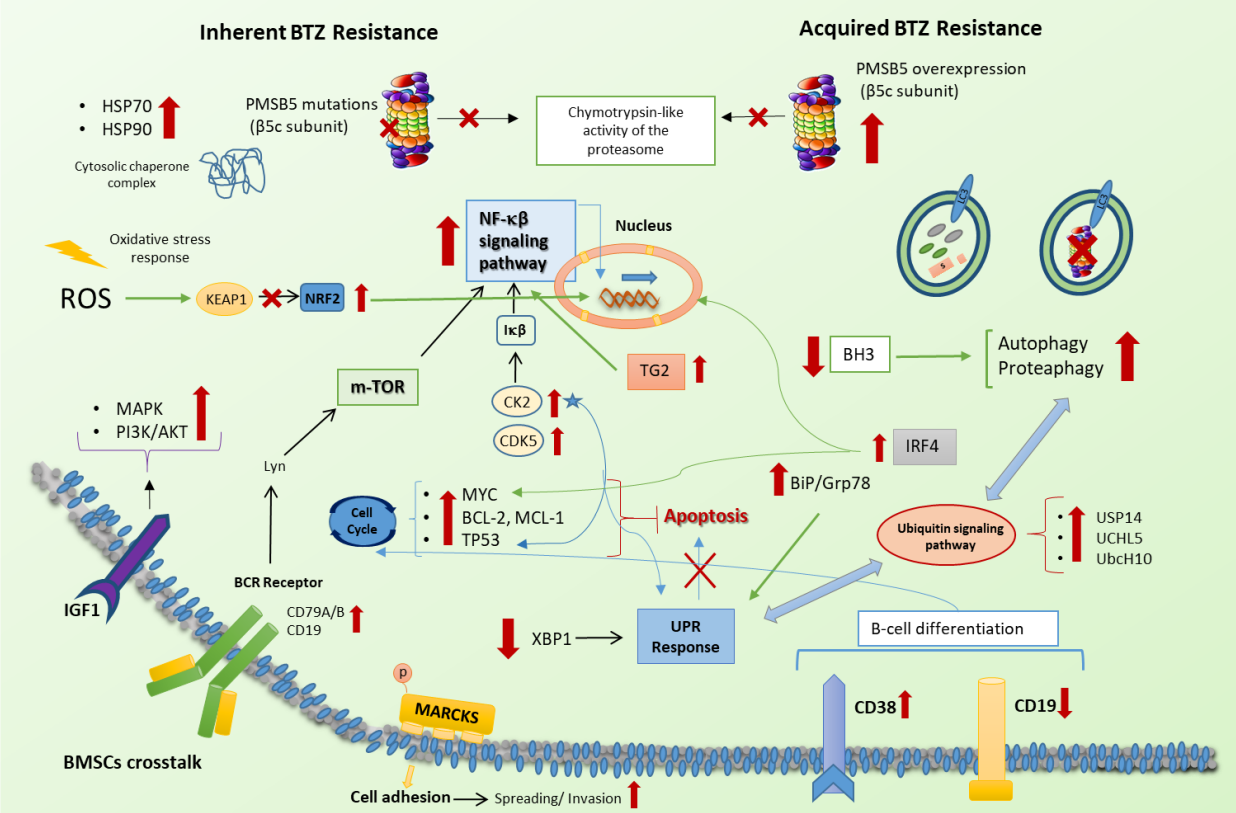

Figure 4: Molecular mechanisms associated with BTZ resistance in acquired and inherent resistant MCL and MM cell models. The pathways involved are: UPS and ALS degradation systems, UPR response, apoptosis, B cell differentiation, cell cycle regulation and mutations in the β5 subunit of the proteasome. Arrows indicate up- or downregulation of the different molecular mechanisms. *Modified from* (Gonzalez-Santamarta et al., 2020).

It is known that proteasome inhibition, induces autophagy activation in order to eliminate UPS substrates avoiding protein accumulation (Ding et al., 2007). Interestingly and supporting Quinet's results (Grégoire Quinet et al, 2021), the Ub-binding cargo autophagy receptor sequestrosome 1 (SQSTM1) or p62 is a key element in the UPS/ALS crosstalk (Cohen-Kaplan et al., 2016a). It has been proved that SQSTM1/p62 expression is elevated triggering a pro-survival autophagy in MM cells resistant to CFZ (Riz et al., 2016).

High expression of deubiquitylating enzymes (DUBs) and autophagy related proteins has been detected in MM patients resistant to BTZ. These alterations in enzymes that are involved in deubiquitylating misfolded/unfolded proteins and in the turnover of proteins by the autophagy-lysosome system (ALS), suggest that Ub signalling pathways play an important role in BTZ resistance. They include USP14 and UCHL5 (Niewerth et al., 2015) but also the Ub-conjugating enzyme H10 (UbcH10) (Wang et al., 2015).

A dysregulation of the intracellular stress machinery can also affect BTZ sensitivity. ER homeostasis is controlled by the immunoglobulin heavy chain binding protein (BiP), also referred as 78-kDa glucose-regulated protein (Grp78) (Ni and Lee, 2007). Under non-stressed conditions, BiP/Grp78 binds to the ER transmembrane PKR-like ER kinase, IRE1, and ATF6 maintaining and inactive monomeric state (Kaufman, 2002). After proteasome inhibition, the accumulation of polyubiquitylated proteins leads to the dissociation of BiP/Grp78 from the luminal domains and the initiation of UPR and apoptosis (Szegezdi et al., 2006). The intracellular accumulation of BiP/Grp78 has been related to acquired and primary resistance to BTZ in MCL, avoiding the apoptotic outcome that would follow in normal conditions (Roué et al., 2011).

Plasmacytic differentiation can be another source of BTZ resistance in MCL cells. BTZ-resistant MCL cells display some of the characteristics of the plasma cells, such as the over-expression of interferon regulatory factor 4 (IRF4) and elevated membrane levels of CD38 and CD138 cell surface markers (Pérez-Galán et al., 2011). Mouse xenograft models of MCL demonstrated a tight correlation between increased tumorigenicity of BTZ-resistant tumours with a plasmacytic differentiation phenotype including an upregulation of IRF4, PR domain zinc finger protein 1 (PRDM1/BLIMP-1) and CD38, and loss of the B cell markers PAX5 and CD19 (Moros et al., 2014).

The identification of key elements of BTZ resistance is far for being a consensus among the scientific community. Different targets and drug treatments have been proposed to recover BTZ sensitivity. Nevertheless, most of them lack the scientific support to reach a clinical benefit and efficient approach directly impacting MCL patients.

8.5 Potential targets to recover PI sensitivity.

Proteasome inhibition affects a wide range of cellular factors, including important signalling cascades, oncogenes, or epigenetic regulators. Given the resistance to PIs observed in some patients, alternative drugs have been tested to overcome resistance as single or combinatorial treatments. Some of them will be briefly discussed in this section.

The dual PI3K and mTOR inhibitor dactoslisib (NVP-BEZ235) showed great results in MCL BTZ-resistant cell lines (Kim et al., 2012). Following this clue, a new generation of mTOR inhibitors, such as temsirolimus and deforolimus have been also proposed for MCL, nevertheless obtaining limited clinical impact (Rizzieri et al., 2008; Witzig et al., 2005).

The NF-κB pathway can be modulated by different compounds to recover sensitivity in PI-MM and MCL resistance cells. Selinexor, a reversible inhibitor of exportin 1 (XPO1), blocks the nuclear export of NF-κB /IκBα complexes leading to NF-κB pathway inactivation (Turner et al., 2016). Transglutaminase 2 (TG2), a calcium-dependent enzyme, hampers high NF-κB expression in BTZ-resistant cells. Moreover, the combination of both molecules with BTZ improved cytotoxicity in MCL cells (Jung et al., 2012). In addition, synergic apoptosis in MCL has been detected when BTZ was combined with degrasyn, a compound that targets constitutive NF-κB and STAT3 (Pham et al., 2010).

BTK inhibitors lead to the NF-κB inactivation and downregulation of MYC (de Claro et al., 2015). Therefore, promising preclinical results were obtained combining ibrutinib and BTZ in MCL and MM BTZ-resistant cells (Murray et al., 2015). BH3 mimetic compounds like obatoclax also showed great results in relapsed MCL, by neutralizing BTZ-induced MCL-1 accumulation (Pérez-Galán et al., 2007).

Histone deacetylase 6 (HDAC6) links the UPS and autophagy by facilitating the transport of protein aggregates to juxtanuclear microtubule organizing centres (McConkey et al., 2012). Cells that lack HDAC6 were found to be defective to remove protein aggregates. Consequently, the combination HDAC inhibitors with BTZ sensitized MM resistant cells to proteasome inhibition (Catley et al., 2006). Although ricolinostat (ACY-1215), a specific inhibitor of HDAC6, showed a good response among BTZ refractory MM patients when combined with BTZ and dexamethasone, this effects is still under investigation in MCL (Amengual et al., 2015; Gonzalez-Santamarta et al., 2020). Other combinations involving HDAC inhibitors are under investigation, like the DNA methyltransferase inhibitor decitabine with BTZ in PI-resistant MCL, showing promising synergistic activity (Leshchenko et al., 2015).

Additionally, deubiquitylating enzymes (DUBs) from the Ub signalling pathway have been considered to be good options to develop therapeutic targets to overcome BTZ resistance, such as P5091 a selective inhibitor of USP7 (Chauhan et al., 2012), b-AP15 a selectively inhibitor for USP14 and UCHL5 (Tian et al., 2014) and SJB3-019A inhibitor for USP1 (Das et al., 2017), showed antitumoral activity and synergic toxicity when combined with BTZ.

9. Protein Homeostasis or Proteostasis.

Proteins exist in a dynamic equilibrium called proteostasis, in which their abundance, folding, and activity is highly regulated. To maintain cell viability, proteostasis (Figure 5) needs to be achieved, through the implication and modulation of multiple pathways and enzymes. When this equilibrium is preserved, cells can respond to stress conditions and different internal stimuli. However, if disrupted, different pathologies appear depending on the cell type and pathway involved, such as inflammatory, neurodegenerative, infectious diseases, and different cancer types. This inner equilibrium is regulated by cellular processes that control the synthesis, folding, assembly/disassembly, and posttranslational modifications (PTMs) regulating localization, degradation and protein-protein interactions (Ballar Kirmizibayrak et al., 2020).

Many enzymes and proteostasis regulators have been described to be dysregulated in various cancers, and there is increasing evidence linking them to tumorigenesis, cancer progression, metastasis and resistance to anticancer therapies (Gâtel et al., 2020). In addition, proteostasis disequilibrium is a common hallmark found in the most aggressive types of tumours like pancreas, lung, prostate cancer, but also in hematologic malignancies like MM or MCL.

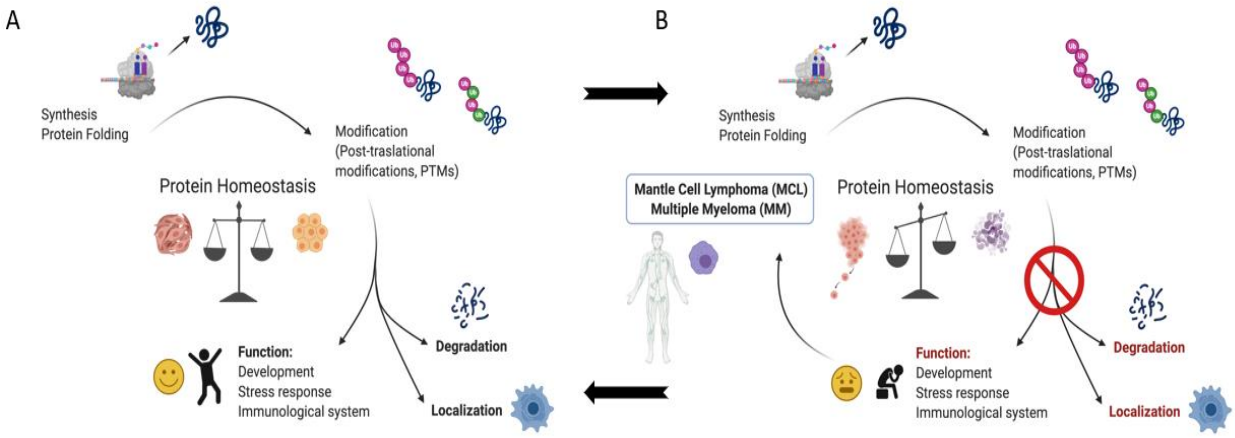

Figure 5: Protein homeostasis or Proteostasis regulation. Functions involved in maintaining the balance: synthesis, folding, PTMs, degradation, localization, and function. Panel A: physiology balance, because of a proper equilibrium the cells can respond to external stress and stimuli. Panel B: pathology outcome (Mantle Cell Lymphoma and Multiple Myeloma as examples) as the result of disrupting this proteostasis balance.
Created with BioRender.com.

Interestingly, protein misfolding, aggregation and accumulation of intra or extracellular proteins are a common characteristic found in neurodegenerative diseases, in particular to those associated with dementia (also called proteinopathies). They appear or develop, as a disruption in the proteolytic internal machinery like the Ub proteasome system, being protein degradation the center of attention for the investigation of those diseases in the lasted decades (Harris et al., 2020).

As already mentioned, proteostasis is affected by many regulatory processes, including the PTMs of proteins like phosphorylation, acetylation, and modification by the Ub family members. PTMs control the half-life of proteins, their localization, activity or even their interactions with other intracellular components or proteins. PTMs involve the addition of small chemical groups, peptides or even complex molecules, and they are characterized generally by their reversibility, a key factor that enables reversible switches between different functional states (Hochstrasser, 2006).

One of those PTMs is the modification made by Ub, and Ub-like proteins (UbLs). The diversity of processes regulated by those modifications is quite extent in scientific literature, growing steadily, and ranging from cell cycle control, cell proliferation, apoptosis, development, infection, and even cilia assembly/disassembly functions (Akutsu et al., 2016). Ub-protein modifications can lead to proteasomal degradation of cell cycle regulator proteins or transcription factors, but also regulate non-proteolytic processes, such as DNA repair, assembly of signalling complexes, membrane protein endocytosis, intracellular trafficking and chromatin mediated transcription regulation (Hochstrasser, 2009).

Proteolysis plays a crucial role in the regulation of many transcription factors, as their steady-state levels are maintained by a tightly controlled and highly regulated balance between synthesis and degradation. In that context, protein degradation via ubiquitylation represents a dynamic and coordinated mechanism that the cell employs to modulate those regulatory factors, and ultimately the cell cycle (Desterro et al., 2000).

Two main proteolytic systems exist in eukaryotic cells: the Ub proteasome system (UPS) and the autophagy lysosome system (ALS). Those intracellular degradation machineries are essential for cell survival under proteotoxic stress conditions, as they are mainly in charge of the clearance of pathogens and misfolded internal aggregates. Additionally, the protein quality control (PQC) system, assisted by molecular chaperones as key players (Ciechanover and Kwon, 2017), is another mechanism involved in this equilibrium inside the cells, dealing with misfolded, aggregated or non-functional proteins, providing ultimately a timely and controlled degradation. Abnormal proteins can be refolded because of the action of different chaperones and co-chaperones, but proteins that cannot be refolded must be degraded, highlighting the importance of those proteolytic systems to relieve cells from proteotoxic stress (Shiber and Ravid, 2014).

10. The Ubiquitin CODE.

Eukaryotic proteins are subjected to a variety of PTMs, including modifications by UbLs. Ten eukaryotic UbL-modification systems have been described so far. Among them, the Ub system was the first one to be described and is the most thoroughly investigated. Protein ubiquitylation is a process involved in nearly all aspects of eukaryotic biology and cellular processes. Ubiquitylation can regulate macromolecular interactions such as proteasome-substrate recognition and protein binding to chromatin to regulate gene expression (Hochstrasser, 2009). It can also be involved in other processes since its implications are continuously discovered in DDR (DNA damage response), autophagic degradation signalling, innate and adaptative immune responses, inflammation and cell death (Akutsu et al., 2016; Spit et al., 2019).

Ub is a highly conserved 76-residue protein that exists in cells either free, or covalently linked to other proteins. It was first isolated by Goldstein and co-workers from the thymus and was thought to be a thymic hormone. However, in subsequent work, it was found in all tissues and all eukaryotic organisms, and its ubiquitous distribution gave the protein its name. All UbLs share the same three-dimensional core structure, the β-grasp fold. They use distinct but evolutionary related enzymes to catalyse the attachment of the UbL proteins, highlighting a common ancestry to all systems (Hochstrasser, 2009).

Ubiquitylation is the addition of a Ub moiety into the target protein through Lys-linked isopeptide bonds. As the Ub molecule has seven lysine residues in its structure (K6, K11, M1, K27, K29, K33, K48, and K63), it can be subjected to further modifications, creating different chain topologies that act as signals encoding information to regulate different processes. Newly synthetized proteins have the capacity to be attached to different functional groups

or molecules at least once in their lifetime, to specify different cellular functions (Akutsu et al., 2016).

All possible Ub linkage types are used for chain assembly and signal propagation inside the cells (Akutsu et al., 2016). This language, in which Ub is used as the minimal entity to drive different outcomes (Pérez Berrocal et al., 2019), has been referred by the scientific community as the Ub Code, the UbiCODE. This code is reliant on the interplay of its "writers, editors and readers" (Figure 6) (Pérez Berrocal et al., 2019; Swatek and Komander, 2016).

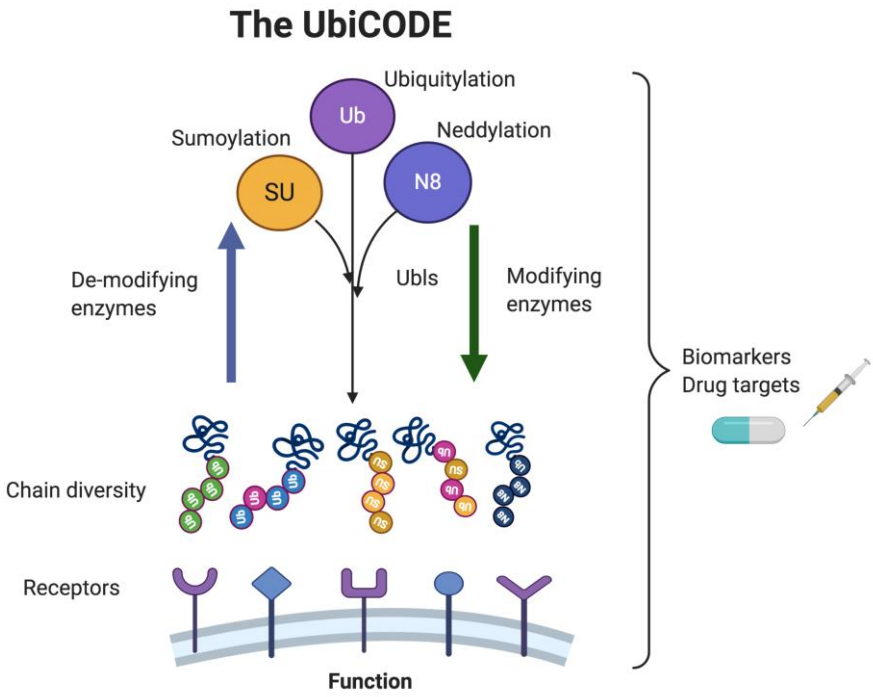

Figure 6: Ubiquitin Code complexity scheme. Cells respond to different stress and stimuli by promoting protein modification, made by modifying enzymes, also called the "writers" of the code. Apart from the ubiquitylation, there are other Ub-like proteins like Nedd8 and SUMO (represented in dark purple and yellow), that can modify target substrates creating a complex chain diversity. Those modifications can be removed or remodelled by the action of de-modifying enzymes, or "editors". The balance of those will drive different cellular functions decoded by specific receptors, "readers", that translate and decipher the code encrypted in the different chains formed in different outcomes inside the cells. To note, receptors indicated in the figure are not on the cell membrane; this schematic representation was made to highlight the importance of their function inside the cells. The involvement of those signals in an increasing number of cellular processes, and their alteration in multiple diseases, underline their biological relevance, making the UbiCODE a new field to explore new biomarkers and discover new drug targets.
Created with BioRender.com.

Ub is not only attached as a monomer, but also as polyUb chains, in which different linkages can be mixed increasing the complexity and morphology. MonoUb can occur with straight or modified Ub, and chains can be formed by one Ub linkage type (homotypic chains), or

different ones (heterotypic chains). Ub chains can also be ubiquitylated at multiple Lys residues forming branched chains (Swatek and Komander, 2016). Another layer of complexity is added when Ub is subjected to other modifications like acetylation or phosphorylation (Akutsu et al., 2016).

All those different possibilities and combinations can dictate the fate of the modified substrate (Hochstrasser, 2009). Additionally, the structural features of the different Ub chains can be used to explain their involvement in a wide variety of cellular processes, as Ub surface patches can be positioned differently depending on the chain type. Usually K6, K11, K29, K33 and K48 form intramolecular interfaces between two Ub moieties, while K63 and M1 adopt open conformations. This surface and its way of exposure is a key step in the propagation of the encoded information, as Ub Binding Domains (UBD) are going to recognise the Ub linkage in a specific manner not only by the Lysine residue (topology) but also by the structural patch formed. Therefore, the topology, morphology and structure of the Ub signals are factors that contribute to drive internal functions (Akutsu et al., 2016).

Additionally, other Ub-like molecules can modify Lys residues, like SUMO (Small Ubiquitin-like Modifier) and NEDD8 (Neural precursor cell expressed developmentally down-regulated protein 8), providing more complexity to this code (Figure 6) (Swatek and Komander, 2016). Hybrid Ub/UbLs chains can be generated under both, physiological and stress conditions, playing specific roles in cellular signalling still to be identified (Pérez Berrocal et al., 2019).

For this code to be fully functional, the signals encrypted in the different Ub chains must be read by different protein adaptors or “readers”, that have UBD in their structure. The UBD-Ub interaction modulates substrate interaction, but also formation and processing, therefore additional chain elongation (Pérez Berrocal et al., 2019; Swatek and Komander, 2016).

When discovered, Ub was mostly associated with degradative functions. However, it has been repeatedly proved in the last decade that it is also connected to non-degradative events, like localization and involved in protein affinity changes (Akutsu et al., 2016; Mendes et al., 2020).

Ubiquitylation is a reversible process, regulated continuously, by modifying enzymes/ “writers”; E1 (Ubiquitin-activating enzyme) encoded by two genes, E2 (Ubiquitin-conjugating enzyme) encoded by at least 37 genes, and E3 (Ubiquitin ligase) encoded by ~800 genes. All eukaryotic species express multiple E2 and E3 isozymes than can vary from dozens of E2s to hundreds of E3s, allowing the different specific modifications to be formed (Hochstrasser, 2009). These enzymes create a cascade of chemical reactions (Figure 7/A) to form an isopeptide bond between the C-terminal (K6, K11, K27, K29, K33, K48, and K63) of the Ub moiety to the Lysine residue in the target protein. An additional type of Ub linkage can be created when Ub is attached to the N-terminus forming Met1-linked (M1) or so-called linear chains.

DUBs, De-ubiquitylating enzymes/ “erasers” also contribute to this regulation by deconjugating Ub from the substrate proteins, providing reversibility to this process. Altogether, these key players in the Ub Code provide a rapid and versatile manner of fine-

tuning countless signalling cascades and molecules (Komander and Rape, 2012; Spit et al., 2019).

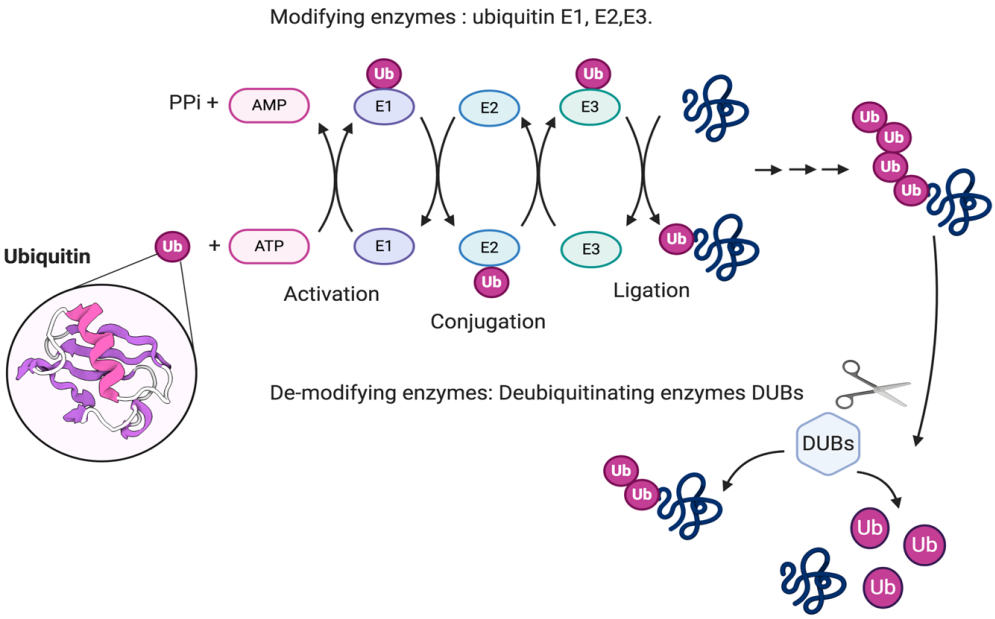

Figure 7/A: Ubiquitylation chemical reaction, enzymatic cascade. The Ub protein conjugation cycle involves (after Ub activation with the E1 activating-enzyme) a E3 ligase, necessary to stimulate the Ub transfer from the E2 to a substrate, generally to a lysine ε-amino group. Additional Ub molecules can be added either to other lysine side chains on the substrate or to the Ub already attached, forming polymers with different topology and conformation. Ub modifications can be removed or remodelled by DUBs or deubiquitylating enzymes.
Created with BioRender.com.

Conjugation of Ub begins with an ATP-dependent activation of the C-terminal glycine residue (G76) of the Ub molecule. The C-terminus is adenylated by an E1 enzyme, with the Ub-AMP remaining bound to the enzyme. Then the E1 cysteine side chain attacks the C-terminal, releasing the AMP and creating a E1-thioester intermediate. The activated Ub is then transferred to the active site on the E2 enzyme. While the E1 enzymes activate the Ub molecule, E2 and E3 enzymes in conjunction are in charge of catalysing substrate ubiquitylation (Hochstrasser, 2009).

The last step of substrate ubiquitylation is carried out by the formation of a complex, consisting of Ub-loaded E2 and a specific E3 to which the substrate protein is bound. It is then transferred from the E2 either directly to a lysine residue of the substrate when the E3 is a RING-(really interesting new gene) finger type, or previously to the target protein, to an internal cysteine residue in the E3 when the enzyme is a HECT (homologous to E6-associated protein C-terminus)-domain type (Hochstrasser, 2009). In addition to those two largest families of E3 enzymes, we can also find in literature the RING-Between-RING (RBR)E3 Ub-ligase (Arpalahti et al., 2020), and the UFD2 homologous (U-box) E3 Ub-ligase (Ballar Kirmizibayrak et al., 2020) acting biochemically in a different manner but with the same goal.

E3 enzymes play a role in substrate recognition, a step not always required in some pathways (Hochstrasser, 2009).

Additional Ub molecules are then added by the same cascade, creating Ub chains that can be further elongated by an additional type of ligase—E4, also termed the "Ub-chain elongation factor" (Komander and Rape, 2012).

DUBs, also called UbL-specific proteases (ULPs), are enzymes that specifically recognise and remove Ub and UbLs from their substrates. They hydrolyse ester, thiol ester, and amido bonds to the carboxyl group of G76 of Ub, cleaving it, but also processing the C-terminally extended precursors forms of these, removing, and modifying Ub chains. To date, nearly 100 DUBs have been described in humans (Ronau et al., 2016).

They are classified in Ub-specific proteases (USPs), Ub C-terminal hydrolases (UCH), ovarian tumour domain proteases (OTUs), Machado-Josephin disease proteases (MJD), motif interacting with Ub novel DUB family (MINDY), Zinc finger with UFM1-specific peptidase domain protein (ZUFSP), and JAB1/MPN/MOV34 (JAMM) domain metalloproteases. These enzymes act at different levels in the Ub pathway: in the generation of free Ub by processing linear precursor or branched chain polyUb, in the removal of Ub from ubiquitylated target protein, and in clearing the proteasome of remnants peptides conjugated to Ub chains (Mennerich et al., 2019).

Mechanistically speaking, we can classify DUBs into thiol proteases, which are related to the well-studied cysteine protease papain and rely on a nucleophilic cysteine in the active site for catalysis, and metalloproteases, which coordinate a Zn2+ ion in the active site and use a nucleophilic water ligated to the metal to hydrolyse the isopeptide bond. Usually, members of the USP family cleave all Ub linkage types without a clear preference while the members of the OUT enzymes can be linkage-specific. As E3 enzymes can specifically recognise the substrate to modify, DUBs can also act in a selective manner removing Ub moieties or chains. However, some DUBs can exhibit promiscuous activity for Ub linkages, and against other UbLs. How DUBs distinguish the different topologies and morphologies on the target substrate is not well understood. However, it appears to be linked to different factors such as Ub chain topology morphology or specific substrate features (Ronau et al., 2016).

Different proteomics studies show that all possible Ub linkage types co-exist inside the cells (Figure 7/B), the Lys48-linked (K48) Ub chain being the predominant linkage type usually displaying a close conformation when forming polyUb chains. This type of linkage generally targets proteins to be degraded by the proteasome. K48 Ub chains are rapidly enriched when the proteasome is inhibited. However, some evidences suggest their involvement in non-degradative roles, as well as the involvement of other Ub chains in proteasomal degradation like Ub K63 and Ub K11 (Ohtake et al., 2018; Swatek and Komander, 2016).

Ohtake et al, showed recently K48-K63 branch chains driving the proteasomal degradation of the apoptotic regulator TXNIP, involving also the recruitment and interaction with the UBR5 Ub ligase mediating the formation of those chains (Ohtake et al., 2018). The same author also showed K48-K63 branch chains regulating the NF-κB signalling. In this context, the E3 Ub ligase HUWE1 generates K48 Ub branches on the initially formed K63 Ub-linkage on TRAF6,

resulting in the amplification of the pathway (Ohtake et al., 2016). Although some authors suggest that heterotypic/branch and hybrid chains may have a major role in signal transduction that may be associated with the elevated level of complexity in its structure, new methods to monitor endogenous polymers are needed to fully validate this hypothesis (Pérez Berrocal et al., 2019; Yau et al., 2017).

K48-K63 heterotypic Ub chains have been associated with cell-cycle regulation and protein quality control, being formed by UBR4 and UBR5 (N-recognin) E3 ligases to prevent accumulation of neurotoxic proteins (Yau et al., 2017). K48-K11 Ub chains have also been related to cell-cycle control, in this case by controlling the proteasomal degradation of regulatory proteins such as Cyclin B1 (Akutsu et al., 2016).

Recent studies show that the Ub composition may be different between the nucleus and the cytoplasm, being K48 Ub-linked misfolded substrates degraded in the nucleus in contrast to K48-K11 Ub modified substrates, that are degraded by cytoplasmic proteasomes (Samant et al., 2018). More detailed Ub chain studies are needed to fully understand what constitutes the unique signal for proteasomal degradation. Consequently to that gap of knowledge, the ubiquitylation threshold model hypotheses that the amount of polyUb rather than the type is important in such decision (Swatek and Komander, 2016).

The second more abundant Ub chain type is Ub-K63, which holds an extended conformation (Ronau et al., 2016) and performs various roles, such as intracellular signalling, DNA damage response, cellular trafficking (Pontrelli et al., 2019), and autophagy degradation (Nam et al., 2017).

K63 Ub-linked Ub chains are required for Double Strand Breaks (DSB) repair systems, as they are abundant at DNA damage sites. The E3 ligases RNF8/RNF168, assisted by the combined activity of a specific E1 enzyme, the heterodimeric E2 Mms2-Ubc13, promotes Ub-K63 chain conjugation and consequently recognition and recruitment of repairing proteins such as RAP80 (Lee et al., 2017). At the same time, Ub-K63 chains can decorate many plasma membrane proteins, providing a signal often required for their internalization. Also, several channels, transporters and receptors can be modified by those types of Ub chains, being recognised by different UBD-proteins in the plasma membrane to be invaginated and trafficked using the trans Golgi network (Erpapazoglou et al., 2014).

Quite recently, the scientific community has begun to characterize the remaining non-as abundant Ub linkages, called atypical linkages; K6, K11, K27, K29, K33 and M1. The understanding of this expanded code has advanced rapidly in recent years. However, there is still need for new methods and molecular tools in order to fully understand their biological implications (Swatek and Komander, 2016).

M1 linked Ub chain are used as positive regulators for NF-κB signalling. They are modulators of innate and adaptative immune responses, by regulating inflammation and cell death signalling pathways. M1 linked chains are usually formed by the linear ubiquitylation assembly complex (LUBAC), the only E3 Ub ligase known for being able to form those chains *de novo*. LUBAC promotes the M1 ubiquitylation on NF-kappa-B essential modulator (NEMO), part of the IKK complex that phosphorylates the IKB-α inhibitor, releasing p50 and

p60 subunits resulting in the NF-κB translocation to the nucleus and transcription activation of proinflammatory proteins (canonical activation of the NF-κB pathway). In addition, M1-K63 Ub chains on NEMO have been proved to serve as a platform to recruit other interacting proteins involved in the pathway, evidence that suggests a diversification in their structure and functional impact. However, the mechanism underlying those heterotypic chains has not been uncovered in detail (Dittmar and Winklhofer, 2019; van Huizen and Kikkert, 2019).

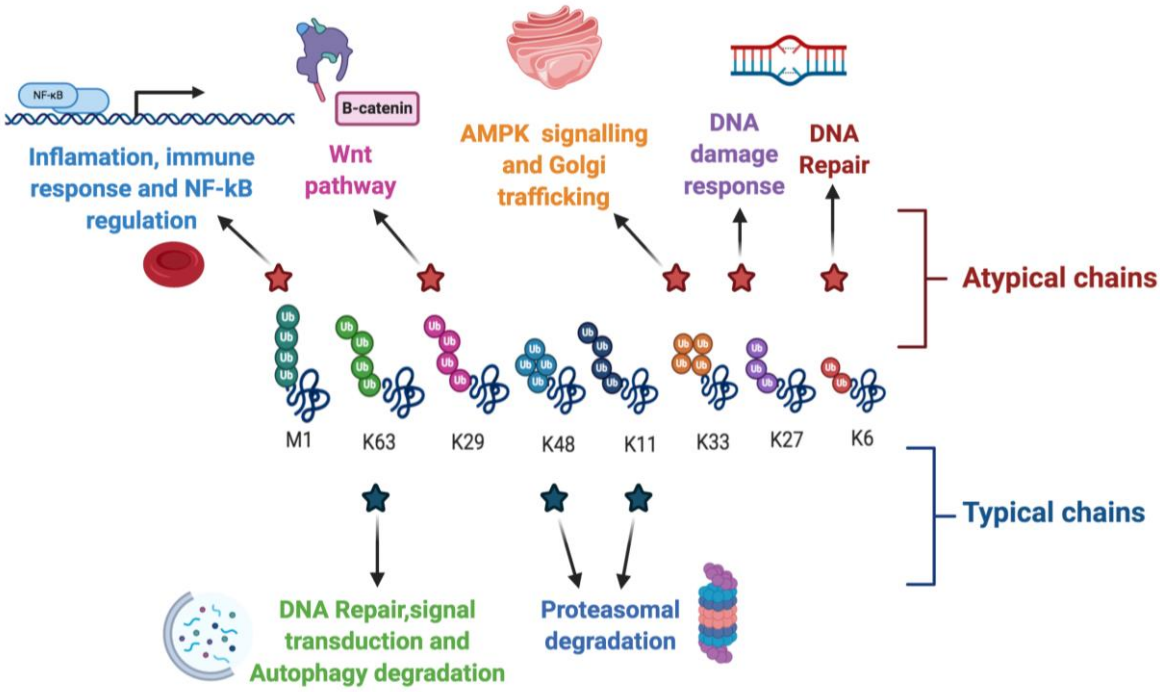

Figure 7/B: **Ubiquitin chain complexity and functions associated.** Upper part: Atypical chains where Ub-M1 is associated with inflammation, immune response, and NF-kB pathways regulation. Ub-K29 associated with Wnt pathway. Ub-K33 is associated with Golgi trafficking and AMPK. Ub-K27 associated with regulating DNA damage response, and Ub-K6 to DNA repair. In the lower part of the panel, typical Ub linkages are indicated and associated with specific functions. Ub-K63 is associated with signal transducing, DNA repair and autophagy. Ub-K11 and K48 associated with proteasomal degradation. Ub chain types and its implication are biological functions are further developed in the main text. Created with BioRender.com.

K6 Ub-linked chains may emerge in other processes such as xenophagy, and mitochondrial homeostasis. In this context, the Parking enzyme, a well-known E3 ligase, assembles K63 but also K6 on the surface of mitochondria for its depolarization. K6 abundance is not increased by proteasome inhibition, but along with K33, are enriched upon UV radiation stress. That may suggest its involvement in non-degradative processes such as DNA repair. Few E3 Ub ligases have been found to mediate those chains like BRCA-BARD1 that conjugates Ub-K6 on substrates and itself to promote a DNA repair response (Akutsu et al., 2016).

K33 Ub-linked chains has been related to post-Golgi membrane protein trafficking as negative regulators in the T-cell antigen receptor and AMPK pathway. In contrast, K29 Ub-linked chains, predominantly being part of heterotypic chains, have been related to proteasomal degradation, also forming polymers on the Axin protein surface repressing Wnt signalling (Akutsu et al., 2016).

K11 Ub-linkages together with M1-linear chains are the most studied atypical Ub linkages (Swatek and Komander, 2016). In contrast, the K27 Ub-linked chains is the least understood. However, different evidences suggest that those may have a role in protein recruitment in the DDR, and host immune response (Akutsu et al., 2016).

Due to the high amount of information gathered by proteomics studies indicating a great amount of ubiquitylation sites in different proteins, it can be suggested that most proteins experience ubiquitylation at least once in their lifetime (Swatek and Komander, 2016). Due to the high complexity, level of regulation and reversibility, ubiquitylation is believed to control the majority of cellular processes, being implicated in pathophysiological states and diseases (van Wijk et al., 2019). Therefore, paying a special attention to the key players in the different PTMs systems (writers, erasers, and readers) will be critical in years to come.

11. The Ubiquitin Proteasome System (UPS).

The Ub Proteasome System is one of the main mechanisms for intracellular protein degradation. This proteolytic mechanism is tightly regulated, in order to ensure the correct turnover of substrates involved in a wide variety of cellular processes. The proteasome plays a central role controlling protein homeostasis, as it is involved in the regulation of almost all cellular pathways through the degradation of different regulatory components. Moreover, due to its high abundance inside the cells, small changes in proteasome abundance and activity can have a major impact on cellular protein turnover (Olivier Coux et al., 2020). The proteasome acts as a central hub of cellular proteolysis, having an impact on multiple processes such as cell cycle, DNA repair, cell differentiation, immune response, amino acid recycling and apoptosis. For this reason, the proteasome has become a privileged target for drug development in order to treat diverse disorders including cancer, infections and inflammation-related diseases (Mata-Cantero et al., 2016; Roeten et al., 2018).

The proteasome is a large complex multidomain (2.5MDa) (Figure 8) protease, found in nucleus and cytosolic cellular compartments, that commonly drives the degradation of short-lived proteins that need an accurate turnover (Tanaka, 2009). The proteasome system is an efficient degradation system of smaller polyubiquitylated proteins, as large proteins cannot enter into this organelle (Nam et al., 2017). However, previous ubiquitylation of the target proteins is usually required for their proteasomal degradation (Komander, 2009; Swatek and Komander, 2016). Ub chains, recognised by proteasome subunits and cofactors, promote polyubiquitylated proteins to enter the proteolytic/catalytic core of the proteasome, in order to be destroyed and recycled as a new pool of amino acids (Tanaka, 2009).

The 26S proteasome (also called "*the proteasome*") is a barrel-shaped proteolytic organelle consisting of: the 20S core particle (CP) and the 19S regulatory capping particles (RPs), that can be at one or both end sides of the CP. 19S complexes bind cargo-proteins, deubiquitylating them and channelling them into the inner core (proteolytic sites) (Nam et al., 2017).

The 20S CP is composed of two outer α-rings, each containing seven α-subunits (α1–α7) and two inner β-rings, each consisting of seven β-subunits (β1–β7). The α-rings form a closed structure which prevents big and unspecific proteins to enter into the inner chamber of the β-rings (Bard et al., 2018). The access to this catalytic chamber is possible through axial pores of the 20S only allowing the entrance to unfolded proteins. Although 20S alone can degrade substrate by themselves, they associate with RP to control substrate specificity. The RP recognizes and tethers targeted polyubiquitylated proteins, removes Ub chains attached to them, unfolds protein substrates, opens the α-ring, and allow unfolded proteins to enter into the CP. The proteasome mostly uses ATP hydrolysis to disrupt higher-order structures of substrates, to translocate the unfolded polypeptides into the internal degradation chamber for proteolytic cleavage (Bard et al., 2018). However, the existing so-called "hybrid 26S proteasomes" can degrade proteins in a ATP and Ub-independent manner (Olivier Coux et al., 2020).

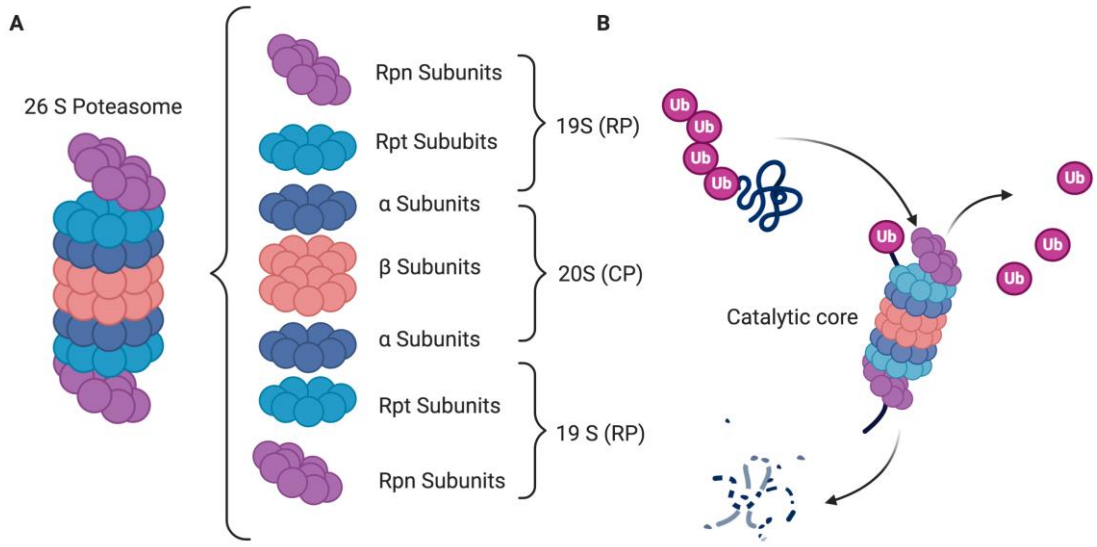

Figure 8: The proteasome and the Ubiquitin proteasome system. Panel A: 26S Proteasome structure; one 20 (CP) core particle and two 19 regulatory particles (RP) at one or both sides. The RP is sub-formed by the lid and the base complexes, containing three Ub/UbL receptors, deubiquitylation (DUB) enzymes, and hexameric ATPase subunits involved in processing substrate proteins. The proteolytic active sites are within the chamber of the CP (proteolytic β subunits). Substrate proteins are unfolded and translocated into the proteolytic active sites through the ATPase and CP channel. Panel B: The Ub Proteasome System (UPS).
Created with BioRender.com.

The proteolytic function of the proteasome is mediated by three catalytic β-subunits—β1, β2, and β5—with distinct peptidase activities, chymotrypsin-like, trypsin-like, and peptidyl-

glutamyl peptide-hydrolysing activity, respectively. The 19S RP, composed of six AAA-ATPase (Rpt) and four non-ATPase (Rpn) subunits, is responsible for the recognition, unfolding, and subsequent translocation of ubiquitylated substrates into the 20S CP (Cohen-Kaplan et al., 2016a).

To efficiently capture ubiquitylated proteins, the 19S RP contains several Ub receptors, specific domains, in charge of the recognition of ubiquitylated substrates through specific UBDs. Those 3 intrinsic Ub receptors of the 19S are Rpn1, Rpn10 and Rpn13. The Ub-interacting motif (UIM) located at the C-terminus of Rpn10 binds selectively mono-Ub but also K48 and K63 polyUb chains (Riedinger et al., 2010), Rpn13 binds di-Ub but through a pleckstrin-like receptor for Ub (Pru) (Schreiner et al., 2008), and Rpn1 carries a UBD that binds both Ub and UbL proteins (Chojnacki et al., 2017).

Several extrinsic Ub receptors such as Rad23, Dsk2, Ddi1 and Sem1 contain both UbL and UBA (Ub-associated) domains in their structure to interact with specific Ub signals. Their UbL domains allow their interaction with some proteasome subunits (Fu et al., 2010; Paraskevopoulos et al., 2014). In particular, the UBD of Rpn1 interacts with the UbL domain of Rad23 and triggers its tethering to the proteasome (Rosenzweig et al., 2012; Shi et al., 2016). These adaptor proteins ensure the highly regulated selectivity of proteasomal degradation.

In contrast to this canonical proteasomal degradation, other Ub independent proteasomal degradation mechanisms do not require ubiquitylation and/or ATP hydrolysis, usually mediated by “hybrid 26 proteasomes” (Klionsky et al., 2016).

In addition, alternative subunits named β5i, β2i and β1i, are expressed in hematopoietic cells in response to pro-inflammatory signals such as cytokines or interferon, integrating the immunoproteasome. These are inducible proteasomal β subunits, that are activated to activate the immune response, replacing their counterparts in the constitutive 20S. This alternative form of 20S proteasome is essential for the major histocompatibility complex (MHC)-I antigen processing. Its degradative action is at the origin of antigenic peptides (Ferrington and Gregerson, 2012). The 20S core can also associate with 11S, another regulatory particle also known as PA28, REG or PA26 which contributes to the action of the immunoproteasome but can also drive proteolysis in other cellular compartments such as the nucleus (Budenholzer et al., 2017).

12. The Autophagy Lysosome System (ALS).

The autophagy lysosome system (ALS) is the other proteolytic mechanism that eukaryotic cells use for protein degradation and removal of misfolded proteins and aggregates along with the UPS. ALS functions through a double-membrane vesicle which sequesters cytosolic proteins or aggregates to be degraded after the fusion with the lysosome by lysosomal enzymes. Dysregulation of autophagy, apart from UPS dysregulation, is also related to several human pathologies, such as neurodegenerative diseases and cancer (Lilienbaum, 2013). The broad conservation of the autophagy pathway from yeast to humans underscores

the pivotal role of autophagy in maintaining cellular homeostasis. Accumulating evidence suggests that mammalian autophagy is required for cell cleansing and remodelling, and selective autophagy mediated by specific receptor proteins seems to be instrumental in these processes (Dikic and Elazar, 2018).

The autophagy contribution to cancer development and progression is contradictory and complex, as autophagy can mediate promotion or inhibition of tumorigenesis (Mancias and Kimmelman, 2016). Although it appears to be tumour-suppressive upon normal cellular homeostatic state, autophagy can mediate tumour cell survival under stress conditions (White and DiPaola, 2009). Failure in selective autophagy is likely to cause an accumulation of protein aggregates and damaged organelles that may mediate neoplastic transformation. In contrast, established tumours depend on autophagy for covering their increased metabolic needs. In this context, selective autophagy may ensure tumour survival via degradation of misfolded proteins and damaged organelles that accumulate in genetically instable tumour cells (Dikic et al., 2010).

Autophagy (from Greek “self-eating”) (Figure 9) digests long-lived protein aggregates and abnormal cytoplasmic or damaged organelles. The generic term ‘‘autophagy’’ comprises several processes by which the lysosome acquires cytosolic cargo. So far, three types of autophagy have been differentiated in the literature: (1) macroautophagy (referred as autophagy), characterized by the formation of a crescent-shaped structure (the phagophore) that expands to form the double-membrane layer autophagosome; (2) microautophagy, in which lysosomes invaginate cytosolic components; and (3) chaperone-mediated autophagy (CMA), which involves the translocation of unfolded proteins across the lysosomal membrane with the cooperation of HSC70 (Takeshige et al., 1992).

Autophagosomes sequester cytosolic material in a non-specific manner as a response to cellular stress situations like starvation (canonical pathway). However, there is evidence for a selective autophagic degradation process which may include protein aggregate, mitochondria, and microbes targeting (Mancias and Kimmelman, 2016). Structures that need to be degraded can be exclusively recognized and eliminated by the ALS system (Zaffagnini and Martens, 2016). For example, mitophagy is selective for mitochondria degradation, xenophagy is for pathogens, aggregaphagy for protein aggregates, proteaphagy for proteasomes, etc. (Kirkin et al., 2009).

Growing evidences suggest that there are specific mechanisms to drive selectivity contributing to maintain intracellular homeostasis in non-starved cells. The autophagy selectivity is modulated by different regulators, but also by the “Ub Code” which acts by forming degradation signals in a similar way to the UPS (Gatica et al., 2018). Historically, it was suggested that short-lived proteins, which are degraded by the proteasome, are marked selectively by K48-linked Ub chains (it was later shown that all Ub chain types are probably involved in proteasomal degradation). In contrast, K63-linked Ub chains act as degradation signals, among other Ub chains continuously and recently being discovered as signals for selective autophagy (Cohen-Kaplan et al., 2016a).

The regulatory components involved in autophagy initiation are the ULK1 (for unc-51 like autophagy activating kinase 1, also called ATG1) and Beclin1 complexes, whose

phosphorylation is modulated by signalling proteins such as mTOR, Akt and AMPK (Xie et al., 2015). Upon induction, proteins of the ULK complex assemble and initiate phagophore nucleation. The induction of autophagy triggers isolation and elongation of a double membrane structure, that forms the growing phagophore. Although the origin of this membrane is not clear, various intracellular sources have been proposed such as the ER, the Golgi complex, or the mitochondria (Wei et al., 2018). The autophagosome elongation, maturation and recruitment of substrates is controlled by the Autophagy related (ATG) genes or ATG proteins, leading ultimately to the fusion with vacuoles, endosomes or lysosomes forming the autophagolysosome. It degrades targeted substrates, using a series of lysosomal/vacuolar acidic hydrolases (He and Klionsky, 2009; Tanida et al., 2004).

Although autophagy was believed to be a cellular adaptative stress response in mammalian cells, basal levels of autophagy are detected in some cells subjected to further activation and giving rise to a variety of selective autophagic events. Starvation-induced autophagy is activated by signalling components that interpret cellular energy (5' AMP-activated protein kinase, AMPK) and nutrient/amino acid levels (Mammalian Target of Rapamycin, mTOR). These pathways converge towards the ULK1 (Atg1 ortholog) complex, promoting autophagy induction. Following induction, the class III phophatidylinositol 3-kinase [PI(3) KC3)] complex (PI3P) nucleates autophagosome formation and the ATG9 transmembrane protein mediates trafficking of source membrane components for autophagosome elongation. Selective autophagy is engaged to the canonical autophagy through a molecular link between selective autophagy receptors and ULK1.

In that scenario, the Huntingtin (HTT) protein acts as a scaffold to bind selective autophagy receptors and activating the ULK1/Atg1 kinase complexes. However, there are also non-canonical modes of autophagy activation that do not involve ULK1 or other core autophagy machinery. It reflects the diversity of mechanisms by which the autophagy program can be initiated (Mancias and Kimmelman, 2016).

The ATG8 protein family is composed of 6 members in mammalian cells, LC3A, B and C, GABARAP, GABARAP L1 and GABARAP L2. ATG8 proteins contain the conserved β grasp folding of the Ub-like protein domains, but also a supplementary hydrophobic pocket that engages interaction networks with autophagy and membrane trafficking components (Shpilka et al., 2011).

LC3/GABARAP proteins are conjugated to phosphatidylethanolamine (PE) in an enzymatic manner (Rockenfeller et al., 2015). PE functions as an anchor for autophagosomal membranes (Xie et al., 2008; Yang et al., 2013). During autophagy induction, ATG8 proteins are lipidated and localize at both sides of the phagophore membrane, controlling the size of the mature autophagosome (Kabeya et al., 2000; Xie et al., 2008). This UbLs-protein lipidation system catalyses the conjugation of phosphatidylethanolamine to the C-terminus of ATG8 and consequently facilitates the attachment of ATG8 proteins to the emerging autophagosomal membrane. In this system, ATG7 acts as an E1 enzyme with ATG10 as the interacting E2, to conjugate the Ub-like ATG12 to ATG5. This ATG12-ATG5, localised in the autophagosomal membranes by WIPI2, acts in a complex with ATG16L1 to facilitate the final ATG8 lipidation. Elongation and maturation steps include the recruitment of the substrate mammalian receptor LC3 (ATG8 in yeast). ATG8s are synthesized in a pro-ATG8 form called

the pro-LC3B-I form, in which a phosphatidylethanolamine is conjugated to the C-terminus forming the LC3B-II form, associated with the expanding autophagosomal membranes (Mancias and Kimmelman, 2016) and binding different adaptor proteins in order to facilitate the selective sequestration of substrates (Cohen-Kaplan et al., 2016a).

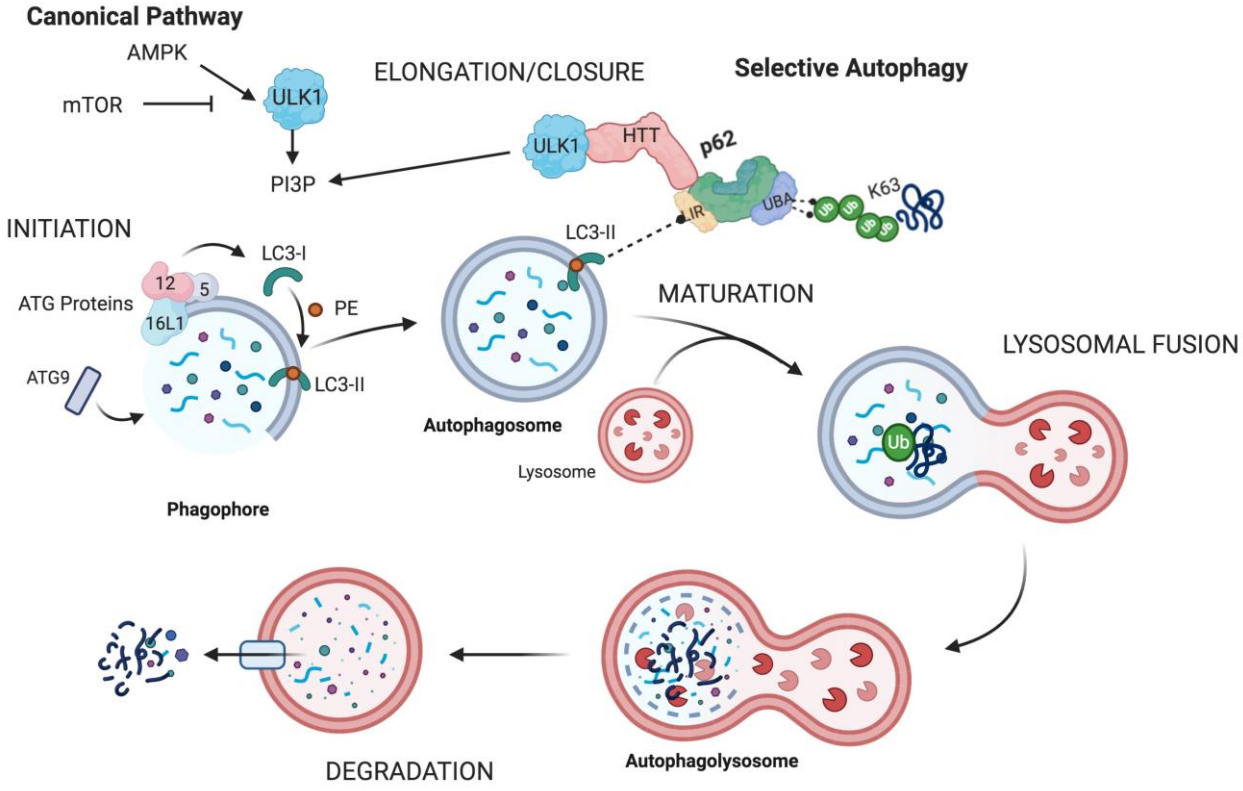

Figure 9: Stages of autophagy (initiation, elongation, closure, maturation, and degradation). Canonical and regulation of selective autophagy. Starvation-induced or canonical autophagy is activated by 5' AMP-activated protein kinase, (AMPK) and Mammalian Target of Rapamycin, (mTOR). These pathways converge towards the unc-51 like autophagy activating kinase 1 (ULK1) complex that mediates autophagy induction. Following induction, the class III phophatidylinositol 3-kinase [PI (3) KC3)] (PI3P) complex nucleates autophagosome formation. The ATG9 transmembrane protein mediates trafficking of source membrane components for autophagosome elongation. The Huntingtin (HTT) protein acts as a scaffold to bind selective autophagy receptors and activates the ULK1/Atg1 kinase complexes. Phosphatidylethanolamine (PE) functions as an anchor to autophagosomal membranes. After the lipidation process of ATG8s localizes at both sides of the phagophore membrane to control the size of the mature autophagosome. In selective autophagy, different adaptor proteins (autophagy receptors) mediate substrate recognition through UBD and promote autophagy degradation by LIR-LC3B autophagy interaction.
Created with BioRender.com.

The phagophore expansion involves actin reorganization, but also the Ub-like ATG8 protein family member and ATG4, being the latest required for autophagy regulation as it deconjugates ATG8s promoting its release from the membrane, limiting phagophore

expansion. Following the expansion of the phagophore, the autophagosome undergoes maturation, which involves gradual release of ATGs components from the autophagosome, and recruitment of machinery responsible for lysosomal fusion and final protein degradation (microtubule-based kinesin motors) (Dikic and Elazar, 2018).

Selective autophagy regulates the abundance of specific cellular components via autophagy receptors, that target protein complexes, aggregates, and whole organelles. Many proteins work as autophagy receptors: p62, NBR1, OPTN or NDP52-also called Sequestosome-1-like receptors (SLRs). Autophagy receptors bind LC3/GABARAP proteins on the phagophore and autophagosome membranes. They recognize signals on protein cargoes to deliver them to the autophagy proteolytic machinery (Khaminets et al., 2016). The diversity of these receptors widen the possible regulation of the selective autophagy, being involved in both Ub-dependent and independent mechanisms (Quinet et al., 2020).

Ubiquitylation not only generates a cargo recognition signal but also targets the core autophagy machinery that controls the rate of autophagosome formation and maturation, such as the ubiquitylation of components of the PI3K/beclin 1 complex affecting and regulating both assembly and autophagy progression (Chen et al., 2019).

The Autophagic Receptor p62/SQSTM1 is a multifunctional adaptor protein that has been implicated in cell signalling and differentiation. It carries a UBA domain that binds to ubiquitylated cargoes. The UBA domain of p62 can bind both K48-linked and K63-linked Ub chains but with a higher affinity for K63 chains. p62/SQSTM1 can mediate degradation of many substrates, such as aggregated proteins or cytosolic bacteria. It has proved to be useful as a marker for autophagic vesicle turnover by different studies (Zaffagnini and Martens, 2016).

p62 protein contains in its structure a LC3 Interacting Region (LIR) motif, and a N-Terminal PB1 domain that triggers p62 polymerization promoting protein aggregation. p62 participates in targeting misfolded aggregated proteins and in the subsequent sequestration and recruitment to the phagophore (Dikic and Elazar, 2018). In addition, different studies have shown that the presence and integrity of the oligomerization promoting by the PB1 domain is crucial for a stable binding to the receptor to both Ub and LC3 (Atg8) (Lu et al., 2017). The PB1 domain forms helical filaments of p62 polymers interacting with both ATG8s and long Ub chains stabilizing their interactions. These large polymers of p62 provide a large molecular scaffold for autophagosome and ensure ubiquitylated cargo recruitment (Ciuffa et al., 2015).

p62 protein has also been shown to drive cargoes to autophagosomes, in a Ub independent manner. p62 is an N-recognin whose ZZ domain binds to the N-terminal arginine and other N-degrons of the N-end rule pathway. The N-end rule pathway is a Ub-dependent proteolytic system, in which single N-terminal amino acids function as a determinant of degrons, called N-degrons that are generated by endoproteolytic cleavage associated with PTMs of otherwise stabilizing N-terminal residues such as deamidation, oxidation, and arginylation. In this system, UBR box-containing (1-7) E3 ligases, like UBR1 and UBR2 ligases, recognize those N-degrons to promote their ubiquitylation. This modification results in their degradation by the proteasome. Alternatively, under proteotoxic stress conditions and

through its ZZ domain, p62 is able to bind selectively to N-degrons, promoting the oligomerization of p62 leading to the co-delivery of this cargoes to the autophagosome. This interaction can also act as an inducer of autophagosome biogenesis and autophagic flux (Cha-Molstad et al., 2018).

Ub-dependent and independent selective autophagy function in concert with other cellular membrane-trafficking pathways, protein complexes, and organelles. Every step-in selection, transport, and degradation of protein aggregates is controlled by additional auxiliary factors. Good examples are molecular chaperones that bind exposed hydrophobic surfaces of misfolded proteins, thereby preventing them from forming aggregates. If proteins fail to adopt a proper conformation, chaperones direct them either to the proteasome or to autophagy for degradation (Khaminets et al., 2016).

Autophagy plays different and complex roles in cancer development and progression. Its cytoprotective function is believed to have tumor-suppressive potentiality before the onset of tumorigenesis, and loss of autophagy has been associated with an increase in the risk of cancer in a lot of patients. Moreover, autophagy has also been shown to allow premalignant cells to escape genotoxic stress and inflammation that promote tumorigenesis. Many types of advanced cancers exhibit high autophagic activity, and it was proposed that certain tumors are highly dependent on autophagy, such as pancreatic tumors or cancers with mutant RAS (Dikic et al., 2010).

In contrast, the tumor-suppressive role of autophagy was first shown in mice heterozygous for the Beclin-1 autophagy protein. These mice showed reduced autophagy and increased cellular proliferation, which translated into the increased incidence of spontaneous malignancies, such as lymphomas, lung, and liver cancers (Dikic et al., 2010).

The controversial view on autophagy as a cell death mechanism has been also supported by the tumor-suppressing role of this pathway. Interestingly, the accumulation of p62 in autophagy-deficient cells was shown to inhibit degradation of cancer-relevant proteins whose expression levels are primarily regulated by the Ub-proteasomal pathway (p53 and B-catenin). p62 does so by sequestering ubiquitylated proteins and consequently preventing their accession to the proteasome. The fact that p62 accumulation acts as a consequence of autophagy inhibition could enhance tumorigenic properties suggest that in addition to clearing harmful cellular junk, selective autophagy may limit tumor formation by directly affecting cell signalling (Dikic et al., 2010).

Autophagy seems to be a double-edged sword in the context of cancer therapies, and it remains to be established whether it can be successfully targeted — inhibited or induced — for therapeutic benefit. Decisions as to whether autophagy activity should be upregulated or downregulated in certain diseases conditions, particularly in cancer, are not trivial and require careful evaluation of the tumor type, stage, and microenvironment (Dikic and Elazar, 2018).

13. Crosstalk between UPS and ALS.

Although the UPS and the ALS have been initially considered as independent proteolytic mechanisms, their interconnection has been supported by an increasing number of studies. The similarity and overlapping of regulatory components in these two pathways have led the scientific community to consider one single proteolytic network comprising the UPS and ALS operating in a coordinate manner inside the cells (Ji and Kwon, 2017). In order to adapt to the environment and its variable changes, cells may operate an accurate and highly regulated network of molecular mechanisms to modulate a functional and efficient crosstalk (Quinet et al, 2021).

Ub is at the centre of this crosstalk, as different types of Ub conjugation processes (K48/K63) can drive different forms of degradation (UPS/ALS). It was firstly suggested that short-lived proteins degraded by the proteasome, modified with K48 Ub may be involved in this process, in contrast to K63 Ub chains that serve as degradation signals for a selective autophagy. However, recent evidences suggest the involvement of other Ub chain types, as the deletion of autophagy genes (ATG5 and ATG7) leads to the accumulation of almost all Ub chain types inside the cells (Cohen-Kaplan et al., 2016a).

The interconnexion between those mechanism (UPS/ALS) was initially detected by the notion that proteasome inhibition induces a compensatory activation mechanism in autophagy. However, this process is not fully understood.

In addition, mitochondria and ER are also key elements of this crosstalk as they are the two cellular organelles in charge of detecting reduced proteasome activity.

13.1 Central role of Ubiquitin

Ub is the molecule that both systems (UPS/ALS) share for driving a selective and coordinated degradation of their target substrates. As a general view, it can be established that K48 Ub-linkages, representing half of all Ub linkages found inside the cells, are associated with short-lived substrates and UPS degradation. In contrast, K63 Ub-linkages are associated with autophagy degradation. Additionally, other Ub linkages have been described to be involved in targeting proteins for UPS, like K11 and K29; and for ALS, K6 Ub chains. Atypical linkages can act as signals for autophagy degradation as well, although little is known about their specific mechanism. The M1 linear Ub chain is one example, that acts as a signal for autophagy degradation during bacterial xenophagy (Ji and Kwon, 2017).

Different regulatory proteins that carry UBD can link those ubiquitylated proteins to the proteasome (RNP10 and RNP13), or to autophagy vacuoles [p62/SQSTM-1/Sequestosome-1, neighbour of BRCA1 gene 1 (NBR1) and histone deacetylase 6 (HDAC6)] (Ji and Kwon, 2017; Nam et al., 2017).

Different examples show that both pathways can recognize the same type of Ub chains, suggesting that they could handle degradation of common substrates. For example, although the p62 protein can recognize K48 Ub linkages, its binding affinity for K63 linkages

seems to be higher. In this context, it has been proposed that a competition between p62 and p97/VCP (Ub binding ER-associated degradation protein) determines the degradation of K48 ubiquitylated proteins (Kocaturk and Gozuacik, 2018). More evidences are needed to fully understand if one linkage would be enough to determine the degradation fate (Ji and Kwon, 2017).

Besides common degradation signals, the two machineries also share common regulatory components like Ub ligases ("writers"). For example, the E3 Ub ligase Parkin conjugates K48 polyUb chains to the substrates that are going to be degraded by the proteasome, whereas its autophagic substrates, like the mitochondria itself, are modified with K63 and K27 Ub chains to promote degradation by the autophagy lysosome system (Cohen-Kaplan et al., 2016b).

E3 Ub ligases can also act as key point connectors between UPS and ALS, as they can target core autophagy complexes like the ULK1 and PI3K, as a way of turning off and on autophagy under different cellular contexts (Chen et al., 2019). For example, the Ub ligase TRAF6 promotes K63 Ub-linkage chains on ULK1 and Beclin-1 to enhance their stability and autophagy induction. In contrast, the RNF216 Ub ligase conjugates K48 and K11 Ub-linkage chains on Beclin-1 and K48 on AMBRA1 driving their proteasomal degradation and therefore autophagy inhibition. Moreover, when the stress condition is resolved upon autophagy activation, cells must recover their basal state promoting autophagy termination to avoid excessive degradation. In this context AMBRA1 can be auto-ubiquitylated (K48 Ub-linked chains) and degraded by the proteasome to control autophagy termination. In conclusion, we can say that while K63 ubiquitylation promotes autophagy induction in response to stress conditions or accelerates autophagy initiation, K48 or K11 ubiquitylation impairs autophagy by promoting the degradation of core autophagy proteins (Chen et al., 2019).

At the same time, Ub ligases can themselves be targets to be degraded by autophagy. One example is the E3 ligase E124. This enzyme is responsible for targeting Ub ligases for degradation by the ALS. It has been proved that E124 promotes the degradation of several E3 enzymes (most of them belonging to the RING type), such as TRAF2, RINCK2 and several tripartite motif-containing (TRIM) enzymes: TRIM28, TRIM21 and TRIM1 among others. Different transcription factors like FOXOs and NF-κB that promote autophagy initiation, are known to be regulated by different E3 enzymes and degraded by the proteasome. Therefore, the modulation of cellular signalling pathways and Ub enzyme abundance by autophagy or proteasome degradation may as well regulate the UPS-ALS crosstalk (Kocaturk and Gozuacik, 2018).

Interestingly, proteins of the TRIM family have been recently described to be involved in different cellular processes such as intracellular signalling, development, apoptosis, protein quality control, innate immunity, autophagy, and carcinogenesis. Consequently, their dysregulation has been shown to promote the development of several diseases such as cancer, developmental disorders, and immunological diseases. There are 80 different TRIM-containing proteins found in the human genome, most of them carrying a RING-finger in the N-terminal domain. Additionally, they carry one or two zinc-finger domains called B boxes (B1 and B2 box), crucial domains for their homo/heterodimerization, a key player process for their activation (Hatakeyama, 2017).

Recent reports have showed that TRIM proteins can regulate autophagy, acting as autophagy receptors and regulators of the autophagosome formation, as knockdown of different TRIM proteins has demonstrated to reduce LC3B puncta formation in Hela cells. TRIM proteins can interact with adaptor proteins such as p62, forming a platform called the "TRIMosome", a complex in charge of regulating the autophagosome formation and interaction with the ULK1 complex and Beclin1 (Hatakeyama, 2017; Mandell et al., 2020).

Most of these proteins have the ability to interact with p62 and LC3. However, the specific mechanism in which each TRIM protein is involved in the autophagy mechanism is still to be discerned. Surprisingly, TRIM proteins have not been identified in yeast, the model organism to study autophagy, highlighting the importance of discovering their role in mammalian autophagy (Hatakeyama, 2017).

As autophagy is related to carcinogenesis, it is not surprising to find aberrant expression of these proteins in different cancer models. Recent evidences support that changes in TRIM protein expression patterns is strongly correlated with cancer malignancy and bad prognosis. For example, TRIM24, a negative regulator of p53, has been described with higher proliferation in prostate cancer, and is related with resistance to antiandrogen therapy, promoting malignancy in castration-resistant prostate cancer (CRPC). There is need for more detailed information about the role of those proteins under different cellular contexts, using biochemical and genetic approaches. However, there is no doubt that due to their involvement in autophagy and carcinogenesis TRIM proteins would be attractive drug targets for different diseases affected by proteostasis disruption (Hatakeyama, 2017).

The p62 protein, as already mentioned in previous sections, is also present in the UPS/ALS crosstalk. The N-end rule pathway apart from proteasome degradation can regulate autophagy degradation by modulation of p62 and autophagy biogenesis (Cha-Molstad et al., 2018). Accumulation of proteins because of proteotoxic stress may induce the N-terminal Arginylation of ER-resident chaperones such as BiP/GRP78. The consequent Arg-BiP is associated with misfolded proteins, and its N-terminal Arg binds to the ZZ-domain of p62. This binding promotes a conformational change in p62 in order to expose the PB1 domain and LC3-interacting region resulting in self-oligomerization and autophagosome targeting (Ji and Kwon, 2017).

13.2 UPS and ALS compensatory mechanisms.

The strongest, and one of the first evidence of UPS/ALS interconnection, comes with the notion that autophagy is activated if the proteasome activity is compromised. In line with this data, different PIs have been reported to activate autophagy in order to relieve cells from protein accumulation and proteotoxicity (Zhu et al., 2010). How this compensatory mechanism is regulated is not well understood. However, different mechanisms have been proposed, including the UPS-ER-autophagy circuit or the tumour suppressor protein p53.

Some transcriptional mechanisms have been shown to connect the UPS and the ALS. That is the case of the p53 protein that is regulated (among others) by the E3 ligase HDM2/MDM2

and UPS mediated degradation. In addition, this protein has a dual role in autophagy, depending on its cellular localization. In the nucleus, p53 accumulates to act as a transcription factor for autophagy-related genes such as ATG2, ATG4, ATG7, and the ULK1 complex, known as autophagy activators. Moreover, under starvation and proteasome impairment, cytosolic p53 leads to the activation of the AMPK pathway, that in turn inhibits the mTOR pathway, leading to autophagy activation (Ji and Kwon, 2017; Kocaturk and Gozuacik, 2018).

Autophagy inhibition causes an accumulation of protein aggregates mediated through p62. These aggregates are thought to sequester proteasomal substrates but also positive regulators of the UPS, leading to a disruption in the proteasomal flux. Therefore, p62 plays a negative role when autophagy is blocked due to its ability to oligomerize (Marshall et al., 2015). However, although this compensatory mechanism could be influenced by the internal cell state (pathology), it seems that this compensatory activity may be only achieved in one direction (Ji and Kwon, 2017; Nam et al., 2017), as ATG knockout assays have showed an accumulation of ubiquitylated proteins in different tissues and cell types (Kocaturk and Gozuacik, 2018).

The UPS has been a target for anti-cancer therapy for several decades, and resistance mechanisms are suggested to appear because of ALS compensatory activation among other factors depending on the cell type and pathology. The treatment failure in this context highlights the importance of tackling ALS and UPS as complementary systems (Nam et al., 2017).

13.3 Autophagic degradation of proteasomes: Proteaphagy.

Upon nutrient starvation, autophagy can be fastly induced to face nutrient limitation. However, during starvation, proteasomes might play a minor role in protein degradation because they are only able to degrade one peptide at a time (Wójcik and DeMartino, 2003). Interestingly, a quite recent quantitative proteomic analysis revealed that proteasomes can be degraded by both basal and starvation-induced conditions in a process called proteaphagy (Dengjel et al., 2012; Zhang et al., 2016). Nevertheless, proteasomes are mainly located in the nucleus. They must thus be translocated out of the nucleus to be degraded by the ALS in the cytoplasm (Marshall et al., 2015; Waite et al., 2016). The way in which these proteasomes come out of the nucleus to be degraded is not very clear, but multiple evidences support a dissociation of CP and RP prior to their nuclear exportation (Waite et al., 2016).

As an evidence, Cohen-Kaplan et al revealed in mammalian cells that proteaphagy induced by amino acid starvation is preceded by an increased polyubiquitylation of proteasomes, mostly in RPN1, RPN2, RPN10 and RPN13 subunits (Cohen-Kaplan et al., 2016a). It is still unclear whether proteaphagy induced by chemical inhibitors can drive degradation of CP and RP proteasomes separately, or in contrast target the whole complex. However, both scenarios can be considered (Quinet et al, 2021).

Other evidences in Marshall et al. publication reveal that mutations in α5 subunit trigger a turnover of the CP only, and mutations in Rpn5 subunit trigger a turnover of the RP (Marshall et al., 2015). Therefore, the role of specific ubiquitylation of proteasome subunits ensured by some associated E3 ligases must play a role in the regulation of proteasome degradation by autophagy (Quinet et al, 2021).

In MCL, proteaphagy has been linked to resistance to the proteasome inhibitor BTZ, as proteasome subunits from both CP and RP are permanently degraded by autophagy in cells with either acquired or innate BTZ resistance. Targeting autophagy to overcome BTZ resistance has been already proposed in these models, since it also affects levels of important cellular factors such as NOXA or NF-κB (Heine et al., 2018; Kawaguchi et al., 2011). In this context, the p62 inhibitor Verteporfin (VTP) has been shown to hamper proteaphagy in BTZ-resistant MCL cells, inducing synergistic cytotoxic effects when combined with BTZ in resistant cells, and reducing tumor growth xenografts models. Targeting the proteaphagy mechanism with pharmacological approaches can thus be considered as a relevant strategy to overcome chemoresistance in these patients (Grégoire Quinet et al, 2021).

13.4 UPS-ER-autophagy circuit, chaperons, and mitochondria mechanisms.

When proteins are synthesized, they are properly folded in the ER. When misfolded proteins are accumulated into the ER, they are retro-translocated to the cytoplasm where they are targets for UPS degradation. Autophagy can be activated to compensate an overload of the UPS system in the context of ER stress [ER-associated degradation (ERAD)]. Consequently, ER-stress can result in the final upregulation of NRF2 target genes, which induce autophagy (Nam et al., 2017).

In the UPS-ER-autophagy circuit, accumulated misfolded proteins promote the dissociation of the chaperon protein GRP78/BiP from the ER membrane. At the same time, different membrane receptors activate the upregulation of ATG genes, as well as LC3 lipidation and autophagosome biogenesis (Ji and Kwon, 2017). Chaperone proteins, such as the C-terminus of HSP-70-interacting protein (CHIP), and BCL-2 associated anthanogene (BAG1 and 3) also determine the fate of protein degradation in the context of misfolding events (Nam et al., 2017).

Another chaperon involved is BAG. While BAG1 mediates proteasomal degradation, BAG3 interacts with Hsp70, CHIP and p62 for autophagy degradation. Moreover, during aging stress, the BAG1/3 ratio is known to modulate autophagy activity (Ji and Kwon, 2017).

As mitochondria senses the ATP status inside the cells, the state of cellular energy reserve is an important factor to regulate degradation. The Parkin protein, a known E3 ligase, plays a critical role by mediating proteasomal degradation of mitochondrial substrates. At the same time, it has been reported that mitochondria can be a shuttling hub of misfolded proteins to be degraded by mitophagy (selective autophagy) when the UPS is overloaded (Nam et al., 2017).

Recent studies showed that mitophagy involves both the UPS and autophagy. In fact, the UPS is believed to be a prerequisite in the preparation of mitochondria for autophagy. Other examples of the UPS/ALS cooperation are present in other selective autophagy processes, such as xenophagy (clearance of pathogens) and pexophagy (clearance of peroxisomes). However, further studies are required to understand the details of this UPS/ALS crosstalk under these conditions (Kocaturk and Gozuacik, 2018).

Additionally, the immuno-proteasome and the autophagy system participate in the regulation of the cell-mediated immune response via the generation of antigenic and self-peptides which are presented on the major histocompatibility complex (MHC), class I and II, respectively (Cohen-Kaplan et al., 2016a).

There is no doubt that the UPS and autophagy function in parallel during cells' life through multiple points of communication and different layers of regulation. In addition to their system-specific functions, both are also involved in the regulation of similar cellular processes. Both systems coordinately act to ensure protein homeostasis, but also development, differentiation, antigen presentation and apoptosis.

14. Molecular tools to study and modulate the ubiquitome.

PTMs are regulatory mechanisms that are very important to maintain protein homeostasis, also involved in controlling a wide number of cellular processes and biological functions. In cells, proteins play key roles in almost all processes and functions, and although proteolytic systems have caught less attention than protein synthesis among the scientific community, the appropriate activity of proteins is known to be regulated by their proper degradation (Cohen-Kaplan et al., 2016a).

Given the variety of UbLs, the different types of monotypic chains that they can potentially form, and the existence of hybrid chains containing different types of UbLs, a complex "Ub code" may underlie numerous biological and cellular processes. This has prompted researchers to develop different systems to isolate UbL-modified proteins using cultured cells, model organisms, and clinical tissue samples. However, the reversibility and heterogeneity of Ub signals have complicated their isolation, quantification, and characterization (Mattern et al., 2019). Moreover, ubiquitylation characterization is a double challenge that involves the mapping of ubiquitylation sites, determination of Ub chain topology (Sylvestersen et al., 2013), but also the discovery of the related biological functions. Deciphering the "Ub code" through the study of the ubiquitome (Ub-modified proteome or profiling of ubiquitylated proteins inside the cells in a specific physiological state) has become a priority in clinical research and biomedicine because of its potential to discover specific biomarkers and new targets for drug development (Mattern et al., 2019).

Historically, most approaches used for the analysis of the ubiquitome of specific cell types included epitope tagged Ub-overexpression (HIS, HA, Myc, GST, GFP and FLAG), being the size of the tag potentially interfering with purification steps. Furthermore, under overexpression conditions, there is additional risk of obtaining results that do not mimic the

natural/basal state of cells. As a result, Ub signals could be detected as exogenous stress responses, altering Ub internal pathways and cellular dynamics (Mattern et al., 2019).

Alternative approaches (Figure 10) have been developed by the scientific community in order to study endogenous Ub modifications, like monoclonal antibodies directed against the di-Gly residual peptide found on Ub substrates after deubiquitylation, or molecular traps formed from tandem Ub-binding domains (TUBEs) repetitions (Hjerpe et al., 2009).

In addition, Avitag, a short peptide, can be used followed by a biotinylating step (using Biotin and promiscuous BirA enzyme from *E.coli*) to be consequently captured by a streptavidin column. Biotin-Streptavidin interactions allow denaturing purification conditions in culture cells and transgenic animals, with the advantage of quite reducing background obtained by endogenous biotinylated proteins (Pirone et al., 2017). Two different tags in two sequential steps had been proposed to increase the purity of samples in precipitation assays. However, the specific negative background expected under those conditions can increase, and the size of the tag can interfere with conjugation/deconjugation dynamics (Mattern et al., 2019).

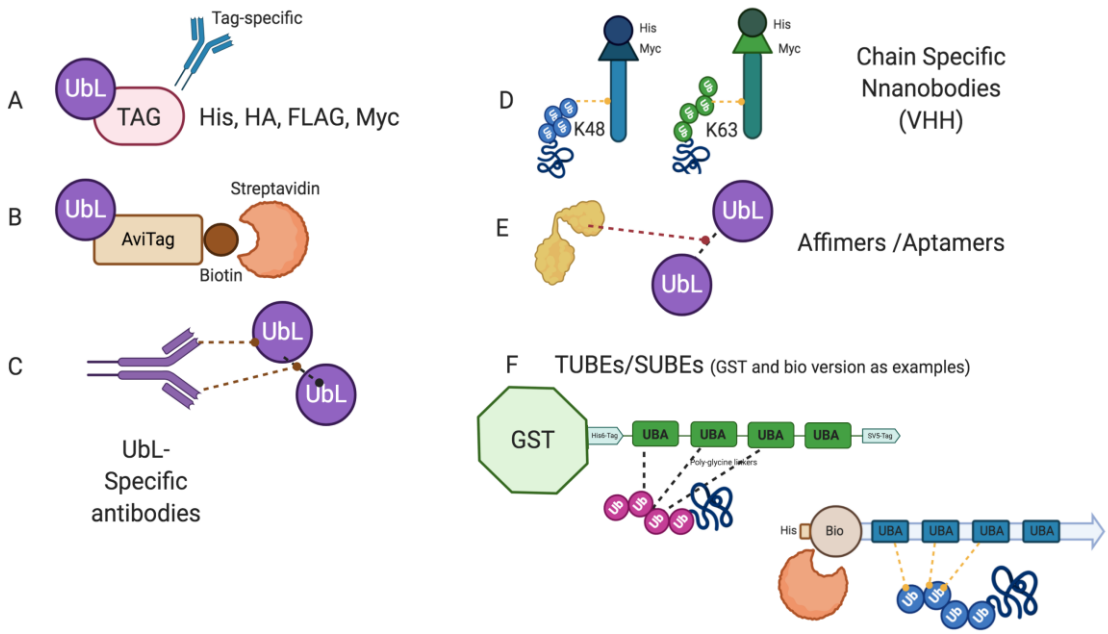

Figure 10: Molecular tools developed to identify ubiquitylated proteins: A: Tagged versions of Ubiquitin (Ub) or Ub-Like proteins (UbLs) like poly-histidine (His), B: AviTag-Biotin-Streptavidin. C: Antibodies against the di-Gly signature recognizing various Ub family members and specific antibodies. Binding tools based in small proteins/peptides with affinity for Ub or UbL: D and E, chain-specific nanobodies and Aptamers/Affimers. F: Tandem Ub Binding Entities (TUBEs), GST and bio version.
Created with BioRender.com.

Additionally, several emerging methods show promising results in allowing a more detailed characterization of Ub chain topologies. Peptide aptamers, affirmers or chain-specific antibodies (minibodies/nanobodies) recognizing specific Ub linkages can be used to immunoprecipitate specific substrates for a subsequent Mass Spectrometry (MS) identification in addition to cell imaging (Chakravarty et al., 2014; Michel et al., 2017).

The isolation and identification of modified proteins via MS has become a fundamental step toward understanding cellular processes and diseases, being therefore a crucial step for unravelling the Ub code and its implications. However, MS presents difficulties as the proportion of modified versus the total pool of a given protein is usually low and modifications can be highly transient and sensitive to the action of DUBs and deconjugation internal dynamics. Nonetheless, different strategies and techniques have being developed over the years to overcome these difficulties (Mattern et al., 2019).

There is no doubt that the improvement in the isolation of endogenous ubiquitylated proteins would help to obtain more accurate data to identify Ub sites and substrates in complex samples. Ub-binding enrichment strategies can contribute to improving our knowledge of the role of these modifications in molecular and cellular processes. Due to the interest in Ub/UbL pathways as sources for discovering new drug targets and biological markers, the scientific community has been motivated during the last years to develop a broad toolbox for studying UbL modified proteins (Figure 10) (Mattern et al., 2019).

14.1 Tandem-repeats Ubiquitin-binding entities / TUBEs.

Weak binding affinities of individual UBDs for Ub suggest that cells may use a multivalent binding mechanism to drive different cellular functions. Following that clue, a significant improvement in Ub-affinity techniques were made with the multimerization of UBDs as in the case of the TUBEs technology (Hjerpe et al., 2009).

TUBEs (Figure 11) were designed by using four tandem UBA domains, separated by flexible linkers to facilitate the purification of endogenous poly-ubiquitylated proteins from cell extracts, as they recognize tetra-Ub entities with higher affinity that single UBA domains (Hjerpe et al., 2009). Interestingly, this multivalent topology has been found in some proteins indicating an evolutionary advantage. This is probably achieved by a co-operative binding effect, and once a Ub linkage is bound to the UBA domain, it positions the second UBA domain favourably to the nearby Ub (Lopitz-Otsoa et al., 2012).

This proteomic tool that behaves as a Ub trap (Lopitz-Otsoa et al., 2010) is a powerful and reliable system for the characterization of the ubiquitome. It can be combined with other Ub-enrichment techniques as MS to provide insights into different cellular processes that involve ubiquitylation events.

TUBEs protect ubiquitylated proteins from DUBs cleavage and proteasomal degradation. Moreover, using TUBEs allows to avoid tag overexpression that could affect internal molecular mechanisms leading to the formation of aberrant Ub chains (Hjerpe et al., 2009).

Since some UBDs show preference for certain linkages, TUBEs can be designed to capture protein-substrates enriched in a particular linkage type. For example, appart from the classical TUBE based on the HR23A (From Rad23 protein) UBA domains, immobilized recombinant Ub binding domains (UBDs) for the specific enrichment of K63 ubiquitylated proteins in combination with TUBEs have been developed to bind certain types of Ub linkages with high affinity, hereby enhancing the enrichment (Mattern et al., 2019).

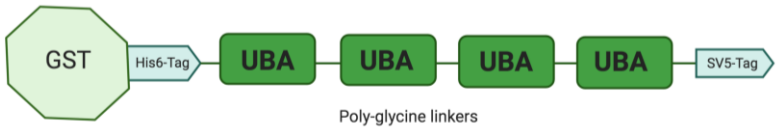

Figure 11: Schematic representation of a GST-TUBE (Tandem-repeats Ubiquitin-binding entities). The tandem disposition increases their Ub-binding capacity. UBA domains are separated by a flexible linker and tagged with GST, His6 and SV5 to be detected in different assays. Created with BioRender.com.

These molecular tools have been proved to be essential elements in multiple studies including in the search of disease biomarkers and drug targets. The HR23A TUBE, based in the UBA domain from the UV excision protein HR23A, has been used to demonstrate the role of Ub in chemotherapy, and K63-TUBEs have been used in mitophagy studies to demonstrate the role of Parkin (Mattern et al., 2019). These tools can be used efficiently for the analysis of ubiquitylation of crucial endogenous factors in different cell events and under different stress conditions (Hjerpe et al., 2009).

Apart from the study of ubiquitylated proteins in enrichment or immunoprecipitation assays, TUBEs can be used in MS analysis. TUBE-enrichment under native conditions can preserve the interactions and protein complexes built around ubiquitylated proteins. In that context, TUBE-MS analysis allows to identify the ubiquitome interplay of cells, the Ub-interactome (Lopitz-Otsoa et al., 2010; Mattern et al., 2019).

TUBEs can also be used in detection methods, to replace antibodies, for example in far western immunoblots or immunofluorescence assays for cellular imaging (transient TUBEs transfection). Alternatively, they can be used for high-throughput screenings, arrays, and drug discovery, as TUBEs-based microarrays can be used for the analysis of cellular processes regulated by ubiquitylation and for the detection of pathologies and aberrant ubiquitylation patterns (Serna et al., 2016). Despite these numerous applications, this tool has limitations and they development may be a challenge as multiple efforts planning, and validation steps must be followed.

14.2 Aptamers/Nanobodies.

Peptide aptamers are small combinatorial proteins (5-20 amino acids residues) embedded in a stable protein scaffold that binds specific sites to their target molecules. These peptide

aptamer scaffolds have become relevant recently, due to their biomedical, bioimaging and bioanalytical applications (Reverdatto et al., 2015). One of the biggest challenges nowadays in the field of biomedicine, and in modern biology research in general, is to design molecules for modulate and investigate specific internal cellular processes. Aptamers emerge as an alternative to conventional antibodies, and with the purpose of overcome some of their disadvantages (considerable size, temperature sensitiveness, dependence on animal immunization, limited life…). Moreover, aptamers are less immunogenic, smaller (10-50Kda), and are characterized by high stability, high solubility, fast folding and kinetics. Nevertheless, the identification and isolation of high affinity ligands from combinatorial libraries is still a challenge (Reverdatto et al., 2015). As an alternative, and with similar characteristics and advantages, Ub chain-specific nanobodies have just recently appeared in the scene.

One strategy to create those combinatory libraries is to use synthetic libraries, based on keeping a common conserved structure and randomly varying the CDR (complementary determining region) sequence. This degree of variation is higher than using naive libraries by immunization. In addition, phage display is a method used to present polypeptides on the surface of bacteriophages, with the purpose of selecting them in terms of specificity and ability to recognize and bind specific targets. The bacteriophage genome can tolerate genomic inserts into coat proteins, presenting these combinatorial libraries into the phage surface. The phage population is presented to the target of interest, and the unbound fraction is washed away. The binding candidate is usually selected after 3 to 10 cycles for the identification of high affinity ligands (Reverdatto et al., 2015).

In vitro selection of antibodies is usually used to obtain highly functional binders, rapidly and at lower cost. In 2016, Moutel et al reported the first fully synthetic phage display library of humanized llama single domain antibody (dsAb) providing high affinity binders without animal immunization. This library was based on the manipulation of antibody fragments retaining binding capacity, a phage display library created and screened against diverse targets for selecting the VHHs Ub chain-specific nanobodies. Additional changes were also be introduced to reduce the distance to the VH human sequence. This humanized synthetic scaffold was created with robustness and high functionality, being Moutel et al, the first to fully address the development of a synthetic single domain antibody library based on a humanized scaffold derived from llama VHH (Moutel et al., 2016).

In contrast to the common antibody structure present in mammals, specimens like camelid or shark have an antigen recognition domain composed by a single VHH domain (referred as nanobodies). They can be easily expressed as recombinant protein fragments and represent attractive alternatives mainly because they are easy to manipulate and are not limited by potential misfolding events (Moutel et al., 2016).

Nanobodies have been developed for therapeutic purposes being very valuable for diagnosis and basic biology research. VHHs can be generated to be used as protein purification ligands, for immunoprecipitation purposes, and to interfere with protein conformation localization, or functioning (*in vivo* immunomodulators). Moreover, due to their monomeric nature and high stability, selectivity, and smaller size (mostly produced in bacteria), nanobodies can be used as sensitive detection probes, even in complex samples (Meyer et al., 2014).

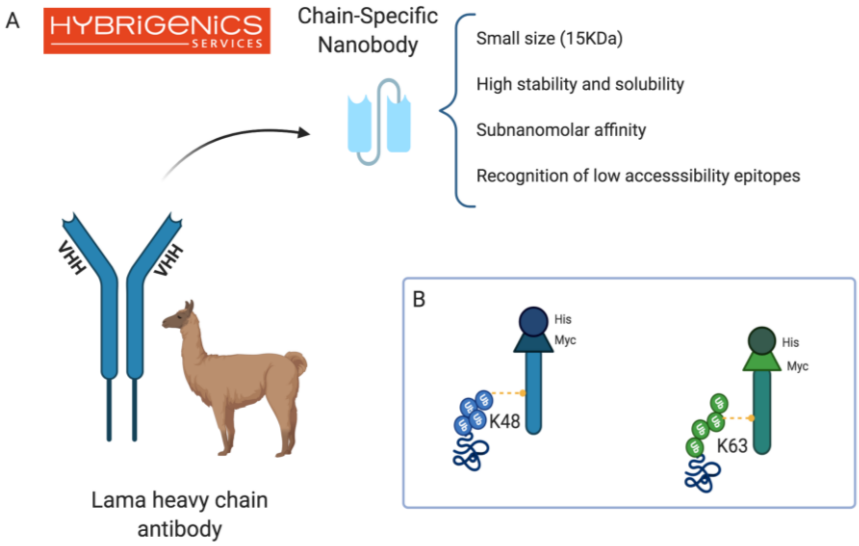

Figure 12: Nanobodies structure (*Hybrigenics*). Panel A: VHH or nanobody is derived from heavy-chain-only antibodies that circulate in the sera of camelids. They have a small size, 15Kda, a single-domain nature, and can be produced as a robust entity very efficiently and with a high solubility (*Hybrigenics* company). Panel B: K48 and K63 chain-specific nanobodies used in this project. Created with BioRender.com.

Chain-specific nanobodies are stable recombinant and highly valued proteins for multiple applications. A combination of nanobody and magnetosome has been proposed for immunoprecipitations assays. But also, by using a fluorescent protein fused to them, they can produce a versatile nano-tracer for imaging, avoiding the necessity to use additional fluorescent tags, like GFP (Thorn, 2017).

Nanobodies were also engineered for molecular imaging applications. Molecular imaging is a very important tool to provide knowledge in cancer research, clinical trials, and medical practice. Due to their smaller size, nanobodies can be used to penetrate solid tumor tissue, a promising technique for non-invasive molecular imaging of specific targets diagnosis, and *in situ* protein-protein interaction studies (Chakravarty et al., 2014).

14.3 Mass spectrometry tools and analysis.

Proteomics usually offer additional and complementary information to genomics analysis. Although in many cases changes in protein abundance and function can be attributed to alterations in gene expression, multiple posttranscriptional and posttranslational mechanisms are implicated in protein regulation. Therefore, proteomes are often much more complex than the corresponding genomes (Zhang et al., 2014).

The central goal of cell biology is to understand the mechanism underlying complex biological processes and dynamic cellular networks. To understand all elements involved in a specific cellular pathway along with its components, it is important to identify the fractional

stoichiometry of the different regulatory modifications and protein assemblies as well as the spatial organization of the different components of the pathway. PTMs and Ub-driven signalling cascades have been, during the last decades, under thorough investigation using different proteomics tools to understand the kinetics and the stoichiometry of individual events and components on these pathways (Ordureau et al., 2015).

MS is a technique that measures the mass-to-charge ratio of ions resulting from the sample ionization by electrospray ionization (ESI), or a matrix assisted-laser (MALDI). ESI produces ions from samples in solution in contrast to MALSI that needs a solid sample crystalized in a chemical matrix. Therefore, ESI-MS is preferred as it can be linked to liquid-separation chromatography (LC) or electrophoresis, allowing the analysis of liquid complex samples (Aebersold and Mann, 2003; Zee and Garcia, 2012).

A mass spectrometer is composed of an ion source from charge species, a mass analyzer that separates analytes by m/z ratio and a detector providing spectra signals, based on the number of ions per m/z. Different m/z separation methods can be found in MS analyzers: TOF or "time of flight", Quadrupole and Orbitrap, that can be coupled with ESI and MALDI indistinctly. However, due to different advantages, MALDI is usually linked to TOF and ESI to quadrupole and orbitrap separation procedures (Aebersold and Mann, 2003).

Protein identification usually involves two MS sequential steps MS1-MS2 (tandem mass spectrometry) using both the same separation method or not. This process is repeated for tandem acquisition depending on the type of mass spectrometer, and data generated is analyzed by a powerful software for protein identification and quantification using MS databases from *in Silico* digestion (Aebersold and Mann, 2003).

There are two broad classes of quantitative measurements that can be made on proteins and complexes using mass spectrometry analysis: relative and absolute quantification methods. These typically involve the combination of multiple labelling and/or enrichment strategies with proteomics workflows designed to reveal the specific characteristics of the molecules being analyzed by being linked to one or more types of MS detection method (Ordureau et al., 2015).

Relative abundance methods allow the detection of a modification and the determination of how the modification changes in response to a perturbation generating ratios or relative changes. Nevertheless, this method does not provide information about the stoichiometry. In contrast, absolute quantification allows stoichiometry but also spatial and sometimes temporal identification of proteins or complexes in the sample. There are two label-based approaches in relative quantification methods: post-trypsinization labelling and stable isotope labelling with amino acids in cell culture (SILAC). Post-trypsinization methods include tandem mass tagging (TMT) and isobaric tags for relative and absolute quantification (iTRAQ). These methods allow an extensive coverage of the proteome and may have the ability to provide a large-scale quantitative analysis of proteins and modifications under different conditions. Label free methods in quantitative measurements also come with advantages and disadvantages. While the method reduces costs, allows unlimited number of samples and provides less complexity in the MS1 analysis, the experiment itself requires a

large amount of time, instrumentation and several runs as they provided low reproducibility (Ordureau et al., 2015).

At the same time, there are two major targeted methods used for absolute quantification measurements. One approach, often referred to as absolute quantification (AQUA) or isotope dilution, uses isotopically heavy proteins or synthetic peptides to measure ion intensities. Alternatively, the multiple reaction monitoring (MRM)—involves targeted analysis of selected peptides whose fragmentation patterns are well described. The use of the last one to quantify Ub chain linkages is increasing as fragmentation patterns for ubiquitylation sites are being discovered and developed rapidly (Ordureau et al., 2015).

MS has emerged as the method of choice for proteome analysis, and more in detail in the study of PTMs and ubiquitylation events. Due to recent technological developments in MS, in combination with novel Ub enrichment strategies, it is now possible to get insights into ubiquitylation sites, but also into their involvement in different biological processes. Great technological progress in MS and liquid chromatography (LC-MS) instrumentation as well as software and sample preparation techniques have substantially improved speed and sensitivity, allowing now the characterization of low-abundant PTMs (Heap et al., 2017).

Apart from the absolute and relative quantification methods, there are two major strategies for the MS bioanalysis of proteins. The bottom-up (commonly called “shotgun” proteomics) approach involves digesting proteins into small peptides to analyze the surrogates by LC-MS/MS. In contrast, the top-down approach analyzes intact proteins by LC-high resolution MS. The principal advantage of bottom-up strategies is the high sensitivity obtained. However, caution is needed to interpret the data, and the specificity in those assays is obtained by using capturing reagents in the sample (Kang et al., 2020).

Classical “bottom-up” (after fragmentation) approaches use enzymatic digestion of the proteins from the sample, followed by separation of the resulting peptide mixture using High-Performance Liquid Chromatography (HPLC) according to their hydrophobicity and eluted into a spray needle from which they are ionised. Peptide ions enter the mass spectrometer and are then analyzed in two ways. First, the mass-to-charge ratio; m/z, and intensities of the peptide ions are determined (MS1). This provides quantitative information about the abundance of the peptide. Secondly, these peptide ions are isolated and fragmented by tandem mass spectrometry (MS2), providing the amino acid sequence information about the peptide. In the final step, protein databases of the studied organism can be searched by specialized software programs using both accurate mass of the peptide and the sequence information leading to the identification of the peptide. If PTMs are targeted, the modification of interest must be included in the peptide search, thereby increasing the search database (Heap et al., 2017).

Peptide spectra are obtained through data-dependent acquisition of the mass spectrometer, and the identity of the analyzed peptide is derived by matching the measured peptide mass and the corresponding MS/MS masses against a database consisting of known protein sequences digested in silico (Figure 13) (Sylvestersen et al., 2013).

For PTMs, ubiquitylated peptides must be enriched prior to MS analysis. Different enrichment methods have emerged, like the His- or FLAG- tagged version of Ub. Other enrichment strategies involve the use of molecular traps like TUBEs or different specific antibodies or aptamers/affirmers (Figure 10). However, it should be noted that although the TUBEs enrichment strategy is a very sensitive and powerful approach to identify proteins, it may not be the method of choice for the identification of ubiquitylation sites depending on the sample size and complexity (Heap et al., 2017).

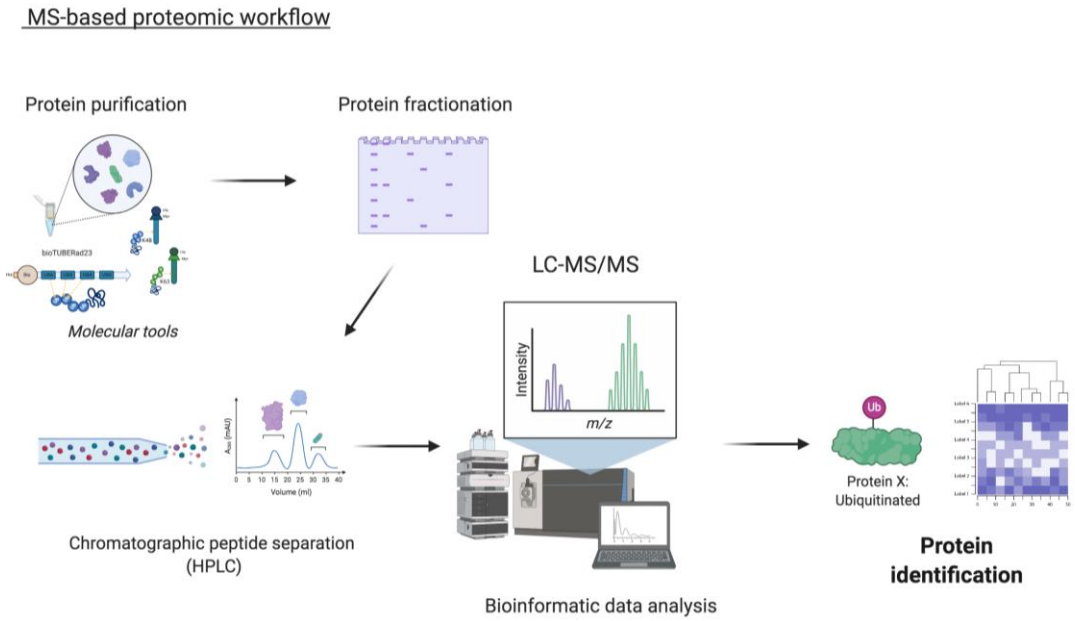

Figure 13: Schematic representation of a general MS proteomic workflow. Protein purification, protein enrichment using different methods and protocols. Protein fractionation or digestion following by a chromatography separation and MS/MS analysis and bioinformatic search of proteins/subtrates identified. Bottom-up will include a previous fragmentation of the sample in contrast to the top-down strategy. Further explained in the main text.
Created with BioRender.com.

Another widespread method of enrichment is the use of the monoclonal antibody against di-Gly remnants, which since its discovery has been used extensively for ubiquitylation proteomics discoveries. This immunoprecipitation approach is a versatile tool as it can be used in conjunction with MS. However, other UbLs like NEDD8 can release the same di-Gly motif after tryptic digestion rendering the distinction impossible to achieve (Heap et al., 2017).

Although proteomic platforms allow to identify many proteins present in complex mixtures, it is not usual for samples to contain co-eluting peptides at various abundances and overlapping m/z masses. To confidently identify as many low-abundant and overlapping peptides as possible, technological advances in speed, sensitivity and mass accuracy of the mass spectrometer are further required. This becomes important in the analysis of PTMs, as

these are predominantly present in complex mixtures at sub-stoichiometric levels. With the introduction of the latest generation of mass spectrometers, several of these analytical requirements have been significantly improved, as the recent development of the Q Exactive mass spectrometer allows the identification of thousands of proteins from a whole human cell extract in just one hour (Sylvestersen et al., 2013).

MS has emerged during the last decades as the method of choice for comprehensive proteome analysis employed for the identification of proteins from complex samples (Sylvestersen et al., 2013). Nevertheless, rapid technological and enrichment advancements improving sample preparation, MS-detection, and data analysis are essential for a robust protein quantification (Macklin et al., 2020).

14.4 PROTAC strategy to drive proteasome degradation/proteolysis.

Proteolysis-targeting chimeric molecules (PROTACs) represent an emerging technique with great prospects in the development of new therapeutic approaches and interventions. The mechanism is based on the inhibition of the protein function by the recruitment of a Ub E3 ligase for its ubiquitylation and consequent protein degradation (Gu et al., 2018). They exploit the intracellular Ub-proteasome system to selectively induce a rapid and sustained protein degradation (Figure 14) (An and Fu, 2018).

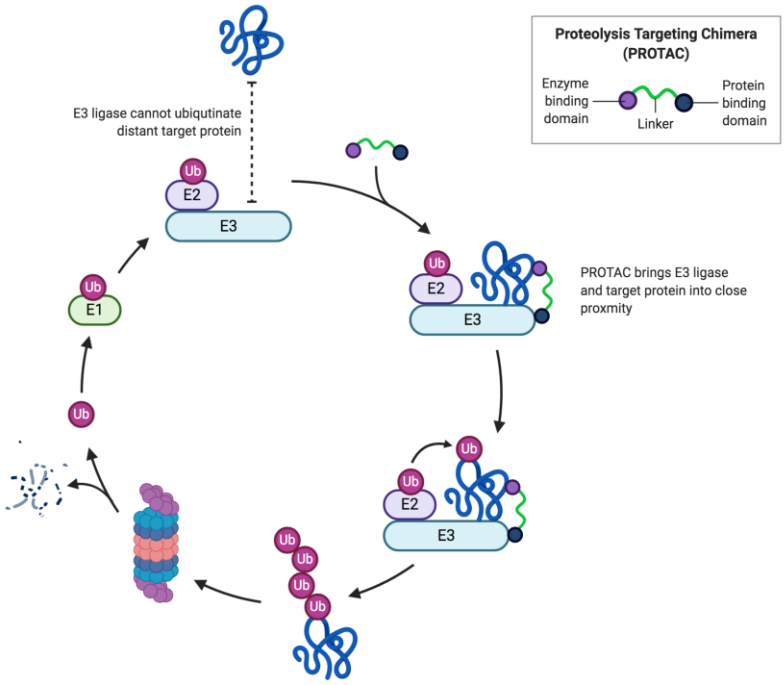

Figure 14: Schematic representation of a PROTAC (Proteolysis Targeting Chimera) molecule and its mechanism of action using the UPS: A ligand for recruiting the E3 ligase or enzyme binding domain, the linker and an additional motif or protein binding domain to target the specific protein. PROTAC molecules use the Proteasome system to degrade targeted ubiquitylated proteins.
Created with BioRender.com.

PROTACs contain a ligand for recruiting an E3 ligase enzyme, a linker, and another binding domain to target the protein of interest. They have displayed profound potential in targeting “undruggable” proteins, such as transcription factors, scaffold proteins and non-enzymatic proteins, which cannot be targeted by small molecules (Gu et al., 2018).

Small molecule inhibitors used to target therapy have manifested several limitations. First, the target proteins must be enzymes or receptors that have pockets or active sites. Second, sustainable, and high drug levels are needed to maintain the intracellular concentration and therapeutic efficacy. This usually leads to off-target and side effects due to the competition with other intracellular molecules. Third, small molecules typically only disrupt the activity of one domain of multidomain scaffolding proteins, and functional activities of other domains and their interactions with other proteins are preserved (An and Fu, 2018; Gechijian et al., 2018). For example, when using the bromodomain inhibitor of multidomain and bromo-containing proteins like TRIM24, effective anti-proliferative responses were not displayed, suggesting that the inhibition of the bromodomain is insufficient as an anti-cancer strategy (Gechijian et al., 2018).

In contrast, the PROTACs strategy triggers a pronounced effect by eliminating target proteins via ubiquitylation and degradation, rather than by inhibiting the activity of these proteins. Moreover, this strategy has been continuously improved during the last years to overcome certain limitations, like stability, cellular permeability, solubility, and tissue distribution (Gu et al., 2018). From 2015, more than thirty small-molecule PROTACs have been reported, many of those showing nanomolar affinity, and exploiting VHL and CRBN E3 ligases. In these cases, protein degradation is induced soon after the treatment, and the depletion of the target protein can be seen within an hour. This reduction is sustained in time, and different reports show a reduction in vivo maintained for more than 24 hours. The downstream proteins and the signalling cascades of the target protein of interest are inhibited with the same persistence in time. Compared with small inhibitors, PROTAC treatments result in more significant and prolonged suppression of downstream proteins including more dramatic cell proliferation suppression/apoptotic cell death, and greater in vivo cancer regression (An and Fu, 2018).

Different examples show high in vitro proliferation suppression, stronger in vivo growth inhibition, and the induction of greater survival improvement. For example, the BET-targeting PROTAC ARV-771 caused a greater reduction of Bromodomain extra-terminal protein (BETP) in MCL cells, and improved survival of mice compared to the treatment with the small BET inhibitor OTX015 (Sun et al., 2018). As another example, the bifunctional PROTAC ARV-825 has been shown to mediate rapid degradation of BRD4, leading to proliferation suppression and apoptosis induction in Burkitt's lymphoma (BL) cell lines (Lu et al., 2015).

As a result, two PROTAC drugs are being tested currently in clinical trials for prostate and breast cancer, due to the potential displayed in vivo and vitro assays (An and Fu, 2018). Quite interestingly, by using a similar strategy, autophagy-targeting chimera (AUTACs) have been recently developed for a selective clearance via autophagy degradation (Takahashi et al., 2019).

15. Scientific Context and preliminary data.

Bortezomib (BTZ) is commonly used to treat Mantle Cell Lymphoma and exerts its antitumor activity by impairing the degradation of crucial factors regulating cell cycle, tumor progression and apoptosis. However, BTZ resistance in hematopoietic cancer cells has been extensively reported and studied due to its high incidence after chemotherapy. Although the molecular mechanisms of BTZ resistance are not fully characterized, the role of proteostasis and the activation of autophagy to avoid BTZ-induced cell death have been addressed in different lymphoma and multiple myeloma studies (Lopez-Reyes et al., 2021; Selimovic et al., 2013).

In a recent publication from the host lab, Quinet et al hypothesized that the ubiquitylation machinery could be involved in the response/resistance to this drug by observing differences in the Ub pattern between sensible and resistant cell lines. By using a comparative Ub-proteome analysis, using GST-TUBEs traps to enrich the Ub proteomic fraction, they detected a reduction in proteasome subunits as well as an increase in autophagy-related proteins in the BTZ-resistant ZBR cell line, compared to the BTZ-sensitive Z138 cell line. This suggests a disrupted balance between the two major proteolytic pathways inside the cells; the Ub Proteasome System (UPS), and the Autophagy Lysosome System (ALS) (Figure 15). In this analysis, different enrichment in Ub enzymes were also detected, though not fully explored yet. Data also indicated a different distribution of Ub signatures/chains (Figure 16), however without statistical significance.

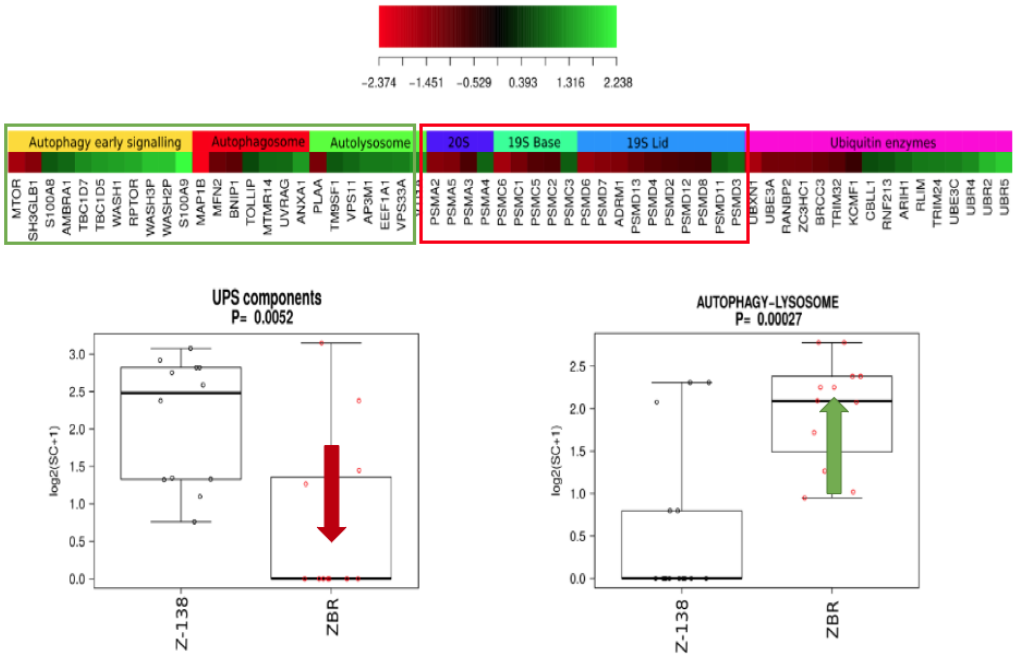

Figure 15: A comparative Ub-proteome analysis, using GST-TUBEs traps in Z138 (sensitive) versus ZBR (BTZ-resistant cell line). The enriched Ub proteomic fraction identified a reduction in proteasome subunits as well as an increase in autophagy-related proteins in the ZBR cell line, compared to the sensitive Z138 cell line (Quinet et al, 2021).

In this analysis, in the Z138 cell line, K11 and K48 Ub linkages were more prominently detected in contrast to the K63, more pronounced detected in the ZBR cell line. Suggesting that a remodeling of chains, could be the cause or the consequence of the disequilibrium between the UPS and ALS (Figure 16), therefore contributing to the resistant phenotype. However, new molecular tools and optimized protocols to enrich specific Ub chains are needed to validate this hypothesis.

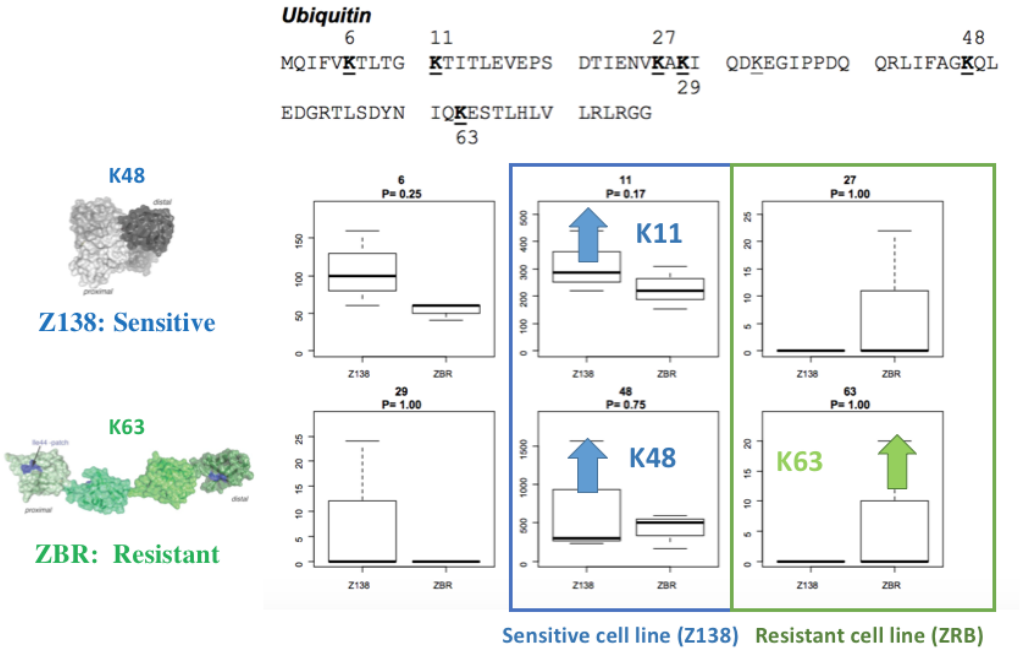

Figure 16: Differences in Ubiquitin signatures detected in the Z138 comparing to the ZBR cell line. As displayed in the figure, K11 and K48 Ub linkages were more prominently detected in the Z138 sensitive cell line, in contrast to the K63 detected in the ZBR cell line. Poor significance in the statistical analysis as indicated by the p values (a lot of dispersion). Data not shown from (Quinet et al, 2021).

In this study, Quinet also demonstrated an accumulation of proteasome subunits into autophagosomes vacuoles by using different autophagy inhibitors Bafilomicin A (BafA) and Cloroquine (CQ), indicating a constitutively activated proteophagy (degradation of the proteasome by the ALS) in MCL BTZ-resistant cells. In fact, testing a variety of resistant cell lines derived from MCL patients (MINO AND REC-1), they showed that the dependence on proteaphagy for survival is higher in more resistant phenotypes, as the combined treatment of autophagy inhibitors with BTZ showed to recover or increase the level of apoptosis similarly to the sensitive counterpart cell line (GRANTA) (Figure 17/ A y B).

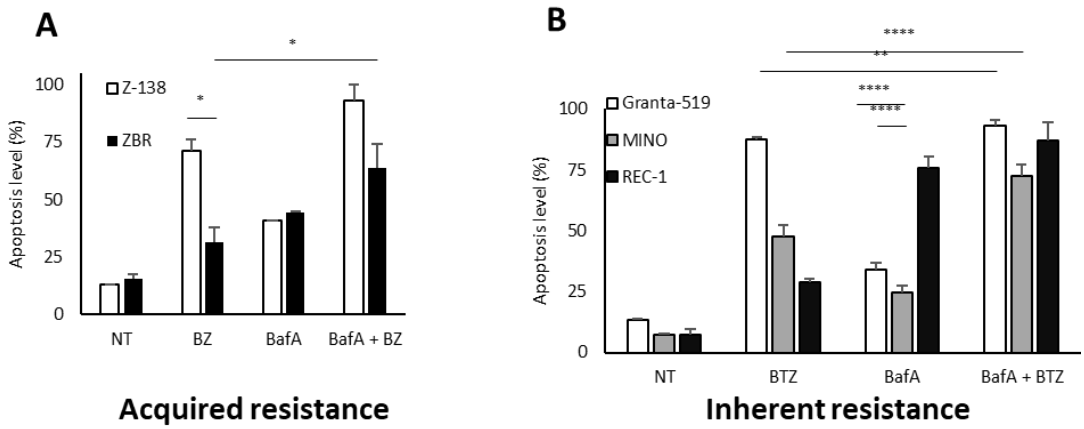

Figure 17/A: Autophagy dependency on BTZ MCL cell lines. A: Acquired BTZ-resistant cell line ZBR and its counterpart after BafA treatment display synergistic activity in combination with BTZ, increasing apoptotic response. B: Cell lines with inherent resistance MINO and REC-1, GRANTA cell lines used as a control without resistance. The more resistant a phenotype is (REC1>MINO), the higher dependent on proteaphagy for survival, and more apoptosis displayed when blocking autophagy. FACS analysis after 24h treatment. From (Quinet et al, 2021).

By using a recent commercially available drug targeting the p62 protein and consequently autophagy, named Verteporfin (VTP), they further corroborated proteaphagy dependency and the involvement of p62 autophagy receptor in the phenotype. They also suggested a more significant involvement of VTP response in the BTZ-resistant phenotype, as in vivo mouse xenografts treated with VTP showed therapeutic potential in limiting tumor growth, opening new possibilities to discover mechanistic implications in the MCL disease and in the proteaphagy phenotype (Figure 17/B) (Quinet et al, 2021).

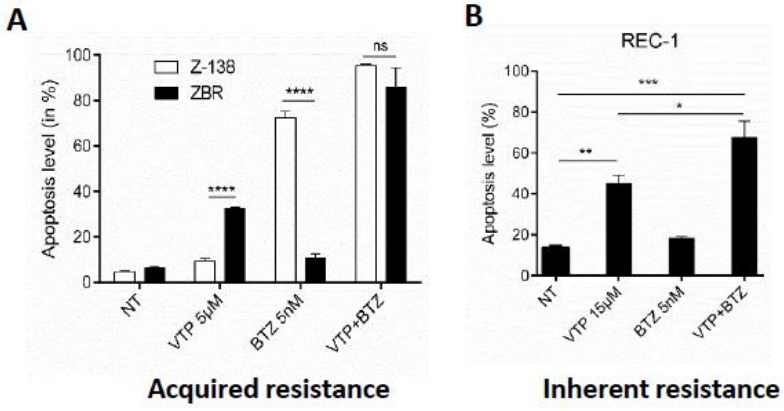

Figure 17/B: Autophagy dependency on BTZ MCL cell lines. A: Acquired BTZ-resistant cell line ZBR and its counterpart after VTP treatment display an increased apoptotic response in contrast to the sensitive cell line. B: Cell line with the higher inherent resistance phenotype REC-1. The more resistant phenotype treated with VTP alone or in combination with BTZ. FACS analysis after 24h treatment. From (Quinet et al, 2021).

16. Hypothesis and Objectives:

Although BTZ resistance is a multifactorial process that is not well understood, different evidences highlight the impact of protein equilibrium or proteostasis, as being dysregulated in multiple diseases and implicated in resistant mechanisms (Gonzalez-Santamarta et al., 2020).

A previous proteomic study performed by the hosting group using the GST-TUBEs technology in BTZ-resistant ZBR and BTZ-sensitive Z138 cells revealed a dysregulation between proteasome subunits and autophagy factors, between these two cell lines. This led to the identification of proteophagy as a driving mechanism on which BTZ-resistant cells could hold dependence for surviving, therefore making autophagy an important contributing factor (Quinet et al, 2021). In this analysis, differences in Ub signatures distribution were also observed between BTZ sensitive and resistant cell lines, indicating that a UPS/ALS disequilibrium could be accompanied by a different Ub distribution or pattern in each cell line. However, more powerful, and specific tools are needed to confirm this information.

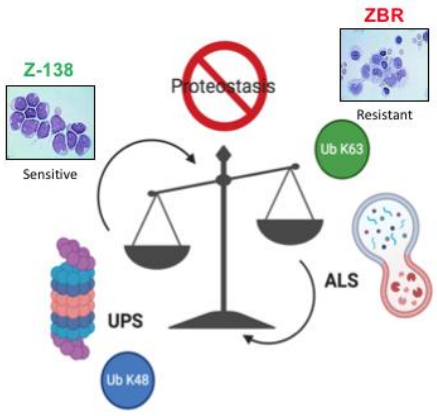

Figure 18: Schematic representation of our main hypothesis in Bortezomib resistant Mantle Cell Lymphoma cells. A disrupted balance between the two major degradative pathways, the Proteasome, and the Autophagy-Lysosome System, determines BTZ sensitivity in MCL cells, with the Ub remodeling being the cause or the consequence of this proteostasis disruption. Created with BioRender.com.

Therefore, and taking all this previous data and the scientific context into account, we have established the general hypothesis (Figure 18) and specific sub-hypotheses leading this project.

We hypothesized that a disrupted balance between the two major degradative pathways, the Ubiquitin Proteasome System (UPS) and the Autophagy-Lysosome System (ALS), contributes to establishing resistance to BTZ in MCL cells.

We considered the possibility that Ubiquitin chain remodeling could be the cause or the consequence of this disequilibrium, contributing to regulating processes implicated in the resistance. More in detail, we explored if the K63 enrichment found in ZBR was contributing to permanently activate autophagy in these cells.

In addition, we also hypothesized that the regulation of Ubiquitin enzymes, implicated or with a major role in UPS/ALS crosstalk or in Ubiquitin chain formation, could be targeted to overcome BTZ resistance.

After establishing our hypothesis, we planned our **objectives** as follows.

In this project, we aim at understanding the **Ubiquitin chain composition** in BTZ-resistant MCL cells. In addition, we are also interested in the **identification of Ubiquitin enzymes** responsible of this chain remodeling, and in **understanding their role** in proteasome autophagy crosstalk and in the response to BTZ.

In parallel, in order to study the ubiquitome of our ZBR BTZ-resistant cells and due to the necessity of the scientific community for new and innovative tools our objective was to **develop and validate Ubiquitin chain-specific nanobodies,** more specifically **K48 and K63** because mayor changes were described in our model. The objective of using those tools in this project was to **validate previous information** using this new technology, but also to bring more information and **understand VTP response** as was described as promising in mouse xenografts, and other mechanism apart form p62 targeting may underlay the apoptotic response in ZBR cells.

More in detail the objectives of this project are listed:

1. **Identifying enzymes** contributing to BTZ resistance in ZBR cells. Potential candidates to validate from the list obtained in the proteomics analysis performed following the GST-TUBE-MS protocol (previous data from the lab).

2. **Targeting** the degradation or chemical inhibition of those potential candidates to recover BTZ response in resistant cells.

3. **Identifying the mechanisms** in which those enzymes contribute to BTZ-resistant phenotype. Autophagy, proteaphagy or other processes.

4. Developing new molecular tools designed to enrich and analyze the ubiquitome in cells. More specifically **Ubiquitin chain-specific K48 and K63 nanobodies**. This part of the project was developed in collaboration with the company *Hybrigenics.*

5. **Optimizing** and validating these Ubiquitin chain-specific nanobodies to use them in combination with Mass Spectrometry, Western Blotting identification and Immunofluorescence or cell imaging.

6. Identifying other processes **mediating VTP apoptosis** in ZBR BTZ-resistant cells apart form p62 targeting promoting high molecular aggregates.

17. Materials and methods.

The following section details the materials and methodology used for the development of this project.

17.1 Antibodies.

(A)					
Primary antibody	**Company**	**Reference**	**Host**	**Dilution**	**Technique**
Annexin 5	BD science	S1-65874	Mouse	1:1000	FACS
Caspase-3	Cell Signalling	#9662	Rabbit	1:1000	WB
Caspase-9	Cell Signalling	#9502	Rabbit	1:1000	WB
ENO1	Cell Signalling	#3810	Rabbit	1:1000	WB
GAPDH	Cell Signalling	#97166	Mouse	1:1000	WB
Lamin A/C	Abcam	ab108595	Rabbit	1:1000	WB
LC3B	Cell Signalling	#2775	Rabbit	1:1000; 1:200	WB, IF
P53 (DO-1)	SantaCruz	SC-126	Mouse	1:1000; 1:100	WB, IF
PGK1	Cell Signalling	#68540	Rabbit	1:1000	WB
PSMA2 (α2)	Cell signalling	11864	Rabbit	1:200	IF
PSMB2 (β2)	Santa Cruz biotech	sc-515006	Mouse	1:1000, 1:100	WB, IF
PSMB5 (β5)	Cell Signaling	12919	Rabbit	1:1000	WB
PSMD2 (RPN1)	Santa Cruz biotech	sc-271775	Mouse	1:1000; 1:100	WB, IF
PSMD4 (RPN10)	Invitrogen	PA5-30136	Rabbit	1:1000	WB
RLIM	Santa Cruz	SC-101117	Rabbit	1:1000	WB
SQSTM1 (p62)	Santa Cruz biotech	Sc-28359	Mouse	1:1000; 1:100	WB, IF
TRIM24	Invitrogen	PA-34561	Rabbit	1:1000; 1:200	WB, IF
Tubulin	Sigma-Aldrich	T3526	Rabbit	1:1000	WB

Ub K48 (A4.1) Hybribody	Hybrigenics	(Not commercially available yet)	RabbitFc IgG2	1:20	IF
Ub K63 (D1.1) Hybribody	Hybrigenics	(Not commercially available yet)	Mouse Fc IgG2	1:20	IF
Ubiquitin (E4I2J)	Cell Signalling	#43124	Rabbit	1:1000; 1:200	WB, IF
Ubiquitin (P4D1)	Cell Signaling	3936	Mouse	1:1000; 1:100	WB, IF
UBR2	Invitrogen	PA5-37161	Rabbit	1:1000	WB
UBR4	Novus	NBP1-28730	Rabbit	1:1000	WB
UBR5	Cell Signalling	#65344	Rabbit	1:1000	WB
UBXN1	ThermoFisher	**#** A303-416A	Rabbit	1:1000	WB
β-actin	Abgent	AM1829B-EV	Mouse	1:1000	WB
Vinculin	Cell Signalling	#13901	Rabbit	1:1000	WB
(B)					
Donkey anti-Mouse IgG (H+L) Cross-Adsorbed Secondary Antibody, Alexa Fluor 568	Invitrogen	A10037	Donkey/Rabbit	1:200; 1/500	IF
Donkey anti-Mouse IgG (H+L) Highly Cross-Adsorbed Secondary Antibody, Alexa Fluor Plus 488	Invitrogen	A32766	Donkey/Mouse	1:200; 1:500	IF
Donkey anti-Rabbit IgG (H+L) Cross-Adsorbed Secondary Antibody,	Invitrogen	A-11011	Donkey/Rabbit	1:200; 1/500	IF

Alexa Fluor 568					
Donkey anti-Rabbit IgG (H+L) Cross-Adsorbed Secondary Antibody, Alexa Fluor 488	Invitrogen	A32790	Donkey/Rabbit	1:200; 1:500	IF
Peroxidase Goat Anti-Rabbit IgG (H+L)	Jackson Immuno research	711-035-045	Goat/Rabbit	1:5 000	WB
Peroxidase Rabbit Anti-Mouse IgG (H+L)	Jackson Immuno research	315-035-003	Rabbit/Mouse	1:5 000	WB

Table 1: List of primary (A) and secondary (B) antibodies.

17.2 Cell lines, plasmids, and bacteria strains.

The following tables detail Mantle Cell Lymphoma cell lines, plasmids, and bacteria strains to produce recombinant proteins (molecular traps) used in this study.

MCL cell lines	Phenotype	Source
Z-138	BTZ-sensitive, WT-p53, WT-ATM	Collaboration. Fully characterized in (Beà et al., 2013; Roué et al., 2011).
ZBR	BTZ acquired resistant, WT-p53, WT-ATM	Collaboration. Fully characterized in (Beà et al., 2013; Roué et al., 2011).
HeLa	ATCC	Collaboration with Dr J.D Sutherland.
JeKo-1	BTZ-sensitive, p53 mutant, WT-ATM	Collaboration. Fully characterized in (Beà et al., 2013; Roué et al., 2011).
JBR	BTZ acquired resistant, p53 mutant, WT-ATM	Collaboration. Fully characterized in (Beà et al., 2013; Roué et al., 2011).

Table 2: List of cell lines.

Bacteria strains	Genotype	Source
Escherichia coli WK6	F' lacIq delta(lacZ)M15 proA+B+ delta(lac-proAB) galE rpsL	This Project: Nanobodies production and purification
Escherichia coli C41- DE3	F – ompT hsdSB (rB- mB-) gal dcm (DE3)	This Project: bioTUBES and GST-*BirA* production and purification

Table 3: List of bacteria strains.

Plasmids	Features	Source
pHEN2- (for K48: A4-1, C5-2, C7-2, E11-2, F5-2, F11-2, F12-1, G1-1, G9-2. H1-2)- (for K63: F10-1, F2-1, E5-1, D10-1, D1-1. B2-1, B4-1, C2-1, C4-1).	Nanobodies K48 and K63 Name of the clones used for each nanobody Sequence protected by MTA	Hybrigenics services
BioTUBERad23 and p62	Sequence from the host lab (no available).	This project. No results for publication (not fully optimized).

Table 4: List of plasmids.

17.3 Reagents and materials.

Reagents and drugs used for protein characterization and Mass Spectrometry analysis are listed here below.

Reagent	Company and reference	Used in
30% Acrylamide/Bis Solution	BioRas #1610156	WB (Gel production)
Amicon Ultra Centrifugal Filters 3 KDa MWCO	Milipore (UFC5003)	Protein purification protocol
Annexin Buffer	BD pharmingen (556454)	FACS
ATP (Adenosine 5'-triphosphate (ATP) disodium salt hydrate)	Sigma-Aldrich A1852	Biotinylation in vitro
Benzamidine	Sigma-Aldrich 12072	bioTUBEs purification
Biotin	Sigma-Aldrich B4501	Biotinylation in vitro

Bradford Solution	BioRad (23236)	Protein quantification
BS3 (bis(sulfosuccinimidyl)suberate) (Thermofisher 21586)	Thermo Fisher (21586)	Crosslinking strategies
Complete protease inhibitor cocktail (Mini, EDTA-free Protease Inhibitor Cocktail)	Roche, (04693159001)	Capture protocols
DAPI	Invitrogen (P36931)	Immunofluorescence (IF)
Dialysis sacks. MWCO 12,000 Da	Sigma-Aldrich (D6191)	Protein purification protocol
Dialysis tubing, benzoylated	Sigma (D7884-10FT)	Dialysis (Nanobodies and bioTUBEs).
dimethyl pimelimidate dihydrochloride (DMP)	Sigma-Aldrich (D8388)	Crosslinking protocols
DTT (1,4-Dithiothreito)	Sigma-Aldrich (3483-12-3)	Protein production and purification protocol
Dulbecco's Modified Eagle Medium (DNEM)	Thermo Fisher (11965084)	Cell culture
FBS (Fetal bovine serum)	Thermo Fisher	Cell culture
FITC Annexin V	BD pharmingen (556420)	FACS
Glass slides	Immunocell (61.100.58)	Immunofluorescence (IF)
Glutathion agarose beads. Glutathione Sepharose® 4B	Sigma-Aldrich (GE17-0756-01)	GST-BirA purification.
IAA (Iodoacetamide)	Sigma Aldrich (I1149)	Capture protocols
IGEPAL	Sigma (I3021)	Detergent for binding and lysis steps
Immobilon-P PVDF transfer membrane	Merck (IPVH00010)	WB
IPTG (Isopropyl β-D-1-thiogalactopyranoside)	Sigma-Aldrich (I6758)	Protein production and purification protocol
LB Broth (Lennox) Media	Sigma-Aldrich (L3022)	Bacteria culture
NEM (N-ethylmaleimide)	Thermo Fisher (23030)	Capture protocols
NE-PER™ Nuclear and Cytoplasmic Extraction Reagents	Thermo Fisher (78833)	Nuclear/cytoplasmic extraction
Ni-NTA Agarose Beads (High Density Nickel)	ABT Technologies (6BCL-QHNi-X)	Protein purification protocol
Ni-NTA Magnetic Agarose Beads	Quiagen (36113)	Nanobodies capture

PBS 1X	Thermo Fisher (10010015)	Cell culture
Poly-L-lysine	Sigma (P8920)	Immunofluorescence (IF)
Polymyxin B	Fluka (81334)	Protein purification protocol
Protein A magnetic beads	Thermo Fisher (88845)	In vitro immunoprecipitation
RPMI 1640 Medium	Thermo Fisher (12633012)	Cell culture
Silver staining kit	Thermo Fisher (10404005)	Silver staining for MS (Background in the negative control)
Strep Magnetic Beads. True Blot@Rockland	Tebubio (S000-18-2)	BioTUBE captures protocol
Super signal west Femto (West Femto ECL)	Thermo Fisher (34096)	WB
TEMED (tetramethylethylenediamine)	BioRad #1610801	WB (Gel polymerization)
Terrific Broth Media	Supelco (T0918)	Bacteria culture
Triton-100X	Sigma-Aldrich (T8787)	Capture protocols.
Ubiquitin commercial chains K48 and K63	Boston Biochem (UC220, UC320)	In vitro immunoprecipitation

Table 5: List of chemicals

Drug	Company	Reference	Stock concentration	Vehicle
Bafilomycin-A1 (BafA)	InvivoGen	tlrl-baf1	100 µM, 1mM.	DMSO
Bortezomib (BTZ)	Sigma Aldrich	CAS 179324-69-7	1 mM	DMSO
dTRIM24 (PROTAC)	MedChem	HY-111519	1mM	DMSO
Luperox@TBH70X (tert-Butyl hydroperoxide)	Sigma Aldrich	458139-100ml	7.3M	Water
NAC (N-Acetyl-L-cysteine)	Sigma Aldrich	A9165-25G	10mM	Water
Verteporfin (VTP)	Sigma Aldrich	129497-78-5	2 mM	DMSO
ZZ p62 inhibitor/XRK3F2	MedChem	HY-112904	10mM	DMSO

Table 6: List of drugs.

17.4 Cell culture.

Cells were cultured in Gibco Roswell Park Memorial Institute (RPMI) 1640 Medium with 2 mM L-glutamine, 100 Units/mL penicillin, 100 µg/mL streptomycin and 10% fetal bovine serum (FBS), previously decomplemented (heated 30min at 56ºC). Cells were incubated at 37°C and 5% CO2 conditions, and passed at 0.3-0.5 million cells/mL, three times a week (Monday, Wednesday, and Friday).

To avoid loss of BTZ resistance in the acquired resistant phenotype, ZBR cultures were treated after the defrost of a new vial with 0,5-1nM of BTZ for 1-2 weeks and checked viability by Flow cytometry (FACS). This protocol was implemented and improved in this project to ensure the phenotype of the cells used in the different experiments and was performed periodically in the lab to ensure the reproducibility of the experiments.

HeLa cells were cultured at 37 °C and 5% CO2 in Dulbecco's modified Eagle Medium (DMEM) supplemented with 10% fetal bovine serum (FBS) and 1% penicillin/streptomycin.

17.5 Western Blotting.

Mammalian cell extracts were lysed by resolving and intense heating (95ºC and shacking) in 1.5X Boiling Buffer (4% SDS, 20% glycerol, 120 mM Tris-HCl pH 6.8). Cell lysate were loaded in 8%–15% acrylamide gels, depending on the size of the protein to analyze and characterize.

Proteins were separated electrophoretically at 80V during 30min in Laemmli Buffer for SDS PAGE (25mM Tris, 192mM Glycine, 0.1% SDS, pH 8.6), then at 120V 1-2h until the migration front (blue front) reached the bottom of the gel, disappearing.
Protein wet-transfers were performed to PVDF membrane (0.45µm pore size, Immobilon-P, Merck) in buffer containing 20% ethanol and 80% 1x transfer buffer (transfer buffer 10x: 240mM Tris, 2M Glycine), either for 1.5h (335mA per two gels at 4°C) or overnight (65mA per two gels, 4°C). Membranes were blocked for 1h in 5% milk, diluted in 1x Tris-buffered saline (TBS).

Membranes were incubated with specific primary antibodies (diluted in TBS 1x) overnight at 4°C. Secondary antibodies were added for 1h at room temperature (RT) in 2,5% milk or in TBS only. Membranes were washed 5 times, 10min with TBS after incubation with primary and secondary antibodies. Pictures were acquired using West Femto ECL (34096 Thermofischer) and/or Clarity Western (ECL Substrate, #1705061) with PXI4 (Syngene), GeneTools (Syngene), Odyssey Fc (LICOR), ChemiDoc Imaging System (BioRad), or Invitrogen iBright Imaging System. Quantification was performed using ImageJ, a specific statistic software.

17.6 Immunofluorescence microscopy.

Immunofluorescence of Z-138 and ZBR cell lines was performed following the following protocol. Glass slides (61.100.58 Immunocell) were incubated 1h at RT with poly-L-lysine (Sigma), then incubated with cells resuspended in 1XPBS (1 million cells/mL). Fixation was

performed with 4% PFA, 10min, and permeabilization in cold methanol 100% for 5min. Samples were then incubated in blocking solution (10% BSA, 0.1% Triton 100X in 1X PBS) 1h at RT. Primary antibodies were incubated overnight, and secondary (1/500) antibodies 30min, at RT in 5% BSA blocking solution. Primary and secondary antibodies used are indicated in methodology section 17.1. Nuclei were stained using DAPI (P36931, Invitrogen).

Immunofluorescence of HeLa cells was performed on 11mm coverslip (25000 cells per well: 24 well plate). Cells were fixed in 4% PFA for 10-15min, wash with PBS 1X, permeabilized in 100% cold methanol for 3min, and washed with 0,1% TX-100 in 1XPBS.

Coverslips were washed 3 times with 1X PBS. Blocking was performed for 30min at RT in Blocking Buffer (2%FBS, 1% of BSA and 1X PBS). Primary antibodies were incubated 1h at 37ºC, or 2h at RT. Secondary antibodies (1:200) were incubated 30min at 37ºC, or 1h at RT, followed by a nuclear staining with DAPI (P36931, Invitrogen). Primary and secondary antibodies are used in section 17.1.

Images were acquired using the Axio Imager D1 Zeiss Microscope (40x, and 63X), or super-resolution microscopy Leica SP8 Lightning and Zeiss LSM 880 Fast Airyscan and assembled with Adobe Photoshop 7.0. Proper controls for each experiment have been performed to discern overlapping of channels and background provided by the secondary antibody (images not shown). Images were not modified other than adjustments of levels, brightness, and magnification.

17.7 Flow Cytometry, apoptosis assay. Fluorescence-activated single cell sorting (FACS).

To measure cell death under different treatments/conditions, or calculate the IC50 of new drugs compounds, we have performed an apoptosis assay using Annexin 5 on a fluorescence-activated cell sorter (FACS) analysis.

One mL of media culture at 4.10^5 cells per mL density was plated in a 24-wells plate. The day after, cells were treated with the indicated drug, time and concentration. After testing the different treatments, cells were pelleted by centrifugation at 125 g for 3-5min and washed with 1mL PBS to remove any media left that could affect the measurement in the flow cytometer.Pellets were re-suspended and stained 5-10min with 100-200 µL 1X Annexin Buffer (556454, BD pharmingen) with 1:100 FITC Annexin V (556420, BD Pharmingen) at RT and covered to avoid light.

BD Accuri C6(BD Bioscience-US), and Cytometre BD Fortessa were used to analyze samples. 10.000 events were collected for each experiment. Forward versus side-scatter gating were used to identify cells of interest. H and W parameters were used to exclude possible droplets. Apoptotic cells stained with FITC were identified on a side-scatter-area versus FSC-A (P4) scatter.

17.8 Molecular trap production.

Bacteria were used to produce the different recombinant proteins/molecular traps used in this project (bioTUBES and nanobodies). *E.Coli* C41-DE3 and WK6 chimiocompetent strains were respectively used for the production of bioTUBEs and nanobodies.

After a rudimentary chemical transformation with specific plasmids to introduce into the bacteria strains (heat shock in a water bath at 42°C during 2min), clones properly transformed were grown upon antibiotic (*Ampicillin*) selection overnight. The day after, the colonies were further expanded in an increasing volume of LB (bioTUBE) or TB media (nanobodies). The confluence of the culture was measured at different times until they reached a confluence of 0.8 O.D (Optical Density) measured at 600nm. Under those conditions, we determined the culture to be in the best conditions to promote the expression of the proteins of interest.

Protein production was induced using 1mM IPTG (Isopropyl β-D-1-thiogalactopyranoside) for 16/overnight at 28°C. Bacteria were pelleted at 6000 gs for 20min at 4°C (Centrifuge Beckman Coulter), washed with 10 ml of PBS1X , and lysed with sonication, to promote the liberation/availability of the exogenous proteins expressed. Proteins of interest were purified using different columns/resins depending on the tag attached to the protein for this purpose. Not induced and induced samples were recollected to verify the proper induction using IPTG by Coomassie staining. Beads were washed several times before a final elution, and dialysis with a buffer exchange to remove uninteresting/targeted proteins (non-specific fraction bound to the proteins). Final concentration obtained was measured, using Nanodrop at 280 nm absorbance. Aliquots were supplemented with 10% glycerol to store at -80°C and avoid any damage to the proteins to use in the different experiments developed in this project.

Differences in the protocols used for the bioTUBES and nanobodies production were optimized (as the different proteins have different properties, solubility, and saturation limits) in this project to obtain the best material to use in our captures and different assays. These specific conditions are indicated in the following sections.

17.8.1 bioTUBEs purification protocol.

After the induction, each bacteria pellet (50ml) was re-suspended in 10 ml of Lysis Buffer (20 ml PBS 0.5 mM NaCl, 2 mM Benzamide and 1 mM PMSF).

The sonication was made 6 times/cycles of 30sec on, 10sec off (amplitude of 30%, using 10µm probe) to obtain a clear and fainter solution. We added 1% of Triton and mixed it well until full homogeneity (20min rotating at 4°C°). We centrifugated the samples at 20.000 RPM for 1h at 4°C and kept the supernatant (Input fraction). The supernatant fraction was then subjected to glutathione or streptavidin agarose affinity purification beads (GST or bio version of the traps) (supplemented with 1mM of DTT Sigma), both rotating overnight at 4°C. The beads were loaded in a column and washed 4-8 times with 5-10 mL of (PBS 1X; 0.8mM NaCl; Triton 1%). Flow through (FT) and washed samples were kept to further

analysis. Proteins of interest were then eluted (10 times) with 1 mL (50mM Tris pH9.5; 0.8M NaCl; 0.05% Triton and 10mM of reduced glutathione) until the elution fraction did not contain proteins detectable by Bradford Solution.

A buffer exchange was performed by dialysis ON at 4°C in 5L of (PBS 1X ; 0.8M NaCl; 0.05% Triton), using a 12kDa tubing, and further concentrated using Amicon Ultra 3 KDa MWCO (Millipore). Protein concentrations were measured by Nanodrop, and protein expressions and purification steps were controlled by Blue Coomassie. For the bio version of those TUBEs, the solubility was reduced to 5mg/ml, and for the bioTUBEp62 we could not work with more than a 1mg/ml concentration to avoid their precipitation.

17.8.2 Nanobodies purification protocol.

E. coli WK6 chimiocompetent bacteria were used to produce the different clones of Ub chain-specific nanobodies.

After a rudimentary chemical transformation with the specific plasmids to introduce into the bacteria (heat shock in a water bath at 42°C during 2min), clones properly transformed were grown upon antibiotic (*Ampicillin*) selection overnight. The day after, colonies were further expanded in an increasing volume of TB media (supplemented with 1% of glucose). The confluence of the culture was measured at different times until they reached a confluence of 0.8 O.D (Optical Density) measured at 600nm. Under those conditions, we determined the culture to be in the best conditions to promote the expression of the proteins of interest.

Protein production was induced using 2mM IPTG (Isopropyl β-D-1-thiogalactopyranoside) for 16h or overnight at 28°C. Bacteria were pelleted at 6000 gs for 20 mins at 4°C (Centrifuge Beckman Coulter), washed with 10 ml of PBS1X , and lysed (Lysis Buffer-10 mM Imidazole, 1 mg/mL of Polymyxin B, PMSF 1Mm, Lysozyme Cf 1.2mg/ml, DTT 2Mm in 1X PBS) with sonication, to promote the liberation/availability of the exogenous proteins expressed. The clarified supernatant after centrifugation was incubated with Ni-NTA agarose-beads, overnight, rotating at 4°C. Not induced and induced samples were recollected to verify the proper induction using IPTG by Coomassie staining.

Beads were washed several times before a final elution, 10 times with 10ml of Washing Buffer (50mM Tris pH8, 500mM NaCl, 10mM Imidazole). The elution was made (10x) with 1ml of Elution Buffer (50mM Tris pH8,500mM NaCl,200mM Imidazole,10 mM DTT). Dialysis with a buffer exchange was made to remove uninteresting/targeted proteins (non-specific fraction bound to the proteins), and then the final concentration obtained was measured using Nanodrop at 280 nm absorbance. The buffer exchange for the dialysis overnight was made with 50mM Tris pH8 and 500mM NaCl.

Proteins were concentrated at 1-5 mg/ml, and aliquots were supplemented with 10% glycerol to store at -80°C and avoid any damage to the proteins to use in the different experiments developed in this project.

17.9 *In vitro* immunoprecipitation.

In vitro immunoprecipitation (IP), using Ub commercial chains (K63 and K48), was used to test the specificity and affinity of the different nanobody clones provided by the company *Hybrigenics*.

Protein A magnetic beads (Thermofisher 88845) were crosslinked to anti-Myc antibody hybridomas (clone 9E10) following the dimethyl pimelimidate dihydrochloride (DMP) (Sigma-Aldrich D8388) protocol. Beads were washed twice with 1X PBS, and once with Binding Buffer (50mM Tris pH8.5, 150mM NaCl, +0.5% Igepal (Sigma I3021). 1ml of hybridomas supernatant was incubated per 100ul of magnetic beads, (per sample point) for 2h rotating at 4°C. When using magnetic beads, a magnetic holder is used for removing non-coupled proteins instead of centrifugation.

Beads were washed twice with 1ml of 1X PBS, and twice with 500ul of Coupling Buffer (200mM borate, 3M NaCl, final pH 9). 500ul of 50mM of DMP prepared in Coupling Buffer was used to incubate the beads for 10min rotating, at room temperature (RT), and then 30min with fresh DMP. Beads were washed twice with 1ml Coupling Buffer, and active groups were blocked with 1ml of 200mM ethanolamine pH8.2 incubation for 1h rotating. Beads were washed twice with 1ml of 1X PBS, and then incubated 3min in 1ml of 1M NaCl made in Binding Buffer to remove non-coupled proteins. This step was repeated twice under rotation conditions. After that step, beads were washed twice in 1ml of 1X PBS, and then incubated 3min in 200mM Glycine pH2.5. This step was performed three times. To block unspecific sites, beads were incubated with 500ul of BSA 1% in Binding Buffer for 1h. Three washes with 1ml of Binding Buffer were performed to equilibrate the beads.

Chain specific nanobodies were incubated with Ubiquitin commercial chains: poly K48 chains (Boston Biochem, UC 320), and poly K63 chains (Boston Biochem UC220). 50ul fraction was taken for the input control sample. After that step, we added the crosslinked magnetic beads, and incubated 1h at 4°C, while rotating.

After that incubation, a 50ul fraction was taken for Flow through (FT) control sample. Beads were washed 5 times with 1ml of Binding buffer, 0.05% Tween-20. Dry beads were re-suspended in 50ul of Boiling Buffer (4% SDS, 20% glycerol, 120 mM Tris-HCl pH 6.8) and boiled 15min at 95°C (capture fraction). Polyacrylamide gels were tested for all fractions using the P4D1 Anti-Ub antibody.

17.10 bioTUBE capture protocol.

Previously to the capture using mammalian cells, a GST-*BirA* purification and *in-vitro* biotinylation steps must be performed and are described in the following section.

The bacteria strain C41-DE3 was transformed using the plasmid for the induction of GST-*BirA* tagged protein. After that, a bacteria culture was grown in 500ml of LB medium with Ampicillin 20ug/ml at 37ºC to reach the optimal density (OD 600nm) of 0,6. Then the expression of GST-*BirA* was induced by the addition of 1Mm IPTG for 3h. Bacteria culture (50ml) was centrifuged at 6693g 30min at 4ºC, and pellets were washed with 25ml of PBS1X,

to freeze, store and be aliquoted, at -20ºC. Each pellet was re-suspended in 1ml of cold PBS 1X, supplemented with 2mM Benzamidine, and sonicated at 30% amplitude with 6 pulses of 10s. After the sonication, lysates Triton was added to a final concentration of 1% to maintain in rotation for 30min.

After that step, samples were centrifuged 2h, at 13.000rpm, and the clarified supernatant was incubated overnight at 4ºC with 200ul of Glutathione agarose beads supplemented with DTT 0.1M. Beads were loaded into a column and washed five times with 10ml of cold PBS1X supplemented with Triton 1%. GST beads, attached to our GST-*BirA*, were stored in PBS 1X and Glycerol 10% at -20ºC, to use the same batch purified in all our experiments and setting conditions steps performed with the bioTUBERad23/p62. GST-BirA protein concentration was measured using the BSA standard calibration curve method. Different BSA aliquots, from 0,5 ug/ul, to 15ug/ul concentration was measured using 1ml of Bradford solution, to measure the absorbance at 600 nm. With the data obtained, a standard curve was plotted, and the concentration of our GST-*BirA* was calculated, by measuring the absorbance in 1ml of Bradford solution (data not shown).

In-vitro biotinylation reaction was set for 5h in rotation, at RT using 5mM ATP, 0.5mM Biotin, 400ug of Bio-TUBE, and 40ul of GST-*BirA*. Samples were spinned down 1000rpm for 5min, to remove GST-*BirA*, and the supernatant was incubated for dialysis into benzoylated tubing and incubated overnight against 5L of PBS1X at 4ºC.

After that a DMP crosslinking protocol (see *in-vitro* immunoprecipitation section) was performed using 100ul of TrueBlot@Rockland streptavidin magnetic beads and 400ug of bio-TUBE trap. The rudimentary protocol (see in *in-vitro* immunoprecipitation section) was changed, and Glycine washes were not necessary as this step is specifically for antibodies assays.

Samples (40 million cells pellets) were re-suspended in 500ul of Lysis Buffer (See nanobodies capture section) on ice for 10min. Samples were centrifuged at 13000 rpm for 10min (4°C), and the supernatant was incubated with the crosslinked beads, rotating at 4°C for 2h. 50ul fraction of this supernatant was taken for the Input sample and after the incubation, 50ul for the FT sample. Beads were washed 3 times with 1mL of PBS Tween 0.05%, and once with 1ml of 1X PBS. Dry beads were re-suspended in 100ul of Boiling Buffer (4% SDS, 20% glycerol, 120 mM Tris-HCl pH 6.8), and heated 45min 95°C with strong agitation to separate the proteins using the magnetic holder. Samples were tested using a polyacrylamide gel and using anti-Ub antibodies in WB. The captured fraction was analyzed by silver staining or blue Coomassie.

Different commercial streptavidin magnetics beads were tested in this project. However, due to inherent background, none of them were selected to further optimize for MS Analysis.

17.11 Nanobodies capture protocol.

In this project, different capture protocols have been implemented in order to use Ub molecular traps to analyze the ubiquitome of our biological model, ZBR and Z138 MCL cell

lines. Different crosslinking strategies have been tested, as well as different binding times. This optimized protocol can be used for an analysis using other cell lines and/or biological models.

40 million cells were used in each condition along with 250ug of each nanobody (K48 and K63). Previously to the binding step using mammalian cell lines, a BS3 (bis(sulfosuccinimidyl)suberate) (Thermofisher 21586) crosslinking protocol was perform using Ni-NTA Magnetic Agarose Beads (Quiagen, 36113). 640ul of dry beads were used per sample point. Those were incubated with 250ug of chain-specific nanobodies in 500 µl of Binding Buffer (50mM Tris pH8.5, 150mM NaCl, +0.5% Igepal) rotating 1-2h at. 4ºC. The non-binding fraction was removed, and beads were washed twice with 1ml of 1X PBS. Beads were incubated with 1ml of 5mM BS3 at RT for 1h. After that, beads were washed with 1ml of 1X PBS and then incubated with 500ul of Blocking Buffer (1.5 M Tris, pH 7.5) at RT for 15min. Beads were washed with 1ml of 1X PBS, and then washed with 500 µl of 0.5M K2HPO4. Beads were washed three times with 1ml 1XPBS, and then with Binding Buffer to equilibrate them.

Cells were lysed in 500ul (each cell pellet of 40Million cells) of Lysis Buffer [(50mM sodium fluoride, 5 mM tetra-sodium pyrophosphate, 10 mM β-glyceropyrophosphate, 1% Igepal, 2 mM EDTA, 20 mM NaH2PO4, 1mM Pefablock, 1.2 mg/mL, a complete protease inhibitor cocktail (Mini, EDTA-free Protease Inhibitor Cocktail-Roche, 04693159001), 10µM PMSF, 10Mm NEM (N-ethylmaleimide, Thermo Scientific 23030) and 10mM IAA (Iodoacetamide, Sigma Aldrich I1149)] on ice for 10min. Tubes were centrifuged at 13000 rpm for 10min (4°C), and the supernatant was incubated with the crosslinked beads, rotating at 4°C for 2h. 50ul fraction of this supernatant were taken for the Input sample. After that, 50ul of non-binding fraction was taken for the FT sample. Beads were washed 4 times with 1mL of PBS Tween 0.05%, and one time with 1ml of 1X PBS. Beads were re-suspended in 100ul of Boiling Buffer (4% SDS, 20% glycerol, 120 mM Tris-HCl pH 6.8), and heated 45min 95°C with strong agitation to separate the proteins of interest from the beads using the magnetic holder. Samples were tested using a polyacrylamide gel and using anti-Ub antibodies in WB, and the capture fraction was analyzed by silver staining or blue Coomassie.

For WB validation of substrates identified using the crosslinking protocol and the magnetic beads, we have optimized the previous protocol but added some modifications: an overnight binding without BS3 crosslinking step and an increased stringency by adding more salt in the binding and washing steps. Specific modifications are indicated below.

Ub chain-specific nanobodies were pre-incubated with (precleared) Ni-NTA agarose-beads for 1h rotating at 4ºC. Centrifugation steps (for washing the beads) are made at 1200rpm, 3-5min.

Binding step was made at 4ºC using the binding buffer previously mentioned but adding 200mM of NaCl. rotating overnight (O/N). Washing steps were made as follow: 3 washes PBS1X-Tween 0,1% 300mM NaCl, 2 washes PBS 1X-Tween 0,05%, and 2 washes PBS 1X.

17.12 Nuclear cytoplasmic extraction protocol.

The Thermo Scientific™ NE-PER™ Nuclear and Cytoplasmic Extraction Protocol was followed for the separation of cytoplasmic and nuclear extracts from mammalian cultured cells (Z138 and ZBR).

Cells were pelleted after 3 washes with PBS 1X. 8-10 × 10^6 cells was pelleted by centrifugation at 500 × g for 2-3 minutes. CERI (reagent from the commercial kit) was added (200ul), and pellets were vortexed vigorously for 15sec to fully re-suspend the cells. Then it was incubated on ice for 10min. CER II (11 ul) was added to the tubes, vortexed and incubated on ice for 1min. Tubes were centrifuged for 5min at maximum speed in a microcentrifuge (~16,000 × g). Supernatant was kept as the cytoplasmic extract (mixed with Boiling Buffer for WB testing). Pellets were re-suspended (insoluble fraction, nucleus) in cold NER (50ul). Samples were on ice and continued vortexing for 15sec every 10min, for a total of 40min. Tubes were centrifuged at maximum speed (~16,000 × g) for 10min. The supernatant (nuclear extract) was kept, mixed with BB and/or stored at -80°C until use.

17.13 Ubiquitin-chain specific nanobody Mass Spectrometry.

17.13.1 Peptide sample preparation.

Captured proteins were loaded into ultra-centrifugal filters with 30 kDa cut off and spin 25 min at 14 000 *xg*. Proteins in the retentate are washed with 0.2 mL of 0.1M HEPES, 8M Urea, pH 8.0, six times by spinning 25 min at 14 000 *xg*. Proteins in the retentate are incubated with 0.1 mL of 0.05 M iodoacetamide for 20 min. Proteins in the retentate are spun 35 min at 14 000 *xg*. Proteins in the retentate are washed with 0.1 mL of 0.1M HEPES, 8M Urea, pH 8.0, four times by spinning 25 min at 14 000 *xg*. Proteins in the retentate are washed with 0.1 mL of 0.04M ammonium bicarbonate, pH 8.0, four times by spinning 25 min at 14 000 *x g*. Proteins in the retentate are incubated with 40 µL 0.01 ug/uL of trypsin overnight at 37°C. Digested proteins are collected by adding 40 µL of 0.04M ammonium bicarbonate, pH 8.0, two times by spinning 25 min at 14 000 *xg*. Peptides are desalted using reverse phase C18 and then stored at -20 °C, before MS analysis.

17.13.2 Nano-LC-MSMS analysis.

Peptide samples were analysed by nano-LC-MSMS (Dionex RSLCnano 3000) coupled to a Q-Exactive Orbitrap mass spectrometer (Thermo Scientific). Briefly, the samples (5 µL) were loaded onto a custom made fused capillary pre-column (2 cm length, 360 µm OD, 75 µm ID) with a flow of 5 µL per minutes for 7 minutes. Trapped peptides were separated on a custom made fused capillary column (20 cm length, 360 µm outer diameter, 75 µm inner diameter) packed with ReproSil Pur C18 3-µm resin (Dr. Maish, Ammerbuch-Entringen, Germany) with a flow of 300 nL per minute using a linear gradient from 92 % A (0.1% formic acid) to 28 % B (0,1% formic acid in 100 acetonitrile) over 93 min followed by a linear gradient from 28 % B to 35 % B over 20 min at a flowrate of 300 nl per minute.

Mass spectra were acquired in positive ion mode applying automatic data-dependent switch between one Orbitrap survey MS scan in the mass range of 400 to 1200 m/z followed by

HCD fragmentation and Orbitrap detection of the 15 most intense ions observed in the MS scan. Target value in the Orbitrap for MS scan was 1,000,000 ions at a resolution of 70,000 at m/z 200. Fragmentation in the HCD cell was performed at normalized collision energy of 31 eV. Ion selection threshold was set to 25,000 counts and maximum injection time was 100 ms for MS scans and 300 and 500 ms for MSMS scans. Selected sequenced ions were dynamically excluded for 45 seconds.

17.13.3 Database dependent search.

Mass accuracy was set to 5 ppm on the peptide level and 10 Da on the fragment ions. A maximum of four missed cleavages was used. Carbamidomethyl (C) was set as a fixed modification. Selected variable modifications included methionine oxidation, N-terminal protein acetylation, di-glycine tagged lysine, and LRGG tagged lysine. The MSMS data was searched against all proteins in UniProt (3AUP000005640) with concatenation of all the sequences in reverse maintaining only lysine and arginine in place. The data was searched and quantified with VEMS (Carvalho et al., 2014).

17.13.4 Quantitative analysis.

The data were analyzed in R statistical programming language. Estimated IBAQ values were subtracted with average of ZBR and Z138 control samples. Negative values were set to zero. The resulting background adjusted quantitative values were preprocessed by three approaches: 1) removing common MS contaminants followed by $\log_2(x + 1)$ transformation, 2) removing common MS contaminants followed by $\log_2(x + 1)$ transformation and quantile normalization, 3) removing common MS contaminants followed by $\log_2(x + 1)$ transformation, quantile normalization and abundance filtering to optimize overall Gaussian distribution of the quantitative values. This led to three quantitative matrices. The $\log_2(x + 1)$ transformed and quantile normalized data were subjected to statistical analysis utilizing R package limma (Smyth, 2004) where contrast between the different conditions were specified. Correction for multiple testing was applied using the method of Benjamini & Hochberg (Benjamini and Hochberg, 1995).

17.13.5 Functional analysis.

Details of how we define functional enrichment based on the hypergeometric probability test have previously been described (Carvalho et al., 2016; Hackenberg and Matthiesen, 2008). Functional enrichment was made by extracting all functional categories for which at least one of the samples showed a significant enrichment based on the hypergeometric probability test followed by multiple corrections of P values by the method of Benjamini & Hochberg (Benjamini and Hochberg, 1995). The analysis was performed for all significantly regulated proteins, significantly up-regulated proteins and significantly down regulated proteins against cellular component (CC), biological process (BP), molecular function (MF) and KEGG pathways.

17.14 Quantification and statistical analysis.

Quantification and statistical analysis were performed using the Image J software and three independent experiments (biological replicates), unless indicated otherwise in the figure legend for some preliminary results. GAPDH/Actin or Vinculin normalization or No treatment sample (NT) Fold change has been used for statistical purposes. Two-Way ANOVA with multiple comparisons or T-tests were applied for comparisons between conditions using the GraphPad software for statistical analysis and visualization. The data are presented as the means ± SD or SEM. The $*p < 0.05$, $**p < 0.01$ or $***p < 0.001$ values were considered as statistically significant. Combination index (CI) was calculated using the Compusyn software.

18. Results.

18.1 Chapter I: Identification and targeting of Ubiquitin enzymes to recover bortezomib sensitiveness: molecular mechanism regulating BTZ resistance.

BTZ is used for the treatment of MM and MCL (Kane et al., 2003; Raedler, 2015). Molecular mechanisms associated with BTZ resistance are still unclear. Different mechanisms have been proposed, including mutations in the β5-subunit (Balsas et al., 2012; Lü and Wang, 2013) and also quite recently dysregulation in proteolytic pathways (Grégoire Quinet et al, 2021; Lü and Wang, 2013).

In the MS analysis reported by Quinet et al, (Grégoire Quinet et al, 2021), differences in the enrichment of Ub E3 enzymes were identified in the BTZ-resistant cell line ZBR in comparison to its sensitive counterpart Z138. In this study, we have investigated the possible contribution of these E3 enzymes to the MCL BTZ-resistant phenotype. The strategy used in this project considered the inhibition/modulation of these enzymes to analyse the impact in Ub chains composition, proteaphagy activation and BTZ resistance. This knowledge should contribute to develope new therapeutic options for patients that do not respond to BTZ.

The ZBR cell line was developed by exposing Z138 cells to BTZ during 5 months (Moros et al., 2014; Roué et al., 2011), providing a good model to study mechanisms underlying BTZ resistance. This pair of cells (BTZ sensitive and resistant) was the main but not the only model used in this research project (see results below). Our strategy included the use of Z138 and ZBR for proteome comparison with the objective to validate proteins/molecules associated to the BTZ-resistant phenotype using different approaches.

18.2 Selection of potential target candidates in whole cell extracts in Z138 and ZBR cell lines.

Data previously obtained by the hosting laboratory highlighted important differences in the proteome identified by TUBE-MS approach between ZBR and Z138 cell lines. The average log ratios of some proteins belonging to the Ub pathway were significantly distinct between cell lines (Z138/ZBR). It was decided to concentrate our efforts in the proteins with the higher enrichment. In figure 19, highly enriched proteins in ZBR cells are indicated in the green scale and red boxes indicate the proteins decided to explore (Figure 19). Among the top-most enriched proteins, we found UBR2, UBR4 and UBR5, the Tripartite motif (TRIM) 24 and RLIM, all E3 Ub ligases. We excluded the analysis of the Ub-protein ligase E3C (UBE3C) as it is difficult to obtain reagents to analyse its function (chemical inhibitors, antibodies). In addition, we selected UBXN1 (UBX domain-containing protein 1) to validate its enrichment in the sensitive cell line Z138 (Figure 19).

In order to validate the enrichment of potential candidates previously identified by TUBE-MS analysis, we analysed by Western blot (WB) the level of enzymes that presented higher differences between ZBR and Z138 cell lines. This step was required to validate protein enrichment previously identified(Figure 19). In this assay, we focused on the identification of

these proteins in whole cell extracts without treatment (basal conditions) but also after BTZ treatment as we were interested in identifying changes in protein stability after blocking this proteolytic pathway.

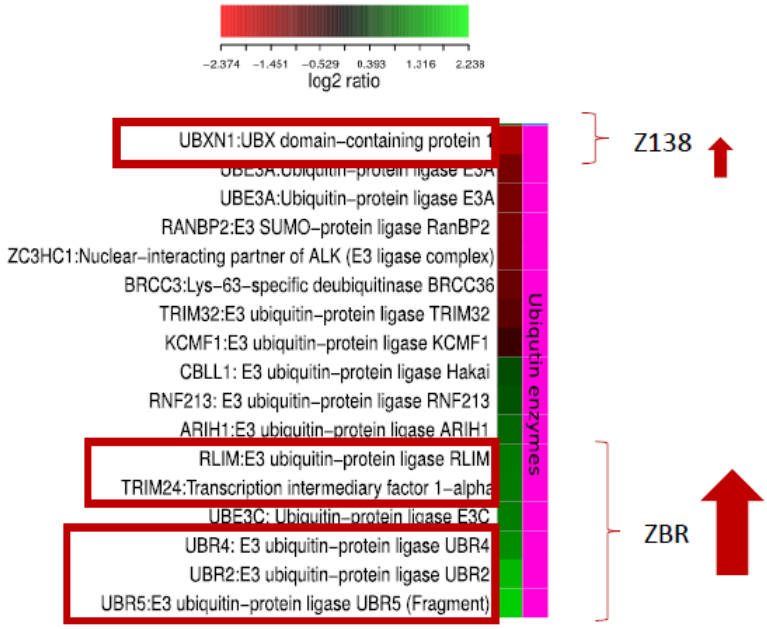

Figure 19: Enriched Ubiquitin enzymes found in the proteome of ZBR cells. Data previously obtained using a GST-TUBE MS analysis (Grégoire Quinet et al, 2021)**.** Heat map representation of enriched Ub enzymes in the BTZ-resistant ZBR cell line compared to the parental Z138 cell line. Red = low enrichment; Green = high enrichment.

UBR enzymes contribute to regulate the N-end rule pathway. In particular, they determine the half-life of proteins containing N-degrons which destabilize the N-terminal residue. The N-end rule pathway is considered to be part of the UPS, as E3 ligases (N-recognins) are in charge of recognising those degrons in the target protein promoting their ubiquitylation and subsequent proteasomal degradation. In this pathway, the UBR domain N-recognins (UBR1/UBR2/UBR4 AND UBR5) recognises Arg/N-terminal modified substrates (Varshavsky, 2011).

There are two different branches inside this pathway: The Ac/N-end rule and the Arg/N-end rule pathway. The Ac/N-end rule pathway targets proteins containing Nt-acetylated, residues, while the Arg/N-end rule pathway involves N-terminal arginylation. More than 80% of human proteins harbour a specific degradation signal termed Ac/N-degrons, that will lead to its Nt-acetylation/arginylation when needed, by the action of different enzymes like methionine-aminopeptidases, caspases, calpains, Nt-acetylases, Nt-amidases, arginyl-transferases, and leucyl-transferases. Therefore, this system can determine the degradation of a great number of proteins inside the cells, mediating physiological functions like: selective elimination of misfolded proteins; DNA repair, fat metabolism, viral and bacterial infection, apoptosis, meiosis, spermatogenesis, neurogenesis and cardiovascular development, among others (Chen et al., 2017; Varshavsky, 2011). Due to those important

functions and their participation to the Ub proteasome system, UBR proteins became interesting to further investigate in this project.

Levels of UBR2, UBR4 and UBR5 proteins were tested in whole cell extracts from ZBR compared to the Z138 cell line (Figure 20). Under basal conditions, they were higher in the ZBR cell line, with UBR2 and UBR4 enrichment showing statistical significance (using two-tailed Student's t-test). In contrast, UBR5 enzyme levels were only slightly higher in ZBR cells. When treated with BTZ, 5nM for 8h, Z138 cells accumulated UBR2, UBR4 and UBR5 indicating that the stability of these enzymes is regulated by proteasomal degradation. However, the level of these enzymes did not increase in ZBR cells treated with BTZ, supporting the notion of a dysregulated UPS/ALS phenotype in ZBR cells, and that UBR proteins could contribute to this phenotype (Grégoire Quinet et al, 2021).

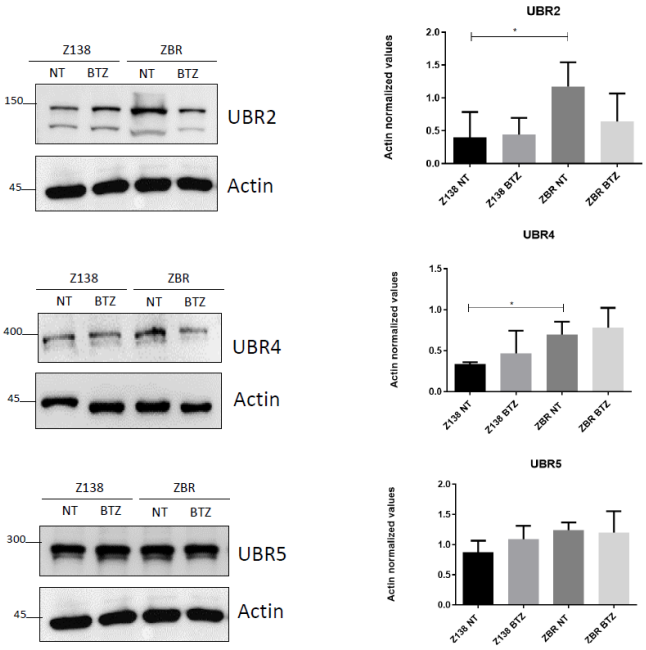

Figure 20: Analysis of UBR proteins level in Z138 and ZBR cells. Z138 and ZBR cell lines (10 million cells per pellet/condition) were treated or not (NT) during 8 hours with a 5nM BTZ treatment (BTZ). Whole cell extracts were analysed by WB with UBR2, UBR4, UBR5 and Actin antibodies. Images quantified with Image J (n≥3; mean ± SEM; two-tailed Student's t-test, *P<0.05, **P<0.01, P***<0.001).

Levels of TRIM24, RLIM and UBXN1 were also investigated (Figure 21). At basal level, TRIM24 was confirmed to be increased in ZBR compared to the Z138 cell line. This difference showed statistical significance using the two-tailed Student's t-test. Interestingly, TRIM24 decreased only in ZBR after BTZ treatment.

In the absence of treatment, the level of the RLIM protein was higher in ZBR BTZ-resistant cells whereas UBXN1 was increased in Z138 sensitive cells (Figure 21), validating the information obtained using the TUBEs-MS methodology. After an 8-hour treatment with BTZ, RLIM was increased while UBXN1 was reduced in ZBR cells.

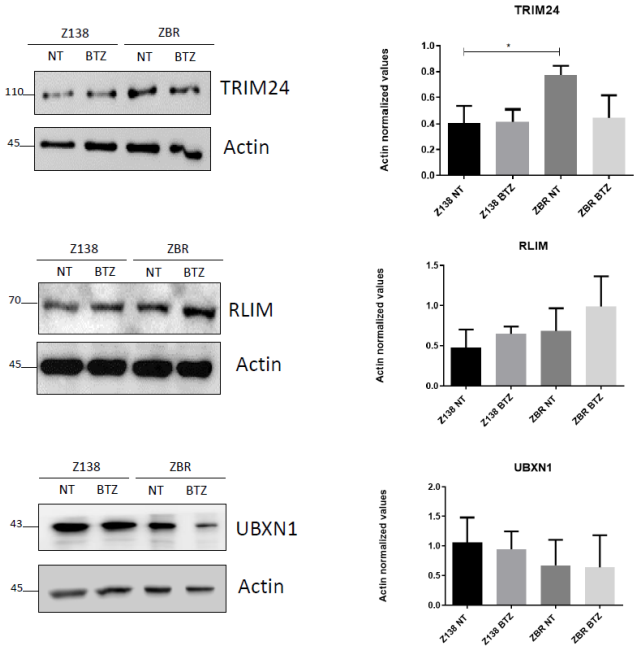

Figure 21: Validation of TRIM24 and other cellular factors enriched in ZBR cells. Z138 and ZBR cell lines were treated or not (NT) during 8 hours with 5nM BTZ treatment (BTZ) (10 million cells per pellet/condition). Whole cell extracts were analysed WB with TRIM24, RLIM, UBXN1 and Actin antibodies. Images quantified with Image J (n≥3; mean ± SEM; two-tailed Student's t-test, *P<0.05, **P<0.01, P***<0.001).

Since autophagy is a mechanism that can be activated when the proteasome system is compromised, it was decided to investigate how the stability, localization, and function of some of the identified proteins was affected in the ZBR cell line after pharmacologic inhibition of these proteolytic pathways.

18.3 TRIM24 stability and localization in Z138 and ZBR cell lines.

The tripartite motif (TRIM) family of E3 ligases is a subfamily of the RING-type E3 Ub ligases, described to be involved in multiple cellular processes such as intracellular signalling, apoptosis, protein quality control, autophagy, and carcinogenesis. Moreover, their dysregulation has been linked to the development of diseases including cancer (Hatakeyama, 2017).

TRIM24, called transcriptional intermediary factor 1α (TIF1 α), is a multidomain protein that has been described to be a co-regulator of transcription, a nuclear histone PTM reader that binds to chromatin via its PHD-bromodomain (Appikonda et al., 2018). TRIM24 also negatively regulates p53 levels by mediating its ubiquitylation (Jain et al., 2014).

Aberrant expression of this protein has been associated with different cancer types, and has been proposed to be a good prognostic cancer usually correlating with increasing proliferation, oncogenic transformation and aggressive malignant phenotypes (Groner et al., 2016; Li et al., 2012, 2012; Liu et al., 2014; Tsai et al., 2010; Zhang et al., 2015).

Due to its role in cancer, we have selected TRIM24 as a good candidate to further characterize in our disease model. In particular, we investigated if TRIM24 could have a role in autophagy impacting proteaphagy, a mechanism recently found to contribute to develop BTZ resistance in MCL cells (Grégoire Quinet et al, 2021).

We performed immunofluorescence (IF) and WB analysis in HeLa cells treated or not with proteasome or autophagy inhibitors to investigate the TRIM24 localization in a cell line distinct from MCL (Figure 22). TRIM24 levels were highly increased after autophagy blockade (Figure 22, A) and its localization was mainly in the nucleus, most likely associated to its nuclear functions (Jain et al., 2014).

When treated with BTZ or BafA, the accumulation of small TRIM24 puncta appears mainly in the nucleus but also in the cytoplasm. With the combined BTZ/BafA treatment, TRIM24 staining was similar to the one observed with BTZ. p62 staining is increased after BafA treatment, highlighting its correct accumulation in the cytoplasm. However, TRIM24 did not colocalize with p62 under the different conditions tested (Figure 22, B).

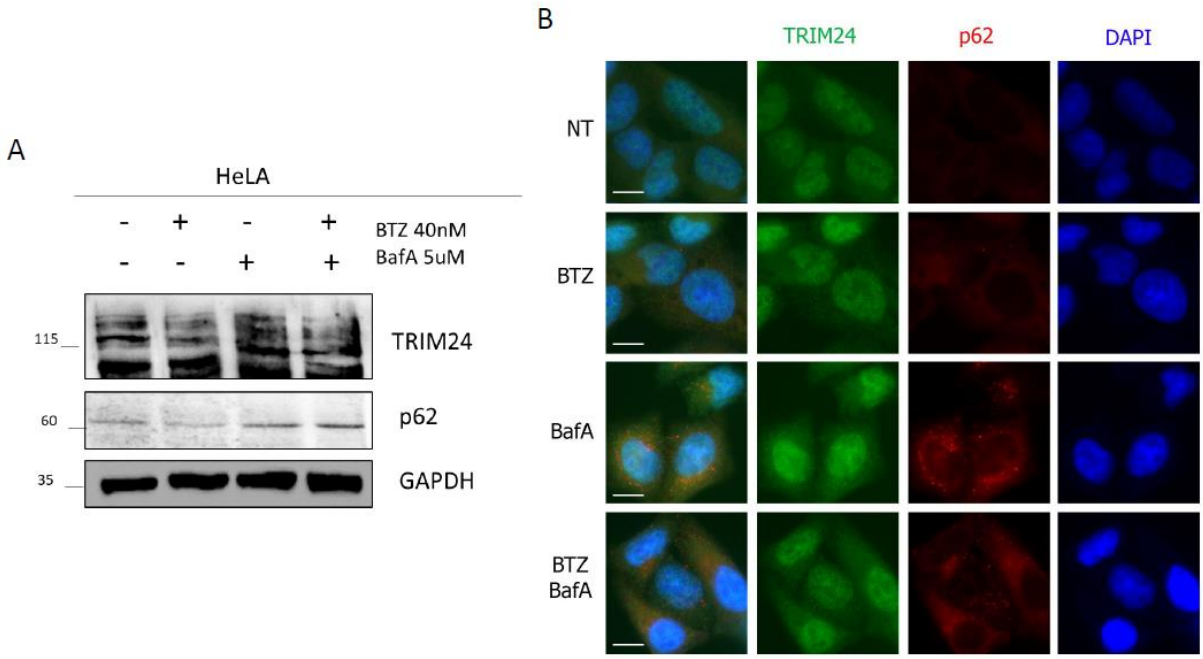

Figure 22: TRIM24 levels and localization in HeLa cells upon proteasome and autophagy inhibition. A: WB analysis of TRIM24 and p62 proteins from total cell extracts (5 million cells per pellet/sample). HeLa cells treated with BTZ 40nM, BafA 5uM or both treatments for 4 hours. GAPDH was used as charge control. Triplicate experiments were performed. B: Immunofluorescence analysis using HeLa cells with no treatment (NT), BTZ 40nM, BafA 5uM or both treatments for 4 hours (1 million cells per cover/sample). TRIM24 was detected with an anti-rabbit antibody and a secondary antibody Alexa anti-donkey/rabbit 488 (Green). p62 was stained with an anti-mouse antibody using as secondary antibody an Alexa anti-donkey mouse 568 (Red). Images were analysed using Axio Imager D1 Zeiss Microscope (40x, and 63X) and assembled with Adobe Photoshop 7.0. (Scale bar: 10um).

We analysed the stability and localization of TRIM24 and p62 in Z138 and ZBR cells by WB and IF (Figure 23). The settings used for both analyses in both cell lines were the same to be able to directly compare results. Under BTZ/BafA treatment, TRIM24 staining was highly increased in Z138 cells. In contrast, in the ZBR cell line, TRIM24 was highly reduced under the same conditions (Figure 23).

WB analysis of TRIM24 and p62 proteins showed that protein levels were consistent with IF images. A significant reduction of TRIM24 was observed only in ZBR cells when treated with BTZ and BafA. Quantifications of the integrated density of the IF images (Figure 24) support the reduction of TRIM24 in ZBR cells observed by WB analysis performed in triplicates.

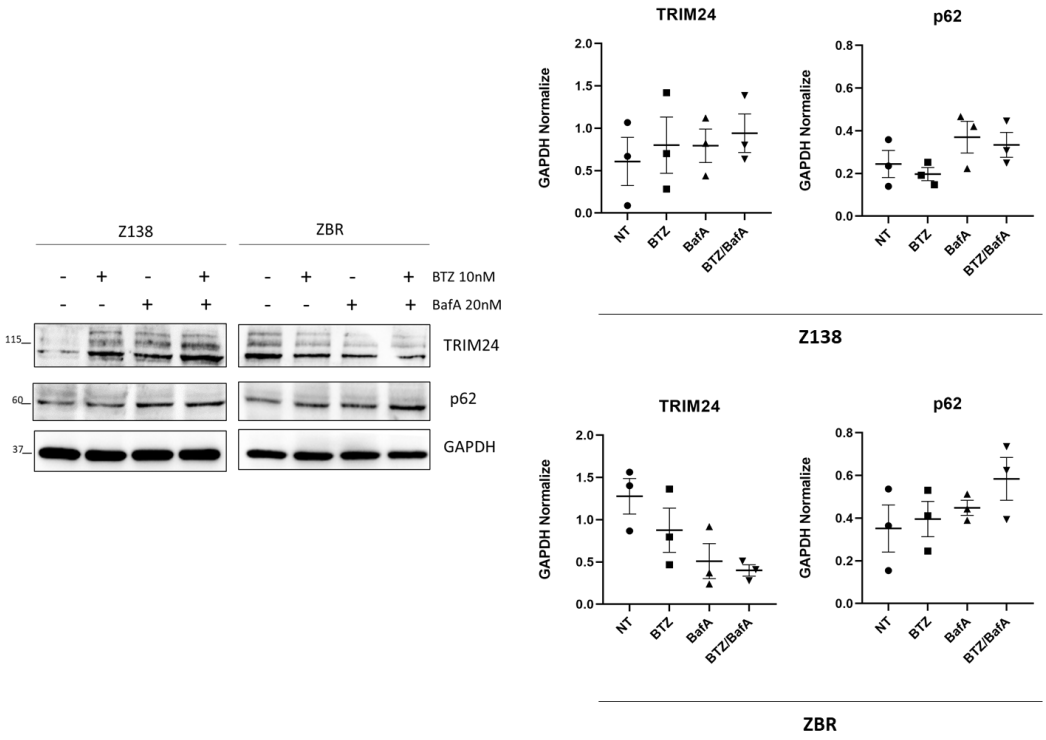

Figure 23: WB analysis of TRIM24 and p62 protein levels in Z138 and ZBR MCL cells upon BTZ and BafA treatment. WB analysis of TRIM24, p62 and GAPDH proteins upon BTZ 10nM, BafA 20nM or the combination of both for 4 hours (10 million cells per pellet/sample). Graphics with the GAPDH normalize values (n≥3; mean ± SD; two-way T-test , *P<0.05, **P<0.01, P***<0.001).

In order to better characterize the localization of TRIM24 in our biological model, we performed an in-depth analysis using concurrence analysis (Image J software). We analysed the amount of TRIM24 intensity (integrated pixel density), that are gathered in the pictures taken inside the area where DAPI staining is observed, indicating nuclear localization. These analyses showed a different distribution of the TRIM24 in both cell lines, with more TRIM24 present in the cytoplasm of ZBR cells (Figure 25, A).

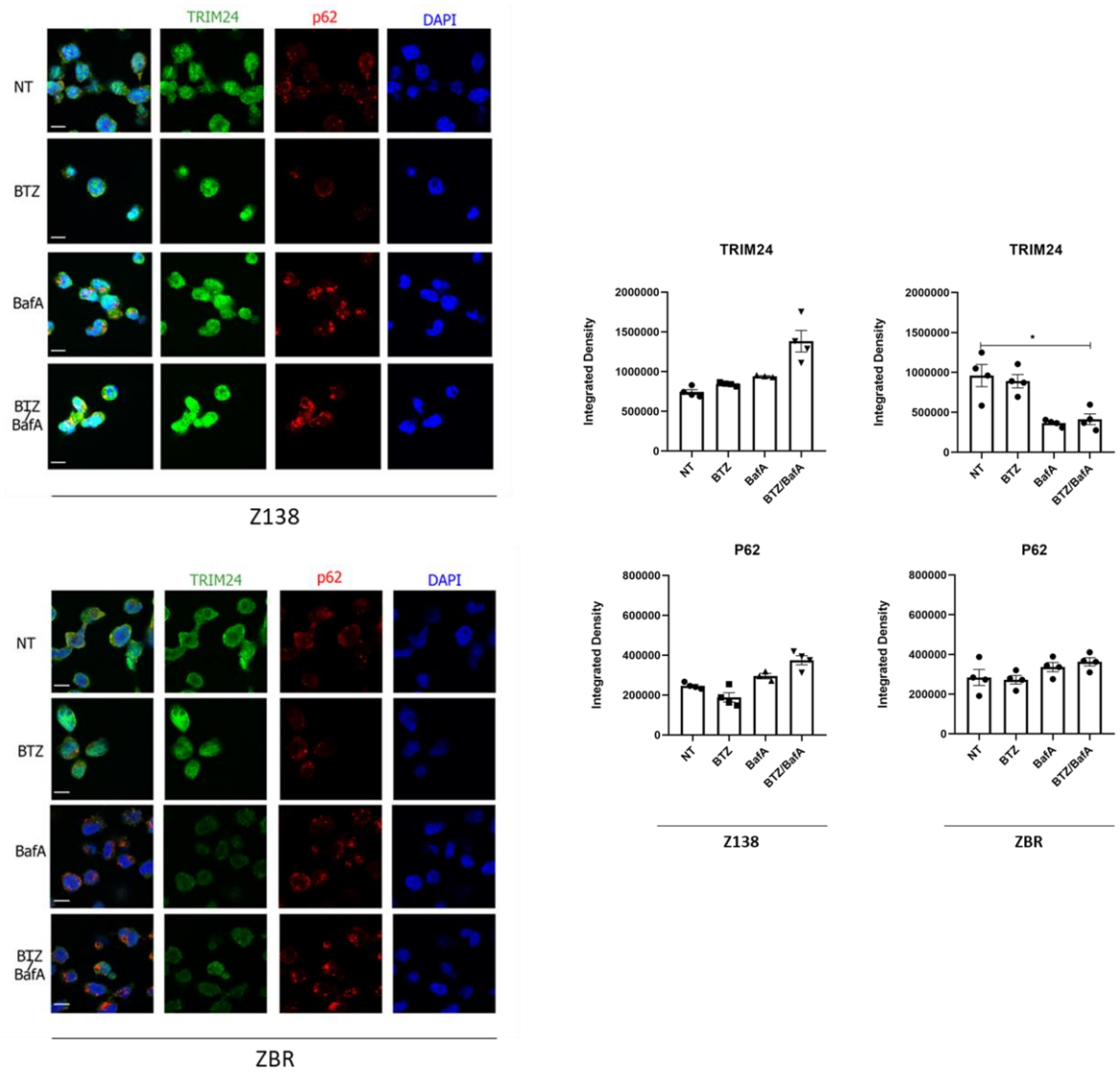

Figure 24: Cellular localisation of TRIM24 and p62. Immunofluorescence analysis of Z138 and ZBR MCL cell lines, with no treatment (NT), BTZ 40nM 4H, BafA 5uM 4 hours or the combination of both (2 million cells per cover/sample). Visualization of TRIM24 anti-rabbit using as the secondary antibody Alexa anti-donkey/rabbit 488 (Green), and p62 anti-mouse using as the secondary Alexa anti donkey mouse 568 (Red) (Scale bar: 10um). Each image was normalized against the number of cells (nuclear staining DAPI) (n≥3; mean ± SD; two-way T-test , *P<0.05, **P<0.01, P***<0.001). Quantification of the integrated density perform with Image J software. Images were acquired using super-resolution microscopy Leica SP8 Lightning and Zeiss LSM 880 Fast Airyscan and assembled with Adobe Photoshop 7.0. (Scale bar: 10um).

This cytoplasmic localization of TRIM24 in ZBR cells could indicate a possible role of this E3 enzyme in this subcellular compartment. Since we know that proteaphagy is permanently activated in ZBR cells (Grégoire Quinet et al, 2021), our first hypothesis was that TRIM24 could directly act on autophagy regulators such as p62 or on proteasome subunits. Nevertheless, TRIM24 and p62 were not co-localised in any of the conditions tested (Figure 24), indicating that p62 might not be a direct TRIM24 target.

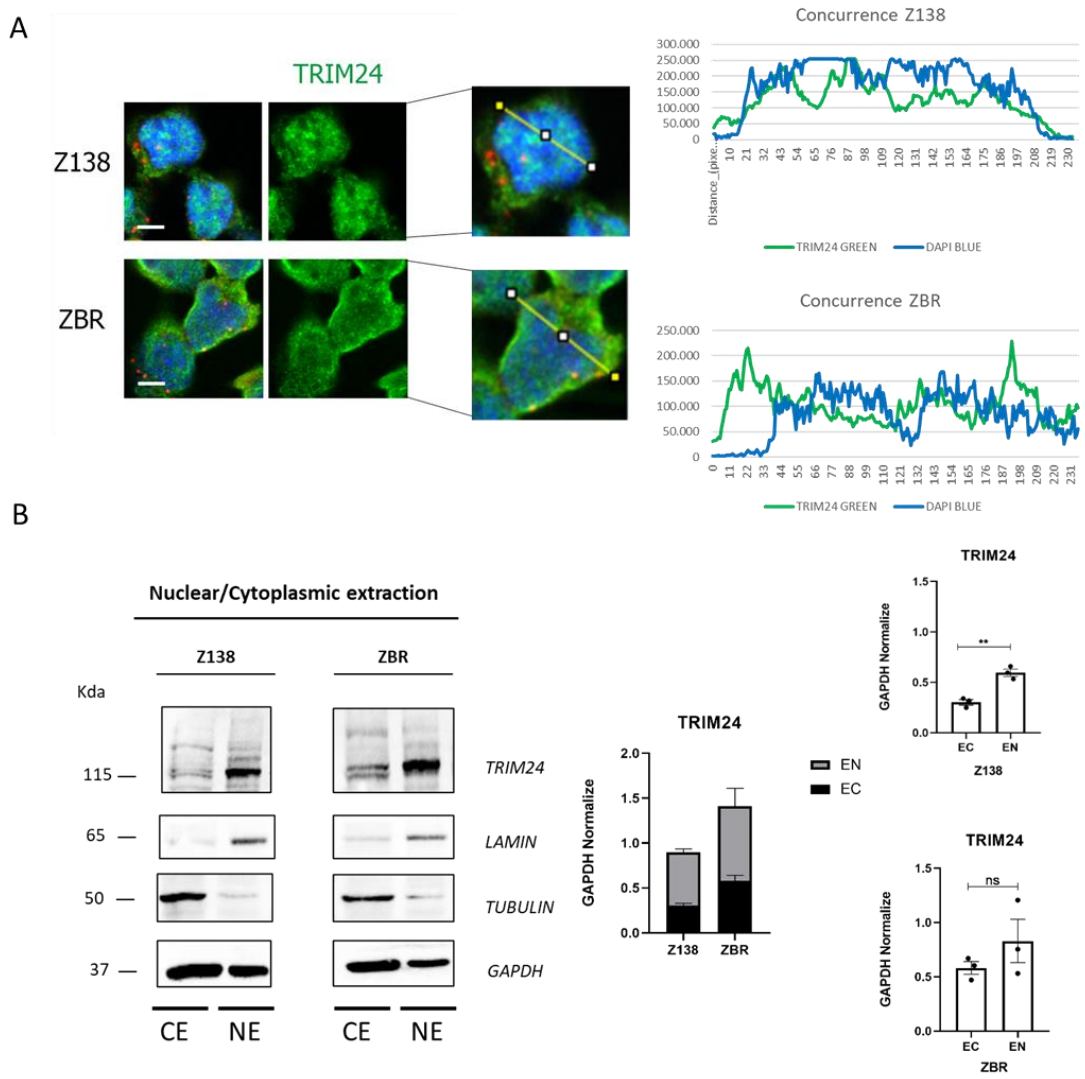

Figure 25: TRIM24 is enriched in the cytoplasm of ZBR cells. A: Immunofluorescence images show the localisation of TRIM24 in Z138 and ZBR cell lines under basal conditions (no treatment). TRIM24 was detected (green) with a specific anti-rabbit antibody and a secondary donkey rabbit antibody coupled Alexa (488). DAPI stain the nucleus in blue. Concurrence analysis (Image J software) displayed at the right part of the panel show the distribution of TRM24 inside the nucleus when overlaps with DAPI in both cell lines. Images were acquired using super-resolution microscopy Leica SP8 Lightning and Zeiss LSM 880 Fast Airyscan and assembled with Adobe Photoshop 7.0. (Scale bar: 10um). B: WB analysis of TRIM24 in Z138 and ZBR MCL cell lines (40 million cells per sample/pellet) upon cytoplasmic/nuclear fractionation. Soluble (CE, Cytoplasmic extract), and Insoluble (NE, Nuclear extract) fractions were obtained following instructions of the manufacturer (materials and methods). Lamin was used to control nuclear enrichment, and Tubulin was used to control the cytoplasmic fractionation. Quantification of TRIM24 using GAPDH from the soluble fraction to normalize values. Graphics were made using GraphPad Prism Software. Data from the NE and CE fraction are recollected in an additional graphic for a better visualization of NE/CE distribution in each cell line. (n≥3; mean ± SD; two-way T-test, *P<0.05, **P<0.01, P***<0.001).

In order to validate the cytoplasmic localization of TRIM24 in ZBR cells observed by IF analysis, we performed a cytoplasmic/nuclear fractionation assay comparing Z138 and ZBR cells following the instructions provided by the manufacturer (see materials and methods section). WB analysis (Figure 25, B) showed an enrichment of TRIM24 in the cytoplasm of

ZBR cells, confirming IF observations. Under these extraction conditions, Lamin was localized mainly in the nuclear fraction, and tubulin mainly in the cytoplasmic fraction validating the efficiency of this fractionation protocol. In sum, these results suggested a different TRIM24 subcellular localization, and a possible distinct function executed by this E3 enzyme can be expected in Z138 compared to ZBR cells.

To continue exploring the meaning of the distinct enrichment and localization of TRIM24 in ZBR, we considered multiple approaches aiming to find the link between this ligase, proteaphagy and the sensitivity/response to BTZ. These results will be presented in the next sections.

18.4 PROTAC degradation strategy to target TRIM24 in MCL cells.

Bromodomains inhibitors have been developed as potential anti-cancer therapy agents. However, these inhibitors do not show negative effects in cancer proliferation (Zhan et al., 2015). The proteolysis targeting chimera (PROTAC) degradation strategy offers a new alternative to target proteins in which chemical inhibition does not exert any therapeutical effect (Qi et al., 2021) even if the protein of interest regulates aberrant proliferation and/or malignancy. Recently, Gechijian et al have developed a cell permeable heterobifunctional TRIM24 degrader (PROTAC), by linking a chemical VHL E3 ligase binder to a bromodomain binder. This PROTAC efficiently drives TRIM24 (bromodomain-containing transcriptional regulator) degradation, and loss on chromatin localization when compared to the dimethyl benzimidazolone inhibitor IACS-9571 (Palmer et al., 2016). This strategy was shown to be successful as a potential treatment for human acute leukemia (Gechijian et al., 2018). Considering these results, we selected this strategy to target TRIM24 degradation and investigate its role, if any, in our BTZ-resistant MCL model cell line.

We used a TRIM24 PROTAC (referred in this document as dTRIM24) for 24 hours, at different concentrations to evaluate its efficiency to target TRIM24 for proteasomal degradation. TRIM24 reduction was evaluated by WB analysis with a specific antibody (Figure 26, A). We tested distinct concentrations of dTRIM24 since our previous results showed that the levels of this E3 enzyme in Z138 and ZBR cells was not the same. Our results indicate that it almost disappears in both Z138 and ZBR cell lines when using 10uM dTRIM24 concentration. These results can be better observed after quantification of the signal detected by WB analysis as displayed in the graphic (Figure 26, B).

We evaluated the effect of dTRIM24 on cell death (apoptosis) using two distinct approaches. We firstly quantified cleaved caspases: Caspase-3 and Caspase-9 detected by WB analysis (Figure 26, C). This was done after 8 hours of dTRIM24 treatment and revealed a significant enrichment of caspases.

The second approach was the analysis of Annexin 5 by Flow cytometry/FACS (see materials and methods section). We tested 5, 7.5, 10 and 15uM dTRIM24 concentrations, to visualize a dose-response curve, and calculate the IC50 for both cell lines (Figure 26, D). Similar results

were obtained using both approaches and no significant differences in apoptosis were observed for Z138 and ZBR cell lines (Figure 26, D).

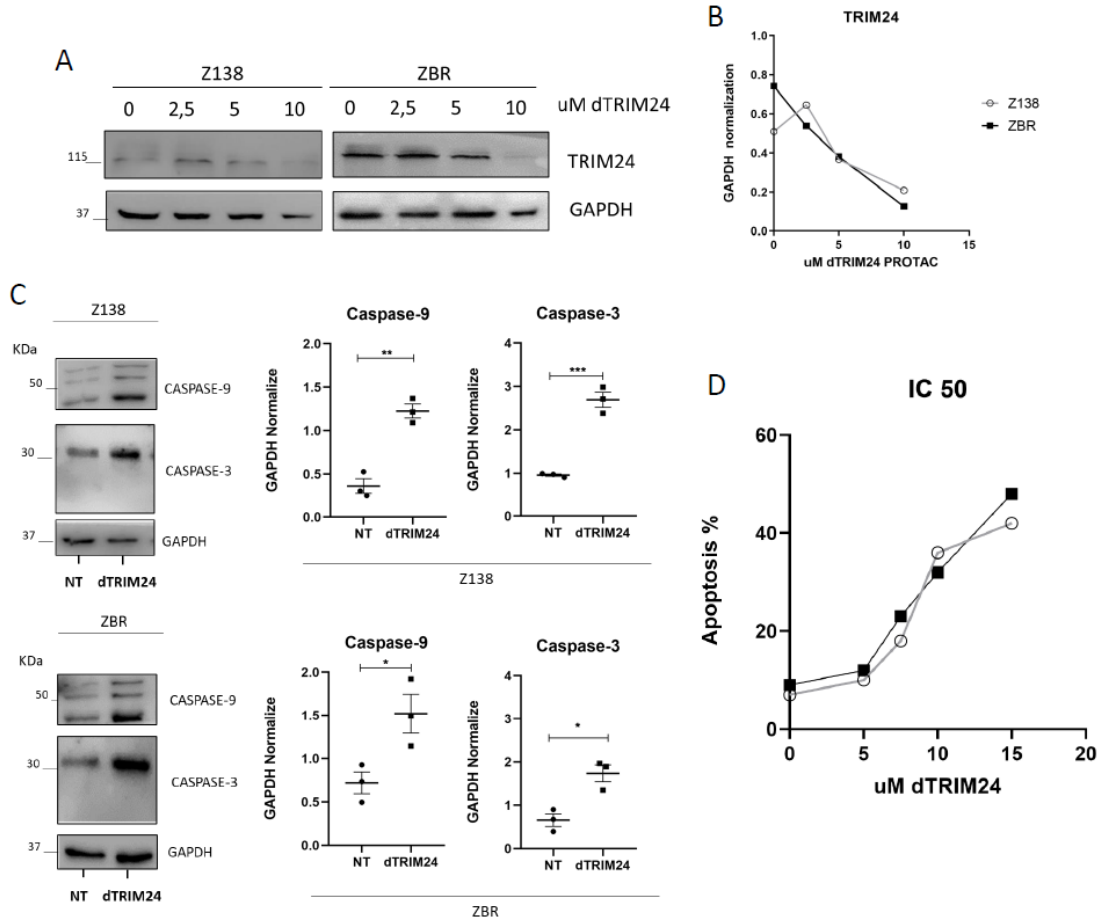

Figure 26: dTRIM24 PROTAC strategy to target TRIM24 in Z138 and ZBR cell lines. A: Z138 and ZBR cells were treated during 24 hours with distinct concentrations of dTRIM24 PROTAC (2.5, 5 and 10uM) (10 million cells per point/sample). TRIM24 protein level was analysed by WB analysis. GAPDH was used as charge control. B: TRIM24 signal was quantified in both cell lines and normalized using GAPDH (graphic visualization of TRIM24 depletion in Z138 and ZBR cell lines). C: Z138 and ZBR cells treated with 10uM dTRIM24 for 8 hours. Cleaved caspases 3 and 9 were analysed by WB analysis. Caspase-9 antibody recognizes both uncleaved (50 kDa) and cleaved (45 kDa) forms. GADPH was used to normalize values. (n≥3; mean ± SD; two-tailed Student's t-test, *P<0.05, **P<0.01, P***<0.001). D: FACS Analysis- measuring Annexin 5. Apoptosis values IC50 for Z138 and ZBR cell lines after 24-hour treatment of dTRIM24 PROTAC (5, 7. 5, 10 and 15uM concentrations).

In 2018, Zhang et al demonstrated that the inhibition of TRIM28 expression enhanced the sensitivity to BTZ of B-cell non-Hodgkin lymphoma cells by favouring p53 activity and therefore apoptosis induction (Zhang et al., 2018). These results suggested a role for TRIM28 in BTZ response and proposed a novel target to increase BTZ efficiency. TRIM28 is a bromodomain TRIM protein, that negatively regulates p53. It has been associated to different cancer types and malignancy progression similarly to TRIM24 (Hatakeyama, 2017; Zhang et al., 2018). In addition, TRIM28 overexpression has been associated with the activation of autophagy, promoting cell proliferation in glioma cells (Peng et al., 2019).

Considering all this information, we decided to investigate whether the depletion of TRIM24 in combination with BTZ would affect cell viability of the ZBR cell line in a different manner.

18.5 Efficient cooperation between BTZ and dTRIM24 in the ZBR cell line.

Since the individual dTRIM24 PROTAC treatment promoted the same level of apoptosis response in both Z138 and ZBR cell lines (Figure 26), it was decided to evaluate the apoptotic effect of the combined dTRIM24/BTZ treatment. We used suboptimal doses of these inhibitors to be able to analyse a possible cooperativity. We used 5 nM BTZ and 10 uM of dTRIM24 PROTAC. Under these conditions the double treatment significantly enhanced cell death only in the ZBR cell line (Figure 27), indicating cooperative effects.

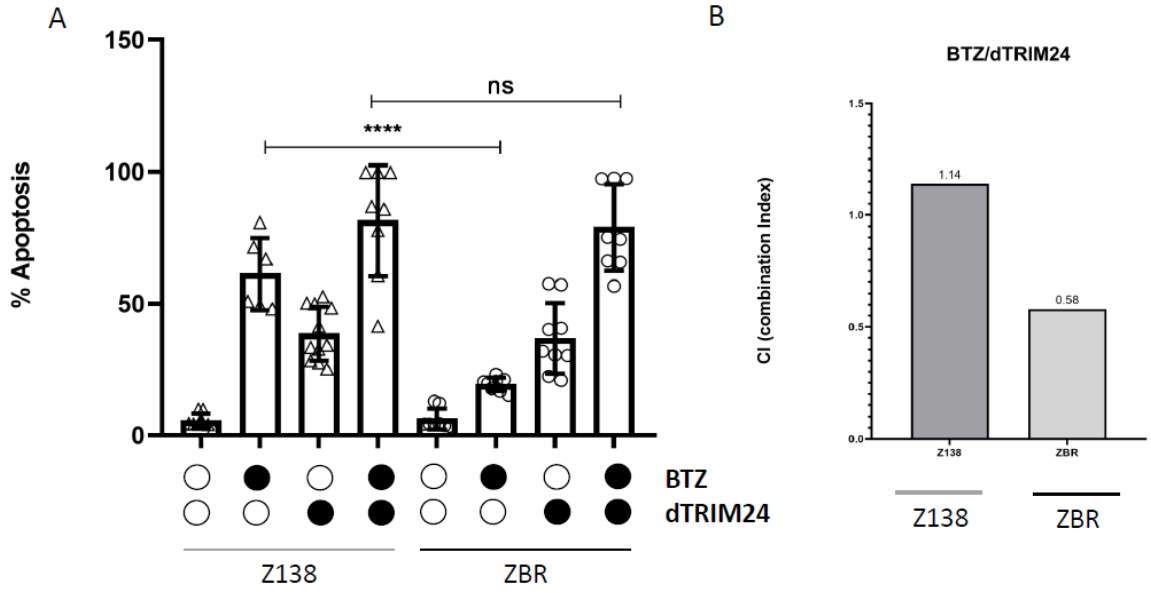

Figure 27: Apoptosis effect of the combined dTRIM24/BTZ treatment in Z138 and ZBR cells. A: Z138 and ZBR cells were treated during 24 hours with 10 uM dTRIM24 PROTAC, 5nM BTZ or the combined treatment (1 million cells per point/sample). Apoptosis levels were measured by FACS (Annexin 5) after 24-hour treatment (n≥3; mean ± SEM; two-way ANOVA test to compare conditions, *P<0.05, **P<0.01, P***<0.001). B: Combination index of the dTRIM24/BTZ treatment in Z138 and ZBR cell lines. Combination index was measured using Compusyn software.

Indeed, if we compare the effect of individual treatments on Z138 and ZBR cells, 5nM BTZ promoted 60% cell death in Z138 and 10% in ZBR while 10 mM dTRIM24 induced 35-40% in both cell lines. The combined treatment induced 80% apoptosis in both cell lines but since BTZ effect on ZBR is low, the cooperativity with dTRIM24 is higher in this BTZ-resistant cell line (Figure 27, A).

The combination index (CI) was calculated using the Compusyn software. Consistently, the CI were lower than 1 in ZBR cells meaning that depletion of TRIM24 shows enhanced apoptotic effects induced by BTZ in this cell line. On the contrary, the CI value was more than 1 in Z-138 suggesting only an additive effect in this cell line (Figure 27, B

18.6 TRIM24 is a crucial autophagy regulator in MCL cells.

It was decided to examine how the dTRIM24 treatment affected autophagy in order to investigate the molecular mechanisms regulated by TRIM24 in ZBR cells compared to Z138. We particularly looked into the stability of core proteasome subunits since they are regulated by the permanently activated proteaphagy in ZBR cells (Figure 28). Cells were treated during 8 hours with dTRIM24, BTZ or dTRIM24/BTZ at the concentrations indicated in Figure 28.

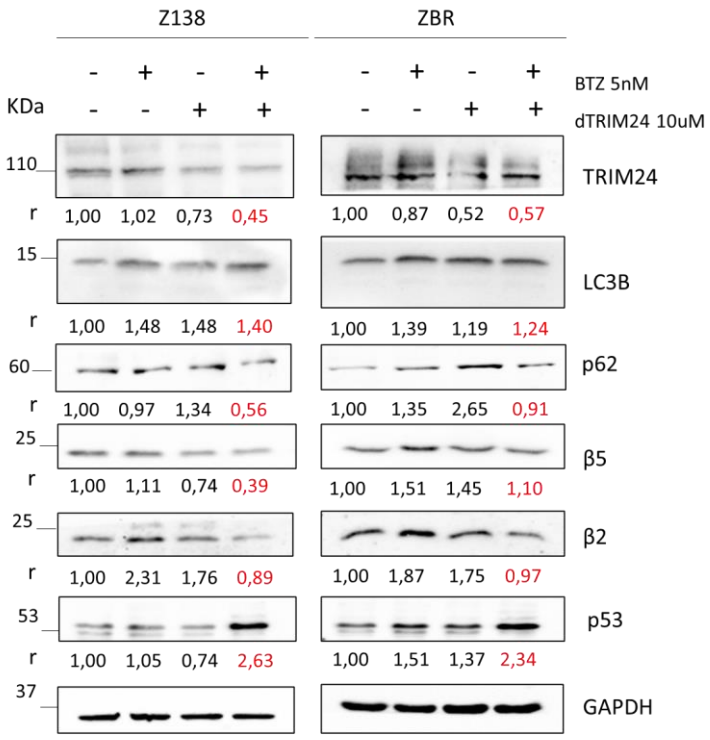

Figure 28: Impact of TRIM24 degradation on autophagy activation and proteasomal subunits in ZBR compared to Z138 cells. Z138 and ZBR cells (10 million cells per point/sample) were treated during 8h with the indicated doses of dTRIM24, BTZ or dTRIM24/BTZ. Whole cell extracts were analysed by WB to detect TRIM24, p53, p62, LC3B, β5 and β2 proteins. Protein levels were quantified using GAPDH to normalize values. Differences in fold change were calculated normalizing against NT values of three independent replicates. The media of those values are indicated below each WB panel as r. Ratio values from the combined treatment are indicated in red.

Whole cell extracts were analysed by WB to detect proteins of interest. While 8 hours of dTRIM24 treatment accumulated both LC3B and p62 in Z138 and ZBR cells, p62 was consistently more accumulated in ZBR cells. The accumulation of β5 was also more prominent in ZBR cells than in Z138 but β2 appeared equally affected in both cell lines. Interestingly, protein levels of p53, a typical substrate of TRIM24, was more prominent in ZBR cells after dTRIM24 treatment. These results suggest that dTRIM24 could contribute to inhibiting proteaphagy while enhancing p53 activity more efficiently in ZBR cells than in Z138.

Even if basal levels of TRIM24 are higher in ZBR and the impact of dTRIM24 on TRIM24 levels appears to be limited, reducing the amount of this E3 Ub ligase could be more crucial in the BTZ-resistant cell line. To understand why the dTRIM24/BTZ treatment induced apoptosis more efficiently in ZBR than in Z138 cells, we analysed its impact on proteaphagy. While the double treatment increased LC3B and p53 levels compared to the single dTRIM24 treatment, p62, β5, and β2 proteins were reduced in both Z138 and ZBR cells under the same conditions (Figure 28) as indicated in the ratio (r) values. Therefore, the combination of BTZ with dTRIM24 equally affected proteaphagy in both cell lines suggesting that a compensatory mechanism could be promoted when blocking the proteasome and targeting TRIM24 for a Ub-proteasome mediated degradation process using this PROTAC.

18.7 TRIM24 regulates the formation of K48 and K63 chains, the Ubiquitin-associated fraction of p62 and proteasome subunits in ZBR cells.

We decided to analyse the impact of dTRIM24 on Ub chain formation in ZBR cells to further explore the molecular mechanisms implicating TRIM24 in the regulation of autophagy, and in particular proteaphagy. Since autophagy activation and termination have been respectively associated with K63 and K48 chains (Gonzalez-Santamarta et al 2021), we analysed these chains using Ub chain-specific nanobodies, optimized and validated for this project (see chapter II of results). Autophagy termination is mostly associated with the degradation of cellular factors implicated in autophagy via the UPS (Gonzalez-Santamarta et al 2021). We first analysed the presence of K63 and K48 chains in both unstimulated Z138 and ZBR cells by nanobody precipitation followed by WB detection (Figure 29).

Our results show that while K48 chains appear equally abundant in both cell lines, K63 were more abundant in ZBR cells, confirming the results observed using the TUBEs-MS approach (Quinet et al 2021). Our results also confirmed that the TRIM24 fraction bound to both Ub chains is more enriched in ZBR than in Z138 cells, enrichment also revealed using the same TUBEs-MS approach (Quinet et al). Interestingly, we also observed that cellular factors implicated in proteaphagy (p62, β2, and β5) were better immunoprecipitated in ZBR cells by the K48 nanobody, even if these proteaphagy factors were modestly and consistently bound to K63 (Figure 29).

We then tested how the depletion of TRIM24 affected Ub chain composition in Z138 and in ZBR cells (Figure 30). Cells were treated or not with 10uM of dTRM24 for 8 hours. Precipitated fractions with K48 and K63 chain-specific nanobodies were analysed to detect ubiquitylation, TRIM24, p62, β2, and β5 proteins by WB. Our results clearly indicate that after dTRIM24 treatment K48 and K63 chains are heavily increased only in the ZBR cell line, suggesting that this Ub E3 regulates the abundance of Ub chains when cells are resistant to BTZ. Surprisingly, TRIM24 does not appear to play an important role in the regulation of Ub chains abundance in BTZ-sensitive Z138 cells.

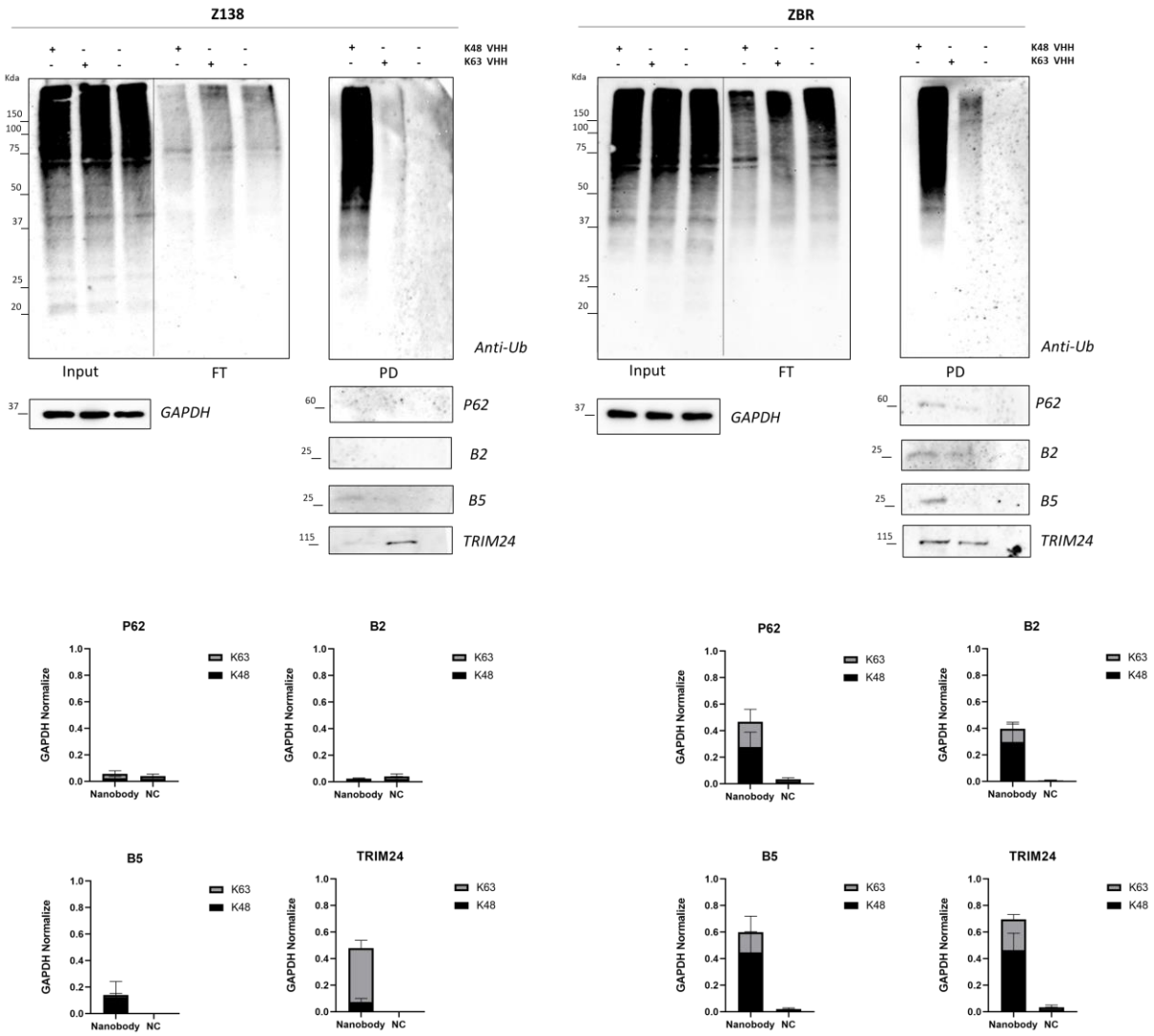

Figure 29: Enrichment of K63 Ubiquitin chains and Ubiquitin associated TRIM24, p62, β2, and β5 proteasomal subunits in ZBR cells. Whole cell extracts from 20 million of unstimulated Z138 and ZBR cells were precipitated using K48 and K63 Ub chain-specific nanobodies. A: Input, FT (Flow Through) and bound fractions (PD) were analysed by WB analysis to detect total ubiquitylation levels using a Ub antibody (P4D1). B: GAPDH from the input fraction was used as charge control. Precipitated TRIM24, p62, β2, and β5 proteins were detected with specific antibodies. Proteins were quantified and normalized against GAPDH. Graphics were made using GraphPad Prism Software. Negative control (NC) values were efficiently low, and nanobody signal was display in the graphics for a better visualization of how much of the total amount of protein identified is coming from K48 or K63 chain-specific nanobody.

We could also observe that in ZBR cells the dTRIM24 treatment increases the fraction of p62, β2 and β5 bound to K48 and K63 chains while in Z138 cells, under the same conditions, these proteins were not detected, or even being reduced like in the case of β5. Altogether these results indicate that TRIM24 negatively regulates K48 and K63 Ub chains and factors implicated in proteaphagy in ZBR cells. Thus, TRIM24 could be one sensor that would contribute to regulating proteaphagy and UPS-ALS crosstalk in cells that resist to BTZ.

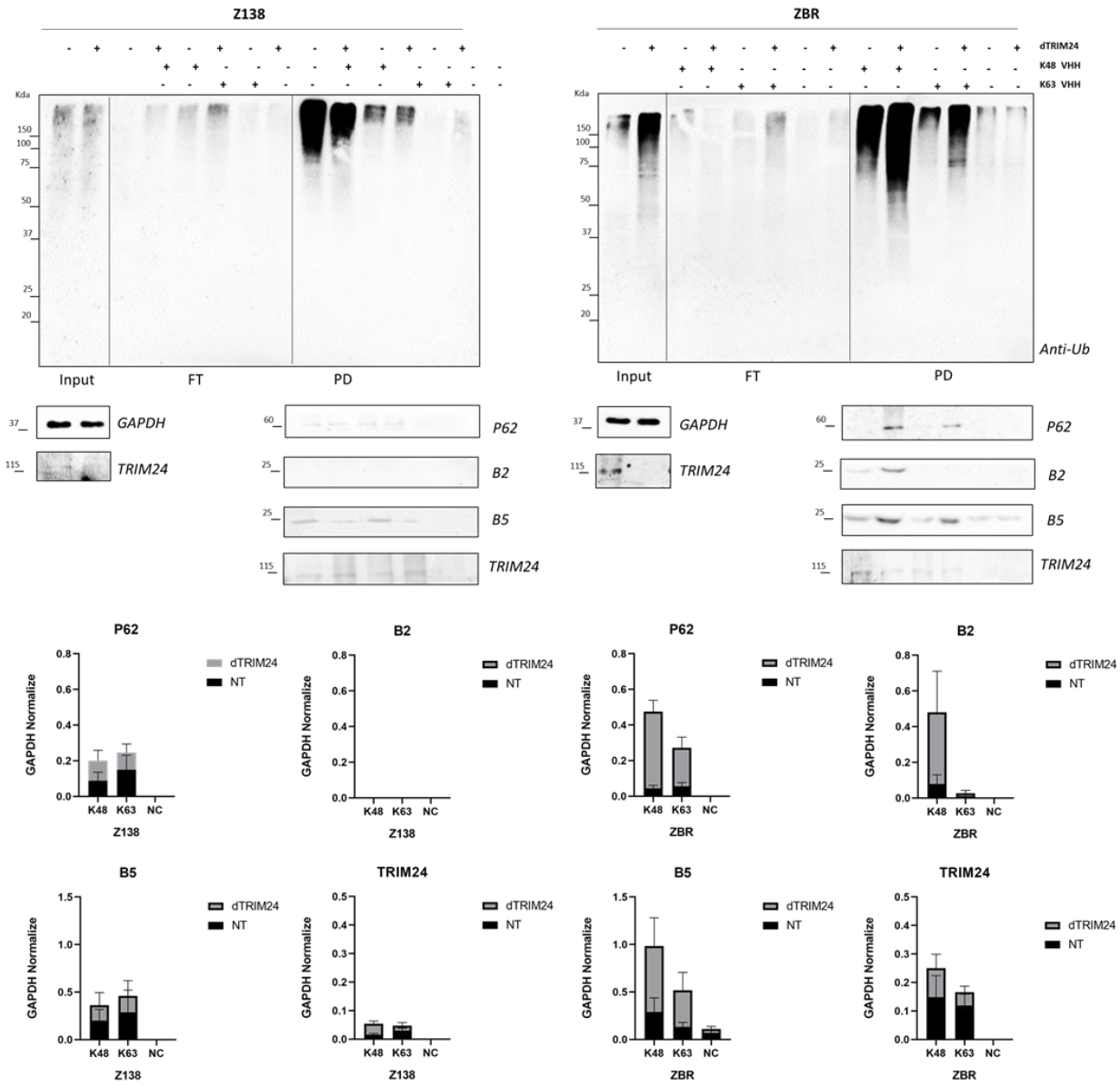

Figure 30: dTRIM24 treatment enhances the formation of K48 and K63 chains and ubiquitylation of proteins implicated in proteaphagy in ZBR cells. 20 million of Z138 and ZBR cells were treated or not (NT) during 8 hours with 10uM dTRIM24. Nanoprecipitations made with K48 and K63 Ub chain-specific nanobodies recognising K48 and K63 Ub chains. WB analysis of Input, FT and PD (nanobody precipitation) to detect total ubiquitylation levels using a Ub antibody (P4D1). WB analysis of TRIM24, p62, β2, and β5 proteins. Proteins of interest were quantified using Image J software and normalized using GAPDH from the input. Graphics were made using GraphPad Prism Software. Negative control (NC) values were efficiently low, and nanobody signal was displayed in the graphics for a better visualization of how much of the total amount of protein identified is coming from K48 or K63 chain-specific nanobody after dTRIM24 treatment or no treatment (NT) conditions.

18.8 p62 is a crucial factor regulating cell viability in ZBR cells.

As previously mentioned, Quinet et al demonstrated the involvement of p62 (AKA SQSTM1) in the regulation of BTZ resistance in ZBR cells. We could demonstrate that the silencing of p62 contributes to regulate BTZ-mediated toxicity (Figure 31), suggesting a major role of this autophagy receptor in this process, underlining its potential as a therapeutic target (Grégoire Quinet et al, 2021). The potential use of p62 as a drug target in cancer treatments was already suggested by other authors (Islam et al., 2018).

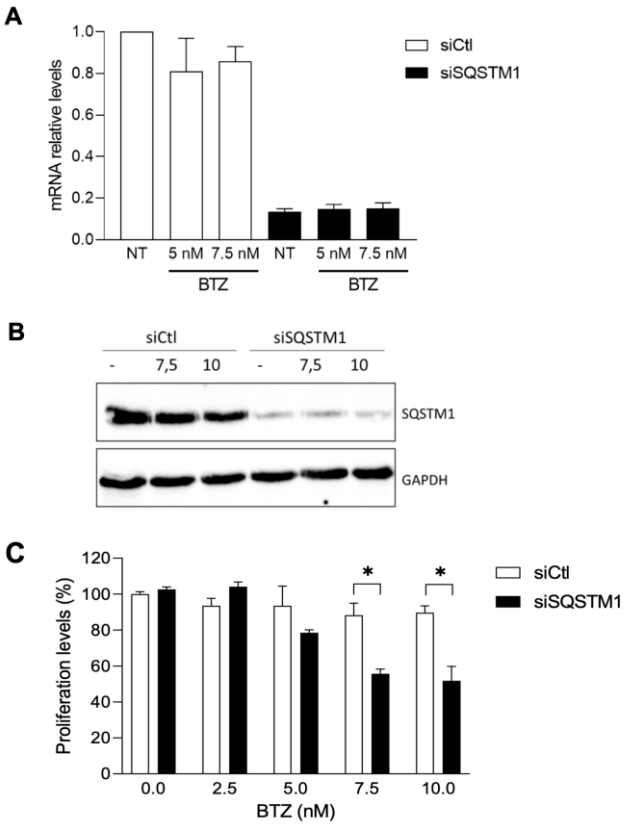

Figure 31: Silencing of p62 recovers sensitivity to BTZ in ZBR cells. ZBR cells were transfected with siRNA against SQSTM1 (s) and non-targeted (scramble) sequence (siCtl) and treated 8 hours after transfection with BTZ at 2.5, 5, 7.5, and 10nM concentrations. A: SQSTM1 mRNA relative levels using quantitative real-time PCR (qRT-PCR). B: SQSTM1 protein were isolated after 24 hours of incubation with different concentrations of BTZ. C: Proliferation levels determined by the Cell Titer-Glo Luminiscent Cell Viability Assay (Grégoire Quinet et al, 2021).

Due to the limited number of chemical molecules blocking p62, our laboratory started working with VTP. We could demonstrate that VTP was very efficient to block p62-mediated proteaphagy and apoptosis in BTZ-resistant cells *in vitro* and *in vivo* mouse xenografts (Quinet et al 2021).

However, as we will see in the following sections, this inhibitor also activates ROS, making it difficult to separate the effects mediated by p62 targeting from others. For this reason, it

was decided to use a novel p62 inhibitor called XRK3F2. The particularity of this inhibitor is that it binds to the ZZ-type zinc finger domain of p62. The ZZ zinc finger domain of p62 is known to be the binding site for the RING finger protein tumour necrosis factor (TNF) receptor-associated factor 6 (TRAF6). It is involved in the regulation of the NF-κB and p38MAPK signalling pathway but has also been proposed to regulate innate immune response as it binds the innate defence regulator 1 (IDR-1). The ZZ domain of p62 has been proposed to be significant for self-oligomerization, which can activate the NF-κB signalling pathway resulting in selective degradation of p62 (Islam et al., 2018). In addition, this domain is also implicated in macroautophagy by regulating the N-end rule pathway and inducing autophagosome biogenesis (Cha-Molstad et al., 2017).

p62 is considered as a N-recognin that can bind type 1 and type 2 N-degrons through its ZZ domain upon proteotoxic stress conditions, resulting in the delivery of cargoes to the autophagy machinery for its degradation. The ZZ domain was proposed to mediate drug resistance in ovarian cancer as its deletion restored sensitivity to cisplatin in ovarian resistant cells through the modulation of the NF-κB pathway (Yan et al., 2017). More importantly, in proteasome inhibitor-resistant MM cells, the combination of the ZZ inhibitor XRK3F2 with proteasome inhibitors reduced cell viability by activating multiple death pathways (Marino et al., 2019).

In this context, we tried using XRK3F2 to promote apoptosis in BTZ sensitive and resistant cells. When used individually, XRK3F2 treatment promoted the same apoptotic response in Z138 and ZBR cell lines at the concentrations tested, as it can be observed in the dose-response curve and the calculated IC50 (Figure 32, A).

When XRK3F2 was combined with suboptimal doses of BTZ (5nM), the induced apoptotic response in Z138 was higher (80%) than in ZBR cells (60%). These differences showed low statistically significance (Figure 32, B). However, in this context the response to BTZ is lower in ZBR cells as the BTZ/XRK3F2 treatment indicates a better additive effect in ZBR than in Z138 (Figure 32). Since the concentrations of XRK3F2 used were already high, we could not increase them because of the low solubility of this compound. Our group is currently developing analogues of XRK3F2 that could improve solubility, efficacy and reduce possible side effects.

In order to better characterise the molecular mechanisms affected by XRK3F2 (and in future analogues being developed in the hosting laboratory), it was decided to investigate the impact of this inhibitor in the stability of p62 and a group of UBR Ub E3 enzymes found enriched in ZBR cells using a TUBE-MS approach. As previously mentioned, these UBR enzymes regulate the N-end rule pathway and could potentially contribute to coordinate the UPS-ALS crosstalk.

Z138 and ZBR cells were treated with 10uM XRK3F2 during 4h. Whole cell extracts were analysed by WB to detect the proteins of interest. Our results clearly show that the stability of p62 is increased in both cell lines indicating that XRK3F2 efficiently targeted p62 (Figure 33). Interestingly, the stability of UBR enzymes appears to be more affected in the ZBR than in Z138 cells. Indeed, UBR2 and UBR5 protein levels are highly accumulated in ZBR but not in Z138 cells (Figure 33).

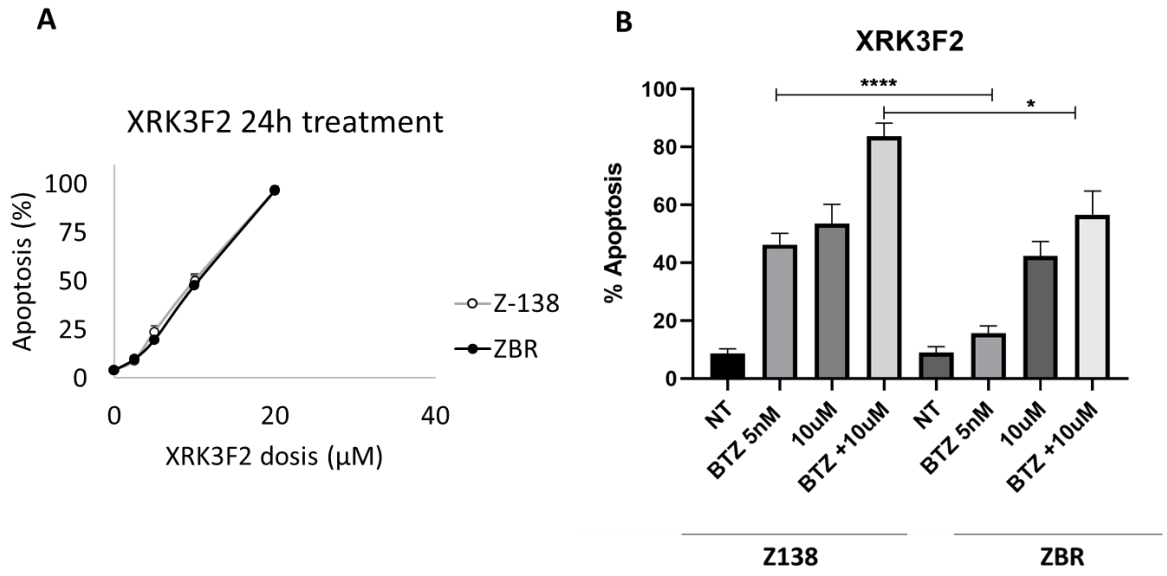

Figure 32: Apoptosis effect of the inhibition of ZZ domain of p62 domain using XRK3F2, and its combination with BTZ in Z138 and ZBR cells. A: IC50 calculated from the dose-curve response of Z138 and ZBR cells (1 million per point/sample) treated with 2.5, 5, 10, and 20 uM of XRK3F2. Apoptosis was measured by FACS (Annexin 5) after 24-hour treatment (n≥3; mean ± SEM; two-way ANOVA test to compare conditions, *P<0.05, **P<0.01, P***<0.001). B: Z138 and ZBR cells (1 million cells per point/sample) treated with 5nM BTZ, 10uM XRK3F2 or the combination of both for 24 hours. Apoptotic values measured by FACS (Annexin 5) (n≥3; mean ± SEM; two-tailed Student's t-test, *P<0.05, **P<0.01, P***<0.001).

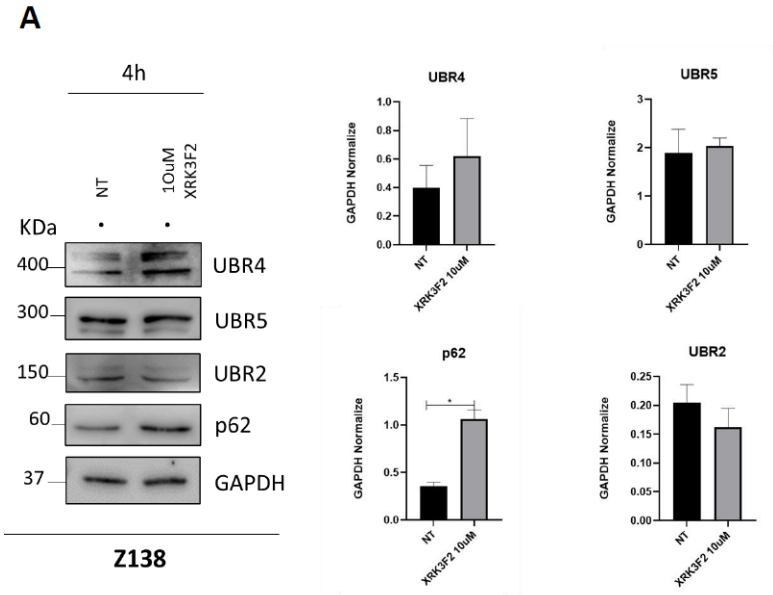

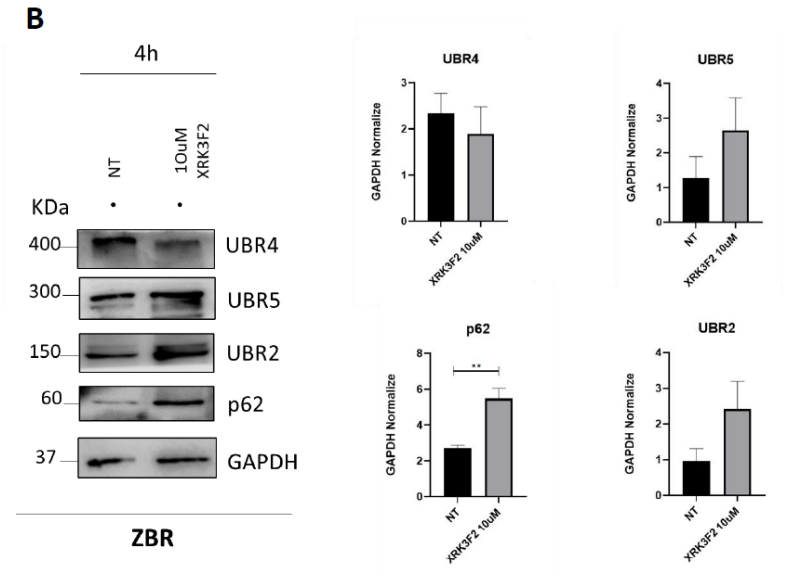

Figure 33: Effect of XRK3F2 on the stability of p62 and UBR enzymes in Z138 and ZBR cells. Z138 and ZBR cells (10 million cells per point/sample) were treated with 10uM of XRK3F2 for 8 hours. Whole cell extracts were analysed by WB to detect p62, UBR2, UBR4 and UBR5 proteins using specific antibodies. A: Z138 cell line and B: ZBR cell line. Proteins were quantified using Image J software and normalized using GAPDH values. (n≥3; mean ± SEM; two-tailed Student's t-test, *P<0.05, **P<0.01, P***<0.001).

On the contrary, UBR4 was more accumulated in Z138 than in ZBR cells. Even though UBR2 and UBR5 regulation by p62 appears to be highly regulated in ZBR cells, interfering with this interaction does not significantly contribute to recover BTZ sensitivity in ZBR cells. This lack of effect could mean that XRK3F2 is not efficiently impacting all UBR enzymes or that this is not a key mechanism contributing to regulating resistance to BTZ in ZBR cells. The new XRK3F2 analogues with higher specificity, solubility and affinity could contribute to prove this hypothesis.

18.9 ROS contribution in the response of ZBR cells to VTP.

As previously mentioned, VTP was used in our laboratory to efficiently recover BTZ sensitivity in BTZ-resistant MCL cells (Quinet et al 2021). VTP is known for promoting p62 aggregation forming high molecular-weight p62 forms, but also for inducing ROS (Konstantinou et al., 2017). Can p62 inhibition and ROS effects induced by VTP be dissociated? To address this question, we decided to investigate the role of ROS in the VTP mechanism of action to induce apoptosis in our ZBR cells. With this purpose, we used N-acetylcysteine (NAC), a widely used ROS inhibitor or scavenger (Halasi et al., 2013). We decided to use suboptimal doses of VTP to be able to observe positive or negative effects in apoptosis.

When combined with NAC 10mM, the VTP apoptosis effect was reduced with statistical significance in both cell lines (Figure 34). This reduction was more pronounced in ZBR cells, suggesting a more important contribution of ROS induced by VTP in this BTZ-resistant cell line. The impact of this ROS inhibitor in the VTP induced aggregation of p62, proteaphagy

and Ub chains observed in ZBR cells remains to be investigated. This last aspect (Ub chains formation) will be partially investigated in the following section.

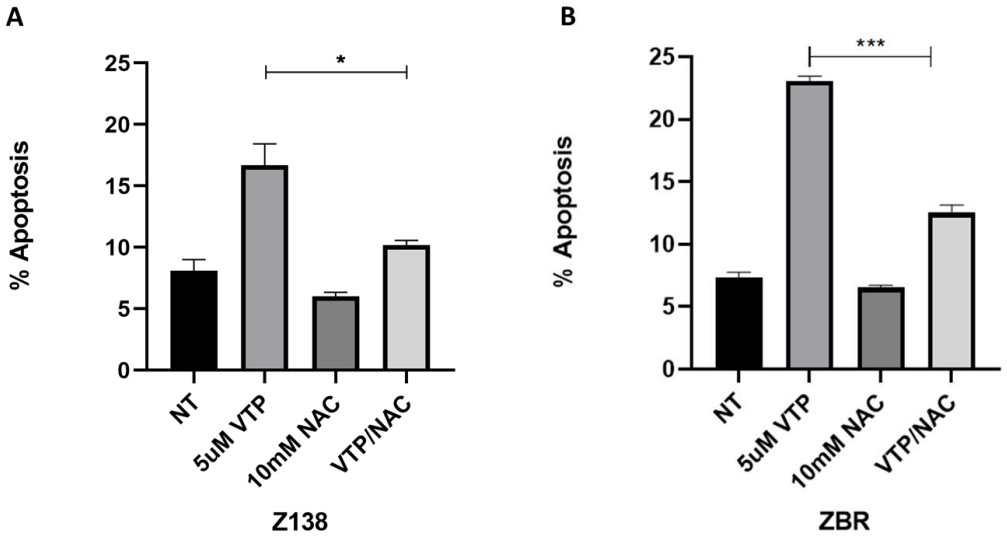

Figure 34: ROS contribution in the VTP-mediated apoptosis in Z138 and ZBR cells. Z138 and ZBR cells (1 million cells per point/sample) were treated with 5uM and/or NAC 10 mM for 24 hours. Apoptotic values measured by FACS (Annexin 5). (n≥3; mean ± SEM; two-tailed Student's t-test, *P<0.05, **P<0.01, P***<0.001).

Since the contribution of ROS appeared to be important for the VTP-mediated apoptosis, we explored the possibility that ROS induction could improve the apoptotic effects observed with XRK3F2. Even if there is no published information that XRK3F2 can induce ROS, we decided to explore this hypothesis by combining XRK3F2 with Luperox, a *tert*-Butyl hydroperoxide (tBHP) (Figure 35), a molecule that activate the oxidative stress response by inducing ROS formation (Chamoto et al., 2017; Ewald et al., 2017).

Z138 and ZBR cells were treated or not with individual and combined treatments of XRK3F2/Luperox/NAC at the indicated doses (Figure 35). As expected, Luperox alone induced apoptosis in both cell lines and this effect was efficiently reverted by NAC. Surprisingly, the XRK3F2/Luperox treatment did not improved but decreased the apoptosis effects observed by Luperox alone suggesting that XRK3F2 behaves like a ROS inhibitor (Figure 35).

All this data suggest that the mechanisms of action induced by VTP and XRK3F2 are not the same. Even if both molecules target p62 stability and function, ROS is induced by VTP, but it is inhibited by XRK3F2. Could these differences explain why VTP more efficiently induced apoptosis in BTZ-resistant cells? To progress in this sense, we decided to further explore the mechanisms of action induced by VTP treatment.

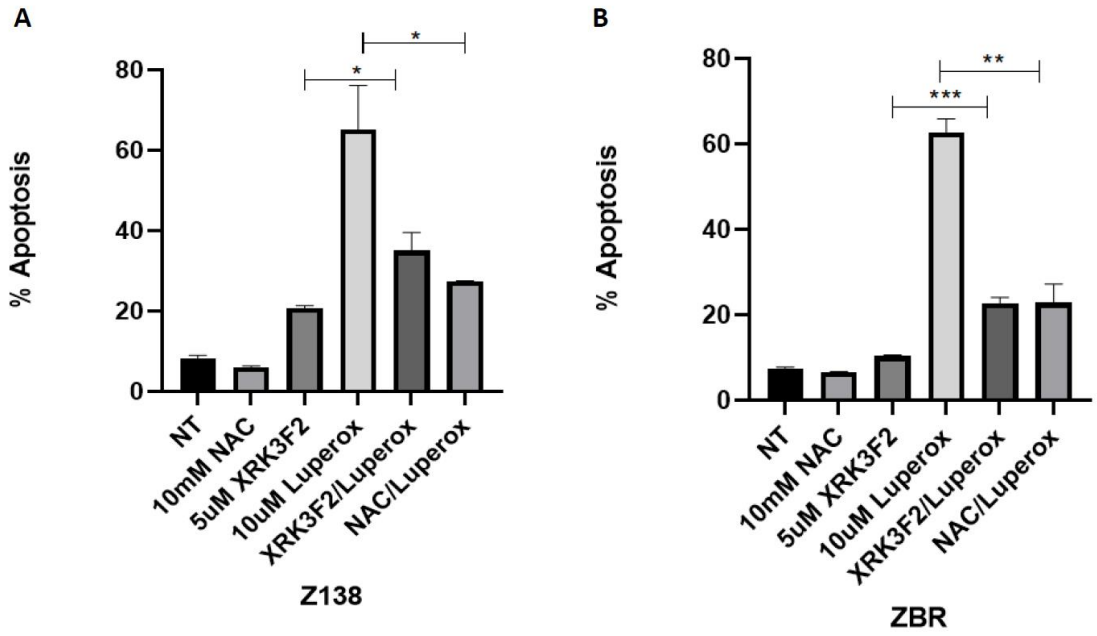

Figure 35: Effect of the ROS inducer Luperox in the XRK3F2-mediated apoptosis in Z138 and ZBR cells. Z138 and ZBR cells (1 million cells per point/sample) were treated with NAC 10 mM, 5 uM XRK3F2, 10uM Luperox, 5 uM XRK3F2/10uM Luperox and NAC 10 mM/10uM Luperox for 24 hours. Apoptotic values measured by FACS (Annexin 5). (n≥3; mean ± SEM; two-tailed Student's t-test, *P<0.05, **P<0.01, P***<0.001).

19. Chapter II: Development of new molecular tools to analyse the ubiquitome: Ubiquitin chain-specific nanobodies.

Protein ubiquitylation is a transient and highly dynamic process subjected to remodelling due to the simultaneous action of multiple DUBs. Therefore, understanding the specific role of distinct Ub chains in regulating different cellular processes is quite important and represents a huge scientific challenge (Mattern et al., 2019). During the last decade, great progress has been made to improve MS-based proteomics technologies for PTMs analysis, including enrichment strategies, computational data analysis and MS/MS methods (Zhao and Jensen, 2009). Different strategies have emerged to isolate endogenous ubiquitylated proteins, such as TUBEs. Our team developed engineered proteins, also called molecular traps, by combining interacting domains/motifs (such as UBDs and SIMs) to enhance the affinity to recognise specific PTMs, allowing their efficient purification/enrichment (Aillet et al., 2012; Da Silva-Ferrada et al., 2013; Hjerpe et al., 2009, 2009; Lopitz-Otsoa et al., 2012). In addition to their high specificity and affinity, some of these tools have the advantage to protect against the action of DUBs and proteasome which increases the capture efficiency of modified targets.

Antibody-based strategies appeared as a good alternative, that can also be used for the analysis of tissues and samples derived from patients in which overexpression methods cannot be applied. The systematic use of polyclonal and monoclonal antibodies is limited by their cost. To overcome this obstacle, small-size polypeptides with high binding affinity have been developed such as affimers, aptamers and more specifically nanobodies and minibodies (Mattern et al., 2019). The high stability, solubility, and affinity of these small polypeptides allow to use them in enrichment protocols followed by MS analysis, but also in high resolution imaging (Chakravarty et al., 2014; Mattern et al., 2019; Michel et al., 2017).

In this project, we have developed Ub chain-specific nanobodies directed against K48 and K63 Ub chains in collaboration with *Hybrigenics*. K48 or K63 chains were used to screen a humanize synthetic peptide phage display library (Moutel et al., 2016). Selected peptides were used as single VHHs and cloned in different vectors to generate nanobodies or minibodies. As shown in the previous section, we used nanobodies to study the role of K63 and K48 chains in BTZ-sensitive and resistant cell lines. In addition, we also used these tools to analyse the Ub proteome in our model, Z138 and ZBR MCL cell lines. This approach will help us to confirm the proteome previously identified by our group using a GST-TUBE/MS approach (Lopitz-Otsoa et al., 2012; Mata-Cantero et al., 2016) in the same cells (Quinet et al 2021). In addition, this new strategy will help us to distinguish functions associated to K48 or K63 chains that cannot be distinguished by the TUBEs-MS approach. Finally, this strategy will be also used to further explore functions affected by the VTP treatment in Z138 and ZBR cell lines.

Our previous TUBEs-MS analysis showed differences in Ub signatures found in Z138 and ZBR cells (Figure 16). However, those differences did not show statistical significance due to high variability. Our first intention was then to confirm that ZBR cells were more enriched with K63 than Z138 cells at basal level. As shown in the previous section, we could confirm these results by WB analysis (Figure 29). The different distribution of K63 Ub chains, when comparing Z138 and ZBR cell lines, supported the hypothesis that autophagy was

upregulated in the BTZ-resistant cell line. This could justify why proteaphagy is permanently activated in ZBR cells. In this project, we were also interested in understanding the functions associated with K63 and K48 chains in both cell lines. Therefore, we implemented a proper methodology to explore these Ub-chain specific functions by coupling precipitation protocols using nanobodies with MS analysis. We finally validated part of the results obtained while bringing new information that could be further explored by the hosting group.

19.1 Purification and *in vitro* characterization of K63 and K48 chain-specific nanobodies.

Using K48 or K63 Ub commercial chains as bait, different clones were isolated after phage display screening (Moutel et al., 2016). The list of all K48 and K63 nanobodies tested are indicated in Table 7. They were produced and purified from bacteria following the protocol indicated in the corresponding materials and methods section. These nanobodies contain two tags at the N-terminus, His6 and Myc that can be used for different affinity purifications steps. The different fractions obtained during the purification of chain-specific nanobodies were analysed by WB and stained by Coomassie blue. One example is illustrated in Figure 36.

VHH AntiK63

Clone	Vector	Purification	IP
F10.1	pHEN2	YES	YES
F2.1	pHEN2	YES	NO
E5.1	pHEN2	YES	NO
D10.1	pHEN2	YES	YES
D1.1	pHEN2	YES	YES
B2.1	pHEN2	YES	NO
B4.1	pHEN2	YES	NO
C2.1	pHEN2	YES	YES
C4.1	pHEN2	YES	YES

VHH AntiK48

Clone	Vector	Purification	IP
A4-1	pHEN2	YES	YES
C5-2	pHEN2	YES	NO
C7-2	pHEN2	YES	YES
E11-2	pHEN2	YES	NO
F5-2	pHEN2	YES	YES
F11-2	pHEN2	*NO*	*NO*
F12-1	pHEN2	YES	NO
G1-1	pHEN2	YES	NO
G9-2	pHEN2	YES	YES
H1-2	pHEN2	YES	YES

Table 7: List of K48 and K63 Ubiquitin chain-specific nanobody clones produced and analysed. A summary of purification, and *in vitro* precipitation results is indicated in this table. List of nanobody clones and vectors used for their expression. Precipitations were performed *in vitro* using K63 or K48 Ub commercial chains. NO indicates that the procedure failed. YES indicates that the procedure was successful.

After the purification of the different clones, *in vitro* precipitations using commercial Ub chains (materials and methods section) were performed for each individual clone (data not shown). With the clones that provided a positive signal, new precipitations were simultaneously performed to compare the amount of Ub chains purified by each of them and select clones with the best affinity for K48 and K63 Ub chains (Figure 37). Capture or pull-down (PD) fractions are used instinctively to indicate bound material from nanobody precipitation assays. As a control of specificity, the same clones were used to precipitate the opposite K63 or K48 Ub chains. The best clones were retained for further characterization and optimisation.

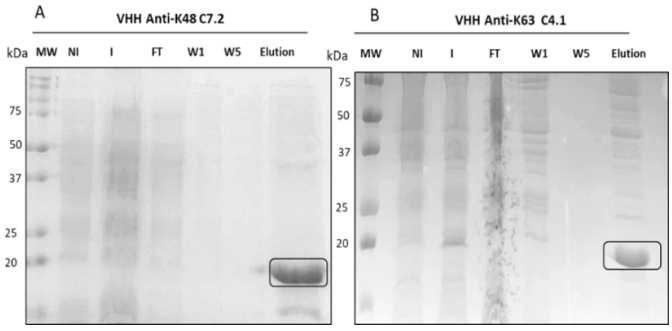

Figure 36: Example of production and purification from bacteria of Ubiquitin chain-specific K48 and K63 nanobodies. Nanobodies were purified from bacteria using a nickel-beads purification procedure (see material and methods section). Fraction of each purification step was analysed by Coomassie blue staining. NI: non-induced, I: IPTG-Induced, FT: Flow though, W1: wash 1, W5: wash 5, and Elution fractions of A: K48 C7.2 and B: K63 C4.1 clones are shown. Nanobody purified estimated size: 18 kDa.

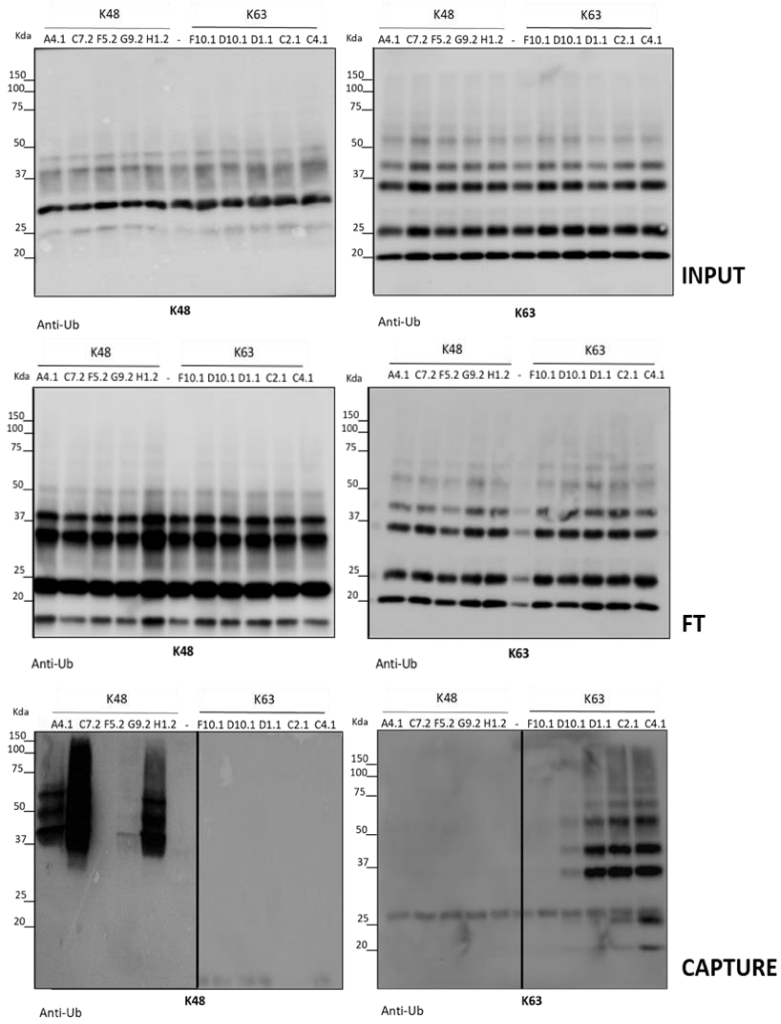

Figure 37: Characterisation of K48 and K63 Ubiquitin chain-specific nanobodies by *in vitro* Ub chain precipitation. Clones tested in this assay were selected after a first screening of all clones. Identical amount of K48 and K63 Ub chains (see material and methods section) were precipitated with the indicated K48 (A4.1, C7.2, F5.2, G9.2 and H1.2) and K63 clones (F10.1, D10.1, D1.1, C2.1, and C4.1) using the Myc tag. To verify the specificity of the clones, they were also used to precipitate the

opposite K63 or K48 Ub chains. Input, FT, and Capture (nanobody precipitation) fractions were analysed by WB using anti-Ub antibody (P4D1).

Among K48 Ub nanobodies, A4.1, C7.2 and H1.2 showed higher affinity for these Ub chains. For the K63 Ub nanobodies, D1.1, C2.1 and C4.1 displayed the best affinity. Our results were consistent with previous results performed with non-absorbed phage ELISA assays (*Hybrigenics,* data not shown). Based on these observations, we selected the clones A4.1 and C7.2 for K48 nanobodies and clones D1.1 and C4.1 for K63 nanobodies to continue working. Nanobody pull-down assay was performed using Z138 and ZBR cell lines, upon basal (NT, no treatment) and BTZ treatment conditions to increase the ubiquitylation fraction inside these cells (Figure 38).

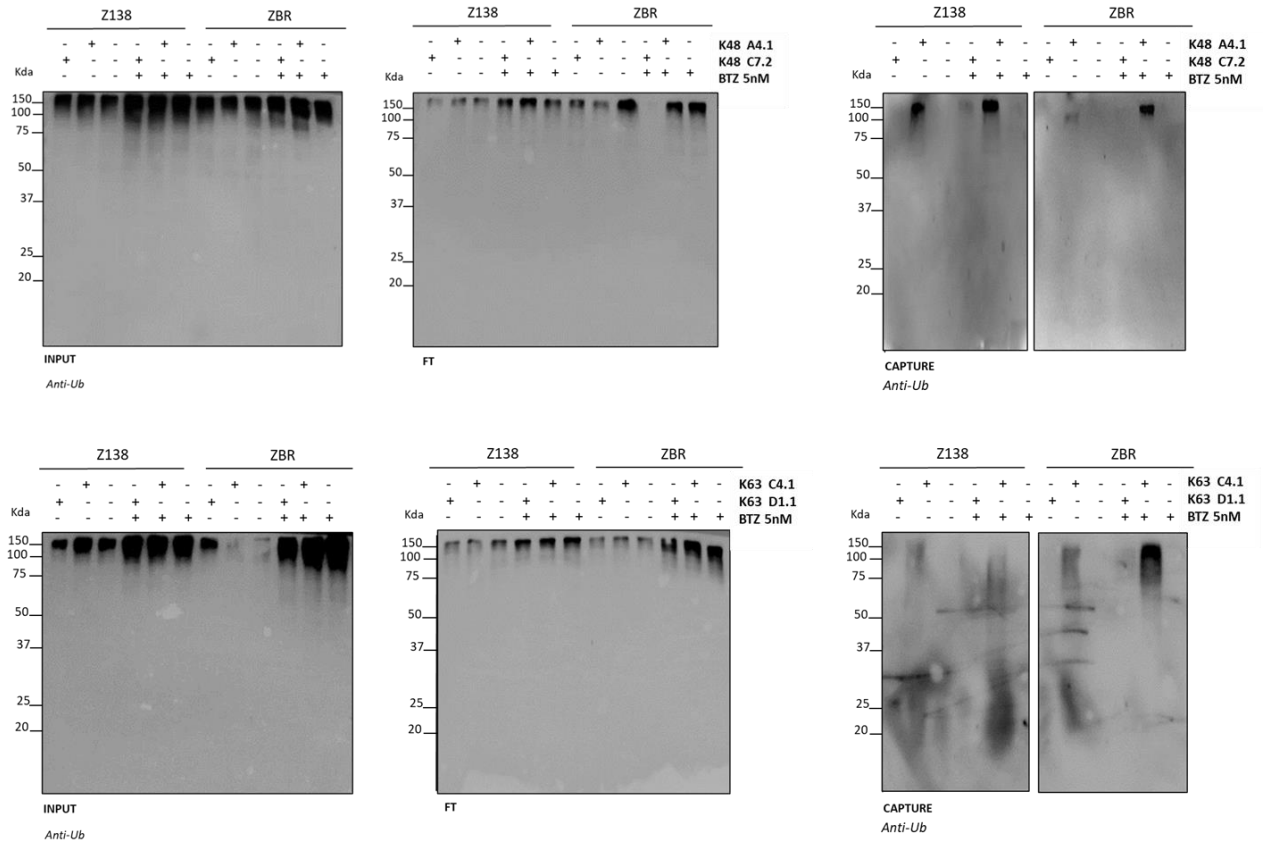

Figure 38: Capture of ubiquitylated proteins from Z138 and ZBR cell lines using the best clones from K48 and K63 Ubiquitin chain-specific nanobodies. Z138 and ZBR cells (10 million cells per point/sample) were treated or not with 5nM of BTZ for 8 hours. Cell extracts were precipitated with A: K48 nanobodies clones A4.1 and C7.2 or B: K63 nanobodies clones C4.1 and D1.1. Input, FT, and Capture (nanobody precipitation) fractions were analysed by WB to detect ubiquitylated proteins using the P4D1 antibody.

These results show that the A4.1 (K48) and D1.1 (K63) Ub chain-specific nanobodies were the best ones to precipitate these Ub chains from our model. In these assays, the His6 tag was used to precipitate the ubiquitylated material using nickel beads. The His6 tag was preferred since it gave less background.

Thus, the A4.1 (K48) and D1.1 (K63) clones showed higher affinity, solubility and stability for the precipitation of Ub chains from our model cell lines. With the aim to explore K48 and

K63 Ub chain-specific functions, we used these nanobodies to implement various methodologies including applications for localising these chains with proteins of interest by IF and MS applications that will be presented in the following sections.

19.1 Validation of the use of Ubiquitin chain-specific minibodies for Cell Imaging.

After validating Ub chain-specific nanobodies for Ub enrichment in cells using precipitations, we further validated the use of the same K48 and K63 clones to identify specific Ub linkages/signatures by cell imaging. As previously mentioned, the peptides identified can be cloned into different vectors to generate single chain antibodies called minibodies. We used mouse (Fc IgG2) and rabbit (Fc IgG2) minibodies containing respectively the UbK63 clone D1.1 and UbK48 clone A4.1. VHH nanobodies fused with Fc fragments from mouse and rabbit include the same binding region and therefore the same affinity to recognise the antigen while adding the possibility to use commercially available fluorescent secondary antibodies (anti-mouse or rabbit). Minibodies were provided by our collaborators from *Hybrigenics*.

Our idea was to generate evidence supporting some of our previous conclusions obtained in our MCL cell lines. However, giving the complexity to work with suspension cells, we decided to set conditions first in a standard cell line such as HeLa. Before the analysis, we established a situation in which autophagy was activated in HeLa cells. A combination of 16-hour serum starvation and 4 hours of 2,5uM BafA treatment gave us the best results to activate autophagy and accumulate lipidated forms of LC3B (Klionsky et al., 2016) (Figure 39, A). This condition is expected to accumulate K63 chains due to autophagy blockage making easier to visualize them by IF. We also generated a situation in which we could easily detect K48 chains. With this purpose, we treated HeLa cells with 40nM BTZ for 4 hours to block the proteasome and accumulate substrates modified by K48 Ub chains. We decided to analyse the accumulation of p53 and ubiquitylated forms of this tumour suppressor by WB, a well-known substrate of the proteasome (Tsvetkov et al., 2010) (Figure 39, B).

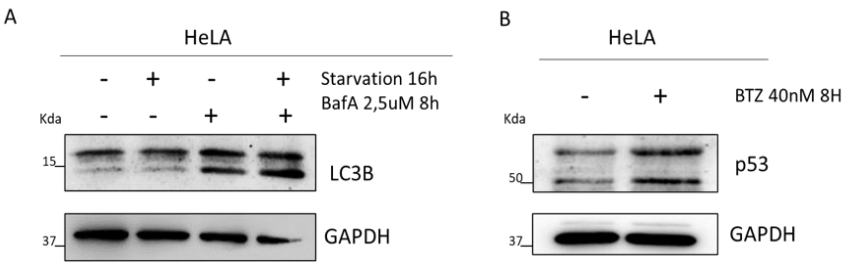

Figure 39: Setting conditions to accumulate K63 and K48 Ubiquitin chains in HeLa cells. A: Autophagy was induced in HeLa cells to accumulate K63 Ub chains. Cells were serum starved for 16 hours and treated or not with 2,5uM BafA for 8 hours. WB analysis was performed to detect LC3B and its lipidated form. B: Proteasomal inhibition was used to accumulate K48 chains in HeLa cells after BTZ 40nM treatment for 8 hours. WB analysis of a typical substrate of the UPS, the tumour suppressor p53 that was accumulated after BTZ treatment.

After setting conditions for the accumulation of K63 and K48 chains, we used minibodies to specifically detect these Ub chains by IF (Figure 40 and 41). In conditions where autophagy is activated, enrichments in LC3B (Red channel) and K63 Ub chains puncta (green channel) were observed. Importantly, some yellow dots marked inside white boxes can be observed indicating that LC3B and K63 chains partially co-localise (Figure 40).

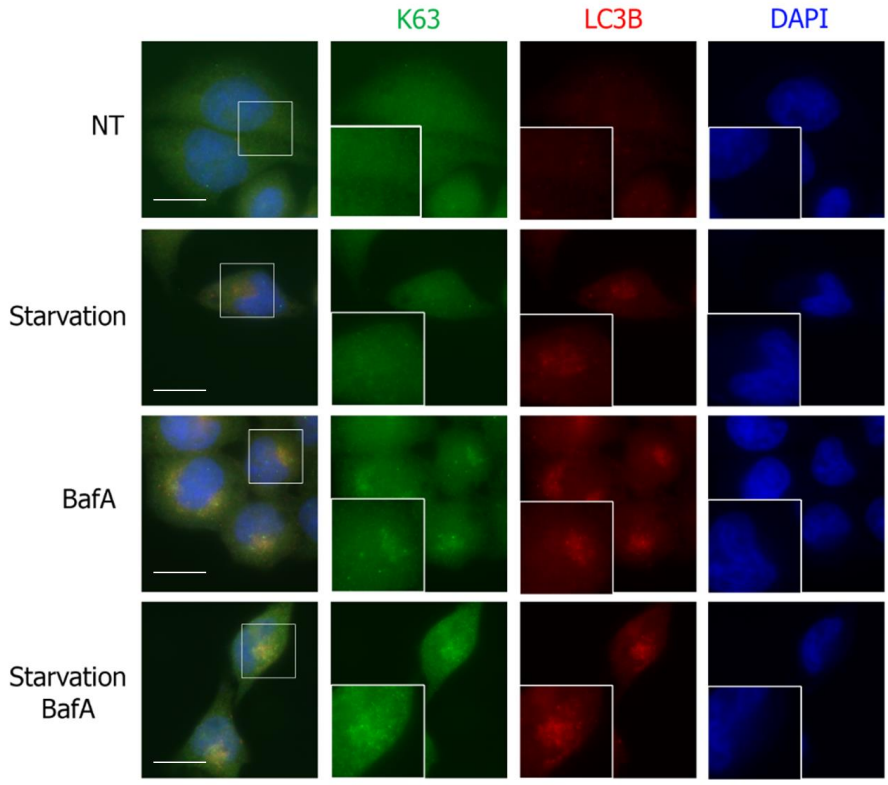

Figure 40: Co-localisation of LC3B and K63 Ubiquitin chain-specific minibodies in HeLa cells under autophagy induction conditions. Immunofluorescence images using HeLa cells under starvation 16 hours, 5uM BafA treatment for 4 hours, the combination of both or no treatment (basal) conditions. K63 minibodies were detected using an anti-mouse secondary antibody (donkey mouse) coupled to Alexa 488 (Green). LC3B anti-rabbit antibody was detected with a donkey anti-rabbit secondary antibody coupled to Alexa 568 (Red). Images were analysed using Axio Imager D1 Zeiss Microscope (40x, and 63X), and assembled with Adobe Photoshop 7.0. (Scale bar: 10um).

After BTZ treatment, K48 puncta are visualized in green and under the same conditions p53 was accumulated in red puncta indicating the accumulation of both after proteasome inhibition (Figure 41). Some of these puncta co-localised in yellow spots when merging both signals indicating that at least some K48 Ub chains are overlapping with p53 under these conditions.

To further validate the use of those K63/K48 Ub chain-specific minibodies for cell imaging, we compared this staining with commercially available anti-Ub antibodies widely used: E4I2J (Cell Signalling) and P4D1 (Santa Cruz) (Figure 42 and 43). The Ub specific antibody E4I2J is known to recognise Ub chains in a selective manner. In contrast, the P4D1 antibody can also

recognise NEDD8 because it shares a high level of identity with Ub. The E4I2J antibody did not provide a strong signal when used in IF assays (Figure 42). Our K63 Ub minibody did not co-localise with E4I2J even if it presented a similar enrichment pattern upon the different treatment conditions. In contrast, the P4D1 antibody presented a good staining when used in IF assays, and puncta co-localisation with our K48 Ub minibody (Figure 43).

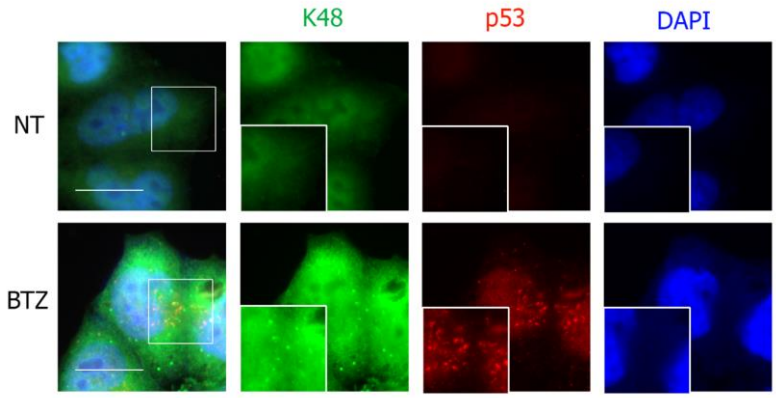

Figure 41: Co-localisation of p53 with K48 Ubiquitin chain-specific minibodies in HeLa cells treated with BTZ. Immunofluorescence images using HeLa cells under proteasome inhibition conditions or no treatment (basal) conditions. BTZ was used at 40nM for 4 hours to block the proteasome. Detection of K48 minibodies was performed using as secondary donkey anti-rabbit antibody coupled to Alexa 488 (Green). The anti-p53 antibody was detected with donkey anti-mouse secondary antibody coupled to Alexa 568 (Red). Images were analysed using Axio Imager D1 Zeiss Microscope (40x, and 63X), and assembled with Adobe Photoshop 7.0. (Scale bar: 10um).

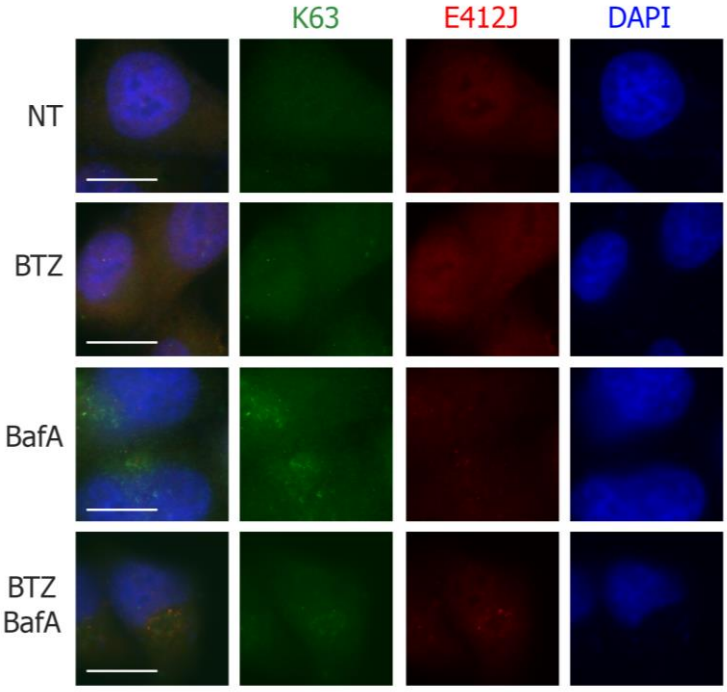

Figure 42: Validation of the use of K63 minibodies for IF. Immunofluorescence images using HeLa cells, K63 Ub minibodies and E4I2J Ub commercially antibody. Immunofluorescence images using HeLa cells with no treatment, starvation 16 hours, BafA treatment 5uM, and the combination of both for 4 hours. Visualization of K63 anti-mouse using as the secondary antibody Alexa anti-donkey mouse

488 (Green), and E4I2J anti-rabbit using as the secondary Alexa anti-donkey rabbit 568 (Red). Images were analysed using Axio Imager D1 Zeiss Microscope (40x, and 63X), and assembled with Adobe Photoshop 7.0. (Scale bar: 10um).

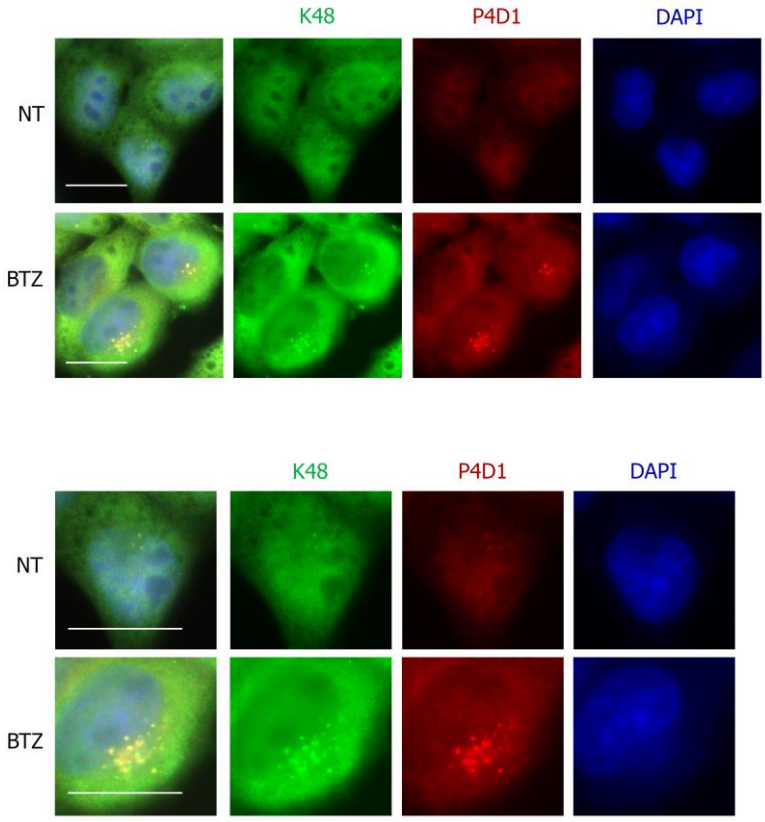

Figure 43: Validation of the use of K48 minibodies for IF. Immunofluorescence images using HeLa cells, K48 Ub minibodies and P4D1 Ub commercially antibody. Immunofluorescence images using HeLa cells with no treatment and BTZ 40nM treatment for 4 hours. Visualisation of K48 anti-rabbit using as the secondary antibody Alexa anti-donkey rabbit 488 (Green), and P4D1 anti-mouse using as the secondary Alexa anti donkey mouse 568 (Red) Images were analysed using Axio Imager D1 Zeiss Microscope (40x, and 63X), and assembled with Adobe Photoshop 7.0. (Scale bar: 10um).

After validating the use of Ub chain-specific minibodies in HeLa cells to visualise K48 and K63 Ub chains, we used these tools to visualise K48 and K63 enrichment in MCL cells. We aimed to visualise proteophagy (mechanism already validated by the lab in ZBR cells). Nevertheless, after BafA treatment of ZBR cells, we did not obtain clear data (not shown) regarding co-localisation of K48 or K63 minibodies in combination with proteasomal markers. Most likely, our IF procedure must be better adapted to these suspension cells.

19.2 Optimisation of a crosslinking protocol to isolate Ubiquitin chains from Z138 and ZBR cell lines.

It was decided to test different crosslinking protocols in order to use our K48 and K63 chain-specific nanobodies for MS applications. Crosslinking of His6-nanobodies to nickel beads will better fix these tools to the column and more stringent washes can be envisaged. More importantly, the stringency of the washes allows to reduce the background level obtained from the unspecific binding of proteins unrelated to Ub chains. We also increased the number of cells used in our precipitation assays to improve the specific signal obtained and facilitate MS detection.

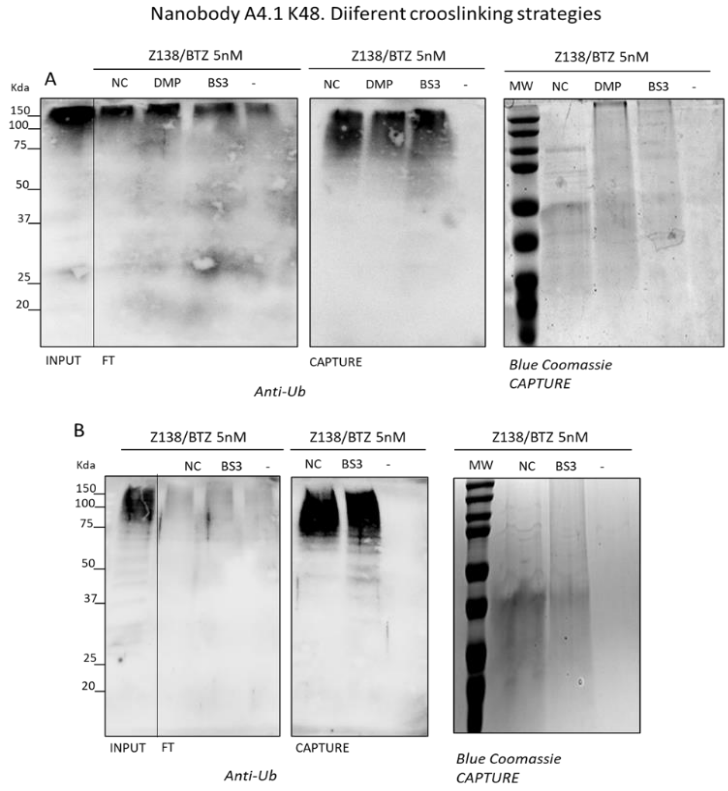

Figure 44: Optimisation of Ubiquitin chain-specific nanobodies enrichment using different crosslinking strategies. Z138 cells (20 million cells per point/sample) were treated with 5nM BTZ for 8 hours. Total cell extracts were precipitated using the K48 A4.1 Ub chain-specific nanobody. A: Results comparing crosslink protocols using DMP and BS3. B: Results comparing protocols without crosslinking (NC) of and using BS3 crosslinking protocol. WB Analysis to detect Ub using Anti-Ub antibody (P4D1) in the Input, FT, and Capture (nanobody precipitation) fractions. In addition, the total amount of protein precipitated was analysed using blue Coomassie staining of the captured fraction.

We tested the dimethyl pimelimidate (DMP) and the bis (sulfosuccinimidyl) suberate (BS3) protocols (Figure 44). In this test, we used only the K48 (A4.1) Ub chain-specific nanobody and Z138 cells treated with BTZ to accumulate ubiquitylated proteins. Crosslinked nanobodies were incubated with these cell extracts and the different fractions were analysed by WB using anti-Ub antibody and blue Coomassie staining for detecting the total amount of protein enriched using this protocol (Figure 44). Our results show that the BS3 protocol provided a stronger signal in the nanobody precipitated fraction (compared to

DMP) with an extended Ub modification pattern, suggesting that a mild crosslinking is more efficient than a stronger one (DMP) (Figure 44, A). In some cases, stronger crosslinking procedures can compromise the structure of small peptides.

Considering these results, we decided to explore if the crosslinking was indeed required to optimize our MS protocol. We therefore used similar cell extracts to compare the precipitations obtained with and without the BS3 crosslinking protocol strategy. Our WB results showed that the BS3 protocol was better to enrich Ub specific fraction in our experiments (Figure 44, B).

The Coomassie staining showed that the total material precipitated could be sufficient for MS analysis, nevertheless upon BTZ treatment. For this reason, an experiment scaling up the number of cells used was introduced, and cell extracts from untreated Z138 cells were used to test the limit of detection of precipitated ubiquitylated proteins (Figure 45) in our settings. This was in part due to the fact that we were also interested in identifying Ub linkages and substrates at basal levels (no treatment conditions). Our results show that under these conditions, K48 Ub chains can be precipitated very efficiently as observed by WB but also that the total ubiquitylation is efficiently detected by Coomassie blue staining almost undetectable in the negative control.

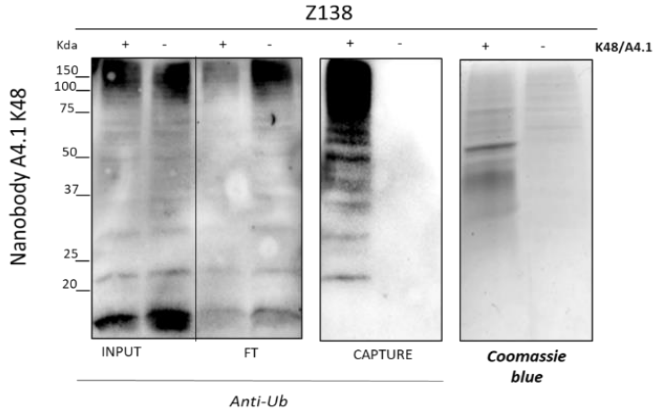

Figure 45: Capture of K48 Ubiquitin chain substrates with the A4.1 chain-specific nanobody using the BS3 crosslinking protocol. 40 million untreated Z138 cells were used to pull down K48 Ub chain modified substrates using or not K48 Ub chain-specific nanobody (clone A4.1). All fractions were analysed by WB using an anti-Ub (P4D1). Input, FT, capture (nanobody precipitation), and blue Coomassie of the capture fraction are shown.

These samples were sent for MS analysis to evaluate the quality of the information that we could obtain for these specific precipitation conditions (data not shown). Since statistic differences could not be obtained with a single sample compared to the negative control, this analysis was not performed. However, more than 500 proteins were identified in this preliminary analysis. These conditions confirmed that we were using good conditions to perform MS analysis.

19.3 Efficient enrichment of K63 and K48 Ubiquitin chain substrates from Z138 and ZBR cells using Ubiquitin chain-specific nanobodies.

Using the conditions set in the previous section, we scaled up while using crosslinked Ub K48 and K63 specific nanobodies to enrich ubiquitylated proteins from our model, Z138 and ZBR (Figure 46 and 47) cell lines. For these experiments, we used 40 million cells to be able to analyse the quality of the sample before sending to MS analysis. Since we were interested in comparing the data obtained using TUBEs with the data obtained with Ub K48 and K63 Ub chain-specific nanobodies, non-stimulated basal conditions were analysed.

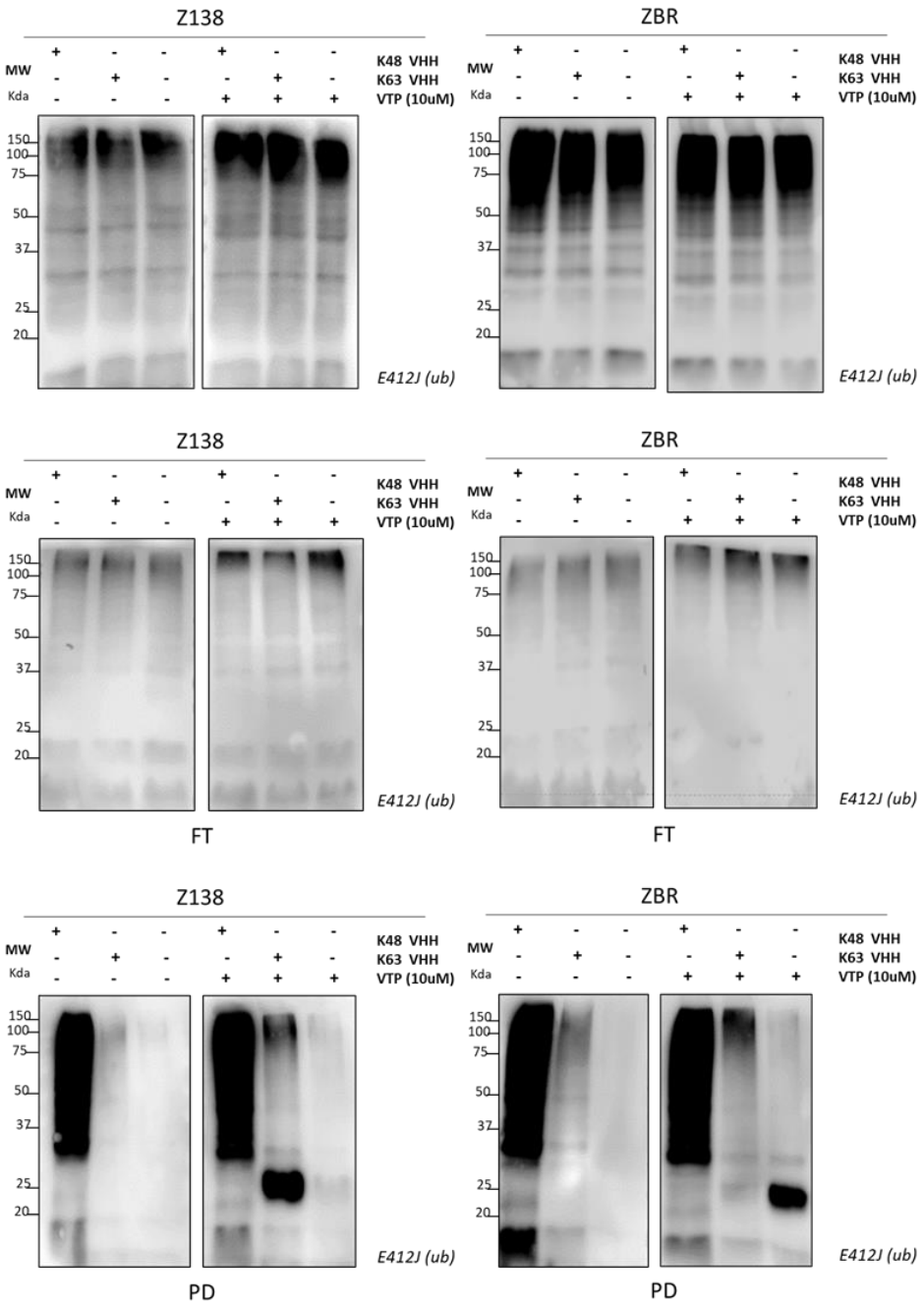

Figure 46: K48 and K63 Ubiquitin chain modified substrates captured with Ubiquitin chain-specific nanobodies in Z138 and ZBR cells treated or not with VTP. 40 million cells were used for each

condition in triplicates. Cells were treated or not with 10uM VTP for 2 hours. Ubiquitylated proteins were precipitated using K48 (A4.1) and K63 (D1.1) nanobodies. WB analysis with anti-Ub (E4I2J) of the input, FT and PD (nanobody precipitation) fractions. These samples were submitted for MS analysis.

In addition, we were also interested in better understanding the mechanisms induced by VTP that was at this moment the best candidate inhibitor of p62 used in our laboratory targeting the activity of this autophagy receptor in cell cultures and *in vivo* (Quinet et al 2021).

VTP induces high molecular weight forms of p62 aggregates, considered to be its mechanism of action (Donohue et al., 2011, 2014; Grégoire Quinet et al, 2021). However, the fact that under these conditions p62 is also captured by TUBEs suggests that at least some of these free forms can be ubiquitylated. Exploring the VTP mechanism of action could help us to understand the contribution of ROS species in the cell-killing response to this drug in BTZ-resistant cells (Konstantinou et al., 2017) (See results from the 18.8 section).

For the MS analysis, we purified ubiquitylated chains using K48 and K63 nanobodies from Z138 and ZBR cells. Cells were treated or not with 10uM VTP for 2 hours and all fractions were analysed by WB with a Ub specific antibody (E4I2J). Figure 46 shows the WB Anti-Ub of the Input, FT, and PD.

We observed an enrichment of K63 Ub chains at basal levels in ZBR cells confirming our previous observations. Also, when p62 is inhibited with VTP, we can see an enrichment of K63 Ub chains in both cell lines, even if these chains are consistently increased in ZBR cells. These results indicate that K63-regulated functions such as signalling cascades or autophagy pathway might be activated at early stages of VTP stimulation.

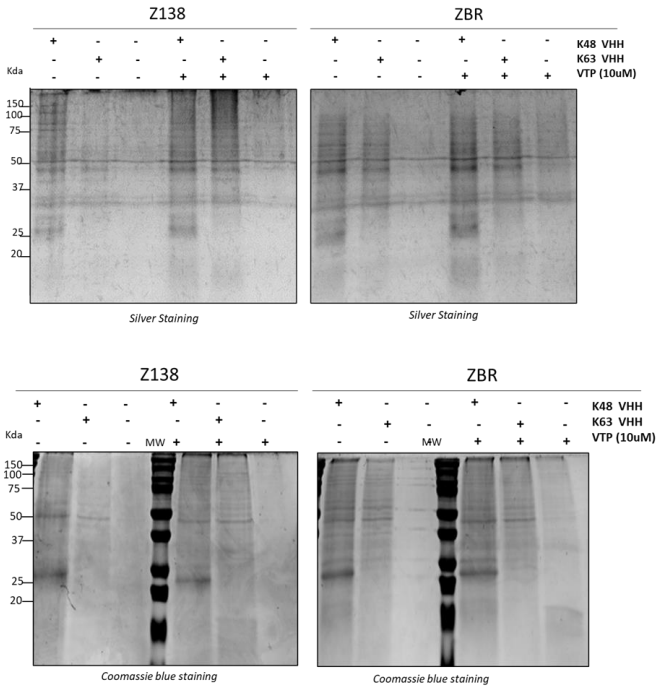

Figure 47: Capture of total proteins using K48 and K63 Ubiquitin chain-specific nanobodies from Z138 and ZBR treated or not with VTP. 40 million cells treated or not with 10uM of VTP for 2 hours were used. Nanobody precipitation of total proteins was performed with K48 (A4.1) and

K63 (D1.1) Ub chain-specific nanobodies. 1/20 of these fractions were submitted to WB analysis and stained with Silver or Coomassie staining. These samples were submitted for MS analysis.

We also stained the total amount of proteins precipitated with Coomassie blue and Silver staining to estimate the total amount of proteins submitted to MS analysis and to evaluate the background obtained only with the beads (Figure 47). Since the fraction loaded in these gels corresponded to 1/20 of the total capture, we could estimate that we submitted between 20-30 μg of total protein to MS analysis. The background level obtained with the control beads was low even if more easily detected by silver staining.

19.4 Mass Spectrometry analysis and Ubiquitin proteome using Ubiquitin chain-specific K48 and K63 nanobodies, from Z138 and ZBR cells.

Proteins purified using K48 and K63 Ub chain-specific nanobodies were analysed by MS to identify ubiquitylated proteins and interactors (proteome and interactome). Three independent replicates were performed to generate a statistically relevant analysis. Altogether this analysis allowed us to identify around 10,000 protein isoforms corresponding to 4,000 genes. A statistical and functional analysis was performed using a Gene Ontology (GO) analysis (http://geneontology.org/docs/go-enrichment-analysis/) and the R package limma.

We performed volcano plots for better visualise the results obtained from the different tested conditions. Proteins with a good level of significance are indicated as red dots in the graphics. Two steps thresholds were considered to guarantee a good level of significance: -log10 (p value) >1.3, and logFC >-1, >1. The top 10 most enriched proteins were indicated as well as proteins related to the Ub pathway (known substrates or E3 ligases).

Consistently with previous proteomic data obtained using the TUBEs-MS approach, basal levels K63 Ub modified proteins were more enriched in ZBR than in Z138 cells. These results can also be observed when comparing results obtained with both nanobodies (K48 vs K63). These analyses confirmed and added statistical significance to the enrichment of K63 substrates purified from ZBR cells at basal levels (Figure 48). Since these chains are implicated in autophagy, these results are coherent with an increased proteolysis mediated by this proteolytic pathway.

Our new MS results also support our previous proteomic study where TRIM24, TRIM28 and proteasomal subunits (such as PSMB2, PSMB10, PSMB9, PSMA6) were enriched in ZBR cells (Quinet et al, 2021). These proteins were detected when purifying ubiquitylated proteins from ZBR cells using K48 nanobodies compared to proteins precipitated using the K63 nanobody in the same cells.

In the ZBR cell line, the TRIM24 protein appears enriched in the Ub-K48 fraction (Figure 48). These results were confirmed in the previous section when using a K48 nanobody precipitation followed by WB analysis to detect TRIM24 (Figure 29). In contrast, MS results obtained in the BTZ-sensitive Z138 cells only detected TRIM24 when the K63 nanobody was used confirming our previous data (Figure 48). Using volcano plot analysis, we could confirm that in addition to TRIM24, factors implicated in proteaphagy were detected in unstimulated

ZBR cells including p62 and proteasome subunits (Figure 48). Altogether, our MS data obtained with K48 and K63 nanobodies confirm most of the results obtained using a TUBEs-MS approach such as Ub K63 chains enrichment, the presence of several enriched Ub E3 enzymes (eg. TRIMs) and support the previously proposed permanently activated proteaphagy in ZBR cells.

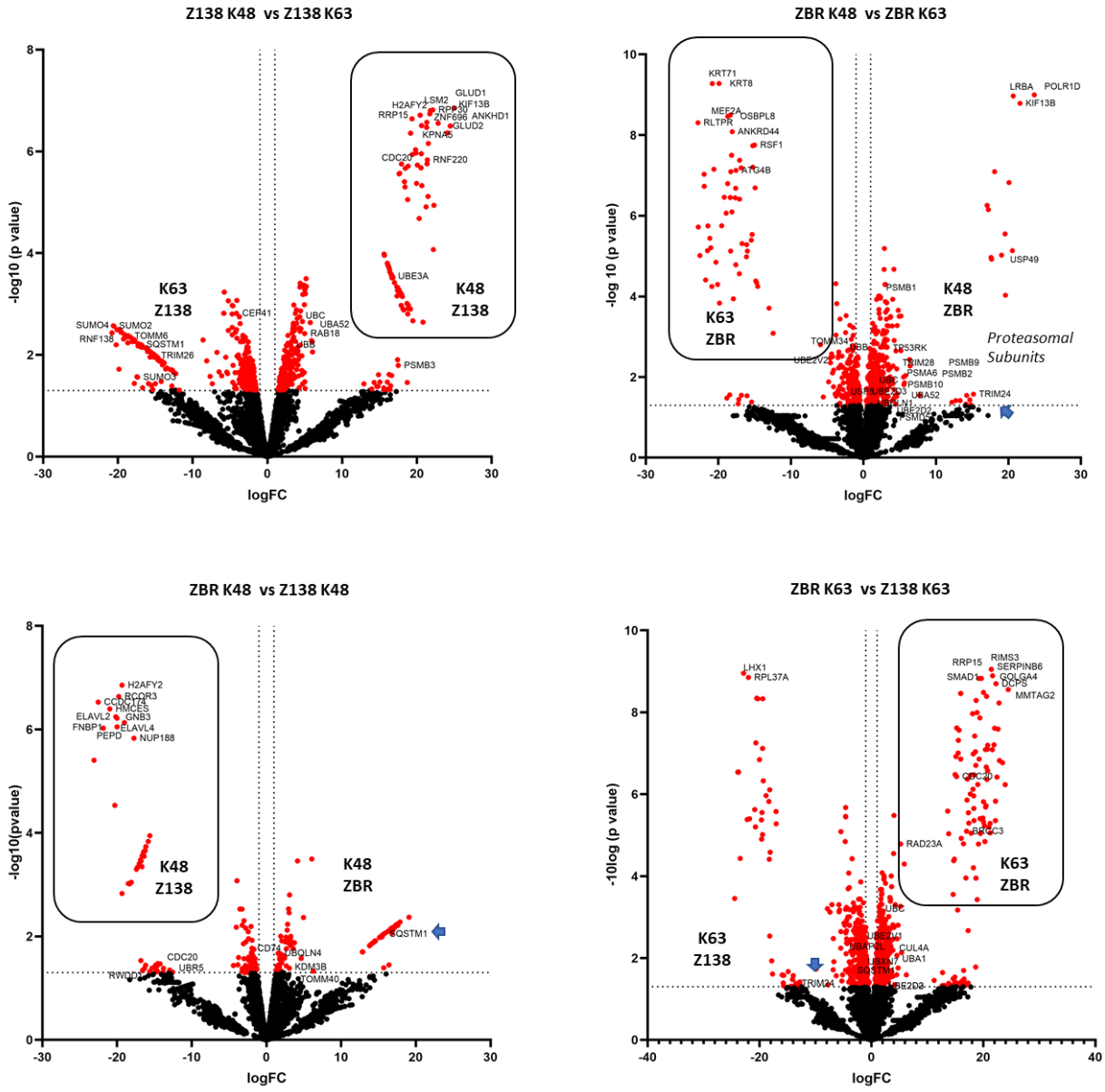

Figure 48: Mass spectrometry K48 and K63 Ubiquitin proteome profiling from Z138 and ZBR cells. Proteins identified were precipitated using K48 or K63 Ub chain-specific nanobodies from ZBR and Z138 cells. Volcano plot of enriched proteins identified using K48 or K63 nanobodies in both cell lines as indicated. Two thresholds in the volcano plots selected to guarantee statistic identification: -log10 (p value) >1.3, and logFC >-1, >1. Protein names represent the top 10 most enriched proteins or related to the Ub pathway such as proteasomal subunits and TRIM proteins.

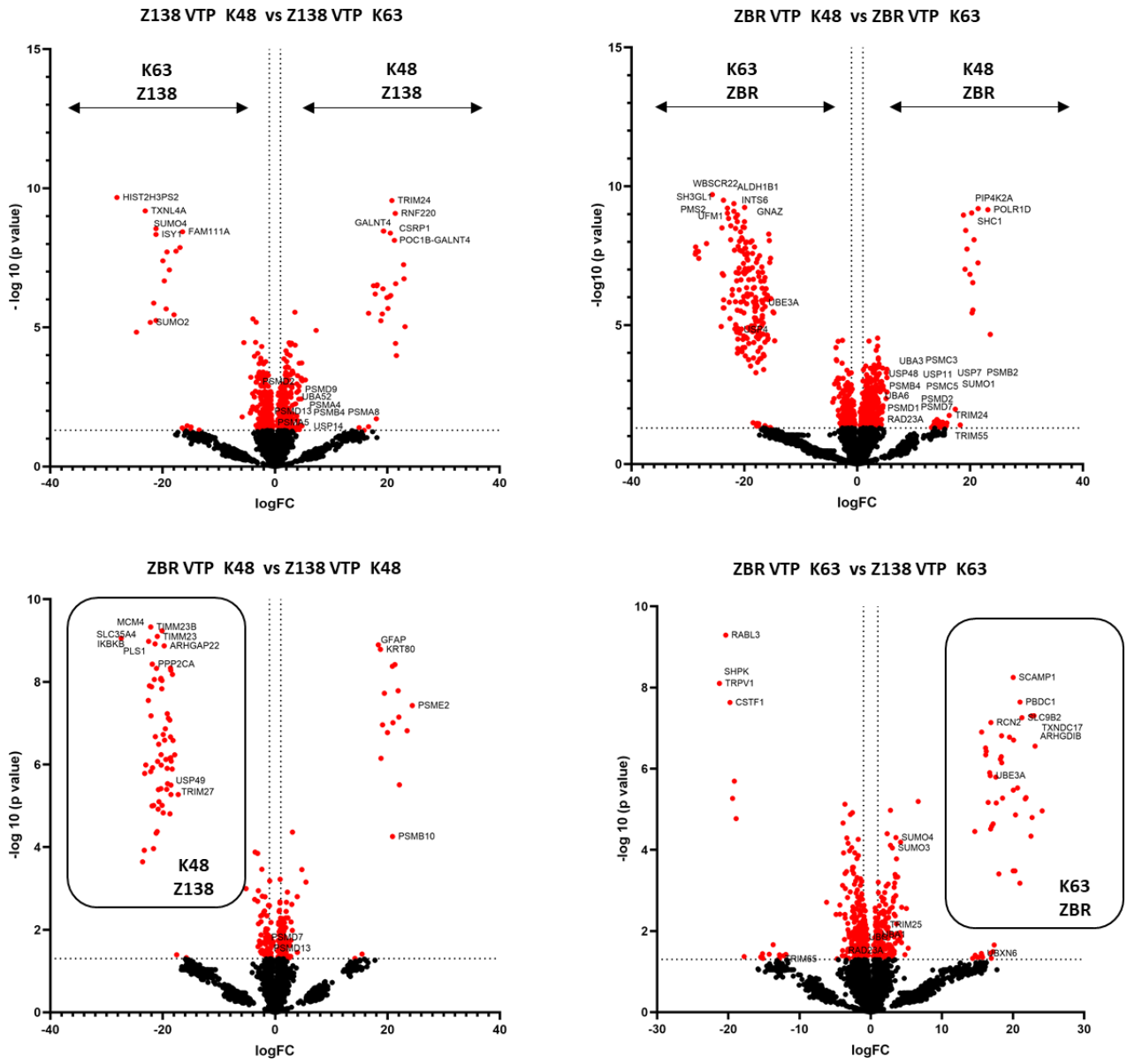

Figure 49: Proteome profiling of proteins identified my MS using K48 and K63 Ubiquitin Chain-Specific nanobodies from Z138 and ZBR cells stimulated with VTP. Volcano plot shows the enriched proteins identified. Two thresholds selected to guarantee the statistic identification: -log10 (p value) >1.3, and logFC >-1, >1. Names of the 10 most enriched proteins are indicated as well as cellular factors implicated the Ub pathway like proteasomal subunits and TRIM E3 ligases.

We also identified proteins enriched by K48 and K63 nanobodies from cells treated with VTP. The aim here was to better understand the mechanisms of action of this drug to identify the reason for a better apoptotic response in ZBR cells. Our results clearly indicate that while in Z138 an equilibrium between K48 and K63 modified proteins was observed after VTP treatment, in ZBR cells this balance was shifted to proteins modified with K63 Ub chains (Figure 49). This situation was also observed in ZBR cells at basal conditions (Figure 48).

A GO analysis allowed us to identify the cellular and molecular processes that were most enriched in Z138 and ZBR cell lines. These GO categories were integrated into a heatmap to easily observe proteins implicated in these processes. The log2FC scale illustrates proteins enriched in green and reduced in red. We selected some of the most interesting processes affected including proteins enriched under the explored experimental VTP response. Particular attention was dedicated to further characterize functions and proteins enriched or reduced in our ZBR cell line (Figure 50).

Consistent with the previous TUBEs-MS analysis performed in these cells, phagosome, endoplasmic reticulum, and proteasome proteins were enriched at basal levels in the ZBR cell line, when using the K63 nanobody (Figure 50, B). RNA transport, translation and amino acid synthesis appears to be also upregulated in this cell line, bringing new information about our BTZ-resistant phenotype.

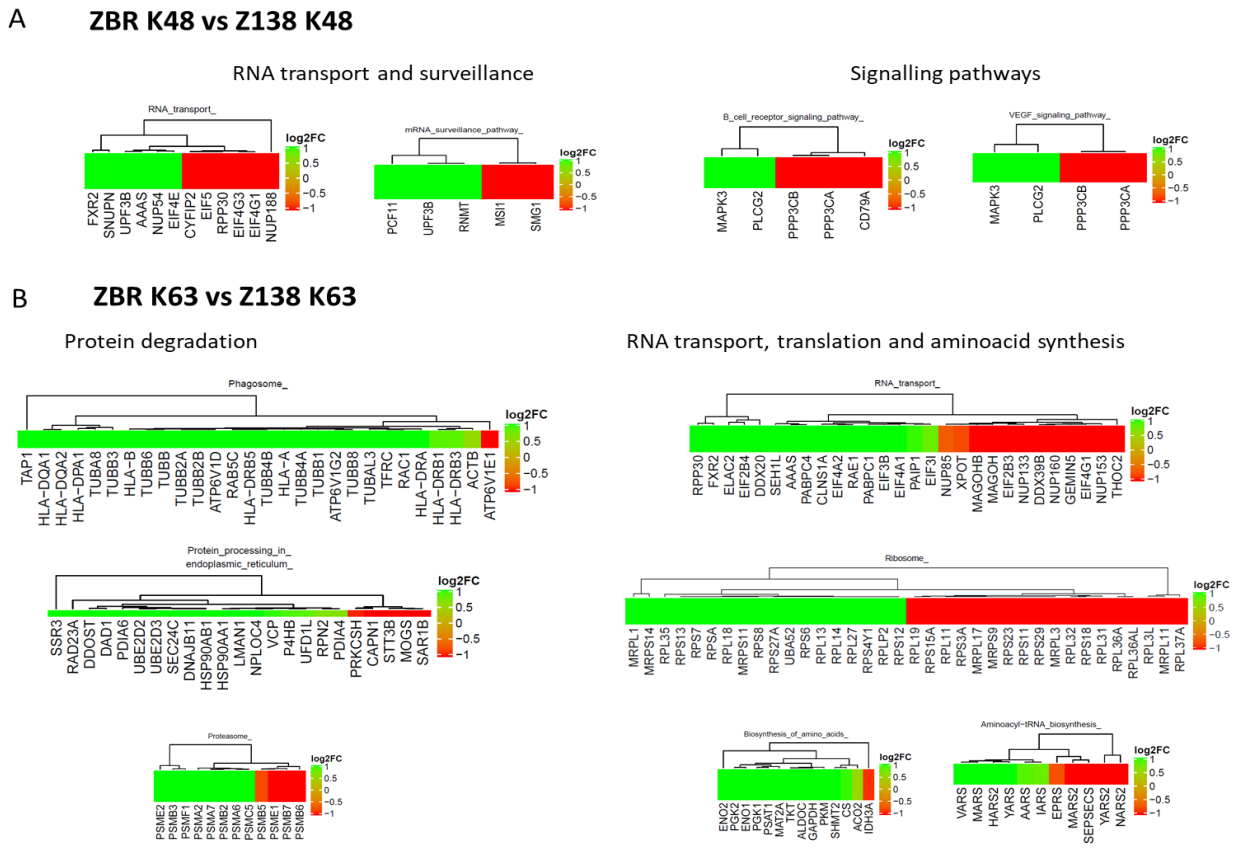

Figure 50: Heatmaps illustrating proteins enriched in ZBR unstimulated cells using K48 and K63 Ubiquitin chain- specific nanobodies. Some of the most interesting functions were integrated in heat maps. The most enriched factors were plotted in a log2FC scale where proteins in green were the most enriched and proteins in red the most reduced. The conditions compared in the heatmaps were A: ZBR K48 vs Z138 K48 and B: ZBR K63 vs Z138 K63 under basal conditions.

When VTP was used to treat ZBR and Z138 cells (Figure 51, A and B), proteins enriched by both nanobodies were completely different. We found ribosomes and endoplasmic

reticulum (ER) proteins reduced in the ZBR cells when using the K48 Ub chain-specific nanobody. These results could mean that the functions associated with ribosomes and ER are down regulated (Figure 51, A). We can speculate that after VTP treatment the functions affected in ZBR cells could be protein synthesis and ER-associated degradation (ERAD) that might contribute to establishing a new homeostatic equilibrium.

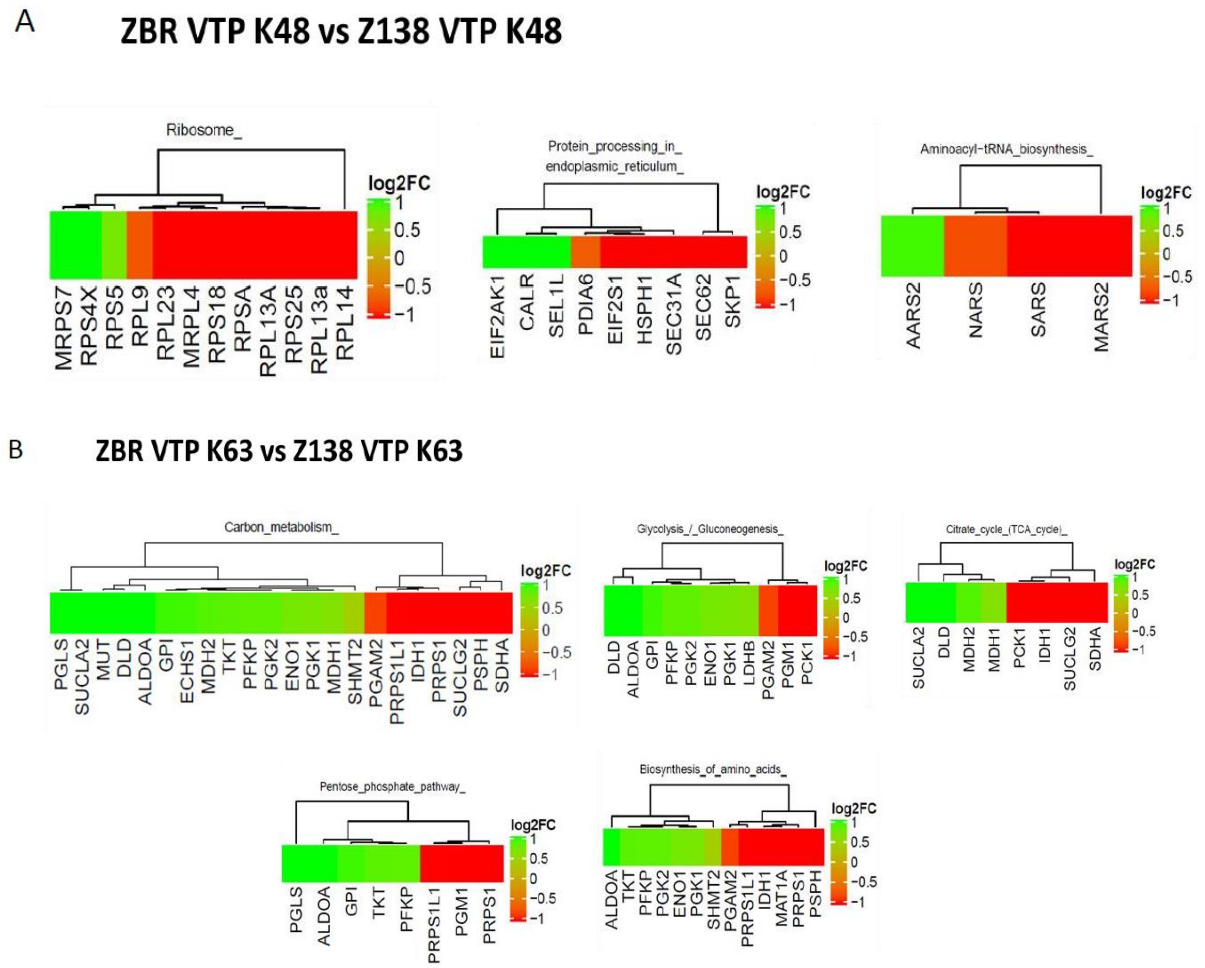

Figure 51: Heatmaps illustrating proteins enriched in ZBR cells stimulated with VTP using K48 and K63 nanobodies. Some of the most interesting functions were integrated in heatmaps. The most enriched factors were plotted in a log2FC scale where proteins in green were the most enriched and proteins in red the most reduced. The conditions compared in the heatmaps were A: ZBR VTP K48 vs Z138 VTP K48 and B: ZBR VTP K63 vs Z138 VTP K63.

When purifying K63 Ub chains from both cells treated with VTP, we observed an enrichment of proteins involved in metabolism in the ZBR cell line (carbon metabolism, glycolysis, and citrate cycle) (Figure 51, B). Surprisingly, when proteins purified using the K63 nanobody from cells treated or not with VTP, a drastic reduction in proteins related to metabolic pathways was observed in ZBR cells, more specifically those involved in glycolysis like ENO1, PGK1 and GAPDH (Figure 51, C and D). These results suggest that these pathways are involved in the response to VTP and could contribute to increase its apoptotic response.

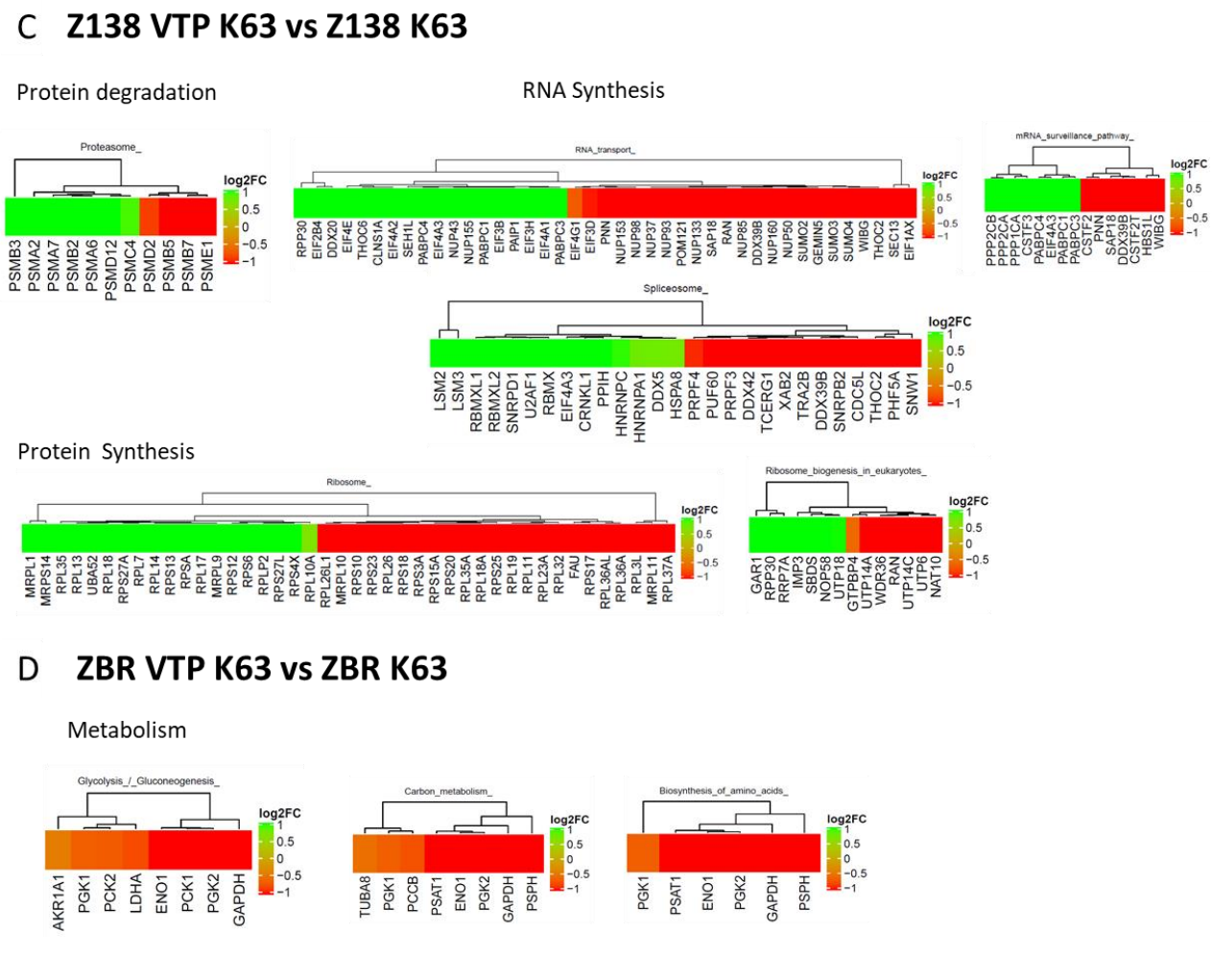

Figure 51: Heatmaps illustrating proteins enriched in ZBR cells stimulated with VTP using K48 and K63 nanobodies. Some of the most interesting functions were integrated in heatmaps. The most enriched factors were plotted in a log2FC scale where proteins in green were the most enriched and proteins in red the most reduced. The conditions compared in the heatmaps were C:Z138 VTP K63 vs Z138 K63 and D: ZBR VTP K63 vs ZBR K63.

To validate the results obtained with VTP, we performed precipitations with nanobodies to detect the proteins of interest (PGK1, ENO1 and GAPDH) by WB (Figure 52). Our results indicate that these glycolytic enzymes precipitated with both nanobodies at basal levels are more enriched in ZBR cells. After VTP treatment, these proteins were less enriched in ZBR, but the reductions appear to be more important when using K63 nanobodies to precipitate ubiquitylated proteins. Since GAPDH is affected by the VTP treatment, we used Vinculin as charge control and to normalize protein levels when quantifying our results (Figure 52). Altogether these results confirm our MS data and GO analysis.

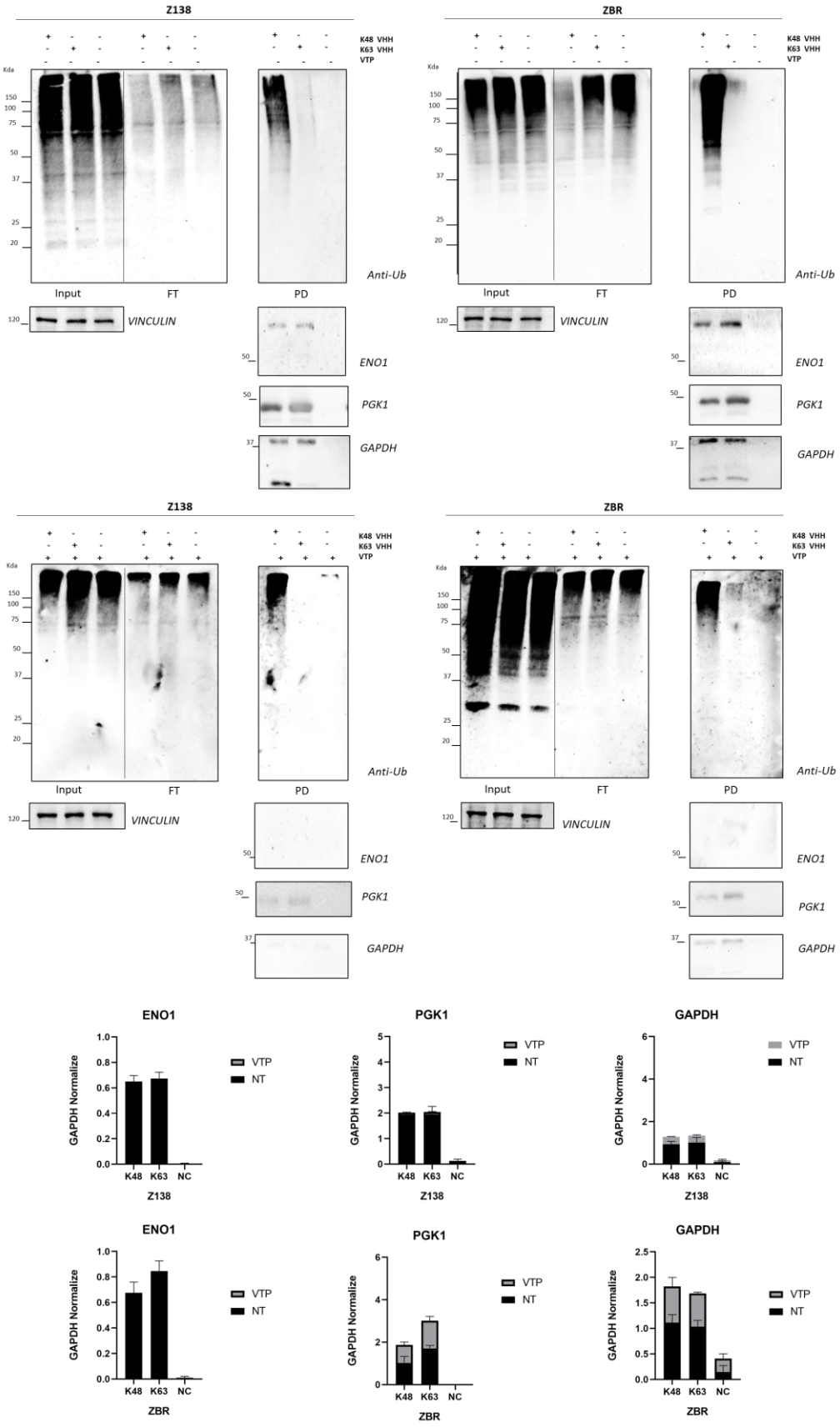

Figure 52: Validation of glycolytic enzymes decreased in the K63 Ubiquitin chain fraction purified from ZBR cells. 20 million Z138 and ZBR cells were treated or not with 10um of VTP for 2 hours. Total cell extracts were precipitated using K48 and K63 nanobodies. Input, FT and PD (nanobody precipitation) fractions were analysed

by WB with anti-Ub antibody, input fraction with Vinculin for normalisation and PD fraction with the indicated antibodies (ENO1, PGK1 and GAPDH). For the quantifications, Vinculin was used to normalise values. Graphics were made using GraphPad Prism Software. Negative control (NC) values were efficiently low, and nanobody signal was displayed in the graphics for a better visualisation of how much of the total amount of protein identified is coming from K48 or K63 chain-specific nanobody after VTP treatment or no treatment (NT) conditions.

20. Discussion.

20.1 UPS/ALS dysregulation in Mantle Cell Lymphoma: proteaphagy contribution to BTZ resistance.

The disruption of the homeostatic protein equilibrium and Ub chain remodelling have been linked to different pathologic situations affecting DNA repair, activation of NF-κB pathway or autophagy, to cite some examples (Gonzalez-Santamarta et al.,2022). Multiple diseases have been associated to deletions, translocations and mutations affecting Ub chain synthesis, deconjugation and chain recognition, altering the proper regulation of different functions. However, the clinical relevance of these PTMs must be better understood before developing new possibilities for therapeutic intervention.

This project used BTZ-sensitive Z138 and BTZ-resistant ZBR MCL cell lines as major models. They were developed in the laboratory after BTZ exposition, to be able to compare cells with the same genetic background in order to identify molecular changes acquired after Z138 cells became resistant to BTZ (Roué et al., 2011).

This project started by exploring some of the results obtained with the comparative proteome analysis performed to study differences in ubiquitylation profiles between Z138 and ZBR cell lines (Figure 15 and 16). This analysis revealed important alterations in the UPS and the ALS, suggesting a dysregulation between these two degradative pathways, as well as changes in the general ubiquitylation distribution such as an enrichment of K63 Ub chains in ZBR cells. Different Ub enzymes were also identified as enriched in ZBR cells, and their possible role if any in the BTZ-resistant phenotype has been explored in this project.

Recently, Quinet et al. reported a permanent activation of proteaphagy in ZBR cells that could allow to develop new therapies for patients not responding to PI by targeting autophagy (Grégoire Quinet et al, 2021). In this context, the autophagy receptor p62 showed to be a key player (Cohen-Kaplan et al., 2016; Quinet et al., 2021), as p62 targeting with VTP significantly enhance the response of BTZ-resistant MCL cells to BTZ (Figure 17, B) (Quinet et al. 2021). However, the nature of the Ub chains implicated in this apoptotic response and Ub enzymes regulating proteaphagy needs to be deeply investigated.

Our research project allowed us to provide evidence supporting a major role of Ub enzymes, in particular the role of the TRIM24 Ub ligase in the control of protein homeostasis and Ub chain composition in ZBR cells. We also contributed to the development of new molecular tools for the enrichment and analysis of the ubiquitome. Using these tools, we validated previous information while bringing new findings that open considerable possibilities to

further investigate the phenotype of BTZ resistance in MCL cells. All this evidence, its relevance and scientific background will be discussed in the following sections.

20.2 TRIM24 involvement in UPS-ALS crosstalk in BTZ-resistant cells.

Recent reports have shown that several TRIM proteins are involved in autophagy regulation, as they can act as autophagy receptors or regulators of autophagy formation. Hatakeyama also suggests that each of these TRIM proteins may have a unique non-redundant roles in autophagy, not being able to function by compensation between them. However, sophisticated biochemical and genetic assays are needed to differentiate specific roles in autophagy for each TRIM protein, specifically in mammalian models as its ancestor or equivalent in yeast has not been discovered (Hatakeyama, 2017).

Since TRIM24 was found enriched in ZBR cells (Figure 21), we investigated the contribution of this enzyme to the development or regulation of the BTZ-resistant phenotype in these cells. In addition, we explored the possible implications of the TRIM24 protein in autophagy regulation and BTZ sensitivity in our model. Our results indicate that TRIM24 is playing a major role in the UPS-ALS crosstalk in ZBR cells with implications at the level of total ubiquitylation, regulation of autophagy and sensitivity to BTZ.

- **TRIM24 stability and localisation in Z138 and ZBR cells.**

TRIM24, also called transcriptional intermediary factor 1α (TIF1 α), is a multidomain protein that has been described to be a co-regulator of transcription, a nuclear histone PTM reader (epigenetic reader) that binds to chromatin through its PHD and bromo domains (Appikonda et al., 2018). Additionally it has been described to be a negative regulator of p53 as it behaves as a E3 Ub ligase mediating its ubiquitylation (Jain et al., 2014). In fact, Jain et al, showed a TRIM24 p53 regulation independently of MDM2 (first identified E3 Ub ligase for p53), in which TRIM24 activates p53 in response to DNA damage through an autoregulatory loop where TRIM24 undergoes ubiquitylation-mediated degradation in the nucleus, mediated as well by phosphorylation of S786 by ATM kinase (Jain et al., 2014).

Considering the possible implications of TRIM24 in different functions related to different cancer types, we first investigated TRIM24 stability and localization at basal levels, but also upon proteasome (BTZ) or autophagy inhibition (BafA).

We observed striking differences in TRIM24 stability between Z138 and ZBR cells. At basal levels, higher protein levels of TRIM24 were found in ZBR compared to Z138 cells, confirming the data obtained in the initial proteome analysis (Figure 23). Used as individual or combined treatments, proteasome or autophagy inhibitors accumulated TRIM24 only in Z138 cells. Since the accumulation is even more important with the double treatment, our results suggest that this Ub E3 is simultaneously regulated by both proteolytic pathways in sensitive cells. In sharp contrast, BTZ, BafA or the combined treatment decrease TRIM24 levels in ZBR cells.

Under the same experimental conditions, p62/SQTSM1 was accumulated in ZBR cells suggesting that the reduction of TRIM24 levels could be linked to a disruption of the autophagy flux promoting p62 accumulation (Figure 23). Interestingly, a reduction of TRIM24 was also observed by IF after BTZ, BafA or the combined treatment in ZBR cells. However, no TRIM24/p62 co-localisation was found under these conditions, suggesting that p62 might not be a direct target or interactor for this Ub E3 enzyme.

We also found that the stability and localisation of TRIM24 in the MCL-unrelated HeLa cell line was similar to the one observed in Z138 cells (Figure 22). Our results strongly suggest that the reduced stability and localisation of TRIM24 found in ZBR cells was linked to the BTZ-resistant phenotype.

When analysing in detail, the TRIM24 protein was more enriched in the cytoplasm of ZBR cells as indicated in the nuclear/cytoplasmic fractionation assay and the concurrence analysis performed with the IF images (Figure 25). Nevertheless, IF analyses for these suspension cells must be optimised to analyse the intensity of the staining using stacking and higher resolution techniques.

TRIM24 was found in cell lines like U2OS and HEK293T mainly in the nuclear fraction, possibly due to its capacity to bind to chromatin and heterochromatin-associated factors through its PHD and bromo domain. In this subcellular compartment, it is supposed to mediate DNA damage response by regulating p53 ubiquitylation through its E3 domain (Jain et al., 2014). TRIM24 staining in the nucleus was found in prostate cancer cell lines, indicating that even in pathological conditions this protein still localises predominantly in the nucleus. In this context, TRIM24 is enhancing tumorigenesis acting as a transcriptional co-activator recruiting and activating STAT3, functioning as a signal relay for oncogenic signalling (Fong et al., 2018). In addition, TRIM24 has been described in prostate cancer to enhance transcriptional activity of AR (Androgen Receptor) (Kikuchi et al., 2009), indicating a strong role of this protein in the nucleus. Our observations indicating a basal enhanced cytoplasmic localisation of TRIM24 in ZBR MCL cells has not been described in any other models. Nevertheless, TRIM24 translocation from the nuclear compartment to the cytoplasm has been described upon virus infection in HEK293T cells to activate the antiviral signalling response. In this scenario, TRIM24 binds TRAF3 to mediate its K63 ubiquitylation, highlighting the importance of understanding the E3 role of this protein (Zhu et al., 2020).

Taking this information into account, we focused on understanding the possible role of TRIM24 in the cytoplasm of ZBR cells in order to identify mechanisms regulating BTZ resistance. Can TRIM24 act by mediating K63 ubiquitylation events in the cytoplasm of these cells, upregulating autophagy and therefore promoting BTZ resistance? This question will be addressed in the next sections.

- **TRIM24 PROTAC treatment sensitises ZBR cells to BTZ.**

TRIM proteins are characterised by a N-terminal containing the RING domain, one or two zinc-finger domains named B-boxes, and a coiled-coil region usually related to TRIM homo-oligomerization and activation. In addition, at the C-terminus different kinds of domains

have been reported, like the Bromodomain (BROMO) observed in TRIM24, TRIM28 and TRIM33. These proteins are classified in seven subfamilies sharing the C-terminus domain (Hatakeyama, 2017; Mandell et al., 2020). Nevertheless, not all known TRIM proteins (80 in the human genome) (Mandell et al., 2020) have a RING domain, and eight RING-less TRIM proteins have been described.

Like TRIM24, TRIM28 is a bromodomain TRIM E3 ligase that negatively regulates p53 by its ubiquitylation, also found upregulated in different cancer types. In addition, TRIM28 has been described by Peng et al. to have a positive role in autophagy and cancer proliferation, promoting enhanced proliferation in glioma tumour cells as a consequence of its upregulation (Peng et al., 2019). Although TRIM24 shares evident similarities with TRIM28 regarding protein domains and regulated functions, its possible role in autophagy has not been addressed in any cell model supporting our encouragement to characterise the role of this protein in our BTZ-resistant phenotype, and possible involvement in autophagy.

To investigate if TRIM24 could contribute to regulate cell survival in BTZ-resistant cells, a validated proteolysis targeting chimera (PROTAC) targeting TRIM24 (dTRIM24) was used (Gechijian et al., 2018). Knowing that the levels of TRIM24 are distinct in both cell lines, different and increasing concentrations of dTRIM24 were tested to select the best doses to effectively reduce TRIM24 levels in both cell lines (Figure 26, A and B). This test is particularly important because it is well-known that this type of bivalent therapeutic molecules work efficiently only when there is an equilibrium between the 3 partners collaborating in this scenario: the PROTAC molecule interacting with both the targeted protein and the Ub ligase. If low concentrations of PROTAC are used, the drug is not efficient and could mainly form dimers with either the target or the enzyme. However, if too much PROTAC is used the formation of dimers can also be favoured and the therapeutic molecules are not efficient. This effect is known as “the hook effect” and has been reported for many PROTACs (An and Fu, 2018; Gu et al., 2018).

Since the level of TRIM24 is not the same in Z138 and ZBR cells, the concentration/dose selected could be more efficient to inactivate TRIM24 in one but not in the other cell line. After several experiments, we selected the dose of 10uM dTRIM24 as the more effective one to deplete TRIM24 in both Z138 and ZBR cell lines. Nevertheless, this treatment could be more efficient in one or the other cell line on some occasions and give variations in the results obtained. For this reason, we generated a TRIM24 KO cell line to better evaluate the TRIM24 contribution in ZBR cells. This cell line would give us more reproducible results while providing the tool to validate the specificity of this PROTAC treatment. Unfortunately, different TRIM24 KO clones were still under sequencing at the time of writing this thesis report.

We used two distinct methods to analyse the impact of dTRIM24 on apoptosis, one by analysing cleaved caspases 3 and 9, and the other by quantifying Annexin 5 by flow cytometry (Figure 26, C and D). The increased level of cleaved caspases indicated a proper apoptosis induction. However, not significant differences were observed between sensitive and BTZ-resistant cell lines in the FACS analysis, indicating the same apoptotic response for both cell lines (Z138 and ZBR).

We then explored if the depletion of TRIM24 in our BTZ-resistant cells could re-sensitise resistant cells to BTZ treatment. We tested the combined dTRIM24/BTZ treatment in both Z138 and ZBR cells, and measured apoptosis by FACS analysis after 24h treatment. We observed that the double treatment significantly enhanced apoptosis in ZBR cells (Figure 27, A). Indeed, the combinatorial index when using both inhibitors was lower than 1.0 in ZBR cells compared to Z138 cells, indicating a synergistic effect in the BTZ-resistant cells instead of an additive effect corresponding to the BTZ-sensitive cell line (Figure 27, B). Therefore, the inhibition of TRIM24 appears to increase the sensitivity to BTZ in ZBR cells, suggesting a participation of this Ub E3 ligase in this apoptotic context.

- **Is TRIM24 a positive regulator of autophagy?**

Since the combination of dTRIM24/BTZ enhanced apoptosis in ZBR cells, it was decided to investigate the molecular mechanisms implicated in this sensitivity and enhanced apoptosis. We explored how this combination could impact the crosstalk between both proteolytic pathways (UPS/ALS) while contributing to explain the cell killing effect in ZBR cells.

Since we knew that there is a permanently activated proteaphagy in ZBR cells, we investigated if this selective autophagy was implicated in the enhancement of apoptosis after the combined dTRIM24/BTZ treatment. To explore this hypothesis, we analysed the level of autophagy markers p62 and LC3B, well-known indicators of autophagic activity (Klionsky et al., 2016), proteasome subunits (β2 and β5) (Quinet et al., 2021) and p53 (Jain et al., 2014) after dTRIM24 treatment. As a single treatment, dTRIM24 modestly but consistently accumulated autophagy markers LC3B, p62 in ZBR and Z138 cells. The accumulation of autophagy markers was commonly observed when autophagy inhibitors such as BafA or CQ were used in ZBR and Z138 cells (Quinet et al., 2021), suggesting that dTRIM24 acts as an autophagy inhibitor. This evidence suggests that TRIM24 is playing a role of positive regulator of autophagy, maybe by promoting the formation of Ub chains linked to autophagy activation (see next section). The dTRIM24 treatment also accumulated p53 that could favour its tumour suppressor activity. Interestingly, when combined with BTZ treatment, TRIM24 depletion favoured the decrease of autophagy markers, as well as the corresponding proteasomal subunits analysed. This reduction could be due to compensatory mechanisms such as effects at transcriptional levels (Groner et al., 2016, 2016; Lv et al., 2017), changes in proteasome subunits composition, or crosstalk with other proteolytic or signalling pathways (Quinet et al., 2021), options that we did not explore. However, since the double treatment reduced proteasome levels, this could explain the high accumulation of p53 (a typical UPS-target) and apoptosis improvement after dTRIM24/BTZ combination (Figure 28).

Even if the qualitative analysis of p53 by WB did not show differences in the accumulation of this tumour suppressor found in Z138 and ZBR cells, the apoptosis observed in ZBR was more efficient with the dTRIM24/BTZ treatment, suggesting that TRIM24 may have additional consequences in these BTZ-resistant cells.

- **TRIM24 as coordinator of ubiquitin-regulated functions in BTZ-resistant cells.**

We investigated how distinct Ub chains could be formed in ZBR cells to further understand how TRIM24 can regulate proteaphagy and perhaps other functions in these BTZ-resistant cells. Since we knew that the level of K63 chains was more abundant in ZBR, our first hypothesis was that a dTRIM24 treatment could contribute to reduce these chains in these cells.

After a TRIM24 depletion in both cell lines, K48 and K63 Ub chains were purified using Ub chain-specific nanobodies (K48 and K63 nanobodies). To our surprise, both K48 and K63 chains were increased after the dTRIM24 treatment only in ZBR cells indicating that the presence of this Ub E3 may contribute to controlling the formation of both Ub chain types in those BTZ-resistant cells. However, since the amount of K48 Ub was more abundant than K63 chains after dTRIM24 treatment, we can speculate that the depletion of TRIM24 is favouring Ub chain balance towards K48-mediated functions in ZBR cells. By affecting the Ub chain balance, dTRIM24 would favour proteasome-mediated proteolysis while the less abundant K63 chains would not favour the activation of autophagy/proteaphagy. If this hypothesis is true, TRIM24 would be an activator of autophagy under conditions where the proteasome is impaired but also a major coordinator of the UPS-ALS crosstalk by regulating the abundance of distinct Ub chains (Figure 30).

Supporting this hypothesis, we found that when the dTRIM24 treatment blocks autophagy, more p62 and proteasome subunits are captured with both K48 and K63 nanobodies. The association of the catalytic β5 proteasome subunit with both chains was more important in ZBR cells, suggesting that this particular subunit could be regulated by TRIM24. Evidence that proteasome complexes can be regulated in a different way after distinct stress signals such as proteasome inhibition (Marshall et al., 2015; Nemec et al., 2017; Welk et al., 2016), supports the possibility that complexes containing β5 subunits that are insensitive to BTZ could be the first ones targeted to proteaphagy. However, further investigations are required to have clear conclusions about the regulation of distinct proteasome complexes affected by proteaphagy in cells that do not respond to proteasome inhibition.

Which other functions can be affected by the massive ubiquitylation changes observed after dTRM24 treatment? The one that immediately comes to our mind is p53 which is a known target of this ligase (Jain et al., 2014). Indeed, our evidence indicates that this treatment alone accumulates p53 in ZBR cells. However, this accumulation is not that visible in Z138 cells suggesting that perhaps other Ub E3 ligases could compensate p53 degradation in these cells. Nevertheless, the combination of dTRIM24/BTZ cooperates in the accumulation of p53 in both Z138 and ZBR cells (Figure 28).

With such a massive accumulation of K48 and K63 Ub chains in ZBR cells, it is likely that other TRIM24 targets not yet identified could be affected after dTRIM24 treatment. Further investigations are required to better understand the role of TRIM24 in BTZ-resistant cells beyond our MCL models.

Other functions that can be affected by the dTRIM24 treatment involve co-regulation of transcriptional activation. The TRIM24 upregulation mediates tumorigenesis in glioblastoma

through the activation of STAT signalling (Lv et al., 2017). These authors also described that although TRIM24 does not directly bind to the p65 subunit of the nuclear factor κB (NF-κB), TRIM24 significantly alters the expression of NF-κB target genes. Other studies involving viral infection describe TRIM24 to regulate RNA virus–induced activation of IFN-I signalling, without affecting NF-κB or MAPK activation (Zhu et al., 2020). However, TRIM24 has been widely described as a promotor of tumorigenesis (Groner et al., 2016; Lv et al., 2017).

Other TRIM proteins have been reported as regulators of the NF-κB signalling pathway, like TRIM22 known to activate two critical regulators of NF-κB signalling in glioma cells, by mediating K48 ubiquitylation on the NF-κB inhibitor alpha (IκBα), and K63 ubiquitylation on the NF-κB upstream regulator IKKγ (Ji et al., 2021). In addition, in the endoplasmic reticulum, TRIM13 enhances NF-κB activity through selective regulation of p65 and c-Rel (NF-κB family members) (Hatchi et al., 2014).

Altogether, our results indicate that the UPS/ALS crosstalk can be targeted by regulating TRIM24 levels and/or activity when combined with BTZ. This treatment will compromise the activity of both autophagy and proteasome and at the same time increase the level of the tumour suppressor p53 to ultimately promote cell death. Since the NF-κB signalling pathway appears to play an important role in the BTZ response, understanding the possible involvement of TRIM24 in NF-κB signalling will be important as well to fully explore the therapeutic potential of this protein in the context of PI resistance.

- **Is TRIM24 an indirect regulator of p62?**

p62 ubiquitylation and expression has been observed after proteasomal inhibition with BTZ in HeLa or 293FT cells after autophagy activation. In addition to PI, upon Ub stress or heat shock, p62 undergoes an E2-dependent ubiquitylation disrupting the dimerization of the UBA domain of p62, liberating its ability to recognize polyubiquitylated cargoes for selective autophagy being critical for autophagy activation (Peng et al., 2017; Sha et al., 2018). In addition, p62 can be a target for proteasomal degradation. Song et al. reported Parkin as a new E3 ligase modifying p62 mediating its proteasomal degradation, while describing Parkin/p62 axis dysregulation at the onset of Parkinson pathogenesis (Song et al., 2016). Interestingly, p62 ubiquitylation on lysine 435 by the UBE2J1/RNF26 complex has been quite recently related to an endosomal reorganization promoting downregulation of Akt signalling (Cremer et al., 2021). p62 ubiquitylation on specific sites can promote selectivity towards different cellular functions, highlighting the multifunctionality of this autophagy receptor under normal/basal and stress conditions.

Our results indicate that TRIM24 could be a Ub ligase directly or indirectly regulating p62 stability since the dTRIM24 treatment increases the level of p62, more importantly in ZBR cells. However, our IF results did not show co-localisation of TRIM24 and p62 at basal levels but also after proteasome or autophagy inhibition suggesting that this ligase does not act directly on p62 (Figure 24). Further experiments with transfected cells and/or in vitro reconstitution approaches with purified proteins should help to confirm these observations.

How can the depletion of TRIM24 affect p62? There are various possible mechanisms that

could affect p62 stability. It could first limit the formation of K63 and/or K48 chains to regulate its activity as autophagy receptor (Peng et al., 2017) but also by regulate its proteasomal degradation (Song et al., 2016). A second possibility is that TRIM24 could be regulating other Ub ligases or complexes conditioning the activity of the ALS and/or UPS. Supporting this last possibility, it has been proposed that TRIM ligases can coordinate autophagy by forming the TRIMosome, a complex binding different autophagy regulator proteins like p62, Beclin1 or ULK1 (Hatakeyama, 2017). Further investigations are necessary to better understand the specific mechanism by which TRIM24 regulates Ub chains, p62 and proteasome stability in ZBR cells.

- **TRIM24 and its interaction with other TRIM E3 ligases.**

Due to the high number of processes involving TRIM proteins, it is not surprising that their targeting has been suggested for multiples disorders, like cancers, allergies, inflammation, and carcinogenesis (Valletti et al., 2019).

Since TRIM proteins have multiple active domains, they show an elevated multifunctionality. In addition, TRIMs are subjected to multiple regulation mechanisms by interaction with different proteins or substrates, including other TRIM proteins. Growing evidence highlights the existence of a crosstalk between TRIM family proteins (Mandell et al., 2020).

As previously mentioned, TRIM24 collaborates with other TRIM proteins to regulate protein substrate stability and activity. In this way, TRIM24 and TRIM28 contribute to control p53 function. However, while TRIM24 directly targets p53 ubiquitylation, TRIM28 mediates the same outcome through its interaction with MDM2. Other TRIM proteins have been identified to module the stability of this tumour suppressor by their E3 ligase activity such as TRIM11 and TRIM25 (Valletti et al., 2019). However, since TRIM11 and TRIM25 are RING-less ligases, this questions the necessity to have this domain to regulate p53. The functional roles of TRIMs can be diverse as they can act at different steps in the p53 pathway and show cooperative effects. Because of the multiple contribution of TRIMs on the regulation of this tumour suppressor, the TRIM-p53 axis has been proposed and considered as a good strategy to better understand chemoresistance and to increase effectiveness of anticancer therapies (Hatakeyama, 2017; Valletti et al., 2019).

Our results show that the dTRIM24/BTZ treatment enhanced the apoptotic response in ZBR cells, likely by impacting autophagy and p53 stability. However, to fully elucidate p53 dependency, further investigations will be required using the same genetic background but with an inactivated p53. Because of that, we are currently performing experiments with a large collection of BTZ-resistant MCL cells to validate this hypothesis. We do have a couple of cell lines, JEKO and the BTZ-resistant counterpart JBR, where p53 is mutated (Amin et al., 2003). These cell lines will be used to explore the p53-dependency on the cell killing effect induced by dTRIM24/BTZ in BTZ-resistant MCL cells. This information will be crucial to propose TRIM24 targeting-based strategy to re-sensitise MCL cells to BTZ treatment.

One important aspect that we did not explore in this study is the impact of the dTRIM24 treatment on the stability of other bromodomain proteins like TRIM28 and TRIM33. These

TRIM proteins have been described in the literature to regulate autophagy (Mandell et al., 2020). Since our PROTAC targets TRIM24 through its bromodomain, this strategy could have a direct or indirect impact on TRIM28 or TRIM33 stability and function, contributing to modulate the autophagy pathway in our ZBR model, a hypothesis already suggested by Mandell et al. (Mandell et al., 2020).

In addition, an indirect effect of dTRIM24 on TRIMs could be obtained by affecting interactions mediated by TRIM dimerization events, typically observed between TRIM proteins. The functionality of TRIMs can also be modulated by other PTMs like SUMOylation, and NEDDylation (Valletti et al., 2019). TRIM24, TRIM28 and TRIM33 have been identified as strong SUMO1-interactors using a new innovative SUMO-ID technology, being localised at the nucleus of U2OS inside PML also called nuclear bodies (Promyelocytic Leukemia Nuclear Bodies). PML are membrane-less ring-like protein structures found in the nucleus usually associated with transcriptionally active genomic regions. The composition of this structure is still under discussion and believed to be highly heterogeneous depending on the cellular status or stress condition (Barroso-Gomila et al., 2021). Other SUMO-proteome studies have also found these TRIM proteins SUMOylated after IFNα response regulating antiviral response (Chelbi-Alix and Thibault, 2021).

A full view on the regulation of TRIM ligases involving not only Ub modifications but also SUMO has already suggested for acute myeloid leukemias (AMK) (Gâtel et al., 2020).

- **TRIM24 as a potential therapeutic target in cancer.**

The aberrant expression of TRIM24 has been associated with different cancer types, and has been proposed to be a good cancer prognostic factor, usually correlated with increasing proliferation, oncogenic transformation, aggressive malignant phenotypes (Groner et al., 2016; Li et al., 2012, 2012; Liu et al., 2014; Tsai et al., 2010; Zhang et al., 2015). It has also been found to mediate chemo-resistant mechanisms in gastric cancer and glioblastoma (Miao et al., 2015; Zhang et al., 2015).

So far, TRIM24 aberrant expression has been directly associated with prostate cancer by acting as a oncogenic transcriptional activator (Groner et al., 2016), with breast cancer used as a good prognostic marker (Chambon et al., 2011; Tsai et al., 2010), with the onset of hepatocellular carcinoma trough AMPK signalling upregulation (Liu et al., 2014; Zhu et al., 2018), with tumour progression in non-small cancer cell lung carcinoma (Li et al., 2012), in neck squamous cell carcinoma (Cui et al., 2013), in glioblastoma (Lv et al., 2017), in colorectal (Wang et al., 2017), and cervical cancer (Lin et al., 2017). It has also being directly related to resistance in glioma and gastric cancer by the regulation of the Akt signalling pathway (Miao et al., 2015; Zhang et al., 2015), to name a few examples.

It is important to highlight that TRIM24 is involved in these different cancer types through different mechanisms, therefore showing the importance of TRIM24 as a multifunctional protein, and the need to identify their specific functions depending on the cell type and specific biological context.

Evidence presented here suggests that tackling TRIM24 will have a negative impact on the permanently activated autophagy observed in ZBR cells. This new equilibrium will reduce proteaphagy and contribute to recovering sensitivity to BTZ. Our results show that the dTRIM24/BTZ treatment enhanced the apoptotic response in ZBR cells not only by inhibiting autophagy but also by stabilizing p53. Therefore, TRIM24 can be proposed as a potential target in the context of PI resistance.

20.3 p62 targeting strategy to overcome BTZ resistance

p62 has been proposed as a target to develop new cancer therapies, since it behaves as an oncoprotein usually upregulated in cancer (Yan et al., 2017).

Since proteaphagy was found to be permanently activated in BTZ-resistant MCL cells, several autophagy inhibitors like BafA and CQ provided interesting results (Quinet et al., 2021). However, the most efficient treatment to recover BTZ sensitivity in cell cultures and *in vivo* xenografted models was verteporfin (VTP), that targets p62. These results highlighted the major role of p62 in recognising proteasomal subunits that will be targeted to autophagy degradation (proteaphagy), but also the relevance of this process in BTZ-resistant phenotypes. Since the number of p62 inhibitors available is limited, we have explored an alternative molecule in this project, XRF3F2 that specifically targets the ZZ domain of p62. The results obtained in this double effort will be discussed in the next section.

- **VTP, a successful treatment to enhance apoptosis in BZT-resistant cells.**

VTP is known to promote the formation of p62 aggregates through its PB1 domain (Donohue et al., 2011, 2014) This aggregation alters the p62 surface that binds ubiquitylated substrates therefore hampering its function as an autophagy receptor. Our group generated evidence indicating that VTP impairs proteaphagy, that in the context of BTZ resistance was described as a cytoprotective mechanism upon BTZ treatment (Quinet et al., 2021). The use of VTP recovered sensitivity of BTZ-resistant cells. However, since VTP has been described to generate ROS (Donohue et al., 2014; Konstantinou et al., 2017), we investigated if the silencing of p62 alone was sufficient to block autophagy and promote apoptosis in combination with BTZ. Our results showed that the silencing of p62 increased the BTZ-induced apoptosis of ZBR cells (Figure 31), indicating that p62 was indeed an interesting molecule to inactivate to recover sensitivity to this PI.

Even if our evidence suggested that the silencing of p62 was sufficient to improve apoptosis after BTZ-treatment in ZBR cells, we cannot ignore the possible contribution of ROS generated after VTP treatment (Donohue et al., 2014; Konstantinou et al., 2017), that could have an impact on many other molecules including members of the Ub family such as Ub and SUMO among others (Bossis et al., 2014).

- **ROS contribution in VTP ZBR apoptosis response.**

Due to the promising results obtained with VTP when used in combination with BTZ to recover sensitivity to this PI, we explored the possible contribution of ROS to this apoptotic response. We tested different ROS inducers (Luperox@) or inhibitors (NAC) to determine how important the contribution of ROS was in the apoptosis response in Z138 and ZBR cells after VTP treatment (Figure 34 and 35).

ROS can be formed from various endogenous sources, including mitochondrial electron transport chain and NAD(P)H oxidases. ROS include superoxide ($O_2^{\bullet -}$), hydrogen peroxide (H_2O_2), hydroxyl radical ($OH^{\bullet}$), singlet oxygen ($^1O_2$), peroxyl radical ($LOO^{\bullet}$), alkoxyl radical ($LO^{\bullet}$), lipid hydroperoxide (LOOH), peroxynitrite ($ONOO^-$), hypochlorous acid (HOCl), and ozone (O3), among others (Li et al., 2016). ROS exist inside the cells in an equilibrium promoted by antioxidant mechanims (Li et al., 2016; Redza-Dutordoir and Averill-Bates, 2016). Low doses of ROS species are considered to be essential for the maintenance and regulation of normal physiological functions such as cell cycle progression, proliferation, differentiation, migration and cell death. The proper maintenance of this redox balance has been implicated in the activation of various cellular signalling pathways. In contrast, excessive levels of ROS lead to the activation of cell death pathways such as apoptosis, promoted by irreversible DNA damage (Caillot et al., 2020a; Redza-Dutordoir and Averill-Bates, 2016).

Perez-Galan et al. showed a loss of apoptosis when using BTZ in combination with the ROS inhibitor NAC (Pérez-Galán et al., 2006), highlighting the contribution of ROS in BTZ-mediated apoptosis in BTZ-resistant MCL cells. However, since the inhibition of proteasome affects multiple cellular events, the exact mechanism by which the oxidative stress response is generated is not fully understood. Later in time, Halasi et al. described a dual nature of NAC, directly interacting and antagonizing the activity of PIs (Halasi et al., 2013). Nevertheless, using alternative ROS inhibitors or inducers like VAS3947 (VAS), and auranofin (AUR), an inhibitor of the antioxidant enzyme thioredoxinmreductase (TXNRD1), Caillot et al. showed that ROS unbalance contributes to re-sensitising MM cells to BTZ (Caillot et al., 2020a). These findings highlight the importance of ROS in the cell killing effect of BTZ.

To identify contribution of ROS in the VTP-induced cell killing response, no combination with PI was considered to evaluate our hypothesis. We used NAC as a general ROS inhibitor. NAC is an important antioxidant, a precursor of intracellular cysteine glutathione (GSH), the most abundant non-protein thiol playing an important role in the regulation of apoptosis (Sun, 2010).

VTP/NAC treatment reduced the percentage of cell death in Z138 cells, but with a higher difference in the reduction of the apoptotic response in ZBR cells (Figure 34). This indicates that p62 targeting may not be the only mechanism in which VTP promotes toxicity, suggesting an important ROS contribution, and a higher ROS susceptibility to these BTZ-resistant cells.

Donohue et al. reported that ROS induced by VTP corresponded specifically to singlet oxygen species (O2). This type of singlet oxygen species, that can be generated by Rose Bengal, produced high-molecular p62 aggregates. Since p62 is susceptible to exogenous and

endogenous oxidants, this mechanim may act as sensor of oxidate stress by promoting the formation of crosslinked p62 oligomers (Donohue et al., 2014).

The involvement of autophagy in maintaining the cells redox status has been reported (Ornatowski et al., 2020). This proteolytic pathway was found to alleviate cells with intensive oxidative damage upon ROS induction. Supporting this hypothesis, the p62 protein has been found to play important roles in activating oxidative stress responses. In the absence of p62, NRF2 is ubiquitylated by KEAP1, and degraded by the proteasome, therefore inhibiting the transcription of a number of cytoprotective genes involved in antioxidant responses (Donohue et al., 2014). In the scenario of VTP promoting p62 oligomerization and ROS induction, p62 could be sequestered to prevent antioxidant responses therefore favouring an early apoptosis response. How is this response better enhanced by VTP in ZBR cells in comparison to Z138 cells? This question was partially addressed in this project (see below).

Quantification of the generation of reactive species using specific probes linked to a highly sensitive approach like liquid chromatography coupled to mass spectrometry (Tsamesidis et al., 2020) could be a strategy to use in order to understand the ROS response promoted by VTP or PI more in detail in our BTZ-resistant MCL cells.

Our comprehension of the ROS-autophagy crosstalk and the role of p62 in the context of BTZ-resistant MCL cells will be important to extrapolate this information to other cancer models. Indeed, the VTP/BTZ combination has been proved to reduce tumour growth in different cancers like breast carcinoma (Li et al., 2013; Mathew et al., 2009; Wei et al., 2014).

- **Inhibition of the p62 ZZ domain in MCL cells.**

Different Ub E3 enzymes were found to be upregulated in ZBR cells using a TUBE-MS approach, in addition to the TRIM24 protein. Among the most enriched E3 ligases, we found 3 UBR enzymes (UBR2, UBR4 and UBR5) (Figure 19) involved in the N-end rule pathway (Varshavsky, 2011). The level of these enzymes was also found enriched in whole extracts from ZBR cells (Figure 20), validating MS results. We initially reasoned that the accumulation of UBR enzymes was a consequence of the dysfunctionality of the proteasome-mediated degradation found in ZBR cells and their inhibition could contribute to reequilibrate the UPS-ALS balance (Quinet et al., 2021). However, we soon realised that the ZZ domain of p62 is also involved in the N-end rule pathway upon proteotoxic stress, acting as a N-recognin to target proteins for autophagy degradation (Cha-Molstad et al., 2018). The action of p62 in this context would alleviate proteotoxic stress due to proteasomal impairment (chemically or pathologically) and is coherent with the activation of autophagy to compensate this proteolytic impairment (Nam et al., 2017).

With these arguments, we investigated the possible contribution of the p62 ZZ domain in our phenotype, hypothesizing that UBR proteins dysregulation could be indirectly affected by interfering at this level. Our experiments using XRF3F2 showed that this ZZ p62 domain inhibitor differently affected the stability of UBR2, UBR4 and UBR5 in Z138 and ZBR cells (Figure 33). XRF3F2 also affected p62 levels and this effect was more important in ZBR cells. XRF3F2 better accumulates UBR5 and UBR2 in ZBR cells even if quantifications did not

support statistical significance. We would have expected that in ZBR cells the XRF3F2 would also destabilise UBR enzymes to reach similar levels than the ones found in Z138, partially reverting the BTZ-resistant phenotype. We found that only UBR4 appears to be reduced in ZBR cells after XRF3F2 treatment, but with no statistical significance. To validate the role of UBR enzymes in this equilibrium we are currently developing XRF3F2 analogues to improve the effect on p62 and perhaps better interfere with their action. Alternatively, specific inhibitors for each UBR protein could be used (Lee et al., 2008). However, the number of commercially available UBR inhibitors is currently limited. Since functional redundancy of UBR enzymes could be expected, tackling various E3s at the same time could be tempted if low concentrations of these chemical inhibitors proved to show efficacy and are well-tolerated.

Coherent with the lack of impact of XRF3F2 on UBR enzymes stability, we did not observe differences in the apoptotic response of Z138 and ZBR cells to different concentrations of this inhibitor. The combination of XRF3F2 with BTZ provided a better apoptotic response in Z138 with low statistical significance. However even if not quantified, the combinatorial index between XRF3F2 and BTZ appears to be better in Z138 cells (Figure 32). Considering that the higher doses of XRF3F2 used in these experiments are at the limit of solubility of this drug, we could not increase its concentration. This also justifies the development of XRF3F2 analogues to improve solubility and efficacy of this treatment. Interestingly, XRK3F2 has been proposed to decrease cell viability in PI-resistant MM cells, when used in combination with BTZ (Marino et al., 2019), justifying our current efforts to develop new ZZ-domain p62 inhibitors.

20.4 Development of new molecular tools to analyse K48 and K63 ubiquitome.

Despite all the progress made on new technology and methodology for MS analysis to unveil the Ub chain complexity, the study of PTMs and its implications in physiology and pathology is still challenging. One of the major obstacles that our community faces is the lack of tools to identify Ub chains and discover the functions to which these chains are connected. An additional complication is the heterologous composition of some Ub chains that can also include other UbLs proteins. Furthermore, the dynamic formation and remodelling of these chains in which the action of multiple DUBs could be involved, limits our understanding of functions associated with complex chains.

Multiple tools have appeared over the last 10 years including molecular traps (e.g. TUBEs), peptide aptamers (e.g. nanobodies) or affirmers, among others. All these tools have advantages and shortcomings and perhaps the combination of all of them will help us to better integrate Ub signals in distinct biological contexts.

In this project we focused our efforts on the validation and optimisation of the K63 and K48 Ub chain-specific nanobodies. These tools are small polypeptides that recognise in a specific manner free Ub chains and Ub-modified target substrates. This part of the project was conducted in collaboration with *Hybrigenics*. These tools are now commercially available at *Nanotag Biotechnologies* as Ubiquitin K63 selector (https://nano-tag.com/products/ubiquitin-k63-selector) and Ubiquitin K48 selector (https://nano-

tag.com/products/ubiquitin-k48-selector), for the benefit of the scientific community. We invested efforts to develop applications for these nanobodies, including precipitations for WB analysis of Ub chains and protein targets. We also implemented a protocol for MS analysis and cell imaging.

- **Using Ubiquitin chain-specific nanobodies for the analysis of the ubiquitome.**

After the characterisation of different K48 and K63 nanobodies clones, we retained A4.1 (K48) and D1.1 (K63) to set up all methodologies. These nanobodies are specific for these chains and do not cross-react with other Ub chains. We first optimised them to perform precipitations using Z138 and ZBR cell extracts. With the purpose to use these nanobodies for MS analysis, we tested distinct crosslinking protocols allowing us to use stringent washing conditions if required.

We tested DMP (dimethyl pimelimidate dihydrochloride) and BS3 (bis(sulfosuccinimidyl)suberate) crosslinking strategies. The DMP crosslinking protocol had already been used in our group to stabilize GST-TUBE to the affinity column before MS analysis (Azkargorta et al., 2016; Xolalpa et al., 2016). Nevertheless, and due to the different characteristics of the nanobodies, we also implemented the BS3 crosslinking protocol. BS3 is a homo-bifunctional cross-linker reagent that promotes the binding of amino groups (Alegria-Schaffer, 2014; Miyake et al., 2019). These protocols were also tested in parallel to attach biotinylated version (Lang et al., 2016) of TUBEs (called bioTUBE-Rad23) to streptavidin columns. Due to technical problems with the commercial beads, we were not able to reduce the background signal coming from free streptavidin even in the negative column control. For this reason, we chose not to present these results in this manuscript. Nevertheless, I could contribute to different publications were GST-TUBEs based on the UBA domain from Rad23 and p62 were used (Quinet et al., 2021; Lopez-Reyes et al., 2021). These manuscripts are listed at the end of this document.

Histidine tags have a limited affinity for metal ions like Ni2+ which are included in nickel-nitrilotriacetic acid (Ni-NTA) beads used in this project. Binding of His-tags can occur under native and denaturing conditions such as urea and guanidinium. However, even under denaturing conditions, background can be obtained from endogenous histidinylated proteins naturally present in eukaryotic cells. Since we saturated our Ni-NTA beads with our His6 tagged nanobodies before the crosslinking, this background was reduced. Furthermore, exhaustive washes can also be performed to remove unspecific protein binding. A clear benefit from this protocol was reached by obtaining clean Ub-captured fractions using the BS3-crosslinking strategy in our precipitations (Figure 44). With this protocol, we obtained a good enrichment of ubiquitylated fractions that will be described in the next sections. The use of these molecular tools for MS has been recently demonstrated to be a powerful enrichment option for protein immunoprecipitation when comparing immunoprecipitation with a K-ε-GG antibody (diGly) with a Ub pan selector nanobody (pan Ub from “Nanotag Biotechnologies”) recognizing all Ub chains (Laigle et al., 2021).

Additionally, we used K48 and K63 Ub chain-specific minibodies for IF purposes in HeLa cells. Different treatment conditions were optimized using WB to better detect K48 or K63-

mediated ubiquitylation events. A combination of 16h starvation and BafA (2,5uM) 8h treatment provided us the proper condition to test the K63 minibody. Moreover, BTZ 40nM treatment for 8h proved to accumulate ubiquitylated forms of p53, a well-known protein described to be degraded by the proteasome (Figure 39) (Roeten et al., 2018).

Upon these conditions, we demonstrated the accumulation of yellow puncta in the merge panel of LC3B (red), and minibody K63 (green) (Figure 40). Co-localisation of puncta was not observed when using the commercial anti-Ub E412J in combination with our K63 Ub-minibodies. Nevertheless, a validated anti Ub-K63 antibody must be used to fully validate the use of this K63 specific Ub-minibody for IF applications. In addition, K48 Ub-minibody (green) staining provided an accumulation of signal as well as an increase of the p53 (red) staining upon proteasome blockage. Some of the red and green dots co-localised in a small proportion, coherently with the notion that p53 is not the only K48 modified protein that accumulates when this proteolytic pathway is inhibited (Figure 41). Nevertheless, strong co-localisation (yellow puncta) of the K48 minibody (green), with a commercial anti-Ub antibody P4D1 (red) was observed validating the use of this tool for cell imaging (Figure 43).

These Ub-minibodies were tested to stain our MCL cells however, without providing a resolution good enough for high quality images (data not shown). The optimisation of the fixation and permeabilisation and stacking steps using suspension cells must be carried out to obtain any conclusion.

- **Enrichment of K63 ubiquitin chains in ZBR cells.**

Once we implemented our nanobodies-MS protocol, we used this approach to explore Ub-regulated processes in Z138 and ZBR cells at basal levels but also in response to VTP. At basal levels (no treatment), an enrichment of proteins was observed with K63 nanobodies in ZBR compared to Z138 cells. In contrast, proteins were more enriched with the K48 nanobody in Z138 cells. These observations were also confirmed when comparing K48 to K63 substrate identification within the same cell line or when comparing K63 or K48 in Z138 and ZBR cell lines (Figure 48).

WB analysis of proteins precipitated with K48 or K63 nanobodies was performed to validate the enrichment of identified proteins. Our results further validated the implemented nanobodies-MS protocol (Figure 39). Among the proteins we could identify p62, β2 and β5 enriched in ZBR cells according to the volcano plots (substrates identified enriched in ZBR in the volcano plots displayed: PSMB1, PSMB2, PSMB9, PSM10, PSMA6 and SQSTM1).

Interestingly, TRIM24 was also found enriched in ZBR using a nanobodies-MS analysis, which is coherent with the previous TUBE-MS analysis. TRIM24 was enriched by both K48 and K63 nanobodies in ZBR cells, suggesting the role of this E3 in the synthesis or coordination of both chains in these BTZ-resistant cells. In sharp contrast, TRIM24 was predominantly captured by K63 Ub chains in Z138. Our volcano plots analysis also supports the different TRIM24 distribution associated to these Ub chains in Z138 and ZBR cell lines. This different Ub chains repartition found in Z138 and ZBR cell lines could be associated with the distinct subcellular localisation of TRIM24 found in these cells (Figure 48).

The enrichment of Ub K63-linked functions found here is coherent and supports the notion that autophagy, and in particular proteaphagy, is permanently activated in ZBR cells (Quinet et al., 2021). Moreover, the heat maps integrating affected GO (Gene Ontology) functions showed similar results to the ones obtained with the TUBE-MS approach. Among these common results, we found phagosome, protein processing in the endoplasmic reticulum, and the proteasome pathway (Figure 50).

- **Identification of metabolic pathways mediating VTP response in ZBR cells.**

The use of our nanobodies-MS protocol revealed a drastic change in protein enrichment after VTP treatment. Volcano plots made with the proteins identified after VTP treatment revealed an important enrichment of K63 substrates in ZBR cells (Figure 49). Interestingly, when specific functions were analysed by GO and integrated into heat maps (Figure 51), an important decrease in proteins related to the ribosome and metabolism (glycolysis, carbon metabolism and biosynthesis of amino acids) was identified.

We confirmed the reduction of glycolytic enzymes identified reduced using nanobody precipitation followed by WB analysis: ENO1, PGK1 and GAPDH after VTP treatment (Figure 52). The involvement of glycolysis was demonstrated in BTZ-resistant MM cells by other authors. Sanchez et al. reported the use of Dichloroacetate (DCA), a glycolytic suppressor to increase sensitivity to BTZ while inducing superoxide production or ROS formation (Sanchez et al., 2013). A metabolic shift towards oxidative glycolysis for ATP production was observed in multiple tumours, also called the “Warburg Effect”. This process is observed even under aerobic conditions conferring a survival benefit to multiple cancer cells, and therefore has been explored for therapeutic development (Pavlides et al., 2012; Sanchez et al., 2013). If VTP is able to inhibit glycolysis and promote ROS apoptosis at the same time, this could explain, at least in part, why this treatment is efficiently inhibiting tumour grow (Quinet et al., 2021).
Recent evidence also suggests a crosstalk between autophagy and glycolysis. Both play essential roles in a great number of pathologies and regulators of these pathways are frequent cancer hallmarks (Chu et al., 2020). Understanding the molecular mechanisms regulating this interconnection is challenging since they are associated with specific pathological status (Chu et al., 2020; Jiao et al., 2018). Exploring the contribution of glycolysis in our BTZ-resistant MCL cells could be the next step to perform in this research project. Since the “Warburg Effect” observed in Myeloma cells is induced by Cyclin D1 and this cyclin is overexpressed in MCL, it would be interesting to explore this possible regulation mechanism (Caillot et al., 2020b).

Furthermore, TRIM24 was described to bind the promoter region of Cyclin D1 mediating its expression and regulating glucose metabolism in Head and Neck Squamous Cell Carcinoma (Wang et al., 2018). In addition, the regulation of glycolysis by autophagy through a p62-mediated ubiquitylation in liver cancer was also reported (Jiao et al., 2018). It is therefore worthy to note the importance of an equilibrium implicating the regulation of multiple interconnected processes, such as autophagy, glycolysis and ROS production under stress conditions to regulate apoptosis. Understanding the relationship between all possible

factors involved in response to distinct treatments is crucial to develop new therapeutic strategies and understand pathological situations more in detail. This knowledge can also be extrapolated to other diseases with common molecular features, favouring the development of new clinical interventions.

20.5 Conclusions and future perspectives.

This PhD project shows evidence indicating that the Ub-ligase TRIM24 found enriched in BTZ-resistant cells contribute to regulating the UPS-ALS crosstalk, playing an important role in proteaphagy and apoptosis regulation. The depletion of TRIM24 in ZBR cells promoted an enhanced apoptosis response when these cells were simultaneously treated with BTZ, suggesting a recovery of the sensitivity to this antitumoral agent. Interestingly, we have observed differences in stability and localisation of TRIM24 when comparing Z138 to the ZBR cell line. The reduction of TRIM24 levels using dTRIM24 alone accumulate autophagy factors and proteasome subunits in ZBR cells behaving as an autophagy inhibitor. An interesting possibility is that dTRIM24-induced remodelling of Ub chains favours autophagy termination (K48 chains) rather than induction (K63 chains). This new Ub chain equilibrium will simultaneously favour the activity of the UPS.

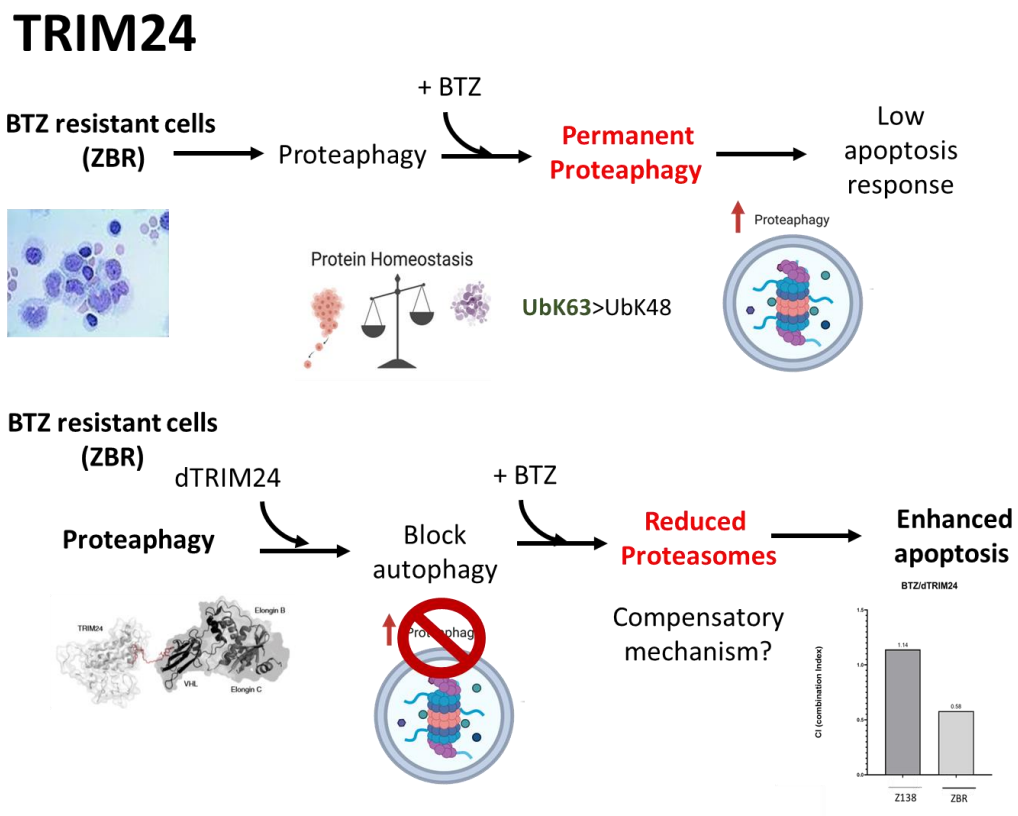

Figure 53 : Proposed mechanism of action of dTRIM24 in ZBR MCL cells. ZBR cells are characterised by an increase of autophagy and K63 enrichment, accompanied by permanently activated proteaphagy. Using dTRIM24 (PROTAC), the autophagy pathway is blocked promoting an accumulation of p62, LC3B and proteasome subunits. When this treatment is combined with BTZ, proteasomes are reduced by unknown

mechanisms and apoptosis is enhanced. The cooperative index calculated when both treatments were used in ZBR cells was significant.

When dTRIM24 is combined with BTZ, this treatment has a negative impact on the stability of the proteasome and autophagy factors in ZBR compared to Z138 cells. These results suggest that a more important reduction of TRIM24 levels driven by the dTRIM24/BZT combination activates compensatory mechanisms that decrease factors implicated in proteaphagy (LC3, p62 and proteasome subunits) in ZBR cells.

Altogether, our results indicate that the UPS-ALS crosstalk is not regulated in the same way in Z138 and ZBR cell lines. TRIM24 regulates proteaphagy and perhaps other selective autophagy pathways in ZBR cells. Our results highlight the important participation of this Ub ligase in the regulation of apoptosis in BTZ-resistant cells (Figure 53). Further experiments are required to determine if TRIM24 is also important in other BTZ-resistant MCL cells and if the apoptosis observed after dTRIM24 treatment alone or in combination with BTZ is p53-dependent.

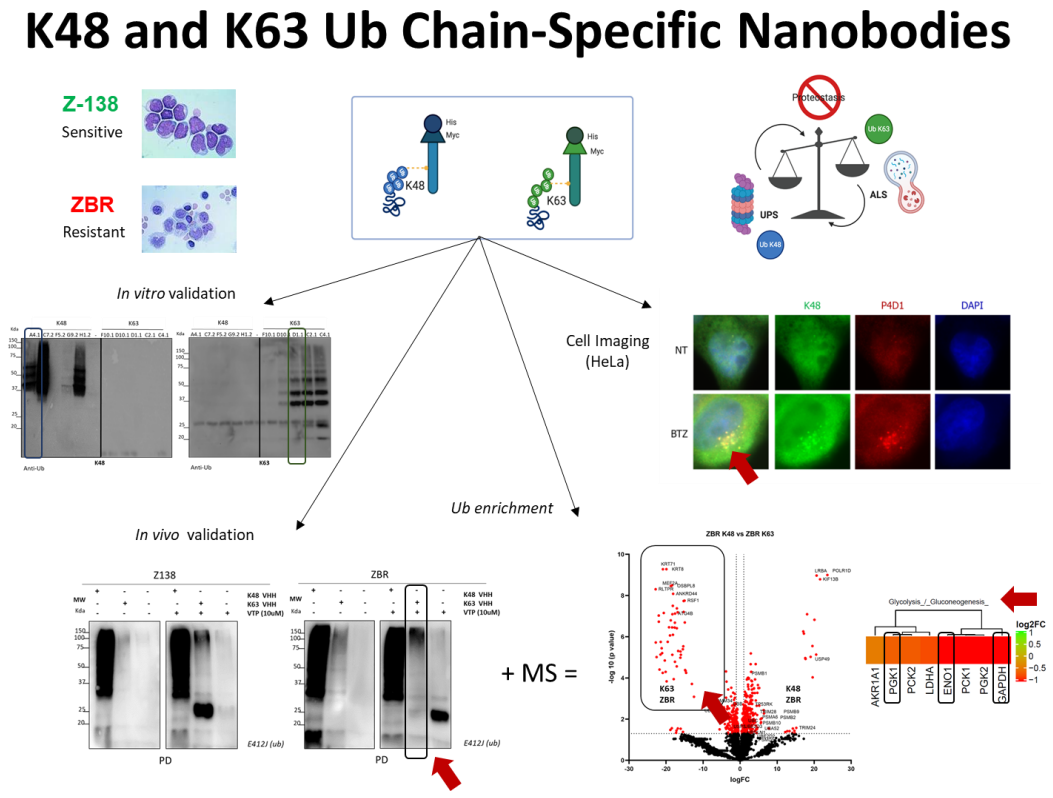

Figure 54 : Ub chain-specific nanobodies applications. Schematic representation of K48 and K63 Ub chain-specific nanobodies applications used for the analysis of the ubiquitome in our biological model, sensitive Z138 and ZBR cells lines and cell imaging in HeLa cells. K48 and K63 nanobodies were used to validate a K63 Ub chain enrichment in ZBR cells and provided new insights into new possible molecular pathways (e.g. glycolysis) that are altered in response to VTP and might contribute to enhancing apoptosis in BTZ-resistant cells.

In a parallel manner, we focused on validating the use of K48 and K63 Ub chain-specific nanobodies for different applications like precipitations followed by WB or MS analysis. We have also invested efforts in the implementation of indirect fluorescence protocols even if we did not have the time to use them in our MCL model cell lines. Thus, K48 and K63 nanobodies represent a reliable new tool that can be used to answer challenging questions explored by the scientific community interested in the study of ubiquitylation events and associated pathologies (Figure 54). K48 and K63 nanobodies, also validated K63 Ub chain enrichment in our ZBR cells found with a TUBE-MS approach (Quinet et al., 2021).

VTP/BTZ treatment is as the best treatment in our hands to induce apoptosis in BTZ-resistant cell cultures and *in vivo* mouse xenografts models. VTP not only targets p62 but also induces ROS production. The use of the inhibitor XKR3F2, that acts at the level of p62 ZZ domain, did not display the same intensity on apoptosis-induction as VTP. Since XKR3F2 accumulated well p62 but did not decrease the levels of UBR enzymes, its efficacy could perhaps be improved with new analogues (Figure 55). Another possibility is that ROS induction after VTP treatment is important (Caillot et al., 2020a) to induce an efficient apoptosis in BTZ-resistant cells (Pérez-Galán et al., 2006). Understanding ROS involvement, and the different reactive oxygen species generated after VTP in BTZ-resistant cells could also be crucial to extrapolate our results to other cancers where resistance to BTZ has also been observed such as MM.

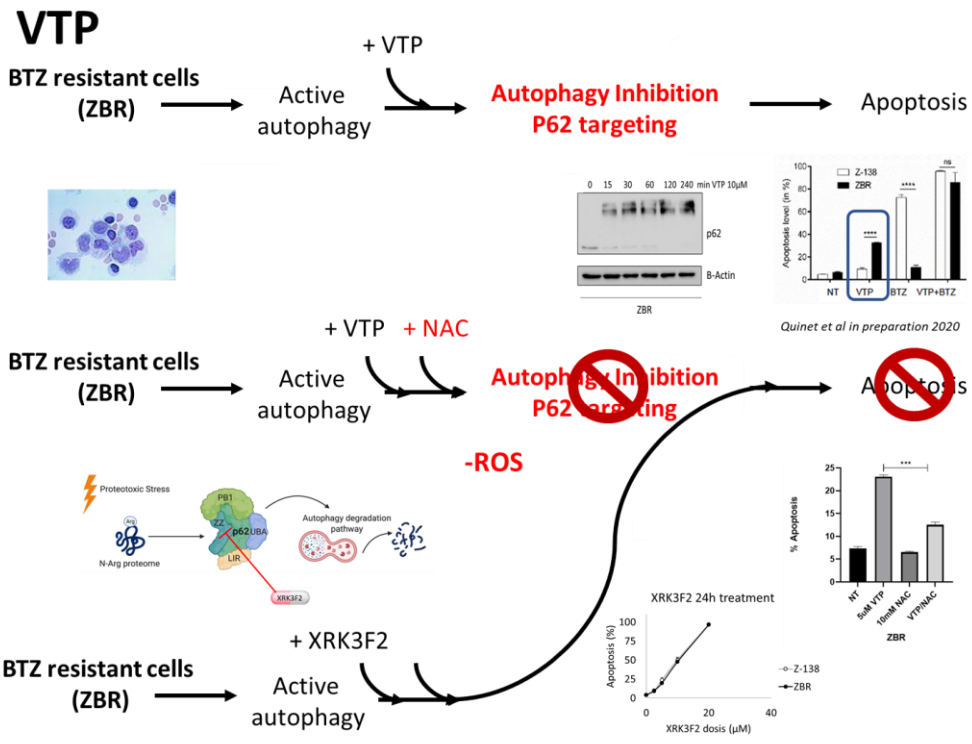

Figure 55 : New insights into VTP-induced response in ZBR cells. Schematic representation gathering results obtained by targeting p62 through different chemical strategies. VTP treatment promoted p62 aggregation and apoptosis in ZBR cells. In addition, VTP treatment has been proved to mediate this apoptotic response through ROS induction. XRK3F2 that targets the ZZ domain of p62 is not sufficient to promote an efficient apoptotic response in ZBR cells.

The glycolytic enzymes downregulated after VTP treatment found in our MS analysis (Figure 54) suggest that they could contribute to regulate apoptosis in BTZ-resistant cells when using this p62 inhibitor. If this new mechanism is confirmed, these enzymes could be directly inhibited using available inhibitors. Although glycolysis has been linked to autophagy regulation, further investigations are required to validate the role of this metabolic pathway in proteaphagy regulation and BTZ resistance.

21. Bibliography.

Abraham, I., Jain, S., Wu, C.-P., Khanfar, M.A., Kuang, Y., Dai, C.-L., Shi, Z., Chen, X., Fu, L., Ambudkar, S.V., et al. (2010). Marine sponge-derived sipholane triterpenoids reverse P-glycoprotein (ABCB1)-mediated multidrug resistance in cancer cells. Biochem. Pharmacol. *80*, 1497–1506.

Aebersold, R., and Mann, M. (2003). Mass spectrometry-based proteomics. Nature *422*, 198–207.

Aillet, F., Lopitz-Otsoa, F., Hjerpe, R., Torres-Ramos, M., Lang, V., and Rodríguez, M.S. (2012). Isolation of ubiquitylated proteins using tandem ubiquitin-binding entities. Methods Mol. Biol. Clifton NJ *832*, 173–183.

Akutsu, M., Dikic, I., and Bremm, A. (2016). Ubiquitin chain diversity at a glance. J. Cell Sci. *129*, 875–880.

Alegria-Schaffer, A. (2014). General protein-protein cross-linking. Methods Enzymol. *539*, 81–87.

Amengual, J.E., Johannet, P., Lombardo, M., Zullo, K., Hoehn, D., Bhagat, G., Scotto, L., Jirau-Serrano, X., Radeski, D., Heinen, J., et al. (2015). Dual targeting of protein degradation pathways with the selective HDAC6 inhibitor, ACY-1215, and bortezomib is synergistic in lymphoma. Clin. Cancer Res. Off. J. Am. Assoc. Cancer Res. *21*, 4663–4675.

Amin, H.M., McDonnell, T.J., Medeiros, L.J., Rassidakis, G.Z., Leventaki, V., O'Connor, S.L., Keating, M.J., and Lai, R. (2003). Characterization of 4 mantle cell lymphoma cell lines. Arch. Pathol. Lab. Med. *127*, 424–431.

An, S., and Fu, L. (2018). Small-molecule PROTACs: An emerging and promising approach for the development of targeted therapy drugs. EBioMedicine *36*, 553–562.

Appikonda, S., Thakkar, K.N., Shah, P.K., Dent, S.Y.R., Andersen, J.N., and Barton, M.C. (2018). Cross-talk between chromatin acetylation and SUMOylation of tripartite motif-containing protein 24 (TRIM24) impacts cell adhesion. J. Biol. Chem. *293*, 7476–7485.

Arpalahti, L., Haglund, C., and Holmberg, C.I. (2020). Proteostasis Dysregulation in Pancreatic Cancer. Adv. Exp. Med. Biol. *1233*, 101–115.

Azkargorta, M., Escobes, I., Elortza, F., Matthiesen, R., and Rodríguez, M.S. (2016). TUBEs-Mass Spectrometry for Identification and Analysis of the Ubiquitin-Proteome. Methods Mol. Biol. Clifton NJ *1449*, 177–192.

Balaji, S., Ahmed, M., Lorence, E., Yan, F., Nomie, K., and Wang, M. (2018). NF-κB signaling and its relevance to the treatment of mantle cell lymphoma. J. Hematol. Oncol.J Hematol Oncol *11*, 83.

Ballar Kirmizibayrak, P., Erbaykent-Tepedelen, B., Gozen, O., and Erzurumlu, Y. (2020). Divergent Modulation of Proteostasis in Prostate Cancer. Adv. Exp. Med. Biol. *1233*, 117–151.

Balsas, P., Galán-Malo, P., Marzo, I., and Naval, J. (2012). Bortezomib resistance in a myeloma cell line is associated to PSMβ5 overexpression and polyploidy. Leuk. Res. *36*, 212–218.

Bard, J.A.M., Goodall, E.A., Greene, E.R., Jonsson, E., Dong, K.C., and Martin, A. (2018). Structure and Function of the 26S Proteasome. Annu. Rev. Biochem. *87*, 697–724.

Barrio, S., Stühmer, T., Da-Viá, M., Barrio-Garcia, C., Lehners, N., Besse, A., Cuenca, I., Garitano-Trojaola, A., Fink, S., Leich, E., et al. (2018). Spectrum and functional validation of PSMB5 mutations in multiple myeloma. Leukemia.

Barroso-Gomila, O., Trulsson, F., Muratore, V., Canosa, I., Merino-Cacho, L., Cortazar, A.R., Pérez, C., Azkargorta, M., Iloro, I., Carracedo, A., et al. (2021). Identification of proximal SUMO-dependent interactors using SUMO-ID. Nat. Commun. *12*, 6671.

Beà, S., and Amador, V. (2017). Role of SOX11 and Genetic Events Cooperating with Cyclin D1 in Mantle Cell Lymphoma. Curr. Oncol. Rep. *19*, 43.

Benjamini, Y., and Hochberg, Y. (1995). Controlling the False Discovery Rate: A Practical and Powerful Approach to Multiple Testing. J. R. Stat. Soc. Ser. B Methodol. *57*, 289–300.

Besse, A., Stolze, S.C., Rasche, L., Weinhold, N., Morgan, G.J., Kraus, M., Bader, J., Overkleeft, H.S., Besse, L., and Driessen, C. (2018). Carfilzomib resistance due to ABCB1/MDR1 overexpression is overcome by nelfinavir and lopinavir in multiple myeloma. Leukemia *32*, 391–401.

Bossis, G., Sarry, J.-E., Kifagi, C., Ristic, M., Saland, E., Vergez, F., Salem, T., Boutzen, H., Baik, H., Brockly, F., et al. (2014). The ROS/SUMO axis contributes to the response of acute myeloid leukemia cells to chemotherapeutic drugs. Cell Rep. *7*, 1815–1823.

Budenholzer, L., Cheng, C.L., Li, Y., and Hochstrasser, M. (2017). Proteasome Structure and Assembly. J. Mol. Biol. *429*, 3500–3524.

Caillot, M., Zylbersztejn, F., Maitre, E., Bourgeais, J., Hérault, O., and Sola, B. (2020a). ROS Overproduction Sensitises Myeloma Cells to Bortezomib-Induced Apoptosis and Alleviates Tumour Microenvironment-Mediated Cell Resistance. Cells *9*, 2357.

Caillot, M., Bourgeais, J., Dakik, H., Costé, É., Mazure, N.M., Lelièvre, É., Coqueret, O., Hérault, O., Mazurier, F., and Sola, B. (2020b). Cyclin D1 targets hexokinase 2 to control aerobic glycolysis in myeloma cells. Oncogenesis *9*, 1–13.

Camacho, E., Hernández, L., Hernández, S., Tort, F., Bellosillo, B., Beà, S., Bosch, F., Montserrat, E., Cardesa, A., Fernández, P.L., et al. (2002). ATM gene inactivation in mantle

cell lymphoma mainly occurs by truncating mutations and missense mutations involving the phosphatidylinositol-3 kinase domain and is associated with increasing numbers of chromosomal imbalances. Blood *99*, 238–244.

Carvalho, A.S., Ribeiro, H., Voabil, P., Penque, D., Jensen, O.N., Molina, H., and Matthiesen, R. (2014). Global mass spectrometry and transcriptomics array based drug profiling provides novel insight into glucosamine induced endoplasmic reticulum stress. Mol. Cell. Proteomics MCP *13*, 3294–3307.

Carvalho, A.S., Molina, H., and Matthiesen, R. (2016). New insights into functional regulation in MS-based drug profiling. Sci. Rep. *6*, 18826.

Catley, L., Weisberg, E., Kiziltepe, T., Tai, Y.-T., Hideshima, T., Neri, P., Tassone, P., Atadja, P., Chauhan, D., Munshi, N.C., et al. (2006). Aggresome induction by proteasome inhibitor bortezomib and alpha-tubulin hyperacetylation by tubulin deacetylase (TDAC) inhibitor LBH589 are synergistic in myeloma cells. Blood *108*, 3441–3449.

Chakravarty, R., Goel, S., and Cai, W. (2014). Nanobody: the “magic bullet” for molecular imaging? Theranostics *4*, 386–398.

Chambon, M., Orsetti, B., Berthe, M.-L., Bascoul-Mollevi, C., Rodriguez, C., Duong, V., Gleizes, M., Thénot, S., Bibeau, F., Theillet, C., et al. (2011). Prognostic Significance of TRIM24/TIF-1α Gene Expression in Breast Cancer. Am. J. Pathol. *178*, 1461–1469.

Cha-Molstad, H., Yu, J.E., Feng, Z., Lee, S.H., Kim, J.G., Yang, P., Han, B., Sung, K.W., Yoo, Y.D., Hwang, J., et al. (2017). p62/SQSTM1/Sequestosome-1 is an N-recognin of the N-end rule pathway which modulates autophagosome biogenesis. Nat. Commun. *8*, 102.

Cha-Molstad, H., Lee, S.H., Kim, J.G., Sung, K.W., Hwang, J., Shim, S.M., Ganipisetti, S., McGuire, T., Mook-Jung, I., Ciechanover, A., et al. (2018). Regulation of autophagic proteolysis by the N-recognin SQSTM1/p62 of the N-end rule pathway. Autophagy *14*, 359–361.

Chamoto, K., Chowdhury, P.S., Kumar, A., Sonomura, K., Matsuda, F., Fagarasan, S., and Honjo, T. (2017). Mitochondrial activation chemicals synergize with surface receptor PD-1 blockade for T cell-dependent antitumor activity. Proc. Natl. Acad. Sci. U. S. A. *114*, E761–E770.

Chauhan, D., Tian, Z., Nicholson, B., Kumar, K.G.S., Zhou, B., Carrasco, R., McDermott, J.L., Leach, C.A., Fulcinniti, M., Kodrasov, M.P., et al. (2012). A small molecule inhibitor of ubiquitin-specific protease-7 induces apoptosis in multiple myeloma cells and overcomes bortezomib resistance. Cancer Cell *22*, 345–358.

Chelbi-Alix, M.K., and Thibault, P. (2021). Crosstalk Between SUMO and Ubiquitin-Like Proteins: Implication for Antiviral Defense. Front. Cell Dev. Biol. *9*, 956.

Chen, R.-H., Chen, Y.-H., and Huang, T.-Y. (2019). Ubiquitin-mediated regulation of autophagy. J. Biomed. Sci. *26*, 80.

Chen, S.-J., Wu, X., Wadas, B., Oh, J.-H., and Varshavsky, A. (2017). An N-end rule pathway that recognizes proline and destroys gluconeogenic enzymes. Science *355*.

Chojnacki, M., Mansour, W., Hameed, D.S., Singh, R.K., El Oualid, F., Rosenzweig, R., Nakasone, M.A., Yu, Z., Glaser, F., Kay, L.E., et al. (2017). Polyubiquitin-Photoactivatable Crosslinking Reagents for Mapping Ubiquitin Interactome Identify Rpn1 as a Proteasome Ubiquitin-Associating Subunit. Cell Chem. Biol. *24*, 443-457.e6.

Chu, Y., Chang, Y., Lu, W., Sheng, X., Wang, S., Xu, H., and Ma, J. (2020). Regulation of Autophagy by Glycolysis in Cancer. Cancer Manag. Res. *12*, 13259–13271.

Ciechanover, A., and Kwon, Y.T. (2017). Protein Quality Control by Molecular Chaperones in Neurodegeneration. Front. Neurosci. *11*, 185.

Ciuffa, R., Lamark, T., Tarafder, A.K., Guesdon, A., Rybina, S., Hagen, W.J.H., Johansen, T., and Sachse, C. (2015). The selective autophagy receptor p62 forms a flexible filamentous helical scaffold. Cell Rep. *11*, 748–758.

de Claro, R.A., McGinn, K.M., Verdun, N., Lee, S.-L., Chiu, H.-J., Saber, H., Brower, M.E., Chang, C.J.G., Pfuma, E., Habtemariam, B., et al. (2015). FDA Approval: Ibrutinib for Patients with Previously Treated Mantle Cell Lymphoma and Previously Treated Chronic Lymphocytic Leukemia. Clin. Cancer Res. Off. J. Am. Assoc. Cancer Res. *21*, 3586–3590.

Cohen-Kaplan, V., Livneh, I., Avni, N., Cohen-Rosenzweig, C., and Ciechanover, A. (2016a). The ubiquitin-proteasome system and autophagy: Coordinated and independent activities. Int. J. Biochem. Cell Biol. *79*, 403–418.

Cohen-Kaplan, V., Livneh, I., Avni, N., Fabre, B., Ziv, T., Kwon, Y.T., and Ciechanover, A. (2016b). p62- and ubiquitin-dependent stress-induced autophagy of the mammalian 26S proteasome. Proc. Natl. Acad. Sci. *113*, E7490–E7499.

Cremer, T., Jongsma, M.L.M., Trulsson, F., Vertegaal, A.C.O., Neefjes, J., and Berlin, I. (2021). The ER-embedded UBE2J1/RNF26 ubiquitylation complex exerts spatiotemporal control over the endolysosomal pathway. Cell Rep. *34*, 108659.

Cui, Z., Cao, W., Li, J., Song, X., Mao, L., and Chen, W. (2013). TRIM24 Overexpression Is Common in Locally Advanced Head and Neck Squamous Cell Carcinoma and Correlates with Aggressive Malignant Phenotypes. PLoS ONE *8*, e63887.

Da Silva-Ferrada, E., Xolalpa, W., Lang, V., Aillet, F., Martin-Ruiz, I., de la Cruz-Herrera, C.F., Lopitz-Otsoa, F., Carracedo, A., Goldenberg, S.J., Rivas, C., et al. (2013). Analysis of SUMOylated proteins using SUMO-traps. Sci. Rep. *3*.

Das, D.S., Das, A., Ray, A., Song, Y., Samur, M.K., Munshi, N.C., Chauhan, D., and Anderson, K.C. (2017). Blockade of Deubiquitylating Enzyme USP1 Inhibits DNA Repair and Triggers Apoptosis in Multiple Myeloma Cells. Clin. Cancer Res. Off. J. Am. Assoc. Cancer Res. *23*, 4280–4289.

Davenport, E.L., Moore, H.E., Dunlop, A.S., Sharp, S.Y., Workman, P., Morgan, G.J., and Davies, F.E. (2007). Heat shock protein inhibition is associated with activation of the unfolded protein response pathway in myeloma plasma cells. Blood *110*, 2641–2649.

Dengjel, J., Høyer-Hansen, M., Nielsen, M.O., Eisenberg, T., Harder, L.M., Schandorff, S., Farkas, T., Kirkegaard, T., Becker, A.C., Schroeder, S., et al. (2012). Identification of autophagosome-associated proteins and regulators by quantitative proteomic analysis and genetic screens. Mol. Cell. Proteomics MCP *11*, M111.014035.

Desterro, J.M., Rodriguez, M.S., and Hay, R.T. (2000). Regulation of transcription factors by protein degradation. Cell. Mol. Life Sci. CMLS *57*, 1207–1219.

Diefenbach, C.S.M., and O'Connor, O.A. (2010). Mantle cell lymphoma in relapse: the role of emerging new drugs. Curr. Opin. Oncol. *22*, 419–423.

Dikic, I., and Elazar, Z. (2018). Mechanism and medical implications of mammalian autophagy. Nat. Rev. Mol. Cell Biol. *19*, 349.

Dikic, I., Johansen, T., and Kirkin, V. (2010). Selective autophagy in cancer development and therapy. Cancer Res. *70*, 3431–3434.

Ding, W.-X., Ni, H.-M., Gao, W., Yoshimori, T., Stolz, D.B., Ron, D., and Yin, X.-M. (2007). Linking of Autophagy to Ubiquitin-Proteasome System Is Important for the Regulation of Endoplasmic Reticulum Stress and Cell Viability. Am. J. Pathol. *171*, 513–524.

Dittmar, G., and Winklhofer, K.F. (2019). Linear Ubiquitin Chains: Cellular Functions and Strategies for Detection and Quantification. Front. Chem. *7*, 915.

Donohue, E., Tovey, A., Vogl, A.W., Arns, S., Sternberg, E., Young, R.N., and Roberge, M. (2011). Inhibition of autophagosome formation by the benzoporphyrin derivative verteporfin. J. Biol. Chem. *286*, 7290–7300.

Donohue, E., Balgi, A.D., Komatsu, M., and Roberge, M. (2014). Induction of Covalently Crosslinked p62 Oligomers with Reduced Binding to Polyubiquitinated Proteins by the Autophagy Inhibitor Verteporfin. PloS One *9*, e114964.

Dreyling, M., Klapper, W., and Rule, S. (2018). Blastoid and pleomorphic mantle cell lymphoma: still a diagnostic and therapeutic challenge! Blood *132*, 2722–2729.

Edwin, N.C., and Kahl, B. (2018). Evolving treatment strategies in mantle cell lymphoma. Best Pract. Res. Clin. Haematol. *31*, 270–278.

Erpapazoglou, Z., Walker, O., and Haguenauer-Tsapis, R. (2014). Versatile Roles of K63-Linked Ubiquitin Chains in Trafficking. Cells *3*, 1027–1088.

Ewald, C.Y., Hourihan, J.M., and Blackwell, T.K. (2017). Oxidative Stress Assays (arsenite and tBHP) in Caenorhabditis elegans. Bio-Protoc. *7*.

Ferrington, D.A., and Gregerson, D.S. (2012). Immunoproteasomes: structure, function, and antigen presentation. Prog. Mol. Biol. Transl. Sci. *109*, 75–112.

Finlayson, A.E., and Freeman, K.W. (2009). A Cell Motility Screen Reveals Role for MARCKS-Related Protein in Adherens Junction Formation and Tumorigenesis. PLOS ONE *4*, e7833.

Fong, K., Zhao, J.C., Song, B., Zheng, B., and Yu, J. (2018). TRIM28 protects TRIM24 from SPOP-mediated degradation and promotes prostate cancer progression. Nat. Commun. *9*, 5007.

Franke, N.E., Niewerth, D., Assaraf, Y.G., van Meerloo, J., Vojtekova, K., van Zantwijk, C.H., Zweegman, S., Chan, E.T., Kirk, C.J., Geerke, D.P., et al. (2012). Impaired bortezomib binding to mutant β5 subunit of the proteasome is the underlying basis for bortezomib resistance in leukemia cells. Leukemia *26*, 757–768.

Fu, H., Lin, Y.-L., and Fatimababy, A.S. (2010). Proteasomal recognition of ubiquitylated substrates. Trends Plant Sci. *15*, 375–386.

Gâtel, P., Piechaczyk, M., and Bossis, G. (2020). Ubiquitin, SUMO, and Nedd8 as Therapeutic Targets in Cancer. Adv. Exp. Med. Biol. *1233*, 29–54.

Gatica, D., Lahiri, V., and Klionsky, D.J. (2018). Cargo recognition and degradation by selective autophagy. Nat. Cell Biol. *20*, 233–242.

Gauthier, J., and Maloney, D.G. (2020). Allogeneic Transplantation and Chimeric Antigen Receptor-Engineered T-Cell Therapy for Relapsed or Refractory Mantle Cell Lymphoma. Hematol. Oncol. Clin. North Am. *34*, 957–970.

Gechijian, L.N., Buckley, D.L., Lawlor, M.A., Reyes, J.M., Paulk, J., Ott, C.J., Winter, G.E., Erb, M.A., Scott, T.G., Xu, M., et al. (2018). Functional TRIM24 degrader via conjugation of ineffectual bromodomain and VHL ligands. Nat. Chem. Biol. *14*, 405–412.

Gelebart, P., Anand, M., Armanious, H., Peters, A.C., Dien Bard, J., Amin, H.M., and Lai, R. (2008). Constitutive activation of the Wnt canonical pathway in mantle cell lymphoma. Blood *112*, 5171–5179.

Gonzalez-Santamarta, M., Quinet, G., Reyes-Garau, D., Sola, B., Roué, G., and Rodriguez, M.S. (2020). Resistance to the Proteasome Inhibitors: Lessons from Multiple Myeloma and Mantle Cell Lymphoma. Adv. Exp. Med. Biol. *1233*, 153–174.

Gonzalez-Santamarta et al.,2022 Ubiquitin-chain dynamics in physiology and pathology. Semin. Cell Dev. Biol.

Grégoire Quinet et al (2021). Targeting p62/Sequestosome-1 impairs constitutively active proteaphagy and enhances apoptosis in bortezomib-resistant mantle cell lymphoma.

Groner, A.C., Cato, L., de Tribolet-Hardy, J., Bernasocchi, T., Janouskova, H., Melchers, D., Houtman, R., Cato, A.C.B., Tschopp, P., Gu, L., et al. (2016). TRIM24 Is an Oncogenic Transcriptional Activator in Prostate Cancer. Cancer Cell *29*, 846–858.

Gu, S., Cui, D., Chen, X., Xiong, X., and Zhao, Y. (2018). PROTACs: An Emerging Targeting Technique for Protein Degradation in Drug Discovery. BioEssays News Rev. Mol. Cell. Dev. Biol. *40*, e1700247.

Hackenberg, M., and Matthiesen, R. (2008). Annotation-Modules: a tool for finding significant combinations of multisource annotations for gene lists. Bioinforma. Oxf. Engl. *24*, 1386–1393.

Halasi, M., Wang, M., Chavan, T.S., Gaponenko, V., Hay, N., and Gartel, A.L. (2013). ROS inhibitor N-acetyl-L-cysteine antagonizes the activity of proteasome inhibitors. Biochem. J. *454*, 201–208.

Harris, L.D., Jasem, S., and Licchesi, J.D.F. (2020). The Ubiquitin System in Alzheimer's Disease. Adv. Exp. Med. Biol. *1233*, 195–221.

Hatakeyama, S. (2017). TRIM Family Proteins: Roles in Autophagy, Immunity, and Carcinogenesis. Trends Biochem. Sci. *42*, 297–311.

Hatchi, E.M., Poalas, K., Cordeiro, N., N'Debi, M., Gavard, J., and Bidère, N. (2014). Participation of the E3-ligase TRIM13 in NF-κB p65 activation and NFAT-dependent activation of c-Rel upon T-cell receptor engagement. Int. J. Biochem. Cell Biol. *54*, 217–222.

Hayes, J.D., and Dinkova-Kostova, A.T. (2014). The Nrf2 regulatory network provides an interface between redox and intermediary metabolism. Trends Biochem. Sci. *39*, 199–218.

He, C., and Klionsky, D.J. (2009). Regulation mechanisms and signaling pathways of autophagy. Annu. Rev. Genet. *43*, 67–93.

Heap, R.E., Gant, M.S., Lamoliatte, F., Peltier, J., and Trost, M. (2017). Mass spectrometry techniques for studying the ubiquitin system. Biochem. Soc. Trans. *45*, 1137–1148.

Heine, S., Kleih, M., Giménez, N., Böpple, K., Ott, G., Colomer, D., Aulitzky, W.E., van der Kuip, H., and Silkenstedt, E. (2018). Cyclin D1-CDK4 activity drives sensitivity to bortezomib in mantle cell lymphoma by blocking autophagy-mediated proteolysis of NOXA. J. Hematol. Oncol.J Hematol Oncol *11*.

Hjerpe, R., Aillet, F., Lopitz-Otsoa, F., Lang, V., England, P., and Rodriguez, M.S. (2009). Efficient protection and isolation of ubiquitylated proteins using tandem ubiquitin-binding entities. EMBO Rep. *10*, 1250–1258.

Hochstrasser, M. (2006). Lingering mysteries of ubiquitin-chain assembly. Cell *124*, 27–34.

Hochstrasser, M. (2009). Origin and Function of Ubiquitin-like Protein Conjugation. Nature *458*, 422.

Hoster, E., Network, for the G.L.G.L.S.G. (GLSG) and the E.M.C.L., Dreyling, M., Network, for the G.L.G.L.S.G. (GLSG) and the E.M.C.L., Klapper, W., Network, for the G.L.G.L.S.G. (GLSG) and the E.M.C.L., Gisselbrecht, C., Network, for the G.L.G.L.S.G. (GLSG) and the E.M.C.L., van Hoof, A., Network, for the G.L.G.L.S.G. (GLSG) and the E.M.C.L., et al. (2008). A new prognostic index (MIPI) for patients with advanced-stage mantle cell lymphoma. Blood *111*, 558–565.

Hsi, E.D. (2014). The SOX11-PDGFA axis in mantle cell lymphoma. Blood *124*, 2165–2166.

van Huizen, M., and Kikkert, M. (2019). The Role of Atypical Ubiquitin Chains in the Regulation of the Antiviral Innate Immune Response. Front. Cell Dev. Biol. *7*, 392.

Islam, Md.A., Sooro, M.A., and Zhang, P. (2018). Autophagic Regulation of p62 is Critical for Cancer Therapy. Int. J. Mol. Sci. *19*.

Jain, A.K., Allton, K., Duncan, A.D., and Barton, M.C. (2014). TRIM24 is a p53-induced E3-ubiquitin ligase that undergoes ATM-mediated phosphorylation and autodegradation during DNA damage. Mol. Cell. Biol. *34*, 2695–2709.

Jares, P., Colomer, D., and Campo, E. (2012). Molecular pathogenesis of mantle cell lymphoma. J. Clin. Invest. *122*, 3416–3423.

Ji, C.H., and Kwon, Y.T. (2017). Crosstalk and Interplay between the Ubiquitin-Proteasome System and Autophagy. Mol. Cells *40*, 441–449.

Ji, J., Ding, K., Luo, T., Zhang, X., Chen, A., Zhang, D., Li, G., Thorsen, F., Huang, B., Li, X., et al. (2021). TRIM22 activates NF-κB signaling in glioblastoma by accelerating the degradation of IκBα. Cell Death Differ. *28*, 367–381.

Jiao, L., Zhang, H.-L., Li, D.-D., Yang, K.-L., Tang, J., Li, X., Ji, J., Yu, Y., Wu, R.-Y., Ravichandran, S., et al. (2018). Regulation of glycolytic metabolism by autophagy in liver cancer involves selective autophagic degradation of HK2 (hexokinase 2). Autophagy *14*, 671–684.

Jung, H.J., Chen, Z., Wang, M., Fayad, L., Romaguera, J., Kwak, L.W., and McCarty, N. (2012). Calcium blockers decrease the bortezomib resistance in mantle cell lymphoma via manipulation of tissue transglutaminase activities. Blood *119*, 2568–2578.

Kabeya, Y., Mizushima, N., Ueno, T., Yamamoto, A., Kirisako, T., Noda, T., Kominami, E., Ohsumi, Y., and Yoshimori, T. (2000). LC3, a mammalian homologue of yeast Apg8p, is localized in autophagosome membranes after processing. EMBO J. *19*, 5720–5728.

Kane, R.C., Bross, P.F., Farrell, A.T., and Pazdur, R. (2003). Velcade: U.S. FDA approval for the treatment of multiple myeloma progressing on prior therapy. The Oncologist *8*, 508–513.

Kang, L., Weng, N., and Jian, W. (2020). LC-MS bioanalysis of intact proteins and peptides. Biomed. Chromatogr. BMC *34*, e4633.

Kaufman, R.J. (2002). Orchestrating the unfolded protein response in health and disease. J. Clin. Invest. *110*, 1389–1398.

Kawaguchi, T., Miyazawa, K., Moriya, S., Ohtomo, T., Che, X.-F., Naito, M., Itoh, M., and Tomoda, A. (2011). Combined treatment with bortezomib plus bafilomycin A1 enhances the cytocidal effect and induces endoplasmic reticulum stress in U266 myeloma cells: crosstalk among proteasome, autophagy-lysosome and ER stress. Int. J. Oncol. *38*, 643–654.

Khaminets, A., Behl, C., and Dikic, I. (2016). Ubiquitin-Dependent And Independent Signals In Selective Autophagy. Trends Cell Biol. *26*, 6–16.

Kikuchi, M., Okumura, F., Tsukiyama, T., Watanabe, M., Miyajima, N., Tanaka, J., Imamura, M., and Hatakeyama, S. (2009). TRIM24 mediates ligand-dependent activation of androgen receptor and is repressed by a bromodomain-containing protein, BRD7, in prostate cancer cells. Biochim. Biophys. Acta BBA - Mol. Cell Res. *1793*, 1828–1836.

Kim, M., Lee, S.H., Kim, J., Lee, S.-E., Kim, Y.-J., and Min, C.-K. (2015). Copy number variations could predict the outcome of bortezomib plus melphalan and prednisone for initial treatment of multiple myeloma. Genes. Chromosomes Cancer *54*, 20–27.

Kirkin, V., McEwan, D.G., Novak, I., and Dikic, I. (2009). A Role for Ubiquitin in Selective Autophagy. Mol. Cell *34*, 259–269.

Klener, P. (2019). Advances in Molecular Biology and Targeted Therapy of Mantle Cell Lymphoma. Int. J. Mol. Sci. *20*.

Klionsky, D.J., Abdelmohsen, K., Abe, A., Abedin, M.J., Abeliovich, H., Acevedo Arozena, A., Adachi, H., Adams, C.M., Adams, P.D., Adeli, K., et al. (2016). Guidelines for the use and interpretation of assays for monitoring autophagy (3rd edition). Autophagy *12*, 1–222.

Kocaturk, N.M., and Gozuacik, D. (2018). Crosstalk Between Mammalian Autophagy and the Ubiquitin-Proteasome System. Front. Cell Dev. Biol. *6*, 128.

Komander, D. (2009). The emerging complexity of protein ubiquitination. Biochem. Soc. Trans. *37*, 937–953.

Komander, D., and Rape, M. (2012). The ubiquitin code. Annu. Rev. Biochem. *81*, 203–229.

Konstantinou, E.K., Notomi, S., Kosmidou, C., Brodowska, K., Al-Moujahed, A., Nicolaou, F., Tsoka, P., Gragoudas, E., Miller, J.W., Young, L.H., et al. (2017). Verteporfin-induced formation of protein cross-linked oligomers and high molecular weight complexes is mediated by light and leads to cell toxicity. Sci. Rep. *7*, 46581.

Ladha, A., Zhao, J., Epner, E.M., and Pu, J.J. (2019). Mantle cell lymphoma and its management: where are we now? Exp. Hematol. Oncol. *8*, 2.

Laigle, V., Dingli, F., Amhaz, S., Perron, T., Chouchène, M., Colasse, S., Petit, I., Poullet, P., Loew, D., Prunier, C., et al. (2021). Quantitative ubiquitylome analysis reveals specificity of RNF111/Arkadia E3 ubiquitin ligase for its degradative substrates SKI and SKIL/SnoN in TGF-β signaling pathway. Mol. Cell. Proteomics MCP 100173.

Lang, V., Da Silva-Ferrada, E., Barrio, R., Sutherland, J.D., and Rodriguez, M.S. (2016). Using Biotinylated SUMO-Traps to Analyze SUMOylated Proteins. Methods Mol. Biol. Clifton NJ *1475*, 109–121.

Lee, B.L., Anamika, Glover, J.N.M., Hendzel, M.J., and Spyracopoulos, L. (2017). Molecular basis for K63-linked ubiquitination processes in double-strand DNA break repair: A focus on kinetics and dynamics. J. Mol. Biol. *429*, 3409–3429.

Lee, M.J., Pal, K., Tasaki, T., Roy, S., Jiang, Y., An, J.Y., Banerjee, R., and Kwon, Y.T. (2008). Synthetic heterovalent inhibitors targeting recognition E3 components of the N-end rule pathway. Proc. Natl. Acad. Sci. U. S. A. *105*, 100–105.

Lennert, K., Mohri, N., Stein, H., and Kaiserling, E. (1975). The Histopathology of Malignant Lymphoma. Br. J. Haematol. *31*, 193–203.

Leshchenko, V.V., Kuo, P.-Y., Jiang, Z., Weniger, M.A., Overbey, J., Dunleavy, K., Wilson, W.H., Wiestner, A., and Parekh, S. (2015). Harnessing Noxa demethylation to overcome Bortezomib resistance in mantle cell lymphoma. Oncotarget *6*, 27332–27342.

Li, H., Sun, L., Tang, Z., Fu, L., Xu, Y., Li, Z., Luo, W., Qiu, X., and Wang, E. (2012). Overexpression of TRIM24 correlates with tumor progression in non-small cell lung cancer. PloS One *7*, e37657.

Li, R., Jia, Z., and Trush, M.A. (2016). Defining ROS in Biology and Medicine. React. Oxyg. Species Apex NC *1*, 9–21.

Li, X., Wu, N., and Li, B. (2019). A high mutation rate of immunoglobulin heavy chain variable region gene associates with a poor survival and chemotherapy response of mantle cell lymphoma patients. Medicine (Baltimore) *98*.

Li, Z., Agharkar, P., and Chen, B. (2013). Therapeutic enhancement of vascular-targeted photodynamic therapy by inhibiting proteasomal function. Cancer Lett. *339*, 128–134.

Lilienbaum, A. (2013). Relationship between the proteasomal system and autophagy. Int. J. Biochem. Mol. Biol. *4*, 1–26.

Lin, L., Zhao, W., Sun, B., Wang, X., and Liu, Q. (2017). Overexpression of TRIM24 is correlated with the progression of human cervical cancer. Am. J. Transl. Res. *9*, 620–628.

Liu, X., Huang, Y., Yang, D., Li, X., Liang, J., Lin, L., Zhang, M., Zhong, K., Liang, B., and Li, J. (2014). Overexpression of TRIM24 is associated with the onset and progress of human hepatocellular carcinoma. PloS One *9*, e85462.

Lopez-Reyes, R.G., Quinet, G., Gonzalez-Santamarta, M., Larrue, C., Sarry, J.-E., and Rodriguez, M.S. (2021). Inhibition of the proteasome and proteaphagy enhances apoptosis in FLT3-ITD-driven acute myeloid leukemia. FEBS Open Bio *11*, 48–60.

Lopitz-Otsoa, F., Rodríguez, M.S., and Aillet, F. (2010). Properties of natural and artificial proteins displaying multiple ubiquitin-binding domains. Biochem. Soc. Trans. *38*, 40–45.

Lopitz-Otsoa, F., Rodriguez-Suarez, E., Aillet, F., Casado-Vela, J., Lang, V., Matthiesen, R., Elortza, F., and Rodriguez, M.S. (2012). Integrative analysis of the ubiquitin proteome isolated using Tandem Ubiquitin Binding Entities (TUBEs). J. Proteomics *75*, 2998–3014.

Lü, S., and Wang, J. (2013). The resistance mechanisms of proteasome inhibitor bortezomib. Biomark. Res. *1*, 13.

Lu, J., Qian, Y., Altieri, M., Dong, H., Wang, J., Raina, K., Hines, J., Winkler, J.D., Crew, A.P., Coleman, K., et al. (2015). Hijacking the E3 Ubiquitin Ligase Cereblon to Efficiently Target BRD4. Chem. Biol. *22*, 755–763.

Lu, K., den Brave, F., and Jentsch, S. (2017). Receptor oligomerization guides pathway choice between proteasomal and autophagic degradation. Nat. Cell Biol. *19*, 732–739.

Luanpitpong, S., Chanthra, N., Janan, M., Poohadsuan, J., Samart, P., U-Pratya, Y., Rojanasakul, Y., and Issaragrisil, S. (2018). Inhibition of O-GlcNAcase Sensitizes Apoptosis and Reverses Bortezomib Resistance in Mantle Cell Lymphoma through Modification of Truncated Bid. Mol. Cancer Ther. *17*, 484–496.

Lv, D., Li, Y., Zhang, W., Alvarez, A.A., Song, L., Tang, J., Gao, W.-Q., Hu, B., Cheng, S.-Y., and Feng, H. (2017). TRIM24 is an oncogenic transcriptional co-activator of STAT3 in glioblastoma. Nat. Commun. *8*, 1454.

Macklin, A., Khan, S., and Kislinger, T. (2020). Recent advances in mass spectrometry based clinical proteomics: applications to cancer research. Clin. Proteomics *17*, 17.

Maddocks, K. (2018). Update on mantle cell lymphoma. Blood *132*, 1647–1656.

Mancias, J.D., and Kimmelman, A.C. (2016). Mechanisms of Selective Autophagy in Normal Physiology and Cancer. J. Mol. Biol. *428*, 1659–1680.

Mandell, M.A., Saha, B., and Thompson, T.A. (2020). The Tripartite Nexus: Autophagy, Cancer, and Tripartite Motif-Containing Protein Family Members. Front. Pharmacol. *11*, 308.

Manni, S., Brancalion, A., Tubi, L.Q., Colpo, A., Pavan, L., Cabrelle, A., Ave, E., Zaffino, F., Di Maira, G., Ruzzene, M., et al. (2012). Protein kinase CK2 protects multiple myeloma cells from ER stress-induced apoptosis and from the cytotoxic effect of HSP90 inhibition through regulation of the unfolded protein response. Clin. Cancer Res. Off. J. Am. Assoc. Cancer Res. *18*, 1888–1900.

Marino, S., Petrusca, D.N., Simpson, E., Anderson, J.L., Xie, X.-Q., Liu, Y., Chirgwin, J., and Roodman, G.D. (2019). Targeting the p62-ZZ/N-End Rule Pathway in Multiple Myeloma Overcomes Proteasome Inhibitor-Resistance Via Induction of Necroptosis and Enhances the Bone Anabolic Effects of Proteasome Inhibitors. Blood *134*, 4391–4391.

Marshall, R.S., Li, F., Gemperline, D.C., Book, A.J., and Vierstra, R.D. (2015). Autophagic Degradation of the 26S Proteasome Is Mediated by the Dual ATG8/Ubiquitin Receptor RPN10 in Arabidopsis. Mol. Cell *58*, 1053–1066.

Mata-Cantero, L., Azkargorta, M., Aillet, F., Xolalpa, W., LaFuente, M.J., Elortza, F., Carvalho, A.S., Martin-Plaza, J., Matthiesen, R., and Rodriguez, M.S. (2016). New insights into host-parasite ubiquitin proteome dynamics in P. falciparum infected red blood cells using a TUBEs-MS approach. J. Proteomics *139*, 45–59.

Mathew, R., Karp, C.M., Beaudoin, B., Vuong, N., Chen, G., Chen, H.-Y., Bray, K., Reddy, A., Bhanot, G., Gelinas, C., et al. (2009). Autophagy suppresses tumorigenesis through elimination of p62. Cell *137*, 1062–1075.

Mattern, M., Sutherland, J., Kadimisetty, K., Barrio, R., and Rodriguez, M.S. (2019). Using Ubiquitin Binders to Decipher the Ubiquitin Code. Trends Biochem. Sci. *44*, 599–615.

McConkey, D.J., White, M., and Yan, W. (2012). HDAC inhibitor modulation of proteotoxicity as a therapeutic approach in cancer. Adv. Cancer Res. *116*, 131–163.

Mendes, M.L., Fougeras, M.R., and Dittmar, G. (2020). Analysis of ubiquitin signaling and chain topology cross-talk. J. Proteomics *215*, 103634.

Mennerich, D., Kubaichuk, K., and Kietzmann, T. (2019). DUBs, Hypoxia, and Cancer. Trends Cancer *5*, 632–653.

Meyer, T., Muyldermans, S., and Depicker, A. (2014). Nanobody-based products as research and diagnostic tools. Trends Biotechnol. *32*.

Miao, Z.-F., Wang, Z.-N., Zhao, T.-T., Xu, Y.-Y., Wu, J.-H., Liu, X.-Y., Xu, H., You, Y., and Xu, H.-M. (2015). TRIM24 is upregulated in human gastric cancer and promotes gastric cancer cell growth and chemoresistance. Virchows Arch. Int. J. Pathol. *466*, 525–532.

Michel, M.A., Swatek, K.N., Hospenthal, M.K., and Komander, D. (2017). Ubiquitin Linkage-Specific Affimers Reveal Insights into K6-Linked Ubiquitin Signaling. Mol. Cell *68*, 233-246.e5.

Mimura, N., Fulciniti, M., Gorgun, G., Tai, Y.-T., Cirstea, D., Santo, L., Hu, Y., Fabre, C., Minami, J., Ohguchi, H., et al. (2012). Blockade of XBP1 splicing by inhibition of IRE1α is a promising therapeutic option in multiple myeloma. Blood *119*, 5772–5781.

Miyake, S., Irikura, D., and Yamasaki, T. (2019). Detection of Mast Cells Expressing c-Kit Using Antibody Covalently Bound to Gelatin Elongated from Surface of Immunosensor Based on Surface Plasmon Resonance. Anal. Sci. *35*, 811–813.

Moros, A., Rodríguez, V., Saborit-Villarroya, I., Montraveta, A., Balsas, P., Sandy, P., Martínez, A., Wiestner, A., Normant, E., Campo, E., et al. (2014). Synergistic antitumor activity of lenalidomide with the BET bromodomain inhibitor CPI203 in bortezomib-resistant mantle cell lymphoma. Leukemia *28*, 2049–2059.

Motokura, T. (2019). Turning Point in the Treatment of Mantle Cell Lymphoma. Yonago Acta Med. *62*, 1–7.

Moutel, S., Bery, N., Bernard, V., Keller, L., Lemesre, E., de Marco, A., Ligat, L., Rain, J.-C., Favre, G., Olichon, A., et al. (2016). NaLi-H1: A universal synthetic library of humanized nanobodies providing highly functional antibodies and intrabodies. ELife *5*.

Murray, M.Y., Zaitseva, L., Auger, M.J., Craig, J.I., MacEwan, D.J., Rushworth, S.A., and Bowles, K.M. (2015). Ibrutinib inhibits BTK-driven NF-κB p65 activity to overcome bortezomib-resistance in multiple myeloma. Cell Cycle *14*, 2367–2375.

Nam, T., Han, J.H., Devkota, S., and Lee, H.-W. (2017). Emerging Paradigm of Crosstalk between Autophagy and the Ubiquitin-Proteasome System. Mol. Cells *40*, 897–905.

Nemec, A.A., Howell, L.A., Peterson, A.K., Murray, M.A., and Tomko, R.J. (2017). Autophagic clearance of proteasomes in yeast requires the conserved sorting nexin Snx4. J. Biol. Chem. *292*, 21466–21480.

Ni, M., and Lee, A.S. (2007). ER chaperones in mammalian development and human diseases. FEBS Lett. *581*, 3641–3651.

Niewerth, D., Jansen, G., Assaraf, Y.G., Zweegman, S., Kaspers, G.J.L., and Cloos, J. (2015). Molecular basis of resistance to proteasome inhibitors in hematological malignancies. Drug Resist. Updat. Rev. Comment. Antimicrob. Anticancer Chemother. *18*, 18–35.

Nunes, A.T., and Annunziata, C.M. (2017). Proteasome Inhibitors: Structure and Function. Semin. Oncol. *44*, 377–380.

Ohtake, F., Saeki, Y., Ishido, S., Kanno, J., and Tanaka, K. (2016). The K48-K63 Branched Ubiquitin Chain Regulates NF-κB Signaling. Mol. Cell *64*, 251–266.

Ohtake, F., Tsuchiya, H., Saeki, Y., and Tanaka, K. (2018). K63 ubiquitylation triggers proteasomal degradation by seeding branched ubiquitin chains. Proc. Natl. Acad. Sci. *115*, E1401–E1408.

Olivier Coux, Barbara A. Zieba, and Silke Meiners (2020). The Proteasome System in Health and Disease. In Proteostasis and Disease. Advances in Experimental Medicine and Biology, p. Ordureau, A., Münch, C., and Harper, J.W. (2015). Quantifying ubiquitin signaling. Mol. Cell *58*, 660–676.

Ornatowski, W., Lu, Q., Yegambaram, M., Garcia, A.E., Zemskov, E.A., Maltepe, E., Fineman, J.R., Wang, T., and Black, S.M. (2020). Complex interplay between autophagy and oxidative stress in the development of pulmonary disease. Redox Biol. *36*, 101679.

Palmer, W.S., Poncet-Montange, G., Liu, G., Petrocchi, A., Reyna, N., Subramanian, G., Theroff, J., Yau, A., Kost-Alimova, M., Bardenhagen, J.P., et al. (2016). Structure-Guided Design of IACS-9571, a Selective High-Affinity Dual TRIM24-BRPF1 Bromodomain Inhibitor. J. Med. Chem. *59*, 1440–1454.

Paraskevopoulos, K., Kriegenburg, F., Tatham, M.H., Rösner, H.I., Medina, B., Larsen, I.B., Brandstrup, R., Hardwick, K.G., Hay, R.T., Kragelund, B.B., et al. (2014). Dss1 is a 26S proteasome ubiquitin receptor. Mol. Cell *56*, 453–461.

Pavlides, S., Vera, I., Gandara, R., Sneddon, S., Pestell, R.G., Mercier, I., Martinez-Outschoorn, U.E., Whitaker-Menezes, D., Howell, A., Sotgia, F., et al. (2012). Warburg Meets Autophagy: Cancer-Associated Fibroblasts Accelerate Tumor Growth and Metastasis via Oxidative Stress, Mitophagy, and Aerobic Glycolysis. Antioxid. Redox Signal. *16*, 1264–1284.

Peng, H., Yang, J., Li, G., You, Q., Han, W., Li, T., Gao, D., Xie, X., Lee, B.-H., Du, J., et al. (2017). Ubiquitylation of p62/sequestosome1 activates its autophagy receptor function and controls selective autophagy upon ubiquitin stress. Cell Res. *27*, 657–674.

Peng, Y., Zhang, M., Jiang, Z., and Jiang, Y. (2019). TRIM28 activates autophagy and promotes cell proliferation in glioblastoma. OncoTargets Ther. *12*, 397–404.

Pérez Berrocal, D.A., Witting, K.F., Ovaa, H., and Mulder, M.P.C. (2019). Hybrid Chains: A Collaboration of Ubiquitin and Ubiquitin-Like Modifiers Introducing Cross-Functionality to the Ubiquitin Code. Front. Chem. *7*, 931.

Pérez-Galán, P., Roué, G., Villamor, N., Montserrat, E., Campo, E., and Colomer, D. (2006). The proteasome inhibitor bortezomib induces apoptosis in mantle-cell lymphoma through generation of ROS and Noxa activation independent of p53 status. Blood *107*, 257–264.

Pérez-Galán, P., Roué, G., Villamor, N., Campo, E., and Colomer, D. (2007). The BH3-mimetic GX15-070 synergizes with bortezomib in mantle cell lymphoma by enhancing Noxa-mediated activation of Bak. Blood *109*, 4441–4449.

Pérez-Galán, P., Dreyling, M., and Wiestner, A. (2011). Mantle cell lymphoma: biology, pathogenesis, and the molecular basis of treatment in the genomic era. Blood *117*, 26–38.

Pham, L.V., Tamayo, A.T., Li, C., Bornmann, W., Priebe, W., and Ford, R.J. (2010). Degrasyn potentiates the antitumor effects of bortezomib in Mantle cell lymphoma cells in vitro and in vivo: therapeutic implications. Mol. Cancer Ther. *9*, 2026–2036.

Pirone, L., Xolalpa, W., Sigurðsson, J.O., Ramirez, J., Pérez, C., González, M., de Sabando, A.R., Elortza, F., Rodriguez, M.S., Mayor, U., et al. (2017). A comprehensive platform for the analysis of ubiquitin-like protein modifications using in vivo biotinylation. Sci. Rep. *7*, 40756.

Podar, K., Chauhan, D., and Anderson, K.C. (2009). Bone marrow microenvironment and the identification of new targets for myeloma therapy. Leukemia *23*, 10–24.

Pontrelli, P., Conserva, F., and Gesualdo, L. (2019). The Role of Lysine 63-Linked Ubiquitylation in Health and Disease. Ubiquitin Proteasome Syst. - Curr. Insights Mech. Cell. Regul. Dis.

Qi, S.-M., Dong, J., Xu, Z.-Y., Cheng, X.-D., Zhang, W.-D., and Qin, J.-J. (2021). PROTAC: An Effective Targeted Protein Degradation Strategy for Cancer Therapy. Front. Pharmacol. *12*, 1124.

Quinet, G., Gonzalez-Santamarta, M., Louche, C., and Rodriguez, M.S. (2020). Mechanisms Regulating the UPS-ALS Crosstalk: The Role of Proteaphagy. Mol. Basel Switz. *25*.

Raedler, L. (2015). Velcade (Bortezomib) Receives 2 New FDA Indications: For Retreatment of Patients with Multiple Myeloma and for First-Line Treatment of Patients with Mantle-Cell Lymphoma. Am. Health Drug Benefits *8*, 135–140.

Redza-Dutordoir, M., and Averill-Bates, D.A. (2016). Activation of apoptosis signalling pathways by reactive oxygen species. Biochim. Biophys. Acta *1863*, 2977–2992.

Reverdatto, S., Burz, D.S., and Shekhtman, A. (2015). Peptide Aptamers: Development and Applications. Curr. Top. Med. Chem. *15*, 1082–1101.

Riedinger, C., Boehringer, J., Trempe, J.-F., Lowe, E.D., Brown, N.R., Gehring, K., Noble, M.E.M., Gordon, C., and Endicott, J.A. (2010). Structure of Rpn10 and Its Interactions with Polyubiquitin Chains and the Proteasome Subunit Rpn12. J. Biol. Chem. *285*, 33992–34003.

Riz, I., Hawley, T.S., Marsal, J.W., and Hawley, R.G. (2016). Noncanonical SQSTM1/p62-Nrf2 pathway activation mediates proteasome inhibitor resistance in multiple myeloma cells via redox, metabolic and translational reprogramming. Oncotarget *7*, 66360–66385.

Rizzieri, D.A., Feldman, E., Dipersio, J.F., Gabrail, N., Stock, W., Strair, R., Rivera, V.M., Albitar, M., Bedrosian, C.L., and Giles, F.J. (2008). A phase 2 clinical trial of deforolimus (AP23573, MK-8669), a novel mammalian target of rapamycin inhibitor, in patients with relapsed or

refractory hematologic malignancies. Clin. Cancer Res. Off. J. Am. Assoc. Cancer Res. *14*, 2756–2762.

Robak, P., Drozdz, I., Szemraj, J., and Robak, T. (2018). Drug resistance in multiple myeloma. Cancer Treat. Rev. *70*, 199–208.

Rockenfeller, P., Koska, M., Pietrocola, F., Minois, N., Knittelfelder, O., Sica, V., Franz, J., Carmona-Gutierrez, D., Kroemer, G., and Madeo, F. (2015). Phosphatidylethanolamine positively regulates autophagy and longevity. Cell Death Differ. *22*, 499–508.

Roeten, M.S.F., Cloos, J., and Jansen, G. (2018). Positioning of proteasome inhibitors in therapy of solid malignancies. Cancer Chemother. Pharmacol. *81*, 227–243.

Ronau, J.A., Beckmann, J.F., and Hochstrasser, M. (2016). Substrate specificity of the ubiquitin and Ubl proteases. Cell Res. *26*, 441–456.

Rosenzweig, R., Bronner, V., Zhang, D., Fushman, D., and Glickman, M.H. (2012). Rpn1 and Rpn2 Coordinate Ubiquitin Processing Factors at Proteasome. J. Biol. Chem. *287*, 14659–14671.

Roué, G., Pérez-Galán, P., Mozos, A., López-Guerra, M., Xargay-Torrent, S., Rosich, L., Saborit-Villarroya, I., Normant, E., Campo, E., and Colomer, D. (2011). The Hsp90 inhibitor IPI-504 overcomes bortezomib resistance in mantle cell lymphoma in vitro and in vivo by down-regulation of the prosurvival ER chaperone BiP/Grp78. Blood *117*, 1270–1279.

Rule, S. (2019). The modern approach to mantle cell lymphoma. Hematol. Oncol. *37 Suppl 1*, 66–69.

Samant, R.S., Livingston, C.M., Sontag, E.M., and Frydman, J. (2018). Distinct proteostasis circuits cooperate in nuclear and cytoplasmic protein quality control. Nature *563*, 407–411.

Sanchez, W.Y., McGee, S.L., Connor, T., Mottram, B., Wilkinson, A., Whitehead, J.P., Vuckovic, S., and Catley, L. (2013). Dichloroacetate inhibits aerobic glycolysis in multiple myeloma cells and increases sensitivity to bortezomib. Br. J. Cancer *108*, 1624–1633.

Schreiner, P., Chen, X., Husnjak, K., Randles, L., Zhang, N., Elsasser, S., Finley, D., Dikic, I., Walters, K.J., and Groll, M. (2008). Ubiquitin docking at the proteasome through a novel pleckstrin-homology domain interaction. Nature *453*, 548–552.

Selimovic, D., Porzig, B.B.O.W., El-Khattouti, A., Badura, H.E., Ahmad, M., Ghanjati, F., Santourlidis, S., Haikel, Y., and Hassan, M. (2013). Bortezomib/proteasome inhibitor triggers both apoptosis and autophagy-dependent pathways in melanoma cells. Cell. Signal. *25*, 308–318.

Serna, S., Xolalpa, W., Lang, V., Aillet, F., England, P., Reichardt, N., and Rodriguez, M.S. (2016). Efficient monitoring of protein ubiquitylation levels using TUBEs-based microarrays. FEBS Lett. *590*, 2748–2756.

Sha, Z., Schnell, H.M., Ruoff, K., and Goldberg, A. (2018). Rapid induction of p62 and GABARAPL1 upon proteasome inhibition promotes survival before autophagy activation. J. Cell Biol. *217*, 1757–1776.

Shi, Y., Chen, X., Elsasser, S., Stocks, B.B., Tian, G., Lee, B.-H., Shi, Y., Zhang, N., de Poot, S.A.H., Tuebing, F., et al. (2016). Rpn1 provides adjacent receptor sites for substrate binding and deubiquitination by the proteasome. Science *351*.

Shiber, A., and Ravid, T. (2014). Chaperoning Proteins for Destruction: Diverse Roles of Hsp70 Chaperones and their Co-Chaperones in Targeting Misfolded Proteins to the Proteasome. Biomolecules *4*, 704–724.

Shpilka, T., Weidberg, H., Pietrokovski, S., and Elazar, Z. (2011). Atg8: an autophagy-related ubiquitin-like protein family. Genome Biol. *12*, 226.

Smyth, G.K. (2004). Linear models and empirical bayes methods for assessing differential expression in microarray experiments. Stat. Appl. Genet. Mol. Biol. *3*, Article3.

Song, P., Li, S., Wu, H., Gao, R., Rao, G., Wang, D., Chen, Z., Ma, B., Wang, H., Sui, N., et al. (2016). Parkin promotes proteasomal degradation of p62: implication of selective vulnerability of neuronal cells in the pathogenesis of Parkinson's disease. Protein Cell *7*, 114–129.

Soriano, G.P., Besse, L., Li, N., Kraus, M., Besse, A., Meeuwenoord, N., Bader, J., Everts, B., den Dulk, H., Overkleeft, H.S., et al. (2016). Proteasome inhibitor-adapted myeloma cells are largely independent from proteasome activity and show complex proteomic changes, in particular in redox and energy metabolism. Leukemia *30*, 2198–2207.

Spit, M., Rieser, E., and Walczak, H. (2019). Linear ubiquitination at a glance. J. Cell Sci. *132*.
Sun, S.-Y. (2010). N-acetylcysteine, reactive oxygen species and beyond. Cancer Biol. Ther. *9*, 109–110.

Sun, B., Fiskus, W., Qian, Y., Rajapakshe, K., Raina, K., Coleman, K.G., Crew, A.P., Shen, A., Saenz, D.T., Mill, C.P., et al. (2018). BET protein proteolysis targeting chimera (PROTAC) exerts potent lethal activity against mantle cell lymphoma cells. Leukemia *32*, 343–352.

Swatek, K.N., and Komander, D. (2016). Ubiquitin modifications. Cell Res. *26*, 399–422.

Swerdlow, S.H., Campo, E., Pileri, S.A., Harris, N.L., Stein, H., Siebert, R., Advani, R., Ghielmini, M., Salles, G.A., Zelenetz, A.D., et al. (2016). The 2016 revision of the World Health Organization classification of lymphoid neoplasms. Blood *127*, 2375–2390.

Sylvestersen, K.B., Young, C., and Nielsen, M.L. (2013). Advances in characterizing ubiquitylation sites by mass spectrometry. Curr. Opin. Chem. Biol. *17*, 49–58.

Szegezdi, E., Logue, S.E., Gorman, A.M., and Samali, A. (2006). Mediators of endoplasmic reticulum stress-induced apoptosis. EMBO Rep. *7*, 880–885.

Takahashi, D., Moriyama, J., Nakamura, T., Miki, E., Takahashi, E., Sato, A., Akaike, T., Itto-Nakama, K., and Arimoto, H. (2019). AUTACs: Cargo-Specific Degraders Using Selective Autophagy. Mol. Cell *76*, 797-810.e10.

Takeshige, K., Baba, M., Tsuboi, S., Noda, T., and Ohsumi, Y. (1992). Autophagy in yeast demonstrated with proteinase-deficient mutants and conditions for its induction. J. Cell Biol. *119*, 301–311.

Tanaka, K. (2009). The proteasome: Overview of structure and functions. Proc. Jpn. Acad. Ser. B Phys. Biol. Sci. *85*, 12–36.

Tanida, I., Ueno, T., and Kominami, E. (2004). LC3 conjugation system in mammalian autophagy. Int. J. Biochem. Cell Biol. *36*, 2503–2518.

Thorn, K. (2017). Genetically encoded fluorescent tags. Mol. Biol. Cell *28*, 848–857.

Tian, Z., D'Arcy, P., Wang, X., Ray, A., Tai, Y.-T., Hu, Y., Carrasco, R.D., Richardson, P., Linder, S., Chauhan, D., et al. (2014). A novel small molecule inhibitor of deubiquitylating enzyme USP14 and UCHL5 induces apoptosis in multiple myeloma and overcomes bortezomib resistance. Blood *123*, 706–716.

Tsai, W.-W., Wang, Z., Yiu, T.T., Akdemir, K.C., Xia, W., Winter, S., Tsai, C.-Y., Shi, X., Schwarzer, D., Plunkett, W., et al. (2010). TRIM24 links a noncanonical histone signature to breast cancer. Nature *468*, 927–932.

Tsamesidis, I., Egwu, C.O., Pério, P., Augereau, J.-M., Benoit-Vical, F., and Reybier, K. (2020). An LC-MS Assay to Measure Superoxide Radicals and Hydrogen Peroxide in the Blood System. Metabolites *10*, E175.

Tsvetkov, P., Reuven, N., and Shaul, Y. (2010). Ubiquitin-independent p53 proteasomal degradation. Cell Death Differ. *17*, 103–108.

Turner, J.G., Kashyap, T., Dawson, J.L., Gomez, J., Bauer, A.A., Grant, S., Dai, Y., Shain, K.H., Meads, M., Landesman, Y., et al. (2016). XPO1 inhibitor combination therapy with bortezomib or carfilzomib induces nuclear localization of IκBα and overcomes acquired proteasome inhibitor resistance in human multiple myeloma. Oncotarget *7*, 78896–78909.

Valentin, R., Grabow, S., and Davids, M.S. (2018). The rise of apoptosis: targeting apoptosis in hematologic malignancies. Blood *132*, 1248–1264.

Valletti, A., Marzano, F., Pesole, G., Sbisà, E., and Tullo, A. (2019). Targeting Chemoresistant Tumors: Could TRIM Proteins-p53 Axis Be a Possible Answer? Int. J. Mol. Sci. *20*.

Varshavsky, A. (2011). The N-end rule pathway and regulation by proteolysis. Protein Sci. Publ. Protein Soc. *20*, 1298–1345.

Veloza, L., Ribera-Cortada, I., and Campo, E. (2019). Mantle cell lymphoma pathology update in the 2016 WHO classification. Ann. Lymphoma *3*.

Vincenz, L., Jäger, R., O'Dwyer, M., and Samali, A. (2013). Endoplasmic reticulum stress and the unfolded protein response: targeting the Achilles heel of multiple myeloma. Mol. Cancer Ther. *12*, 831–843.

Waite, K.A., De-La Mota-Peynado, A., Vontz, G., and Roelofs, J. (2016). Starvation Induces Proteasome Autophagy with Different Pathways for Core and Regulatory Particles. J. Biol. Chem. *291*, 3239–3253.

Wang, C., Pan, Y.-H., Shan, M., Xu, M., Bao, J.-L., and Zhao, L.-M. (2015). Knockdown of UbcH10 Enhances the Chemosensitivity of Dual Drug Resistant Breast Cancer Cells to Epirubicin and Docetaxel. Int. J. Mol. Sci. *16*, 4698–4712.

Wang, F.-Q., Han, Y., Yao, W., and Yu, J. (2017). Prognostic relevance of tripartite motif containing 24 expression in colorectal cancer. Pathol. Res. Pract. *213*, 1271–1275.

Wang, H., Xue, W., and Jiang, X. (2018). Overexpression of TRIM24 Stimulates Proliferation and Glucose Metabolism of Head and Neck Squamous Cell Carcinoma. BioMed Res. Int. *2018*, e6142843.

Wei, H., Wang, C., Croce, C.M., and Guan, J.-L. (2014). p62/SQSTM1 synergizes with autophagy for tumor growth in vivo. Genes Dev. *28*, 1204–1216.

Wei, Y., Liu, M., Li, X., Liu, J., and Li, H. (2018). Origin of the Autophagosome Membrane in Mammals. BioMed Res. Int. *2018*, 1012789.

Weinkauf, M., Zimmermann, Y., Hartmann, E., Rosenwald, A., Rieken, M., Pastore, A., Hutter, G., Hiddemann, W., and Dreyling, M. (2009). 2-D PAGE-based comparison of proteasome inhibitor bortezomib in sensitive and resistant mantle cell lymphoma. Electrophoresis *30*, 974–986.

Welk, V., Coux, O., Kleene, V., Abeza, C., Trümbach, D., Eickelberg, O., and Meiners, S. (2016). Inhibition of Proteasome Activity Induces Formation of Alternative Proteasome Complexes. J. Biol. Chem. *291*, 13147–13159.

Weniger, M.A., Rizzatti, E.G., Pérez-Galán, P., Liu, D., Wang, Q., Munson, P.J., Raghavachari, N., White, T., Tweito, M.M., Dunleavy, K., et al. (2011). Treatment-induced oxidative stress and cellular antioxidant capacity determine response to bortezomib in mantle cell lymphoma. Clin. Cancer Res. Off. J. Am. Assoc. Cancer Res. *17*, 5101–5112.

White, E., and DiPaola, R.S. (2009). The Double-edged Sword of Autophagy Modulation in Cancer. Clin. Cancer Res. Off. J. Am. Assoc. Cancer Res. *15*, 5308–5316.

van Wijk, S.J., Fulda, S., Dikic, I., and Heilemann, M. (2019). Visualizing ubiquitination in mammalian cells. EMBO Rep. *20*.

Witzig, T.E., Geyer, S.M., Ghobrial, I., Inwards, D.J., Fonseca, R., Kurtin, P., Ansell, S.M., Luyun, R., Flynn, P.J., Morton, R.F., et al. (2005). Phase II trial of single-agent temsirolimus (CCI-779) for relapsed mantle cell lymphoma. J. Clin. Oncol. Off. J. Am. Soc. Clin. Oncol. *23*, 5347–5356.

Wójcik, C., and DeMartino, G.N. (2003). Intracellular localization of proteasomes. Int. J. Biochem. Cell Biol. *35*, 579–589.

Xie, Y., Kang, R., Sun, X., Zhong, M., Huang, J., Klionsky, D.J., and Tang, D. (2015). Posttranslational modification of autophagy-related proteins in macroautophagy. Autophagy *11*, 28–45.

Xie, Z., Nair, U., and Klionsky, D.J. (2008). Atg8 controls phagophore expansion during autophagosome formation. Mol. Biol. Cell *19*, 3290–3298.

Xolalpa, W., Mata-Cantero, L., Aillet, F., and Rodriguez, M.S. (2016). Isolation of the Ubiquitin-Proteome from Tumor Cell Lines and Primary Cells Using TUBEs. Methods Mol. Biol. Clifton NJ *1449*, 161–175.

Yan, X.-Y., Zhang, Y., Zhang, J.-J., Zhang, L.-C., Liu, Y.-N., Wu, Y., Xue, Y.-N., Lu, S.-Y., Su, J., and Sun, L.-K. (2017). p62/SQSTM1 as an oncotarget mediates cisplatin resistance through activating RIP1-NF-κB pathway in human ovarian cancer cells. Cancer Sci. *108*, 1405–1413.

Yang, A., Li, Y., Pantoom, S., Triola, G., and Wu, Y.-W. (2013). Semisynthetic lipidated LC3 protein mediates membrane fusion. Chembiochem Eur. J. Chem. Biol. *14*, 1296–1300.

Yang, D.T., Young, K.H., Kahl, B.S., Markovina, S., and Miyamoto, S. (2008). Prevalence of bortezomib-resistant constitutive NF-kappaB activity in mantle cell lymphoma. Mol. Cancer *7*, 40.

Yang, Y., Chen, Y., Saha, M.N., Chen, J., Evans, K., Qiu, L., Reece, D., Chen, G.A., and Chang, H. (2015). Targeting phospho-MARCKS overcomes drug-resistance and induces antitumor activity in preclinical models of multiple myeloma. Leukemia *29*, 715–726.

Yau, R.G., Doerner, K., Castellanos, E.R., Haakonsen, D.L., Werner, A., Wang, N., Yang, X.W., Martinez-Martin, N., Matsumoto, M.L., Dixit, V.M., et al. (2017). Assembly and Function of Heterotypic Ubiquitin Chains in Cell-Cycle and Protein Quality Control. Cell *171*, 918-933.e20.
Yong, K., Gonzalez-McQuire, S., Szabo, Z., Schoen, P., and Hajek, R. (2018). The start of a new wave: Developments in proteasome inhibition in multiple myeloma. Eur. J. Haematol.

Zaffagnini, G., and Martens, S. (2016). Mechanisms of Selective Autophagy. J. Mol. Biol. *428*, 1714–1724.

Zee, B.M., and Garcia, B.A. (2012). Discovery of lysine post-translational modifications through mass spectrometric detection. Essays Biochem. *52*, 147–163.

Zhan, Y., Kost-Alimova, M., Shi, X., Leo, E., Bardenhagen, J.P., Shepard, H.E., Appikonda, S., Vangamudi, B., Zhao, S., Tieu, T.N., et al. (2015). Development of novel cellular histone-binding and chromatin-displacement assays for bromodomain drug discovery. Epigenetics Chromatin *8*, 37.

Zhang, L.-H., Yin, A.-A., Cheng, J.-X., Huang, H.-Y., Li, X.-M., Zhang, Y.-Q., Han, N., and Zhang, X. (2015). TRIM24 promotes glioma progression and enhances chemoresistance through activation of the PI3K/Akt signaling pathway. Oncogene *34*, 600–610.

Zhang, P.-P., Ding, D.-Z., Shi, B., Zhang, S.-Q., Gu, L.-L., Wang, Y.-C., and Cheng, C. (2018). Expression of TRIM28 correlates with proliferation and Bortezomib-induced apoptosis in B-cell non-Hodgkin lymphoma. Leuk. Lymphoma *59*, 1–11.

Zhang, T., Shen, S., Qu, J., and Ghaemmaghami, S. (2016). Global Analysis of Cellular Protein Flux Quantifies the Selectivity of Basal Autophagy. Cell Rep. *14*, 2426–2439.

Zhang, Z., Wu, S., Stenoien, D.L., and Paša-Tolić, L. (2014). High-Throughput Proteomics. Annu. Rev. Anal. Chem. *7*, 427–454.

Zhao, Y., and Jensen, O.N. (2009). Modification-specific proteomics: Strategies for characterization of post-translational modifications using enrichment techniques. Proteomics *9*, 4632–4641.

Zhu, K., Dunner, K., and McConkey, D.J. (2010). Proteasome inhibitors activate autophagy as a cytoprotective response in human prostate cancer cells. Oncogene *29*, 451–462.

Zhu, Q., Yu, T., Gan, S., Wang, Y., Pei, Y., Zhao, Q., Pei, S., Hao, S., Yuan, J., Xu, J., et al. (2020). TRIM24 facilitates antiviral immunity through mediating K63-linked TRAF3 ubiquitination. J. Exp. Med. *217*, e20192083.

Zhu, Y., Zhao, L., Shi, K., Huang, Z., and Chen, B. (2018). TRIM24 promotes hepatocellular carcinoma progression via AMPK signaling. Exp. Cell Res. *367*, 274–281.

22. Associated publications.

Gonzalez-Santamarta, M., Quinet, G**.,** Reyes-Garau, D., Sola, B., Roué, G., & Rodriguez, M. S. (2020). **Resistance to the Proteasome Inhibitors: Lessons from Multiple Myeloma and Mantle Cell Lymphoma**. *Advances in experimental medicine and biology*, *1233*, 153–174. https://doi.org/10.1007/978-3-030-38266-7_6

Quinet, G., **Gonzalez-Santamarta, M.,** Louche, C., & Rodriguez, M. S. (2020). **Mechanisms Regulating the UPS-ALS Crosstalk: The Role of Proteaphagy**. *Molecules*, *25*(10), 2352. MDPI AG. http://dx.doi.org/10.3390/molecules25102352

Lopez-Reyes, R., Quinet, G., **Gonzalez-Santamarta, M**., Larrue, C., Sarry, J.E, Rodriguez M.S (2020). **New insights into proteasome inhibition-induced proteaphagy in acute myeloid leukemia**. *FEBS Open Bio* https://doi.org/10.1002/2211-5463.12950

Quinet, G., Xolalpa, W., Reyes-Garau D., Azkargorta M., Ceccato L., **Gonzalez-Santamarta M**., Marsal. M, Andilla J., Aillet F., Bosch F, Elortza F., Loza-Alvarez P., Sola B., Coux O., Matthiesen R., Roué G., Rodriguez M.S. **Targeting p62/Sequestosome-1 impairs constitutively active proteaphagy and enhances apoptosis in bortezomib-resistant mantle cell lymphoma.** *(Article in revision 2021)*

Gonzalez-Santamarta M, Xolalpa W, Bouvier C, Rodriguez MS. **Ubiquitin-chains dynamics and its role regulating crucial cellular processes.** *Seminars in Cell and Developmental Biology.* https://www.sciencedirect.com/science/article/abs/pii/S1084952121003050 .

In preparation:

Gonzalez-Santamarta M, Rune Matthiessen, JC Rain, Manuel S. Rodríguez. Isolation and Mass Spectrometry identification of the Ubiquitin Proteome in Mantle Cell Lymphoma cells using Ubiquitin Chain-specific Nanobodies. (Book Methods in Molecular Biology, Springer, 2022).

Gonzalez-Santamarta M, Bouvier C, James. D. Sutherland, Barrio R, Rodriguez MS. The Tripartite Motif Containing protein 24 (TRIM24), regulates apoptosis in bortezomib resistant in Mantle Cell Lymphoma cells. (In preparation to be submitted to Cell Death and Disease. 2022).

Resistance to the Proteasome Inhibitors: Lessons from Multiple Myeloma and Mantle Cell Lymphoma

6

Maria Gonzalez-Santamarta, Grégoire Quinet, Diana Reyes-Garau, Brigitte Sola, Gaël Roué, and Manuel S. Rodriguez

Abstract

Since its introduction in the clinics in early 2000s, the proteasome inhibitor bortezomib (BTZ) significantly improved the prognosis of patients with multiple myeloma (MM) and mantle cell lymphoma (MCL), two of the most challenging B cell malignancies in western countries. However, relapses following BTZ therapy are frequent, while primary resistance to this agent remains a major limitation for further development of its therapeutic potential. In the present chapter, we recapitulate the molecular mechanisms associated with intrinsic and acquired resistance to BTZ learning from MM and MCL experience, including mutations of crucial genes and activation of prosurvival signalling pathways inherent to malignant B cells. We also outline the preclinical and clinical evaluations of some potential druggable targets associated to BTZ resistance, considering the most meaningful findings of the past 10 years. Although our understanding of BTZ resistance is far from being completed, recent discoveries are contributing to develop new approaches to treat relapsed MM and MCL patients.

Keywords

BTZ resistance · Proteasome · Ubiquitin · Mantle cell lymphoma · Multiple myeloma

6.1 Introduction

Proteolysis is tightly regulated in eukaryotes through the superposition of sophisticated molecular mechanisms to ensure protein homeostasis. One of the major proteolytic activities is driven by the 26S proteasome that holds a catalytic core particle (CP) or 20S [1]. The proteolytic activity of the 26S proteasome requires the previous ubiquitylation of protein targets mediated by a cascade of thiol-ester reactions implicating at least 3 enzymes named activating (E1), conjugating (E2) and ubiquitin ligases (E3). Removal or remodelling of ubiquitin chains condition the stability, localisation and function of the modified target proteins. The ubiquitin tagging step and the 26S-mediated proteolysis constitute the Ubiquitin–Proteasome System (UPS). Some proteins directly degraded by the CP do not require ubiquitin tagging and are therefore destroyed by an ubiquitin-independent process. The CP can also include proteasome subunits that are specifically involved in the immune response, constituting the immunoproteasome. Furthermore,

M. Gonzalez-Santamarta · G. Quinet · M. S. Rodriguez (✉)
ITAV-IPBS, CNRS USR3505, Toulouse, France
e-mail: manuel.rodriguez@cnrs.fr

D. Reyes-Garau · G. Roué
Lymphoma Translational Group, Josep Carreras Leukaemia Research Institute (IJC), Badalona (Barcelona), Spain

B. Sola
Normandie University, INSERM UMR1245, UNICAEN, Caen, France

R. Barrio et al. (eds.), *Proteostasis and Disease*, Advances in Experimental Medicine and Biology 1233,
https://doi.org/10.1007/978-3-030-38266-7_6

the CP can be associated to other regulatory subunits such as 11S, which have specialised cellular functions [1]. In sum, the proteasome acts as a central hub of cellular proteolysis, having an impact on multiple processes such as cell cycle, DNA repair, cell differentiation, immune response, amino acid recycling or apoptosis. For this reason, the proteasome became a privileged target for drug development to treat diverse disorders including cancers, infections and inflammation-related diseases, among others [2]. The proteasome inhibitor (PI) bortezomib (BTZ), also known as Velcade, was, in 2003 and 2006, the first Food and Drug Administration (FDA)-approved PI for the treatment of two haematological malignancies: multiple myeloma (MM) and chemotherapy-resistant mantle cell lymphoma (MCL), respectively. Despite the success of BTZ therapy, inherent and acquired resistance in patients were observed, encouraging the development of a new generation of PIs, as well as small molecules targeting enzymes of the UPS. Full understanding of the mechanisms underlying BTZ resistance in cancer is a prerequisite to design new strategies to recover sensitivity to these agents, or to use alternative treatments to lower apoptosis threshold in BTZ-resistant cells. To elucidate these mechanisms several laboratories have characterised a number of patient-derived MM and MCL cell lines with natural or acquired resistance to BTZ. In this chapter we summarise mechanisms of PI resistance reported in the last decade. Even if some of these acquired resistance mechanisms have not yet been confirmed in patients, their discovery may have an impact in upcoming clinical studies. We also review potential strategies to overcome PIs resistance mechanisms, including the use of new signalling pathways inhibitors regulating protein homeostasis.

6.2 Cancers Treated with Proteasome Inhibitors

Resistance to proteasome inhibitors has been observed in various cancer types including haematological, pancreatic or breast cancer [3]. Two of the best responding cancers are MM and MCL and for this reason, more knowledge has been accumulated on BTZ resistance for these haematologic disorders [4].

6.2.1 Multiple Myeloma

MM is a plasma cell malignancy with bone marrow (BM) infiltration of clonal cells and monoclonal immunoglobulin protein in the serum and/or urine of patients. Genomic techniques have allowed a better understanding of the genetic abnormalities of MM by providing a better landscape of this collection of diseases with a common clinical phenotype [5]. Several genetic alterations including chromosomal translocations of the immunoglobulin heavy chain (*IGH*) gene leading to the overexpression of D-type cyclins, have been considered as primary events. Not less important are the secondary mutations and clonal evolution. The most frequent mutations occur in *KRAS, NRAS, FAM46C, DIS3* and *TP53,* among others. These mutations affect multiple signalling pathways by altering the mRNA levels but also protein expression and stability. In the past decade, this knowledge has contributed to remarkable changes in the clinical practices, such as the implementation of more effective therapies including new classes of drugs like PIs. The combination of BTZ with immunomodulatory drugs (IMiDs) such as lenalidomide or dexamethasone are currently among the most effective treatments in MM (see Sect. 6.4). The success of BTZ as a MM treatment underlies its broad impact on the stability and activity of vital cellular factors.

6.2.2 Mantle Cell Lymphoma

MCL is an aggressive non-Hodgkin lymphoma (NHL) arising from pre-germinal centre of mature B cells and is typically incurable due to the inevitable development of drug resistance, leading to the worst prognosis among NHL subtypes [6]. Classical MCL cells show minimal mutations in the IGH variable region gene (*IGHV*) and express the transcription factor SOX11. Patients present tumours in lymph nodes or extra-nodal

sites and cells overexpressing cyclin D1 are prone to acquisition of additional abnormalities in cell cycle, DNA damage response, or cell survival pathways, leading to a more aggressive disease behaviour. Less typical are leukemic non-nodal MCL developed through the germinal centre with IGHV somatic hypermutation and minimal SOX11 expression. These patients present MCL cells in peripheral blood, BM and spleen. Leukemic non-nodal MCL behaves in a more indolent way with genetic stability over time. Secondary genetic abnormalities, such as *TP53* mutations, result in a more aggressive disease associated with poor outcome. Since BTZ was approved by the FDA in 2006 for the treatment of relapsed/refractory (R/R) MCL, numerous phenomena have been described to explain innate or acquired resistance observed in more than half of patients [7]. It is known that the development of resistance to BTZ in MCL is an adaptive process, which takes place gradually and includes metabolic changes and/or deregulated (re)activation of adaptive processes like plasmacytic differentiation, autophagy, or improper activation of intracellular signalling pathways such as PI3K/AKT/mTOR axis or NF-κB, among others.

6.2.3 Proteasomes and Chemical Inhibitors

Proteasomes are macromolecular proteolytic complexes with distinct roles under multiple physiologic or pathologic situations. The 26S proteasome is composed by a 19S regulatory particle that recognises ubiquitin chain as degradation signals [1]. The catalytic core or 20S subunit contains 7 α and 7 β subunits of which β5, β2 and β1 hold the chymotrypsin-like, trypsin-like and peptidyl-glutamyl peptide-hydrolysing activity. Alternative β subunits named β5i, β2i and β1i are expressed in haematopoietic cells in response to pro-inflammatory signals such as cytokines or γ interferon and integrate the immunoproteasome. The 20S core can also associate with 11S, another regulatory particle also known as PA28, REG or PA26 which contributes to the action of the immunoproteasome but can also drive proteolysis in other cellular compartments such as the nucleus [1]. Given the role of the proteasome in the degradation of many critical cellular factors, its potential as therapeutic target attracted the interest of many pharmaceutical companies.

Approved in the 2000s by the FDA, BTZ has been used for decades as one pivotal treatment in MM and MCL. However, its association with neuropathy and the acquisition of resistance in the clinics highlighted the need to develop new PIs that would be more effective, less toxic and would reduce the occurrence of resistance. Each of these aspects was considered for the development of second generation PIs such as marizomib (MRZ), carfilzomib (CFZ), ixazomib (IXZ) and oprozomib (OPZ) [3] (Table 6.1). Unlike BTZ, some of them target all the catalytic sites of the proteasome, like MRZ. They carry a different administration way and reversibility than BTZ, hence reducing off-target effects and toxicities in patients. MRZ and OPZ are in early clinical development, and CFZ and IXZ have been already approved in combined treatment for R/R MM. However, preclinical adaptation to these new agents has already been reported, strengthening the need for alternative strategies to face PI resistance [8].

6.3 Molecular Origin of the Resistance to Bortezomib

In the last decade, several molecular mechanisms involved in BTZ resistance have been proposed. During the progression of the disease, complex genomic alterations promote the activation of different signalling cascades that contribute to the development of the resistant phenotype. These include defects in the initiation/regulation of cellular stress, cell differentiation, apoptosis and autophagy, in combination with mutations and alterations in the expression of the drug target. On the other hand, microenvironmental factors and epigenetics can be another source of inherent resistance mechanism, as these events can modulate the expression of critical genes, including

Table 6.1 Proteasome inhibitors

PI	Action	Family	Target	IC_{50} (nM)
Bortezomib	Reversible	Boronate	β5c β5i β1c	7 4 74
Carfilzomib	Irreversible	Epoxyketone	β5c β5i	5 33
Oprozomib CFZ oral analogue	Irreversible	Epoxyketone	β5c β5i	36 82
Ixazomib	Reversible	Boronate	β5c β5i	3 31
Marizomib	Irreversible	β-Lactone	β5c β2c β1c	2.5 26 330
ONX0914	Irreversible	Epoxyketone	β5c β5i	28 280

Data presented in the table have been compiled from [4]

tumour suppressors [9]. The acquired resistance to BTZ is also multifactorial including, among others alterations, the levels of expression of proteasome subunits, crosstalk with other proteolytic pathways or overexpression of efflux pumps (Fig. 6.1).

6.3.1 Inherent Resistance

In this part of the chapter, we will review available data about molecular mechanisms that have been proposed so far to be at the origin of the inherent BTZ-resistant phenotype in MM and MCL.

6.3.1.1 Mutations in PSMB5 Proteasome Subunit

PSMB5 mutations are known to lower PI binding capacity and to impair the chymotrypsin-like catalytic activity of the 20S proteasome [10, 11] giving a benefit under PI stress. However, both in in vitro and in vivo settings, mutations were detected only in tumour cells that received heavy PI-based therapies, suggesting that the selected mutations emerge lately during the process of clonal selection besides the apparition of the resistant phenotype. Moreover, in vivo, at the time of relapse, cells exhibiting PSMB5 mutations could partially or totally disappear, questioning the role of such mutations at late stages of the disease [12]. Finally, the relevance of *PSMB5* gene mutation in BTZ resistance has recently been challenged. Soriano and colleagues have shown that proteasome activity is dispensable in BTZ- and CFZ-resistant MM cell lines suggesting that *PSMB5* mutations are likewise not required or involved in the development of BTZ resistance [10] (Fig. 6.1).

In support, no mutations of *PSMB5* were found for years in MM primary cells, even using targeted or high-throughput sequencing techniques on large cohorts of patients including refractory patients or in relapse. The relevance of *PSMB5* mutations and their functional impact were suggested recently. Four *PSMB5* mutations were detected in a single MM patient that received prolonged BTZ-based treatments (Table 6.2) [12]. According to the Darwinian model of myeloma evolution, mutations evolved independently in different tumour subclones. For instance, C63Y and A27P are lost during the course of the disease, whereas A20T and M45I are maintained longer. When tested in vitro, all mutations were functionally relevant and provided PI resistance but at different degree according to both the mutation itself (A20 and M45 having a higher impact than C63 and A27), and the tested PI (BTZ, CFZ or IXZ). The response pattern was similar for BTZ and IXZ, but not for CFZ. CFZ response was less affected by *PSMB5* mutations, likely due to its unique structure and binding [12]. No mutations of PSMB5, PSMB6 and PSMB7 were ever described in CFZ-adapted MM cell lines [10].

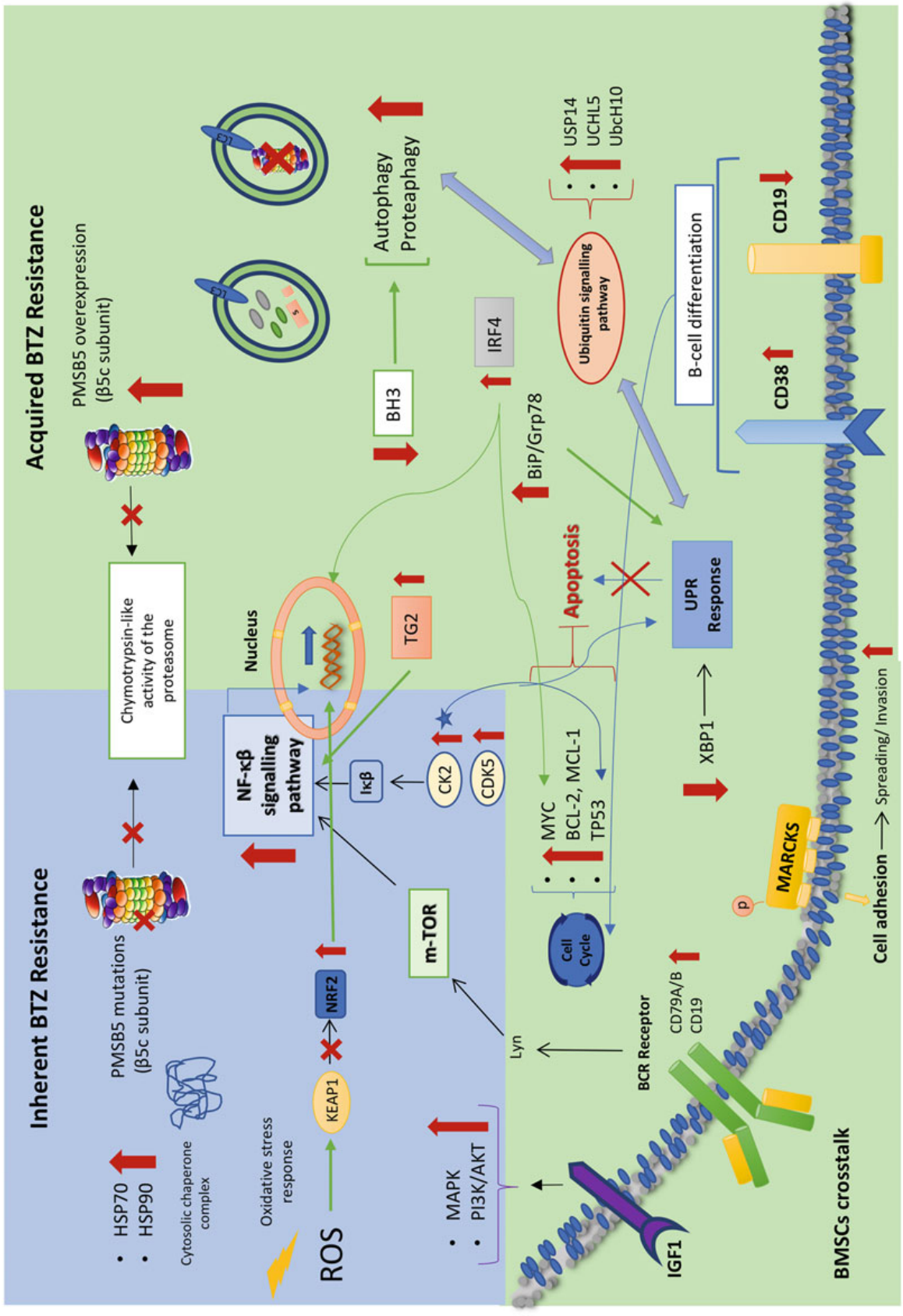

Fig. 6.1 Molecular mechanisms associated to BTZ resistance in acquired and resistant MCL and MM cell models. The pathways involved are: UPS and ALS degradation systems, UPR response, apoptosis, B cell differentiation, cell cycle regulation and mutations in the β5 subunit of the proteasome. Arrows indicates up- or downregulation of the different molecular mechanisms when compared with non-pathological conditions. See main text for further details

Table 6.2 PSMB5 mutations associated to BTZ resistance in MCL and MM

Gene	Mutation	Protein	Tumour cells	Pathology	References
PSMB5	c.322G>A	p.A49T	KMS-11	MM	[13]
			OPM-2		
	c.247A>G c.322G>A	p.T21A p.A49T	8226	MM	[11]
	c.310A>G	p.M45V	8226[a]	MM	[4]
	c.310A>G	p.M45V	AMO	MM	[10]
	c.235G>A c.256G>C c.312G>C c.365G>A	p.A20T p.A27P p.M45I p.C63Y	Primary cells	MM	[12]

The indicated cell lines have been exposed to a continuous pressure of BTZ; except those marked with [a], exposed to PR-924, a selective inhibitor of the immunoproteasome

6.3.1.2 Apoptosis Failure

Defective apoptosis signalling is a key oncogenic mechanism of drug resistance in haematological malignancies, mainly attributed to the deregulation of B cell lymphoma-2 (BCL-2) family members. This family of proteins is composed by prosurvival proteins such as BCL-2, BCL-XL, MCL-1, BCLW and BFL1/A1, as well as proapoptotic factors, represented by multidomain (BAX, BAK and BOK) and BH3-only (BIM, PUMA, NOXA, BAD, BID, BMF, BIK and HRK) proteins. Once activated upon cytotoxic or stress signals, the BH3-only proteins interact with their prosurvival counterparts, leading to the release and oligomerisation of BAX and BAK, permeabilisation of the mitochondrial outer membrane, and the cytosolic release of apoptogenic factors, culminating in the activation of the caspase family of proteases and ultimately, cell death [14].

In MCL cells, BTZ has been described to evoke intracellular accumulation of MCL-1, which harbours a PEST sequence at the origin of its targeting to the proteasome for its degradation. As MCL-1 can physiologically interact with and block the proapoptotic signalling of NOXA, which is transcriptionally activated upon cell exposure to BTZ, the increase in MCL-1 levels can counteract NOXA-mediated activation of BAK, thus delaying the onset of cell death. Therefore, blocking NOXA expression or inhibiting MCL-1 was used to modulate the response to BTZ in MCL [15] (See Sect. 6.4).

Despite concomitant overexpression of several antiapoptotic proteins of the BCL-2 family, MM cells depend primarily on MCL-1 for survival as demonstrated by the use of small-molecule MCL-1 inhibitor and the knockdown of MCL-1 [16, 17]. MM cells are tightly dependent on their microenvironment known to promote MCL-1 expression in plasma cells. For example, bone marrow stromal cells (BMSCs) provide survival signals such as interleukin-6 (IL-6), vascular endothelial growth factor and insulin-like growth factor. IL-6 upregulates MCL-1 transcription and induces MCL-1 dependence [18]. Recently, it has been shown that the long non-coding RNA (lncRNA) H19 is present in the serum of MM patients and that an H19/miR-29b-3p axis promotes MCL-1 translation and BTZ resistance [19]. Thus, MCL-1 is certainly an important target for coping with MM drug resistance.

6.3.1.3 Signalling Cascades

The NF-κB pathway is activated via canonical and non-canonical signalling mechanisms. The canonical pathway regulates inflammatory responses, immune regulation, and cell proliferation, whereas the non-canonical signalling cascade leads to B cell maturation and lymphoid organogenesis. These pathways regulate the expression of genes involved in cell survival and tumour-promoting cytokines. Therefore, its activation has a profound impact in tumorigenesis. The NF-κB pathway can be potentially targeted and is expected to have a high impact on the viability of malignant B cells, due to its interplay with other crucial pathways activated during B cell differentiation, such as B cell receptor (BCR), PI3K/AKT/mTOR, and toll-like receptor (TLR) signalling axes. Constitutive NF-κB activity is often present in MCL and MM. The inhibition of

NF-κB is a primary mechanism to induce cell apoptosis after BTZ treatment and plays a role in evading the effect of this treatment in BTZ-resistant phenotypes [20].

A high NF-κB activity was found in tumour cells of BTZ refractory MM patients and in in vitro models of cell adhesion-mediated drug resistance (CAM-DR), reinforcing the notion that the NF-κB pathway signals BTZ resistance [21, 22]. In MCL, this constitutive NF-κB signalling and consequent lack of response to BTZ has been linked to a proteasome-independent degradation of the intrinsic NF-κB inhibitor, IκBα [20]. However, a number of studies have pointed out a lack of correlation between NF-κB activity and BTZ resistance status [23].

NF-κB pathway is also regulated by casein kinase 2 (CK2). CK2 is a multifaceted serine/threonine kinase involved in several cellular processes, and is overexpressed and overactive in many blood tumours. CK2 regulates signalling cascades and molecules that are targeted by BTZ. For instance, it modulates IκBα protein turnover, p53 function, AKT activation, and has a role in the control of endoplasmic reticulum (ER) stress and unfolded protein response (UPR) (see Sect. 6.3.2.3). Inhibition of CK2 enhances BTZ cytotoxic effect in MCL cell lines by down modulating NF-κB and signal transducer and activator of transcription 3 (STAT3) signalling cascades and by potentiating the proteotoxic effects of proteasome blockade. Altogether these results suggest that levels of CK2 are involved in MCL resistance to BTZ [24].

The BCR includes a heterodimer of CD79A/B molecules, and CD19, a key co-receptor. The upregulation of those molecules have been proposed to promote BTZ resistance in MCL cells. While BCR regulates cell survival and proliferation of MCL cells, in MM it has been only linked to monoclonal gammopathy of undetermined significance (MGUS), a premalignant phase of MM [25]. A human phospho-kinase array further pointed out an overexpression of phosphorylated BCR kinases LYN, LCK, and YES as well as a sustained downstream activation of PI3K/AKT/mTOR axis in BTZ-resistant cells. Among these kinases, LYN was functionally associated with the resistance phenotype, rending cells more sensitive to the SRC kinase inhibitor dasatinib and allowing to synergistic activity of the dasatinib/BTZ combination in vitro [26].

In MCL, the redox status has also been pointed out as a crucial mediator of BTZ efficacy, as PIs lead to the generation of large amounts of reactive oxygen species (ROS), modulating at least in part the transcription of *NOXA* and thus contributing to the cytotoxic activity of proteasome inhibition [27]. The nuclear factor NF-E2 p45-related factor 2 (NRF2) was identified as a key regulator of this response. Indeed, while under physiological conditions it is sequestrated by Kelch-like ECH-Associated Protein 1 (KEAP1) in the cytosol, when KEAP1 is oxidised by ROS, NRF2 is released to the nucleus where it initiates the transcription of genes involved in the adaptive oxidative stress response. Upon BTZ exposure, BTZ-sensitive MCL cells display a sharp increase in the expression of NRF2 target genes, as well as genes related to protein ubiquitylation or proteasome components, while resistant tumours show minimal changes. Accordingly, an elevated expression of NRF2 target genes at the basal level, predicts a poor sensitivity to proteasome inhibition [28]. In line with this, a recent study has highlighted the capacity of ROS to modulate some cancer stem cells (CSCs)-like subpopulations in MCL cell lines and primary cultures and to regulate cell sensitivity to BTZ. Authors showed that O_2- was involved in the inhibition of CSC-like cells and in the sensitisation of MCL to BTZ, while H_2O_2 favoured a CSC-like phenotype, impairing BTZ-induced cell death [29]. This process was associated with transcriptional regulation of two O_2- and H_2O_2 targets, namely MCL-1, and ZEB-1, a WNT-regulated transcription factor that interfered with MCL response to chemotherapeutics. This resulted in the activation of proliferation-associated genes including *MYC* and *CCND1* and the induction of an antiapoptotic gene signature [30].

6.3.2 Acquired Resistance

PI-acquired resistance has multifactorial and interconnected causes and PI-resistant cells show cross-resistant profiles. Among the main

mechanisms recognised in MM and/or MCL are upregulation of 20S proteasome subunits including β5c, downregulation of 19S proteasome subunits and overexpression of efflux pumps. Adaptive metabolic changes, modulation of the unfolded protein response, and alteration of autophagy signalling contribute also to PI resistance in MM cells.

6.3.2.1 Overexpression of Proteasome Subunits

Beside *PMBS5* mutations, overexpression of *PMBS5* and (to a lesser extent) *PMBS6* are frequent alterations found in MM cell lines adapted to increased concentrations of BTZ [11, 31, 32]. *PSMB5* is overexpressed in one MM patient with clinical resistance to BTZ, compared to three BTZ-sensitive patients [33]. Franke and colleagues demonstrated a tight relationship between impaired proteasome activity carried on by a mutated β5c subunit and the β5c subunit overexpression. In cells harbouring homozygous *PSMB5* mutations, the upregulation of β5c subunit was even more important when compared to cells harbouring heterozygous mutations. The authors proposed a model in which, the prolonged exposure of MM cells to BTZ leads first to the appearance of *PSMB5* mutations, resulting in decreased BTZ binding. In turn, mutant cells compensate this reduced proteasome activity by upregulation of the β5c subunit. Moreover, in those BTZ-resistant MM cells the upregulation of β5c is associated with the downregulation of β5i to balance the total proteasome units and impairs any possible remaining BTZ-inhibition [11].

In two recent studies, the involvement of the 19S subunits of the proteasome has been highlighted. To identify genes controlling the sensitivity and adaptation of MM cells to CFZ, Acosta-Alvear and colleagues used a new-generation shRNA library screening [34]. They found that the knockdown of several subunits of the 20S proteasome core (including β5c) provides a strong sensitisation to proteasome inhibition. Paradoxically, the genetic depletion of most of the 19S regulatory components confers a marked resistance. They further confirmed that shRNAs-mediated knockdown of *PMSC1*, *PMSC6*, *PMSD1*, *PMSD2*, *PMSD6* and *PMSD12* leads to resistance towards BTZ and CFZ in MM cell lines. Importantly, the authors showed that PSMC2 levels in MM patients seem predictive for the response towards CFZ-based therapy. In the second report, Shi and colleagues used a genome-scale CRIPSR-Cas9 library to identify genes associated with BTZ resistance. They validated *PSMC6* depletion as the strongest hit conferring BTZ resistance in MM cells [35]. *PSMC6* deficiency resulted in reduced BTZ ability to regulate chymotrypsin-like activity of β5c through changes in the proteasome structure. Mutations in other members of the PMSC group also individually impart BTZ resistance albeit less potently. No mutation of *PSMC6* has been reported so far but the analysis was performed on a cohort of untreated MM patients [35].

Recent results from our laboratories comparing BTZ-adapted MCL cell lines and their parental counterparts revealed a reduced expression of 19S proteasome subunits in BTZ-resistant cells. Strikingly, when autophagy was blocked with inhibitors such as bafilomycin A or chloroquine, the level of those proteasome subunits increased in resistant cells only, suggesting an autophagy-mediated degradation. In MCL cell lines that naturally resist to BTZ, the accumulation of proteasome subunits after the chemical inhibition of autophagy was proportional to the level of BTZ resistance observed. The proteasome degradation by autophagy was named proteaphagy and has been observed in response to starvation or proteasome inhibition in several biologic models including human cells [36, 37]. Quinet et al. showed that proteaphagy can contribute to develop resistance to BTZ in MCL cells since inhibited proteasomes are degraded and BTZ reduces its impact on proteasomes and cell death. In other words, BTZ-resistant cells bypass proteasome inhibition relying on autophagy through degradation of proteasomes and perhaps other cellular proteins [38].

6.3.2.2 Metabolic Adaptation

Metabolic reprogramming is a hallmark of cancer that has emerged as an attractive target for novel therapeutic strategies for cancer treatment. O-GlcNAcylation is an abundant, dynamic and

nutrient-sensitive post-translational modification that corresponds to the addition of an O-linked β-N-acetylglucosamine (O-GlcNAc) moiety to the serine or threonine residues in proteins in response to changes in the hexosamine biosynthetic pathway. As this latest depends on various essential nutrients and metabolic intermediates like glucose, glutamine, acetyl-coA, and UTP, it provides an ideal machinery for cells to sense and respond to a variety of microenvironmental conditions [39]. Little was known about its role in MCL, until the recent study of Luanpitpong and collaborators who demonstrated that O-GlcNAcylation of tBID promoted apoptosis in MCL cells exposed to BTZ, and that this process could be amplified by co-treatment with the antifungal drug kenoconazole, an O-GlcNAcase inhibitor that blocks tBID ubiquitylation and subsequent proteasomal degradation [40].

ABC (ATP-binding cassette) transporters such as ABCB1 (multidrug resistance, MDR1 or P-glycoprotein, P-gp) mediate drug resistance by alterations of the absorption and elimination of xenobiotics and drugs. ABCB1 expression correlates with poor prognosis, treatment resistance and aggressiveness of the MM disease [41]. ABCB1 protein is overexpressed in CFZ-resistant compared to sensitive MM cell lines [10]. ABCB1 was expressed by circulating malignant plasma cells of MM patient at diagnosis and its expression increases along the course of CFZ treatment [42]. Overexpressed ABCB1 protein limits the proteasome-inhibiting activity and clearance of poly-ubiquitinated proteins by CFZ and reduces its cytotoxicity. Importantly, ABCB1 overexpression affects the cytotoxic activity of epoxyketone-type PIs (CFZ) significantly stronger than non-epoxyketone PIs (BTZ). Drugs targeting ABCB1 may resensitise MM cells to PI, in particular CFZ.

Soriano and colleagues analysed by a combined quantitative and functional proteomics approach CFZ- and BTZ-adapted MM cell lines [10]. They found that resistance to BTZ/CFZ was independent of proteasome activity but relied on energy metabolism, redox homeostasis, protein folding and degradation. PI-resistant cells adapted themselves to a very low proteasome activity while continuing to synthesise immunoglobulins. In turn, the level of metabolic intermediates involved in oxidative glycolysis (pyruvate kinase), redox state (superoxide dismutase, glutathione peroxidase, peroxiredoxin), mitochondrial respiration (cytochrome c) were increased thus maintaining high stringent redox conditions. In agreement with previous studies, authors also confirmed that the most upregulated proteins in CFZ-resistant cells were ABCB1 [41, 42] and the heat-shock proteins HSP70 and HSP90, whose transcriptional regulator, HIF1, is involved in BTZ resistance in MM cells [43]. Conversely, the positive apoptosis regulators BAX, CASP and DIABLO were downregulated [10].

Similarly to Soriano et al., Dytfeld and colleagues conducted a comparative proteomic profiling of R/R patients vs. naïve MM patients [44]. In the proteomic signature associated with BTZ resistance, four sets of proteins were characterised including proteasomal proteins, some factors regulating the redox status, proteins signalling apoptosis, and proteins involved in the inflammation response. In particular, regulatory and catalytic components of the proteasome, including part of the 11S complex, were upregulated. The antioxidant thioredoxin, peroxiredoxin, and thioredoxin reductase were upregulated whereas annexins A1 and A2, that regulate the apoptotic process, were downregulated. PI resistance may thus be alleviated by manipulating the redox status and the energy metabolism.

Although not revealed by the above proteomic studies, NRF2 seems to be a node for BTZ and CFZ resistance in MM. As it maintains redox homeostasis by inducing antioxidant and detoxification genes and by modulating energy metabolism [45], NRF2 indirectly regulates: (a) chaperoning activity [46]; (b) redox, metabolic and translational reprogramming [47]; and (c) activation of prosurvival autophagy. These major functions are supported by clinical data showing *NRF2* upregulation in a subgroup of relapsed patients [47]. Other studies showed that high glutathione (GSH), whose levels are controlled by NRF2, dampens BTZ toxicity in MM cells [48].

In the last decade, numerous studies have indicated that components of the BM stroma, extracellular matrix (ECM), cytokines, chemokines and growth factors are involved in BTZ resistance in MM cells [49]. The membrane protein myristoylated alanine-rich C-kinase substrate (MARCKS) is a protein that plays an important role in cell adhesion, spreading and invasion, and is crucial for metastasis [50]. MARCKS is overexpressed in MM cell lines and is involved in the cross-resistance to the farnesyltransferase inhibitor R115777 and BTZ, as well as in MM patients that do not reach a sustained response to BTZ therapy. In addition, the inhibition of MARCKS phosphorylation increases cytotoxicity in BTZ-resistant cells [51].

The insulin-like growth factor IGF-1, known as a growth factor for MM cells [52], is produced by plasma cells, and is present in the BM microenvironment. IGF-1 has been proposed to promote proliferation and drug resistance in MM cells through the activation of MAPK and PI3K/AKT-signalling pathways [49]. According to these data, the IGF-1/IGF-1R signalling axis was detected to be upregulated in three BTZ-resistant MM cell lines, compared to parental cells. Kuhn et al. proved that a small molecule responsible for the inhibition of IGF-1R has the capacity to sensitise BTZ-resistant MM cells to the proteasome inhibitor [53].

6.3.2.3 Protein Homeostasis

Because of their high capacity to synthesise and secrete immunoglobulins, MM cells exhibit an expanded ER network and an increased ability to cope with unfolded or misfolded proteins that accumulate in the ER. These conditions are referred to as ER stress. As a consequence, MM cells activate the UPR pathway as an adaptive strategy and are rendered dependent on this mechanism for their survival [54]. ER stress upregulates three UPR signalling branches: activating transcription factor 6 (ATF6), protein kinase R (PKR)-like ER kinase (PERK)-ATF4 and inositol-requiring enzyme 1 (IRE1)-X box binding protein 1 (XBP1) which suppress global translation and promote protein folding and degradation. During ER stress, ATF6 translocates into the nucleus and activates the *XBP1* promoter allowing an upregulation of the protein. At the same time, IRE1 oligomerizes and autophosphorylates, resulting in the activation of its endonuclease activity that cleaves XBP1 mRNA. This results in a frameshift that modifies the unspliced inactive XBP1 form (XBP1u) into an active XBP1s form. XBP1s acts as transcription factor and activates genes encoding protein folding and chaperones (see Sect. 6.3.2.5). Previous studies done on cohorts of MM patients and confirmed in vitro on BTZ-adapted cell lines, defined a 'low IRE1-XBP1' phenotype that predicts a poor response to BTZ [55, 56]. Moreover, *XBP1* knockdown experiments in MM cell lines showed correlation with BTZ resistance, as the suppression of XBP1 lowers both the basal ER stress and the ER stress due to proteasome inhibition [56].

High expression of deubiquitinating enzymes (DUBs) and autophagy-related proteins have been detected in MM patients resistant to BTZ. These alterations in enzymes that are involved in deubiquitinating misfolded/unfolded proteins and in the turnover of proteins by the autophagy–lysosome system (ALS) suggest an important role of ubiquitin signalling pathways in BTZ resistance. Niewerth et al. showed that inhibition of USP14 and UCHL5 promotes apoptosis and helps to overcome BTZ resistance in MM patients [4]. Another enzyme that can be regulated to recover sensitivity to BTZ is the ubiquitin-conjugating enzyme H10 (UbcH10). Wang et al. proved that through the expression of hsa-miR-631, the negative regulation of UbcH10 transcription prevents MM cells to develop resistance against proteasome inhibitors [57].

6.3.2.4 UPS–ALS Crosstalk

Eukaryotic cells have two interconnected mechanisms for protein degradation and removal of misfolded proteins and aggregates, the UPS and the macroautophagy (here referred to as ALS). Autophagy functions by double-membrane vesicles known as autophagosomes which sequester cytosolic proteins, followed by fusion with lysosomes for degradation. Autophagy is involved in several human diseases, such as neurodegenerative diseases and cancer [58]. While it

appears to be tumour suppressive in normal cellular homeostasis, autophagy can mediate tumour cell survival under stress conditions [59]. For many years, UPS and ALS pathways were thought to function independently, but the recent observation that impairment of either pathway impacts the other has suggested that these two proteolytic systems do collaborate [58]. It is thought that upon proteasome inhibition, autophagy is initiated as a survival mechanism to eliminate UPS substrates [60], and thus, upregulated autophagy could play a role in BTZ resistance [61].

The ubiquitin-binding cargo autophagy receptor sequestrosome 1 (SQSTM1) or p62 is a critical link between UPS and ALS [62]. In CFZ-adapted MM cells, SQSTM1/p62 is elevated triggering a prosurvival autophagy however through two different mechanisms according to the settings. In the first model, the pluripotency-associated transcription factor Kruppel-like factor 4 (KLF4), is overexpressed and contributes to CFZ resistance by activating the *SQSTM1* gene [47]. In the second model, elevated levels of SQSTM1/p62 conduct CFZ resistance through both a prosurvival autophagy involving GABARAPL1 upregulation and the activation of the NRF2 pathway [47]. However, since KLF4 is also a target of NRF2, both factors could cooperate for maintaining a high level of *SQSTM1* transcription. The activation of NRF2 occurs through the activation of the PERK-eukaryotic translation initiation factor-2α (eIF2α) axis of the UPR [47]. As stated before (see paragraph 3.2.2), NRF2 is a major actor for PI resistance through the reprogramming of metabolism and the control of redox status [10, 47]. In addition to eIF2α, another NRF2 target and translation initiation factor, eIF4E3 is overexpressed in CFZ-resistant cells, and increased EIF4E3 expression was found in a subgroup of patients with chemoresistant minimal residual disease and in R/R patients [47].

Interestingly, deficiency in BIM has been shown to contribute to adaptive resistance to BTZ in MM cells, mediated by increased autophagy, and that autophagy disruption by means of chloroquine could sensitise these cells to BIM-mediated cell death [63]. Of special interest, upon exposure to pharmacological inhibitors of autophagy like chloroquine or bafilomycin A, BTZ-resistant MCL cells can undergo a blockade of proteaphagy, leading to the stabilisation of proteasome subunits, and the recovery of BTZ sensitivity [38]. Importantly, sensitivity to autophagy inhibitors requires a significant degree of BTZ resistance, thus suggesting that modulating proteaphagy with specific inhibitors may be considered as a strategy to resensitise resistant cells to PI.

6.3.2.5 Stress Signals

Subsequent studies have been focused to determine the interplay between the deregulation of the intracellular stress machinery and MCL loss of sensitivity to BTZ. A key defect in BTZ-dependent cell death was first identified within the ER stress pathway, because its activation in MCL cells exposed to BTZ is required to elicit *NOXA* transcription [64]. ER homeostasis is controlled by the immunoglobulin heavy chain binding protein (BiP), also referred as 78-kDa glucose-regulated protein (Grp78). BiP/Grp78 forms a large multiprotein complex with a set of other ER molecular chaperones, including the Hsp90 ER homologue, Grp94, protein disulphide isomerase, calcium binding proteins, and cyclophilin B [65]. Under non-stressed conditions, BiP/Grp78 binds to and maintains in an inactive monomeric state the ER transmembrane PKR-like ER kinase, IRE1, and ATF6 [66]. After proteasome inhibition, the accumulation of polyubiquitylated and misfolded proteins within the ER lumen leads to BiP/Grp78 dissociation from the luminal domains of these sensor proteins and the initiation of UPR (see Sect. 6.3.2.3) [67]. This coordinated cellular response initially promotes cell survival, but ultimately triggers apoptosis if cytoprotective mechanisms are overwhelmed. Supporting the observation that accumulation of some HSP proteins can promote cellular resistance to PIs, a correlation has been made between acquired and primary resistance to BTZ in MCL, and intracellular accumulation of BiP/Grp78 in proteasome-compromised MCL cells [68]. For this reason inhibitors of HSP90

have been used to improve the BTZ-mediated cell death induction in BZT-resistant cells (see Sect. 6.4) [68].

In line with this study, deregulated expression of several cytosolic HSP70 family members has also been associated with BTZ resistance in MCL [69] and MM [70]. Supporting a role of HSP70 protein in MCL cell resistance to chemotherapeutic agents, B cells modified to overexpress cyclin D1, the genomic hallmark of MCL, presented strong alterations in their response to growth factor withdrawal [71]. Acquired BTZ resistance is also attributed to the upregulation of other HSPs such as HSP90 and HSP27, that promotes NF-κB activity [21].

6.3.2.6 B Cell Differentiation Programme

It has been proposed that MM cells also achieve BTZ resistance via the dedifferentiation of plasma cells. A pool of $XBP1^{low/-}$ tumour progenitors or CSCs pre-exists drug treatment, contributing to tumour diversity [55]. CSCs recapitulate maturation stages between B cells and plasma cells. Tumour B cells and pre-plasmablasts survive PI treatment preventing cure, while maturation arrest of MM before the plasmablast stage enables progressive disease on PI treatment. These tumour progenitors should be targeted to allow a complete cure for MM patients.

Although MCL was originally considered a neoplasm of naive lymphocytes that have not passed through the germinal centre (GC), a significant number of cases present somatic mutations in the immunoglobulin genes, suggesting that they have been in contact with the antigen in the GC. Some cases were also described that presented evidences of plasmacytic differentiation in patients harbouring the characteristic *t*(11;14) translocation [72]. A couple of studies have related the resistance to BTZ with the plasmacytic differentiation programme in MCL cells. Plasma cells are the final effectors of humoral immunity, which are devoted to the synthesis and secretion of immunoglobulins. BTZ-resistant MCL cells display some of the characteristics of the plasma cells, such as the overexpression of interferon regulatory factor 4 (IRF4) and elevated membrane levels of CD38 and CD138 cell surface markers, but they do not present splicing of XBP1 or increase in immunoglobulin production [6]. It is postulated that during the acquisition of resistance to BTZ, the balance between the protein load and the proteasomal activity is key. When plasmacytic differentiation is induced through stimulation of TLR9 receptor, the sensitivity to BTZ changed throughout the process of B cell differentiation to final plasma B cell phenotype with the capacity to manage the future increase in protein loads. Since the cells do not acquire full secretory capacities, this mechanism granted them with an advantage against the antitumour activity of BTZ. Once MCL have completed this process of differentiation, they return to a BTZ-sensitive state [6]. Mouse xenograft models of MCL using different cell lines with different sensitivity to BTZ, including cells with acquired or primary resistance to the PI, demonstrated a tight correlation between increased tumorigenicity of BTZ-resistant tumours with a plasmacytic differentiation phenotype including upregulation of IRF4, PR domain zinc finger protein 1 (PRDM1/BLIMP-1) and CD38, and loss of the B cell markers PAX5 and CD19 [73]. Of note, beside its role as a transcription factor that represses the expression of proteins needed for B cell identity and proliferation, and that helps to drive B cells through their final differentiation stage to become antibody-secreting cells, BLIMP-1 is also a mediator of NOXA-induced apoptosis in MCL and is required for BTZ-induced apoptosis in MCL cell lines and primary tumour samples [74]. This finding further strengthens the interplay between NOXA and plasmacytic differentiation in BTZ-mediated anticancer activity in MCL.

6.4 Potential Targets to Recover Proteasome Inhibitors Sensitivity

Given the resistance to PIs observed in some patients, alternative drugs have been tested to overcome resistance as single or combinatorial

treatments. Many agents have shown promising preclinical results in terms of safety, specificity and efficacy to treat PI-resistant MM and MCL cells. Already existent or new therapeutic drugs are used to tackle the adaptation of the cells to PIs (Table 6.3). Cellular mechanisms involved in PI resistance are hence targeted by a wide range of drugs, some of the most relevant are described below.

6.4.1 Deubiquitinases

Because proteasome degradation and UPR implicate ubiquitin signal, targeting factors regulating ubiquitin signal could potentially contribute to increase the sensitivity to BTZ and therefore be an option to overcome PI resistance. In this context, DUBs have been considered as therapeutic targets to overcome BTZ resistance. P5091 is a selective inhibitor of USP7, a DUB that targets the E3 ligase HDM2. Treatment of MM cell lines and primary cells from MM patient with P5091 inhibited growth and induced apoptosis in tumour cells including those resistant to BTZ, without affecting the viability of normal PBMCs [75]. The 19S regulatory particle inhibitor b-AP15 selectively blocked deubiquitinating activity of USP14 and UCHL5 without inhibiting proteasome activity. This led to an activated UPR and an inhibited tumour growth, in MM xenografts resistant to BTZ [76]. The antitumoral effects of b-AP15 were also demonstrated in MCL [77]. Another USP inhibitor, SJB3-019A tackling USP1 showed synergic toxicity in MM when combined with BTZ [78]. Song et al. found contribution of RPN11, a proteasomal deubiquitinase, in MM pathogenesis using gene expression analysis. Pharmacological inhibition of RPN11 with *O*-phenanthroline (OPA) or capzimin blocked proteasome function, induced apoptosis in MM cells and overcame resistance to BTZ [79].

USP9X is also highly expressed in MM patients and in particular in those with as short progression-free survival. The partially selective USP9X inhibitor WP1130 induced apoptosis through the downregulation of MCL-1. However, this effect was transient due to the compensatory upregulation of USP24 who sustains MM cell survival. By contrast, a novel compound EOAI3402143 with a dual USP9X/USP24 inhibiting activity displayed promising anti-myeloma activity [80]. Associated with the inhibition of USP14 activity, VLX1570 led to an extended survival of xenografts models of myeloma including BTZ-resistant cells [81].

6.4.2 Transport Modulators

PI cellular intake is regulated by transport modulators, and treatment efficiency is directly linked to intracellular concentration of drug. Specific inhibitors of ABCB1 such as verapamil and reserpine showed increased proteotoxic stress in CFZ-resistant MM cells [10]. The two HIV inhibitors nelfinavir and lopinavir counteract ABCB1 overexpression in CFZ-resistant MM, via the modulation of the mitochondria transition pore. This promising preclinical results encourage the clinical evaluation of both treatments [42]. Thanks to its capacity to modulate the UPR pathway, nelfinavir has also attested a safe and promising activity in combination with BTZ and/or dexamethasone, in a phase I clinical trial involving advanced BTZ-refractory MM patients [82].

6.4.3 Autophagy Signalling

Ubiquitin and ubiquitin-like molecules play an important role on the regulation of autophagy. In BTZ-resistant MCL cells, the use of autophagy inhibitors such as bafilomycin A and chloroquine, and the p62 inhibitor verteporfin revealed increased cytotoxicity and synergistic activity with BTZ, mediated by the reversion of the proteaphagic process [38]. Blocking autophagy also leads to multiple changes in the cell such as the accumulation of IκBα, which prevents BTZ-induced NF-κB activation. The combination of bafilomycin A with BTZ might therefore contribute to increase cytotoxicity in MM cells in this manner [83]. Finally, orlistat, a fatty acid

Table 6.3 Drugs currently used to recover sensitivity to BTZ

Drug name(s)	Mechanism	Molecular target	Pathology	References
P5091	Ubiquitin signal	USP7	MM	[75]
b-AP15	Ubiquitin signal	USP14 and UCHL5	MM MCL	[76, 77]
SJB3-019A	Ubiquitin signal	USP1	MM	[78]
O-phenanthroline	Ubiquitin signal	RPN11	MM	[79]
Capzimin	Ubiquitin signal	RPN11	MM	[79]
WP1130	Ubiquitin signal	USP9X, USP5	MM	[80]
EOAI3402143	Ubiquitin signal	USP9X and USP24	MM	[80]
VLX1570	Ubiquitin signal	USP14	MM	[81]
Verapamil	Drug transport	ABCB1	MM	[9]
Reserpine	Drug transport	ABCB1	MM	[9]
Nelfinavir	Drug transport	ABCB1	MM	[42, 82]
Lopinavir	Drug transport	ABCB1	MM	[42]
Bafilomycin A	Autophagy	Vacuolar ATPase ATP6V1A	MM, MCL	[38, 83]
Chloroquine	Autophagy	Lysosome	MCL	[38]
Verteporfin	Autophagy	p62	MCL	[38]
Orlistat	Autophagy	Fatty acid synthase	MCL	[84]
Perifosine	mTOR/Akt	Akt, PI3K	MM	[85]
Dactolisib NVP-BEZ235	mTOR/Akt	PI3K, mTOR	MCL	[86]
Temsirolimus (Torisel)	mTOR/Akt	mTOR	MCL	[87]
Deforolimus (Ridaforolimus)	mTOR/Akt	mTOR	MCL	[88]
Perillyl alcohol	NF-κB	TG2 signalling	MM MCL	[89]
Selinexor	NF-κB	XPO1	MM	[90]
Ibrutinib (Imbruvica)	NF-κB	BTK	MM MCL	[91–93]
Degrasyn	NF-κB	STAT, DUBs	MCL	[94]
Obatoclax	Bcl-2 proteins	NOXA	MCL	[15, 95]
cAMP	Bcl-2 proteins	Mcl-1	MM	[96]
Lenalidomide (Revlimid)	IMiD	CRBN, TNFSF11, CDH5, PTGS2	MCL	[97, 98]
Pomalidomide	IMiD	CRBN, TNF, PTGS2	MM	[99–101]
Dexamethasone	Glucocorticoid Immunosuppressant	NR3C1, NR0B1, ANXA1, NOS2	MM	[99, 100, 102]
JQ1	BET bromodomain inhibitors	BRD4	MM	[103, 104]
CPI203	BET bromodomain inhibitors	BRD4	MM MCL	[73, 104]
PROTACs (ARV-825)	BET-specific target	BRD4 and other BET	MM	[105]
Birabresib (OTX015)	BET bromodomain inhibitors	BRD2,3,4	MM	[101]
Ricolinostat (ACY-1215)	Epigenetic regulators	HDAC6	MM MCL	[102, 106]
Decitabine	Epigenetic regulators	DNA methyl transferase	MCL	[107]
Vorinostat	Epigenetic regulators	HDACI	MM MCL	[108]

synthase inhibitor that affects autophagy, sensitises MCL cells to BTZ through the inhibition of the autophagic degradation of NOXA [84].

6.4.4 Oncogenes and Signalling Pathways

Proteasome inhibition has pleiotropic effect within the cells. It affects a wide range of cellular factors, including important signalling cascades, oncogenes or epigenetic regulators. This modulation of critical factors during BTZ treatment can hamper the apoptotic effect of PI, and leads to resistance. As described above, adaptation of signalling pathways including mTOR and NF-κB, or modulation of important oncogenes such as BCL-2 or MYC proteins, have been directly linked to BTZ resistance in MM and MCL. Therapeutics agents targeting these factors have been proposed to overcome BTZ resistance.

6.4.4.1 mTOR/AKT Pathway

Modulating mTOR/AKT, key proteins of a complex signalling cascade, has successfully reverted malignant cell adaptation to BTZ in preclinical studies. The dual PI3K and mTOR inhibitor dactoslisib (NVP-BEZ235) showed great results in MCL BTZ-resistant cells lines [86]. A new generation of mTOR inhibitors, such as temsirolimus and deforolimus have been also proposed for MCL treatment but limited clinical impact was obtained [87, 88]. The AKT inhibitor perifosine combined with BTZ revealed increase cytotoxicity in R/R MM patients previously treated with BTZ [85], warranting its use in BTZ-resistant cancers.

6.4.4.2 NF-κB Pathway

Since NF-κB pathway is overactivated under BTZ treatment, its modulation has been used to treat PI-resistant MM and MCL. Selinexor is a reversible inhibitor of exportin 1 (XPO1) that blocks the nuclear export of NF-κB/IκBα complexes leading to NF-κB pathway inactivation [109]. Selinexor associated with BTZ or CFZ overcomes acquired PI resistance in MM models and patients. MM drug resistance to CFZ and BTZ is enhanced in hypoxic conditions [90]. In such conditions, selinexor is capable to overcome PI resistance [90]. Because Transglutaminase 2 (TG2) is a calcium-dependent enzyme, calcium blockers have been proposed to hamper high NF-κB expression in BTZ-resistant cells. The combination of such molecules with BTZ indeed improves cytotoxicity in MCL [89]. Degrasyn has been also proposed to target constitutive NF-κB and STAT3, and combined treatment with BTZ showed a synergic apoptosis in MCL [94].

Within the BCR pathway, Bruton's tyrosine kinase (BTK) inhibitors lead to NF-κB inactivation and downregulation of MYC. Ibrutinib (Imbruvica), a first-in-class BTK inhibitor, was approved by the FDA in 2013 as second line treatment for MCL patients [91]. This promising drug leads to the best complete remission rate as a single agents when compared to the other three drugs licensed at that time for use in MCL (BTZ, temsirolimus (Torisel) and the IMiD drug, thalidomide-derivative lenalidomide (Revlimid)) [110]. Promising preclinical results were obtained combining ibrutinib and BTZ in MCL and MM BTZ-resistant cells [92]. Ibrutinib alone or in combination with dexamethasone went very recently through a phase II trial with R/R MM patients, with some positive results [93].

6.4.4.3 NOXA/BCL-2 Proteins

BH3 mimetic compounds like obatoclax showed great results alone or in combination with BTZ in relapsed MCL. By neutralising BTZ-induced MCL-1 accumulation, obatoclax sensitises MCL cells to low doses of the PI [15]. A phase I/II study substantiated the tolerance of a combined treatment BTZ/obatoclax in patient with R/R MCL. However the synergism supported by the preclinical studies was not confirmed in patients [95]. Treatment of MM cell lines including BTZ-resistant cells and primary cells with cyclic adenosine monophosphate (cAMP) induces downregulation of MCL-1 and degradation of cyclin D1. Moreover, a synergy between BTZ and cAMP showed promising results in a murine xenograft model, warranting this strategy to overcome BTZ resistance [96].

6.4.4.4 IRF4/MYC Signalling

As described before, exacerbated de novo IRF4 signalling has been associated with MCL resistance to BTZ in vitro and in vivo, thus supporting the preclinical/clinical evaluation of IRF4-targeting drugs. Following first observations in MM preclinical models where it efficiently suppressed IRF4-expressing cells [111], lenalidomide was found to be effective in vitro and in vivo in BTZ-resistant MCL tumours harbouring high IRF4 levels, while sparing IRF4 negative cases. Lenalidomide activity relied on a functional interaction with the component of the E3 ligase complex, cereblon (CRBN), and CRBN-dependent lowering of IRF4 expression, leading to the blocking of B cell differentiation programme, as shown by increase in PAX5 and loss of CD38 and BLIMP-1. Consequently, BTZ-lenalidomide combination could overcome BTZ resistance [73]. Lenalidomide single agent was further validated in a phase II trial involving R/R MCL patients, including cases refractory to BTZ [97]. In contrast, in MM patients, therapy combining lenalidomide with BTZ failed in phase II trial [98]. Among the IMiD family, pomalidomide has been approved by the FDA for the treatment of R/R MM with at least two prior treatments, including BTZ. When added to BTZ or MRZ in combination with low dose dexamethasone, this agent went through successful phase I trial on heavily pretreated, high risks relapsing MM [99, 100].

Beside these approaches, the inhibition of the IRF4 target gene, *MYC*, in BTZ-resistant MCL cultures has been studied either with siRNA-mediated gene knockdown or with treatment with an inhibitor of BRD4, a bromodomain and extraterminal domain (BET) protein. BET proteins mainly regulate epigenetics marks. They impact gene expression and in turn, participate in cancer pathogenesis. BET inhibitors (BETis) are very promising novel anticancer agents, and combinatory therapy with these inhibitors has been suggested. Because BETis target the NF-κB pathway, their impact on BCL-2 and c-MYC proteins among others, has been tested preclinically in MCL and MM. As a proof-of-concept, inhibition of BRD4 synergistically induced cell death in vitro and in vivo when combined with lenalidomide. This confirmed that exacerbated IRF4/MYC signalling is associated with MCL resistance to BTZ and warranted the clinical evaluation of the IMiD-BETi combination in MCL cases refractory to the inhibition of proteasome [73].

Also, the BETi birabresib (OTX015) significantly synergises with BTZ, CFZ, IXZ and IMiD to improve MM response and overcomes resistance to PIs. It triggers the suppression of NF-κB pathway and decrease in c-MYC signalling. The birabresib/pomalidomide combination demonstrated great results to overcome adaptive resistance in MCL [101].

Moreover, JQ1, a thieno-triazolo-1,4-diazepine has been characterised as the first indirect inhibitor c-MYC transcriptional network in MM cells [103]. Thereafter, the combination of BTZ with the JQ1 derivative, CPI203, was found to be synergistic in BTZ-resistant MM cell lines and in a primary culture from a MM patient refractory to BTZ therapy [104]. These studies supported the clinical evaluation of the IMiD-BETis combination in MM and in MCL cases refractory to PIs. An alternative approach to directly inhibit BRD4 was to promote its degradation. This was recently achieved by the use of the protein-targeting chimeric molecule (PROTAC), ARV-825, which specifically induces BRD4 ubiquitination and degradation, granting activity and overcoming PI resistance in MM [105].

6.4.5 Epigenetic Modulators

Histone deacetylase 6 (HDAC6) mechanistically links the UPS and autophagy by facilitating the transport of protein aggregates along tubulin to juxtanuclear microtubule organising centres [112]. Aggregated ubiquitinated proteins are transferred to lysosomes via autophagy, and BTZ treatment contributes to aggresome formation. Cells that lack HDAC6 were found to be defective in the removal of protein aggregates and are not able to form large aggresomes. The combination HDAC inhibitors with BTZ sensitises MM-resistant cells to proteasome inhibition [113]. Ricolinostat (ACY-1215) is a specific

inhibitor of HDAC6. When ricolinostat is combined with BTZ and dexamethasone, the response rate among BTZ-refractory MM patients raised up to 20%. This combined treatment appeared well tolerated, supporting the use of HDAC6 inhibitors to overcome PI resistance in patient [102]. In MCL, combined PI and ricolinostat treatments are still under preclinical investigations [106].

Vorinostat is an inhibitor of class I and II HDAC. In combination with BTZ, vorinostat revealed limited results in clinical phase II and I, respectively, for relapsing MCL and MM [108]. Others combinations involving this HDAC inhibitor are under investigation, and epigenetic regulation mechanisms such as DNA methylation have been subject of preclinical studies. Because NOXA and BCL-2 are demethylated during BTZ treatment, the DNA methytransferase inhibitor decitabine showed synergic effect with BTZ in PI-resistant MCL [107].

6.5 Concluding Remarks

Molecular mechanisms that explain inherent or acquired BTZ resistance have been essentially explored in MM and MCL. The identified alterations include mutations in proteasomal subunits and activation of prosurvival signalling pathways that have impact in cell cycle, cell differentiation, apoptosis, and stabilisation of critical cellular factors. Inside the cell, UPS and ALS are major regulators of protein homeostasis and contribute to maintain the balance required to accomplish all protein functions, including the capacity of the cells to respond to BTZ. Beside the malignant cell itself, microenvironment is a crucial factor for impairing PI activity, especially in MM cells, which are heavily dependent on external factors for their growth and response to drugs.

New molecular mechanisms are regularly discovered that have been associated with drug resistance. Some of these mechanisms could be implicated in PI resistance, enhancing the complexity of this process. In the hypothesis of a multifactorial origin, the conception of new and more efficient approaches tackling PI resistance should include combinatorial approaches simultaneously targeting multiple cellular mechanism. In the case of MCL and MM, the development of new types of drug such as IMiDs and BETis used in combination with PIs led to promising results in vivo. Nevertheless, combinatorial treatment could also increase off-target effects and for this reason a better assessment of these treatments has to be performed before been used in patients. The perfect strategy to overcome drug resistance in MM, MCL and other cancer types is far from being identified. Improving our knowledge on the molecular mechanisms implicated in resistance would also open the possibility to elaborate more efficient treatments while reducing the undesired side effects on healthy cells.

Acknowledgments MGS and MSR are part of the UbiCODE project and received funding from the European Union's Horizon 2020 research and innovation program under the Marie Skłodowska-Curie grant agreement No 765445. GQ is a fellow from the French Ministry of Education. MSR is also funded by the Institut National du Cancer, France (PLBIO16-251), LASSERLAB-EUROPE grant number 654148 and CONACyT-SRE (Mexico) grant 0280365.
BS acknowledges support from Ligue contre le Cancer and Fondation Française pour la Recherche contre le Myélome et les Gammapathies. GR was financially supported by Fondo de Investigación Sanitaria PI15/00102 and PI18/01383, European Regional Development Fund (ERDF) 'Una manera de hacer Europa'.

References

1. Budenholzer L, Cheng CL, Li Y, Hochstrasser M (2017) Proteasome structure and assembly. J Mol Biol 429:3500–3524. https://doi.org/10.1016/j.jmb.2017.05.027
2. Mata-Cantero L, Lobato-Gil S, Aillet F et al (2015) The ubiquitin-proteasome system (UPS) as a cancer drug target: emerging mechanisms and therapeutics. In: Wondrak GT (ed) Stress response pathways in cancer. Springer, New York, pp 225–264
3. Roeten MSF, Cloos J, Jansen G (2018) Positioning of proteasome inhibitors in therapy of solid malignancies. Cancer Chemother Pharmacol 81:227–243. https://doi.org/10.1007/s00280-017-3489-0
4. Niewerth D, Jansen G, Assaraf YG et al (2015) Molecular basis of resistance to proteasome inhibitors in hematological malignancies. Drug Resist Updat Rev Comment Antimicrob Anticancer

Chemother 18:18–35. https://doi.org/10.1016/j.drup.2014.12.001
5. Kumar SK, Rajkumar V, Kyle RA et al (2017) Multiple myeloma. Nat Rev Dis Primer 3:17046. https://doi.org/10.1038/nrdp.2017.46
6. Pérez-Galán P, Dreyling M, Wiestner A (2011) Mantle cell lymphoma: biology, pathogenesis, and the molecular basis of treatment in the genomic era. Blood 117:26–38. https://doi.org/10.1182/blood-2010-04-189977
7. Diefenbach CSM, O'Connor OA (2010) Mantle cell lymphoma in relapse: the role of emerging new drugs. Curr Opin Oncol 22:419–423. https://doi.org/10.1097/CCO.0b013e32833d58f2
8. Yong K, Gonzalez-McQuire S, Szabo Z et al (2018) The start of a new wave: developments in proteasome inhibition in multiple myeloma. Eur J Haematol 101:220–236. https://doi.org/10.1111/ejh.13071
9. Robak P, Drozdz I, Szemraj J, Robak T (2018) Drug resistance in multiple myeloma. Cancer Treat Rev 70:199–208. https://doi.org/10.1016/j.ctrv.2018.09.001
10. Soriano GP, Besse L, Li N et al (2016) Proteasome inhibitor-adapted myeloma cells are largely independent from proteasome activity and show complex proteomic changes, in particular in redox and energy metabolism. Leukemia 30:2198–2207. https://doi.org/10.1038/leu.2016.102
11. Franke NE, Niewerth D, Assaraf YG et al (2012) Impaired bortezomib binding to mutant β5 subunit of the proteasome is the underlying basis for bortezomib resistance in leukemia cells. Leukemia 26:757–768. https://doi.org/10.1038/leu.2011.256
12. Barrio S, Stühmer T, Da-Viá M et al (2018) Spectrum and functional validation of PSMB5 mutations in multiple myeloma. Leukemia. https://doi.org/10.1038/s41375-018-0216-8
13. Ri M, Iida S, Nakashima T et al (2010) Bortezomib-resistant myeloma cell lines: a role for mutated PSMB5 in preventing the accumulation of unfolded proteins and fatal ER stress. Leukemia 24:1506–1512. https://doi.org/10.1038/leu.2010.137
14. Valentin R, Grabow S, Davids MS (2018) The rise of apoptosis: targeting apoptosis in hematologic malignancies. Blood 132:1248–1264. https://doi.org/10.1182/blood-2018-02-791350
15. Pérez-Galán P, Roué G, Villamor N et al (2007) The BH3-mimetic GX15-070 synergizes with bortezomib in mantle cell lymphoma by enhancing Noxa-mediated activation of Bak. Blood 109:4441–4449. https://doi.org/10.1182/blood-2006-07-034173
16. Kotschy A, Szlavik Z, Murray J et al (2016) The MCL1 inhibitor S63845 is tolerable and effective in diverse cancer models. Nature 538:477–482. https://doi.org/10.1038/nature19830
17. Morales AA, Kurtoglu M, Matulis SM et al (2011) Distribution of Bim determines Mcl-1 dependence or codependence with Bcl-xL/Bcl-2 in Mcl-1–expressing myeloma cells. Blood 118:1329–1339. https://doi.org/10.1182/blood-2011-01-327197
18. Gupta VA, Matulis SM, Conage-Pough JE et al (2017) Bone marrow microenvironment-derived signals induce Mcl-1 dependence in multiple myeloma. Blood 129:1969–1979. https://doi.org/10.1182/blood-2016-10-745059
19. Pan R, Ruvolo VR, Wei J et al (2015) Inhibition of Mcl-1 with the pan–Bcl-2 family inhibitor (–)BI97D6 overcomes ABT-737 resistance in acute myeloid leukemia. Blood 126:363–372. https://doi.org/10.1182/blood-2014-10-604975
20. Yang DT, Young KH, Kahl BS et al (2008) Prevalence of bortezomib-resistant constitutive NF-kappaB activity in mantle cell lymphoma. Mol Cancer 7:1–14. https://doi.org/10.1186/1476-4598-7-40
21. Markovina S, Callander NS, O'Connor SL et al (2008) Bortezomib-resistant nuclear factor-kappaB activity in multiple myeloma cells. Mol Cancer Res 6:1356–1364. https://doi.org/10.1158/1541-7786.MCR-08-0108
22. Annunziata CM, Davis RE, Demchenko Y et al (2007) Frequent engagement of the classical and alternative NF-kappaB pathways by diverse genetic abnormalities in multiple myeloma. Cancer Cell 12:115–130. https://doi.org/10.1016/j.ccr.2007.07.004
23. Rizzatti EG, Mora-Jensen H, Weniger MA et al (2008) Noxa mediates Bortezomib induced apoptosis in both sensitive and intrinsically resistant mantle cell lymphoma cells and this effect is independent of constitutive activity of the AKT and NF-kappaB pathways. Leuk Lymphoma 49:798–808. https://doi.org/10.1080/10428190801910912
24. Manni S, Brancalion A, Mandato E et al (2013) Protein kinase CK2 inhibition down modulates the NF-κB and STAT3 survival pathways, enhances the cellular proteotoxic stress and synergistically boosts the cytotoxic effect of bortezomib on multiple myeloma and mantle cell lymphoma cells. Clin Cancer Res 18:1888–1900. https://doi.org/10.1371/journal.pone.0075280
25. Chattopadhyay S, Thomsen H, da Silva Filho MI et al (2018) Enrichment of B cell receptor signaling and epidermal growth factor receptor pathways in monoclonal gammopathy of undetermined significance: a genome-wide genetic interaction study. Mol Med 24:30. https://doi.org/10.1186/s10020-018-0031-8
26. Kim A, Seong KM, Kang HJ et al (2015) Inhibition of Lyn is a promising treatment for mantle cell lymphoma with bortezomib resistance. Oncotarget 6:38225–38238
27. Pérez-Galán P, Roué G, Villamor N et al (2006) The proteasome inhibitor bortezomib induces apoptosis in mantle-cell lymphoma through generation of ROS and Noxa activation independent of p53 status. Blood 107:257–264. https://doi.org/10.1182/blood-2005-05-2091
28. Weniger MA, Rizzatti EG, Pérez-Galán P et al (2011) Treatment-induced oxidative stress and cellular antioxidant capacity determine response to bortezomib in

mantle cell lymphoma. Clin Cancer Res 17:5101–5112. https://doi.org/10.1158/1078-0432.CCR-10-3367
29. Luanpitpong S, Poohadsuan J, Samart P et al (2018) Reactive oxygen species mediate cancer stem-like cells and determine bortezomib sensitivity via Mcl-1 and Zeb-1 in mantle cell lymphoma. Biochim Biophys Acta Mol Basis Dis 1864:3739–3753. https://doi.org/10.1016/j.bbadis.2018.09.010
30. Sánchez-Tilló E, Fanlo L, Siles L et al (2014) The EMT activator ZEB1 promotes tumor growth and determines differential response to chemotherapy in mantle cell lymphoma. Cell Death Differ 21:247–257. https://doi.org/10.1038/cdd.2013.123
31. Balsas P, Galán-Malo P, Marzo I, Naval J (2012) Bortezomib resistance in a myeloma cell line is associated to PSMβ5 overexpression and polyploidy. Leuk Res 36:212–218. https://doi.org/10.1016/j.leukres.2011.09.011
32. Rückrich T, Kraus M, Gogel J et al (2009) Characterization of the ubiquitin-proteasome system in bortezomib-adapted cells. Leukemia 23:1098–1105. https://doi.org/10.1038/leu.2009.8
33. Shuqing L, Jianmin Y, Chongmei H et al (2011) Upregulated expression of the PSMB5 gene may contribute to drug resistance in patient with multiple myeloma when treated with bortezomib-based regimen. Exp Hematol 39:1117–1118. https://doi.org/10.1016/j.exphem.2011.09.003
34. Acosta-Alvear D, Cho MY, Wild T et al (2015) Paradoxical resistance of multiple myeloma to proteasome inhibitors by decreased levels of 19S proteasomal subunits. eLife 4:e08153. https://doi.org/10.7554/eLife.08153
35. Shi C-X, Kortüm KM, Zhu YX et al (2017) CRISPR genome-wide screening identifies dependence on the proteasome subunit PSMC6 for bortezomib sensitivity in multiple myeloma. Mol Cancer Ther 16:2862–2870. https://doi.org/10.1158/1535-7163.MCT-17-0130
36. Bartel B (2015) Proteaphagy-selective autophagy of inactive proteasomes. Mol Cell 58:970–971. https://doi.org/10.1016/j.molcel.2015.06.004
37. Marshall RS, Vierstra RD (2018) Autophagy: the master of bulk and selective recycling. Annu Rev Plant Biol 69:173–208. https://doi.org/10.1146/annurev-arplant-042817-040606
38. Quinet G, Rodriguez MS (2019) Evidences for an active proteaphagy in Bortezomib resistant mantle cell lymphoma cells. Manuscript Preparation
39. Bond MR, Hanover JA (2013) O-GlcNAc cycling: a link between metabolism and chronic disease. Annu Rev Nutr 33:205–229. https://doi.org/10.1146/annurev-nutr-071812-161240
40. Luanpitpong S, Chanthra N, Janan M et al (2018) Inhibition of O-GlcNAcase sensitizes apoptosis and reverses Bortezomib resistance in mantle cell lymphoma through modification of truncated bid. Mol Cancer Ther 17:484–496. https://doi.org/10.1158/1535-7163.MCT-17-0390
41. Abraham I, Jain S, Wu C-P et al (2010) Marine sponge-derived sipholane triterpenoids reverse P-glycoprotein (ABCB1)-mediated multidrug resistance in cancer cells. Biochem Pharmacol 80:1497–1506. https://doi.org/10.1016/j.bcp.2010.08.001
42. Besse A, Stolze SC, Rasche L et al (2018) Carfilzomib resistance due to ABCB1/MDR1 overexpression is overcome by nelfinavir and lopinavir in multiple myeloma. Leukemia 32:391–401. https://doi.org/10.1038/leu.2017.212
43. Fok JHL, Hedayat S, Zhang L et al (2018) HSF1 is essential for myeloma cell survival and a promising therapeutic target. Clin Cancer Res 24:2395–2407. https://doi.org/10.1158/1078-0432.CCR-17-1594
44. Dytfeld D, Luczak M, Wrobel T et al (2016) Comparative proteomic profiling of refractory/relapsed multiple myeloma reveals biomarkers involved in resistance to bortezomib-based therapy. Oncotarget 7:56726–56736. https://doi.org/10.18632/oncotarget.11059
45. Hayes JD, Dinkova-Kostova AT (2014) The Nrf2 regulatory network provides an interface between redox and intermediary metabolism. Trends Biochem Sci 39:199–218. https://doi.org/10.1016/j.tibs.2014.02.002
46. Zong Z-H, Du Z-X, Zhang H-Y et al (2015) Involvement of Nrf2 in proteasome inhibition-mediated induction of ORP150 in thyroid cancer cells. Oncotarget 7:3416–3426. https://doi.org/10.18632/oncotarget.6636
47. Riz I, Hawley TS, Marsal JW, Hawley RG (2016) Noncanonical SQSTM1/p62-Nrf2 pathway activation mediates proteasome inhibitor resistance in multiple myeloma cells via redox, metabolic and translational reprogramming. Oncotarget 7:66360–66385. https://doi.org/10.18632/oncotarget.11960
48. Starheim KK, Holien T, Misund K et al (2016) Intracellular glutathione determines bortezomib cytotoxicity in multiple myeloma cells. Blood Cancer J 6:e446. https://doi.org/10.1038/bcj.2016.56
49. Podar K, Chauhan D, Anderson KC (2009) Bone marrow microenvironment and the identification of new targets for myeloma therapy. Leukemia 23:10–24. https://doi.org/10.1038/leu.2008.259
50. Finlayson AE, Freeman KW (2009) A cell motility screen reveals role for MARCKS-related protein in adherens junction formation and tumorigenesis. PLoS One 4:e7833. https://doi.org/10.1371/journal.pone.0007833
51. Yang Y, Chen Y, Saha MN et al (2015) Targeting phospho-MARCKS overcomes drug-resistance and induces antitumor activity in preclinical models of multiple myeloma. Leukemia 29:715–726. https://doi.org/10.1038/leu.2014.255
52. Sprynski AC, Hose D, Caillot L et al (2009) The role of IGF-1 as a major growth factor for myeloma cell lines and the prognostic relevance of the expression of its receptor. Blood 113:4614–4626. https://doi.org/10.1182/blood-2008-07-170464

53. Kuhn DJ, Berkova Z, Jones RJ et al (2012) Targeting the insulin-like growth factor-1 receptor to overcome bortezomib resistance in preclinical models of multiple myeloma. Blood 120:3260–3270. https://doi.org/10.1182/blood-2011-10-386789
54. Vincenz L, Jäger R, O'Dwyer M, Samali A (2013) Endoplasmic reticulum stress and the unfolded protein response: targeting the Achilles heel of multiple myeloma. Mol Cancer Ther 12:831–843. https://doi.org/10.1158/1535-7163.MCT-12-0782
55. Leung-Hagesteijn C, Erdmann N, Cheung G et al (2013) Xbp1s-negative tumor B cells and pre-plasmablasts mediate therapeutic proteasome inhibitor resistance in multiple myeloma. Cancer Cell 24:289–304. https://doi.org/10.1016/j.ccr.2013.08.009
56. Mimura N, Fulciniti M, Gorgun G et al (2012) Blockade of XBP1 splicing by inhibition of IRE1α is a promising therapeutic option in multiple myeloma. Blood 119:5772–5781. https://doi.org/10.1182/blood-2011-07-366633
57. Wang C, Pan Y-H, Shan M et al (2015) Knockdown of UbcH10 enhances the chemosensitivity of dual drug resistant breast cancer cells to epirubicin and docetaxel. Int J Mol Sci 16:4698–4712. https://doi.org/10.3390/ijms16034698
58. Lilienbaum A (2013) Relationship between the proteasomal system and autophagy. Int J Biochem Mol Biol 4:1–26
59. White E, DiPaola RS (2009) The double-edged sword of autophagy modulation in cancer. Clin Cancer Res 15:5308–5316. https://doi.org/10.1158/1078-0432.CCR-07-5023
60. Ding W-X, Ni H-M, Gao W et al (2007) Linking of autophagy to ubiquitin-proteasome system is important for the regulation of endoplasmic reticulum stress and cell viability. Am J Pathol 171:513–524. https://doi.org/10.2353/ajpath.2007.070188
61. Amaravadi RK, Lippincott-Schwartz J, Yin X-M et al (2011) Principles and current strategies for targeting autophagy for cancer treatment. Clin Cancer Res 17:654–666. https://doi.org/10.1158/1078-0432.CCR-10-2634
62. Cohen-Kaplan V, Livneh I, Avni N et al (2016) The ubiquitin-proteasome system and autophagy: coordinated and independent activities. Int J Biochem Cell Biol 79:403–418. https://doi.org/10.1016/j.biocel.2016.07.019
63. Chen S, Zhang Y, Zhou L et al (2014) A Bim-targeting strategy overcomes adaptive bortezomib resistance in myeloma through a novel link between autophagy and apoptosis. Blood 124:2687–2697. https://doi.org/10.1182/blood-2014-03-564534
64. Wang Q, Mora-Jensen H, Weniger MA et al (2009) ERAD inhibitors integrate ER stress with an epigenetic mechanism to activate BH3-only protein NOXA in cancer cells. Proc Natl Acad Sci USA 106:2200–2205. https://doi.org/10.1073/pnas.0807611106
65. Ni M, Lee AS (2007) ER chaperones in mammalian development and human diseases. FEBS Lett 581:3641–3651. https://doi.org/10.1016/j.febslet.2007.04.045
66. Kaufman RJ (2002) Orchestrating the unfolded protein response in health and disease. J Clin Invest 110:1389–1398. https://doi.org/10.1172/JCI16886
67. Szegezdi E, Logue SE, Gorman AM, Samali A (2006) Mediators of endoplasmic reticulum stress-induced apoptosis. EMBO Rep 7:880–885. https://doi.org/10.1038/sj.embor.7400779
68. Roué G, Pérez-Galán P, Mozos A et al (2011) The Hsp90 inhibitor IPI-504 overcomes bortezomib resistance in mantle cell lymphoma in vitro and in vivo by down-regulation of the prosurvival ER chaperone BiP/Grp78. Blood 117:1270–1279. https://doi.org/10.1182/blood-2010-04-278853
69. Weinkauf M, Zimmermann Y, Hartmann E et al (2009) 2-D PAGE-based comparison of proteasome inhibitor bortezomib in sensitive and resistant mantle cell lymphoma. Electrophoresis 30:974–986. https://doi.org/10.1002/elps.200800508
70. Davenport EL, Moore HE, Dunlop AS et al (2007) Heat shock protein inhibition is associated with activation of the unfolded protein response pathway in myeloma plasma cells. Blood 110:2641–2649. https://doi.org/10.1182/blood-2006-11-053728
71. Roué G, Pichereau V, Lincet H et al (2008) Cyclin D1 mediates resistance to apoptosis through upregulation of molecular chaperones and consequent redistribution of cell death regulators. Oncogene 27. https://doi.org/10.1038/onc.2008.126
72. Orchard J, Garand R, Davis Z et al (2003) A subset of t(11;14) lymphoma with mantle cell features displays mutated IgVH genes and includes patients with good prognosis, nonnodal disease. Blood 101:4975–4981. https://doi.org/10.1182/blood-2002-06-1864
73. Moros A, Rodríguez V, Saborit-Villarroya I et al (2014) Synergistic antitumor activity of lenalidomide with the BET bromodomain inhibitor CPI203 in bortezomib-resistant mantle cell lymphoma. Leukemia 28:2049–2059. https://doi.org/10.1038/leu.2014.106
74. Desai S, Maurin M, Smith MA et al (2010) PRDM1 is required for mantle cell lymphoma response to bortezomib. Mol Cancer Res MCR 8:907–918. https://doi.org/10.1158/1541-7786.MCR-10-0131
75. Chauhan D, Tian Z, Nicholson B et al (2012) A small molecule inhibitor of ubiquitin-specific protease-7 induces apoptosis in multiple myeloma cells and overcomes bortezomib resistance. Cancer Cell 22:345–358. https://doi.org/10.1016/j.ccr.2012.08.007
76. Tian Z, D'Arcy P, Wang X et al (2014) A novel small molecule inhibitor of deubiquitylating enzyme USP14 and UCHL5 induces apoptosis in multiple myeloma and overcomes bortezomib resistance. Blood 123:706–716. https://doi.org/10.1182/blood-2013-05-500033

77. Kropp KN, Maurer S, Rothfelder K et al (2018) The novel deubiquitinase inhibitor b-AP15 induces direct and NK cell-mediated antitumor effects in human mantle cell lymphoma. Cancer Immunol Immunother 67:935–947. https://doi.org/10.1007/s00262-018-2151-y
78. Das DS, Das A, Ray A et al (2017) Blockade of deubiquitylating enzyme USP1 inhibits DNA repair and triggers apoptosis in multiple myeloma cells. Clin Cancer Res 23:4280–4289. https://doi.org/10.1158/1078-0432.CCR-16-2692
79. Song Y, Li S, Ray A et al (2017) Blockade of deubiquitylating enzyme Rpn11 triggers apoptosis in multiple myeloma cells and overcomes bortezomib resistance. Oncogene 36:5631–5638. https://doi.org/10.1038/onc.2017.172
80. Peterson LF, Sun H, Liu Y et al (2015) Targeting deubiquitinase activity with a novel small-molecule inhibitor as therapy for B-cell malignancies. Blood 125:3588–3597. https://doi.org/10.1182/blood-2014-10-605584
81. Wang X, Mazurkiewicz M, Hillert EK et al (2016) The proteasome deubiquitinase inhibitor VLX1570 shows selectivity for ubiquitin-specific protease-14 and induces apoptosis of multiple myeloma cells. Sci Rep 6:26979. https://doi.org/10.1038/srep26979
82. Driessen C, Kraus M, Joerger M et al (2016) Treatment with the HIV protease inhibitor nelfinavir triggers the unfolded protein response and may overcome proteasome inhibitor resistance of multiple myeloma in combination with bortezomib: a phase I trial (SAKK 65/08). Haematologica 101:346–355. https://doi.org/10.3324/haematol.2015.135780
83. Kawaguchi T, Miyazawa K, Moriya S et al (2011) Combined treatment with bortezomib plus bafilomycin A1 enhances the cytocidal effect and induces endoplasmic reticulum stress in U266 myeloma cells: crosstalk among proteasome, autophagy-lysosome and ER stress. Int J Oncol 38:643–654. https://doi.org/10.3892/ijo.2010.882
84. Heine S, Kleih M, Giménez N et al (2018) Cyclin D1-CDK4 activity drives sensitivity to bortezomib in mantle cell lymphoma by blocking autophagy-mediated proteolysis of NOXA. J Hematol Oncol 11:112. https://doi.org/10.1186/s13045-018-0657-6
85. Richardson PG, Eng C, Kolesar J et al (2012) Perifosine, an oral, anti-cancer agent and inhibitor of the Akt pathway: mechanistic actions, pharmacodynamics, pharmacokinetics, and clinical activity. Expert Opin Drug Metab Toxicol 8:623–633. https://doi.org/10.1517/17425255.2012.681376
86. Kim A, Park S, Lee J-E et al (2012) The dual PI3K and mTOR inhibitor NVP-BEZ235 exhibits antiproliferative activity and overcomes bortezomib resistance in mantle cell lymphoma cells. Leuk Res 36:912–920. https://doi.org/10.1016/j.leukres.2012.02.010
87. Witzig TE, Geyer SM, Ghobrial I et al (2005) Phase II trial of single-agent temsirolimus (CCI-779) for relapsed mantle cell lymphoma. J Clin Oncol 23:5347–5356. https://doi.org/10.1200/JCO.2005.13.466
88. Rizzieri DA, Feldman E, Dipersio JF et al (2008) A phase 2 clinical trial of deforolimus (AP23573, MK-8669), a novel mammalian target of rapamycin inhibitor, in patients with relapsed or refractory hematologic malignancies. Clin Cancer Res 14:2756–2762. https://doi.org/10.1158/1078-0432.CCR-07-1372
89. Jung HJ, Chen Z, Wang M et al (2012) Calcium blockers decrease the bortezomib resistance in mantle cell lymphoma via manipulation of tissue transglutaminase activities. Blood 119:2568–2578. https://doi.org/10.1182/blood-2011-09-377598
90. Muz B, Azab F, de la Puente P et al (2017) Selinexor overcomes hypoxia-induced drug resistance in multiple myeloma. Transl Oncol 10:632–640. https://doi.org/10.1016/j.tranon.2017.04.010
91. de Claro RA, McGinn KM, Verdun N et al (2015) FDA approval: Ibrutinib for patients with previously treated mantle cell lymphoma and previously treated chronic lymphocytic leukemia. Clin Cancer Res 21:3586–3590. https://doi.org/10.1158/1078-0432.CCR-14-2225
92. Murray MY, Zaitseva L, Auger MJ et al (2015) Ibrutinib inhibits BTK-driven NF-κB p65 activity to overcome bortezomib-resistance in multiple myeloma. Cell Cycle 14:2367–2375. https://doi.org/10.1080/15384101.2014.998067
93. Richardson PG, Bensinger WI, Huff CA et al (2018) Ibrutinib alone or with dexamethasone for relapsed or relapsed and refractory multiple myeloma: phase 2 trial results. Br J Haematol 180:821–830. https://doi.org/10.1111/bjh.15058
94. Pham LV, Tamayo AT, Li C et al (2010) Degrasyn potentiates the antitumor effects of bortezomib in mantle cell lymphoma cells in vitro and in vivo: therapeutic implications. Mol Cancer Ther 9:2026–2036. https://doi.org/10.1158/1535-7163.MCT-10-0238
95. Goy A, Hernandez-Ilzaliturri FJ, Kahl B et al (2014) A phase I/II study of the pan Bcl-2 inhibitor obatoclax mesylate plus bortezomib for relapsed or refractory mantle cell lymphoma. Leuk Lymphoma 55:2761–2768. https://doi.org/10.3109/10428194.2014.907891
96. Wang Y, Tang Y, Hang H et al (2018) cAMP induces cell apoptosis in multiple myeloma and overcomes bortezomib resistance. Am J Cancer Res 8:16–29
97. Desai M, Newberry K, Ou Z et al (2014) Lenalidomide in relapsed or refractory mantle cell lymphoma: overview and perspective. Ther Adv Hematol 5:91–101. https://doi.org/10.1177/2040620714532124
98. Morrison VA, Jung S-H, Johnson J et al (2015) Therapy with bortezomib plus lenalidomide for relapsed/refractory mantle cell lymphoma: final results of a phase II trial (CALGB 50501). Leuk Lymphoma 56:958–964. https://doi.org/10.3109/10428194.2014.938333
99. Richardson PG, Hofmeister CC, Raje NS et al (2017) Pomalidomide, bortezomib and low-dose

dexamethasone in lenalidomide-refractory and proteasome inhibitor-exposed myeloma. Leukemia 31:2695–2701. https://doi.org/10.1038/leu.2017.173
100. Spencer A, Harrison S, Zonder J et al (2018) A phase 1 clinical trial evaluating marizomib, pomalidomide and low-dose dexamethasone in relapsed and refractory multiple myeloma (NPI-0052-107): final study results. Br J Haematol 180:41–51. https://doi.org/10.1111/bjh.14987
101. Tarantelli C, Bernasconi E, Gaudio E et al (2018) BET bromodomain inhibitor birabresib in mantle cell lymphoma: in vivo activity and identification of novel combinations to overcome adaptive resistance. ESMO Open 3:e000387. https://doi.org/10.1136/esmoopen-2018-000387
102. Vogl DT, Raje N, Jagannath S et al (2017) Ricolinostat, the first selective histone deacetylase 6 inhibitor, in combination with Bortezomib and dexamethasone for relapsed or refractory multiple myeloma. Clin Cancer Res 23:3307–3315. https://doi.org/10.1158/1078-0432.CCR-16-2526
103. Delmore JE, Issa GC, Lemieux ME et al (2011) BET bromodomain inhibition as a therapeutic strategy to target c-Myc. Cell 146:904–917. https://doi.org/10.1016/j.cell.2011.08.017
104. Siegel MB, Liu SQ, Davare MA et al (2015) Small molecule inhibitor screen identifies synergistic activity of the bromodomain inhibitor CPI203 and bortezomib in drug resistant myeloma. Oncotarget 6:18921–18932
105. Zhang X, Lee HC, Shirazi F et al (2018) Protein targeting chimeric molecules specific for bromodomain and extra-terminal motif family proteins are active against pre-clinical models of multiple myeloma. Leukemia 32:2224–2239. https://doi.org/10.1038/s41375-018-0044-x
106. Amengual JE, Johannet P, Lombardo M et al (2015) Dual targeting of protein degradation pathways with the selective HDAC6 inhibitor ACY-1215 and bortezomib is synergistic in lymphoma. Clin Cancer Res 21:4663–4675. https://doi.org/10.1158/1078-0432.CCR-14-3068
107. Leshchenko VV, Kuo P-Y, Jiang Z et al (2015) Harnessing Noxa demethylation to overcome Bortezomib resistance in mantle cell lymphoma. Oncotarget 6:27332–27342. https://doi.org/10.18632/oncotarget.2903
108. Yazbeck V, Shafer D, Perkins EB et al (2018) A phase II trial of bortezomib and vorinostat in mantle cell lymphoma and diffuse large B-cell lymphoma. Clin Lymphoma Myeloma Leuk 18:569–575.e1. https://doi.org/10.1016/j.clml.2018.05.023
109. Turner JG, Kashyap T, Dawson JL et al (2016) XPO1 inhibitor combination therapy with bortezomib or carfilzomib induces nuclear localization of IκBα and overcomes acquired proteasome inhibitor resistance in human multiple myeloma. Oncotarget 7:78896–78909. https://doi.org/10.18632/oncotarget.12969
110. Campo E, Rule S (2015) Mantle cell lymphoma: evolving management strategies. Blood 125:48–55. https://doi.org/10.1182/blood-2014-05-521898
111. Lopez-Girona A, Heintel D, Zhang L-H et al (2011) Lenalidomide downregulates the cell survival factor, interferon regulatory factor-4, providing a potential mechanistic link for predicting response. Br J Haematol 154:325–336. https://doi.org/10.1111/j.1365-2141.2011.08689.x
112. McConkey DJ, White M, Yan W (2012) HDAC inhibitor modulation of proteotoxicity as a therapeutic approach in cancer. Adv Cancer Res 116:131–163. https://doi.org/10.1016/B978-0-12-394387-3.00004-5
113. Catley L, Weisberg E, Kiziltepe T et al (2006) Aggresome induction by proteasome inhibitor bortezomib and alpha-tubulin hyperacetylation by tubulin deacetylase (TDAC) inhibitor LBH589 are synergistic in myeloma cells. Blood 108:3441–3449. https://doi.org/10.1182/blood-2006-04-016055

molecules

MDPI

Review

Mechanisms Regulating the UPS-ALS Crosstalk: The Role of Proteaphagy

Grégoire Quinet, Maria Gonzalez-Santamarta, Clara Louche and Manuel S. Rodriguez *

ITAV-CNRS USR 3505 IPBS-UPS, 1 Place Pierre Potier, 31106 Toulouse, France; Gregoire.QUINET@itav.fr (G.Q.); Maria.GONZALEZ-SANTAMARTA@itav.fr (M.G.-S.); clara.louche@itav.fr (C.L.)

* Correspondence: manuel.rodriguez@itav.fr

Academic Editors: Cécile Polge and Alfred Vertegaal

Received: 26 April 2020; Accepted: 16 May 2020; Published: 18 May 2020

Abstract: Protein degradation is tightly regulated inside cells because of its utmost importance for protein homeostasis (proteostasis). The two major intracellular proteolytic pathways are the ubiquitin-proteasome and the autophagy-lysosome systems which ensure the fate of proteins when modified by various members of the ubiquitin family. These pathways are tightly interconnected by receptors and cofactors that recognize distinct chain architectures to connect with either the proteasome or autophagy under distinct physiologic and pathologic situations. The degradation of proteasome by autophagy, known as proteaphagy, plays an important role in this crosstalk since it favours the activity of autophagy in the absence of fully active proteasomes. Recently described in several biological models, proteaphagy appears to help the cell to survive when proteostasis is broken by the absence of nutrients or the excess of proteins accumulated under various stress conditions. Emerging evidence indicates that proteaphagy could be permanently activated in some types of cancer or when chemoresistance is observed in patients.

Keywords: ubiquitin proteasome system; autophagy; ubiquitin-like; proteaphagy; pathology

1. Introduction

In order to maintain cell viability, protein homeostasis (proteostasis) needs to be tightly controlled. Proteostasis is regulated by many mechanisms, including various post-translational modifications (PTM). PTMs can affect the half-life of proteins, their localization, their activity or even their interactions with other cellular components. Protein PTM are highly dynamic and controlled by the action of modifying/de-modifying enzymes that attach/detach small chemical groups, peptides or even complex molecules. The best-known protein modification by a small polypeptide is ubiquitin (Ub), which together with other ubiquitin-like (UbL) proteins integrates a family sharing the same β-grasp folding [1]. Ubiquitin family members are about 10 to 20 kDa in size when free. The C-terminal glycine residues of Ub or UbL moieties are attached or conjugated to a lysine residue (in most cases) on the substrate protein. The conjugation of Ub and UbL to protein substrates is mediated by a three-step enzymatic thiol-ester cascade that involves distinct sets of enzymes. A first ATP-dependent step occurs with the action of an E1 activating enzyme. The Ub or UbL moiety is then transferred to an E2 conjugating enzyme, to finally be specifically attached to a protein substrate with the help of an E3 ligase [2]. As mentioned, those modifications are reversible and each modification can be cleaved by specific enzymes such as deubiquitylating (DUB) [3], SUMO specific proteases (SUSPs) [4] or deNEDDylating (NEDP1) enzymes [5], among other isopeptidases.

The ubiquitin proteasome system (UPS) and the autophagy lysosome system (ALS) are the two major intracellular proteolytic machineries in eukaryotic cells [6]. The UPS system relies on the polyubiquitylation of target proteins and their subsequent degradation by the proteasome [7,8]. While ubiquitylation also contributes to recruiting cargoes that are targeted to the ALS for degradation,

the chain topology appears to be different to the one recognized by the proteasome. In particular, the ALS drives the degradation of cellular components, such as organelles, but also large protein aggregates. Selective autophagy events (macroautophagy) require the formation of autophagosomes that will fuse with lysosomes to degrade sequestered components [9].

PTMs contribute to coordinating the action of the UPS and ALS under distinct cellular stress situations such as multiple infections, inflammations, degenerative diseases, cancers or in response to medical treatments. This review presents some of the major roles of the UPS and ALS in protein homeostasis and the cooperation mechanisms activated in various pathologic situations that help the cell to cope with a disrupted proteostasis. Recent findings on proteaphagy will be discussed. In particular, its role in the ALS–UPS exchanges under nutrient starvation or after proteasome inhibition.

2. The Ubiquitin Proteasome System (UPS)

The ubiquitin proteasome system (UPS) is one of the main mechanisms for intracellular protein degradation and is essential to maintain protein homeostasis. This proteolytic mechanism is tightly controlled, to ensure the correct turnover of substrates involved in a wide variety of cellular processes. Ubiquitylated cargoes are recognized by proteasome subunits and cofactors that present substrates to the catalytic core of the proteasome [7,10]. Protein ubiquitylation and degradation is tightly regulated by a large number of cellular factors including Ub and UbL, enzymes involved in the modification/de-modification of substrates, chaperones and permanent or transient components of the proteasome [11,12].

2.1. The 20S Proteasome

The proteasome is a large complex multidomain protein (2.5 MDa) that drives the degradation of short-lived proteins in need of accurate turnover control. Proteasomes are found in nuclear and cytosolic compartments, associated or not to organelles [13].

The core particle (CP) of this barrel-shaped complex is also known as the 20S proteasome. It stacks two outer rings composed of seven α-subunits (α1–7) and two inner rings of seven β-subunits (β1–7) (Figure 1). The catalytic sites within the proteolytic chamber are present in three β subunits (β1, β2 and β5) and respectively display trypsin-like, post–glutamyl peptide hydrolase–like and chymotrypsin-like activities. Structural studies revealed that α-rings form a closed structure which prevents proteins from entering the inner chamber of the β-rings [14]. Narrow axial pores of the 20S barrel allow access to this catalytic chamber so that only unfolded proteins can enter for degradation [15]. Although 20S alone are found in cells and degrade unstructured substrates in the absence of ubiquitylation [16], their association with 19S tightly controls the specific degradation of ubiquitin modified substrates [10].

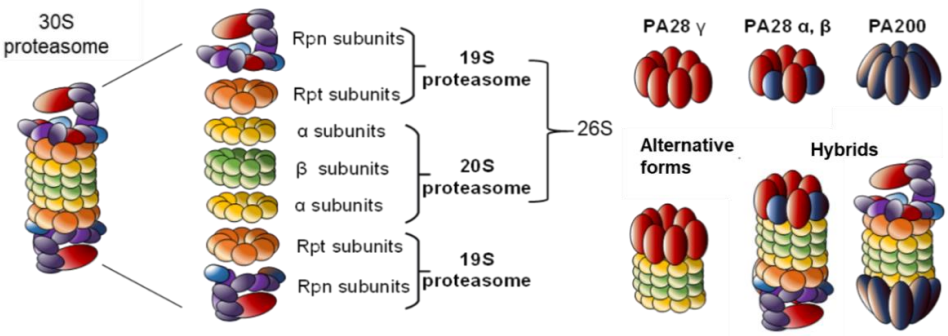

Figure 1. Proteasome complexity. The 26S proteasome is the most studied proteasome. However, alternative regulatory particles 19S, PA28 or PA200 are able to cap the core 20S proteasome to modulate its proteolytic activity. All these proteasome complexes (20S, 26S, 30S or hybrids) have been found in cells.

Cytokines that activate immune response can induce several isoforms of 20S subunits. The genes encode for inducible proteasomal β subunits, so-called β1i, β2i and β5i. These subunits replace their counterparts in the constitutive 20S, building the immunoproteasome [17]. This alternative form of 20S proteasome has different substrate selectivity compared to the normal proteasome. In particular, it is essential for the MHC-I antigen processing, since its degradative action is at the origin of antigenic peptides [18]. The thymoproteasome has also been described as an alternative form of the CP. A β5t expressed specifically in the thymus is incorporated into the 20S, together with β1i and β2i subunits. This thymoproteasome has a specific role in thymic positive selection of CD8+ T cells [19].

2.2. The 19S Complex

Proteasomes exist in several complexes, depending on the association between a CP and one or two regulatory particles (RP). The CP associated to the RP 19S is the most abundant and best characterized form of cellular proteasome, the so-called 26S proteasome [14]. The 19S, also known as P700 complex, not only recognizes and tethers targeted polyubiquitylated proteins but also removes ubiquitin chains [20], unfolds protein substrates [21], opens the closed α-ring [22], and allow unfolded proteins to enter into the CP for proteolysis. The 19S caps one or both ends of the CP, forming respectively the 26S or the 30S proteasomes (Figure 1). A base and a lid subcomplexes form the 19S [10]. At least nine non-ATPase (RPN) subunits form the lid complex: RPN3, RPN5, RPN6, RPN7, RPN8, RPN9, RPN11, RPN12 and RPN15. The base of the 19S complex includes four non-ATPase subunits (RPN1, RPN2, RPN10 and RPN13) and six homologous AAA + ATPase subunits (RPT1–RPT6) [10]. The base has various roles including the opening of the channel of the α-ring. The six ATPase subunits of the base form a hexameric ring that controls the entry of substrates into the catalytic sites of the CP [15]. RPN subunits have an important structural role, since recent evidence revealed that these subunits contribute to complex conformational changes to process specific substrates [15,23]. For instance, RPN1 and RPN2 work together to create a surface for substrate recruitment and interaction with the 20S [24]. These regulatory particles also ensure deubiquitylation of protein substrates by the action of several DUBs. While RPN11 is essential for RP-CP assembly [25], this subunit also cleaves polyubiquitin chains at a proximal site and contributes to recycling ubiquitin chains [26,27]. The C-terminal domain of RPN13 also has a DUB activity that optimises the cleavage of ubiquitin chains when close to the proteasome. Other DUBs cleave at distal sites including Usp14 anchored to RPN1 [12,14] or Uch37 associated to RPN2, bound itself to RPN13 [28].

The 19S contains several ubiquitin receptors to efficiently capture ubiquitylated proteins. The docking and the recognition of ubiquitylated substrates is performed through ubiquitin binding domains (UBD), located either within intrinsic proteasomal ubiquitin receptors or extrinsic ubiquitin receptors. The three intrinsic ubiquitin receptors of the 19S are RPN1, RPN10 and RPN13. The Ub-interacting motif (UIM) located at the C-terminus of RPN10 binds selectively monoubiquitin but also K48 and K63 polyubiquitin chains [29]. Ubiquitylation of RPN10 modulates substrate recruitment to proteasome [30] and its association with the 19S [31]. RPN13 binds di-ubiquitin through a pleckstrin-like receptor for ubiquitin (Pru) domain located at its N-terminus [32]. RPN1 carries a UBD that binds both ubiquitin and UbL proteins [33]. RPT5 also binds polyubiquitylated proteins in vitro, but in vivo evidence is still lacking [34]. Several extrinsic ubiquitin receptors such as Rad23, Dsk2, Ddi1 and Sem1 contain in their structure both UbL and UBA (ubiquitin-associated) domains. Their UBA domains interact with a specific ubiquitin signal, while their UbL domains allow interaction with proteasome subunits [35,36]. In particular, the UBD of RPN1 interacts with the UbL domain of Rad23 and triggers its tethering to proteasome [24,37]. Other ubiquitin receptors include VCP (AKA Cdc48 or p97 ATPase) that binds proteasome and polyubiquitylated substrates. This highly conserved AAA + ATPase is essential for proteasomal degradation of well-folded proteins. VCP carries a protein-unfoldase activity that is able to extract ubiquitylated proteins from complexes, unfolds the target to finally ensure its processing into the catalytic core of the 26S proteasome [38].

2.3. Other CP Regulators

The CP can also be regulated by several RP such as PA28 (AKA 11S or REG) and PA200 (AKA Blm10), two complexes with distinct characteristics and biological roles (Figure 1). Three structurally related PA28 proteins known as α, β and γ share around 50% of homology. While PA28α and PA28β assembled into hetero-oligomeric complexes with alternating α and β subunits, PA28γ forms homopolymers [39]. PA28α and PA28β are located in the cytoplasm, whereas PA28γ is mainly located in the nucleus and in perinuclear areas. PA28α/β complexes activate peptidase activities of the 20S proteasome and contribute to the production of cytotoxic T lymphocyte (CTL) epitopes [18]. Some evidence indicates that PA28γ functions as a regulator of cell proliferation and body growth in mice. In PA28$\gamma^{-/-}$ mice, neither PA28α nor PA28β compensate for PA28γ deficiency, suggesting their non-redundant roles [40]. PA28γ is implicated in various functions such as DNA damage response, apoptosis signalling, or transcriptional regulation of metabolism: it is involved in both ubiquitin-dependent and -independent recognition of substrates, to mediate proteasome-mediated protein turnover [41]. In yeast, PA200 has been shown to regulate proteasome assembly, maturation and/or proteolytic activity. This regulatory particle binds to the 20S but it is also found in hybrid proteasomes together with the 19S [14,42] (Figure 1).

2.4. The Hybrid Proteasome

Hybrid proteasomes are composed of two distinct regulators capping both ends of the CP. They contribute to an efficient coordination of cell proteolysis. For instance, PA28 and 19S can simultaneously bind to the two extremes of the 20S particle, forming the 19S–20S–PA28 "hybrid proteasome" complex (Figure 1) [39,43]. The RP first recognizes protein substrates to be internalized into the cavity of the 20S with an enhanced cleavage activity when bound to the PA28 complex. PA28 has been shown to activate the ATP-dependent degradation of ornithine decarboxylase (ODC) even in the absence of ubiquitylation but in the presence of antizyme (ODC inhibitor) [43]. Hybrid proteasomes also enhance the hydrolysis of small peptides that are different from those typically processed by the 26S proteasome. This has been associated to the capacity of PA28 to enhance antigen presentation. Interestingly, IFN-γ enhances the expression of the PA28αβ complex, favoring the formation of a hybrid proteasome and justifying its role in the processing of intracellular antigens [44].

All of these proteasomes create a large variety of complexes that can adapt for an optimized intracellular proteolysis activity. Proteasomes play major roles to face cellular stresses, and their dysregulation causes many pathologies, including neurodegenerative and cardiovascular disorders, respiratory diseases, and cancers [45]. Therefore, efficient proteasome activity is essential to maintain proteostasis in healthy cells.

3. Autophagy Lysosome System (ALS)

The autophagy lysosome system (ALS) is, together with the UPS, one of the main intracellular degradation systems. Literally meaning self-eating in Greek, autophagy digests long-lived, protein aggregates, stress RNA granules, and abnormal cytoplasmic organelles, including mitochondria, among others. Three types of autophagy have been identified so far: the chaperone-mediated autophagy, the microautophagy and the macroautophagy. The chaperone-mediated autophagy uses HSC70 to sequester into lysosomes proteins containing a KFERQ motif. Microautophagy is a direct lysosomal uptaking of substrates, whereas during macroautophagy (here referred as autophagy), cytosolic cargos are sequestered by a double membrane vesicle within which a portion of the cytoplasm is trapped in a complex multistep process. A tight regulation of autophagy leads to the selective degradation of substrates by the lysosome [9]. Therefore, the ALS plays a wide range of physiological and pathological roles.

3.1. Basal and Induced Autophagy

Early studies reported autophagy as a non-selective pathway, in which cargoes were randomly degraded. Indeed, autophagy was initially considered as a bulk degradation pathway, activated during nutrient deprivation, to ensure recycling of building blocks [46]. However, growing evidence supports the existence of an intricate selective process that contributes to intracellular homeostasis in non-starved cells [47]. Only one selective autophagy pathway can exclusively recognize and eliminate particular structures that must be degraded [46]. Hence, mitophagy drives mitochondria degradation, xenophagy targets pathogens, aggrephagy destroys aggregates, proteaphagy degrades proteasomes, etc. Different regulators modulate the selectivity of autophagy, including ubiquitin, which serves as a major degradation signal for this pathway [48]. However, a variety of cargoes are committed selectively to autophagy, in an ubiquitin-independent manner [49].

Basal level autophagy runs continuously under normal conditions [47], but stresses such as starvation, multiple infections, heat or drug treatment can strongly activate the process. The signalling pathways involved in autophagy regulation are centralized around the ULK1 (for unc-51 like autophagy activating kinase 1, also called ATG1) and Beclin1 complexes (Figure 2). ULK1 and Beclin1 phosphorylation is modulated by signalling proteins such as mTOR, Akt, AMPK and other PKA kinases. These phosphorylation steps regulate the initiation of the autophagic machinery [50]. The induction of autophagy triggers the isolation and elongation of a large cup-shaped double membrane that forms the growing phagophore (Figure 2). Although the origin of this membrane is not clear, various intracellular sources have been proposed, such as the endoplasmic reticulum (ER), the Golgi complex or the mitochondria [51]. Around 20 AuTophaGy (ATG) genes mediate the autophagy process [52]. These proteins are recruited to the phagophore and regulate the later autophagosome formation and maturation. During autophagy induction, ATG8 proteins are modified by phosphatidylethanolamine (PE). The lipidated ATG8 proteins localize at both sides of the phagophore, controlling the size of the future autophagosome [53,54]. Autophagosome maturation and the subsequent recruitment of substrates driven by ATG proteins (see below) lead to the late fusion with either vacuoles, endosomes or lysosomes (Figure 2). The autolysosome formed degrades targeted substrates using a series of lysosomal/vacuolar acid hydrolases such as cathepsins in mammalian cells. These degradation events produce small molecules such as amino acids that are transported back in the cytosol for recycling [55,56].

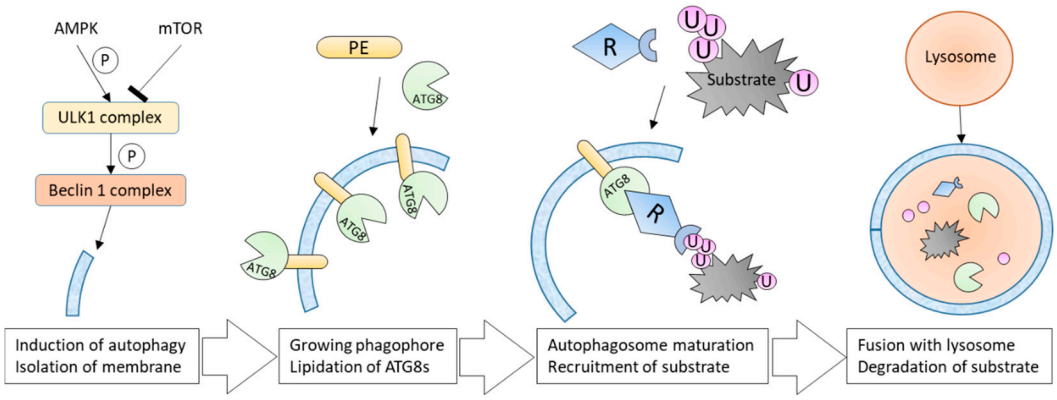

Figure 2. Selective autophagy pathways ensure the degradation of specific cargoes but also bulk of proteins. A complex signaling pathway regulates autophagy and induces the lipidation of ATG8 proteins within the newly formed cup shaped membrane, called phagophore. Recruitment of the autophagy substrate marks the maturation of the autophagosome. The substrate tethering to lipidated ATG8 is ensured by autophagy receptors (R). Autophagosomes then fuse with lysosomes, forming autolysosomes in which trapped substrates are degraded.

3.2. ATG8 Proteins Family, Characteristics and Functions

ATG8s are central components of autophagy regulation because of their essential role in autophagosome formation and maturation. This protein family is composed of six members in mammalian cells, LC3A, B and C, GABARAP, GABARAP L1 and GABARAP L2. The β grasp folding of ubiquitin is well conserved among the members of the ATG8 family and plays an essential role in protein–protein interactions. However, ATG8 proteins contain a supplementary hydrophobic pocket that engages interaction networks with autophagy and membrane trafficking components [57]. During the autophagy process, LC3/GABARAP proteins are conjugated to PE in an enzymatic manner. The mature form of ATG8, which will be covalently linked to PE, is generated through the processing of a high molecular weight precursor that is cleaved by the protease ATG4 [58]. To get conjugated to PE, ATG8 has to be first activated by ATG7 (E1). The conjugation requires the action of ATG3 (E2) and a mature E3 complex integrated by ATG5, ATG12 and ATG16. The integration of this E3 complex is mediated by ATG10 (E2) that covalently links ATG12 and ATG5 [59]. Since PE is the second-most abundant phospholipid found in biological membranes in mammals, its abundance positively regulates autophagy [60]. PE functions as an anchor of ATG8 to autophagosome membranes. ATG8s integration to phagophore through PE mediates the membrane fusion needed for a proper autophagosome formation [48,61].

A recent study showed that blocking the ATG8 conjugation system by knocking out ATG5 or ATG7 dramatically reduces membrane elongation and closure of autophagosomes, although autophagosome formation is not fully abolished [52]. Although Nguyen et al. showed that LC3/GABARAP proteins are not essential during the autophagosome formation, they appear to be crucial for the autophagosome-lysosome fusion [62]. Sometimes considered as proteins with common or redundant functions, the members of the LC3/GABARAP family play specialized and distinct roles. As an example, a recent study reveals a striking opposite role of LC3B/C and GABARAP/GABARAPL1 in autophagy induction. Even if LC3s or GABARAPs binds to the autophagy activation complex ULK1, they respectively trigger a negative or a positive regulation of autophagy [63]. Furthermore, LC3/GABARAP proteins play a pivotal role in selective autophagy by ensuring the docking of specific substrates to autophagosome membranes. LC3/GABARAP proteins act in non-redundant ways together with a large variety of autophagy receptors to tether specific targets for degradation. For instance, the presence of LC3C in autophagosome membranes is crucial for innate immunity during bacterial infection. Its interaction with the autophagy receptor nuclear domain 10 protein 52 (NDP52) drives an antibacterial autophagy, also called xenophagy, that protects host cytoplasm against *Salmonella enterica* [64].

3.3. Autophagy Receptors

The presentation of cargoes to the ALS is driven by more than 30 autophagy receptors, also called sequestosome-1-like receptors (SLRs) after the first described p62/SQSTM1 (sequestosome 1) [65]. Other well studied SLRs include njext to BRCA1 gene 1 protein (NBR1), optineurin (OPTN) or NDP52, that share common functional domains (Table 1). The diversity of receptors underlines the complex regulation of selective autophagy mechanisms. Some of them show functional redundancy for cargo recognition and cooperate with cofactors [66]. Furthermore, SLRs can be involved in both ubiquitin-dependent and -independent mechanisms of autophagy degradation [49].

Table 1. Structure and functions associated to the most studied autophagy receptors. Among more than 30 autophagy receptors known so far in mammalians, structural similarities and preserved functional domains are observed such as the presence of ubiquitin binding domains (UBDs), ATG8s binding domains like LC3 interacting regions (LIRs), oligomerization domains like PB1, or membrane associated domain [65]. Involvement of the displayed autophagy receptors in distinct selective autophagy events and collaborations between them are listed.

Autophagy Receptor	Structure Ubiquitin Binding Domain; Oligomerization Domain; ATG8s Binding Domain; Membrane Associated Domain	Selective Autophagy	Collaboration	References
p62/SQSTM1		Aggrephagy; Mitophagy; Xenophagy; Lysophagy; Pexophagy; Proteaphagy	NBR1 (aggregaphagy, pexophagy) NDP52 + OPTN (xenophagy)	[66–68]
NBR1		Pexophagy; Aggrephagy	p62 (aggregaphagy, pexophagy);	[64,66,67]
NDP52		Mitophagy	p62 + OPTN (xenophagy)	[67,69]
OPTN		Mitophagy; Xenophagy	NDP52 + p62 (xenophagy)	[67,69,70]
BNIP3/NIX	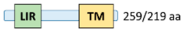	Mitophagy		[71]
ALFY		Aggrephagy	p62 (aggrephagy)	[72,73]
RTN3	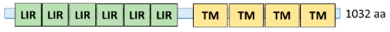	ER-phagy		[74]
FAM134B	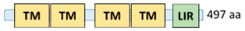	ER-phagy; Aggrephagy		[75]

The human cargo receptor p62 mediates the degradation of many substrates, such as aggregated proteins or cytosolic bacteria. P62 carries a ubiquitin-associated domain (UBA), a UBD that binds ubiquitylated cargoes. The UBA domain of p62 can homodimerize, modulating its interaction with monoubiquitin [9]. P62 and other autophagy receptors contain LC3 interacting regions (LIR). This affinity domain interacts with ATG8 proteins tethered into the autophagosome membrane (Table 1). Furthermore, p62 display a N-Terminal PB1 domain that triggers its polymerization. The scaffolding of these PB1 domains forms helical filaments of p62 polymers of variable lengths, that interact with both ATG8s and long ubiquitin chains enhancing their interactions. These large polymers of p62 provide a large molecular scaffold for autophagosome and ensure ubiquitylated cargo recruitment to structures where ATG8 proteins are lipidated [68]. Interestingly, oligomeric p62 preferentially binds to linear and K63-linked ubiquitin chains, compared to K48-linked chains. For this reason, K63 ubiquitin chains are commonly admitted as the signal for autophagy degradation. In contrast, K48 ubiquitin chains have been proposed to disrupt p62 oligomers, suggesting that they are not the preferred targets for p62-mediated degradation in vivo [76]. p62 has also been shown to drive cargoes to autophagosomes, in a ubiquitin-independent manner. A protein that needs to be degraded can get its N-terminus cleaved or modified by PTMs, building a signal for degradation called N-degron. Through its ZZ domain, p62 is able to bind selectively N-degrons, oligomerize and deliver these cargoes to autophagosomes [77].

NBR1 is another autophagy receptor carrying UBA, LIR and PB1 domains, with similar folding but distinct amino-acid sequence to the ones of p62. NBR1 plays an essential role in peroxisomes autophagy and works as a specific autophagy receptor for these organelles [66] (Table 1). There is no evidence supporting the idea that the PB1 domain of NBR1 is able to form polymers. However, it has been shown that NBR1 can form hetero-oligomers with p62 and cooperate in autophagy degradation [68]. OPTN acts as an autophagy receptor during xenophagy, mitophagy, as well as in aggrephagy. Considered as ancestral bacteria, mitochondria (mitophagy) uses the same receptor as xenophagy. However, it is clear that distinct signalling pathways and mechanisms activate and regulate these selective autophagy events. In mitophagy, OPTN is recruited to damaged mitochondria along with NDP52, therefore both receptors play redundant roles [78]. Interestingly, mitophagy and xenophagy also involve OPTN and p62, but both receptors lead to independent degradation in separated autophagosomes [79]. This evidence suggests a strong collaboration between autophagy receptors to regulate specificity of lysosome degradation [79] (Table 1). Furthermore, post-translational modifications of autophagy receptors can modulate their activity, adding another layer of complexity in the regulation of selective autophagy events. As an example, the OPTN phosphorylation on serine −177 located upstream of the LIR motif regulates its interaction with ATG8 proteins and is needed for the autophagy of *Salmonella enterica* during infection [70].

3.4. The Role of LIR Motifs

The LIR motif is a small peptide sequence that has affinity for ATG8 proteins. LIR-containing proteins can be autophagy receptors but also members of basal autophagy regulation, vesicle-associated proteins, and specific signalling proteins. The great number of possible LIR sequences are gathered in three consensuses and named depending of the first amino acid of hydrophobic core sequence: tryptophan, phenylalanine or tyrosine. Birgisdottir et al. defined the possible core consensus sequences as [W/F/Y]xx[L/I/V], and displayed variable binding affinities for the hydrophobic pockets of the different LC3/GABARAP proteins. As an example, the structure of p62 LIR motif reveals a W-x-x-L motif that gives a non-exclusive preference for LC3B proteins. OPTN carries the F-x-x-I consensus while NBR1 displays the less common Y-x-x-I consensus [80]. The LIR motif from OPTN shows stronger interaction with GABARAPs than with LC3s [81], although the affinity switches toward LC3B when phosphorylated at S177 by the TANK binding kinase (TBK1) [69].

Non-canonical LIR motifs have also been reported, such as the SKIP carboxyl homology (SKICH) domain of the autophagy receptor NDP52. This domain is essential for selective interaction with LC3C during *Salmonella* infections to drive the antibacterial autophagy [64]. In addition to the four amino

acids of the LIR motif, other adjacent amino acid residues are needed for specificity and affinity toward LC3/GABARAP proteins. For example, the importance of the acidic aspartic residues N-terminal to the LIR motif of p62 was verified by alanine substitutions [82]. Therefore, differences in the amino acids surrounding LIR motifs create different autophagy receptors affinities for LC3/GABARAP proteins.

To sum up, in order to explore the complexity of selective autophagy regulation, one should first consider the ubiquitin-chains present on the tagged substrates and the nature of the UBDs carried by dozens of autophagy receptors. Second, members of the LC3/GABARAP family interact with autophagy receptors through a diversity of LIR sequences to sort and tether autophagy substrates toward autophagosome membranes. Furthermore, homo and hetero polymerizations of autophagy receptors modulate their interactions with ubiquitin signals and/or LC3/GABARAP proteins. Actions of several autophagy receptors during one selective autophagy event can occur, with or without collaboration with other receptors. Finally, PTMs occurring on all these proteins can modulate their activities as well. The number of possible combinations involved in cargo recognition reveals the level of complexity of selective autophagy processes in mammalian cells.

4. Crosstalk between ALS and UPS

Although the UPS and the ALS have been initially considered to be independent proteolytic mechanisms, their interconnection has been supported by increasing evidence. The level of similarity and overlapping of regulatory components in these two pathways supports the notion that they belong to a single coordinated proteolytic network [83]. In order to adapt to the changing cellular environment, in particular during pathologies, a highly regulated network of molecular mechanisms modulates an efficient crosstalk. The following section will review some of the most important mechanisms involved in the regulation of the interconnection between the UPS and the ALS [83–85].

4.1. Central Role of Ubiquitin in UPS/ALS Crosstalk

Ubiquitin chain architecture appears to be determinant to drive protein substrates to one or the other proteolytic pathway. In addition to K48, K11 and K29 ubiquitin linkages appear to contribute to UPS degradation [86]. In contrast, K63 and K6 ubiquitin linkages have been considered as autophagy degradation signals [87]. Other atypical ubiquitin linkages have been proposed as signals for autophagy degradation, although little is known about their specific mechanism. One example is the Met1 linear ubiquitin chain that acts as a signal for autophagy degradation during bacterial xenophagy [83]. Although p62 protein shows a higher binding affinity for K63 ubiquitin linkages, it can recognize K48 chains as well. A competition for K48-linked ubiquitin chains between p62 and p97/VCP (ubiquitin-binding ER-associated degradation protein) determines the degradation pathway to be taken by protein substrates [86]. Most likely, one ubiquitin linkage will not be enough to determine protein degradation since multiple ubiquitin chain topologies are involved in proteolysis regulation. Furthermore, other post-translational modifications including acetylation, phosphorylation or various UbL proteins would directly affect chain composition with an impact on proteolysis. This large panel of chain possibilities and complexity integrated under the name of "ubiquitin code", is implicated in the final proteolytic decision [83,88]. More information on the role of ubiquitin chains in the UPS/ALS was nicely gathered in recent reviews [84,85].

E3 ligases can also act as key elements to regulate the connection between UPS and ALS, as they build multiple ubiquitin chains but can also be targets of the UPS and ALS. One example is the E3 ligase E124 that is responsible for targeting ubiquitin ligases for degradation by the ALS. It has been proved that E124 promotes the degradation of several E3 enzymes (most of them belonging to the RING type), such as TRAF2, RINCK2 and several Tripartite Motif (TRIM) family enzymes: TRIM28, TRIM21 and TRIM1 among others. Interestingly, TRIM family proteins have been recently shown to act as autophagy receptors and regulators of the autophagosome formation [89]. The biological implications of the degradation of RING ubiquitin ligases and its impact on the regulation of the autophagy system

are not well understood [85]. Some of these E3 ligases control factors activating transcription that promotes autophagy initiation such as the previously mentioned NF-κB or FOXOs [90].

The N-end rule pathway is a proteolytic system in which single amino acids in the N-terminal part of proteins act as signals for degradation (N-degrons). In eukaryotes there are two different pathways. The Ac/N-end rule pathway targets proteins containing N(α)-terminally acetylated (Nt-acetylated) residues. The Arg/N-end rule pathway recognizes unacetylated N-terminal residues and involves N-terminal arginylation. N-terminal arginylated degrons are recognized by UBR box family proteins (UBR1, UBR2, UBR4, UBR5), that promote ubiquitylation to mediate the degradation by the proteasome. Recently, SQSTM1/p62 protein was identified to be a N-recognin that binds N-Arg and other N-degrons (Type 1 and 2). P62 hence mediates autophagic degradation of ER-residing molecular chaperones and their associated protein cargoes [77]. The N-end rule pathway regulates autophagy degradation by limiting the participation of p62 to selective autophagy events. In this context, cellular proteotoxic stress developed after the accumulation of misfolded ER proteins promotes the N-terminal argynilation of cytosolic chaperones like BiP. Argynilated chaperons are recognized by the ZZ domain of p62 and oligomerized. Aggregated p62/chaperons interact with LC3 and are targeted to a ubiquitin-independent mediated autophagy since the UBD of p62 is not involved in this process [83].

4.2. Compensatory UPS-ALS Mechanisms

Some of the strongest evidence of the UPS–ALS interconnection was revealed after the chemical or genetic inactivation of the proteasome that results in the activation of autophagy [91]. Different proteasome inhibitors used in clinic, such as bortezomib (BTZ) or NP-0052, have been reported to activate autophagy, relieving cells from cellular proteotoxicity after protein accumulation [92]. How this compensatory mechanism is regulated is not well understood. However different mechanisms have been proposed, including a role for the N-end rule pathway, the UPS-ER-autophagy circuit or the tumour suppressor protein p53 [93–95].

Various transcription factors have been shown to connect the UPS and the ALS, including processes mediated by p53. p53 is one of the best characterized targets of the UPS that plays a dual role in autophagy, depending on its cellular localization. In the nucleus, p53 acts as a transcription factor for autophagy-related genes such as ATG2, ATG4, ATG7, and ULK1, known to activate autophagy [96]. Under starvation and proteasome impairment, cytosolic p53 leads to the activation of the AMPK, that in turn inhibits the mTOR pathway, leading to autophagy activation [83–97]. Wang et al. revealed that the impairment of autophagy after knock down of ATG genes in colon cancer led to upregulation of proteasomal subunits β5 [98]. However, ATG5 and ATG7 knockouts in mice have been shown to accumulate ubiquitylated proteins in different tissues, although this compensatory mechanism could be influenced by the physio-pathology status of the cell [24,85]. Autophagy inhibition causes the accumulation of protein aggregates containing p62. These aggregates are thought to sequester proteasomal substrates but also positive regulators of the UPS, leading to a disruption in proteasomal flux [99].

The UPS has been a target for anti-cancer therapy for a couple of decades. However, resistance to proteasome inhibitors activate compensatory mechanisms, including a permanent activation of the ALS (see Section 5). Understanding how the ALS and the UPS communicate with each other is an actual challenge to find alternative treatments [85].

4.3. Other Mechanisms Impacting the UPS-ALS Crosstalk

After their synthesis, proteins are folded in the endoplasmic reticulum (ER). Misfolded proteins accumulated into the ER are retrotranslocated to the cytoplasm where they become targets for the UPS. This ER-associated degradation (ERAD) can be compensated by autophagy after ER stress. ER-stress upregulates Nrf2 target genes, which in turn induce autophagy [85]. In the UPS-ER-autophagy circuit, accumulated misfolded proteins promote the dissociation of the chaperon protein GRP78/BiP from the

ER membrane. At the same time, different membrane receptors like PERK, IRE1α, ATF6α [94] activate ATG gene expression, as well as LC3 lipidation and autophagosome biogenesis [83].

Chaperone proteins such as C-terminus of HSP-70-interacting protein (CHIP) and BCL-2 associated athanogenes (BAG1 and 3) also determine the fate of protein degradation when misfolding events occur [85]. CHIP acts as a co-chaperone for Hsp70 and Hsp90, for the degradation of misfolded proteins through the addition of K48-linked ubiquitin chains [100]. However, CHIP can also mediate autophagy degradation by promoting K63 linkages. Associated CHIP-associated chaperones and E2 partners direct substrates to either proteasomal or autophagic degradation. Other chaperones involved are BAG1 and 3, that mediate proteasomal degradation. BAG3 interacts with Hsp70, CHIP and p62 for autophagy degradation. During aging, the BAG1/3 ratio is known to modulate autophagy activity [83].

Mitochondria and ER are the two cellular organelle sensors of reduced proteasome activity. The accumulation of proteins as a consequence of proteasome impairment results in an alteration of mitochondrial proteome, ROS generation, and induction of autophagy via AMPK activation [101]. As mitochondria senses the ATP status inside the cells, the cellular energy reserve is an important factor to regulate degradation. Parkin protein, a known E3 ligase, plays a critical role by mediating proteasomal degradation of mitochondrial substrates. At the same time, it has been reported that mitochondria can be a shuttling hub of misfolded proteins to be degraded by mitophagy when the UPS is overloaded [85].

5. Role of Proteaphagy in the UPS-ALS Crosstalk

One of the most intriguing relationship between the UPS and autophagy is proteaphagy, that was demonstrated in distinct biological models (Figure 3). A restriction of nutrients or an accumulation of proteins disrupts proteostasis and activates this process. Importantly, permanently activated proteaphagy has been observed in certain human pathologies. This section sums up some of these recent findings.

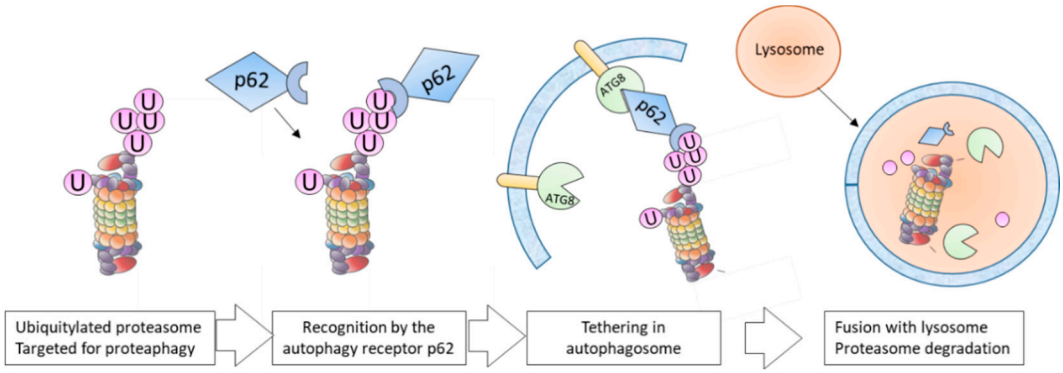

Figure 3. Main steps occurring during proteaphagy. In mammalian cells, ubiquitylated proteasomes are recognized by the autophagy receptor p62 that interacts with lipidated ATG8 proteins tethered into the autophagosome membranes. The late fusion with lysosome ensures the enzymatic degradation of captured proteasomes.

5.1. Proteaphagy upon Nutrient Starvation

Upon nutrient starvation, autophagy is upregulated to face the lack of nitrogen, fixed carbon phosphate, zinc and other nutrients (Figure 3). In these situations, autophagy works as a recycling machine in order to recover the nutrient pool from dysfunctional cellular components [102,103]. During starvation, proteasomes might play a minor role in protein degradation because they are able to degrade one peptide at a time, with high energy cost. Nevertheless, proteasomes are relatively abundant, representing approximately 0.6% of total cell proteins [104]. Autophagy can be quickly induced during starvation and has a bulk protein degradation capacity. For this reason, the autophagic degradation of proteasomes can be seen as an efficient strategy to face nutrient limitation. Immuno-electron microscopy

studies revealed the first hint of autophagic degradation of proteasomes, since proteasomes were observed in rat liver lysosomes upon starvation [105]. Later in time, quantitative proteomic analyses revealed proteasomal proteins among autophagosome-associated-proteins and regulators in basal and starvation-induced autophagy, suggesting that proteasomes are degraded in both conditions [106,107].

Recently, Marshall et al. proved that autophagic degradation of proteasomes occurs in a significant level in both *Arabidopsis taliana* and *Saccharomyces cerevisiae* under nitrogen starvation. In *Arabidopsis Thaliana*, 50% of proteasomes are degraded after 24 h while more than 80% of yeast proteasomes are degraded after 8 h of starvation [108,109]. This bulk autophagy of proteasomes activated under starvation was shown to be independent of autophagy receptors like RPN10 or NBR1, with no coincidence with proteasome ubiquitylation in plant model [108]. In yeast, no receptor that could drive proteasomes to autophagosomes during starvation has been identified [109,110]. This supports the hypothesis that bulk autophagy acts non-selectively without specific autophagy receptors. Nemec et al. revealed that in yeast, nitrogen starvation-induced proteaphagy involved the conserved nexins Snx4/41/42. The complete deletion of Snx4 impaired not only proteaphagy but also autophagy of fatty acid synthetase and ribosomes, indicating that Snx4 is a shared requirement for these selective autophagy events [111].

An important fraction of the proteasomes is located in the nucleus, whereas autophagy occurs in the cytoplasm. Can nuclear proteasomes or distinct proteasome complexes be impacted by proteaphagy? These are open questions for which only little evidence has been published. To be processed through bulk proteaphagy, nuclear proteasomes must be transported out of the nucleus. It is known that autophagy of nuclear components involves specific receptors such as ATG39 and ATG40 [112]. However, it has been excluded that ATG39 is required in nuclear proteasome autophagy upon starvation [108,110]. Some evidence supports a dissociation of CP and 19S prior to nuclear export, in order to allow cytosolic proteaphagy [110]. Waite et al. proposed a model in yeast where proteasomes are disassembled within the nucleus during nitrogen starvation and follow different routes toward autophagic degradation. They revealed that CP autophagy depends on the deubiquitylase Ubp3, while RP export for cytosolic degradation relies on ATG7 and ATG17 factors [110]. By artificially tethering the lid of the 19S proteasome to chromatin, Nemec et al. showed that a dissociation of 19S base and 20S is required prior to proteaphagy in nitrogen-starved yeast [111]. They proposed that proteasome dissociation attenuates CP activity when exported to cytosol, preventing interference with proteostasis in this compartment [111]. However, these mechanisms that ensure dissociation of nuclear proteasomes might not occur for cytosolic proteasomes.

In mammalian cells, proteaphagy is also activated in response to amino acid starvation. Cohen-Kaplan et al. showed a degradation of both CP and 19S RP subunits in starved HeLa cells. Interestingly, they revealed that proteaphagy induced by amino acid starvation is preceded by an increase in polyubiquitylation of proteasomes, mostly in RPN1, RPN2, RPN10 and RPN13 subunits. The autophagy receptor p62 mediates this degradation, making the bridge between lipidated LC3B and ubiquitylated proteasomes [113]. Altogether, these recent studies indicated that proteaphagy can be activated as part of the cellular response to starvation. This participation of distinct autophagy receptors in distinct biological models indicates that while this is a functionally conserved mechanism, the molecules involved can be distinct.

5.2. Proteaphagy of Non-Functional Proteasomes

The elimination of non-functional proteasomes by autophagy has been described in plants, yeast and mammalian cells (Figure 3). Both proteasome inhibitor treatment (bortezomib or MG132) and genetic alteration of proteasome subunits trigger proteaphagy. The extensive ubiquitylation of proteasomes, mainly on the 19S RP, has been highlighted in several studies [108,111]. The identities of modified subunits have not been fully characterized so far, but this ubiquitin signal is thought to mediate the recognition of impaired proteasomes by selective autophagy receptors and their clearance [114]. In *Arabidopsis Thaliana*, Marshall et al. proposed RPN10 to be the selective autophagy

receptor for inactive 26S proteasomes. RPN10 was shown to bind on one hand ATG8 through a ubiquitin-interacting motif (UIM) and on the other hand ubiquitylated proteasomes. Interestingly, proteasome inhibitor-induced proteaphagy was hampered in RPN10 mutant, but starvation-induced proteaphagy was not affected. Furthermore, the deubiquitylase USP2 modulates RPN10 stability during proteasome inhibition, suggesting a central role of proteasome ubiquitylation in this context [108].

In yeast, separate routes are employed for proteaphagy during nitrogen starvation and proteasome inhibition. Proteasome inhibition induces ubiquitylation of proteasome prior to its degradation. Identification of autophagy receptors revealed Cue5 as a mediator of proteaphagy for both chemical inhibition and genetic mutation of 26S proteasomes. Co-immunoprecipitation assays supported that Cue5 tethers ubiquitylated 26S proteasomes to ATG8 [108]. Intriguingly, yeast proteaphagy likewise needs a prior aggregation of 26S proteasome into peri-vacuolar insoluble protein deposit (IPOD)-type structures. The IPOD formation upon proteasome inhibition suggests that there might be some overlap between proteaphagy and aggregaphagy, at least in a yeast model [79]. The chaperone Hsp42 has been shown to deliver dysfunctional proteasomes into IPODs, where extensive ubiquitylation might occur prior to proteaphagy [108]. In a *Dictyostelium discoideum* model, a recent study revealed direct interactions between RPN1 and RPN2 subunits with the core autophagosomal protein ATG16. In this organism, ATG16 appears to be required for RPN1 and RPN2 enrichment in ATG8a positive puncta, suggesting that ATG16 acts as proteaphagy adaptator [115].

It is still unclear whether proteaphagy induced by chemical inhibitors can drive degradation of CP and 19S RP proteasomes separately or target the 26S whole complex. Marshall et al. revealed that mutation in the α5 subunit triggers turnover of the CP only, and mutation in the RPN5 subunit triggers turnover of the 19S RP [108]. Specific ubiquitylation of proteasome subunits ensured by associated E3 ligases could play a crucial role in the regulation of proteaphagy. Furthermore, the involvement of distinct autophagy receptors in different biological models and in a stimuli-dependent manner could provide the quality control required to regulate this selective autophagy route.

6. Proteaphagy in Pathology

Proteaphagy has been shown to be induced by virulent *Pseudomonas syringae* pv tomato strain DC3000 during *Arabidopsis thaliana* infections. The bacterial protein T3E Hrp outer protein M1 (HopM1) works as a putative proteasome inhibitor to increase pathogenicity in plants [116], but also activates proteaphagy during infection [117] to escape host defenses. By enhancing autophagy flux and activating proteaphagy in host cells, *Pseudomonas syringae* suppresses proteasome function to promote virulence. This example is the only one demonstrating that proteaphagy can be manipulated by bacteria to enhance infection. Since it is known that several pathogenic bacteria modulate autophagy to escape their elimination through xenophagy (e.g., *Salmonella*, *Shigella*, *Legionella*, and *Mycobacterium*) [118], it is not excluded that proteaphagy could be part of the mechanisms employed by some other pathogens during human infection.

In yeast, nitrogen starvation or low ATP levels accumulate CP and RP separately in proteasome storage granules (PSG) [114]. Like IPODs, these PSG inclusions were proposed to serve as a proteasome protection mechanism from autophagy. Indeed, blocking delivery of proteasomes into PSGs induces their degradation by proteaphagy. It has thus been proposed that PSGs act as a reservoir of proteasomes for a rapid re-mobilization when proteolytic demand rises [114]. Protein aggregation and clustering, such as proteasome accumulation in PSGs or IPOD, are used by cells to survive under stress conditions. However, inappropriate regulation of cluster formation occurs and can be associated with diseases such as Alzheimer's or Parkinson's. Deregulation of mitophaghy is already associated with these neurodegenerative diseases. Loss of function of the ubiquitin ligase Parkin results in an accumulation of damaged mitochondria and an aggregation of proteins that can lead to neuronal death [118]. Therefore, investigating the link between proteaphagy and clustering regulation could ultimately improve the understanding of protein aggregation in neurodegenerative pathologies [119].

The proteasome inhibitor BTZ has been used to treat hematologic diseases such as multiple myeloma (MM) and mantle cell lymphoma (MCL), even if some patients do not respond or develop resistance to this treatment [120]. In acute myeloid leukaemia (AML), the proteasome inhibitor BTZ activates the autophagy degradation of crucial cellular factors when the FLT3-ITD translocation is present [91]. Proteaphagy has been recently observed in FLT3-ITD positive AML cells after BTZ treatment, and the chemical inhibition of autophagy and proteasome enhances apoptosis in those cells [121]. In MCL, proteaphagy has been easily observed in BTZ-resistant cells [122]. Proteasome subunits from both CP and RP are permanently degraded by autophagy in cells with acquired or innate BTZ resistance, in a p62-dependent manner. Interestingly, the more the cells are resistant to BTZ, the more proteaphagy seems to be activated. Pharmacological inhibition of autophagy by inhibitors such as bafilomycinA or chloroquine enhances BTZ-induced apoptosis in these cells [122]. Targeting autophagy to overcome BTZ resistance has already been proposed in these models, since it affects the stability of important cellular factors such as NOXA or NF-κB [93,94]. Importantly, the p62 inhibitor verteporfin (VTP) hampers proteaphagy in BTZ-resistant MCL cells. Thus, combining BTZ with autophagy inhibitors synergistically induces cytotoxic effects in BTZ-resistant cells and reduces tumor growth in xenografted animal models [122]. Targeting proteaphagy with pharmacological approaches can be considered as a relevant strategy to overcome BTZ-resistance in patients.

7. Conclusions

Maintaining the cellular proteostasis is of the upmost importance for cells health. The UPS and the ALS act in an orchestrated manner to guarantee the correct degradation of a large diversity of substrates such as proteins, aggregates, organelles or macromolecular complexes. Both systems are regulated through different signalling pathways, using different sensor molecules that will activate the most appropriated mechanisms to face aberrant situations. Ubiquitin and ubiquitin-like molecules play an important role in this crosstalk between the two major proteolysis pathways. No less important are the cellular factors and cofactors regulating these events or recognizing the degradation signals, like do the distinct autophagy receptors. Considering all possible combinations of signals and factors involved in the regulation of the UPS–ALS crosstalk, the plasticity of the cell to generate the appropriate response or to get adapted to a specific situation is wide and complex. Proteaphagy appears as an evolutionary conserved functional pathway by which organisms respond to an aberrant protein disequilibrium. Although the molecules implicated in distinct organisms are not necessarily the same, it seems that alternatives to regulate proteaphagy are multiple. The way in which proteaphagy could impact other proteasome complexes and proteasome-regulated events in distinct cellular compartments, such as the nucleus, remains to be investigated. Finally, proteaphagy can help cells to survive stresses like nutrient starvation, since proteasomes work with a high energy cost and represent a potential source of amino acid for recycling. Unravelling the regulation and biological impact of proteaphagy could potentially have clinical implications, as new evidence underlines an important dysregulation of this mechanism in various human pathologies.

Author Contributions: G.Q., M.G.-S., C.L. and M.S.R. wrote this review. G.Q. integrated all sections and prepared illustrations. All authors provided comments and suggestions to improve this manuscript. All authors have read and agreed to the published version of the manuscript.

Funding: G.Q. is a fellow from the French Ministry of Education. M.G.-S. is fellow from the UbiCODE project funded by the EU's Horizon 2020 research and innovation program under the Marie Skłodowska-Curie grant agreement No 765445. M.S.R. is also funded by the Institut National du Cancer, France (PLBIO16-251), CONACyT-SRE (Mexico) grant 0280365 and the REPERE program of Occitanie. C.L. is supported by pre-maturation program of Occitanie.

Acknowledgments: We do thank all members of UbiCARE laboratory, Fabienne Aillet and Clémence Coutelle-Rebut for the critics and proofreading of the manuscript.

Conflicts of Interest: The authors declare no conflicts of interest.

References

1. van der Veen, A.G.; Ploegh, H.L. Ubiquitin-Like Proteins. *Annu. Rev. Biochem.* **2012**, *81*, 323–357. [CrossRef] [PubMed]
2. Zheng, N.; Shabek, N. Ubiquitin Ligases: Structure, Function, and Regulation. *Annu. Rev. Biochem.* **2017**, *86*, 129–157. [CrossRef] [PubMed]
3. Mevissen, T.E.T.; Komander, D. Mechanisms of Deubiquitinase Specificity and Regulation. *Annu. Rev. Biochem.* **2017**, *86*, 159–192. [CrossRef] [PubMed]
4. Seeler, J.-S.; Dejean, A. SUMO and the Robustness of Cancer. *Nat. Rev. Cancer* **2017**, *17*, 184–197. [CrossRef] [PubMed]
5. Mendoza, H.M.; Shen, L.-N.; Botting, C.; Lewis, A.; Chen, J.; Ink, B.; Hay, R.T. NEDP1, a Highly Conserved Cysteine Protease That DeNEDDylates Cullins. *J. Biol. Chem.* **2003**, *278*, 25637–25643. [CrossRef] [PubMed]
6. Kwon, Y.T.; Ciechanover, A. The Ubiquitin Code in the Ubiquitin-Proteasome System and Autophagy. *Trends Biochem. Sci.* **2017**, *42*, 873–886. [CrossRef] [PubMed]
7. Hershko, A.; Ciechanover, A. The Ubiquitin System. *Annu. Rev. Biochem.* **1998**, *67*, 425–479. [CrossRef]
8. Komander, D.; Rape, M. The Ubiquitin Code. *Annu. Rev. Biochem.* **2012**, *81*, 203–229. [CrossRef]
9. Zaffagnini, G.; Martens, S. Mechanisms of Selective Autophagy. *J. Mol. Biol* **2016**, *428*, 1714–1724. [CrossRef]
10. Bard, J.A.M.; Goodall, E.A.; Greene, E.R.; Jonsson, E.; Dong, K.C.; Martin, A. Structure and Function of the 26S Proteasome. *Annu. Rev. Biochem.* **2018**, *87*, 697–724. [CrossRef]
11. Komander, D. The Emerging Complexity of Protein Ubiquitination. *Biochem. Soc. Trans.* **2009**, *37*, 937–953. [CrossRef] [PubMed]
12. Swatek, K.N.; Komander, D. Ubiquitin Modifications. *Cell Res.* **2016**, *26*, 399–422. [CrossRef] [PubMed]
13. Livneh, I.; Cohen-Kaplan, V.; Cohen-Rosenzweig, C.; Avni, N.; Ciechanover, A. The Life Cycle of the 26S Proteasome: From Birth, through Regulation and Function, and onto Its Death. *Cell Res.* **2016**, *26*, 869–885. [CrossRef] [PubMed]
14. Tanaka, K. The Proteasome: Overview of Structure and Functions. *Proc. Jpn. Acad. Ser. B Phys. Biol. Sci.* **2009**, *85*, 12–36. [CrossRef]
15. Finley, D.; Chen, X.; Walters, K.J. Gates, Channels, and Switches: Elements of the Proteasome Machine. *Trends Biochem. Sci.* **2016**, *41*, 77–93. [CrossRef]
16. Ben-Nissan, G.; Sharon, M. Regulating the 20S Proteasome Ubiquitin-Independent Degradation Pathway. *Biomolecules* **2014**, *4*, 862–884. [CrossRef]
17. Ferrington, D.A.; Gregerson, D.S. Immunoproteasomes: Structure, Function, and Antigen Presentation. *Prog. Mol. Biol. Transl. Sci.* **2012**, *109*, 75–112. [CrossRef]
18. Murata, S.; Udono, H.; Tanahashi, N.; Hamada, N.; Watanabe, K.; Adachi, K.; Yamano, T.; Yui, K.; Kobayashi, N.; Kasahara, M.; et al. Immunoproteasome Assembly and Antigen Presentation in Mice Lacking Both PA28α and PA28β. *EMBO J.* **2001**, *20*, 5898–5907. [CrossRef]
19. Xing, Y.; Jameson, S.C.; Hogquist, K.A. Thymoproteasome Subunit-B5T Generates Peptide-MHC Complexes Specialized for Positive Selection. *Proc. Natl. Acad. Sci. USA* **2013**, *110*, 6979–6984. [CrossRef]
20. Dambacher, C.M.; Worden, E.J.; Herzik, M.A.; Martin, A.; Lander, G.C. Atomic Structure of the 26S Proteasome Lid Reveals the Mechanism of Deubiquitinase Inhibition. *eLife* **2016**, *5*, e3027. [CrossRef]
21. Navon, A.; Goldberg, A.L. Proteins Are Unfolded on the Surface of the ATPase Ring before Transport into the Proteasome. *Mol. Cell* **2001**, *8*, 1339–1349. [CrossRef]
22. Smith, D.M.; Chang, S.-C.; Park, S.; Finley, D.; Cheng, Y.; Goldberg, A. Docking of the Proteasomal ATPases' C-Termini in the 20S Proteasomes Alpha Ring Opens the Gate for Substrate Entry. *Mol. Cell* **2007**, *27*, 731–744. [CrossRef] [PubMed]
23. Snoberger, A.; Brettrager, E.J.; Smith, D.M. Conformational Switching in the Coiled-Coil Domains of a Proteasomal ATPase Regulates Substrate Processing. *Nat. Commun.* **2018**, *9*, 1–13. [CrossRef] [PubMed]
24. Rosenzweig, R.; Bronner, V.; Zhang, D.; Fushman, D.; Glickman, M.H. Rpn1 and Rpn2 Coordinate Ubiquitin Processing Factors at Proteasome. *J. Biol. Chem.* **2012**, *287*, 14659–14671. [CrossRef]
25. Yu, Z.; Livnat-Levanon, N.; Kleifeld, O.; Mansour, W.; Nakasone, M.A.; Castaneda, C.A.; Dixon, E.K.; Fushman, D.; Reis, N.; Pick, E.; et al. Base-CP Proteasome Can Serve as a Platform for Stepwise Lid Formation. *Biosci. Rep.* **2015**, *35*, e00203. [CrossRef]

26. Worden, E.J.; Padovani, C.; Martin, A. Structure of the Rpn11-Rpn8 Dimer Reveals Mechanisms of Substrate Deubiquitination during Proteasomal Degradation. *Nat. Struct. Mol. Biol.* **2014**, *21*, 220–227. [CrossRef]
27. Worden, E.J.; Dong, K.C.; Martin, A. An AAA Motor-Driven Mechanical Switch in Rpn11 Controls Deubiquitination at the 26S Proteasome. *Mol. Cell* **2017**, *67*, 799–811.e8. [CrossRef]
28. Lee, M.J.; Lee, B.-H.; Hanna, J.; King, R.W.; Finley, D. Trimming of Ubiquitin Chains by Proteasome-Associated Deubiquitinating Enzymes. *Mol. Cell Proteom.* **2011**, *10*, R110.003871. [CrossRef]
29. Riedinger, C.; Boehringer, J.; Trempe, J.-F.; Lowe, E.D.; Brown, N.R.; Gehring, K.; Noble, M.E.M.; Gordon, C.; Endicott, J.A. Structure of Rpn10 and Its Interactions with Polyubiquitin Chains and the Proteasome Subunit Rpn12. *J. Biol. Chem.* **2010**, *285*, 33992–34003. [CrossRef]
30. Isasa, M.; Katz, E.J.; Kim, W.; Yugo, V.; González, S.; Kirkpatrick, D.S.; Thomson, T.M.; Finley, D.; Gygi, S.P.; Crosas, B. Monoubiquitination of RPN10 Regulates Substrate Recruitment to the Proteasome. *Mol. Cell* **2010**, *38*, 733–745. [CrossRef]
31. Keren-Kaplan, T.; Zeev Peters, L.; Levin-Kravets, O.; Attali, I.; Kleifeld, O.; Shohat, N.; Artzi, S.; Zucker, O.; Pilzer, I.; Reis, N.; et al. Structure of Ubiquitylated-Rpn10 Provides Insight into Its Autoregulation Mechanism. *Nat. Commun.* **2016**, *7*, 12960. [CrossRef] [PubMed]
32. Schreiner, P.; Chen, X.; Husnjak, K.; Randles, L.; Zhang, N.; Elsasser, S.; Finley, D.; Dikic, I.; Walters, K.J.; Groll, M. Ubiquitin Docking at the Proteasome through a Novel Pleckstrin-Homology Domain Interaction. *Nature* **2008**, *453*, 548–552. [CrossRef] [PubMed]
33. Chojnacki, M.; Mansour, W.; Hameed, D.S.; Singh, R.K.; El Oualid, F.; Rosenzweig, R.; Nakasone, M.A.; Yu, Z.; Glaser, F.; Kay, L.E.; et al. Polyubiquitin-Photoactivatable Crosslinking Reagents for Mapping Ubiquitin Interactome Identify Rpn1 as a Proteasome Ubiquitin-Associating Subunit. *Cell Chem. Biol.* **2017**, *24*, 443–457. [CrossRef] [PubMed]
34. Lam, Y.A.; Lawson, T.G.; Velayutham, M.; Zweier, J.L.; Pickart, C.M. A Proteasomal ATPase Subunit Recognizes the Polyubiquitin Degradation Signal. *Nature* **2002**, *416*, 763–767. [CrossRef] [PubMed]
35. Fu, H.; Lin, Y.-L.; Fatimababy, A.S. Proteasomal Recognition of Ubiquitylated Substrates. *Trends Plant. Sci.* **2010**, *15*, 375–386. [CrossRef] [PubMed]
36. Paraskevopoulos, K.; Kriegenburg, F.; Tatham, M.H.; Rösner, H.I.; Medina, B.; Larsen, I.B.; Brandstrup, R.; Hardwick, K.G.; Hay, R.T.; Kragelund, B.B.; et al. Dss1 Is a 26S Proteasome Ubiquitin Receptor. *Mol. Cell* **2014**, *56*, 453–461. [CrossRef]
37. Shi, Y.; Chen, X.; Elsasser, S.; Stocks, B.B.; Tian, G.; Lee, B.-H.; Shi, Y.; Zhang, N.; de Poot, S.A.H.; Tuebing, F.; et al. Rpn1 Provides Adjacent Receptor Sites for Substrate Binding and Deubiquitination by the Proteasome. *Science* **2016**, *351*, aad9421. [CrossRef]
38. Olszewski, M.; Williams, C.; Dong, K.; Martin, A. The Cdc48 Unfoldase Prepares Well-Folded Protein Substrates for Degradation by the 26S Proteasome. *Commun. Biol.* **2019**, *2*, 1–8. [CrossRef]
39. Fort, P.; Kajava, A.V.; Delsuc, F.; Coux, O. Evolution of Proteasome Regulators in Eukaryotes. *Genome Biol Evol.* **2015**, *7*, 1363–1379. [CrossRef]
40. Murata, S.; Kawahara, H.; Tohma, S.; Yamamoto, K.; Kasahara, M.; Nabeshima, Y.; Tanaka, K.; Chiba, T. Growth Retardation in Mice Lacking the Proteasome Activator PA28γ. *J. Biol. Chem.* **1999**, *274*, 38211–38215. [CrossRef]
41. Stohwasser, R. Proteasome Activator 28γ: Impact on Survival Signaling and Apoptosis. In *Current Understanding Apoptosis-Program. Cell Death*; Yusuf, T., Lutfi, T., Eds.; IntechOpen: London, UK, 2018.
42. Ortega, J.; Heymann, J.B.; Kajava, A.V.; Ustrell, V.; Rechsteiner, M.; Steven, A.C. The Axial Channel of the 20S Proteasome Opens upon Binding of the PA200 Activator. *J. Mol. Biol.* **2005**, *346*, 1221–1227. [CrossRef] [PubMed]
43. Tanahashi, N.; Murakami, Y.; Minami, Y.; Shimbara, N.; Hendil, K.B.; Tanaka, K. Hybrid Proteasomes. Induction by Interferon-Gamma and Contribution to ATP-Dependent Proteolysis. *J. Biol. Chem.* **2000**, *275*, 14336–14345. [CrossRef] [PubMed]
44. Cascio, P. PA28αβ: The Enigmatic Magic Ring of the Proteasome? *Biomolecules* **2014**, *4*, 566–584. [CrossRef] [PubMed]
45. Olivier, C.; Barbara, A.Z.; Silke, M. The Proteasome System in Health and Disease. *Adv. Exper. Med. Biol.* **2020**, *1233*, 55–100.

46. Takeshige, K.; Baba, M.; Tsuboi, S.; Noda, T.; Ohsumi, Y. Autophagy in Yeast Demonstrated with Proteinase-Deficient Mutants and Conditions for Its Induction. *J. Cell Biol.* **1992**, *119*, 301–311. [CrossRef] [PubMed]
47. Clarke, A.J.; Simon, A.K. Autophagy in the Renewal, Differentiation and Homeostasis of Immune Cells. *Nat. Rev. Immunol.* **2019**, *19*, 170–183. [CrossRef]
48. Gatica, D.; Lahiri, V.; Klionsky, D.J. Cargo Recognition and Degradation by Selective Autophagy. *Nat. Cell Biol.* **2018**, *20*, 233–242. [CrossRef]
49. Khaminets, A.; Behl, C.; Dikic, I. Ubiquitin-Dependent And Independent Signals In Selective Autophagy. *Trends Cell Biol.* **2016**, *26*, 6–16. [CrossRef]
50. Xie, Y.; Kang, R.; Sun, X.; Zhong, M.; Huang, J.; Klionsky, D.J.; Tang, D. Posttranslational Modification of Autophagy-Related Proteins in Macroautophagy. *Autophagy* **2015**, *11*, 28–45. [CrossRef]
51. Wei, Y.; Liu, M.; Li, X.; Liu, J.; Li, H. Origin of the Autophagosome Membrane in Mammals. *Biomed. Res. Int.* **2018**, *2018*, 1012789. [CrossRef]
52. Tsuboyama, K.; Koyama-Honda, I.; Sakamaki, Y.; Koike, M.; Morishita, H.; Mizushima, N. The ATG Conjugation Systems Are Important for Degradation of the Inner Autophagosomal Membrane. *Science* **2016**, *354*, 1036–1041. [CrossRef] [PubMed]
53. Kabeya, Y.; Mizushima, N.; Ueno, T.; Yamamoto, A.; Kirisako, T.; Noda, T.; Kominami, E.; Ohsumi, Y.; Yoshimori, T. LC3, a Mammalian Homologue of Yeast Apg8p, Is Localized in Autophagosome Membranes after Processing. *Embo J.* **2000**, *19*, 5720–5728. [CrossRef] [PubMed]
54. Xie, Z.; Nair, U.; Klionsky, D.J. Atg8 Controls Phagophore Expansion during Autophagosome Formation. *Mol. Biol. Cell* **2008**, *19*, 3290–3298. [CrossRef] [PubMed]
55. He, C.; Klionsky, D.J. Regulation Mechanisms and Signaling Pathways of Autophagy. *Annu. Rev. Genet.* **2009**, *43*, 67–93. [CrossRef] [PubMed]
56. Tanida, I.; Ueno, T.; Kominami, E. LC3 Conjugation System in Mammalian Autophagy. *Int. J. Biochem. Cell Biol.* **2004**, *36*, 2503–2518. [CrossRef] [PubMed]
57. Shpilka, T.; Weidberg, H.; Pietrokovski, S.; Elazar, Z. Atg8: An Autophagy-Related Ubiquitin-like Protein Family. *Genome Biol.* **2011**, *12*, 226. [CrossRef]
58. Yu, Z.-Q.; Ni, T.; Hong, B.; Wang, H.-Y.; Jiang, F.-J.; Zou, S.; Chen, Y.; Zheng, X.-L.; Klionsky, D.J.; Liang, Y.; et al. Dual Roles of Atg8−PE Deconjugation by Atg4 in Autophagy. *Autophagy* **2012**, *8*, 883–892. [CrossRef]
59. Ichimura, Y.; Kirisako, T.; Takao, T.; Satomi, Y.; Shimonishi, Y.; Ishihara, N.; Mizushima, N.; Tanida, I.; Kominami, E.; Ohsumi, M.; et al. Ubiquitin-like System Mediates Protein Lipidation. *Nature* **2000**, *408*, 488–492. [CrossRef]
60. Rockenfeller, P.; Koska, M.; Pietrocola, F.; Minois, N.; Knittelfelder, O.; Sica, V.; Franz, J.; Carmona-Gutierrez, D.; Kroemer, G.; Madeo, F. Phosphatidylethanolamine Positively Regulates Autophagy and Longevity. *Cell Death Differ.* **2015**, *22*, 499–508. [CrossRef]
61. Yang, A.; Li, Y.; Pantoom, S.; Triola, G.; Wu, Y.-W. Semisynthetic Lipidated LC3 Protein Mediates Membrane Fusion. *Chembiochem* **2013**, *14*, 1296–1300. [CrossRef]
62. Nguyen, T.N.; Padman, B.S.; Usher, J.; Oorschot, V.; Ramm, G.; Lazarou, M. Atg8 Family LC3/GABARAP Proteins Are Crucial for Autophagosome-Lysosome Fusion but Not Autophagosome Formation during PINK1/Parkin Mitophagy and Starvation. *J. Cell Biol.* **2016**, *215*, 857–874. [CrossRef] [PubMed]
63. Grunwald, D.S.; Otto, N.M.; Park, J.-M.; Song, D.; Kim, D.-H. GABARAPs and LC3s Have Opposite Roles in Regulating ULK1 for Autophagy Induction. *Autophagy* **2020**, *16*, 600–614. [CrossRef] [PubMed]
64. von Muhlinen, N.; Akutsu, M.; Ravenhill, B.J.; Foeglein, Á.; Bloor, S.; Rutherford, T.J.; Freund, S.M.V.; Komander, D.; Randow, F. LC3C, Bound Selectively by a Noncanonical LIR Motif in NDP52, Is Required for Antibacterial Autophagy. *Mol. Cell* **2012**, *48*, 329–342. [CrossRef] [PubMed]
65. Kirkin, V.; Rogov, V.V. A Diversity of Selective Autophagy Receptors Determines the Specificity of the Autophagy Pathway. *Mol. Cell* **2019**, *76*, 268–285. [CrossRef] [PubMed]
66. Deosaran, E.; Larsen, K.B.; Hua, R.; Sargent, G.; Wang, Y.; Kim, S.; Lamark, T.; Jauregui, M.; Law, K.; Lippincott-Schwartz, J.; et al. NBR1 Acts as an Autophagy Receptor for Peroxisomes. *J. Cell Sci.* **2013**, *126*, 939–952. [CrossRef] [PubMed]
67. Kim, B.-W.; Kwon, D.H.; Song, H.K. Structure Biology of Selective Autophagy Receptors. *Bmb Rep.* **2016**, *49*, 73–80. [CrossRef]

68. Ciuffa, R.; Lamark, T.; Tarafder, A.K.; Guesdon, A.; Rybina, S.; Hagen, W.J.H.; Johansen, T.; Sachse, C. The Selective Autophagy Receptor P62 Forms a Flexible Filamentous Helical Scaffold. *Cell Rep.* **2015**, *11*, 748–758. [CrossRef]
69. Padman, B.S.; Nguyen, T.N.; Uoselis, L.; Skulsuppaisarn, M.; Nguyen, L.K.; Lazarou, M. LC3/GABARAPs Drive Ubiquitin-Independent Recruitment of Optineurin and NDP52 to Amplify Mitophagy. *Nat. Commun.* **2019**, *10*, 1–13. [CrossRef]
70. Wild, P.; Farhan, H.; McEwan, D.G.; Wagner, S.; Rogov, V.V.; Brady, N.R.; Richter, B.; Korac, J.; Waidmann, O.; Choudhary, C.; et al. Phosphorylation of the Autophagy Receptor Optineurin Restricts Salmonella Growth. *Science* **2011**, *333*, 228–233. [CrossRef]
71. Zhang, J.; Ney, P.A. Role of bnip3 and nix in cell death, autophagy, and mitophagy. *Cell Death Differ* **2009**, *16*, 939–946. [CrossRef]
72. Clausen, T.H.; Lamark, T.; Isakson, P.; Finley, K.; Larsen, K.B.; Brech, A.; Øvervatn, A.; Stenmark, H.; Bjørkøy, G.; Simonsen, A.; et al. P62/SQSTM1 and ALFY Interact to Facilitate the Formation of P62 Bodies/ALIS and Their Degradation by Autophagy. *Autophagy* **2010**, *6*, 330–344. [CrossRef] [PubMed]
73. Isakson, P.; Holland, P.; Simonsen, A. The Role of ALFY in Selective Autophagy. *Cell Death Differ.* **2013**, *20*, 12–20. [CrossRef]
74. Grumati, P.; Morozzi, G.; Hölper, S.; Mari, M.; Harwardt, M.-L.I.; Yan, R.; Müller, S.; Reggiori, F.; Heilemann, M.; Dikic, I. Full Length RTN3 Regulates Turnover of Tubular Endoplasmic Reticulum via Selective Autophagy. *eLife* **2017**, *6*, e25555. [CrossRef] [PubMed]
75. Khaminets, A.; Heinrich, T.; Mari, M.; Grumati, P.; Huebner, A.K.; Akutsu, M.; Liebmann, L.; Stolz, A.; Nietzsche, S.; Koch, N.; et al. Regulation of Endoplasmic Reticulum Turnover by Selective Autophagy. *Nature* **2015**, *522*, 354–358. [CrossRef] [PubMed]
76. Wurzer, B.; Zaffagnini, G.; Fracchiolla, D.; Turco, E.; Abert, C.; Romanov, J.; Martens, S. Oligomerization of P62 Allows for Selection of Ubiquitinated Cargo and Isolation Membrane during Selective Autophagy. *Elife* **2015**, *4*, e0894. [CrossRef]
77. Cha-Molstad, H.; Lee, S.H.; Kim, J.G.; Sung, K.W.; Hwang, J.; Shim, S.M.; Ganipisetti, S.; McGuire, T.; Mook-Jung, I.; Ciechanover, A.; et al. Regulation of Autophagic Proteolysis by the N-Recognin SQSTM1/P62 of the N-End Rule Pathway. *Autophagy* **2018**, *14*, 359–361. [CrossRef]
78. Lazarou, M.; Sliter, D.A.; Kane, L.A.; Sarraf, S.A.; Wang, C.; Burman, J.L.; Sideris, D.P.; Fogel, A.I.; Youle, R.J. The Ubiquitin Kinase PINK1 Recruits Autophagy Receptors to Induce Mitophagy. *Nature* **2015**, *524*, 309–314. [CrossRef]
79. Sharma, V.; Verma, S.; Seranova, E.; Sarkar, S.; Kumar, D. Selective Autophagy and Xenophagy in Infection and Disease. *Front. Cell Dev. Biol.* **2018**, *6*, 147. [CrossRef]
80. Birgisdottir, Å.B.; Lamark, T.; Johansen, T. The LIR Motif - Crucial for Selective Autophagy. *J. Cell Sci.* **2013**, *126*, 3237–3247. [CrossRef]
81. Rogov, V.V.; Stolz, A.; Ravichandran, A.C.; Rios-Szwed, D.O.; Suzuki, H.; Kniss, A.; Löhr, F.; Wakatsuki, S.; Dötsch, V.; Dikic, I.; et al. Structural and Functional Analysis of the GABARAP Interaction Motif (GIM). *EMBO Rep.* **2017**, *18*, 1382–1396. [CrossRef]
82. Noda, N.N.; Kumeta, H.; Nakatogawa, H.; Satoo, K.; Adachi, W.; Ishii, J.; Fujioka, Y.; Ohsumi, Y.; Inagaki, F. Structural Basis of Target Recognition by Atg8/LC3 during Selective Autophagy. *Genes Cells* **2008**, *13*, 1211–1218. [CrossRef] [PubMed]
83. Ji, C.H.; Kwon, Y.T. Crosstalk and Interplay between the Ubiquitin-Proteasome System and Autophagy. *Mol. Cells* **2017**, *40*, 441–449. [CrossRef] [PubMed]
84. Liebl, M.P.; Hoppe, T. It's All about Talking: Two-Way Communication between Proteasomal and Lysosomal Degradation Pathways via Ubiquitin. *Am. J. Physiol. Cell Physiol.* **2016**, *311*, C166–C178. [CrossRef] [PubMed]
85. Nam, T.; Han, J.H.; Devkota, S.; Lee, H.-W. Emerging Paradigm of Crosstalk between Autophagy and the Ubiquitin-Proteasome System. *Mol. Cells* **2017**, *40*, 897–905. [CrossRef] [PubMed]
86. Locke, M.; Toth, J.I.; Petroski, M.D. K11- and K48-Linked Ubiquitin Chains Interact with P97 during Endoplasmic Reticulum-Associated Degradation. *BiochemJ* **2014**, *459*, 205–216. [CrossRef] [PubMed]
87. Tan, J.M.M.; Wong, E.S.P.; Kirkpatrick, D.S.; Pletnikova, O.; Ko, H.S.; Tay, S.-P.; Ho, M.W.L.; Troncoso, J.; Gygi, S.P.; Lee, M.K.; et al. Lysine 63-Linked Ubiquitination Promotes the Formation and Autophagic Clearance of Protein Inclusions Associated with Neurodegenerative Diseases. *Hum. Mol. Genet.* **2008**, *17*, 431–439. [CrossRef] [PubMed]

88. Mattern, M.; Sutherland, J.; Kadimisetty, K.; Barrio, R.; Rodriguez, M.S. Using Ubiquitin Binders to Decipher the Ubiquitin Code. *Trends Biochem. Sci.* **2019**, *44*, 599–615. [CrossRef] [PubMed]
89. Hatakeyama, S. TRIM Family Proteins: Roles in Autophagy, Immunity, and Carcinogenesis. *Trends Biochem. Sci.* **2017**, *42*, 297–311. [CrossRef]
90. Boccitto, M.; Kalb, R.G. Regulation of Foxo-Dependent Transcription by Post-Translational Modifications. *Curr. Drug Targets* **2011**, *12*, 1303–1310. [CrossRef]
91. Larrue, C.; Saland, E.; Boutzen, H.; Vergez, F.; David, M.; Joffre, C.; Hospital, M.-A.; Tamburini, J.; Delabesse, E.; Manenti, S.; et al. Proteasome Inhibitors Induce FLT3-ITD Degradation through Autophagy in AML Cells. *Blood* **2016**, *127*, 882–892. [CrossRef]
92. Zhu, K.; Dunner, K.; McConkey, D.J. Proteasome Inhibitors Activate Autophagy as a Cytoprotective Response in Human Prostate Cancer Cells. *Oncogene* **2010**, *29*, 451–462. [CrossRef] [PubMed]
93. Cha-Molstad, H.; Sung, K.S.; Hwang, J.; Kim, K.A.; Yu, J.E.; Yoo, Y.D.; Jang, J.M.; Han, D.H.; Molstad, M.; Kim, J.G.; et al. Amino-Terminal Arginylation Targets Endoplasmic Reticulum Chaperone BiP for Autophagy through P62 Binding. *Nat. Cell Biol.* **2015**, *17*, 917–929. [CrossRef] [PubMed]
94. Hetz, C.; Chevet, E.; Oakes, S.A. Proteostasis Control by the Unfolded Protein Response. *Nat. Cell Biol.* **2015**, *17*, 829–838. [CrossRef] [PubMed]
95. White, E. Autophagy and P53. *Cold Spring Harb. Perspect. Med.* **2016**, *6*, a026120. [CrossRef] [PubMed]
96. Feng, Y.; Yao, Z.; Klionsky, D.J. How to Control Self-Digestion: Transcriptional, Post-Transcriptional, and Post-Translational Regulation of Autophagy. *Trends Cell Biol* **2015**, *25*, 354–363. [CrossRef] [PubMed]
97. Kocaturk, N.M.; Gozuacik, D. Crosstalk Between Mammalian Autophagy and the Ubiquitin-Proteasome System. *Front. Cell Dev. Biol* **2018**, *6*, 128. [CrossRef]
98. Wang, X.J.; Yu, J.; Wong, S.H.; Cheng, A.S.L.; Chan, F.K.L.; Ng, S.S.M.; Cho, C.H.; Sung, J.J.Y.; Wu, W.K.K. A Novel Crosstalk between Two Major Protein Degradation Systems: Regulation of Proteasomal Activity by Autophagy. *Autophagy* **2013**, *9*, 1500–1508. [CrossRef]
99. Korolchuk, V.I.; Mansilla, A.; Menzies, F.M.; Rubinsztein, D.C. Autophagy Inhibition Compromises Degradation of Ubiquitin-Proteasome Pathway Substrates. *Mol. Cell* **2009**, *33*, 517–527. [CrossRef]
100. McDonough, H.; Patterson, C. CHIP: A Link between the Chaperone and Proteasome Systems. *Cell Stress Chaperones* **2003**, *8*, 303–308. [CrossRef]
101. Zhao, B.; Qiang, L.; Joseph, J.; Kalyanaraman, B.; Viollet, B.; He, Y.-Y. Mitochondrial Dysfunction Activates the AMPK Signaling and Autophagy to Promote Cell Survival. *Genes Dis* **2016**, *3*, 82–87. [CrossRef]
102. Kawamata, T.; Horie, T.; Matsunami, M.; Sasaki, M.; Ohsumi, Y. Zinc Starvation Induces Autophagy in Yeast. *J. Biol. Chem.* **2017**, *292*, 8520–8530. [CrossRef] [PubMed]
103. Thompson, A.R.; Doelling, J.H.; Suttangkakul, A.; Vierstra, R.D. Autophagic Nutrient Recycling in Arabidopsis Directed by the ATG8 and ATG12 Conjugation Pathways. *Plant. Physiol.* **2005**, *138*, 2097–2110. [CrossRef] [PubMed]
104. Wójcik, C.; DeMartino, G.N. Intracellular Localization of Proteasomes. *Int. J. Biochem. Cell Biol.* **2003**, *35*, 579–589. [CrossRef]
105. Cuervo, A.M.; Palmer, A.; Rivett, A.J.; Knecht, E. Degradation of Proteasomes by Lysosomes in Rat Liver. *Eur. J. Biochem.* **1995**, *227*, 792–800. [CrossRef] [PubMed]
106. Dengjel, J.; Høyer-Hansen, M.; Nielsen, M.O.; Eisenberg, T.; Harder, L.M.; Schandorff, S.; Farkas, T.; Kirkegaard, T.; Becker, A.C.; Schroeder, S.; et al. Identification of Autophagosome-Associated Proteins and Regulators by Quantitative Proteomic Analysis and Genetic Screens. *Mol. Cell Proteom.* **2012**, *11*, M111.014035. [CrossRef] [PubMed]
107. Zhang, T.; Shen, S.; Qu, J.; Ghaemmaghami, S. Global Analysis of Cellular Protein Flux Quantifies the Selectivity of Basal Autophagy. *Cell Rep.* **2016**, *14*, 2426–2439. [CrossRef] [PubMed]
108. Marshall, R.S.; Li, F.; Gemperline, D.C.; Book, A.J.; Vierstra, R.D. Autophagic Degradation of the 26S Proteasome Is Mediated by the Dual ATG8/Ubiquitin Receptor RPN10 in Arabidopsis. *Mol. Cell* **2015**, *58*, 1053–1066. [CrossRef]
109. Marshall, R.S.; McLoughlin, F.; Vierstra, R.D. Autophagic Turnover of Inactive 26S Proteasomes in Yeast Is Directed by the Ubiquitin Receptor Cue5 and the Hsp42 Chaperone. *Cell Rep.* **2016**, *16*, 1717–1732. [CrossRef]
110. Waite, K.A.; De-La Mota-Peynado, A.; Vontz, G.; Roelofs, J. Starvation Induces Proteasome Autophagy with Different Pathways for Core and Regulatory Particles. *J. Biol. Chem.* **2016**, *291*, 3239–3253. [CrossRef]

111. Nemec, A.A.; Howell, L.A.; Peterson, A.K.; Murray, M.A.; Tomko, R.J. Autophagic Clearance of Proteasomes in Yeast Requires the Conserved Sorting Nexin Snx4. *J. Biol. Chem.* **2017**, *292*, 21466–21480. [CrossRef]
112. Mochida, K.; Oikawa, Y.; Kimura, Y.; Kirisako, H.; Hirano, H.; Ohsumi, Y.; Nakatogawa, H. Receptor-Mediated Selective Autophagy Degrades the Endoplasmic Reticulum and the Nucleus. *Nature* **2015**, *522*, 359–362. [CrossRef] [PubMed]
113. Cohen-Kaplan, V.; Livneh, I.; Avni, N.; Fabre, B.; Ziv, T.; Kwon, Y.T.; Ciechanover, A. P62- and Ubiquitin-Dependent Stress-Induced Autophagy of the Mammalian 26S Proteasome. *Proc. Natl. Acad. Sci. USA* **2016**, *113*, E7490–E7499. [CrossRef] [PubMed]
114. Marshall, R.S.; Vierstra, R.D. Proteasome Storage Granules Protect Proteasomes from Autophagic Degradation upon Carbon Starvation. *eLife* **2018**, *7*, e34532. [CrossRef] [PubMed]
115. Xiong, Q.; Fischer, S.; Karow, M.; Müller, R.; Meßling, S.; Eichinger, L. ATG16 Mediates the Autophagic Degradation of the 19S Proteasomal Subunits PSMD1 and PSMD2. *Eur. J. Cell Biol.* **2018**, *97*, 523–532. [CrossRef] [PubMed]
116. Üstün, S.; Sheikh, A.; Gimenez-Ibanez, S.; Jones, A.; Ntoukakis, V.; Börnke, F. The Proteasome Acts as a Hub for Plant Immunity and Is Targeted by Pseudomonas Type III Effectors. *Plant. Physiol.* **2016**, *172*, 1941–1958. [CrossRef] [PubMed]
117. Üstün, S.; Hafrén, A.; Liu, Q.; Marshall, R.S.; Minina, E.A.; Bozhkov, P.V.; Vierstra, R.D.; Hofius, D. Bacteria Exploit Autophagy for Proteasome Degradation and Enhanced Virulence in Plants. *Plant. Cell* **2018**, *30*, 668–685. [CrossRef] [PubMed]
118. Pickrell, A.M.; Youle, R.J. The Roles of PINK1, Parkin, and Mitochondrial Fidelity in Parkinson's Disease. *Neuron* **2015**, *85*, 257–273. [CrossRef]
119. Irvine, G.B.; El-Agnaf, O.M.; Shankar, G.M.; Walsh, D.M. Protein Aggregation in the Brain: The Molecular Basis for Alzheimer's and Parkinson's Diseases. *Mol. Med.* **2008**, *14*, 451–464. [CrossRef] [PubMed]
120. Gonzalez-Santamarta; Quinet, G.; Reyes-Garau, D.; Sola, B.; Roué, G.; Manuel, S.R. Resistance to the Proteasome Inhibitors: Lessons from Multiple Myeloma and Mantle Cell Lymphoma. In *Proteostasis and Disease From Basic Mechanisms to Clinics*; Springer International Publishing: Cham, Switzerland, 2020.
121. Lopez, R. New insights into Proteasome Inhibition-Induced Proteaphagy in Acute Myeloid Leukaemia. 2020; unpublished work.
122. Quinet, G. Targeting p62/Sequestosome-1Impairs Constitutively Active Proteaphagy and Enhances Apoptosis of BTZ-Resistant MCL. 2020; unpublished work.

FEBS openbio

FEBS PRESS science publishing by scientists

Inhibition of the proteasome and proteaphagy enhances apoptosis in FLT3-ITD-driven acute myeloid leukemia

Rosa G. Lopez-Reyes[1,2], Grégoire Quinet[1], Maria Gonzalez-Santamarta[1], Clément Larrue[2], Jean-Emmanuel Sarry[2] and Manuel S. Rodriguez[1]

1 Institute of Advanced Technology and Life Sciences (ITAV), IPBS-Centre de la Recherche Scientifique (CNRS), Université Toulouse III Paul Sabatier, Toulouse, France

2 Cancer Research Center of Toulouse Unité Mixte de Recherche (UMR) 1037 INSERM, ERL 5294 Centre de la Recherche Scientifique (CNRS), Toulouse, France

Keywords
AML; bortezomib; FLT3-ITD; leukaemia; proteaphagy; ubiquitin

Correspondence
M. S. Rodriguez, UbiCARE, Institute of Advanced Technology and Life Sciences, 1 Place Pierre Potier, 31000 Toulouse, France
E-mail: manuel.rodriguez@itav.fr

(Received 27 May 2020, revised 15 July 2020, accepted 12 August 2020)

doi:10.1002/2211-5463.12950

Acute myeloid leukaemia (AML) is a clonal disorder that affects hematopoietic stem cells or myeloid progenitors. One of the most common mutations that results in AML occurs in the gene encoding fms-like tyrosine kinase 3 (*FLT3*). Previous studies have demonstrated that AML cells expressing FLT3-internal tandem duplication (ITD) are more sensitive to the proteasome inhibitor bortezomib (Bz) than FLT3 wild-type cells, with this cytotoxicity being mediated by autophagy (Atg). Here, we show that proteasome inhibition with Bz results in modest but consistent proteaphagy in MOLM-14 leukemic cells expressing the FLT3-ITD mutation, but not in OCI-AML3 leukemic cells with wild-type FLT3. Chemical inhibition of Atg with bafilomycin A simultaneously blocked proteaphagy and resulted in the accumulation of the p62 Atg receptor in Bz-treated MOLM-14 cells. The use of ubiquitin traps revealed that ubiquitin plays an important role in proteasome-Atg cross-talk. The p62 inhibitor verteporfin blocked proteaphagy and, importantly, resulted in accumulation of high molecular weight forms of p62 and FLT3-ITD in Bz-treated MOLM-14 cells. Both Atg inhibitors enhanced Bz-induced apoptosis in FLT3-ITD-driven leukemic cells, highlighting the therapeutic potential of these treatments.

Acute myeloid leukaemia (AML) is a clonal disorder that affects hematopoietic stem cells or myeloid progenitors. It is characterized by an accumulation of immature leukemic cells in the bone marrow and peripheral blood and leads to bone marrow failure [1]. AML is a heterogeneous disease with a variety of distinct genetic alterations [2]. One of the most common mutations occurs in the gene encoding fms-like tyrosine kinase 3 (*FLT3*) [3]. This type III receptor tyrosine kinase regulates the normal growth and differentiation of hematopoietic cells via the activation of multiple signalling including Akt, mitogen-activated protein kinase and signal transducer and activator of transcription 5 (STAT5) [4,5]. FLT3 cooperates with other recurrent molecular abnormalities to induce acute leukaemia in preclinical models. Internal tandem duplication (ITD) mutations in the FLT3 gene are found in approximately 30% of AML patients and are associated with a poor clinical outcome. Previous studies have demonstrated that AML cells expressing FLT3-ITD are more sensitive to the proteasome inhibitor (PI) bortezomib (Bz) than FLT3 wild-type cells.

Abbreviations
ALS, autophagy-lysosome system; AML, acute myeloid leukaemia; Atg, autophagy; BafA, bafilomycin A; Bz, bortezomib; FLT3, fms-like tyrosine kinase 3; FT, flow-through; GST, glutathione S-transferase; IP, immunoprecipitation; ITD, internal tandem duplication; LC3B, microtubule-associated proteins 1A/1B light chain 3B; PI, proteasome inhibitor; TUBEs, tandem ubiquitin binding entities; UPS, ubiquitin-proteasome system; VT, verteporfin.

This cytotoxicity is mediated by autophagy (Atg) [6]. Furthermore, the genetic inhibition of early Atg steps or of autophagosome formation blocks FLT3-ITD, STAT5 and Akt degradation induced by Bz [6].

The proteasome has been envisioned as a promising target for the development of anticancer therapeutic drugs [7]. The 26S proteasome is a large multi-subunit protease (1500–2000 kDa) formed by the 20S proteolytic core and one or two 19S regulatory particles [8]. Three proteolytically active subunits integrate the 20S core: β1 with a caspase-like activity, β2 with a trypsin-like activity and β5 with a chymotrypsin-like activity. β5 is the primary target for most PIs that reached a clinical phase [8,9]. Cancer therapy also targets the autophagy-lysosome system (ALS), another proteolytic process that is responsible for the bulk degradation of cytoplasmic components. Amino acid deficiency activates Atg by regulating the signalling cascades controlling this proteolytic pathway [10]. During selective Atg, phagophores engulf cytoplasmic material, and then fuse to form double-membrane autophagosomes. Cargo recruitment occurs through a family of Atg receptors, including p62, OPTN or NBR1, which are often used as markers for Atg activation together with the ubiquitin-like molecule Atg8 [11]. The Atg machinery was first identified in yeast and equivalent molecules reported in mammalian cells [11–13]. Distinct Atg events drive the degradation of organelles or aggregated proteins such as mitophagy (mitochondria), aggrephagy (protein aggregates) or proteasome (proteaphagy), to name a few [14].

Many of the current Atg inhibitors act at a late stage of the system, such as the V-ATPase inhibitor bafilomycin A (BafA). BafA inhibits Atg in a non-selective way, by neutralizing the acidic pH of the lysosomal hydrolases that drive autophagic degradation [15]. Verteporfin (VT) is a drug approved by the US Food and Drug Administration that was identified in a screen for chemicals that prevent autophagosome formation [16]. Unlike BafA, VT inhibits Atg at an early stage and does not allow autophagosome accumulation[16]. A better understanding of the proteolytic regulation mechanism and interplay will allow the exploration of alternative/combined treatments to tackle cancer development and/or drug resistance.

Here, we aimed to better understand the proteolytic cross-talk connecting proteasome with Atg after Bz treatment in FLT3-ITD-positive MOLM-14 AML cells. Using a chemical approach to block Atg at distinct levels together with ubiquitin traps [known as tandem ubiquitin binding entities (TUBEs)] [17], immunoprecipitation (IP) and immunofluorescence, we found that proteaphagy was activated after Bz treatment. Although proteaphagy is a process preserved in distinct species [18–20], we found that the presence of FLT3-ITD predisposes MOLM-14 cells to activate it.

Materials and methods

Cell lines

Human myeloid leukaemia cell lines MOLM-14 and OCI-AML-3 were purchased from the ATCC collection (ATCC, Manassas, VA, USA). AML cell lines were maintained in RPMI supplemented with 10% foetal calf serum in the presence of 100 $U{\cdot}mL^{-1}$ penicillin and 100 $\mu g{\cdot}mL^{-1}$ streptomycin. Cells were incubated at 37 °C with 5% CO_2 [6]. To facilitate Atg analysis, 2% calf serum was used during the chemical inhibitor treatment for a maximum of 8 h.

Antibodies and reagents

The anti-microtubule-associated protein antibodies 1A/1B light chain 3B (LC3B), anti-Erk 1/2, anti-STAT5, anti-Akt, anti-ubiquitin (P4D1) and anti-PSMB5 were purchased from Cell Signaling Technology (Beverly, MA, USA). Anti-FLT3, anti-p62/SQSTM1 and anti-Beta 2 were obtained from Santa Cruz Biotechnology (Dallas, TX, USA) and anti-PSMA6 was obtained from Invitrogen (Carlsbad, CA, USA). Anti-PSMB6 and anti-Rpn10 were purchased from Enzo (Enzo Diagnostics, Farmingdale, NY, USA), anti-PSMD3 was obtained from Thermo Fisher (Waltham, MA, USA) and anti-GAPDH was obtained from Sigma-Aldrich (St Louis, MO, USA).

Bz and chloroquine were purchased from Sigma-Aldrich, BafA was obtained from InvivoGen (InvivoGen, San Diego, CA, USA) and VT was obtained from Sigma-Aldrich.

Western blot analysis

Proteins were resolved using 8–12% PAGE and electrotransferred to poly(vinylidene difluoride) membranes. Membranes were then blocked with 5% skimmed powdered milk in NaCl/Tris or 5% BSA in NaCl/Tris. Membranes were immunostained with appropriate antibodies and horseradish peroxidase-conjugated secondary antibodies and visualized using an enhanced chemiluminescence system.

Apoptosis assay

Cell lines were cultured in RPMI 5% and then treated at different times with Bz, BafA and VT. Then, 5×10^5 cells were washed with NaCl/P_i and resuspended in 100 µL of annexin-V binding buffer. Two microliters of annexin-V-fluorescein isothiocyanate was added at room temperature. All samples were analysed by a fluorescence-activated cell

sorter (FACS Calibur flow cytometer; Becton-Dickinson Biosciences, Franklin Lakes, NJ, USA) [6].

TUBE capture

TUBEs were produced as described by Hjerpe *et al.* [17,21]. Twenty million cells were used for each condition [TUBE p62, TUBE HHR23 or glutathione *S*-transferase (GST) control]. Cells were resuspended in 500 µL of TUBE lysis buffer, maintained for 10 min at 4 °C and spin down at 15 500 ***g***. A fraction of this supernatant was diluted in 3 × boiling buffer (BB) (50 mM Tris-HCl, pH 6.8, 10% glycerol, 2% SDS, bromophenol blue, 10% β-mercaptoethanol) and considered as the input. Supernatant was transferred to the glutathione-agarose beads with TUBEs or GST control, and samples were incubated overnight in rotation at 4 °C. The next day, samples were spin down at 500 ***g*** at 4 °C, a fraction recollected, diluted in BB and considered as the flow-through (FT). Beads were washed three times with 1 mL of NaCl/P_i Tween 0.05%. Beads were resuspended in 100 µL of BB and boiled for 5 min before protein electrophoresis.

Antibody cross-linking

Thirty microliters per point of magnetic beads protein A (Millipore, Billerica, MA, USA) were washed with NaCl/P_i and equilibrated in binding buffer (50 mM Tris pH 8.5, 150 mM NaCl, +0.5% NP40) using a magnetic holder. Antibodies were added to beads and rotated overnight. The next day, 10–20 µL of supernatant was kept to control antibody binding. Beads were washed twice with NaCl/P_i and once with 500 µL of coupling buffer (200 mM borate, 3 M NaCl pH 9). Fifty millimolars of dimethyl pimelimidate was added to the coupling buffer, and samples were rotated for 30 min with this cross-linking solution. Supernatant was discarded, replaced with fresh cross-linking solution and incubated at 4 °C for 30 min. Beads were washed twice with coupling buffer before blocking with 20 mM ethanolamine, pH 8.2. Supernatant was discarded and replaced by fresh ethanolamine and incubated for 1 h. Beads were washed twice with NaCl/P_i. Non-coupled antibodies were removed with two washes of 1 M NaCl/binding buffer. A NaCl/P_i equilibration was performed before washing three times with 200 mM glycine, pH 2.5. Beads were blocked with 0.1% BSA in binding buffer for 90 min. Magnetic beads were equilibrated in binding buffer and maintained in NaCl/P_i until use. A fraction of these beads (10–20 µL) were analyzed by electrophoresis followed by Coomassie blue staining to compare antibodies before and after cross-linking.

IP in the presence of TUBEs

Twenty millions of cells were spin down at 300 ***g*** for 10 min and the dry pellet was resuspended in 500 µL of TUBE lysis buffer including 100 µg of TUBE p62 or TUBE HHR23[17]. Cell lysates were homogenized with 40 strokes at 4 °C using a Dounce homogenizer. The whole sample was centrifuged at 200 ***g*** for 5 min and the supernatant was recovered for IP. A fraction (1/20) of the supernatant was considered as input. The cross-linked antibody was incubated with cell lysates in rotation for 1 h 30 min at 4 °C. Samples were disposed in magnetic holder to separate bound from unbound material. Proteins unbound to cross-linked antibodies were considered as the FT fraction. Magnetic beads were washed with NaCl/P_i/Tween 0.05% three to five times and then resuspended in 30 µL of BB 3× to be analyzed by western blotting.

Statistical analysis

Data from four independent experiments are reported as the mean ± SEM. Statistical analyses were performed using unpaired two-tailed Student's *t*-tests with PRISM, version 4 (GraphPad Software Inc., San Diego, CA, USA). $P < 0.05$ was considered statistically significant.

Results

Proteaphagy activation after proteasome inhibition in FLT3-ITD mutant-driven MOLM-14 leukemic cells

To mechanistically understand the regulation of the cross-talk between the ubiquitin-proteasome system (UPS) and ALS in leukaemia, we investigated the role of proteaphagy, which is known to be activated after proteasome inhibition [22]. The impact of Bz was assessed in MOLM-14 cells with the FLT3-ITD mutation and compared with the FLT3 wild-type cell line OCI-AML3 (Fig. 1). Bz treatment does not always promote an obvious degradation of proteasome subunits because proteolysis can be compensated by the *novo* synthesis of these subunits as reported previously [23,24]. For this reason, proteaphagy was evaluated by the degradation of 20S and 19S proteasomal subunits after Bz treatment and their accumulation with Atg inhibitors. BafA treatment resulted in the accumulation of Atg markers p62 and LC3B in the presence or absence of Bz, indicating that Atg was activated under these experimental conditions in both cell lines (Fig. 1A). Nevertheless, lipidated forms of LC3B were only observed after BafA treatment in MOLM-14 but not in OCI-AML3. The low levels of apoptosis observed after 8 h of individual or combined Bz/BafA treatment excluded the possibility that differences could be due to massive death of MOLM-14 cells (Fig. S1). Our results showed modest but consistent

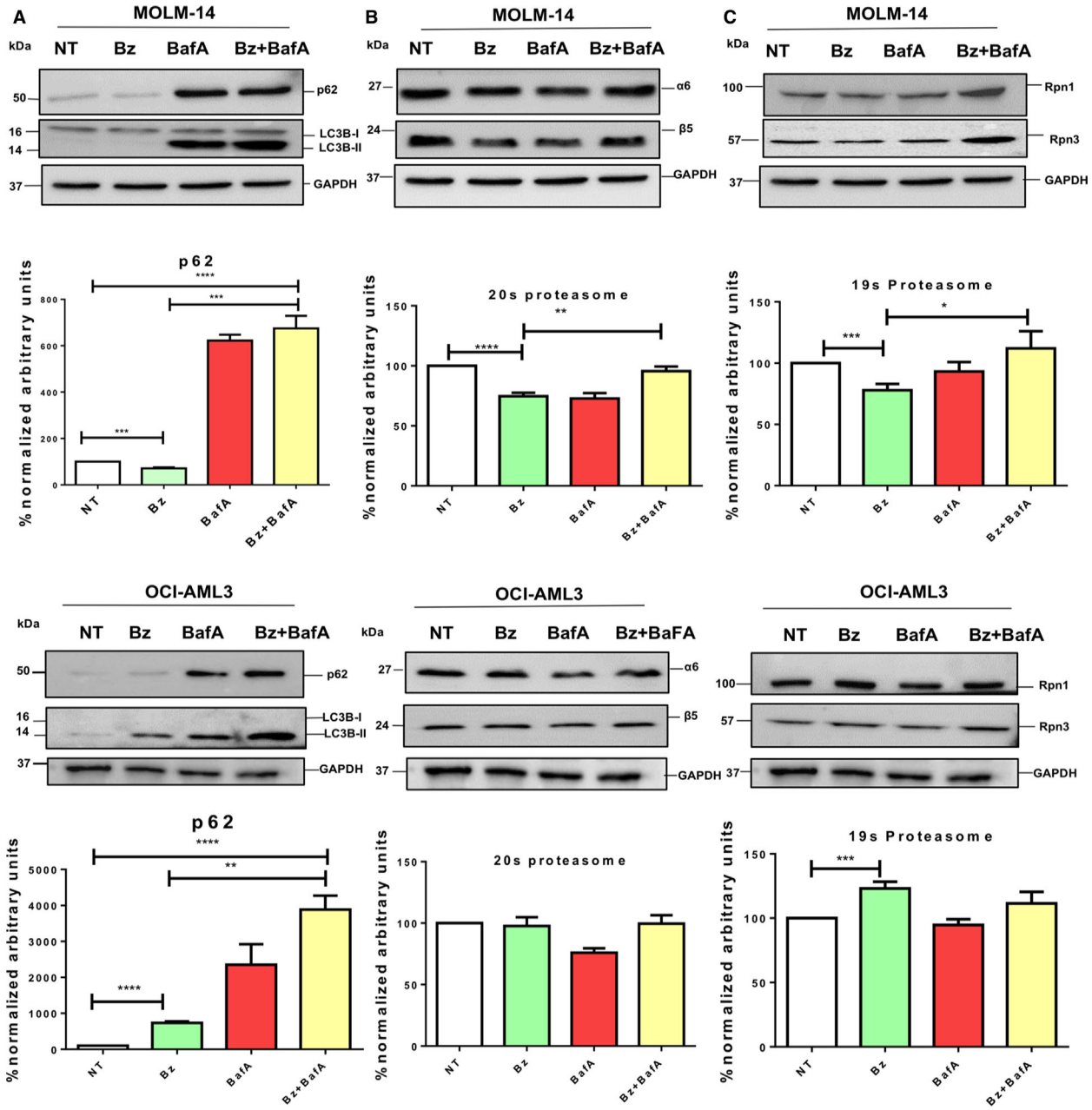

Fig. 1. Bz-driven proteaphagy is enhanced in the FLT3-ITD phenotype. MOLM-14 (FLT3-ITD+/–) or OCI-AML3 (FLT3-WT) cells were treated for 8 h with 10 nM Bz and 20 nM bafilomycin. Total cell lysates were resolved by SDS/PAGE and immunoblotted with the indicated antibodies recognizing the Atg receptor p62 (A), proteasome core subunits α6 and β5 (B) or 19S subunits Rpn1 and Rpn3 (C). Protein expression levels were quantified by densitometry analysis (IMAGEJ; NIH, Bethesda, MD, USA). Statistical analyses were performed using unpaired two-tailed Student's *t*-tests with PRISM, version 4. $*P < 0.05$, $**P < 0.01$, $***P < 0.001$ and $****P < 0.0001$. Data are reported as the mean ± SEM ($n = 4$).

Bz-mediated degradation of 20S proteasome subunits α6s and β5 and 19S subunits Rpn1 and Rpn3, which was blocked by BafA in MOLM-14 (Fig. 1B,C). However, the combination of BafA with Bz did not significantly accumulate proteasome subunits in OCI-AML3 as was the case in MOLM-14 cells (Fig. 1B,C, lower), suggesting that a predisposition for degradation of 26S proteasome could be linked to the presence of FLT3-ITD. These results were also confirmed by immunofluorescence, where proteasomes subunit β2 or α2 colocalized with autophagosomes (Atg8 equivalent LC3B or p62 staining, respectively) after Bz/BafA treatment

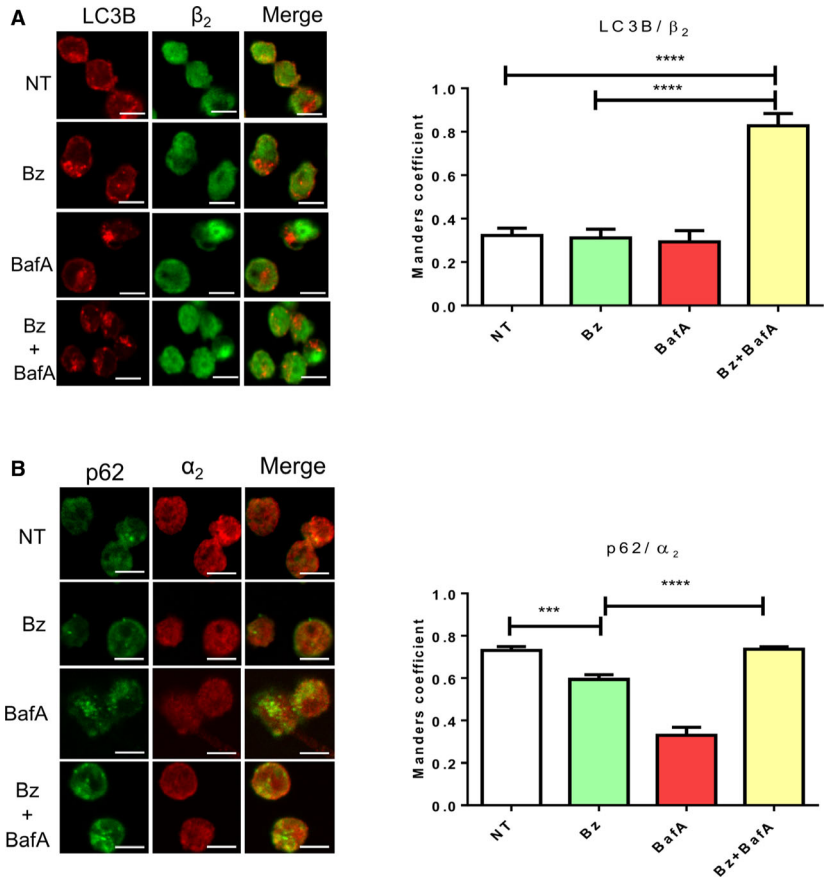

Fig. 2. Colocalization of proteasome and Atg markers after Bz and Atg inhibitor treatment in FLT3-ITD AML cells. Indirect immunofluorescence staining LC3B/β_2 (A)- or p62/α_2 (B)-positive structures in MOLM-14 cells treated for 8 h with 10 nM Bz and 20 nM BafA. Images were captured by confocal microscopy. Scale bar = 10 μm. Immunofluorescence images were quantified from three replicates. Statistical analyses were performed using unpaired two-tailed Student's *t*-tests with PRISM, version 6. ***$P < 0.001$ and ****$P < 0.0001$. Data are reported as the mean ± SEM.

of MOLM-14 cells (Fig. 2). This Bz-induced degradation of proteasome subunits is blocked by BafA, indicating that proteaphagy mediated these proteolytic events.

Role of p62 and ubiquitin in Bz-induced autophagy

To analyse the role of p62 in the Bz-induced autophagic degradation of the proteasomes and FLT3-ITD, the interaction of p62 with proteasome subunits and FLT3-ITD was investigated. IP experiments using a specific p62 antibody were performed using MOLM-14 cells treated (or not) with Bz/BafA. Taking advantage of the protective effects of TUBEs that block the action of proteases, accumulate ubiquitylated proteins and interact with multiple chain types [17,25], IPs were performed in the presence or absence of TUBEs based in the UBA domain of HHR23 (TUBE-HHR23) or the UBA domain of p62 (TUBE-p62) (Fig. 3A). In the absence of TUBEs, p62 was immunoprecipitated without treatment and Bz/BafA reduced the level of precipitated p62. However, in the presence of both TUBEs, p62 was protected from proteasome- and/or Atg-mediated degradation under Bz/BafA conditions (Fig. 3A). Compared to the situation without any TUBEs or TUBE-HHR23, the presence of TUBE-p62 allowed a better coimmunoprecipitation of p62-bound proteasome subunits β2 and but not RPN1. High molecular weight forms most likely representing ubiquitylated forms of RPN1 were better immunoprecipitated in the presence of TUBE-HHR23 (Fig. 3A). Consistent with these observations, FLT3-ITD was also protected by TUBE-p62, although putative ubiquitylated forms of this protein were better immunoprecipitated in the presence of TUBE-HHR23.

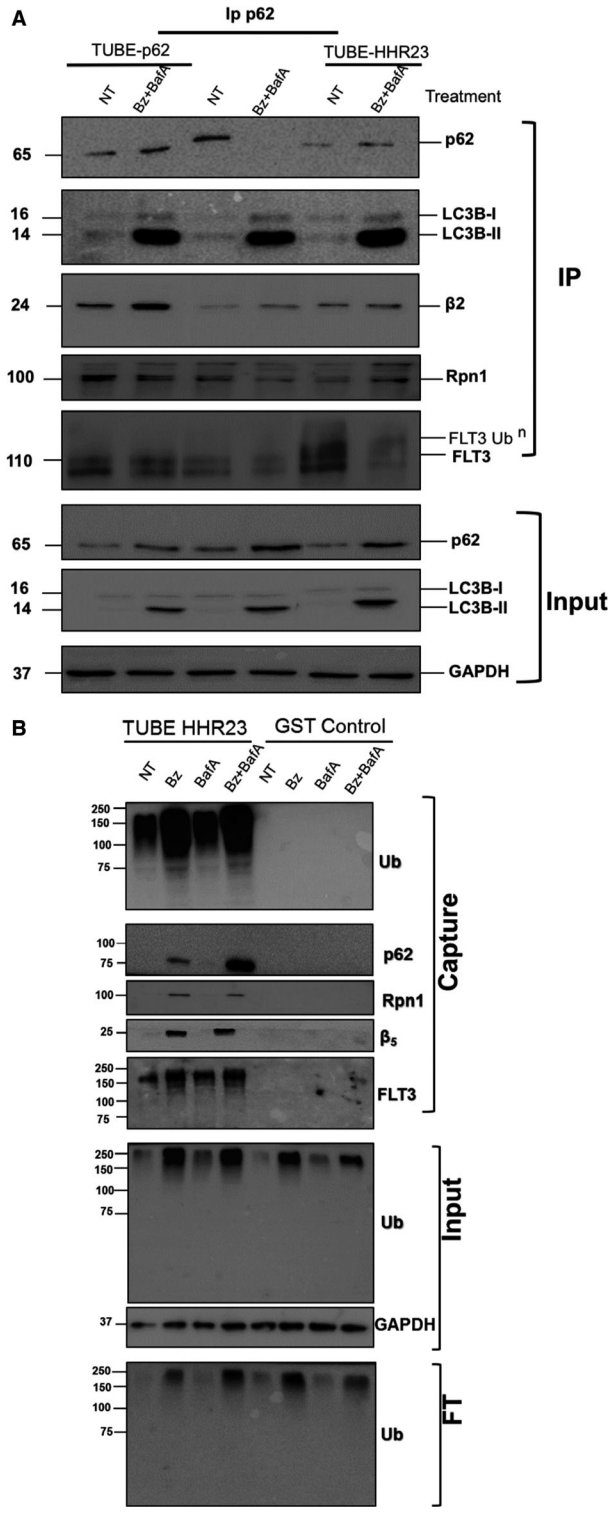

Fig. 3. Ubiquitin role in proteaphagy and degradation of FLT3-ITD under proteasome inhibition conditions. MOLM-14 cells were treated (or not) for 8 h with 10 nM Bz, 20 nM BafA, or both drugs, and cells were lysed as reported [17]. Ubiquitylated proteins were captured using TUBEs-HHR23, TUBEs-p62 or GST control (A). Captured proteins were resolved by SDS/PAGE and immunoblotted with the indicated antibodies. Input and FT fractions were also analysed with anti-ubiquitin antibody. GAPDH was used as the loading control. (B) MOLM-14 cells were treated (or not) with Bz/BafA under the same conditions as in (A). p62-bound proteins were captured by IP with a specific p62 antibody in the presence or absence of TUBE-HHR23 or TUBE-p62. Precipitated material was analysed by western blot with the indicated antibodies. The input fraction was analysed for the indicated proteins.

Because ubiquitin is a major coordinator of UPS and ALS, we investigated its role in the cross-talk of these pathways induced after Bz and BafA treatments. In particular, we were interested in investigating whether the high molecular weight forms of FLT3 co-immunoprecipitated with p62 corresponded to ubiquitylated FLT3. TUBE-HHR23 was used to capture total ubiquitylated proteins from MOLM-14 cells treated (or not) with individual and combined Bz/BafA treatment (Fig. 3B). Total ubiquitylated proteins were efficiently trapped by TUBE-HHR23. BafA treatment alone did not significantly enrich ubiquitylated proteins captured by TUBE-HHR23 compared to Bz or Bz/BafA. Proteasome subunits β5 and Rpn1 were captured by TUBE-HHR23 (Fig. 3B). The p62 receptor was also captured under the same conditions, although the combination of Bz/BafA enriched this protein compared to Bz alone (Fig. 3B). Interestingly, ubiquitylated forms of FLT3-ITD were captured by TUBE-HHR23 under all conditions but were best enriched when Bz/BafA treatment was used (Fig. 3B).

p62 drives proteaphagy and autophagic degradation of FLT3-ITD

To further assess the role of the Atg receptor p62 in proteaphagy, VT was used to treat MOLM-14 cells and western blot analyses were performed to detect distinct proteasome subunits. High molecular weight forms of p62 were detected after VT treatment (Fig. 4A). Interestingly, the lipidated form of LC3B decreased after VT treatment, indicating that this drug reduced the Atg flux. Bz-mediated degradation of 20S or 19S subunits was blocked by VT even if the Bz-mediated degradation of 19S subunits was more prominent than 20S subunits (Fig. 4B,C). The colocalization of p62/α_2 was significantly reduced with VT or Bz/VT, indicating that blocking of p62 could inhibit proteaphagy via a mechanism distinct from BafA (Fig. 4D). To investigate whether the high molecular weight forms of p62 observed in Fig 4A were aggregated and/or ubiquitylated, IP was performed with p62 antibodies in the presence or absence of TUBE-

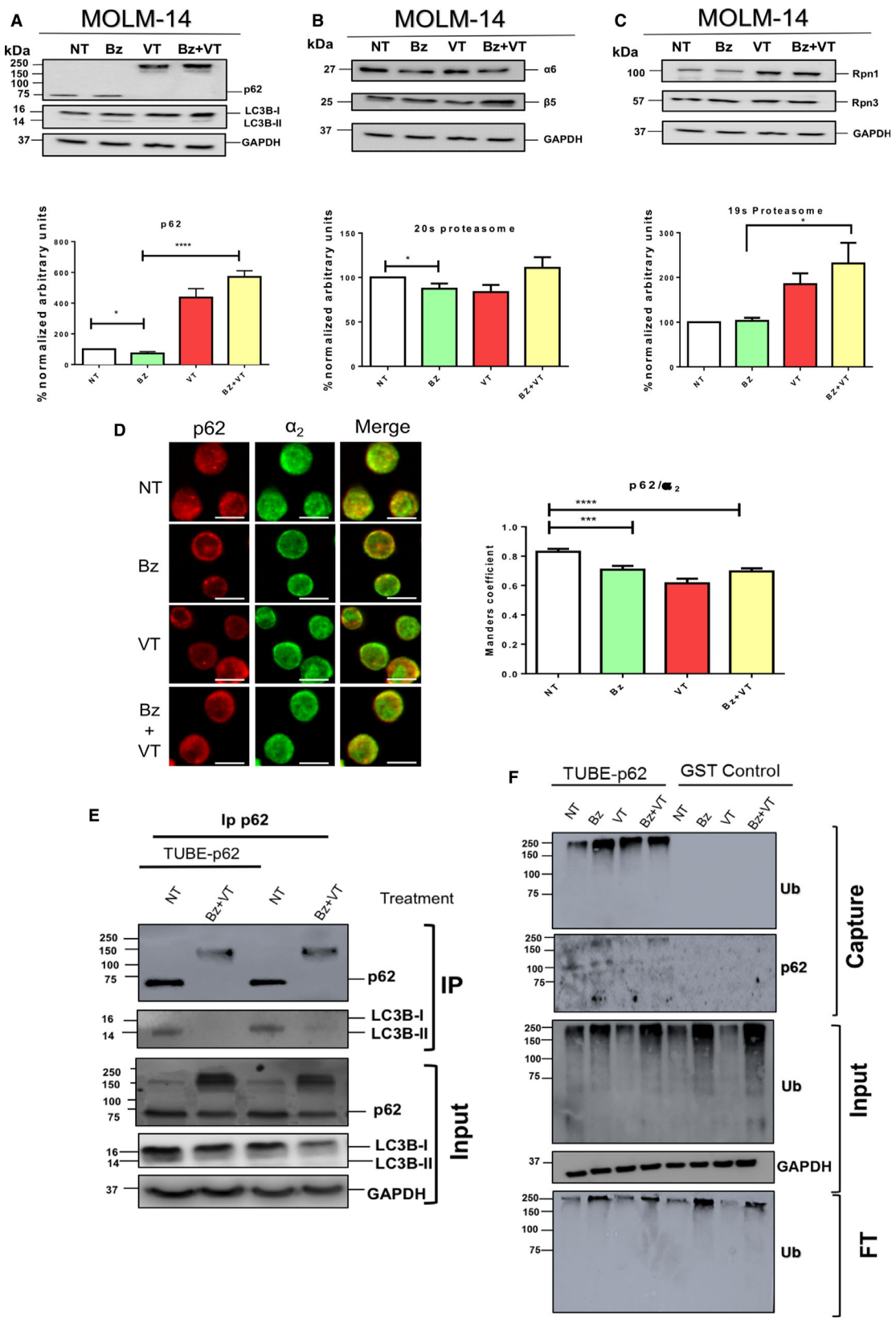

FEBS Open Bio **11** (2021) 48–60 © 2020 The Authors. *FEBS Open Bio* published by John Wiley & Sons Ltd on behalf of Federation of European Biochemical Societies.

Fig. 4. p62 drives proteaphagy in FLT3-ITD AML cells. MOLM-14 cells were treated for 8 h with 10 nM Bz and 1 μM VT. Total cell lysates were resolved by SDS/PAGE and immunoblotted with antibodies against Atg markers LCB3 and p62 (A), proteasome core subunits α6 and β5 (B), and 19 subunits Rpn1 and Rpn3 (C). Protein expression levels were quantified by densitometry analysis (IMAGEJ). (D) Indirect immunofluorescence staining of p62/α_2-positive structures in MOLM-14 cells treated for 8 h with 10 nM Bz and 1 μM VT. Images were captured by confocal microscopy. Scale bar = 10 μm. Immunofluorescence images were quantified from three replicates. Statistical analyses were performed using unpaired two-tailed Student's *t*-tests with PRISM, version 6. $*P < 0.05$, $**P < 0.01$, $***P < 0.001$ and $****P < 0.0001$. Data are reported as the mean ± SEM ($n = 5$). (E) IP of p62 from MOLM-14 cells treated (or not) with 10 nM Bz and 1 μM VT. Experiments were performed in the presence or absence of TUBE-p62. Precipitated material was analysed by western blotting with specific p62 and LC3B antibodies. The input fraction was analysed with the indicated antibodies. (F) Capture of ubiquitylated proteins using TUBE-p62 trap. GST was used as the negative control. Captured proteins were analysed by western blotting with anti-ubiquitin or p62 antibodies. The input and FT fractions were analysed with the indicated antibodies.

p62 (Fig 4E) and TUBE capture of ubiquitylated proteins (Fig. 4F). Interestingly, the aggregated forms of p62 generated after Bz/VT treatment did not interact with the lipidated form of LC3B, indicating that this treatment negatively affected the interaction (Fig. 4E). The lipidated forms of LCB3 were also reduced in the input fraction, indicating that VT stops the Atg flux as observed in Fig. 4A. To explore the ubiquitylation status of p62 after VT treatment, we captured ubiquitylated proteins using TUBE-p62 (Fig. 4F). VT had a negative impact on the total ubiquitylated proteins as can be observed in the input fraction. Nevertheless, the levels of ubiquitylation could be recovered when VT was combined with Bz. These results were also observed with respect to the TUBE capture of total ubiquitylated proteins. Under these experimental conditions, p62 increased its ubiquitylated levels after Bz treatment and decreased when cells were treated with VT (Fig. 4F). Taken together, the evidence indicates that, after VT treatment, aggregated forms of p62 are accumulated and these forms are less ubiquitylated. The reduction of the interaction p62/lipidated LC3B indicates that this p62 was not integrated into autophagosomes after Bz/VT treatment. In a similar manner, VT reduced the localization of p62 with proteasome subunits, supporting the idea that proteaphagy is hampered by this treatment (Fig. 4D). Thus, these data show that p62 plays an important role in the proteaphagy observed in MOLM-14 cells.

Inhibition of UPS and ALS pathways enhances apoptosis of FLT3-ITD cells

Individual or combined treatments were used to investigate whether Bz-induced degradation of FLT3-ITD was blocked by VT in MOLM-14 cells (Fig. 5A). The results obtained indicated that FLT3-ITD and FLT3 were degraded by up to 25% after Bz treatment in MOLM-14 cells (Fig. 5A). FLT3-ITD degradation was blocked by VT, whereas high molecular weight forms of FLT3 were formed under the same conditions in MOLM-14 suggesting a ubiquitin-driven Atg-mediated proteolysis event (Fig. 5A). Interestingly, in OCI-AML3 cells, under the same experimental conditions, FLT3 was not degraded by Bz and VT treatment and, instead, there was an accumulation of high mobility forms of this protein (Fig. 5B). The double Bz/VT treatment did not result in a significant accumulation of FLT3 in OCI-AML3 (Fig. 5B), supporting the idea that proteolytic pathways are not efficiently activated in these cells.

Finally, we investigated the consequences of accumulated proteasome and FLT3-ITD after inhibition of the UPS and ALS pathways in MOLM-14 cells compared to OCI-AML3 cells. Apoptosis was measured by analysing annexin-V-positive cells after single agent or combined treatments (Fig. 5). Bz-induced cell death was always maintained below 50% to differentiate positive or negative effects of BafA on the Bz treatments. To improve the efficiency of Atg inhibition, cells were pre-treated with BafA for 8 h before adding Bz for an additional 16 h at the indicated doses (Fig. 5C,D). The results obtained showed that the toxicity of the individual BafA treatment was approximately 20% (MOLM-14) or below 5% (OCI-AML3) and both drugs efficiently cooperated to enhance the cell killing effect on MOLM-14 (Fig. 5C), although this was not in the case in OCI-AML3 (Fig. 5D). Apoptosis induced by VT also improved the results observed with Bz alone in MOLM-14 cells (Fig. 5E) but not in OCI-AML3 cells (Fig. 5F). In this case, Bz and VT were simultaneously added to cell cultures to work below the VT IC_{50}. This results in an additional 8 h of Bz compared to Fig. 5A, explaining the higher apoptosis observed for the Bz treatment only. Cooperative effects observed with the double Bz/VT treatment were statistically significant in MOLM-14 cells but not in OCI-AML3 (Fig. 5E,F). Taken together, our results show that the inhibition of both proteolytic pathways markedly enhances apoptosis levels in MOLM-14 that express FLT3-ITD (Fig. 6) but not in OCI-AML3 that express WT FLT3.

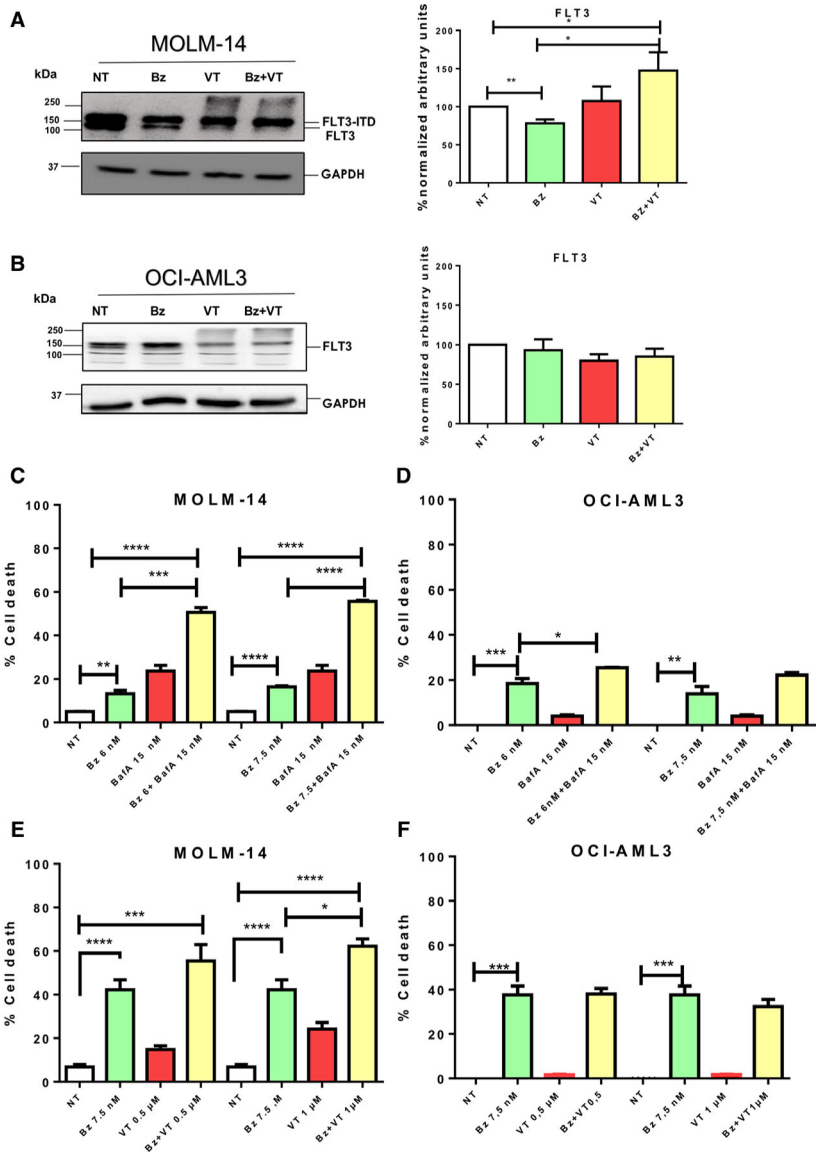

Fig. 5. Proteasome and Atg inhibitors cooperate to improve apoptosis of FLT3-ITD expressing cells. MOLM-14 (A) and OCI-AML3 (B) cells were treated for 8 h with 10 nM Bz and 1 μM VT. Total cell lysates were resolved by SDS/PAGE and immunoblotted with antibodies against FLT3 (A, B). Protein expression levels were quantified by densitometry analysis (IMAGEJ). Statistical analyses were performed using unpaired two-tailed Student's *t*-tests tests with PRISM, version 6. $*P < 0.05$, $**P < 0.01$, $***P < 0.001$ and $****P < 0.0001$. Data are reported as the mean ± SEM. (C, D) MOLM-14 and OCI-AML3 cells were treated for 8 h with 15 nM BafA. Bz was added at a concentration of 6 or 7.5 nM for an additional 16 h. (E, F) MOLM-14 and OCI-AML3 cells were treated with a fixed concentration of 7.5 nM Bz and two distinct doses of VT (0.5 and 1 μM) as indicated. Apoptosis was analysed by FACS. The percentage of cell death was measured from four biological replicates. Statistical analyses were performed using unpaired two-tailed Student's *t*-tests PRISM, version 4. $*P < 0.05$, $**P < 0.01$, $***P < 0.001$ and $****P < 0.0001$. Data are reported as the mean ± SEM ($n = 3$).

Discussion

Multiple mechanisms of interplay between the UPS and ALS have been documented over the last 10 years. In the present study, we have identified proteaphagy as part of the selective autophagic events, which are activated after Bz treatment in FLT3-ITD-positive leukemic cells. Our data showed that this tyrosine kinase translocation facilitates the Bz-mediated proteolysis of 20S and 19S subunits and their colocalization within autophagosomes. FLT3-ITD can potentially predispose to proteaphagy as a result of

FEBS Open Bio **11** (2021) 48–60 © 2020 The Authors. *FEBS Open Bio* published by John Wiley & Sons Ltd on behalf of Federation of European Biochemical Societies.

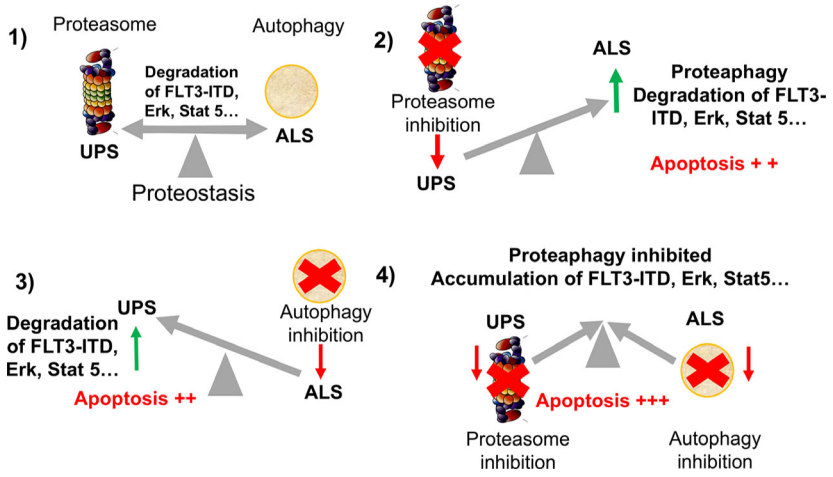

Fig. 6. UPS and ALS cross-talk under proteasome and/or Atg inhibition. (1) Under basal unstimulated conditions, turnover of important cellular factor is ensured by equilibrated proteolytic pathways. (2) Inhibition of proteasome directs crucial cellular factors to ALS for degradation. (3) Atg inhibition drives the degradation of some cellular factors to proteasome-mediated degradation. (4) When both proteolytic pathways are impaired, both UPS and ALS contribute to accumulate cellular factors and increase apoptosis in FLT3-ITD-positive cells.

its capacity to activate multiple signalling cascades that have an impact on Atg activation. Among these are the phosphatidylinositol-3 kinase [26,27]; Akt [28]; mammalian target of rapamycin [29]; Ras; and extracellular signal-related kinase, mitogen-activated protein kinase and STAT5 [5,30] pathways. It remains to be determined whether any (or several) of these signalling pathways has a positive or negative impact on proteaphagy.

Proteaphagy is a complicated process to analyse because not all proteasomes are directly concerned by this type of degradation. Nuclear proteasomes will not be immediately affected because proteaphagy is a cytoplasmic event. According to the literature, only 20–50% of the proteasomes are regulated by proteaphagy depending on the time, intensity and type of stimuli in distinct biologic models [18–20]. Our results demonstrate that the Atg receptor p62 is implicated in the proteaphagy activated by Bz in MOLM-14 cells. However, our data do not exclude the participation of other Atg receptors in this process [14]. For example, both the ubiquitin receptor Cue5 and the chaperon Hsp40 [19] or the proteasome subunit RPN10 [18], respectively, mediate proteaphagy in *Saccharomyces cerevisiae* or *Arabidopsis thaliana*. Nevertheless, the use of VT in leukemic cells showed that the inactivation of p62 stops Bz-induced proteaphagy, supporting a major role for p62 in this process. Interestingly, VT favors the formation of high molecular weight aggregates of p62 [31], which are also observed with FLT3-ITD with the same treatment. However, other effects have been reported for VT, including the activation of ROS, which could affect other processes [32,33] making it difficult to attribute the effects of VT only to its action on p62.

The IP/protection assays [17] revealed that TUBE-p62 protects p62, RPN1, β2 or FLT3-ITD from Bz-driven degradation blocked with BafA in MOLM14 cells. TUBE-HHR23 also protects these factors, although to a lesser extent than TUBE-p62. However, TUBE-HHR23 better accumulates ubiquitylated forms of RPN1 or FLT3-ITD. Similar IP experiments performed with Bz/VT in MOLM-14 showed that high molecular weight forms of p62 did not interact with the lipidated form of LC3B, indicating that p62 was not integrated into autophagosomes under those conditions. This could be associated with the reduction of total ubiquitylated forms observed after VT treatment that might have a negative impact on ubiquitin-regulated events.

The ubiquitin proteome captured with TUBE-HHR23 includes several proteins implicated in proteaphagy such as p62, RPN1 or β5 after Bz or Bz/BafA treatments but not with BafA alone, indicating that this Atg inhibitor does not accumulate ubiquitylated forms of these factors in the absence of proteasome inhibition. TUBE-p62 captures significantly less ubiquitylated proteins than TUBE-HHR23 and specific ubiquitylated forms can only be seen with overexposure. Nonetheless, in this way, we found that, although Bz accumulated ubiquitylated forms of p62,

VT reduces these forms, most likely by interfering with the integration of this receptor into autophagosomes. The use of both TUBEs to investigate UPS and ALS regulated events highlights the need to consider all possibilities with respect to determining which pathway plays a role under distinct experimental settings. Although TUBE-HHR23 recognises almost all types of chains [17,25,34], the UBA domain of p62 recognises mainly K63 ubiquitin chains, explaining the observed differences [35,36].

Taken together, our data indicate that, when both proteolytic pathways are blocked, the accumulation of cellular factors occurs as a result of the functional absence of these degradation machineries (Fig. 6). This contributes to enhanced apoptosis in MOLM-14 but not in OCI-AML3 cells under the same experimental conditions. In conclusion, targeting protein homeostasis could be an alternative for improving current treatments of FLT3-ITD AML cells. Although the crosstalk of these complex proteolytic mechanisms remains to be fully clarified, our results open new possibilities for the treatment of this AML phenotype.

Acknowledgements

We thank Clémence Coutelle-Rebut for proofreading the manuscript submitted for publication. MSR and MGS are funded by UbiCODE a network supported by the European Union's Horizon 2020 Research and Innovation Programme under the Marie Skłodowska-Curie grant agreement No. 765445. MSR also receives funding from the Institut National du Cancer, France (PLBIO16-251), LASSERLAB-EUROPE under the grant No 654148, CONACyT-SRE (Mexico) under the grant No 0280365, and the Occitanie Region, France, through the REPERE and Prematuration programs. GQ and RGLR are, respectively, fellows from The French Ministry of Higher Education and Research and CONACYT (Mexico).

Conflict of interest

The authors declare no conflict of interest.

Data accessibility

The data are available from the corresponding author upon reasonable request.

Author contributions

RGLP, MSR and JES conceived and designed the project. RGLP, GQ and MGS acquired the data. RGLP, GQ, MGS and CL analysed and interpreted the data. MSR and RGLP wrote the pape. All authors approved the final

version of the manuscript submitted for publication.

References

1 Horton SJ and Huntly BJP (2012) Recent advances in acute myeloid leukemia stem cell biology. *Haematologica* **97**, 966–974.

2 Staudt D, Murray HC, McLachlan T, Alvaro F, Enjeti AK, Verrills NM and Dun MD (2018) Targeting oncogenic signaling in mutant FLT3 acute myeloid leukemia: the path to least resistance. *Int J Mol Sci* **19**, 3198.

3 Pratz KW and Luger SM (2014) Will FLT3 inhibitors fulfill their promise in AML? *Curr Opin Hematol* **21**, 72–78.

4 Takahashi S (2011) Downstream molecular pathways of FLT3 in the pathogenesis of acute myeloid leukemia: biology and therapeutic implications. *J Hematol Oncol* **4**, 13.

5 Choudhary C, Müller-Tidow C, Berdel WE and Serve H (2005) Signal transduction of oncogenic Flt3. *Int J Hematol* **82**, 93–99.

6 Larrue C, Saland E, Boutzen H, Vergez F, David M, Joffre C, Hospital M-A, Tamburini J, Delabesse E, Manenti S *et al.* (2016) Proteasome inhibitors induce FLT3-ITD degradation through autophagy in AML cells. *Blood* **127**, 882–892.

7 Liu Y, Huang W-J, Lin M-T, Li J-J and Zhang J-Y (2019) Chapter 13 - Proteasome Inhibitors as Sensitizing Agents for Cancer Chemotherapy. In *Cancer Sensitizing Agents for Chemotherapy, Protein Kinase Inhibitors as Sensitizing Agents for Chemotherapy* (Chen Z-S and Yang D-H, eds), vol. **4**, pp. 207–228. Academic Press. doi: 10.1016/B978-0-12-816435-8.00013-4

8 Finley D, Chen X and Walters KJ (2016) Gates, channels, and switches: elements of the proteasome machine. *Trends Biochem Sci* **41**, 77–93.

9 Orlowski M and Wilk S (2000) Catalytic activities of the 20 S proteasome, a multicatalytic proteinase complex. *Arch Biochem Biophys* **383**, 1–16.

10 Mejlvang J, Olsvik H, Svenning S, Bruun J-A, Abudu YP, Larsen KB, Brech A, Hansen TE, Brenne H, Hansen T *et al.* (2018) Starvation induces rapid degradation of selective autophagy receptors by endosomal microautophagy. *J Cell Biol* **217**, 3640–3655.

11 Rogov V, Dötsch V, Johansen T and Kirkin V (2014) Interactions between autophagy receptors and ubiquitin-like proteins form the molecular basis for selective autophagy. *Mol Cell* **53**, 167–178.

12 Kraft C, Peter M and Hofmann K (2010) Selective autophagy: ubiquitin-mediated recognition and beyond. *Nat Cell Biol* **12**, 836–841.

13 Mizushima N, Yoshimori T and Ohsumi Y (2011) The role of Atg proteins in autophagosome formation. *Annu Rev Cell Dev Biol* **27**, 107–132.
14 Mancias JD and Kimmelman AC (2016) Mechanisms of selective autophagy in normal physiology and cancer. *J Mol Biol* **428**, 1659–1680.
15 Juhász G (2012) Interpretation of bafilomycin, pH neutralizing or protease inhibitor treatments in autophagic flux experiments: novel considerations. *Autophagy* **8**, 1875–1876.
16 Donohue E, Tovey A, Vogl AW, Arns S, Sternberg E, Young RN and Roberge M (2011) Inhibition of autophagosome formation by the benzoporphyrin derivative verteporfin. *J Biol Chem* **286**, 7290–7300.
17 Hjerpe R, Aillet F, Lopitz-Otsoa F, Lang V, England P and Rodriguez MS (2009) Efficient protection and isolation of ubiquitylated proteins using tandem ubiquitin-binding entities. *EMBO Rep* **10**, 1250–1258.
18 Marshall RS, Li F, Gemperline DC, Book AJ and Vierstra RD (2015) Autophagic degradation of the 26S proteasome is mediated by the dual ATG8/ubiquitin receptor RPN10 in arabidopsis. *Mol Cell* **58**, 1053–1066.
19 Marshall RS, McLoughlin F and Vierstra RD (2016) Autophagic turnover of inactive 26S proteasomes in yeast is directed by the ubiquitin receptor Cue5 and the Hsp42 chaperone. *Cell Rep* **16**, 1717–1732.
20 Cohen-Kaplan V, Livneh I, Avni N, Fabre B, Ziv T, Kwon YT and Ciechanover A (2016) p62- and ubiquitin-dependent stress-induced autophagy of the mammalian 26S proteasome. *Proc Natl Acad Sci USA* **113**, E7490–E7499.
21 Aillet F, Lopitz-Otsoa F, Hjerpe R, Torres-Ramos M, Lang V and Rodríguez MS (2012) Isolation of ubiquitylated proteins using tandem ubiquitin-binding entities. *Methods Mol Biol* **832**, 173–183.
22 Waite KA, Mota-Peynado AD-L, Vontz G and Roelofs J (2016) Starvation induces proteasome autophagy with different pathways for core and regulatory particles. *J Biol Chem* **291**, 3239–3253.
23 Meiners S, Heyken D, Weller A, Ludwig A, Stangl K, Kloetzel P-M and Krüger E (2003) Inhibition of proteasome activity induces concerted expression of proteasome genes and de novo formation of Mammalian proteasomes. *J Biol Chem* **278**, 21517–21525.
24 Welk V, Coux O, Kleene V, Abeza C, Trümbach D, Eickelberg O and Meiners S (2016) Inhibition of proteasome activity induces formation of alternative proteasome complexes. *J Biol Chem* **291**, 13147–13159.
25 Altun M, Kramer HB, Willems LI, McDermott JL, Leach CA, Goldenberg SJ, Kumar KGS, Konietzny R, Fischer R, Kogan E *et al.* (2011) Activity-based chemical proteomics accelerates inhibitor development for deubiquitylating enzymes. *Chem Biol* **18**, 1401–1412.
26 Piddock RE, Bowles KM and Rushworth SA (2017) The role of PI3K isoforms in regulating bone marrow microenvironment signaling focusing on acute myeloid leukemia and multiple myeloma. *Cancers* **9**, 29.
27 Nepstad I, Hatfield KJ, Grønningsæter IS and Reikvam H (2020) The PI3K-Akt-mTOR signaling pathway in human acute myeloid leukemia (AML) cells. *Int J Mol Sci* **21**, 2907.
28 Brandts CH, Sargin B, Rode M, Biermann C, Lindtner B, Schwäble J, Buerger H, Müller-Tidow C, Choudhary C, McMahon M *et al.* (2005) Constitutive activation of Akt by Flt3 internal tandem duplications is necessary for increased survival, proliferation, and myeloid transformation. *Cancer Res* **65**, 9643–9650.
29 Tabe Y, Tafuri A, Sekihara K, Yang H and Konopleva M (2017) Inhibition of mTOR kinase as a therapeutic target for acute myeloid leukemia. *Expert Opin Ther Targets* **21**, 705–714.
30 Spiekermann K, Bagrintseva K, Schwab R, Schmieja K and Hiddemann W (2003) Overexpression and constitutive activation of FLT3 induces STAT5 activation in primary acute myeloid leukemia blast cells. *Clin Cancer Res* **9**, 2140–2150.
31 Konstantinou EK, Notomi S, Kosmidou C, Brodowska K, Al-Moujahed A, Nicolaou F, Tsoka P, Gragoudas E, Miller JW, Young LH *et al.* (2017) Verteporfin-induced formation of protein cross-linked oligomers and high molecular weight complexes is mediated by light and leads to cell toxicity. *Sci Rep* **7**, 46581.
32 Lefaki M, Papaevgeniou N and Chondrogianni N (2017) Redox regulation of proteasome function. *Redox Biol* **13**, 452–458.
33 Finkel T (2011) Signal transduction by reactive oxygen species. *J Cell Biol* **194**, 7–15.
34 Xolalpa W, Mata-Cantero L, Aillet F and Rodriguez MS (2016) Isolation of the ubiquitin-proteome from tumor cell lines and primary cells using TUBEs. *Methods Mol Biol* **1449**, 161–175.
35 Long J, Gallagher TRA, Cavey JR, Sheppard PW, Ralston SH, Layfield R and Searle MS (2008) Ubiquitin Recognition by the Ubiquitin-associated Domain of p62 Involves a Novel Conformational Switch. *J Biol Chem* **283**, 5427–5440.
36 Cabe M, Rademacher DJ, Karlsson AB, Cherukuri S and Bakowska JC (2018) PB1 and UBA domains of p62 are essential for aggresome-like induced structure formation. *Biochem Biophys Res Commun* **503**, 2306–2311.

Supporting information

Additional supporting information may be found online in the Supporting Information section at the end of the article.

Fig. S1. Cell death evaluation at 8 h. Treatments using 15 nM Bz and 10 nM BafA with fetal bovine serum 2% MOLM-14 before annexin-V staining and flow cytometry to validate the western blot conditions ($n = 24$), three biological replicates. Statistical analyses were performed using unpaired two-tailed Student's t-tests with PRISM, version 6. $*P < 0.05$, $**P < 0.01$, $***P < 0.001$ and $****P < 0.0001$. Data are reported as the mean ± SEM ($n = 3$).

FEBS Open Bio **11** (2021) 48–60 © 2020 The Authors. *FEBS Open Bio* published by John Wiley & Sons Ltd on behalf of Federation of European Biochemical Societies.

Seminars in Cell and Developmental Biology xxx (xxxx) xxx

Contents lists available at ScienceDirect

Seminars in Cell and Developmental Biology

journal homepage: www.elsevier.com/locate/semcdb

Ubiquitin-chains dynamics and its role regulating crucial cellular processes

Maria Gonzalez-Santamarta [a], Corentin Bouvier [a], Manuel S. Rodriguez [a,*], Wendy Xolalpa [b]

[a] Laboratoire de Chimie de Coordination (LCC) – UPR 8241 CNRS, and UMR 152 Pharma-Dev, Université de Toulouse, IRD, UPS, 31400 Toulouse, France
[b] Departamento de Ingeniería Celular y Biocatálisis, Instituto de Biotecnología, Universidad Nacional Autónoma de México, 62250 Cuernavaca, Morelos, Mexico

ARTICLE INFO

Keywords:
Ubiquitin chains
Ubiquitin enzymes
Proteasome
Autophagy
DNA repair
NF-κB signaling

ABSTRACT

The proteome adapts to multiple situations occurring along the life of the cell. To face these continuous changes, the cell uses posttranslational modifications (PTMs) to control the localization, association with multiple partners, stability, and activity of protein targets. One of the most dynamic protein involved in PTMs is Ubiquitin (Ub). Together with other members of the same family, known as Ubiquitin-like (UbL) proteins, Ub rebuilds the architecture of a protein in a few minutes to change its properties in a very efficient way. This capacity of Ub and UbL is in part due to their potential to form complex architectures when attached to target proteins or when forming Ub chains. The highly dynamic formation and remodeling of Ub chains is regulated by the action of conjugating and deconjugating enzymes that determine, in due time, the correct chain architecture for a particular cellular function. Chain remodeling occurs in response to physiologic stimuli but also in pathologic situations. Here, we illustrate well-documented cases of chain remodeling during DNA repair, activation of the NF-κB pathway and autophagy, as examples of this dynamic regulation. The crucial role of enzymes and cofactors regulating chain remodeling is discussed.

1. Introduction

Proteins form a dynamic equilibrium in cells. Their quality, abundance and function must be highly regulated. This homeostatic protein equilibrium known as proteostasis contributes to maintaining cell viability, granting the ability to cope with external/internal stimuli or stress conditions. Various processes are involved in this equilibrium including protein synthesis, folding, posttranslational modifications (PTMs), assembly/disassembly of complexes, intracellular transport, and degradation. Disruptions of this equilibrium are associated with various pathologies such as inflammatory, neurodegenerative, or infectious diseases and different cancer types. A proteostasis disequilibrium is a common hallmark in the most aggressive types of cancers like those localized in the pancreas, lung, and prostate. Many enzymes and proteostasis regulators have been described to be dysregulated in tumorigenesis, cancer progression, metastasis and resistance to chemotherapy [1]. In addition, neurodegenerative diseases, in particular those associated with dementia, usually display a defective proteolytic activity generating a "proteostatic collapse", a phenotype in which misfolded proteins aggregate together with ubiquitylated inclusion bodies [2].

PTMs like phosphorylation, acetylation, and modification by Ubiquitin (Ub) family members also known as (AKA) Ubiquitin-like proteins (UbLs), regulate the half-life of proteins and their localization, but also their activity and interactions with other cellular factors. The reversibility of PTMs has the great virtue of enabling reversible switches between different functional states, therefore a rapid and versatile manner of fine-tuning countless signaling cascades and cellular events. Historically, Ub was first involved in the regulation of proteasomal degradation, also called "Ub Proteasome System" (UPS). In the last decades, different functions and layers of complexity have however been attributed to this unique modification underlaying a complex language that has been named as "*the Ub Code*", involving different types of ubiquitylation and regulatory mechanisms [3]. The plasticity of the Ub Code allows the control of a large diversity of processes including cell cycle control, protein quality control, cell proliferation, apoptosis, development, DNA repair, autophagy, signal transduction pathways, endocytosis, intracellular trafficking, transcription and the regulation of multiple infections, among others [4–7].

Ub is a 76-residue amino-acid β-grasp structure that is highly conserved across eukaryotic organisms. Ub is generated through the processing of high molecular weight precursors that after cleavage expose the glycine residue 76 (G76) then used to attach it covalently to

* Corresponding author.
E-mail addresses: maria.gonzalez@lcc-toulouse.fr (M. Gonzalez-Santamarta), corentin.bouvier@lcc-toulouse.fr (C. Bouvier), manuel.rodriguez@lcc-toulouse.fr (M.S. Rodriguez), wendy.xolalpa@ibt.unam.mx (W. Xolalpa).

https://doi.org/10.1016/j.semcdb.2021.11.023
Received 16 September 2021; Received in revised form 19 November 2021; Accepted 23 November 2021

lysine or other residues on target proteins [3]. The complexity of Ub signals relies in part on its capacity to be attached as a monomer, one or several times on the target proteins, but also on one or more of the 7 reactive lysine residues present on Ub itself.

Ub attachment to protein substrates, or Ub conjugation, is a highly dynamic reversible process regulated by conjugating and deconjugating enzymes. Conjugation events involve a thiol ester cascade of reactions that are mediated by a group of enzymes that activate (E1), conjugate (E2) or ligate (E3) the Ub moiety to its target. This process is associated with the writing of the Ub Code and involves two E1, at least 37 E2s and around 600 putative ligases in human cells. While E1s and E2s form thiol-ester intermediates, not all E3s do it and Ub can be transferred from E2 directly to the lysine residue on the substrate. In this category of E3, we find the family of really interesting new gene (RING) finger type. Other enzymes like the homologous to E6-associated protein C-terminus (HECT) domain type form a thiol ester intermediate with an internal cysteine residue in the E3 before transferring Ub to the target protein. Literature describes two other major families of E3 ligases: the UFD2 homology (U-box), and the RING-in-between-RING (RBR) [3]. E3s confers specificity to the conjugation process as they control the decision for the substrate to be modified and the lysine residue to be conjugated.

Deconjugating enzymes are editors of this language and are specific for each member of the Ub family. In the case of Ub, these have been called DUBs for deubiquitylating enzymes. This group of enzymes proofread the architecture of Ub chains acting as “erasers” to control the quantity or number of Ub moieties modifying targets and chain architecture required to connect with a specific function. DUBs are proteases that specifically recognize monoubiquitin (monoUb) or polyubiquitin (polyUb) chains on modified targets and remove Ub by hydrolysis of isopeptide bonds from the carboxyl group of Ub G76 attached to the target. Some DUBs process high molecular weight precursors of Ub and others have a role on Ub chain remodeling by its endo- or exo-protease activity. DUBs have been classified in seven families, based on their sequence and structure of their catalytic domain; six are cysteine proteases, the Ub-specific proteases (USP), Ub C-terminal hydrolases (UCH), Machado-Joseph disease proteases (MJD), ovarian tumor domain proteases (OTUs), motif interacting with Ub containing novel DUB family (MINDYs) and the recently discovered zinc finger with UFM1-specific peptidase domain protein proteases (ZUFSPs). The seventh family encompasses the zinc dependent metalloproteases JAB1/MPN/MOV34 (JAMMs) [8,9]. The Ub chain architecture on a particular target protein can be simultaneously proofread by the action of one or more DUBs that will determine the final architecture.

The information encrypted in Ub chains is read and interpreted by different adapter proteins or “readers” [10]. The modulation of the formation and processing of Ub chains is achieved through Ubiquitin Binding Domains (UBD), some of them with a preference for specific Ub chains and topologies [11]. In this way, Ub chains, recognized by multiple UBDs present in effector proteins, can connect with multiple cellular functions. In some cases, this connection might rely on cofactors of different nature that will provide specificity or increase affinity of these temporal interactions. Since the Ub Code can be regulated at the level of writing, editing, reading and interpretation, the complexity of this language is almost limitless. Improving our knowledge of the messages encrypted by distinct chain types is necessary to understand this cellular communication.

2. Ubiquitin chains diversity

Protein substrates can be modified by one Ub moiety over one or multiple amino acids of its target protein, referred to as mono- or multi-monoubiquitylation respectively. Ub attachment generally occurs on lysine (K) residues, but serine (S) and threonine (T) have been found to be ubiquitylated under particular circumstances too [12]. Since Ub has a globular shape, eight exposed residues can be conjugated to the C-terminus of another Ub via isopeptide bonds to form chains of various lengths, linkages, and structures. Seven lysine residues (K6, K11, K27, K29, K33, K48, and K63) and N-terminal methionine residue (M1) force Ub to adopt unique topologies forming distinct binding surfaces. Formation of polyUb chains can hold the same Ub linkage (homotypic chains) or a combination of different K linkages (heterotypic chains). Heterotypic chains provide another layer of complexity as they can be mixed with different Ub linkages and branched when Ub is modified at two or more K residues [11] (Fig. 1). Further complexity is generated by the order in which branched chains are formed resulting in different conformations.

Despite recent efforts, the mechanism underlying the formation of complex Ub chains is not fully understood [13]. To simplify our understanding, generic functions have been attributed to some chain linkages. While the functions of homotypic chains are well-defined, the structures and functions of heterotypic or branched chains have emerged more recently. Even if heterotypic K6/K11, K6/K48, K27/K29 and K29/K33 linkages have been detected in vitro or in cells, only a few examples have been found and their functions need to be better studied to define their role. Evidence also exists for branched M1/K63 and K11/K63 chains, though their structures are still to be identified [14]. Recent studies have shown that branched chains represent a significant fraction of all polyUb chains in cells, with current estimates ranging from 5% to 20% [15]. Finally, Ub moieties can also be modified by other PTMs, including phosphorylation, acetylation, SUMOylation or NEDylation. These PTMs alter the Ub chain architecture and allow new interactions that connect with a distinct set of functions [16,17]. Examples of generic functions established for some Ub chains are summary in the Table 1.

3. Ubiquitin chains implicated in proteasomal degradation

One of the most predominant Ub linkages found inside the cells is K48, which is the major signal for proteasome-mediated degradation. Quantitative mass spectrometry (MS) analyses of cells treated with the proteasome inhibitor MG132 provided evidence to support this idea, since K48-polyUb linkages quickly accumulate in cells after treatment. Initial studies suggested that at least four K48-linked Ub molecules were required for an efficient binding to the 26S proteasome. However, latest data indicate that the number of K48-polyUb chains may be more important than chain length since two di-Ub K48-chains provide a more efficient binding to the proteasome than a single tetraubiquitin K48-chain [18]. The requirement of four or more Ub moieties integrated into a polyUb chain to target proteasomal degradation was challenged by several studies. Ciechanover et al. demonstrated that multiple mono-ubiquitylation can also mimic the patch required for an optimal recognition by dedicated proteasome Ub receptors [19]. Dimova et al. also showed that multiple monoubiquitylation of cyclin B1 is an efficient signal for proteasomal degradation [20]. Consequently, these and other findings proved that multiple Ub moieties can be recognized by the proteasome and imply the existence of monoubiquitylation vs. polyubiquitylation decision mechanisms. Based on these observations, it was suggested that the chain length necessary for proteasomal degradation is mainly determined by the size of the substrate: substrates smaller than 150 residues are degraded via multiple monoubiquitylation, whereas longer substrates need longer chains. Dimova and co-workers proved that by limiting the number of ubiquitylable K residues, the degradation signal can change from multiple monoubiquitylations to polyubiquitylation [20]. These results suggest that masking K residues by protein–protein interactions or PTMs can affect the ubiquitylation pattern.

Since K48-linked chains became a canonical signal for proteasomal proteolysis, an interesting hypothesis proposed that intrinsic proteasome subunits with UBDs, such as Rpn10 and Rpn13, selectively bind with K48-polyubiquitin chains. Proteasome associated subunits with UBDs like hHR23A and hHR23B would also bind with K48-polyubiquitin conjugates to stimulate their binding to the 26S [21].

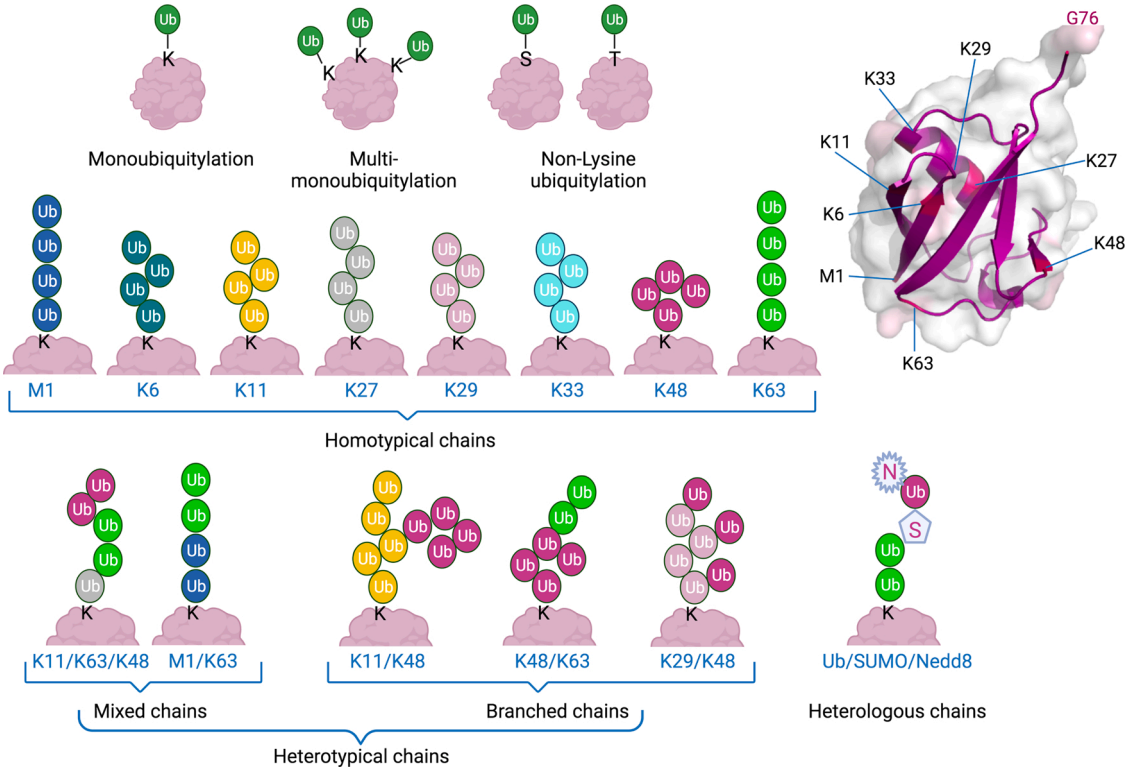

Fig. 1. Ub chains diversity. Monoubiquitylation occurs when the Ub G76 residue is attached to a K residue on a target protein. Multimonoubiquitylation involves the attachment of several Ub molecules on multiple sites on the same target protein. Polyubiquitylation occurs when the first attached Ub is the target of another Ub moiety, which in turn, becomes the target for additional Ub molecules. The architecture and formation of Ub chains depend on the K residue that is used on the proximal Ub (which is the nearest to the substrate), to form the isopeptide link with the G76 residue of the adjacent or distal Ub. Structural diversity and complexity of chains can be appreciated and classified as it is shown in the cartoon representations. A structural view of Ub molecule (PDB:1ubq) is presented to illustrate the position of each K or M1 residues involved in the link formation.

Interestingly, when isolated, these UBDs bind with K48- and K63-linked chains with similar affinity suggesting that other domains or cofactors could contribute to provide K48 Ub chain selectivity. Tsuchiya et al. described how the cell division cycle protein 48 (Cdc48) and its cofactor Npl4 direct K48 ubiquitylated proteins to the proteasome upstream Rad23/Dsk2 and proposed the Cdc48-Rad23/Dsk2 axis as a major route to drive proteasome-mediated proteolysis [22].

DUBs play a crucial role in the regulation of K48 Ub chain-mediated functions. Several members of the OTU family showed remarkable specificity for K48-linked chains including OTUB1, that limits its action towards this chain type even in the context of mixed chain linkages. K48 chains can also be regulated by DUBs associated with the 19 S regulatory particle of the proteasome. This is the case for Ubp6/USP14 and Rpn11/PSMD14 (in yeast and human, respectively).

3.1. *Heterotypic chains in proteasomal degradation*

Different evidences suggest that other Ub linkages are involved in proteasomal degradation as various Ub chain types are accumulated upon proteasome inhibition [3,23]. Among them, K11-linked Ub chains, which are the third most abundant linkages in cells, play a significative role during mitosis. However, in 2015, Grice et al. suggested that homotypic K11 Ub signals are not sufficient to bind the proteasome and drive proteasomal degradation [24]. Heterotypic K11/K48 chains are involved in the degradation of multiple cellular factors, but in the absence of tools and technology to monitor them, their characterization and the assessment of their role in the regulation of different functions remains problematic. By engineering a bi-specific antibody to detect K11/K48 Ub chains, Yau et al. discovered that the multi-subunit RING E3 ligase anaphase-promoting complex (AKA APC/C or cyclosome) assembles K11/K48 heterotypic chains on cell-cycle substrates [25]. They showed that K11/K48 chains were enriched upon proteotoxic stress generated by proteasome inhibition or HSP70/90 blockage. These findings underlined that K11/K48 Ub chains are involved in the control of cell-cycle and protein quality, as they provided a rapid and specific degradation of mitosis regulators like cyclin B and misfolded proteins [13]. The formation of K11/K48 branched chains, during mitosis, is mediated by the APC/C with the cooperation of two E2 conjugating enzymes, UBE2C and UBE2S. First, UBE2C attaches short chains containing mainly mixed K11/K48 linkages to substrates of the APC/C. Then, the K11-specific E2, UBE2S, adds multiple K11 linkages to these short chains, resulting in branched K11/K48. The proteotoxic stress response also involves E3 ligases, UBR4 and UBR5 to generate K11/K48 chains on misfolded and aggregation-prone proteins such as the Huntington's disease-associated HTT variant [25]. These modified proteins bind the p97/VCP complex and the proteasomal adapter hHR23A. K11/K48 polyUb chains adopt conformations that can bind with the proteasome 19S subunit, likely via interaction with the I44 Ub-binding surface, or alternatively by the presence of K48 linkages permitting its association with 26S Ub receptors. It has been shown recently that the Rpn1 proteasomal subunit contains a high affinity towards K11/K48 chains [26]. In 2018, Samant et al. discovered that K48/K11 Ub chains are needed for cytoplasmic degradation in contrast to the K11-nuclear independent degradation of substrates, which only involves K48 Ub chains, also making a distinction in the regulatory elements associated in each proteolytic pathway [27].

The proteasome's capacity to differently degrade proteins modified with homotypic K11 and heterotypic K11/K48 chains has been associated with the capacity of proteasome-associated DUBs to disassemble these chains. Both homotypic K11 and heterotypic K11/K48-polyUb conjugates can be disassembled, but only K11/K48-polyUb conjugates can efficiently drive protein degradation [24]. Thus, the binding of

Table 1
Functions associated to different ubiquitin-chain linkages. Non exhaustive examples.

Type of Ub chain		Ub chain linkage-type	Main described functions	Ref.
Homotypical	Canonical	K48	Proteasomal degradation	[18,22]
		K63	Cell signaling, DNA repair, autophagy, protein trafficking	[30,40,41, 67,150]
	Non-canonical or atypical	M1	NF-κB signaling, cell death regulation, protein quality control	[13, 43–45]
		K6	DNA repair, mitophagy	[6,126]
		K11	Proteasomal degradation, cell cycle, IFN signaling	[24,72]
		K27	Cell signaling, immune regulation, autophagy, DNA repair	[72,151]
		K29	Wnt/β-catenin signaling, immune regulation	[75,76, 152,153]
		K33	Cell signaling, immune regulation, protein trafficking, autophagy	[71,74, 153–156]
Heterotypical	Mixed	K6/K11	unknown	[157]
	Branched	K6/K48	unknown	[14]
	Branched	K11/K48	Proteasomal degradation, cell cycle, protein quality control	[24,25, 157,158]
	Mixed	K11/K63	unknown	[157]
	Branched	K27/K29	unknown	[14]
	Branched	K29/K33	unknown	[14]
	Branched	K29/K48	ER-associated protein degradation (ERAD)	[159]
	Branched	K48/K63	NF-κB signaling	[47,160]
	Mixed	K63/M1	NF-κB signaling	[46]
	Mixed	K48/ K63/K11	Cyclin B1 regulation	[161]

ubiquitylated substrates to 19S receptors is not required to activate the proteasome-associated DUBs for the disassembly of homotypic K11 Ub chains. Deubiquitylation of APC/C substrates is mediated by the K11-linkage-specific DUB Cezanne (OTUD7B), a member of OTU family [28]. Cezanne depletion accelerates APC/C target degradation and provokes errors in mitotic progression. Cezanne also regulates ubiquitylation and stability of the hypoxia inducible factor HIF-1α and HIF-2α [29].

Whether the other Ub chain types can act as signal for proteasomal degradation is still unclear. Whereas K6, K27, K29, and K33 Ub linkages are all detected at low levels in cells, they all increase after treatment with proteasome inhibitors, though in different proportions. This means that their accumulation could be an indirect consequence of proteasome inhibition or that they could be involved in proteasomal degradation.

4. Ubiquitin chains implicated in proteasome-independent functions

Early structural studies demonstrated a drastic conformational distinction between Ub chains driving proteasomal degradation from those that do not. Ub chains recognized by the proteasome mainly adopt a packed "closed" conformation wherein the two neighboring Ub subunits form extensive interactions with each other. In contrast, non-proteolytic Ub chains form an extended configuration with no direct contact between neighboring Ub moieties. The many exceptions to this dogmatic theory argue in favor of other features and regulatory mechanisms determining the role of distinct Ub chains. Non-proteolytic chains are very diverse, and their functions are far from being fully understood. However, their role in the regulation of intracellular signaling cascades is without any doubt one of the most important. Cell signaling allows cells to perceive and respond to the extracellular environment, essential to their development, growth, and immune response. Ubiquitylation has emerged as a key mechanism that regulates signal transduction pathways in most biological processes. For instance, ubiquitylation regulates multiple receptor-mediated signaling cascades implicated in differentiation, cell cycle, innate and adaptive immune responses, among others. The first Ub chain implicated in cell signaling was the K63, reported to regulate the activation of protein kinases and protein trafficking for cell survival and proliferation. Defective formation of K63 chains is associated with the development of various disorders including inflammation, cancer, neurodegeneration and cardiac hypertrophy [30].

One of the best-known examples of signaling pathways regulated by K63 chains is the NF-κB pathway, an important signaling cascade involved in inflammation and cancer development. NF-κB is also regulated by M1 chains that will be discussed below. The following sections how some examples of regulation of crucial functions and cellular pathways by diverse Ub chains implicating multiple Ub E3s and DUBs in a dynamic way.

4.1. Ubiquitin chains in the NF-κB pathway

The nuclear factor κB (NF-κB) was initially described in B cells as a transcription factor that binds the enhancer of the kappa light chain gene. NF-κB is a family of inducible heterodimeric transcription factors found at the center of cell signaling pathways, having a role in immune response, cell growth and apoptosis [31]. NF-κB plays an important role in inflammation since it is activated by cytokines such as interleukin-1 (IL-1) or the tumor necrosis factor α (TNF-α). Under unstimulated conditions NF-κB is retained in the cytosol by natural inhibitors and its nuclear translocation is conditioned to the degradation of these molecules (see text below). The NF-κB pathway involves a signaling cascade starting with the receptor stimulation until the activation of transcription of inflammatory genes [32]. Two pathways lead to NF-κB activation, known as the canonical and non-canonical pathways (Fig. 2) [33, 34]. The canonical one converges into phosphorylation of the inhibitor IkappaB (IκB) by a multi-subunit IκB kinase (IKK) complex. The IKK complex composed by three subunits: IKK1 (AKA, IKKα), IKK2 (AKA, IKKβ) and a regulatory subunit NF-κB essential modulator (NEMO) (AKA, IKKγ) fundamental for NF-κB canonical activation. Phosphorylation on the N-terminal of IκBα is followed by ubiquitylation leading to its proteasomal degradation. A tight control of both pathways is necessary to maintain NF-κB homeostasis. Ubiquitylation and other PTMs participate in this fine regulation at different levels. We dissected the canonical pathway into 3 levels to illustrate the role of distinct Ub chains, E3s and DUBs: 1) Recruitment of adapter proteins after receptor-ligand binding, 2) Recruitment of the main kinase complexes and 3) Release of NF-κB dimer.

4.1.1. Recruitment of adapter proteins after receptor-ligand binding

In the prototype-signaling pathway induced by the tumor necrosis factor alpha (TNF-α), the TNF receptor 1 (TNF-R1) trimerizes and triggers recruitment of different proteins, including many Ub E3s, comprising the TNF-R1-signaling complex. The adapter protein TRADD bound to the TNF-R1 cytoplasmic domain enrolls the receptor-interacting serine/threonine-protein kinase 1 (RIPK1), the adapter protein Sam68, the E3 ligase TNF receptor–associated factor 2 (TRAF2) and possibly also TRAF5 [33]. TRAF2 is a scaffold for two other Ub E3s, the cellular inhibitor of apoptosis protein-1 (c-IAP1) and c-IAP2, which are responsible of conjugation of K63-, K48- and K11-linked Ub chains to

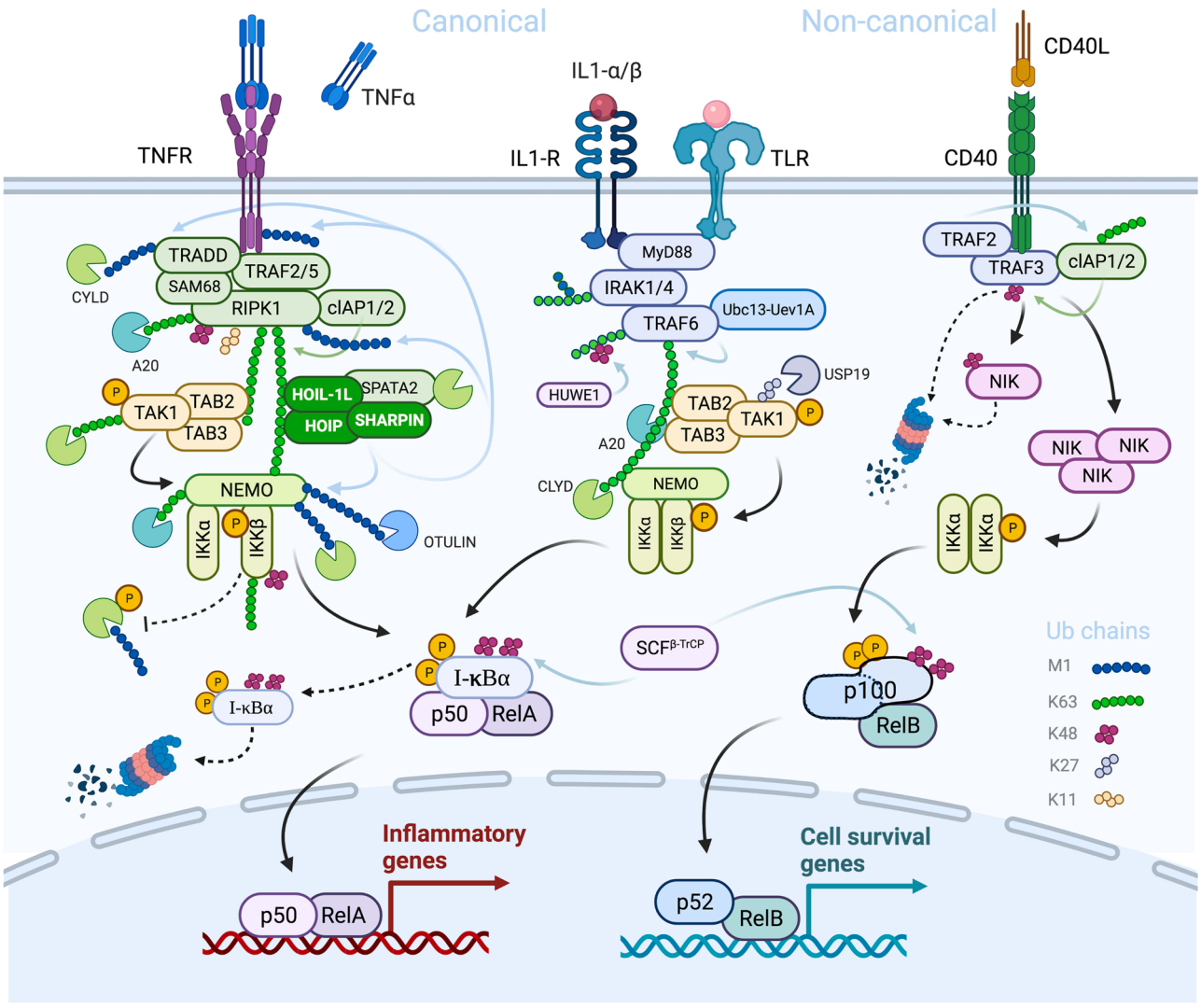

Fig. 2. Highly dynamic regulation of the NF-kB pathway by distinct Ub chains. The two canonical and the non-canonical pathways activating NF-κB are heavily regulated by M1, K63, K48, K27 and K11 Ub chain (illustrated with multiple colors). While the canonical pathway converges into phosphorylation of the inhibitor, IkappaB (IκB), by a multi-subunit IκB kinase (IKK) complex to release the p50/RelA heterodimer, the non-canonical pathway activate the cleavage of p100 that will form the p52/RelB transcription dimer. Ubiquitylation and other posttranslational modifications participate in this fine regulation at the level of the recruitment of adapter proteins after receptor-ligand binding, the activation of main kinase complexes and the NF-κB dimer releasing. The names and roles of regulated factors are well described in the main text.

RIPK1 [35]. Polyubiquitylated RIPK1, particularly with K63 chains, recruits the linear Ub E3 complex (LUBAC) and the TAK1 kinase complex, which are important for the downstream signaling cascade. The stimulation of the IL-1R or toll-like receptors (TLRs) recruits a different set of adapter proteins that leads to the enrollment of TRAF6, an Ub E3 that catalyze the synthesis of K63-linked Ub chains with the help of the Ub E2 Ubc13-Uev1A. These K63 Ub chains are attached to the same TRAF6 (autoubiquitylation) that is necessary for the recruitment of the transforming growth factor-β-activated kinase 1 (TAK1) kinase complex, which in turn phosphorylates and activates the IKK complex [36]. TRAF6 was shown to promote K63- and K27-linked polyubiquitination over TAK1 after IL-1β stimulation [37].

4.1.2. Recruitment of the main kinases complexes

Different stimuli as well as pattern recognition receptors (PRRs) can trigger receptor mediated-signaling transduction, which converges at TAK1 activation. TAK1 is a member of the MAPKKK kinases that exists as a heterotrimer in the complex with the accessory proteins TAK1 binding protein (TAB) 1, TAB2 or TAB3. The complex TAK1/TAB2/TAB3 is recruited to the site of ubiquitylated RIPK1 thanks to the ubiquitin associated (UBA) domain Np14 zinc finger (NZF), present in TAB2 and TAB3, that recognizes K63-linked chains [38]. Free K63-linked Ub chains synthetized by TRAF6 are also able to bind TAB2 [36]. The identification of the K377 site on RIPK1 was shown to be important for the recruitment of TAK1 and IKK complexes, even if other sites were later characterized [39].

On the other hand, the recruitment of the IKK complex is mediated through the ubiquitylated-RIPK1 recognition by NEMO. The N-terminal of NEMO is involved in the interaction with IKKα and IKKβ, while the C-terminal attaches Ub chains. The NEMO C-terminal harbor two different motifs which together form a UBD that specifically recognizes K63-linked Ub chains, the UBAN motif (AKA NOA) and the zinc finger (ZF) motif [40]. Recruited IKK complex is responsible of phosphorylation of IκB through the IKKβ subunit. There is evidence that also IKKβ undergoes ubiquitylation with K48- and K63-linked Ub chains. The role of ubiquitylation in the regulation of this kinase was shown by mutations at the K171 site, which leads to constitutive phosphorylation activity. This particular mutation was previously observed in Multiple Myeloma, Spleen Marginal Zone Lymphoma and Mantle Cell Lymphoma. *In vitro* experiments simulating the K171 mutation showed an increased

K63-linked ubiquitylation of IKKβ on different sites and a persistent activation of STAT3 signaling [41]. Otherwise, IKK3 (AKA IKKε) is a non-canonical IKK family member that is activated by TLRs and intracellular receptors able to recognize viral nucleic acids such as dsRNA. IKK3 plays a role in the phosphorylation and activation of other transcription factors as interferon response factors IRF3 and IRF7, but can also activate NF-κB. IKK3 and Tank-binding kinase 1 (TBK1) are involved in the activation of the NF-**κ**B pathway through phosphorylation of I**κ**B and p65 subunit [42].

LUBAC is currently the only E3 ligase complex that synthetizes linear chains. It is composed of 3 members: HOIL-1L (AKA RBCK1), HOIL-1L-interacting protein (HOIP) (AKA RNF31) and SHANK-associated RH domain interacting protein (SHARPIN). The assembled heterotrimer is required to generate M1 linear chains where HOIP is the catalytic subunit [43]. Once LUBAC is enrolled by ubiquitylated RIPK1, it attaches M1-linked chains to the IKK complex subunit NEMO and to the same RIPK1 leading for an efficient activation of the canonical IKK [44]. MS analyses of ubiquitylated NEMO and mutagenesis experiments showed that K285 and K309 are the acceptors of LUBAC-mediated ubiquitylation. LUBAC can also modify other substrates as TRADD and TNF-R1 and undergo autoubiquitylation. It can synthetize linear Ub conjugates with different E2s as UbcH5, E2–25, and UbcH7. Recruitment of LUBAC is key to stabilizing the TNF-R1-signaling complex since several components harbor UBDs. Indeed, linear Ub chains bind UBDs and retention of cIAP1, TRAF2, RIPK1, and TAK1 was shown to be dependent on LUBAC ligase activity, protecting the complex from falling apart [45]. There is also evidence that the UBAN motif of NEMO binds to M1-linked Ub chains with higher affinity than to K63 chains, and that this interaction is crucial for the TNF-α-induced activation of the IKK complex. Interestingly, hybrid chains were later observed in the pathway mediated by IL-1R stimulation. Emmerich and collaborators found that K63-ubiquitylated substrates, such as the IL-1R1 associated kinase (IRAK) 1, were also ubiquitylated by linear chains. The formation of K63-linked Ub chains was shown to be a prerequisite for the formation of M1-linked chains, with NEMO being able to capture these hybrid chains [46]. Regarding the identification of heterotypic chains, it has been shown that K48–K63 branching Ub chains are formed in substrates as TRAF6 or IRAK1 in cells stimulated with IL-1β. Ubiquitylated TRAF6 with K63-linked chains seems to be remodeled by the action of the E3 ligase HUWE1, which conjugates K48 Ub chains on the preformed chains. Interestingly, there is no interference in the recognition of these K48-K63 branched chains by TAB2; but otherwise, branched chains appear to be protected from cylindromatosis (CYLD)-mediated deubiquitylation, which could contribute to amplifying the NFκB activation [47]. Even if LUBAC has been extensively studied in the context of TNF signaling, it has also been recently associated with oncogenic signaling, antibacterial autophagy and protein quality control [13].

4.1.3. Release of NF-κB dimer

NF-κB dimers can be assembled with two of the five subunits: RelA (AKA p65), RelB, c-Rel, p50 (from precursor p105) and p52 (from p100). Under basal unstimulated conditions, the dimer is retained in the cytoplasm by action of its corresponding inhibitor (an IκB family member). Phosphorylation of IκB takes place once the IKK complex has been activated.

In addition to the p105 and p100 precursors that contain ankyrin repeats, three other proteins inhibit *NF*-κB activity: IκBα, IκBβ and IκBε. Ankyrin repeats allow the interaction with the Rel domain of NF-κB. IκBs share a conserved sequence DSGXXS motif that includes the two serine residues that are targeted by the IKK complex [33]. In the TNF-stimulated cells, phosphorylation at residues S32 and S36 on the N-terminal of I**κ**Bα is followed by K48-linked ubiquitylation that leads to its proteasomal degradation. The phosphorylation signal is recognized by a key E3 Ub ligase complex, the multisubunit Skp, Cullin, F-box, beta-transducin repeat containing protein ($SCF^{\beta\text{-}TrCP}$) E3 ligase, which polyubiquitinates I**κ**Bα mainly on K21 and K22, favors its degradation releasing the NF-κB dimer. Monoubiquitylated forms of IκBα can be found in basal state, in forms that are not degraded by the proteasome after TNF-stimulation, as usually occurs with polyubiquitylated IκBα [48]. The role of this pool of monoubiquitylated IκBα remains to be fully investigated. Furthermore, IκBα is subjected to multiple PTMs beyond phosphorylation and ubiquitylation since SUMOylation, acetylation, glutathionylation and hydroxylation have also been reported [49].

4.1.4. Non-canonical pathway

A non-canonical or alternative pathway has been described in the activation of specific NF-κB family members. The p50/RelA dimer is predominantly translocated to the nucleus in the canonical pathway, while the p52/RelB dimer is particularly activated in the non-canonical pathway. This alternative mechanism relies on the inducible processing of the p100 precursor instead of degradation of IκBα. P100 takes on the inhibiting role of IκB impeding the RelB nuclear translocation, so the p100 processing to p52 allows dimer release and translocation for target genes activation. Resembling to the phosphorylation sites of IκBα, p100 contains two serine residues S866 and S870, which are phosphorylated by the NF-**κ**B-inducing kinase (NIK, AKA MAP3K14). Phoshorylated sites of p100 generate a binding site for βTrCP subunit of $SCF^{\beta\text{-}TrCP}$ E3 ligase that induces p100 ubiquitylation. The p100 modified-site is a Lys residue, K856, which is analogous to the I-κBα K22 residue adjacent to the phosphorylation site S32. Phosphorylation-dependent ubiquitylation promotes p100 processing releasing the p52/RelB dimer to trigger the transcription of a different set of target genes compared than those of the canonical pathway. The stimuli responsible of non-canonical pathway activation are different from those to the canonical pathway. Examples of non-canonical receptors are such as CD40 ligand or lymphotoxin β, that lead to the IKKα activation, phosphorylating p100 at multiple sites to drive p52 processing [50]. IKKα activation in turn depends on kinase activity from the newly synthesized NIK. Under basal conditions, NIK is constantly degraded by the proteasome due to K48 ubiquitylation mediated by the complex TRAF3-TRAF2-cIAP1/cIAP2 [51]. When CD40, which is a TNFR member, is stimulated by its ligand, TRAF2 ubiquitylates cIAPs with K63 chains promoting their ligase activity and targeting TRAF3. Conjugated K48 chains drive TRAF3 to proteasomal degradation and prevent its association with NIK, allowing NIK accumulation and therefore IKKα phosphorylation [34]. The processing of p105 precursor to p50 can also be dependent on ubiquitylation. Recently, the KIP1 ubiquitylation-promoting complex 1 (KPC1 AKA RNF123) was identified to form a heterodimer with KPC2 (AKA UBAC1), acting together as a Ub E3 ligase to promote a limited proteasome-mediated proteolysis of p105 [52].

4.1.5. Role of DUBs in the NF-κB pathway

A strict control of all of these Ub modifications is key to avoid cellular alterations that could result in inflammatory disorders and other NF-**κ**B related diseases. NF-κB is deregulated in numerous tumors. Negative regulation of the NF-**κ**B activation is prompted by the editing deubiquitylating enzymes CYLD and USP19, which are Ub specific protease (USP) family members. Also contributing to the regulation of NF-**κ**B, OTU (ovarian tumor domain) deubiquitinase family members A20 (AKA TNF-α-induced protein 3 (TNFAIP3)) and OTULIN (AKA Gumby or Fam105b), a DUB with linear linkage specificity. The K63- and M1-linked Ub chains can be removed from different ubiquitylated substrates by CYLD, a DUB enzyme that was first identified as a NEMO-interacting protein [53]. Deficiency of this DUB leads to a constitutive NF-**κ**B activation causing proinflammatory gene expression [54]. CYLD is constitutively expressed, but after TNF stimulation it is recruited to LUBAC through the adapter protein spermatogenesis-associated protein 2 (SPATA2), which in turn binds to the subunit HOIP of LUBAC [54,55]. In the pathway triggered by NOD2 that is involved in inflammation by infectious diseases, the DUB activity of CYLD is necessary to regulate K63- and M1-linked ubiquitylation on RIPK2 [56]. The functional role of

CYLD in different pathological processes was well documented prior to understanding its role as a DUB enzyme. Several skin disorders related to CYLD gene mutations were described such as multiple familial cylindromatosis, trichoepithelioma and the Brooke–Spiegler syndrome. In cancers such as multiple myeloma, mutations on CYLD and other genes involved in the NF-κB pathway, as c-IAP1/2, were also reported [57]. CYLD activity was shown to be regulated by IKK3 kinase, which targets CYLD by phosphorylation at S418 decreasing its deubiquitylating activity [58]. Besides CYLD, OTULIN is a DUB that specifically recognizes and deconjugates M1-linked Ub chains; it is currently the only DUB able to cleave exclusively lineal chains [59]. OTULIN interacts directly with the subunit HOIP of LUBAC and regulates LUBAC-mediated processes. The OTULIN function is important to regulate angiogenesis, innate immunity and autoimmunity [60].

The deubiquitylating/E3 Ub ligase enzyme A20, plays an important role in the regulation of the NF-κB pathway [61]. A20 was first described as an inhibitor of TNF-induced apoptosis, but its role as a negative feedback regulator of NF-κB pathway was later well documented. The A20 gene is one of the several target genes that respond to NF-κB. The N-term of A20 harbor an OTU domain with DUB activity that hydrolyzes in vitro K48-, K11- and K63-linked Ub chains. The C-term contains a series of seven ZF motifs, among them, the ZF4 is critical to confer its E3 ligase activity. The NF-κB inhibitory effect of A20 was mainly attributed to its ability to disassemble K63-linked chains from different substrates, including RIPK1, TRAF6 and NEMO [54]. For instance, A20 was shown to remodel Ub chains on RIPK1 by removing K63-linked chains and conjugating K48-linked chains favoring its proteasomal degradation [62]. Although there is evidence that A20 as DUB or E3 ligase enzyme contributes to the regulation of the NF-κB pathway, later studies suggest that also its non-enzymatic features, like the ZF7 motif, play a significant role in the regulation of this pathway as it regulates cell death [63].

The DUB USP19 appears to be also a negative regulator of TNF-α– and IL-1β–triggered NF-kB activation by hydrolyzing K63- but also K27-linked Ub chains from TAK1. TAK1 was recently found to be a substrate of USP19. TRAF6 mediates K27-linked polyubiquitylation of TAK1, which is necessary for the recruitment of TAB2 and TAB3 to TAK1 to generate the TAK1-TABs complex. This deubiquitylation impairs TAK1 phosphorylation and therefore disrupts the TAK1–TAB complex, thus terminating the TAK1-mediated induction of NF-κB downstream genes [37]. The K27 ubiquitylation was first linked to NEMO regulation by the tripartite motif (TRIM) Ub ligase TRIM23, a step required for NF-κB and IRF3 induction [64]. Since then, several TRIM ligases have been shown to form K27 Ub chains that regulate intracellular signaling, transcription, autophagy, and carcinogenesis, among other important processes [65]. TRIM26 and TRIM21 regulate immune responses using distinct mechanisms synthesizing K27 Ub linkages. For instance, TRIM26 can be auto-ubiquitylated with K27 Ub chains to favor its interaction with NEMO while inducing the expression of autoinflammatory cytokines and type I IFNs [66]. The regulation of the NF-κB pathway is an example of complex Ub dynamics that will be regulated in a spatio-temporal manner depending on the physiologic or pathologic situation of the cell.

4.2. Ubiquitin chains in the regulation of Akt pathway

The activity of many kinases is controlled by K63 chains, as we showed with RIPK1 that is implicated in the regulation of cell death besides inflammation [67]. Another example is the serine/threonine kinase Akt (AKA Protein kinase B) that plays key roles in multiple cellular processes such as glucose metabolism, apoptosis, cell proliferation, transcription, and cell migration. Although it is well known that PIP3 produced by PI3K is essential for the membrane recruitment and activation of Akt, K63–linked polyubiquitylation contributes to its hyperactivation and therefore to the regulation of tumorigenesis [68]. TRAF6 is an E3 ligase that ubiquitinates Akt upon stimulation with insulin-like growth factor 1 (IGF 1). CYLD acts on Akt permitting to keep Akt-stimulating activity in balance. By studying the molecular mechanisms of lung injury, Lim et al. discovered that loss of CYLD led to the development of lung fibrosis in mice infected with *Streptococcus pneumoniae*. They found that CYLD deubiquitinates and inactivates K63-polyubiquitylated Akt, leading to inhibition of transforming growth factor–β (TGF-β) signaling by decreasing the stability of the TGF-β effector protein Smad3 [69]. In line with this study, Yang et al. showed that CYLD and Akt are physically associated. They found that, in the absence of growth factors, CYLD keeps Akt hypo-ubiquitylated through direct association and deubiquitylation, whereas growth factor stimulation allows E3 ligases such as TRAF6 to replace CYLD from Akt, thereby promoting its ubiquitylation, membrane translocation, phosphorylation and activation [70]. The E3 ligase Skp2-Skp–cullin–F-box—containing (SCF) complex, also ubiquitylates Akt in response to the activation of the epidermal growth factor family of receptors (ErbB) [70]. These findings show that Akt K63-linked ubiquitylation and activation can be induced by diverse signaling cascades using distinct E3 ligases.

4.3. Atypical ubiquitin chains in signaling and immune related functions

Beyond K63 chains, there are atypical Ub linkages also having non-proteolytic roles in cells mediating signaling, intracellular trafficking, and autophagy among other functions [71,72]. K33 Ub chains regulate T-cell antigen receptor (TCR) and AMP-activated protein kinase (AMPK)-related kinases [4]. E3 Ub ligases such as Cbl-b and Itch synthetize K33 Ub chains on the T cell receptor-zeta (TCR-zeta). Deficient formation of K33 Ub chains increases T cell activation and spontaneous autoimmunity [71], demonstrating their role in regulation of cell surface receptor-mediated signal transduction. K33 Ub signals are also implicated in immune responses upon DNA or RNA virus infection. Viral infection leads to TBK1 K33 poly-ubiquitylation, promoting IRF3 activation and type I Interferon (IFN) signaling. This antiviral response can be reversed by the DUB USP38 that removes K33 Ub chains on K670 of TBK1 and favors the formation of K48 Ub chains at the same position to drive its proteasomal degradation. Lin et al. found that knockout of USP38 increased K33-linked ubiquitylation and decreased K48 Ub-mediated degradation of TBK1 kinase, thus enhancing type I IFN signaling. Conversely, overexpression of USP38 decreased K33-linked ubiquitylation of TBK1 and increased its K48-linked ubiquitylation [73]. Another example of the role of K33 chains is leaded by the Ub E3 RNF2, which generates K33 Ub chains on the STAT1 DNA binding domain allowing its dissociation from the promotor of several interferon stimulated genes (ISG) underlining the role of these chains in the regulation of IFN pathway [74].

K29-linked polyUb chains have been associated with the regulation of inflammation, antiviral immune response, and the regulation of the Wnt/β-catenin pathway at multiple levels. The Wnt/β-catenin pathway is essential to the regulation of events such as cell proliferation, organized migration, self-renewal, and tissue polarity. Various Ub E2s in coordination with E3s attach distinct Ub linkages to different K residues on β-catenin, causing context-specific functional consequences. For example, both the E2 Rad6B and the E3 Ub ligase EDD (identified by differential display) interact with β-catenin and enhance its ubiquitylation, stability and activity. While EDD catalyzes the formation of K29-linked chains on β-catenin, Rad6B adds K63-linked polyUb chains on the same target protein. Under basal conditions, a destruction complex comprising Axin and adenomatous polyposis coli (APC) promotes β-catenin degradation. Wnt ligands lead to the inactivation of this complex, allowing β-catenin to accumulate, and thus activate a transcriptional program [75].

Smad ubiquitylation regulatory factor 1 (Smurf1) commonly serves to regulate Ub-dependent protein degradation in several signaling pathways. It also drives non-proteolytic ubiquitylation through the formation of K29 Ub chains on Axin [76]. Axin ubiquitylation on K789 and K821 negatively regulates Wnt/β-catenin signaling by disrupting Axin interaction with the Wnt co-receptors LRP5/6 that together with

Frizzled receptor initiate this signaling cascade.

K29 ubiquitylation has also been linked to the modification and activation of ASK1 (apoptosis signal-regulating kinase 1), promoting type I interferon production upon viral infection. The F-box only protein Fbxo21, a functionally unknown component of SCF (Skp1-Cul1-F-box protein) complex, mediates ASK1 ubiquitylation. Fbxo21 deficiency impairs the production of proinflammatory cytokines resulting in reduced antiviral response and enhanced virus replication and infection. The Ub Specific Peptidase 9 X-Linked (USP9X) is a C19-peptidase family protein with known DUB activity, which can cleave K48, K63 and K29 linkages. USP9X binds and stabilize ASK1 by removal of Ub chains and prevention of its degradation. Interestingly, ASK1 contains six amino acids identical to the Ub C-terminus (LRLRGG), of which the GG sequence was required for the USP9X-ASK1 interaction [77].

TRIM21 assembles K27 polyUb chains on mitochondrial antiviral signaling protein (MAVS), promoting the recruitment of TBK1 to mitochondrial adapter molecules, or mitochondrial antiviral signaling proteins leading to the upregulation of innate immunity [78]. MAVS is also targeted by RNF34 Ub ligase, that mediates K27 and K29 Ub chains after viral infection, enhancing its autophagic degradation and negatively regulating antiviral immunity [79]. Another example of K27 implication was observed upon microbial DNA invasion, the endoplasmic reticulum (ER) protein AMFR is recruited to interact with stimulator of interferon genes (STING) in an insulin-induced gene 1 (INSIG1)-dependent manner. AMFR and INSIG1 form an E3 Ub ligase complex to catalyze K27 Ub-linked chains on STING. This modification served as a scaffold to recruit TANK-binding kinase 1 (TBK1) triggering the activation of the interferon regulatory factor-3 (IRF3) and/or NF-κB signaling pathway inducing the expression of type I IFNs and proinflammatory cytokines [4]. The DUB USP13 has been reported to remove the K27-linked Ub chains on STING and thereby inhibiting the recruitment of TBK1 to STING, negatively regulating IFN production during DNA virus infection [80]. Other ligases also synthesize K27 Ub chains to regulate immune responses. The TIR domain-containing adapter inducing interferon-β (TRIF), an essential adapter protein required for innate immune responses, was shown to be regulated by K27 ubiquitylation. The RING E3 Ub ligase complex Cullin-3-Rbx1-KCTD10 assembles K27 polyUb chains on TRIF, and the reaction is reversed by USP19 [81]. Tumorigenesis can be also regulated by K27 Ub chains. For example, BRFA (key player in tumorigenesis and MEK/ERK pathway) is modified by K27 Ub chains by the ITCH Ub E3 ligase, regulating proliferation and invasion in melanoma cells [82]. Further investigations are required to evaluate full potential of K27 Ub chains to regulate other functions.

5. Ubiquitin chains dynamics in autophagy regulation

The Autophagy Lysosome System (ALS) is one of the main intracellular degradation systems, together with the UPS. Autophagy digests long-lived, protein aggregates, stress RNA granules, and abnormal cytoplasmic organelles, including among others, mitochondria. Chaperone-mediated autophagy, microautophagy and macroautophagy use distinct mechanisms to drive proteolysis. Chaperone-mediated autophagy uses HSC70 to sequester proteins containing a KFERQ motif into lysosomes. Microautophagy is a direct lysosomal uptake of substrates whereas in macroautophagy (here referred as autophagy), cytosolic cargos are sequestered by a double membrane vesicle including a fraction of the cytoplasm using a complex multistep process. Recent general autophagy reviews give more details on the whole process [83].

5.1. Activation of autophagy by non-proteolytic ubiquitin chains

Several Ub chains and Ub-like molecules play an important role in the regulation of autophagy and in the crosstalk between the UPS and ALS. Nevertheless, their role in distinct mechanisms including the regulation of signaling cascades and targeting cargoes to proteolysis has not been fully elucidated. It has been suggested that non-degradative Ub chains stimulate autophagy induction, whereas degradative Ub chains are needed to restore the basal autophagy flux once the stress situation is resolved [84]. UbE3s and DUBs determine K63 and K48 Ub chains formed on distinct regulatory complexes and define their role in a dynamic reversible manner (Fig. 3) [85]. The initiation of autophagy and autophagosome formation is regulated by ULK1 and PI3K-III kinases whose activity is regulated by mTORC1 and AMPK dependent phosphorylation [86]. Ubiquitylation mediated by the concerted action of various E3 ligases also contributes to regulating autophagy initiation and autophagosome formation [85]. For instance, the Ub E3 TRAF6 can regulate ULK1 and PI3K-III kinases by the formation of K63 chains. Upon starvation, TRAF6 uses unphosphorylated AMBRA1 (Autophagy and BECLIN 1 Regulator 1) to bind ULK1 which is stabilized and activated by K63 chains favoring autophagy (Fig. 3A). K63-activated ULK1 phosphorylates AMBRA1 to set a regulatory autophagy loop. Interestingly mTORC1 also phosphorylates AMBRA1 on distinct sites and controls ULK1 ubiquitylation self-association and function, which has a negative effect on autophagy [87].

The catalytic core of the PI3K–III complex is regulated by TRAF6-mediated K63 ubiquitylation of BECLIN 1 which abolishes its binding to BCL2 and induces autophagy (Fig. 3A). A20, a DUB that hydrolyzes the K63 chain of BECLIN 1, contributes to restore the binding to BCL2 [88,89]. BECLIN 1 phosphorylation by DAPK negatively regulates its association with BCL2, underlining an important interplay between these two PTMs to regulate autophagy [90]. Other Ub E3s such as Rbx1/Cul4-ligase can also form a complex with AMBRA1 to target BECLIN 1 under starvation. ULK1 can also phosphorylate BECLIN 1, increasing the PI3K–III complex activity [91]. Other members of the Ub family such as SUMO contribute to regulating the PI3K-III complex since VPS34, a component of the catalytic core of this complex, is targeted by the SUMO ligase KAP1. SUMOylated VPS34 increases its interactions within the PI3K–III complex and promotes phagophore formation [92].

5.2. Autophagy termination is regulated by degradative ubiquitylation

Under normal growth conditions or when a specific stress situation is finished, autophagy is stopped to avoid the unnecessary destruction of cellular components that could compromise cell viability. Phosphorylation and ubiquitylation also contribute to switch off the activity of the ULK1 and PI3K–III complexes [84]. In particular, K11 and K48 Ub chains have been proposed to promote the proteasomal degradation of autophagy regulators to restore a new equilibrium compatible with the physiological basal autophagy flux. NEDD4, a Ub E3 of the HECT family, uses K11 Ub chains to target BECLIN1 for degradation, limiting autophagy [93] (Fig. 3B). Interestingly, an E3 ligase homologous to NEDD4, called NEDD4L, drives the proteasome degradation of ULK1 via K27 and K29 chains during autophagy [94] (Fig. 3B). The CULLIN3–KHLH20 ligase can also drive the K48 chains-driven degradation of ULK1, BECLIN 1, and VPS34 [95] highlighting the participation of several ligases in the control of both autophagy induction and termination. During starvation, AMBRA1 is another important factor targeted for proteasome-mediated proteolysis by various Ub ligases including CULLIN4–DDB1 [96] or RNF2 [97].

Protein de-ubiquitylation importantly contributes to regulate the degradation of autophagy regulators, like DUBs USP13 and USP10 that protect BECLIN 1 from ubiquitylation. Their chemical inhibition by Spautin-1treatment drives a Ub-proteasome mediated degradation of BECLIN 1. The chemical separation of BECLIN 1 from its chaperone HSP90 by geldanamycin also results in the K48 ubiquitylation of BECLIN 1 [98] (Fig. 3B).

It is clear that the autophagy system uses multiple E3 ligases to regulate different steps inside this pathway like the activation, progression and the termination of the flux. We can speculate that a DUB will be counteracting their role for each ubiquitylation reaction. However, many of these enzymes are still uncharacterized.

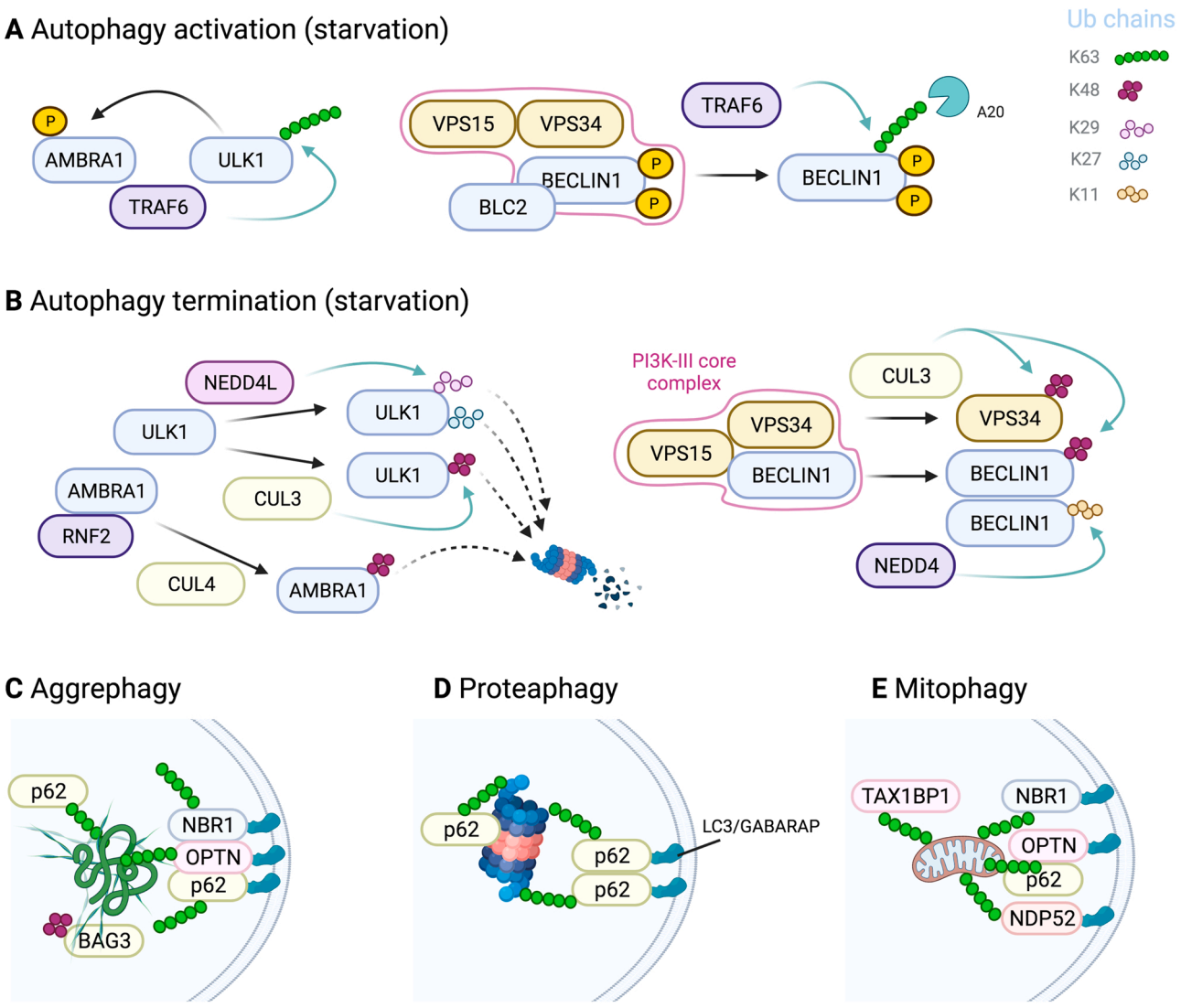

Fig. 3. Multiple steps of autophagy are regulated by Ub chains. Several Ub chains and Ub-like molecules play an important role in the regulation of autophagy and in the crosstalk of the UP and AL systems. While non-degradative Ub chains stimulate autophagy induction (A), degradative Ub chains are needed to terminate it (B). (A) TRAF6 form K63 chains that regulate ULK1 and PI3K-III kinases. TRAF6 also uses AMBRA1 to bind and stabilize ULK1 by forming K63 chains and activate autophagy. DUBs such as A20 regulate ubiquitin chains formed on distinct regulatory complexes and define their role in a dynamic reversible manner (see main text). (B) K11 and K48 Ub chains promote proteasomal degradation of crucial regulators to control autophagy. For example, NEDD4 targets BECLIN1 for degradation to inhibit autophagy and NEDD4L that induce proteasomal degradation of ULK1. Selective autophagy events such as aggrephagy (C), proteaphagy (D) or Mitophagy (E) involve the participation of K63 Ub chains but also degradative chains. The type of chains involved depends in a large proportion in the stimuli activating these proteolytic events. The UbL proteins LC3/GABARAP contribute to the cargo recruitment into the phagophores, illustrated with a double membrane. Several autophagy receptors have been involved in these selective events such as p62, NBR1, OPTN or NDP52. For some of these selective events such as proteaphagy, the information available is still limited (see main text).

5.3. Role of Ub in selective autophagy pathways

The concept of selective autophagy derives from the fact that distinct types of aggregated proteins and damaged organelles are targeted for degradation under distinct physiologic and pathologic situations, implying the existence of specialized pathways. However, some of the enzymes, adapters and cofactors are shared under certain circumstances, complicating our understanding of the selectivity of proteolytic events. This includes the autophagy receptors that bring cargoes into autophagosomes for clearance. More than 30 autophagy receptors, also called Sequestosome-1-like receptors (SLRs) after the first described p62/SQSTM1 (Sequestosome 1) [99]. p62 carries a UBA, a UBD that binds ubiquitylated cargoes. The UBA domain of p62 can homodimerize, modulating its interaction with monoubiquitin. p62 contains LC3 Interacting Regions (LIR) that interact with ATG8 proteins that will be integrated into autophagosomes. Other SLRs with similar architecture include Next to BRCA1 gene 1 protein (NBR1), Optineurin (OPTN) or the nuclear dot protein 52 kDa (NDP52). The diversity of receptors underlines the complex regulation of selective autophagy mechanisms. Some of them show functional redundancy for cargo recognition and cooperate with multiple cofactors [100].

Selective autophagy events can be classified as Ub-dependent or -independent. The receptors involved in Ub-dependent autophagy bind Ub chains through a UBD which is absent in receptors implicated in Ub-independent autophagy. However, some cargos can be transported in a Ub-dependent and independent manner. It is most likely the reason why selective autophagy events are named according to the cargo they transport [101]. K63 Ub chains show preferential binding for the autophagy receptors [102], while K48, K27 and K11 Ub chains target for proteasomal degradation (Fig. 3). Nevertheless, in situations of defective

autophagy, all Ub chains have been found enriched [103], most likely due to the fact that these chain types are also involved in the regulation of other cellular functions. The accumulation of Ub aggregates might also contribute to increasing the affinity of autophagy receptors for the cargoes. The role of Ub chains in the regulation of autophagy is still under investigation. Regardless of their Ub dependency, all autophagy receptors contain LC3-interacting regions (LIRs) that bind other members of the Ub family in mammalians (LC3/GABARAP) or yeast (ATG8) (Fig. 3). These ATG8 molecules contribute to expanding the autophagosomes and providing specificity to selective autophagy events.

Around 20 types of selective autophagy have been reported, half of them driven by Ub [101]. Selective autophagy events include aggrephagy and mitophagy (that will be further developed in this review) but also xenophagy, lysophagy and ERphagy, to name a few. Characterized more recently, proteaphagy is quite intriguing since together with aggrephagy, it importantly contributes to the crosstalk between the UPS and ALS and is activated under similar stress stimuli. The nature of the aggrephagy-proteaphagy interconnection has not been totally explored (Fig. 3).

5.3.1. Aggrephagy

Heat-shock stress or proteotoxic insults generate protein aggregates. Part of these aggregated proteins are degraded by the proteasome via K48 chains while K63 chains activate the aggrephagy machinery to recruit the autophagy receptors p62, OPTN and NBR1 (Fig. 3C) [104]. These autophagy receptors and K63 Ub chains are essential to present proteins aggregates for autophagosome inclusion. The aggregation process itself involves the participation of other UbL molecules such as SUMO-1 and FAT10 [105,106]. BAG3 also interacts with K48 chains and p62, favoring ALS degradation of ubiquitylated proteins. Interestingly, another member of the same family named BAG1 favors the presentation of misfolded proteins to the proteasome underlining the participation of BAG proteins in the balance between both proteolytic pathways [107] (Fig. 3C). Several DUBs are other important actors of the degradation of protein aggregates, including the RPN11 proteasome subunit that recruits HDAC6 to promote autophagy degradation [108,109]. The role of DUBs in the autophagy-dependent degradation of proteins aggregates is still under investigation, but examples, like USP9X that acts on mono-ubiquitylated synuclein to favor aggrephagy rather than proteasomal degradation, illustrate the importance of these enzymes in selecting the proteolytic pathway to be used to eliminate these cargoes [110].

5.3.2. Proteaphagy

Upon nutrient starvation, autophagy works as a recycling machine to recover the nutrient pool from dysfunctional cellular components [111]. Under these circumstances, proteaphagy represents an efficient strategy to face nutrient limitation. Marshall et al. proved that proteaphagy occurs in both *Arabidopsis taliana* and *Saccharomyces cerevisiae* under nitrogen starvation [112]. Nuclear proteasomes are also regulated by proteaphagy but the core particle (CP) and 19S subunit/regulatory particle (RP) have to be dissociated prior to their nuclear export in yeast. The autophagy of the CP depends on the DUB Ubp3, while RP export for cytosolic degradation relies on ATG7 and ATG17 factors [113].

In mammalian cells, proteaphagy is also activated in response to amino acid starvation. Proteaphagy induced by amino acid starvation involves the polyubiquitylation of proteasomes subunits RPN1, RPN2, RPN10 and RPN13. The autophagy receptor p62 is required to drive the degradation of ubiquitylated proteasomes [114]. The participation of distinct autophagy receptors in distinct biological models and stress conditions suggest that the molecules involved can be distinct [115].

Proteaphagy can also be induced when the proteasome activity is impaired by point mutations or chemical inhibition by proteasome inhibitors [115]. After proteasome inhibition, ubiquitylated RP subunits are recognized by the autophagy receptor p62 [112,116,117] (Fig. 3D). In *Arabidopsis,* RPN10 acts as an autophagy receptor to promote the proteaphagy of inactive 26S proteasomes but does not participate in starvation-induced proteaphagy. In this process, USP2 plays a role as a regulator of RPN10 stability [112]. In yeast, Cue5 acts as an autophagy receptor to mediate proteaphagy after chemical inhibition and genetic mutation of 26S proteasomes [118]. The nature of the Ub chains implicated in proteaphagy must be better defined, but while K48 Ub chains are decreased, K63 Ub chains are enriched after proteasome inhibition in Bortezomib resistant cells [116,119].The Ub ligases and DUBs implicated in proteaphagy remains to be identified.

5.3.3. Mitophagy

Mitochondrial degradation is a good example of collaboration between the autophagy and the proteasome, where Ub plays an important role (Fig. 3E). Mitophagy can also be achieved in a Ub-independent manner and involve the autophagy receptors FUNDC1, BNIP3, and NIX [120].

Ub-dependent mitophagy involves the E3 Ub ligase PARKIN, which is activated by PINK1-mediated phosphorylation, increasing the ubiquitylation of mitochondrial outer membrane (MOM) proteins. PINK1 also phosphorylates Ub chains on the mitochondrial surface, increasing mitophagy due to the higher affinity of PARKIN for phospho-Ub chains [121–123]. PARKIN ubiquitylation favors the binding of several autophagy receptors including p62, OPTN, NPD2, TAX1BP1, and NBR1. PARKIN interacts with AMBRA1 that could potentially recruit Ub E3s such as TRAF6 and CUL4–DDB1 to the mitochondria. It also regulates the interaction of BECLIN1 with BCL2 by controlling the monoubiquitylation levels of BCL2 and blocking BECLIN1 function in autophagy [124]. Therefore, PARKIN plays multiple roles by promoting autophagy through the formation of K63 and K48 chains on the mitochondria but also inhibits autophagy when it monoubiquitylates BCL2. The DUB USP30 controls PARKIN activity by removing preferentially K6 and K11 polyUb chains from the mitochondrial surface [125]. K6 Ub linkages have also been detected in MOM proteins. Using Ub linkage-specific affirmers for K6, Michel et al., identified HUWE1 E3 as the major source of K6 Ub chain formation inside the cells. HUWE1 modifies mitofusin-2 (Mfn2), a known substrate required for mitochondrial membrane remodeling during mitophagy [126]. On the other side, a reduced membrane potential leads to the accumulation of the mitochondrial kinase PINK1 and subsequently the E3 Ub ligase PARKIN which predominantly assembles K6-linked Ub chains. Distinct Ub chains appear as key regulators of PARKIN-mediated mitophagy and can be disassembled by DUBs like USP8, USP15, USP30 and USP33 [126,127]. Ub-dependent or independent mitophagy must go through a fission process to be incorporated into autophagosomes.

Ub also plays an important role in mitochondrial fission and fusion since it modifies the MOM proteins MFN1/2, FIS1, DRP1, and OPA1, driving their K48 Ub chain-dependent proteasomal degradation with consequences in the mitochondrial network [128,129]. The degradation of MFN2 and OPA1 favors mitochondrial fission, which is required to isolate a single damaged organelle. Under starvation, healthy mitochondria escape proteasomal degradation by promoting their elongation to preserve ATP production and avoid mitophagy [130].

6. Ubiquitin chains dynamics in DNA repair

Cells possess different mechanisms to contend with exogenous or endogenous events that cause damage to DNA integrity. The DNA damage response encompasses a set of mechanisms involving detection, signaling and initiation of DNA repair. According to the type of damage, a particular pathway is triggered by the cell to repair the lesion. DNA adducts or ultraviolet (UV)-induced DNA lesions are repaired by the nucleotide excision repair (NER) mechanism. The Fanconi anemia pathway (FA) repairs DNA crosslinks, while base lesions are repaired by the base excision repair (BER) pathway [131]. DNA double-strand breaks (DSB) are low-frequency types of DNA damage producing very drastic effects when they are unrepaired or incorrectly repaired, leading

to genome instability promoting subsequent disorders such as cancer. Ubiquitylation regulates multiple steps of these mechanisms as will be reviewed below (Fig. 4).

When a DSB occurs, two major repair mechanisms can be initiated: nonhomologous end-joining (NHEJ) and homologous recombination (HR). Fidelity and template requirements are the main differences between the two ways. NHEJ modifies the broken DNA ends and ligates them together with no homology or reference template, therefore being considered as an error prone mechanism generating deletions or insertions. In contrast, HR requires a DNA template on the sister chromatid or homologous chromosome to repair the DSB and restore the original sequence [131]. After DSB, the ataxia telangiectasia mutated (ATM/ATR) signaling pathway takes place rendering a serial of PTMs over histones and intermediate proteins as H2AX and mediator of DNA damage checkpoint protein 1 (MDC1). Ubiquitylation of histones is essential to select one of the two repairing ways. The E3 ligases RNF8 (RING finger protein 8) and RNF168 have a major role in promoting NHEJ mechanism, while the E3 ligase complex BRCA1/BARD1 (breast cancer susceptibility gene 1/BRCA1-associated RING-domain protein) promotes HR. In both cases, the main target is the histone H2A through ubiquitylation on specific sites. It was first thought that RNF8 had a priming role as E3 ligase, undertaking H2A ubiquitylation, followed by extension of K63-chains by RNF168. However, it became evident that RNF8 in coordination with the Ub E2 UBC13, is responsible of the observed K63 Ub chains generated at DSB sites even if the target substrate was not identified [132]. Thorslund T. and colleagues identified, by proteomics studies, that the isoforms of the linker histone H1 (H1.2 and H1.x) were substrates of the RNF8-UBC13 complex. The

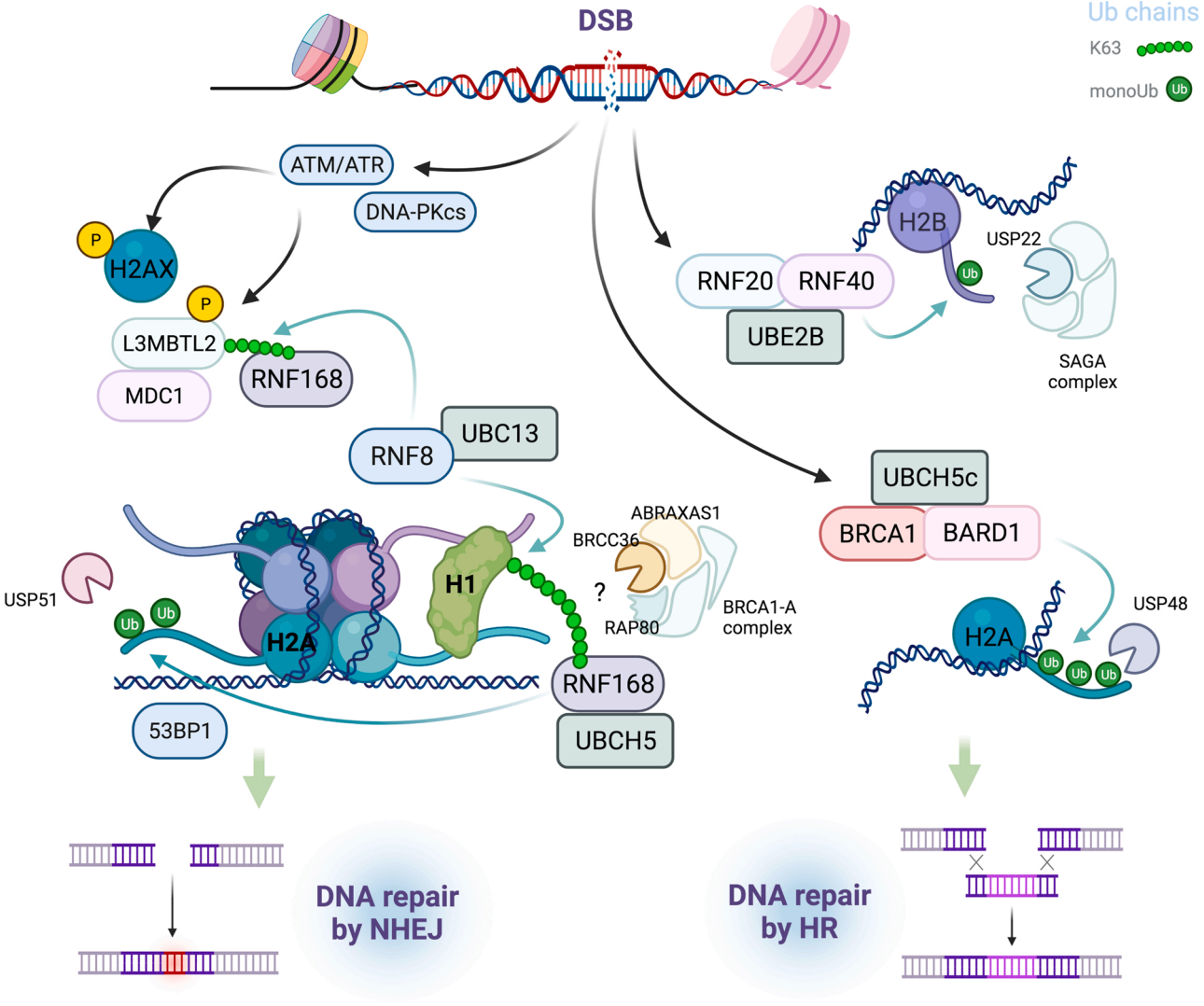

Fig. 4. Regulation of DNA repair by multiple Ub chain types. Protein ubiquitylation regulates the two major DNA repair mechanisms initiated by nonhomologous end-joining (NHEJ) and homologous recombination (HR). The ataxia telangiectasia mutated (ATM/ATR) signaling pathway regulate H2AX and the mediator of DNA damage checkpoint protein 1 (MDC1). Ubiquitylation of histones determine the DNA repair mechanisms that will be used. While the E3 ligases RNF8 and RNF168 promote NHEJ mechanism, the E3 ligase complex BRCA1/BARD1 (breast cancer susceptibility gene 1/BRCA1-associated RING-domain protein) promotes HR. RNF8 and the Ub E2 UBC13 form K63 Ub chains at DSB sites. The K63-polyubiquitylation of histone H1 allows the recruitment of RNF168 and the E2 UBCH5 which initiates the ubiquitylation events on histone H2A at K13 and K15 sites recruiting the repairing protein p53-binding protein 1 (53BP1) towards nucleosomes near sites of broken DNA. RNF168 also promotes non-canonical K27-linked chains on histones H2A/H2A.X which is crucial in the DNA stress response since allow the recruitment of mediators like 53BP1, and BRCA1. The USP51 deubiquitylating enzyme regulate H2A ubiquitylation. DSB induced by ionizing radiation enrolls the E3 heterodimer, RNF20/RNF40 (BRE1 complex). Together with the Ub E2 UBE2B (RAD6), the BRE1 complex to promotes monoubiquitylation on histone H2B which has a critical role in cellular functions. H2B is deubiquitylated by the Spt-Ada-Gcn5-acetyltransferase (SAGA) complex which integrates the DUB ubiquitin-specific protease 22 (Usp22). The complex BRCA1/BARD1 modifies H2A favouring HR mechanism. The USP48 deubiquitylating activity regulates BRCA1–BARD1 modifications and promotes the DNA-end resectioning.

K63-polyubiquitylation of histone H1 at DSB sites is the signal for enrollment of RNF168 which initiates the ubiquitylation events on histone H2A [133]. RNF168, in combination with the E2 UBCH5, directs mono-ubiquitylation of the N-terminal region of histone H2A at K13 and K15 sites; specifically K15 ubiquitylation promotes recruiting of repairing protein p53-binding protein 1 (53BP1) towards nucleosomes near sites of broken DNA [134]. In 2015, Gatti et al., demonstrated that RNF168 also promotes non-canonical K27-linked chains on histones H2A/H2A.X upon DNA damage. This modification appears to be crucial in the DNA stress response, as mutations on Ub K27 prevent DNA damage response activation and the recruitment of mediators like 53BP1, and BRCA1 [4,135]. 53BP1 endorses DNA repair by NHEJ mechanism antagonizing DNA end resection that is the initial step in HR. To counteract H2A ubiquitylation at K13 and K15, the role of USP51 as a deubiquitylating enzyme has been demonstrated [136].

Once DSB triggers the ATM/ATR pathway, kinases guide phosphorylation of histones H2AX, MDC1 and L3MBTL2 (lethal (3) malignant brain tumor-like protein 2). L3MBTL2 is a polycomb group protein essential for embryonic development which is mutated in malignancies such as leukemia. ATM-mediated phosphorylation of L3MBTL2 promotes its interaction with MDC1 and localizes it to the DSB site. In addition to the H1 ubiquitylation by RNF8, this E3 can also conjugate K63-Ub chains into L3MBTL2 that allows its binding to the UDM1 domain of RNF168. UDM1 specifically recognizes K63-linked Ub chains and in this way RNF168 is attracted to the DSB site [137]. The same mechanism allows the UDM1 to interact with polyubiquitylated H1. Therefore, RNF8 and RNF168 are sequentially recruited at DSB sites and K63-linked chains generated by the complex RNF8-UBC13 are necessary for RNF168 participation. K63-Ub chains can be regulated by the deubiquitylating activity of BRCC36 (BRCC3), a DUB member belonging to the JAMM family that forms a heterodimeric complex with ABRAXAS1 (a metalloprotease-like with no activity) [138]. BRCC36 and ABRAXAS1 are scaffold subunits of a macro-multi-protein complex known as BRCA1-A complex, that is also recruited by K63-chains through the UIM domain of the RAP80 subunit [8,139]. Depletion of BRCC36 compromises the G2/M cell cycle checkpoint, inactivating BRCC36 DUB by RNAi and genome editing attenuates BRCA1-A functions at DSBs and leads to unrestrained DSB end resection and hyperactive DNA repair [140].

According to Kaiser S.E. et al., approximately 65% of total Ub (present in cell lines) are conjugated as mono Ub, and from this pool ~ 30% are present on the histones fraction. Histone H2A is probably the most abundant ubiquitylated protein in the cell [141]. Three E3s enable H2A monoubiquitylation including RNF168 that was already mentioned. RING1B/ BMI1 is another E3 which is part of the polycomb repressive complex 1 (PRC1) and is responsible of the canonical K119 site modification. A third E3 is the complex BRCA1/BARD1 which modifies the K125, K127 and K129 sites located at the C-terminal of histone H2A [132]. Ubiquitylation by PRC1 takes part in transcriptional silencing that is more related to chromatin remodeling or epigenetics than DNA repair, while ubiquitylation by BRCA1/BARD1 inclines the balance for the HR mechanism.

BRCA1/BARD1 occupancy at DSBs antagonizes 53BP1. The BRCA1/BARD1 heterodimeric complex harbors a RING domain on each monomer through which it interacts with E2 enzymes [142]. Very recently, the structure of BRCA1/BARD1 heterodimer with the E2 enzyme UBCH5c bound to the nucleosome was resolved by cryo-EM. The H2A K-targeted by BRCA1/BARD1 (125/127/129) are nearby to those targeted by RING1B/BMI1 (118/119) but reside in the fully disordered flexible C-terminal tail of H2A. It is particularly interesting that the BRCA1/BARD1 complex selectively ubiquitylates only K125, K127 and K129 positions. Heterodimer arrangement effectively tilts the BRCA1 E2 interaction site, orienting UBCH5c active site away from the K119 position. This interface is also sensitive to H3 K79 methylation status and mutations found in individuals are associated with cancer [143]. USP48 deubiquitylating activity counters the BRCA1–BARD1 modifications and promotes the DNA-end resectioning [8].

DSB induced by ionizing radiation leads to enrollment of another E3 heterodimer, RNF20/RNF40 (BRE1 complex). This ligase operates with the Ub E2 UBE2B (RAD6) to promote monoubiquitylation on histone H2B at the K120 site. H2B ubiquitylation has a critical role in cellular function, and its impairment has been linked to various cancers [144]. H2B is deubiquitylated by the Spt-Ada-Gcn5-acetyltransferase (SAGA) complex deubiquitylation module, composed of ENY2, ATXN7, ATXN7L3, and the DUB Ub-specific protease 22 (Usp22). There is evidence of the RNF20/RNF40 role in HR as they are required for CtIP- and NBS1-dependent end resection. Observations also point out that BRE1 has a role in NHEJ for repair of I-SceI-induced DSBs which requires repression of resection [144]. A more accepted role for H2B monoubiquitylation is to allow access of repair proteins to DNA by promoting displacement of one H2A/H2B dimer from the nucleosome barrier for transcription activation [145].

If K63-linked chains and monoUb are important for recruiting of repairing factors, other Ub linkages participate in regulating other DNA damage events. It has been reported that RNF8 can conjugate K11-linked Ub chains in coordination with the E2 UBE2S [146]. The K11-linked ubiquitylation plays a critical role in inhibiting transcription at sites of damage and is essential for cellular resistance to ionizing radiation. The DUB enzyme Cezanne (OTUD7B), a member of OTU family, has been shown to catalyze hydrolysis of K11-linked Ub chains even if its role has been mainly described in the regulation of the NF-κB pathway [147]. In response to DSB, Cezanne antagonizes the activity of RNF8 and UBE2S [146].

Searching for K63-linked Ub chain-specific binders, Wu X. and collaborators developed a UBD microarray where UBA domains of Cezanne and Cezanne2 were identified as selective for K63 but not K48- or K11-linked chains. Cells depleted of Cezanne by siRNAs or knockout (KO) cells generated by CRISPR-Cas9, showed diminished ionizing radiation-induced foci of Abraxas and BRCA1 seemingly as occurs with depletion of Rap80, the subunit component of BRCA1-A complex responsible of recruiting towards K63-linked foci. Intriguingly, their experiments suggested that Cezanne promotes Rap80/Abraxas/BRCA1 recruitment to DNA damage sites through its UBA domain binding to K63-conjugates, and its DUB activity disassembled K11-linked Ub chains. A model has been proposed where Cezanne serves as a “reader” of the K63-linkage and “eraser” of the K11-linkage ubiquitylation for the regulation of DNA damage response [148].

7. Conclusions and future perspectives

Over the last 20 years, Ub and UbL proteins have appeared as key regulators of the proteome and cellular plasticity, since these PTMs determine not only stability and localization of modified targets but also their function depending on the stimuli. The clinical relevance of these PTMs is based on the hundreds of reported diseases where deletions, translocations and mutations affect Ub chain synthesis, deconjugation, recognition and connection with effector functions. Understanding the meaning of the Ub language and its regulation will be crucial to better assess the possibilities for therapeutic intervention. Despite the technological progress on mass spectrometry analysis to unveil the Ub chain complexity, our community still faces a lack of tools to identify complex chains. Most of the available tools provide information on homotypic Ub chains. However, we know that distinct and complex Ub-chains exist and some of them include other PTM modifications related to the Ub family (eg. SUMO or NEDD8) or not (eg. phosphorylation or acetylation). Deciphering how Ub moieties are disposed within a complex Ub chain is still challenging [149]. Distinct tools such as molecular traps (eg. TUBEs), peptide aptamers (eg. nanobodies) or affimers, were recently developed to get information on specific chain types. One can expect that in the near future more tools recognizing all Ub chain linkages or modified Ub will be developed and the identification and characterization of non-homotypic, mixed or branched chains will be

possible [15]. The highly dynamic action of DUBs further complicates our understanding of Ub chains. With or without dedicated chain specificity, they indeed remodel Ub polymers depending on the stimuli, time, and cellular space where the substrate is present. It is also important to keep in mind that the concept of one enzyme for one target used, to easily explain or simplify our research paradigms is called into question. Since functional redundancy might exists between Ub enzymes to act on a single target and some targets could be modified by several members of the Ub family, cooperation or opposition could exist to control Ub-driven functions. The identification of enzymes participating in Ub chain synthesis and remodeling in physiology and pathology will be crucial to understand how cells remodel their proteome to face distinct situations. These efforts should allow the selection of the best candidate biomarkers and drug targets.

Declaration of Competing Interest

The authors declare that they have no known competing financial interests or personal relationships that could have appeared to influence the work reported in this paper.

Acknowledgments

We thank Clémence Coutelle-Rebut for the proofreading, Sofia Lobato-Gil for the critical reading of this manuscript and Leticia Olvera-Rodríguez for helping with figures. MGS is fellow from the UbiCODE project funded by the EU's Horizon 2020 research and innovation program under the Marie Skłodowska-Curie grant agreement (No. 765445) and the Association contre le Cancer (ARC). CB is fellow from la ligue contre le Cancer (TAJV22303). WX thanks the support from Consejo Nacional de Ciencia y Tecnología (CONACYT) grant CB-2017-2018-A1-S-22895. MSR is also funded by the Telethon, the REPERE and pre-maturation program of Occitanie and Consejo Nacional de Ciencia y Tecnologia- Secretaria de Relaciones Exteriores CONACYT-SRE (Mexico) Grant 0280365. Biorender was used to draw all figures.

References

[1] P. Gâtel, M. Piechaczyk, G. Bossis, Ubiquitin, SUMO, and Nedd8 as therapeutic targets in cancer, Adv. Exp. Med. Biol. 1233 (2020) 29–54, https://doi.org/10.1007/978-3-030-38266-7_2.

[2] L.D. Harris, S. Jasem, J.D.F. Licchesi, The ubiquitin system in Alzheimer's disease, Adv. Exp. Med. Biol. 1233 (2020) 195–221, https://doi.org/10.1007/978-3-030-38266-7_8.

[3] M.E. Davis, M.U. Gack, Ubiquitination in the antiviral immune response, Virology 479–480 (2015) 52–65, https://doi.org/10.1016/j.virol.2015.02.033.

[4] M. Akutsu, I. Dikic, A. Bremm, Ubiquitin chain diversity at a glance, J. Cell Sci. 129 (2016) 875–880, https://doi.org/10.1242/jcs.183954.

[5] R.-H. Chen, Y.-H. Chen, T.-Y. Huang, Ubiquitin-mediated regulation of autophagy, J. Biomed. Sci. 26 (2019) 80, https://doi.org/10.1186/s12929-019-0569-y.

[6] M.L. Mendes, M.R. Fougeras, G. Dittmar, Analysis of ubiquitin signaling and chain topology cross-talk, J. Proteom. 215 (2020), 103634, https://doi.org/10.1016/j.jprot.2020.103634.

[7] D.A. Pérez Berrocal, K.F. Witting, H. Ovaa, M.P.C. Mulder, Hybrid chains: a collaboration of ubiquitin and ubiquitin-like modifiers introducing cross-functionality to the ubiquitin code, Front. Chem. 7 (2019) 931, https://doi.org/10.3389/fchem.2019.00931.

[8] M.J. Clague, S. Urbé, D. Komander, Breaking the chains: deubiquitylating enzyme specificity begets function, Nat. Rev. Mol. Cell Biol. 20 (2019) 338–352, https://doi.org/10.1038/s41580-019-0099-1.

[9] M.P.C. Mulder, K.F. Witting, H. Ovaa, Cracking the ubiquitin code: the ubiquitin toolbox, Curr. Issues Mol. Biol. 37 (2020) 1–20, https://doi.org/10.21775/cimb.037.001.

[10] K. Kliza, K. Husnjak, Resolving the complexity of ubiquitin networks, Front. Mol. Biosci. 7 (2020) 21, https://doi.org/10.3389/fmolb.2020.00021.

[11] K.N. Swatek, D. Komander, Ubiquitin modifications, Cell Res. 26 (2016) 399–422, https://doi.org/10.1038/cr.2016.39.

[12] A.J. McClellan, S.H. Laugesen, L. Ellgaard, Cellular functions and molecular mechanisms of non-lysine ubiquitination, Open Biol. 9 (2019), 190147, https://doi.org/10.1098/rsob.190147.

[13] G. Dittmar, K.F. Winklhofer, Linear ubiquitin chains: cellular functions and strategies for detection and quantification, Front. Chem. 7 (2019) 915, https://doi.org/10.3389/fchem.2019.00915.

[14] M.E. French, C.F. Koehler, T. Hunter, Emerging functions of branched ubiquitin chains, Cell Discov. 7 (2021) 6, https://doi.org/10.1038/s41421-020-00237-y.

[15] K.N. Swatek, J.L. Usher, A.F. Kueck, C. Gladkova, T.E.T. Mevissen, J.N. Pruneda, et al., Insights into ubiquitin chain architecture using Ub-clipping, Nature 572 (2019) 533–537, https://doi.org/10.1038/s41586-019-1482-y.

[16] Z.-J. Han, Y.-H. Feng, B.-H. Gu, Y.-M. Li, H. Chen, The post-translational modification, SUMOylation, and cancer (review), Int. J. Oncol. 52 (2018) 1081–1094, https://doi.org/10.3892/ijo.2018.4280.

[17] J. Yao, X. Liang, Y. Liu, M. Zheng, Neddylation: a versatile pathway takes on chronic liver diseases, Front. Med. 7 (2020), 586881, https://doi.org/10.3389/fmed.2020.586881 (Lausanne).

[18] Y. Lu, B. Lee, R.W. King, D. Finley, M.W. Kirschner, Substrate degradation by the proteasome: a single-molecule kinetic analysis, Science (2015) 348, https://doi.org/10.1126/science.1250834.

[19] Y. Kravtsova-Ivantsiv, S. Cohen, A. Ciechanover, Modification by single ubiquitin moieties rather than polyubiquitination is sufficient for proteasomal processing of the p105 NF-κB precursor, Adv. Exp. Med. Biol. 691 (2011) 95–106, https://doi.org/10.1007/978-1-4419-6612-4_10.

[20] N.V. Dimova, N.A. Hathaway, B.-H. Lee, D.S. Kirkpatrick, M.L. Berkowitz, S. P. Gygi, et al., APC/C-mediated multiple monoubiquitylation provides an alternative degradation signal for cyclin B1, Nat. Cell Biol. 14 (2012) 168–176, https://doi.org/10.1038/ncb2425.

[21] J.A. Nathan, H.T. Kim, L. Ting, S.P. Gygi, A.L. Goldberg, Why do cellular proteins linked to K63-polyubiquitin chains not associate with proteasomes? EMBO J. 32 (2013) 552–565, https://doi.org/10.1038/emboj.2012.354.

[22] H. Tsuchiya, F. Ohtake, N. Arai, A. Kaiho, S. Yasuda, K. Tanaka, et al., In vivo ubiquitin linkage-type analysis reveals that the Cdc48-Rad23/Dsk2 axis contributes to K48-linked chain specificity of the proteasome, Mol. Cell 66 (2017) 488–502, https://doi.org/10.1016/j.molcel.2017.04.024, e7.

[23] M.J. Clague, S. Urbé, Ubiquitin: same molecule, different degradation pathways, Cell 143 (2010) 682–685, https://doi.org/10.1016/j.cell.2010.11.012.

[24] G.L. Grice, I.T. Lobb, M.P. Weekes, S.P. Gygi, R. Antrobus, J.A. Nathan, The proteasome distinguishes between heterotypic and homotypic lysine-11-linked polyubiquitin chains, Cell Rep. 12 (2015) 545–553, https://doi.org/10.1016/j.celrep.2015.06.061.

[25] R.G. Yau, K. Doerner, E.R. Castellanos, D.L. Haakonsen, A. Werner, N. Wang, et al., Assembly and function of heterotypic ubiquitin chains in cell-cycle and protein quality control, Cell 171 (2017) 918–933, https://doi.org/10.1016/j.cell.2017.09.040, e20.

[26] R. Baur, M. Rape, Getting close: insight into the structure and function of K11/K48-branched ubiquitin chains, Structure 28 (2020) 1–3, https://doi.org/10.1016/j.str.2019.12.004.

[27] R.S. Samant, C.M. Livingston, E.M. Sontag, J. Frydman, Distinct proteostasis circuits cooperate in nuclear and cytoplasmic protein quality control, Nature 563 (2018) 407–411, https://doi.org/10.1038/s41586-018-0678-x.

[28] A. Bremm, S. Moniz, J. Mader, S. Rocha, D. Komander, Cezanne (OTUD7B) regulates HIF-1α homeostasis in a proteasome-independent manner, EMBO Rep. 15 (2014) 1268–1277, https://doi.org/10.15252/embr.201438850.

[29] S. Moniz, D. Bandarra, J. Biddlestone, K.J. Campbell, D. Komander, A. Bremm, et al., Cezanne regulates E2F1-dependent HIF2α expression, J. Cell Sci. 128 (2015) 3082–3093, https://doi.org/10.1242/jcs.168864.

[30] K. Yan, M. Ponnusamy, Y. Xin, Q. Wang, P. Li, K. Wang, The role of K63–linked polyubiquitination in cardiac hypertrophy, J. Cell Mol. Med. 22 (2018) 4558–4567, https://doi.org/10.1111/jcmm.13669.

[31] H. Xu, M. You, H. Shi, Y. Hou, Ubiquitin-mediated NFκB degradation pathway, Cell Mol. Immunol. 12 (2015) 653–655, https://doi.org/10.1038/cmi.2014.99.

[32] J. Chen, Z.J. Chen, Regulation of NF-κB by ubiquitination, Curr. Opin. Immunol. 25 (2013) 4–12, https://doi.org/10.1016/j.coi.2012.12.005.

[33] G. Courtois, M.-O. Fauvarque, The many roles of ubiquitin in NF-κB signaling, Biomedicines 6 (2018), E43, https://doi.org/10.3390/biomedicines6020043.

[34] S.-C. Sun, The non-canonical NF-κB pathway in immunity and inflammation, Nat. Rev. Immunol. 17 (2017) 545–558, https://doi.org/10.1038/nri.2017.52.

[35] B. Dumétier, A. Zadoroznyj, L. Dubrez, IAP-mediated protein ubiquitination in regulating cell signaling, Cells 9 (2020), E1118, https://doi.org/10.3390/cells9051118.

[36] Z.-P. Xia, L. Sun, X. Chen, G. Pineda, X. Jiang, A. Adhikari, et al., Direct activation of protein kinases by unanchored polyubiquitin chains, Nature 461 (2009) 114–119, https://doi.org/10.1038/nature08247.

[37] C.-Q. Lei, X. Wu, X. Zhong, L. Jiang, B. Zhong, H.-B. Shu, USP19 inhibits TNF-α- and IL-1β-triggered NF-κB activation by deubiquitinating TAK1, J. Immunol. 203 (2019) 259–268, https://doi.org/10.4049/jimmunol.1900083.

[38] L. Dai, C. Aye Thu, X.-Y. Liu, J. Xi, P.C.F. Cheung, TAK1, more than just innate immunity, IUBMB Life 64 (2012) 825–834, https://doi.org/10.1002/iub.1078.

[39] D.S. Simpson, A. Gabrielyan, R. Feltham, RIPK1 ubiquitination: evidence, correlations and the undefined, Semin. Cell Dev. Biol. 109 (2021) 76–85, https://doi.org/10.1016/j.semcdb.2020.08.008.

[40] E. Laplantine, E. Fontan, J. Chiaravalli, T. Lopez, G. Lakisic, M. Véron, et al., NEMO specifically recognizes K63-linked poly-ubiquitin chains through a new bipartite ubiquitin-binding domain, EMBO J. 28 (2009) 2885–2895, https://doi.org/10.1038/emboj.2009.241.

[41] L.H. Gallo, A.N. Meyer, K. Motamedchaboki, K.N. Nelson, M. Haas, D. J. Donoghue, Novel Lys63-linked ubiquitination of IKKβ induces STAT3 signaling, Cell Cycle 13 (2014) 3964–3976, https://doi.org/10.4161/15384101.2014.988026.

[42] J.-Y. Kim, A.A. Beg, E.B. Haura, Non-canonical IKKs, IKKε and TBK1, as novel therapeutic targets in the treatment of non-small cell lung cancer, Expert Opin.

Ther. Targets 17 (2013) 1109–1112, https://doi.org/10.1517/14728222.2013.833188.
[43] F. Ikeda, Y.L. Deribe, S.S. Skånland, B. Stieglitz, C. Grabbe, M. Franz-Wachtel, et al., SHARPIN forms a linear ubiquitin ligase complex regulating NF-κB activity and apoptosis, Nature 471 (2011) 637–641, https://doi.org/10.1038/nature09814.
[44] F. Tokunaga, Linear ubiquitination-mediated NF-κB regulation and its related disorders, J. Biochem. 154 (2013) 313–323, https://doi.org/10.1093/jb/mvt079.
[45] B. Gerlach, S.M. Cordier, A.C. Schmukle, C.H. Emmerich, E. Rieser, T.L. Haas, et al., Linear ubiquitination prevents inflammation and regulates immune signalling, Nature 471 (2011) 591–596, https://doi.org/10.1038/nature09816.
[46] C.H. Emmerich, A. Ordureau, S. Strickson, J.S.C. Arthur, P.G.A. Pedrioli, D. Komander, et al., Activation of the canonical IKK complex by K63/M1-linked hybrid ubiquitin chains, Proc. Natl. Acad. Sci. USA 110 (2013) 15247–15252, https://doi.org/10.1073/pnas.1314715110.
[47] F. Ohtake, Y. Saeki, S. Ishido, J. Kanno, K. Tanaka, The K48-K63 branched ubiquitin chain regulates NF-κB signaling, Mol. Cell 64 (2016) 251–266, https://doi.org/10.1016/j.molcel.2016.09.014.
[48] E.D. Silva-Ferrada, M. Torres-Ramos, F. Aillet, M. Campagna, C. Matute, C. Rivas, et al., Role of monoubiquitylation on the control of IκBα degradation and NF-κB activity, PLOS ONE 6 (2011), e25397, https://doi.org/10.1371/journal.pone.0025397.
[49] X. Wang, H. Peng, Y. Huang, W. Kong, Q. Cui, J. Du, et al., Post-translational modifications of IκBα: the state of the art, Front. Cell Dev. Biol. 8 (2020) 1285, https://doi.org/10.3389/fcell.2020.574706.
[50] T. Cartwright, N.D. Perkins, C. L Wilson, NFKB1: a suppressor of inflammation, ageing and cancer, FEBS J. 283 (2016) 1812–1822, https://doi.org/10.1111/febs.13627.
[51] I.E. Wertz, V.M. Dixit, Signaling to NF-kappaB: regulation by ubiquitination, Cold Spring Harb. Perspect. Biol. 2 (2010), a003350, https://doi.org/10.1101/cshperspect.a003350.
[52] Y. Kravtsova-Ivantsiv, I. Shomer, V. Cohen-Kaplan, B. Snijder, G. Superti-Furga, H. Gonen, et al., KPC1-mediated ubiquitination and proteasomal processing of NF-κB1 p105 to p50 restricts tumor growth, Cell 161 (2015) 333–347, https://doi.org/10.1016/j.cell.2015.03.001.
[53] S.-C. Sun, Non-canonical NF-κB signaling pathway, Cell Res. 21 (2011) 71–85, https://doi.org/10.1038/cr.2010.177.
[54] M. Lork, K. Verhelst, R. Beyaert, CYLD, A20 and OTULIN deubiquitinases in NF-κB signaling and cell death: so similar, yet so different, Cell Death Differ. 24 (2017) 1172–1183, https://doi.org/10.1038/cdd.2017.46.
[55] P.R. Elliott, D. Leske, M. Hrdinka, K. Bagola, B.K. Fiil, S.H. McLaughlin, et al., SPATA2 links CYLD to LUBAC, activates CYLD, and controls LUBAC signaling, Mol. Cell 63 (2016) 990–1005, https://doi.org/10.1016/j.molcel.2016.08.001.
[56] M. Hrdinka, B.K. Fiil, M. Zucca, D. Leske, K. Bagola, M. Yabal, et al., CYLD limits Lys63- and Met1-linked ubiquitin at receptor complexes to regulate innate immune signaling, Cell Rep. 14 (2016) 2846–2858, https://doi.org/10.1016/j.celrep.2016.02.062.
[57] J.J. Keats, R. Fonseca, M. Chesi, R. Schop, A. Baker, W.-J. Chng, et al., Promiscuous mutations activate the noncanonical NF-kappaB pathway in multiple myeloma, Cancer Cell 12 (2007) 131–144, https://doi.org/10.1016/j.ccr.2007.07.003.
[58] J.E. Hutti, R.R. Shen, D.W. Abbott, A.Y. Zhou, K.M. Sprott, J.M. Asara, et al., Phosphorylation of the tumor suppressor CYLD by the breast cancer oncogene IKKepsilon promotes cell transformation, Mol. Cell 34 (2009) 461–472, https://doi.org/10.1016/j.molcel.2009.04.031.
[59] L. Verboom, E. Hoste, G. van Loo, OTULIN in NF-κB signaling, cell death, and disease, Trends Immunol. 42 (2021) 590–603, https://doi.org/10.1016/j.it.2021.05.003.
[60] R.B. Damgaard, P.R. Elliott, K.N. Swatek, E.R. Maher, P. Stepensky, O. Elpeleg, et al., OTULIN deficiency in ORAS causes cell type-specific LUBAC degradation, dysregulated TNF signalling and cell death, EMBO Mol. Med. 11 (2019), e9324, https://doi.org/10.15252/emmm.201809324.
[61] A. Dorronsoro, V. Lang, E. Jakobsson, I. Ferrin, J.M. Salcedo, J. Fernández-Rueda, et al., Identification of the NF-κB inhibitor A20 as a key regulator for human adipogenesis, Cell Death Dis. 4 (2013), e972, https://doi.org/10.1038/cddis.2013.494.
[62] I.E. Wertz, K.M. O'Rourke, H. Zhou, M. Eby, L. Aravind, S. Seshagiri, et al., De-ubiquitination and ubiquitin ligase domains of A20 downregulate NF-kappaB signalling, Nature 430 (2004) 694–699, https://doi.org/10.1038/nature02794.
[63] A. Martens, G. van Loo, A20 at the crossroads of cell death, inflammation, and autoimmunity, Cold Spring Harb. Perspect. Biol. 12 (2020), a036418, https://doi.org/10.1101/cshperspect.a036418.
[64] K. Arimoto, K. Funami, Y. Saeki, K. Tanaka, K. Okawa, O. Takeuchi, et al., Polyubiquitin conjugation to NEMO by triparite motif protein 23 (TRIM23) is critical in antiviral defense, Proc. Natl. Acad. Sci. USA 107 (2010) 15856–15861, https://doi.org/10.1073/pnas.1004621107.
[65] S. Hatakeyama, TRIM family proteins: roles in autophagy, immunity, and carcinogenesis, Trends Biochem. Sci. 42 (2017) 297–311, https://doi.org/10.1016/j.tibs.2017.01.002.
[66] Y. Ran, J. Zhang, L.-L. Liu, Z.-Y. Pan, Y. Nie, H.-Y. Zhang, et al., Autoubiquitination of TRIM26 links TBK1 to NEMO in RLR-mediated innate antiviral immune response, J. Mol. Cell Biol. 8 (2016) 31–43, https://doi.org/10.1093/jmcb/mjv068.
[67] Y. Tang, H. Tu, J. Zhang, X. Zhao, Y. Wang, J. Qin, et al., K63-linked ubiquitination regulates RIPK1 kinase activity to prevent cell death during embryogenesis and inflammation, Nat. Commun. 10 (2019) 4157, https://doi.org/10.1038/s41467-019-12033-8.
[68] G. Wang, J. Long, Y. Gao, W. Zhang, F. Han, C. Xu, et al., SETDB1-mediated methylation of Akt promotes its K63-linked ubiquitination and activation leading to tumorigenesis, Nat. Cell Biol. 21 (2019) 214–225, https://doi.org/10.1038/s41556-018-0266-1.
[69] J.H. Lim, H. Jono, K. Komatsu, C.-H. Woo, J. Lee, M. Miyata, et al., CYLD negatively regulates transforming growth factor-β-signalling via deubiquitinating Akt, Nat. Commun. 3 (2012) 771, https://doi.org/10.1038/ncomms1776.
[70] W.-L. Yang, J. Wang, C.-H. Chan, S.-W. Lee, A.D. Campos, B. Lamothe, et al., The E3 ligase TRAF6 regulates Akt ubiquitination and activation, Science 325 (2009) 1134–1138, https://doi.org/10.1126/science.1175065.
[71] H. Huang, M.-S. Jeon, L. Liao, C. Yang, C. Elly, J.R. Yates, et al., K33-linked polyubiquitination of T cell receptor-zeta regulates proteolysis-independent T cell signaling, Immunity 33 (2010) 60–70, https://doi.org/10.1016/j.immuni.2010.07.002.
[72] M. van Huizen, M. Kikkert, The role of atypical ubiquitin chains in the regulation of the antiviral innate immune response, Front. Cell Dev. Biol. 7 (2019) 392, https://doi.org/10.3389/fcell.2019.00392.
[73] M. Lin, Z. Zhao, Z. Yang, Q. Meng, P. Tan, W. Xie, et al., USP38 inhibits type I interferon signaling by editing TBK1 ubiquitination through NLRP4 signalosome, Mol. Cell 64 (2016) 267–281, https://doi.org/10.1016/j.molcel.2016.08.029.
[74] S. Liu, M. Jiang, W. Wang, W. Liu, X. Song, Z. Ma, et al., Nuclear RNF2 inhibits interferon function by promoting K33-linked STAT1 disassociation from DNA, Nat. Immunol. 19 (2018) 41–52, https://doi.org/10.1038/s41590-017-0003-0.
[75] R. Nusse, H. Clevers, Wnt/β-catenin signaling, disease, and emerging therapeutic modalities, Cell 169 (2017) 985–999, https://doi.org/10.1016/j.cell.2017.05.016.
[76] C. Fei, Z. Li, C. Li, Y. Chen, Z. Chen, X. He, et al., Smurf1-mediated Lys29-linked nonproteolytic polyubiquitination of axin negatively regulates Wnt/β-catenin signaling, Mol. Cell Biol. 33 (2013) 4095–4105, https://doi.org/10.1128/MCB.00418-13.
[77] H. Nagai, T. Noguchi, K. Homma, K. Katagiri, K. Takeda, A. Matsuzawa, et al., Ubiquitin-like sequence in ASK1 plays critical roles in the recognition and stabilization by USP9X and oxidative stress-induced cell death, Mol. Cell 36 (2009) 805–818, https://doi.org/10.1016/j.molcel.2009.10.016.
[78] B. Xue, H. Li, M. Guo, J. Wang, Y. Xu, X. Zou, et al., TRIM21 promotes innate immune response to RNA viral infection through Lys27-linked polyubiquitination of MAVS, J. Virol. (2018) 92, https://doi.org/10.1128/JVI.00321-18.
[79] X. He, Y. Zhu, Y. Zhang, Y. Geng, J. Gong, J. Geng, et al., RNF34 functions in immunity and selective mitophagy by targeting MAVS for autophagic degradation, EMBO J. 38 (2019), e100978, https://doi.org/10.15252/embj.2018100978.
[80] H. Sun, Q. Zhang, Y.-Y. Jing, M. Zhang, H.-Y. Wang, Z. Cai, et al., USP13 negatively regulates antiviral responses by deubiquitinating STING, Nat. Commun. 8 (2017) 15534, https://doi.org/10.1038/ncomms15534.
[81] X. Wu, C. Lei, T. Xia, X. Zhong, Q. Yang, H.-B. Shu, Regulation of TRIF-mediated innate immune response by K27-linked polyubiquitination and deubiquitination, Nat. Commun. 10 (2019) 4115, https://doi.org/10.1038/s41467-019-12145-1.
[82] Q. Yin, T. Han, B. Fang, G. Zhang, C. Zhang, E.R. Roberts, et al., K27-linked ubiquitination of BRAF by ITCH engages cytokine response to maintain MEK-ERK signaling, Nat. Commun. 10 (2019) 1870, https://doi.org/10.1038/s41467-019-09844-0.
[83] J.P. Chua, H. De Calbiac, E. Kabashi, S.J. Barmada, Autophagy and ALS: mechanistic insights and therapeutic implications, Autophagy (2021) 1–29, https://doi.org/10.1080/15548627.2021.1926656.
[84] M. Antonioli, M. Di Rienzo, M. Piacentini, G.M. Fimia, Emerging mechanisms in initiating and terminating autophagy, Trends Biochem. Sci. 42 (2017) 28–41, https://doi.org/10.1016/j.tibs.2016.09.008.
[85] C. Reidick, F. El Magraoui, H.E. Meyer, H. Stenmark, H.W. Platta, Regulation of the tumor-suppressor function of the class III phosphatidylinositol 3-kinase complex by ubiquitin and SUMO, Cancers 7 (2014) 1–29, https://doi.org/10.3390/cancers7010001 (Basel).
[86] J. Kim, K.-L. Guan, AMPK connects energy stress to PIK3C3/VPS34 regulation, Autophagy 9 (2013) 1110–1111, https://doi.org/10.4161/auto.24877.
[87] F. Nazio, F. Strappazzon, M. Antonioli, P. Bielli, V. Cianfanelli, M. Bordi, et al., mTOR inhibits autophagy by controlling ULK1 ubiquitylation, self-association and function through AMBRA1 and TRAF6, Nat. Cell Biol. 15 (2013) 406–416, https://doi.org/10.1038/ncb2708.
[88] A. Ashkenazi, C.F. Bento, T. Ricketts, M. Vicinanza, F. Siddiqi, M. Pavel, et al., Polyglutamine tracts regulate beclin 1-dependent autophagy, Nature 545 (2017) 108–111, https://doi.org/10.1038/nature22078.
[89] C.-S. Shi, J.H. Kehrl, TRAF6 and A20 regulate lysine 63-linked ubiquitination of beclin-1 to control TLR4-induced autophagy, Sci. Signal. 3 (2010) ra42, https://doi.org/10.1126/scisignal.2000751.
[90] H. Feng, G.Y. Lopez, C.K. Kim, A. Alvarez, C.G. Duncan, R. Nishikawa, et al., EGFR phosphorylation of DCBLD2 recruits TRAF6 and stimulates AKT-promoted tumorigenesis, J. Clin. Investig. 124 (2014) 3741–3756, https://doi.org/10.1172/JCI73093.
[91] R.C. Russell, Y. Tian, H. Yuan, H.W. Park, Y.-Y. Chang, J. Kim, et al., ULK1 induces autophagy by phosphorylating beclin-1 and activating VPS34 lipid kinase, Nat. Cell Biol. 15 (2013) 741–750, https://doi.org/10.1038/ncb2757.
[92] Y. Yang, W. Fiskus, B. Yong, P. Atadja, Y. Takahashi, T.K. Pandita, et al., Acetylated hsp70 and KAP1-mediated Vps34 SUMOylation is required for autophagosome creation in autophagy, Proc. Natl. Acad. Sci. USA 110 (2013) 6841–6846, https://doi.org/10.1073/pnas.1217692110.

[93] H.W. Platta, H. Abrahamsen, S.B. Thoresen, H. Stenmark, Nedd4-dependent lysine-11-linked polyubiquitination of the tumour suppressor beclin 1, Biochem. J. 441 (2012) 399–406, https://doi.org/10.1042/BJ20111424.
[94] F. Nazio, M. Carinci, C. Valacca, P. Bielli, F. Strappazzon, M. Antonioli, et al., Fine-tuning of ULK1 mRNA and protein levels is required for autophagy oscillation, J. Cell Biol. 215 (2016) 841–856, https://doi.org/10.1083/jcb.201605089.
[95] C.-C. Liu, Y.-C. Lin, Y.-H. Chen, C.-M. Chen, L.-Y. Pang, H.-A. Chen, et al., Cul3-KLHL20 ubiquitin ligase governs the turnover of ULK1 and VPS34 complexes to control autophagy termination, Mol. Cell 61 (2016) 84–97, https://doi.org/10.1016/j.molcel.2015.11.001.
[96] M. Antonioli, F. Albiero, F. Nazio, T. Vescovo, A.B. Perdomo, M. Corazzari, et al., AMBRA1 interplay with cullin E3 ubiquitin ligases regulates autophagy dynamics, Dev. Cell 31 (2014) 734–746, https://doi.org/10.1016/j.devcel.2014.11.013.
[97] P. Xia, S. Wang, G. Huang, Y. Du, P. Zhu, M. Li, et al., RNF2 is recruited by WASH to ubiquitinate AMBRA1 leading to downregulation of autophagy, Cell Res. 24 (2014) 943–958, https://doi.org/10.1038/cr.2014.85.
[98] C. Xu, J. Liu, L.-C. Hsu, Y. Luo, R. Xiang, T.-H. Chuang, Functional interaction of heat shock protein 90 and beclin 1 modulates toll-like receptor-mediated autophagy, FASEB J. 25 (2011) 2700–2710, https://doi.org/10.1096/fj.10-167676.
[99] V. Kirkin, V.V. Rogov, A diversity of selective autophagy receptors determines the specificity of the autophagy pathway, Mol. Cell 76 (2019) 268–285, https://doi.org/10.1016/j.molcel.2019.09.005.
[100] E. Deosaran, K.B. Larsen, R. Hua, G. Sargent, Y. Wang, S. Kim, et al., NBR1 acts as an autophagy receptor for peroxisomes, J. Cell Sci. 126 (2013) 939–952, https://doi.org/10.1242/jcs.114819.
[101] A. Khaminets, C. Behl, I. Dikic, Ubiquitin-dependent and independent signals in selective autophagy, Trends Cell Biol. 26 (2016) 6–16, https://doi.org/10.1016/j.tcb.2015.08.010.
[102] A. Stolz, I. Dikic, PINK1-PARKIN interplay: down to ubiquitin phosphorylation, Mol. Cell 56 (2014) 341–342, https://doi.org/10.1016/j.molcel.2014.10.022.
[103] G.A. Collins, A.L. Goldberg, The logic of the 26S proteasome, Cell 169 (2017) 792–806, https://doi.org/10.1016/j.cell.2017.04.023.
[104] V. Kirkin, T. Lamark, Y.-S. Sou, G. Bjørkøy, J.L. Nunn, J.-A. Bruun, et al., A role for NBR1 in autophagosomal degradation of ubiquitinated substrates, Mol. Cell 33 (2009) 505–516, https://doi.org/10.1016/j.molcel.2009.01.020.
[105] S.-J. Cho, S.-M. Yun, C. Jo, D.-H. Lee, K.J. Choi, J.C. Song, et al., SUMO1 promotes Aβ production via the modulation of autophagy, Autophagy 11 (2015) 100–112, https://doi.org/10.4161/15548627.2014.984283.
[106] B. Kalveram, G. Schmidtke, M. Groettrup, The ubiquitin-like modifier FAT10 interacts with HDAC6 and localizes to aggresomes under proteasome inhibition, J. Cell Sci. 121 (2008) 4079–4088, https://doi.org/10.1242/jcs.035006.
[107] M. Gamerdinger, A.M. Kaya, U. Wolfrum, A.M. Clement, C. Behl, BAG3 mediates chaperone-based aggresome-targeting and selective autophagy of misfolded proteins, EMBO Rep. 12 (2011) 149–156, https://doi.org/10.1038/embor.2010.203.
[108] Y. Kawaguchi, J.J. Kovacs, A. McLaurin, J.M. Vance, A. Ito, T.P. Yao, The deacetylase HDAC6 regulates aggresome formation and cell viability in response to misfolded protein stress, Cell 115 (2003) 727–738, https://doi.org/10.1016/s0092-8674(03)00939-5.
[109] J.-Y. Lee, H. Koga, Y. Kawaguchi, W. Tang, E. Wong, Y.-S. Gao, et al., HDAC6 controls autophagosome maturation essential for ubiquitin-selective quality-control autophagy, EMBO J. 29 (2010) 969–980, https://doi.org/10.1038/emboj.2009.405.
[110] R. Rott, R. Szargel, J. Haskin, R. Bandopadhyay, A.J. Lees, V. Shani, et al., α-Synuclein fate is determined by USP9X-regulated monoubiquitination, Proc. Natl. Acad. Sci. USA 108 (2011) 18666–18671, https://doi.org/10.1073/pnas.1105725108.
[111] T. Kawamata, T. Horie, M. Matsunami, M. Sasaki, Y. Ohsumi, Zinc starvation induces autophagy in yeast, J. Biol. Chem. 292 (2017) 8520–8530, https://doi.org/10.1074/jbc.M116.762948.
[112] R.S. Marshall, F. Li, D.C. Gemperline, A.J. Book, R.D. Vierstra, Autophagic degradation of the 26S proteasome is mediated by the dual ATG8/ubiquitin receptor RPN10 in arabidopsis, Mol. Cell 58 (2015) 1053–1066, https://doi.org/10.1016/j.molcel.2015.04.023.
[113] K.A. Waite, A. De-La Mota-Peynado, G. Vontz, J. Roelofs, Starvation induces proteasome autophagy with different pathways for core and regulatory particles, J. Biol. Chem. 291 (2016) 3239–3253, https://doi.org/10.1074/jbc.M115.699124.
[114] V. Cohen-Kaplan, I. Livneh, N. Avni, B. Fabre, T. Ziv, Y.T. Kwon, et al., p62- and ubiquitin-dependent stress-induced autophagy of the mammalian 26S proteasome, PNAS 113 (2016) E7490–E7499, https://doi.org/10.1073/pnas.1615455113.
[115] G. Quinet, M. Gonzalez-Santamarta, C. Louche, M.S. Rodriguez, Mechanisms regulating the UPS-ALS crosstalk: the role of proteaphagy, Molecules (2020) 25, https://doi.org/10.3390/molecules25102352.
[116] Grégoire Quinet, et al. Targeting p62/Sequestosome-1 Impairs Constitutively Active Proteaphagy and Enhances Apoptosis in Bortezomib-Resistant Mantle Cell Lymphoma 2021.
[117] R.G. Lopez-Reyes, G. Quinet, M. Gonzalez-Santamarta, C. Larrue, J.-E. Sarry, M. S. Rodriguez, Inhibition of the proteasome and proteaphagy enhances apoptosis in FLT3-ITD-driven acute myeloid leukemia, FEBS Open Bio 11 (2021) 48–60, https://doi.org/10.1002/2211-5463.12950.
[118] R.S. Marshall, F. McLoughlin, R.D. Vierstra, Autophagic turnover of inactive 26S proteasomes in yeast is directed by the ubiquitin receptor Cue5 and the Hsp42 chaperone, Cell Rep. 16 (2016) 1717–1732, https://doi.org/10.1016/j.celrep.2016.07.015.
[119] M. Gonzalez-Santamarta, The Tripartite Motif Containing Protein 24 (TRIM24) Ubiquitin Ligase, Regulates the Proteasome-Autophagy Crosstalk (Proteaphagy) and p53-Mediated Apoptosis in Bortezomib Resistant in Mantle Cell Lymphoma ZBR Cells, 2021, n.d. (In preparation).
[120] L. Liu, D. Feng, G. Chen, M. Chen, Q. Zheng, P. Song, et al., Mitochondrial outer-membrane protein FUNDC1 mediates hypoxia-induced mitophagy in mammalian cells, Nat. Cell Biol. 14 (2012) 177–185, https://doi.org/10.1038/ncb2422.
[121] L.A. Kane, M. Lazarou, A.I. Fogel, Y. Li, K. Yamano, S.A. Sarraf, et al., PINK1 phosphorylates ubiquitin to activate Parkin E3 ubiquitin ligase activity, J. Cell Biol. 205 (2014) 143–153, https://doi.org/10.1083/jcb.201402104.
[122] A. Ordureau, S.A. Sarraf, D.M. Duda, J.-M. Heo, M.P. Jedrychowski, V. O. Sviderskiy, et al., Quantitative proteomics reveal a feedforward mechanism for mitochondrial PARKIN translocation and ubiquitin chain synthesis, Mol. Cell 56 (2014) 360–375, https://doi.org/10.1016/j.molcel.2014.09.007.
[123] A. Ordureau, J.-M. Heo, D.M. Duda, J.A. Paulo, J.L. Olszewski, D. Yanishevski, et al., Defining roles of PARKIN and ubiquitin phosphorylation by PINK1 in mitochondrial quality control using a ubiquitin replacement strategy, Proc. Natl. Acad. Sci. USA 112 (2015) 6637–6642, https://doi.org/10.1073/pnas.1506593112.
[124] D. Chen, F. Gao, B. Li, H. Wang, Y. Xu, C. Zhu, et al., Parkin mono-ubiquitinates Bcl-2 and regulates autophagy, J. Biol. Chem. 285 (2010) 38214–38223, https://doi.org/10.1074/jbc.M110.101469.
[125] B. Bingol, J.S. Tea, L. Phu, M. Reichelt, C.E. Bakalarski, Q. Song, et al., The mitochondrial deubiquitinase USP30 opposes parkin-mediated mitophagy, Nature 510 (2014) 370–375, https://doi.org/10.1038/nature13418.
[126] M.A. Michel, K.N. Swatek, M.K. Hospenthal, D. Komander, Ubiquitin linkage-specific affimers reveal insights into K6-linked ubiquitin signaling, Mol. Cell 68 (2017) 233–246, https://doi.org/10.1016/j.molcel.2017.08.020, e5.
[127] K. Niu, H. Fang, Z. Chen, Y. Zhu, Q. Tan, D. Wei, et al., USP33 deubiquitinates PRKN/parkin and antagonizes its role in mitophagy, Autophagy 16 (2020) 724–734, https://doi.org/10.1080/15548627.2019.1656957.
[128] W. Li, M.H. Bengtson, A. Ulbrich, A. Matsuda, V.A. Reddy, A. Orth, et al., Genome-wide and functional annotation of human E3 ubiquitin ligases identifies MULAN, a mitochondrial E3 that regulates the organelle's dynamics and signaling, PLoS One 3 (2008), e1487, https://doi.org/10.1371/journal.pone.0001487.
[129] N. Nakamura, Y. Kimura, M. Tokuda, S. Honda, S. Hirose, MARCH-V is a novel mitofusin 2- and Drp1-binding protein able to change mitochondrial morphology, EMBO Rep. 7 (2006) 1019–1022, https://doi.org/10.1038/sj.embor.7400790.
[130] L.C. Gomes, G. Di Benedetto, L. Scorrano, During autophagy mitochondria elongate, are spared from degradation and sustain cell viability, Nat. Cell Biol. 13 (2011) 589–598, https://doi.org/10.1038/ncb2220.
[131] C. Natarajan, K. Takeda, Regulation of various DNA repair pathways by E3 ubiquitin ligases, J. Cancer Res. Ther. 13 (2017) 157–169, https://doi.org/10.4103/0973-1482.204879.
[132] M. Uckelmann, T.K. Sixma, Histone ubiquitination in the DNA damage response, DNA Repair 56 (2017) 92–101, https://doi.org/10.1016/j.dnarep.2017.06.011 (Amst.).
[133] T. Thorslund, A. Ripplinger, S. Hoffmann, T. Wild, M. Uckelmann, B. Villumsen, et al., Histone H1 couples initiation and amplification of ubiquitin signalling after DNA damage, Nature 527 (2015) 389–393, https://doi.org/10.1038/nature15401.
[134] A. Fradet-Turcotte, M.D. Canny, C. Escribano-Díaz, A. Orthwein, C.C.Y. Leung, H. Huang, et al., 53BP1 is a reader of the DNA-damage-induced H2A Lys 15 ubiquitin mark, Nature 499 (2013) 50–54, https://doi.org/10.1038/nature12318.
[135] M. Gatti, S. Pinato, A. Maiolica, F. Rocchio, M.G. Prato, R. Aebersold, et al., RNF168 promotes noncanonical K27 ubiquitination to signal DNA damage, Cell Rep. 10 (2015) 226–238, https://doi.org/10.1016/j.celrep.2014.12.021.
[136] Z. Wang, H. Zhang, J. Liu, A. Cheruiyot, J.-H. Lee, T. Ordog, et al., USP51 deubiquitylates H2AK13,15ub and regulates DNA damage response, Genes Dev. 30 (2016) 946–959, https://doi.org/10.1101/gad.271841.115.
[137] S. Nowsheen, K. Aziz, A. Aziz, M. Deng, B. Qin, K. Luo, et al., L3MBTL2 orchestrates ubiquitin signalling by dictating the sequential recruitment of RNF8 and RNF168 after DNA damage, Nat. Cell Biol. 20 (2018) 455–464, https://doi.org/10.1038/s41556-018-0071-x.
[138] E. Zeqiraj, L. Tian, C.A. Piggott, M.C. Pillon, N.M. Duffy, D.F. Ceccarelli, et al., Higher-order assembly of BRCC36–KIAA0157 is required for DUB activity and biological function, Mol. Cell 59 (2015) 970–983, https://doi.org/10.1016/j.molcel.2015.07.028.
[139] J. Rabl, R.D. Bunker, A.D. Schenk, S. Cavadini, M.E. Gill, W. Abdulrahman, et al., Structural basis of BRCC36 function in DNA repair and immune regulation, Mol. Cell 75 (2019) 483–497, https://doi.org/10.1016/j.molcel.2019.06.002, e9.
[140] H.-M. Ng, L. Wei, L. Lan, M.S.Y. Huen, The Lys63-deubiquitylating enzyme BRCC36 limits DNA break processing and repair, J. Biol. Chem. 291 (2016) 16197–16207, https://doi.org/10.1074/jbc.M116.731927.
[141] S.E. Kaiser, B.E. Riley, T.A. Shaler, R.S. Trevino, C.H. Becker, H. Schulman, et al., Protein standard absolute quantification (PSAQ) method for the measurement of cellular ubiquitin pools, Nat. Methods 8 (2011) 691–696, https://doi.org/10.1038/nmeth.1649.

[142] R.M. Densham, J.R. Morris, The BRCA1 Ubiquitin ligase function sets a new trend for remodelling in DNA repair, Nucleus 8 (2017) 116–125, https://doi.org/10.1080/19491034.2016.1267092.
[143] S.R. Witus, A.L. Burrell, D.P. Farrell, J. Kang, M. Wang, J.M. Hansen, et al., BRCA1/BARD1 site-specific ubiquitylation of nucleosomal H2A is directed by BARD1, Nat. Struct. Mol. Biol. 28 (2021) 268–277, https://doi.org/10.1038/s41594-020-00556-4.
[144] C.C. So, S. Ramachandran, A. Martin, E3 ubiquitin ligases RNF20 and RNF40 are required for double-stranded break (DSB) repair: evidence for monoubiquitination of histone H2B lysine 120 as a novel axis of DSB signaling and repair, Mol. Cell Biol. 39 (2019), https://doi.org/10.1128/MCB.00488-18 e00488-18.
[145] S. In, Y.-I. Kim, J.E. Lee, J. Kim, RNF20/40-mediated eEF1BδL monoubiquitylation stimulates transcription of heat shock-responsive genes, Nucleic Acids Res. 47 (2019) 2840–2855, https://doi.org/10.1093/nar/gkz006.
[146] A. Paul, B. Wang, RNF8- and Ube2S-dependent ubiquitin lysine 11-linkage modification in response to DNA damage, Mol. Cell 66 (2017) 458–472, https://doi.org/10.1016/j.molcel.2017.04.013, e5.
[147] H. Hu, G.C. Brittain, J.-H. Chang, N. Puebla-Osorio, J. Jin, A. Zal, et al., OTUD7B controls non-canonical NF-κB activation through deubiquitination of TRAF3, Nature 494 (2013) 371–374, https://doi.org/10.1038/nature11831.
[148] X. Wu, S. Liu, C. Sagum, J. Chen, R. Singh, A. Chaturvedi, et al., Crosstalk between Lys63- and Lys11-polyubiquitin signaling at DNA damage sites is driven by Cezanne, Genes Dev. 33 (2019) 1702–1717, https://doi.org/10.1101/gad.332395.119.
[149] M. Mattern, J. Sutherland, K. Kadimisetty, R. Barrio, M.S. Rodriguez, Using ubiquitin binders to decipher the ubiquitin code, Trends Biochem. Sci. 44 (2019) 599–615, https://doi.org/10.1016/j.tibs.2019.01.011.
[150] Y. Sato, A. Yoshikawa, A. Yamagata, H. Mimura, M. Yamashita, K. Ookata, et al., Structural basis for specific cleavage of Lys 63-linked polyubiquitin chains, Nature 455 (2008) 358–362, https://doi.org/10.1038/nature07254.
[151] Q. Zhou, J. Zhang, K27-linked noncanonic ubiquitination in immune regulation, J. Leukoc. Biol. n.d.;n/a. ⟨https://doi.org/10.1002/JLB.4RU0620-397RR⟩.
[152] Y.A. Kristariyanto, S.A. Abdul Rehman, D.G. Campbell, N.A. Morrice, C. Johnson, R. Toth, et al., K29-selective ubiquitin binding domain reveals structural basis of specificity and heterotypic nature of k29 polyubiquitin, Mol. Cell 58 (2015) 83–94, https://doi.org/10.1016/j.molcel.2015.01.041.
[153] M.A. Michel, P.R. Elliott, K.N. Swatek, M. Simicek, J.N. Pruneda, J.L. Wagstaff, et al., Assembly and specific recognition of k29- and k33-linked polyubiquitin, Mol. Cell 58 (2015) 95–109, https://doi.org/10.1016/j.molcel.2015.01.042.
[154] Y.A. Kristariyanto, S.-Y. Choi, S.A.A. Rehman, M.S. Ritorto, D.G. Campbell, N. A. Morrice, et al., Assembly and structure of Lys33-linked polyubiquitin reveals distinct conformations, Biochem. J. 467 (2015) 345–352, https://doi.org/10.1042/BJ20141502.
[155] Y. Nibe, S. Oshima, M. Kobayashi, C. Maeyashiki, Y. Matsuzawa, K. Otsubo, et al., Novel polyubiquitin imaging system, PolyUb-FC, reveals that K33-linked polyubiquitin is recruited by SQSTM1/p62, Autophagy 14 (2018) 347–358, https://doi.org/10.1080/15548627.2017.1407889.
[156] W.-C. Yuan, Y.-R. Lee, S.-Y. Lin, L.-Y. Chang, Y.P. Tan, C.-C. Hung, et al., K33-linked polyubiquitination of coronin 7 by Cul3-KLHL20 ubiquitin E3 ligase regulates protein trafficking, Mol. Cell 54 (2014) 586–600, https://doi.org/10.1016/j.molcel.2014.03.035.
[157] H.-J. Meyer, M. Rape, Enhanced protein degradation by branched ubiquitin chains, Cell 157 (2014) 910–921, https://doi.org/10.1016/j.cell.2014.03.037.
[158] E. Oh, K.G. Mark, A. Mocciaro, E.R. Watson, J.R. Prabu, D.D. Cha, et al., Gene expression and cell identity controlled by anaphase-promoting complex, Nature 579 (2020) 136–140, https://doi.org/10.1038/s41586-020-2034-1.
[159] C. Liu, W. Liu, Y. Ye, W. Li, Ufd2p synthesizes branched ubiquitin chains to promote the degradation of substrates modified with atypical chains, Nat. Commun. 8 (2017) 14274, https://doi.org/10.1038/ncomms14274.
[160] L. Pluska, E. Jarosch, H. Zauber, A. Kniss, A. Waltho, K. Bagola, et al., The UBA domain of conjugating enzyme Ubc1/Ube2K facilitates assembly of K48/K63-branched ubiquitin chains, EMBO J. 40 (2021), e106094, https://doi.org/10.15252/embj.2020106094.
[161] D.S. Kirkpatrick, N.A. Hathaway, J. Hanna, S. Elsasser, J. Rush, D. Finley, et al., Quantitative analysis of in vitro ubiquitinated cyclin B1 reveals complex chain topology, Nat. Cell Biol. 8 (2006) 700–710, https://doi.org/10.1038/ncb1436.

cancers

MDPI

Article

Constitutive activation of p62/Sequestosome-1-mediated proteaphagy regulates proteolysis and impairs cell death in bortezomib-resistant mantle cell lymphoma

Grégoire Quinet[1,a], Wendy Xolalpa[2,a], Diana Reyes-Garau[3], Núria Profitós-Pelejà[3], Mikel Azkargorta[4], Laurie Ceccato[1], Maria Gonzalez-Santamarta[1], Maria Marsal[5], Jordi Andilla[5], Fabienne Aillet[2], Francesc Bosch[6], Felix Elortza[4], Pablo Loza-Alvarez[5], Brigitte Sola[7], Olivier Coux[8], Rune Matthiesen[9,*], Gaël Roué[3,*], Manuel S. Rodriguez[1,*]

[1]Laboratoire de Chimie de Coordination (LCC) CNRS-UPR8241, - UPS, Toulouse, France.

[2]Proteomics Unit, CICbioGUNE, Parque Tecnológico de Bizkaia, Derio, Spain.

[3] Lymphoma Translational group, UBIRed, Josep Carreras Leukaemia Research Institute, Badalona, Spain.

[4]Proteomics Platform CICbioGUNE, CIBERehd, ProteoRed-ISCIII, Parque Tecnológico de Bizkaia, Derio, Spain.

[5]ICFO-Institut de Ciencies Fotoniques, The Barcelona Institute of Science and Technology, 08860 Castelldefels (Barcelona), Spain.

[6]Laboratory of Experimental Hematology, Department of Hematology, Vall d'Hebron Institute of Oncology, Vall d'Hebron University Hospital, Barcelona, Spain

[7]Normandie Univ, INSERM UMR1245, Unicaen, Caen, France. BS_ORCID: 0000-0001-7278-9651

[8]Centre de Recherche de Biologie Cellulaire de Montpellier (CRBM) CNRS-UMR 5237, Université de Montpellier, Montpellier, France.

[9]Computational and Experimental Biology Group, CEDOC-Chronic Diseases Research Center, Faculdade de Ciências Médicas, Universidade Nova de Lisboa, Lisboa, Portugal.

WX Actual address: Departamento de Ingeniería Celular y Biocatálisis, Instituto de Biotecnología, Universidad Nacional Autónoma de México, Cuernavaca, Mor., México.

[a] Equal contribution

Corresponding author and lead contact:

*Manuel S Rodriguez, LCC CNRS-UPR8241, UPS, 205 route de Narbonne, 31400 Toulouse, France. Phone: +33 561333100, manuel.rodriguez@lcc-toulouse.fr

Corresponding authors:

*Rune Matthiesen, Computational and Experimental Biology Group, CEDOC, Chronic Diseases Research Centre, NOVA Medical School, Faculdade de Ciências Médicas, Universidade NOVA de Lisboa, Campo dos Mártires da Pátria, 130, 1169-056 Lisboa, Portugal Phone : +35 1924137220, rune.matthiesen@nms.unl.pt

*Gaël Roué, Josep Carreras Leukaemia Research Institute, Ctra de Can Ruti, Cami de les Escoles s/n, 08916 Badalona (Barcelona), Spain. Phone : +34 93 557 2835, groue@carrerasresearch.org

Received: date; Accepted: date; Published: date

Abstract: Protein ubiquitylation coordinates crucial cellular events in physiologic and pathologic conditions. A comparative analysis of the ubiquitin proteome from bortezomib (BTZ)-sensitive and BTZ-resistant mantle cell lymphoma (MCL) revealed an enrichment of Autophagy-Lysosome System (ALS) in BTZ-resistant cells. Pharmacological inhibition of autophagy at the level of lysosome-fusion revealed a constitutive activation of proteaphagy and accumulation of proteasome subunits within autophagosomes in different MCL cell lines with acquired or natural resistance to BTZ. Inhibition of the autophagy receptor p62/SQSTM1 upon verteporfin (VTP) treatment disrupted proteaphagosome assembly, reduced co-localisation of proteasome subunits with autophagy markers and negatively impacted proteasome activity. Finally, the silencing or pharmacological inhibition of p62 restored the apoptosis threshold at physiological levels in BTZ-resistant cells both in vitro and in vivo. In total, these results demonstrate for the first time a proteolytic switch from Ubiquitin-Proteasome System (UPS) to ALS in B-cell lymphoma refractory to proteasome inhibition, pointing out a crucial role for proteaphagy in this phenomenon and paving the way for the design of alternative therapeutic venues in treatment-resistant tumours.

Keywords: Apoptosis; Autophagy; Proteasome inhibitor; TUBEs; Ubiquitin proteome; Verteporfin.

1. Introduction

Mantle Cell Lymphoma (MCL) is an aggressive subtype of non-Hodgkin lymphoma, for which chemotherapy treatments show poor response and reduced patient survival. The proteasome inhibitor (PI) bortezomib (BTZ) has been used as a new class of agents for treatment of multiple myeloma (MM) and MCL [1,2]. BTZ inhibits the proteasome by targeting the β5 subunit of the 20S core particle (CP), thereby impairing degradation of intracellular proteins, including crucial factors regulating cell cycle, tumour progression and apoptosis [3]. Resistance to BTZ treatment appears in patients and has been extensively investigated in hematologic cancers over the last decade [4]. Point mutations in the β5 catalytic subunits of the proteasome occasionally explain BTZ resistance [5,6]. Nevertheless, such mutations are not always found in BTZ-resistant cells indicating that alternative mechanisms must support drug refractoriness. These alternative mechanisms include dysfunction of oxidative and endoplasmic reticulum stress [7], activation of the cytoprotective arm of the unfolded protein response [8], or re-activation of a plasmacytic differentiation program [9]. Consistently, pharmacological modulation of these pathways can partially re-sensitize resistant MCL cells to BTZ [10].

The Ubiquitin Proteasome System (UPS) and the Autophagy Lysosome System (ALS) constitute the main intracellular proteolytic pathways in eukaryotic cells [11,12]. Proteasomes are large protein complexes that ensure the selective degradation of cytosolic and nuclear proteins in response to a vast diversity of specific signals. The best understood proteasome form is the 26S proteasome, which degrades ubiquitylated proteins. It is formed by the 20S CP carrying the proteolytic activities and the 19S regulatory particle (RP) that recruits the target proteins and injects

them into the CP. The 20S CP possesses three catalytic subunits: β1, β2 and β5 with caspase-like, trypsin-like and chymotrypsin-like peptidase activities, respectively [13,14].

Ubiquitin (Ub) and Ubiquitin-like proteins (UbLs) are also implicated in ALS-mediated proteolysis. In particular, members of the LC3/GABARAP are involved in the formation of lipidic membranes called phagophores that engulf targeted cargos. Subsequently, they fuse with lysosomes to drive substrate degradation [11,12]. Distinct selective autophagy pathways have been reported and named according to the type of substrate that is embedded and degraded such as mitophagy (mitochondria) or proteaphagy (proteasome). Recently, Marshall *et al.* showed in *A. thaliana* that proteaphagy is activated under proteasome inhibition and nutrient starvation [15,16]. Proteaphagy has also been described in mammalian cells [17–19]. These results revealed a novel level of interaction between UPS and ALS.

To analyse the molecular impact of BTZ resistance in MCL, we investigated the Ub-dependent proteome of MCL cells. To this end, Tandem Ubiquitin Binding Entities (TUBEs) coupled to mass spectrometry (MS) analysis were performed [20–22]. Here we report the comparison of TUBEs-associated Ub-proteomes from MCL cell lines refractory (ZBR) or responsive (Z-138) to BTZ. Similar changes were found by comparing other sensitive and resistant MCL cells, highlighting the relevance of our observations. Our results show that ALS compensates a defective UPS found in BTZ-resistant cells by a permanently activated proteaphagy and that autophagy receptor p62 has a key role in the assembly of proteaphagosomes. We further demonstrate that silencing or pharmacological inhibition of p62 reactivates apoptosis signalling *in vitro* and *in vivo* in MCL tumours with intrinsic or acquired resistance to BTZ.

2. Results

2.1. Reduction of UPS is compensated by ALS factors in BTZ-resistant MCL cells

The biological impact of proteasome inhibition in MCL leads to the accumulation of ubiquitylated proteins, inducing proteotoxic stress and affecting crucial signalling pathways [10,23]. We hypothesized that these accumulated proteins could potentially be implicated in the response or resistance to BTZ. To get insight into the nature of these proteins, we compared the Ub-proteome isolated from a representative, BTZ-sensitive MCL cell line (Z138), and from its BTZ-resistant derived sub-clone (ZBR) [8]. We used TUBEs previously shown to be efficient for purification of Ub-proteins [3,21,24,25]. We identified 895 proteins that were specifically bound to TUBEs in Z-138 cells, and 683 in ZBR cells (Figures 1A and S1A-S1E). From these proteins, 263 were reduced or enriched in these cell lines and were retained for analysis (Table S1). Ingenuity Pathway Analysis (IPA) showed protein ubiquitylation, phagosome maturation and unfolding protein response were in the top five of the most represented pathways (Figure S1F). Gene ontology (GO) analysis was used to obtain an integrated heatmap view of the simultaneous Ub-regulated processes occurring in both BTZ-resistant and -sensitive cells (Figure S2). Crucial differences were observed among the 60 proteins of the UPS and ALS. In particular, proteasome subunits were reduced while components of the ALS were enriched in ZBR compared to Z-138 cells (Figures 1B and S3A). Other changes in the UPS included Ub-ligases, de-ubiquitylating enzymes and total protein ubiquitylation (Figure 1B and 1C).

We confirmed the reduced levels of proteasome subunits (α and β subunits of the CP, base and lid subunits of the 19S complex) associated to the Ub-proteome in ZBR cells compared to Z-138

122 cells by Western blot (WB) using specific antibodies (Figures 1D, S3B and S3D). In direct contrast,
123 cellular factors implicated in autophagosome early signalling, autophagosome formation and fusion
124 with the lysosome were enriched in the Ub-proteome of ZBR compared to Z-138 cells (Figures 1D,
125 S3B and S3D). The enrichment of some ALS factors and reduction of proteasome subunits were
126 confirmed by WB in JBR, another BTZ-resistant cell line, when compared to the parental JeKo-1 cell
127 line (Figures 1E, S3C and S3E). In summary, our results indicate that in BTZ-resistant cells, the levels
128 of ALS factors associated to the Ub-proteome are increased concomitantly with a reduction in
129 proteasome subunits levels, suggesting a compensatory mechanism that highlights a regulatory
130 crosstalk between ALS and UPS in these cells.

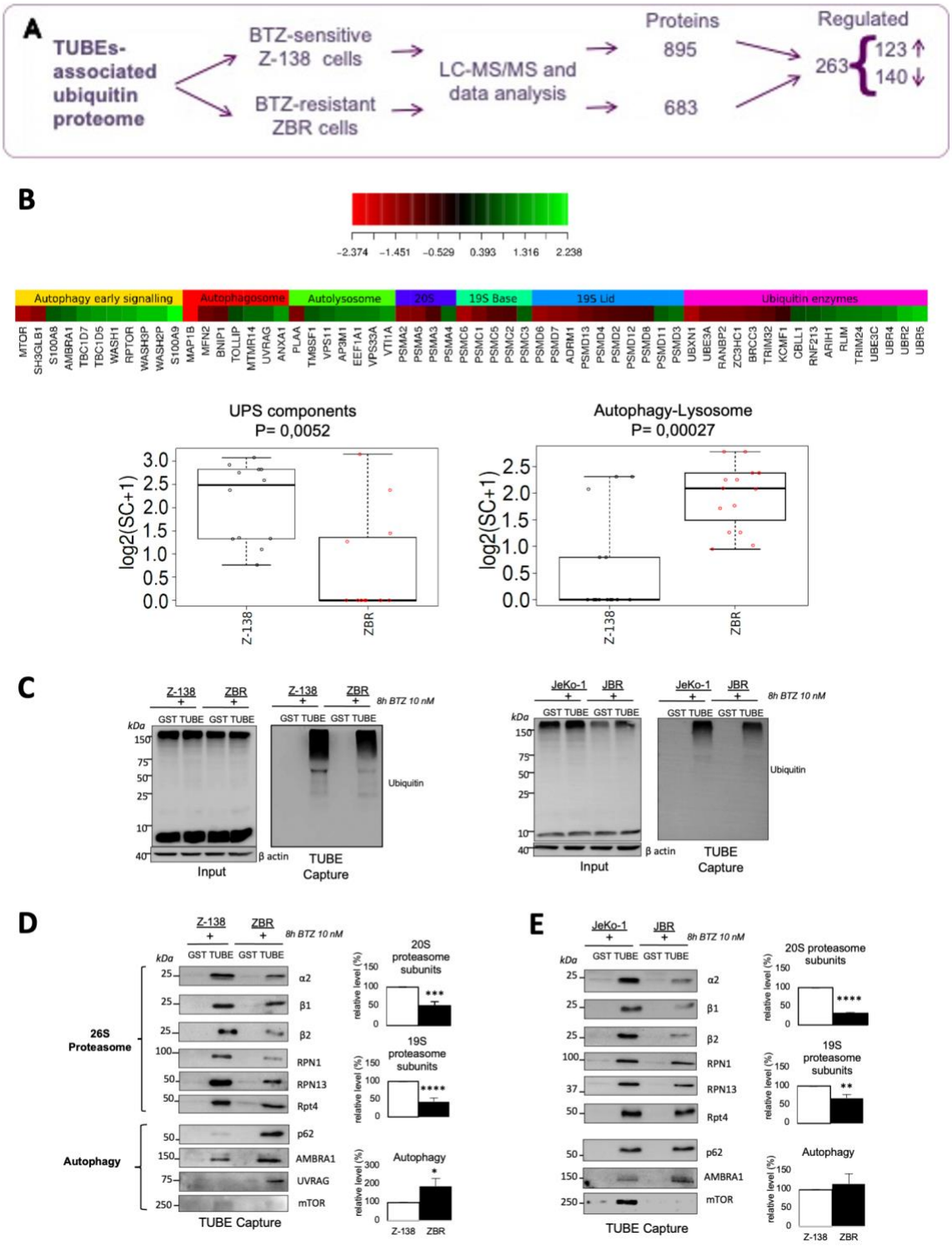

Figure 1. Analysis of the TUBEs-associated Ub proteome of BTZ-resistant MCL cells. (A) Scheme of the strategy used to isolate and compare the Ub proteome of Z-138 and ZBR MCL cells. **(B)** Heat map and boxplots showing significantly functional enriched UPS and ALS categories in BTZ-resistant ZBR cells compared to the parental Z-138 cell line. Red = low enrichment; green = high enrichment. **(C)** Ubiquitylation pattern in Z-138 vs ZBR and JeKo-1 vs JBR cells. Ubiquitylated proteins were captured using TUBEs from Z-138/ZBR **(D)** and JeKo-1/JBR **(E).** GST was used as a control. Indicated

fractions were analysed by WB with the indicated Abs. The densities of proteins calculated for the 19S, 20S and autophagy are the means of all single values. Quantifications were performed using ImageJ software (n ≥ 3; mean ± SD; two-tailed Student's *t*-test, *P < 0.05, **P < 0.01, ***P < 0.001, ****P < 0.0001). "n" represents the mean of three replicates for each of the subunits analysed that were integrated into 20S or 19S subunits".

2.2. Proteaphagy is constitutively active in BTZ-resistant MCL cells

Proteaphagy was proposed to be increased after proteasome inhibition, indicating that this mechanism could be used in physiological conditions to eliminate inactive proteasomes [16,17,26]. We observed that the autophagy inhibitors bafilomycin A (BafA) and chloroquine (CQ) led to the accumulation of autophagy factors (p62 ad LC3B) equally well in all cell lines (Figures 2A, 2B, S4A, S4B). In sharp contrast, they triggered an increase in the whole-cell levels of 26S proteasome subunits in ZBR and JBR cells and a decrease in Z-138 and JeKo-1 parental (BTZ-sensitive) cells. These results strongly supported a constitutive activation of proteaphagy only in BTZ-resistant cells. To extend these results, we evaluated the accumulation of proteasome subunits in the presence of BafA in several MCL cell lines with distinct inherent resistance/sensitivity to BTZ. We found that the MCL cell line REC-1 with the highest intrinsic resistance to proteasome inhibition [8], accumulated proteasome subunits after BafA treatment. This phenomenon was not statistically significant or not observed in MINO and Granta-519 cell lines showing intermediate and null resistance to BTZ, respectively (Figures 2C and S4C-E). Moreover, the accumulation of proteasome subunits was easier to detect when BTZ treatment was combined with BafA or CQ. Our data suggested that proteaphagy was activated in BTZ-resistant cells. Supporting these observations, immunofluorescence studies revealed a substantial increase in proteasome subunits-containing autophagosomes in ZBR and JBR treated with BafA or CQ plus BTZ, when compared to parental Z-138 and JeKo-1 cells (Figures 2D, 2E, S5A-B). In remarkable contrast with the BTZ-sensitive cell line Z-138, the co-localisation of proteasomes with autophagosomes was already observed at basal levels in ZBR cells, and BTZ treatment did not improve this co-localisation as much as autophagy inhibitors (Figure S5A). These results indicated that proteaphagy is functionally active in BTZ-resistant cells in the absence of any stimulus and underline its potential as a hallmark of BTZ-resistance in MCL cells.

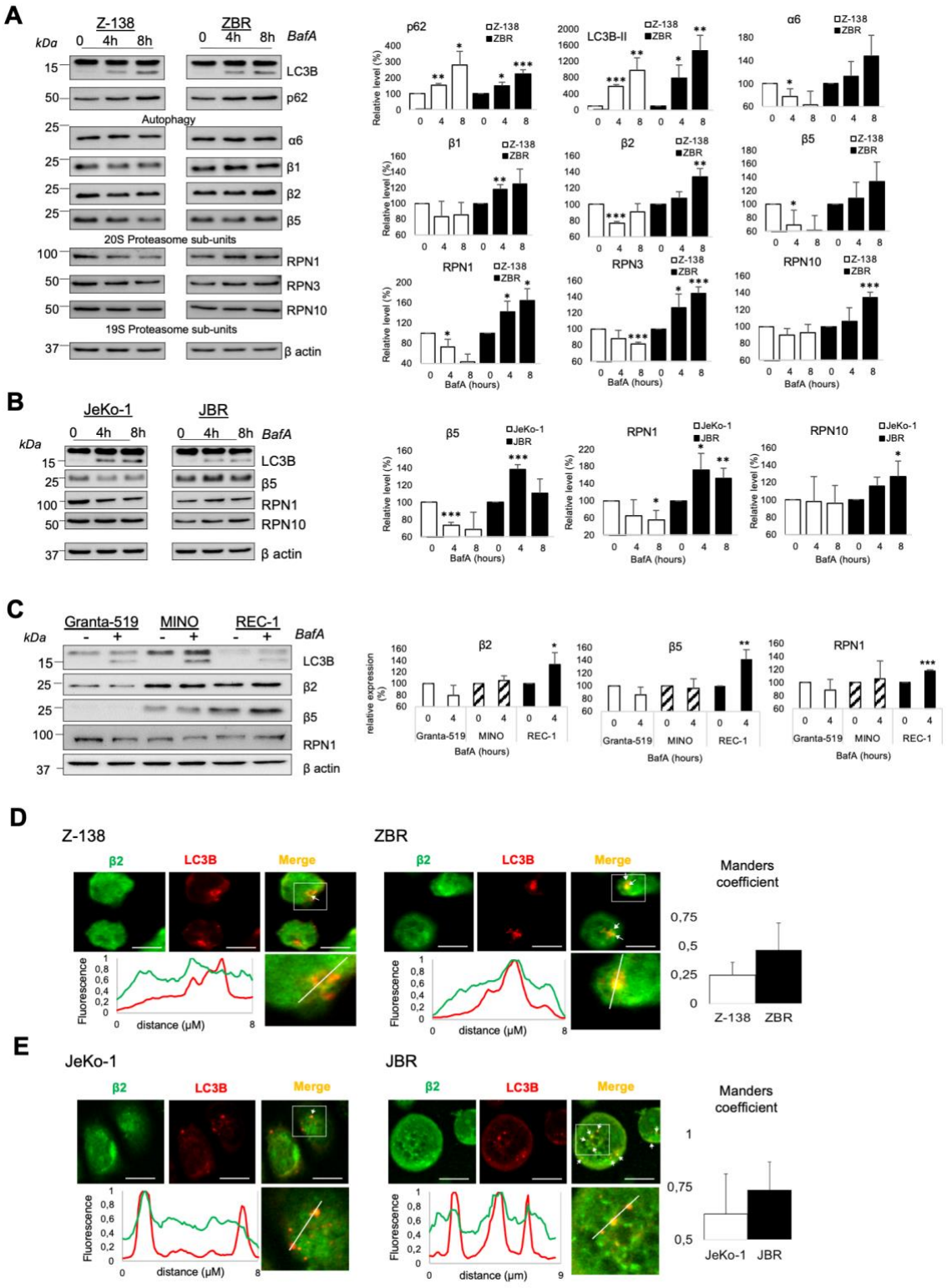

Figure 2. Proteaphagy is activated in BTZ-resistant MCL cells. BTZ-sensitive cells Z-138 **(A)** and JeKo-1 **(B)** and their resistant counterpart ZBR and JBR were treated or not with 20 nM BafA for 4 or 8 hours. Cells with intrinsic sensitivity (Granta-519) or resistance to BTZ (MINO and REC-1) **(C)** were treated or not with 40 nM BafA for 4 hours. WB analyses to detect autophagy or 26S proteasome proteins were performed with the indicated antibodies. Quantifications were performed using ImageJ software (n ≥ 3; means ± SD; two-tailed Student's *t*-test, *P < 0.05, **P < 0.01, ***P < 0.001). Z-

138/ZBR **(D)** and JeKo-1/JBR **(E)** were treated with 40 nM BafA for 8 hours. Fixed cells were stained with anti-β2 (green) or -LC3B (red) Abs and analysed by confocal microscopy, scale bar indicates 10 μM. Primary Abs were used: mouse anti- β2 1:100, mouse anti-p62 1:100, rabbit anti-LC3B 1:200, rabbit anti-α2 1:200. Secondary Abs were diluted 1:500 in blocking solution (5% bovine serum albumine, 0.1% Triton x100 in PBS) and incubated during 30 min at RT. Nuclei were stained with DAPI (P36931, Invitrogen). Looking for co-localisation of proteasome and autophagy proteins, normalized values of fluorescence intensity for LC3B (red) and β2 (green) along the white lines were plotted. Co-localisation was measured with Manders correlation coefficient calculated in regions of interest with LC3B punctates ($n \geq 20$; means ± SD; two-tailed Student's *t*-test, *$P < 0.05$, **$P < 0.01$, ***$P < 0.001$).

2.3. p62/Sequestosome-1 coordinates proteaphagosome assembly

p62 is not only a major autophagy player but it has also been involved in proteaphagy [17] and in proteasome inhibitor susceptibility in multiple myeloma cells [27]. To explore the role of p62 in proteaphagy, verteporfin (VTP, a clinical-grade small molecule inhibitor of this autophagy receptor) was employed [28,29]. Unlike BafA, VTP inhibits autophagy at early stage by aggregation of p62 and reduces autophagosome accumulation that can be assessed by a reduction of the autophagy marker LC3B [30,31]. Whereas the levels of LC3B and its lipidated form decreased, high molecular weight aggregates of p62 accumulated after VTP treatment in both Z-138 and ZBR cells. In contrast, BafA treatment accumulated both LC3B forms and p62 monomers. In agreement with the mechanism of action of these drugs when the double treatment was used, VTP stopped the BafA-induced accumulation of LC3B and p62 (Figure 3A). Interestingly, high molecular weight forms of RPN1, were also observed after VTP treatment. In contrast, β5 and β2 subunits were decreased after VTP treatment in both cell lines (Figure 3B). Accordingly, VTP treatment induced co-localisation of p62 with RPN1 but not with β2 subunits (Figure 3C, D). In contrast, BafA accumulated these proteasomal subunits in regions where punctuated autophagosomes were observed, in ZBR but not in Z138 cells (Figure 3B), highlighting a distinct mechanism of action for each inhibitor.

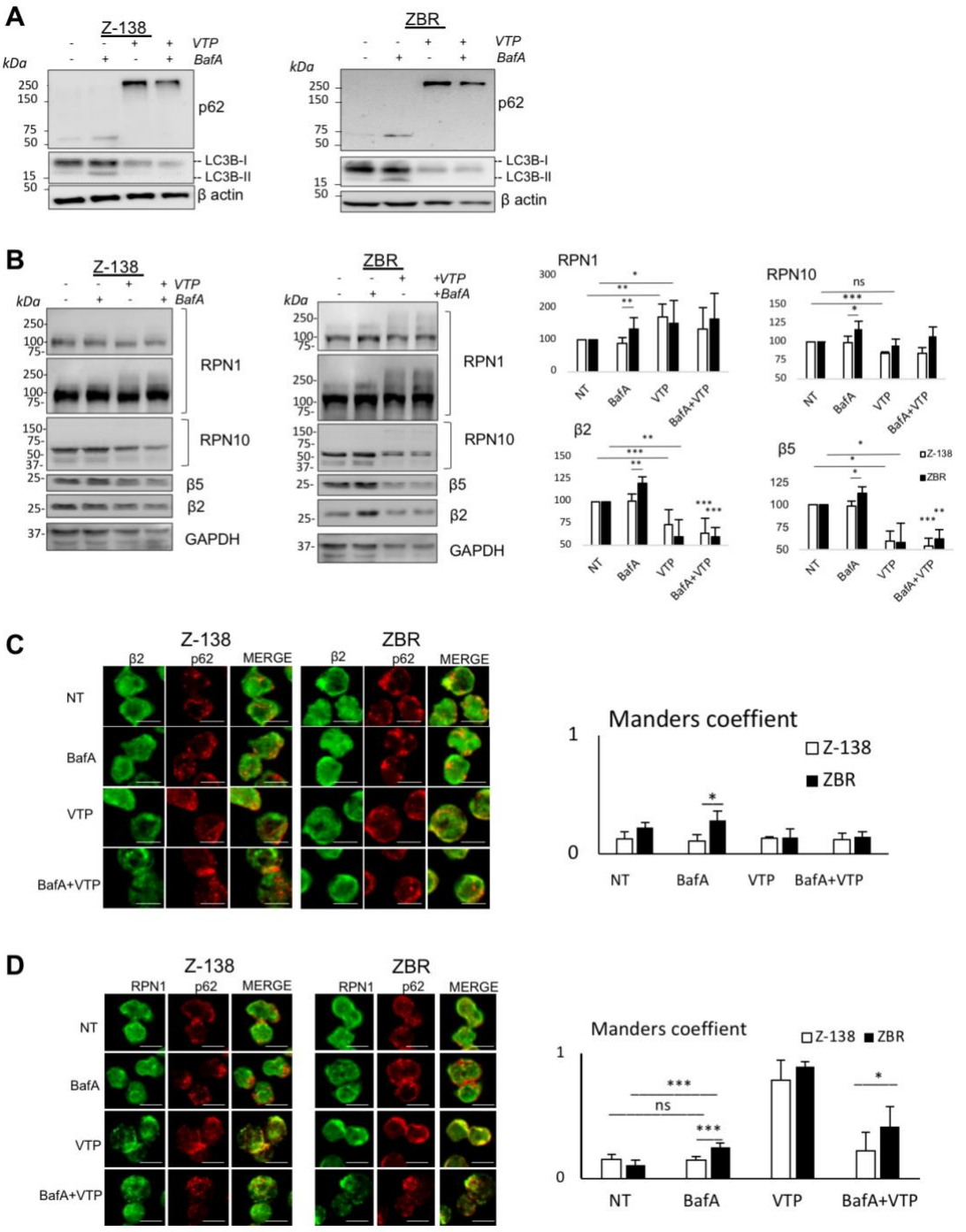

Figure 3. Inhibition of p62 affects the stability and localisation of proteasome subunits. Z-138 and ZBR cells were treated with 40 nM BafA, 10 μM VTP or in combination of BafA/VTP at the same concentrations for 4 or 6 hours, respectively. Whole-cell extracts were analysed by WB to control autophagy flux **(A)** and the total expression of proteasome subunits after treatments **(B).** Bands were analysed in 3 biological replicates using ImageJ software. **(C and D)** Co-localisation of proteasome subunits with autophagosomes after treatment with autophagy inhibitors. Z-138/ZBR were treated or not for 4 hours with 40 nM BafA or 10μM VTP or the combined treatment. Fixed cells were stained with anti-β2 antibody (green) and p62 (red) **(C),** or with anti-RPN1 antibody (green) and anti-p62

(red) **(D)**. Images were analysed by confocal microscopy, scale bar indicates 10 μM. Co-localisation was measured with Manders correlation coefficient calculated in regions of interest containing LC3B or p62 punctates (n ≥ 20; mean ± SD; two-tailed Student's *t*-test, *P<0.05, **P<0.01, ***P<0.001).

To investigate if high molecular weight forms of RPN1 could be ubiquitylated, a TUBEs-capture approach was used (Figure 4A). VTP remarkably altered the total ubiquitylation and had a negative impact on the TUBE-capture of RPN10 and β5 proteasome subunits in ZBR cells. Moreover, VTP enhanced the capture of p62 and RPN1 in both ZBR and Z138 cells (Figure 4A). To investigate how VTP affected p62 interactions with distinct proteasome subunits, immunoprecipitation experiments were performed using cell extracts from Z-138 and ZBR cells treated with BafA, VTP or both drugs (Figure 4B). The amount of RPN1 and β5 associated to p62 after BafA treatment was marginally but consistently increased, specifically in ZBR cells. In sharp contrast, the β5 and RPN1 subunits showed a reduced binding to p62 after VTP treatment (Figure 4B). To confirm these observations, RPN1 immunoprecipitation was performed under identical conditions. The level of RPN1 was increased after VTP treatment and this affected the amount of immunoprecipitated RPN1 (Figure 4C). Under these conditions, high molecular weight forms of p62 were bound to RPN1 while β5 subunits were dissociated (Figure 4C). These results suggest that p62 and RPN1 antibodies recognize distinct complexes differentially affected with BafA or VTP treatments. While the anti-p62 Ab precipitated proteophagosomes in the presence of BafA, the anti-RPN1 Ab precipitated aggregated forms of p62 after VTP treatment. All in all, these results underline the key role of p62 and its association with RPN1 for degradation *via* proteaphagy. Since VTP treatment could reduce the interaction of RPN1 with the 20S catalytic subunits, this raised the question of its impact on the overall proteasome activity. To investigate this point, in-gel chymotrypsin-like activity of proteasome β5 subunit was measured *in vitro* from VTP-treated MCL cells using reporter peptides [32]. Our results showed that 30S, 26S and 20S activities were reduced after a VTP treatment, but were unaffected by BafA (Figure 4D). Native gel-WB analysis of α7, β5 and RPN1 subunits revealed that VTP accumulated RPN1 subunit, whereas 20S CP were reduced and converted into a smaller molecular weight form of 20S subunit (Figure 4E). According to the in-gel proteasome activity assay this low molecular weight form of 20S was not activated (i20S). Overall, our results suggested that p62 contributes to target proteasome subunits to proteaphagic degradation.

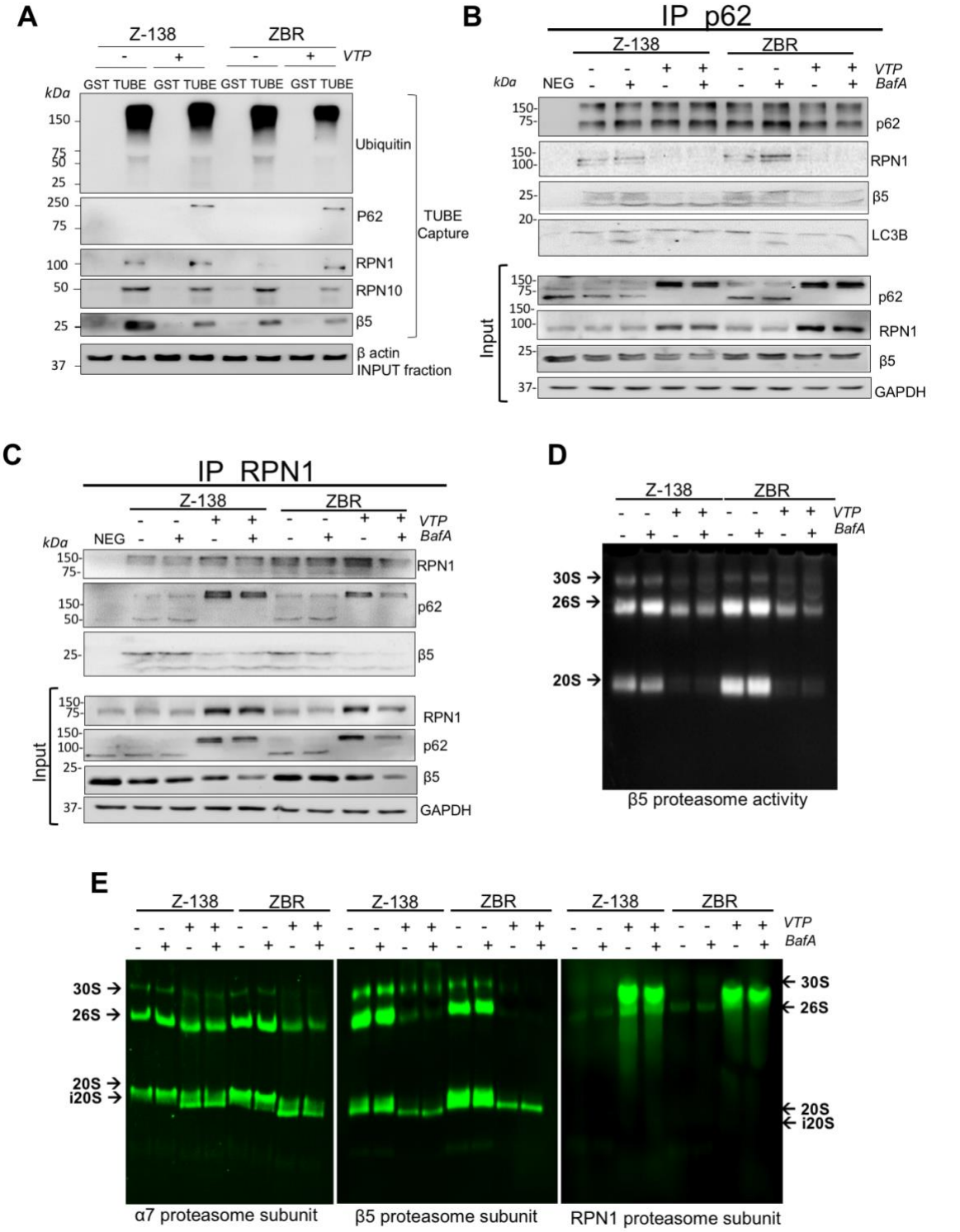

Figure 4. Role of p62 in the proteophagosome assembly. (A) Ubiquitylated proteins were captured using TUBEs from Z-138 and ZBR treated or not with 10 μM VTP for 4 hours. GST was used as a control. Indicated fractions were analysed by WB with the indicated Abs. **(B and C)** Cell lysates from Z-138 and ZBR were immunoprecipitated (IP) with anti-p62 and anti-RPN1 Abs. Immunoprecipitated material and input fractions were resolved and subjected to WB with the indicated Abs. **(D)** Cell extracts from Z-138 and ZBR treated or not with BafA, VTP or combined

253 treatment were run into non-denaturing native gels. In gel proteasome activity assay was measured
254 using fluorogenic peptides. **(E)** Native complexes separated as in **(D)** were transferred onto PDVF
255 membranes and blotted with the indicated Abs (n ≥ 3; mean ± SD; two-tailed Student's *t*-test, *P < 0.05,
256 **P < 0.01, ***P < 0.001)
257
258 *2.4. Autophagy inhibition increases apoptosis in BTZ-resistant MCL cells*
259
260 To explore the impact of autophagy inhibition on the viability of BTZ-resistant cells,
261 pharmacological modulation of apoptosis was evaluated by flow cytometry analysis of ZBR and JBR
262 cells. As expected, compared to their parental cells, both BTZ-resistant cell lines showed a significant
263 reduction in apoptosis levels after a 48h-treatment with 10 nM BTZ (Figures 5A and B). However, the
264 24 h-treatment with 20 nM BafA delivered a stronger apoptosis response in ZBR (around 40%) than
265 in JBR cells (around 12%). Both BTZ- resistant and their parental cell lines responded to the BafA-
266 treatment to the same extent (Figures 4A and S7). Nevertheless, the combined BTZ plus BafA
267 treatment remarkably stimulated apoptosis in ZBR (up to 70% apoptotic cells) and Z-138 cells (up to
268 90% apoptotic cells) while this combination exerted relatively modest anti-apoptotic activity (around
269 40% apoptosis) in JBR cells (Figure 5A and B). Considering the high diversity in MCL genetic
270 backgrounds, we further explored the effects of the same treatments on cell lines that naturally show
271 distinct sensitivity to BTZ (Figure 5C). While BafA alone killed efficiently REC-1 cells (Figure 5C), the
272 BafA/BTZ combo slightly increased the apoptosis rate in these cells, when compared with MINO cells
273 (Figure 5C), suggesting that this combination treatment could be more efficient in cells with high
274 bortezomib resistance.
275 Since p62 is playing a critical role in the assembly of proteaphagosomes, we then explored
276 whether its inhibition upon VTP treatment could favourably impact on BTZ-mediated apoptosis in
277 resistant cells (Figure 5D-F). Although VTP significantly promoted apoptosis when used alone (plus
278 30% or 26% cell death in REC-1 and ZBR, respectively). Its combination with BTZ achieved a
279 significant higher degree of cytotoxicity in both ZBR (plus 80% cell death induction, Figure 5D) and
280 REC1 cells (70% cell death induction) (Figure 5E), with respective drug combination indexes of 0.81
281 +/- 0.15 and 0.76 +/- 0.12, indicative of cooperative effects (Figure 5F). Interestingly, this cooperative
282 effect was statistically similar in ZBR and REC-1 cells.
283 In order to confirm the participation of p62 in the BTZ-mediated cytotoxicity, we used a
284 siRNA approach to knockdown *SQSTM1* (encoding p62) gene in ZBR cells prior to BTZ treatment.
285 As shown in Figure S6A and B, an 80% reduction was observed in p62 mRNA and protein levels after
286 transfection, this level of expression was maintained upon treatment with standard doses of BTZ.
287 Interestingly, upon a 24 h-treatment with BTZ, compared to the cells transfected with a non-targeting
288 siRNA, sensitivity to this inhibitor was restored in siSQSTM1-transfected ZBR cells. Following
289 treatment with 7.5 or 10 nM BTZ, the relative cytotoxic activity was recovered by 32% and 38%,
290 respectively (Figure S6C). Accordingly, knocking-down *SQSTM1* reduced the mean IC_{50} of BTZ
291 down to 7.33 nM at 24 h, reaching a similar value as the one observed in the parental non-resistant
292 Z-138 cells [8]. These results clearly support a role of p62 in the response to BTZ in resistant cells and
293 underline its potential as target for drug development.

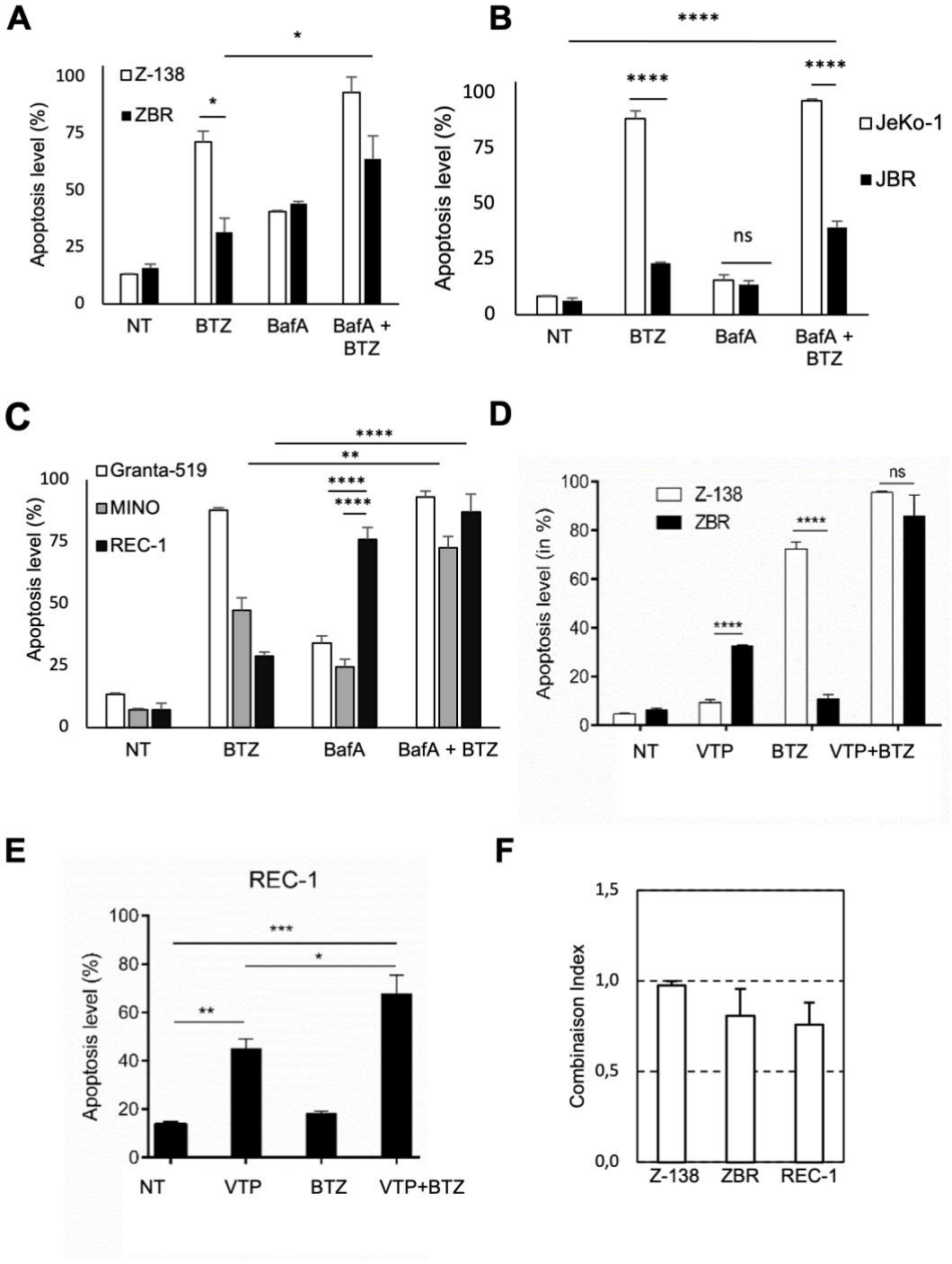

Figure 5. Autophagy inhibition increases apoptosis of BTZ-resistant cells. Flow cytometry analysis of apoptosis in Z-138 and ZBR cells **(A)**, JeKo-1 and JBR **(B)** cells or in Granta-519, MINO and REC-1 **(C)** MCL cells treated or not for 48 hours with 10 nM BTZ, 50 nM BafA or combined drugs as indicated. Apoptosis levels were measured by annexin V staining in Z-138 and ZBR cells (D) treated for 24 hours with 5µM VTP, 5 nM BTZ or the combined treatment and in REC-1 cells (E) treated for 24 hours with 15µM VTP, 5 nM BTZ or the combined treatment (n ≥ 3; means ± SD; two-tailed Student's *t*-test, *P<0.05, **P<0.01, ***P<0.001, ****p<0.0001). **(F)** From these results, we calculated the combination indexes (CIs) for Z-138, ZBR and REC-1 treated with VTP or BTZ using the Compusyn software (http://www.combosyn.com). The CIs between VTP and BTZ were determined at the constant ratios

displayed in **(D)** and **(E)** for Z-138/ZBR and REC-1 respectively. CI values of <1.0 indicate a cooperative effect of the two agents tested in combination.

2.5. Inhibition of p62 reduces the growth of BTZ-resistant MCL tumours in vivo

To evaluate the potential clinical interest of p62 inhibition in the treatment of BTZ-resistant MCL tumours, REC-1-Luc+ mouse xenografts were treated for two weeks with 0.5 mg/kg BTZ, 20 mg/kg VTP or both drugs. Tumour growth was evaluated for two weeks upon bioluminescent signal and tumour volume recorded (Figure 6A-D). Consistent with the resistant phenotype of REC1 cells, administration of BTZ as a single agent did not affect tumour burden. VTP-receiving animals experimented a 38% reduction in tumour growth compared to vehicle- or BTZ-treated mice. VTP administration combined with BTZ treatment reduced tumour growth to 44%, reaching statistical significance (Figure 6A and B). Immunohistochemical and WB analysis of tissue sections in representative tumour specimens revealed that VTP as a single agent was able to reduce the tumour mitotic index and to trigger apoptosis, as shown by a lower phospho-histone H3 staining and by the appearance of some nuclei positive for active caspase-3 within the tumours (Figure 6C, D). Most important, VTP-based treatments were associated with a cytosolic accumulation of p62, indicative of an inhibited autophagy, together with the consequent accumulation of RPN1. Confirming *in vitro* results, VTP/BTZ drug combination was able to improve both p62 and RPN1 accumulation, in association with highest tumour growth inhibition and apoptosis processing (Figure 6C, D). Thus, these *in vivo* results confirm the therapeutic potential of using autophagy inhibitors to recover the antitumor activity of BTZ in MCL tumours primarily resistant to this agent.

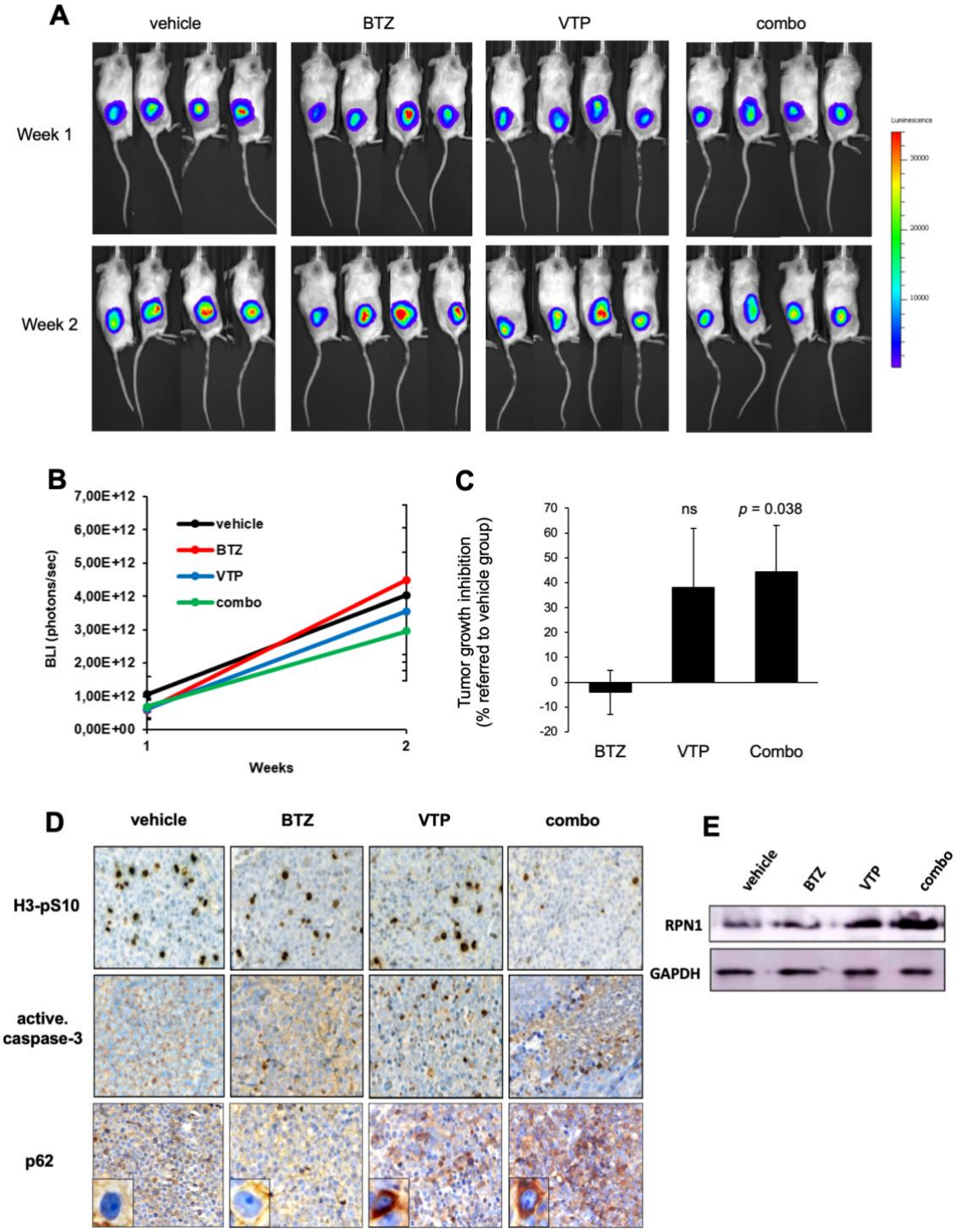

Figure 6. p62 inhibition reduces tumour growth in a BZT-resistant MCL xenograft model. (A) NSG mice were subcutaneously injected with REC1-GFP+Luc+ cells and tumour-bearing mice were randomly assigned to one of the following treatment arms (n = 4 mice per group): BTZ, 0.5 mg/kg twice weekly (i.p.); VTP, 20 mg/kg twice weekly (i.p.), both agents or equal volume of vehicle, for two weeks. Tumour burden was evaluated at week 1 and week 2 by analysis of the bioluminescence signal. **(B)** Luciferase activity was quantified using the Living Image software. **(C)** Tumour volume was

evaluated *ex vivo* using callipers, upon euthanasia of the animals. The inhibition of tumour growth relative to the control group is reported on the histograms. **(D)** Immunohistochemical labelling of phosphorylated histone H3 (H3-pS10) as a marker of proliferating cells and activated (act.) caspase 3 as a marker of apoptosis, and p62 in consecutive tissue sections from four representative tumour specimens (x 500, magnification) after 2 weeks of treatment. **(E)** RPN1 protein levels were evaluated by WB analysis in 4 representative tumour samples after the 2 weeks of treatment. ns, not significant.

3. Discussion

Bortezomib significantly improved the prognosis of patients with MM and MCL. However, relapses following this therapy are frequent, while primary resistance to this agent remains a major limitation for further development of its therapeutic use [10]. Here, using different cellular models of MCL with either acquired or intrinsic resistance, we observed that refractoriness to BTZ is accompanied by ALS activation, and in particular proteaphagy. Reduction of proteasome subunits in the Ub-proteome is a strong hallmark of BTZ-resistant cells and highlight an important crosstalk between these two major proteolytic pathways in these cells. Other studies have proposed that the reduced expression of 19S proteasome subunits are responsible for the BTZ-resistance found in MM cells [33]. Furthermore, low levels of 19S subunits are at the origin of the resistance to the second-generation PI, carfilzomib, in MM cells [33,34]. Upon the blockade of autophagy-mediated degradation, both 19S and 20S subunits were accumulated in BTZ-resistant cells with acquired or intrinsic resistance. In intrinsic resistant models such as REC-1 cells, the accumulation of proteasome subunits upon autophagy inhibition was easier to highlight. The reduction in proteasome subunits within the Ub-proteome was also observed in JBR cells. JBR and its parental cell line JeKo-1 carry mutations/deletions of relevant genes such as *TP53*, *MLL2*, *DCP1B*, *TRMP6* [35]. Despite these genetic alterations, proteaphagy was observed in JBR indicating that active proteaphagy is a well-preserved mechanism present in cells that resist to BTZ-treatment, independently of the genetic background of the tumour cells.

Our co-localisation analyses employing two distinct markers of autophagy (LC3B and p62), clearly indicate that 20S proteasome subunits are accumulated in autophagosomes after treatment with autophagy inhibitors, indicating ongoing proteaphagy. Cells may employ this mechanism in the presence of deficient proteasomes to restore proteostasis [15,16]. Interestingly, the use of distinct autophagy inhibitors (CQ, BafA or VTP) did not lead to the same results in ZBR and JBR in terms of timing and efficiency to accumulate proteasome subunits nor in the capacity to drive apoptosis alone or in combination with BTZ. This suggests that the molecular mechanisms engaged by these drugs are not exactly the same [23,36]. Blocking autophagy at the level of p62 receptor appears to negatively affect the assembly of the 26S proteasome and results in a dissociation of the 20S from 19S subunits. Since VTP could trigger oxidative stress, in a light dependent manner [28] and produce reactive oxygen species (ROS) such as singlet oxygen and radical species [37], ROS contribute to the observed effects on proteasome stability and activity [38]. In any case, RPN1 is likely fulfilling a relevant role in the response to VTP since in contrast to other proteasome subunits tested, its integration in the ubiquitin proteome is increased after treatment with this drug.

The role of p62 in the response to BTZ in multiple myeloma has been previously suggested [27]. Although the mechanism of BTZ-resistance acquisition is not fully clear, it appears that it could

be common to other proteasome inhibitors such as carfilzomib since p62 is directly or indirectly implicated in this process [39]. Indeed, knocking down SQSTM1 in ZBR cells significantly potentiates BTZ cytotoxicity (Figure 6), supporting the role of p62 in BTZ resistance in MCL model. Actual options for chemical inhibitors of p62 are limited. The XRK3F2 inhibitor that specifically targets the ZZ domain of p62 [40] can overcome BTZ resistance in MM, independently of the *TP53* status [41,42]. We therefore tested the p62 inhibitor XRK3F2 in BTZ-resistant MCL cells, but its cytotoxic effects were less pronounced than the ones observed with VTP (data not shown). This suggest that in addition of p62, other factors might play a crucial role in the response/resistance to proteasome inhibitors.

Late stage autophagy inhibitors also induced distinct apoptosis levels in BTZ-resistant MCL cells. In inherent BTZ-resistant cell models, the resistance to BTZ seems positively correlated with their dependency on autophagy, and BafA alone compromises cell viability (e.g. results from REC-1). However, the combined treatment BTZ/BafA could be more efficient to kill cells with intermediate levels of resistance (e.g. results from MINO) [9]. Interestingly, the most efficient single treatment was VTP and the combination index indicated that cooperative effects can be observed when combined with BTZ. These observations were also validated in xenografted mice models using the REC-1 cell line.

4. Materials and Methods

4.1. Antibodies

Antibodies (Abs) anti-P4D1 ubiquitin, -β2, -PSMD2, -p62 were purchased from Santa Cruz Biotechnology (CA). Abs anti-α6 and -PSMD3 were obtained from Invitrogen. Anti-β-actin Ab was from Abgent. Anti-annexin 5 Ab was from BD Science. Abs anti-β1, -RPN10 and -RPT4 were from Enzo Life Science. Anti-β5, -PSMA2, -LC3B, -ADRM1, -AMBRA1 and -HYOU1 were from Cell Signaling Technology (Danvers, MA). Abs anti-mTOR and -S100A9 were from Sigma (St. Louis, MO). Abs anti-UVRAG, -TOLLIP, -VPS33A, and -VTI1A were from ThermoFischer Scientific (Waltham, MA). Donkey anti-rabbit TexRed and donkey anti-mouse FITC secondary Abs were from Jackson Immunoresearch. Goat anti-mouse Star 635 was from Abberior and Donkey anti-Rabbit Alexa Fluor 594 was from Invitrogen. Fluorescent secondary Abs IRDye® 800CW and IRDye® 680RD were from LICOR. Peroxidase Goat Anti-Rabbit IgG and Peroxidase Rabbit Anti-Mouse IgG were from Jackson Immunoresearch.

4.2. Reagents

Ac-nLPnLD-amc, Boc-LSTR-amc and Suc-LLVY-amc peptides were purchased from Bachem AG (Bubendorf, CHE). Marizomib, Chloroquine and Verteporfin were from Sigma (St. Louis, MO), Bortezomib was from Tebu bio (FR), Bafilomycin A1 and Everolimus were from Invivogen (CA).

4.3. Cell Culture

ZBR and JBR were derived from Z-138 and JeKo-1 respectively [8]. All cells were cultured in RPMI 1640 with 2 mM L-glutamine, 100 Units/mL penicillin, 100 μg/mL streptomycin and 10% foetal bovine serum (FCS), excepting JeKo-1 and JBR (20% FCS). Cells were incubated at 37°C, 5% CO_2. Cell lines authentication was based on short tandem repeat (STR) profiling by DSMZ services (Braunschweig,

Germany).

4.4. TUBEs capture

The capture of ubiquitylated proteins for mass spectrometry analysis was performed as described in [3]. For all other TUBE-captures, 10^7 cells were treated and used according to the protocol reported in [20] and [21].

4.5. Mass spectrometry analysis

TUBEs-mass spectrometry analysis was performed as reported [3,44]. Mass spectrometry data are available in the PRIDE database: http://www.ebi.ac.uk/pride Username: reviewer16995@ebi.ac.uk Password: 5aiE0r5b. A stringent protein identification filter was selected retaining only proteins with at least false discovery rate (FDR) < 1%. Spectral counts were summed up for each matching peptide for a given protein and spectral counts obtained in GST control samples were subtracted using the statistical programming language R. Negative and zero values were set to one to enable $\log_2$ transform of the quantitative data. The data were then $\log_2$ transformed and quantile normalized across samples. Proteins with more than two fold regulated between Z-138 and ZBR that could be reproduced in all three replicas were maintained for further Western blot validation and functional evaluation. From the 263 selected proteins with more than two-fold difference between Z-138 and ZBR that could be reproduced in all three replicas, 60 were UPS and ALS factors. Among the 263, 123 were more abundant in ZBR and 140 less abundant in ZBR. These proteins were maintained for further dry and wet analyses.

4.6. IPA analysis

Analysis using Ingenuity Pathway Analysis (IPA®, QIAGEN Redwood City, www.qiagen.com/ingenuity) integrated canonical signalling pathways associated to Z-138 and ZBR cells (p-value < 0.05 calculated by Fishers's exact test). The calculated p-values determine the probability that the association between proteins in the dataset and the canonical pathways is explained by chance alone.

4.7. Database search

The obtained data from the 120 LC-MS runs were searched using VEMS [45] and MaxQuant [46] using both Higher-energy induced collisional dissociation (HCD) and ETD scoring. A standard human proteome database from UniProt (3AUP000005640) including common contaminating proteins [47]. Permutated protein sequences, where Arg and Lys were not permutated, were included in the database. The total number of protein entries in the database was 140149. Trypsin cleavage allowing a maximum of 4 missed cleavages was used. Carbamidomethyl cysteine was included as fixed modification. Methionine oxidation (UNIMOD: 35), N-terminal protein acetylation (UNIMOD: 1), GG tag (UNIMOD: 121) on lysine, LRGG tag (UNIMOD: 535) on lysine deamidation (UNIMOD: 7) of asparagine and glutamine was included as variable modifications. Five ppm mass accuracy was specified for precursor ions and 0.5 m/z for fragment ions. The FDR for protein identification was set to 1% for peptide and protein identifications. No restriction was applied for minimal peptide length for VEMS search. Identified proteins were divided into evidence groups [48].

462 *4.8. Bioinformatics analysis*

463 Gene ontology analysis (http://geneontology.org) was made using the R packages GO.db [49] and
464 KEGG.db [50] the proteins associated to the functional categories in the heatmaps. Venn diagrams
465 were made with the R package VennDiagram [51].
466
467 *4.9. Western blotting*

468 Western blot analysis was performed as previously reported [20,21]. Pictures were acquired using
469 West Femto ECL (34096 Thermofischer), with PXI4 (Syngene) and GeneTools (Syngene).
470 Quantifications were performed using ImageJ. The density of each protein of interest was then
471 normalized against the density of the control housekeeping protein β-actin. Relative protein levels
472 under treatment conditions were calculated with respect the control basal condition.
473
474 *4.10. Immunoprecipitation*

475 Abs (3-5 μg per point) were incubated 2 h at 4°C with 30-40 μl of protein A magnetic beads (Millipore).
476 Abs were then crosslinked as reported [3]. Cells pellets were lysed with 500 μL TUBE lysis buffer [21].
477 After 5 min incubation on ice, samples were centrifugated 30 min at 13 000 rpm at 4°C. Supernatant
478 were incubated 1 h at 4°C with 30 μL of DMP-crosslinked beads-Abs. After 5 washes with PBST 0.05%,
479 pull-downed proteins were eluted in 100 μL 1.5X Boiling Buffer (4% SDS, 20% glycerol, 120 mM Tris-
480 HCl pH 6.8) before analysis by immunoblotting.
481
482 *4.11. Immunofluorescence microscopy*

483 Immunofluorescence analysis of Z-138/ZBR and JeKo-1/JBR was performed with the same reported
484 protocol [8]. Abs were incubated overnight at RT in blocking solution (5% bovine serum albumine,
485 0.1% triton X100 in PBS). Images from Figure 2 and Figure S5 were acquired with Zeiss Observer Z.1
486 Microscope implemented with the Zeiss LSM 510, C-apochromat objective 40X/1.20 W (UV-V15-IR,
487 Torr), using Zen 2009 software package (Zeiss). Images from Figure S5 were acquired with Nikon
488 confocal C1-Si with 40X oil immersion objective 1.3 NA, using NIS-Elements Software (Nikon).
489 Pictures were assembled with Adobe Photoshop 7.0. Images were not modified other than
490 adjustments of levels, brightness and magnification. Co-localisation analyses and Manders co-
491 localisation coefficient calculations were performed using ImageJ.
492
493 *4.12. Native gel electrophoresis and in gel proteasomal activity assay*

494 The analysis of proteasome complexes and activity were performed by native gel electrophoresis as
495 reported [32,52]. Ten million of fresh or rapidly thawed cells were used for each experimental point.
496 Thirty μg of total protein were migrated per well in NuPAGE™ Novex™ 3-8% Tris-Acetate Protein
497 Gel (ThermoFisher). Migrations were performed in native gel electrophoresis buffer (NG buffer) (90
498 mM Tris-borate, 0.1 mM EDTA, 5 mM $MgCl_2$, 0.5 mM ATP, 0.5 mM DTT) at 150 volts for 3 hours. The
499 intrinsic activity of native proteasomes was analysed in gel by 20 min incubation in NG buffer
500 supplemented with 100 μM Suc-LLVY-AMC (Bachem) at 37°C. The amount of cleaved AMC
501 fragment was imaged with Syngene NuGenius. Native gels were then washed during 10 min 2 times
502 in 10x Tris-Glycine/SDS Laemmli buffer (0.25 M Tris, 1.92 M Glycine, 1% SDS, pH 8.6), followed by a
503 last wash in 1x Tris-Glycine/SDS Laemmli buffer. Gels were transferred in PDVF membrane (0.45μm
504 pore size, Immobilon-P, Merck) overnight at 40 volts at 4°C. Membranes were blotted and analysed

for proteins of interest.

4.13. Flow cytometry

Cells seeded at 4 x 10^5/mL in 12- or 24-well plates were collected and pelleted by centrifugation at 125 *g* for 5 min. Pellets were resuspended and cells were stained 20 min with 100 µL 1x Annexin V Buffer (BD Pharmingen) with 1:100 FITC-Annexin V (BD Pharmingen). Three hundred µL of Annexin Buffer were added to samples, and 10^4 events were collected for each experiment. Means ± SD of all events were calculated from the population.

4.14. In vivo experiments

REC1-GFP-Luc cells were produced and inoculated subcutaneously in 7-week old NSG mice as previously described [53]. Animals were randomly assigned into 4 equivalent cohorts and treated intraperitoneally with 0.5 mg/kg BTZ and/or 20 mg/kg VTP, twice weekly, for two weeks. Animals of the control group were dosed with equal volume of vehicle. Tumour engraftment was determined weekly following mice injection with 75 mg/kg D-luciferine (AnaSpec) and bioluminescence recording on a Xenogen IVIS Spectrum (Perkin Elmer). After two weeks, animals were then sacrificed, and tumours were measured *ex vivo* by external calipers. Tumour samples were formalin-fixed and paraffin-embedded and subjected to immunohistochemical analysis following previously described procedure [9]. The primary Abs used were phospho-histone H3 and cleaved-caspase-3 (Cell Signaling Technology) and p62 (Tebu-Bio). Images were acquired using an Eclipse microscope with the NIS-Elements Viewer software (Nikon). One representative tumour of each group was used for the quantification of RPN1 protein levels by SDS-PAGE, as previously published [54], using an anti-RPN1 monoclonal antibody (Tebu-Bio). Animal handling was performed following protocols approved by the Animal Ethics Committee of the Autonomous University of Barcelona (protocol #37/18).

4.15 Quantification and statistical analysis

All experiments were repeated for at least 3 times unless stated in the figure legend. Two-tailed unpaired Student's t-tests was applied for comparisons between two groups. The data are presented as the means ± SD except where stated otherwise. $P < 0.05$ values were considered statistically significant.

5. Conclusions

Our results indicate that manipulating proteaphagy could be used as a strategy to treat BTZ-resistant MCL cells since they become "addicted" to autophagy and therefore hypersensitive to the inhibition of both proteolytic pathways. Since proteaphagy is permanently activated in BTZ-resistant cells but absent from untreated BTZ-sensitive cells, this process might only concern inactive proteasomes under those conditions. However, since BTZ is still blocking some proteasome activity in BTZ-resistant cells further investigations are required to elucidate if proteaphagy distinguish inactive from active proteasomes. Since proteaphagy eliminates the target of BTZ (20S proteasomes), the sensitivity to this treatment is reduced in BTZ-resistant cells. We propose proteaphagy as a new mechanism contributing to the lack of sensitivity to BTZ observed in BTZ-resistant cells. The existence

of other compensatory processes contributing to reduce the efficacy of BTZ cannot be ruled out.

New generation of PIs have been subsequently developed to reduce toxicity and overcome BTZ-resistance [43]. Marizomib constitutes a promising example that acts on the three catalytic subunits of the proteasome and improves apoptosis when combined to distinct autophagy inhibitors on BTZ-resistant cells [34,43]. Therefore, the identification of the multifactorial mechanisms mediating inherent and acquired resistance to BTZ will be instrumental to overcome this problem and enhance the therapeutic efficacy of PIs.

Supplementary Materials:
Supplementary materials contain supplementary methods and supplementary figures and legends as follows: Figure S1. TUBEs-MS procedure to identify the ubiquitin proteome from MCL cells, Figure S2. Heat map representation of the 263 proteins enriched or reduced in studied MCL cell lines, Figure S3. Analysis of the UPS and ALS proteins identified in our TUBEs-MS analysis, Figure S4. Inhibition of autophagy revealed an active proteaphagy in distinct BZT-resistant MCL cell lines, Figure S5. Co-localisation of proteasome subunits with autophagosomes in distinct MCL cell lines, Figure S6. Silencing of p62 improves sensitivity to BTZ in BZT-resistant MCL cells. Supplementary Table 1. Excel file with the following MS data can be obtained at: the PRIDE database: http://www.ebi.ac.uk/pride Username: reviewer16995@ebi.ac.uk Password: 5aiE0r5b.

Author Contributions: WX, MA, FA, FE and MSR established settings and performed MS analysis. GQ, WX, MA, and RM performed bioinformatics and statistics analysis. GQ, LC, MGS and MSR validated TUBE-captured proteins and performed autophagy analysis experiments. Immunofluorescence was performed by GQ, MM, JA and PLA. GQ and OC performed proteasome assays and data analysis. NPP, FB and DRG carried out p62 silencing and in vivo experiments. BS and GR provided know-how and all MCL cell lines used in this project. MSR, GR and RM designed and supervised the project and wrote the first draft of this manuscript. All authors provided comments and suggestions to improve this manuscript.

Funding: This work was supported at early stages by (Spanish MINECO, CTQ2011– 27874 grant). MGS is fellow from the UbiCODE project funded by the EU's Horizon 2020 research and innovation program under the Marie Skłodowska-Curie grant agreement No 765445. MSR and LC were also funded by the Institut National du Cancer, France (PLBIO16-251), CONACyT-SRE (Mexico) grant 0280365 and the REPERE program of Occitanie. OC is funded by "La Ligue contre le cancer du Gard". ICFO authors were supported from Spanish MINECO "Severo Ochoa" program for Centres of Excellence in R&D (SEV-2015-0522), from Fundació Privada Cellex, Fundación Mig-Puig, from Generalitat de Catalunya CERCA program and form LASERLAB Europe (grant agreement No 654148). GR was financially supported by Fondo de Investigación Sanitaria PI15/00102 and PI18/01383, European Regional Development Fund (ERDF) 'Una manera de hacer Europa'. GR and DRG are members of the Spanish Network of Excellence UBIRed funded by the Spanish Ministry Science, Innovation and Universities (SAF2017-90900-REDT).

Acknowledgments:
We do thank all members of UbiCARE laboratory, Sophie Pautot and Renaud Legouis for stimulating discussions and/or technical assistance. We thank Clémence Coutelle-Rebut for the proofreading of this manuscript.

Conflicts of Interest: The authors declare no conflict of interest. The funders had no role in the design of the study; in the collection, analyses, or interpretation of data; in the writing of the manuscript, or in the decision to publish the results.

References

1. Cheah CY, Seymour JF, Wang ML. Mantle Cell Lymphoma. J Clin Oncol. 10 Apr 2016;34(11):1256-69.
2. Kane RC, Bross PF, Farrell AT, Pazdur R. Velcade: U.S. FDA approval for the treatment of multiple myeloma progressing on prior therapy. Oncologist. 2003;8(6):508-13.
3. Xolalpa W, Mata-Cantero L, Aillet F, Rodriguez MS. Isolation of the Ubiquitin-Proteome from Tumor Cell Lines and Primary Cells Using TUBEs. Methods Mol Biol. 2016;1449:161-75.
4. Niewerth D, Jansen G, Assaraf YG, Zweegman S, Kaspers GJL, Cloos J. Molecular basis of resistance to proteasome inhibitors in hematological malignancies. Drug Resist Updat. Jan 2015;18:18-35.
5. Barrio S, Stühmer T, Da-Viá M, Barrio-Garcia C, Lehners N, Besse A, et al. Spectrum and functional validation of PSMB5 mutations in multiple myeloma. Leukemia. Feb 2019;33(2):447-56.
6. Hambley B, Caimi PF, William BM. Bortezomib for the treatment of mantle cell lymphoma: an update. Ther Adv Hematol. Aug 2016;7(4):196-208.
7. Weniger MA, Rizzatti EG, Pérez-Galán P, Liu D, Wang Q, Munson PJ, et al. Treatment-induced oxidative stress and cellular antioxidant capacity determine response to bortezomib in mantle cell lymphoma. Clin Cancer Res. 1 Aug 2011;17(15):5101-12.
8. Roué G, Pérez-Galán P, Mozos A, López-Guerra M, Xargay-Torrent S, Rosich L, et al. The Hsp90 inhibitor IPI-504 overcomes bortezomib resistance in mantle cell lymphoma in vitro and in vivo by down-regulation of the prosurvival ER chaperone BiP/Grp78. Blood. 27 Jan 2011;117(4):1270-9.
9. Moros A, Rodríguez V, Saborit-Villarroya I, Montraveta A, Balsas P, Sandy P, et al. Synergistic antitumor activity of lenalidomide with the BET bromodomain inhibitor CPI203 in bortezomib-resistant mantle cell lymphoma. Leukemia. Oct 2014;28(10):2049-59.
10. Gonzalez-Santamarta M, Quinet G, Reyes-Garau D, Sola B, Roué G, Rodriguez MS. Resistance to the Proteasome Inhibitors: Lessons from Multiple Myeloma and Mantle Cell Lymphoma. Adv Exp Med Biol. 2020;1233:153-74.
11. Dikic I. Proteasomal and Autophagic Degradation Systems. Annu Rev Biochem. 20 2017;86:193-224.
12. Kwon YT, Ciechanover A. The Ubiquitin Code in the Ubiquitin-Proteasome System and Autophagy. Trends Biochem Sci. 2017;42(11):873-86.
13. Collins GA, Goldberg AL. The Logic of the 26S Proteasome. Cell. 18 May 2017;169(5):792-806.
14. Coux O, Zieba BA, Meiners S. The Proteasome System in Health and Disease. Adv Exp Med Biol. 2020;1233:55-100.
15. Marshall RS, Vierstra RD. Eat or be eaten: The autophagic plight of inactive 26S proteasomes. Autophagy. 2015;11(10):1927-8.
16. Marshall RS, McLoughlin F, Vierstra RD. Autophagic Turnover of Inactive 26S Proteasomes in Yeast Is Directed by the Ubiquitin Receptor Cue5 and the Hsp42 Chaperone. Cell Rep. 09 2016;16(6):1717-32.

627 17. Cohen-Kaplan V, Livneh I, Avni N, Fabre B, Ziv T, Kwon YT, et al. p62- and ubiquitin-dependent stress-
628 induced autophagy of the mammalian 26S proteasome. Proc Natl Acad Sci U S A. 22 nov
629 2016;113(47):E7490-9.

630 18. Cohen-Kaplan V, Ciechanover A, Livneh I. Stress-induced polyubiquitination of proteasomal ubiquitin
631 receptors targets the proteolytic complex for autophagic degradation. Autophagy. 3 avr 2017;13(4):759-60.

632 19. Quinet G, Gonzalez-Santamarta M, Louche C, Rodriguez MS. Mechanisms Regulating the UPS-ALS
633 Crosstalk: The Role of Proteaphagy. Molecules. 18 mai 2020;25(10).

634 20. Aillet F, Lopitz-Otsoa F, Hjerpe R, Torres-Ramos M, Lang V, Rodríguez MS. Isolation of ubiquitylated
635 proteins using tandem ubiquitin-binding entities. Methods Mol Biol. 2012;832:173-83.

636 21. Hjerpe R, Aillet F, Lopitz-Otsoa F, Lang V, England P, Rodriguez MS. Efficient protection and isolation of
637 ubiquitylated proteins using tandem ubiquitin-binding entities. EMBO Rep. Nov 2009;10(11):1250-8.

638 22. Mattern M, Sutherland J, Kadimisetty K, Barrio R, Rodriguez MS. Using Ubiquitin Binders to Decipher the
639 Ubiquitin Code. Trends Biochem Sci. July 2019;44(7):599-615.

640 23. Accardi F, Toscani D, Bolzoni M, Dalla Palma B, Aversa F, Giuliani N. Mechanism of Action of Bortezomib
641 and the New Proteasome Inhibitors on Myeloma Cells and the Bone Microenvironment: Impact on
642 Myeloma-Induced Alterations of Bone Remodeling. Biomed Res Int. 2015;2015:172458.

643 24. Lopitz-Otsoa F, Rodriguez-Suarez E, Aillet F, Casado-Vela J, Lang V, Matthiesen R, et al. Integrative
644 analysis of the ubiquitin proteome isolated using Tandem Ubiquitin Binding Entities (TUBEs). J
645 Proteomics. 6 June 2012;75(10):2998-3014.

646 25. Mata-Cantero L, Azkargorta M, Aillet F, Xolalpa W, LaFuente MJ, Elortza F, et al. New insights into host-
647 parasite ubiquitin proteome dynamics in P. falciparum infected red blood cells using a TUBEs-MS
648 approach. J Proteomics. 29 avr 2016;139:45-59.

649 26. Marshall RS, Li F, Gemperline DC, Book AJ, Vierstra RD. Autophagic Degradation of the 26S Proteasome
650 Is Mediated by the Dual ATG8/Ubiquitin Receptor RPN10 in Arabidopsis. Mol Cell. 18 June
651 2015;58(6):1053-66.

652 27. Milan E, Perini T, Resnati M, Orfanelli U, Oliva L, Raimondi A, et al. A plastic SQSTM1/p62-dependent
653 autophagic reserve maintains proteostasis and determines proteasome inhibitor susceptibility in multiple
654 myeloma cells. Autophagy. 2015;11(7):1161-78.

655 28. Donohue E, Balgi AD, Komatsu M, Roberge M. Induction of Covalently Crosslinked p62 Oligomers with
656 Reduced Binding to Polyubiquitinated Proteins by the Autophagy Inhibitor Verteporfin. PLoS One.
657 2014;9(12):e114964.

658 29. Donohue E, Tovey A, Vogl AW, Arns S, Sternberg E, Young RN, et al. Inhibition of autophagosome
659 formation by the benzoporphyrin derivative verteporfin. J Biol Chem. 4 Mar 2011;286(9):7290-300.

660 30. Lopez-Reyes RG, Quinet G, Gonzalez-Santamarta M, Larrue C, Sarry J-E, Rodriguez MS. Inhibition of the
661 proteasome and proteaphagy enhances apoptosis in FLT3-ITD-driven acute myeloid leukemia. FEBS Open
662 Bio. Jan 2021;11(1):48-60.

663 31. Saini H, Sharma H, Mukherjee S, Chowdhury S, Chowdhury R. Verteporfin disrupts multiple steps of
664 autophagy and regulates p53 to sensitize osteosarcoma cells. Cancer Cell Int. 14 Jan 2021;21(1):52.

665 32. Kisselev AF, Goldberg AL. Monitoring activity and inhibition of 26S proteasomes with fluorogenic peptide
666 substrates. Meth Enzymol. 2005;398:364-78.

33. Tsvetkov P, Mendillo ML, Zhao J, Carette JE, Merrill PH, Cikes D, et al. Compromising the 19S proteasome complex protects cells from reduced flux through the proteasome. Elife. 1 Sept 2015;4.

34. Acosta-Alvear D, Cho MY, Wild T, Buchholz TJ, Lerner AG, Simakova O, et al. Paradoxical resistance of multiple myeloma to proteasome inhibitors by decreased levels of 19S proteasomal subunits. Deshaies RJ, éditeur. eLife. 1 Sept 2015;4:e08153.

35. Beà S, Valdés-Mas R, Navarro A, Salaverria I, Martín-Garcia D, Jares P, et al. Landscape of somatic mutations and clonal evolution in mantle cell lymphoma. Proc Natl Acad Sci USA. 5 Nov 2013;110(45):18250-5.

36. Mauthe M, Orhon I, Rocchi C, Zhou X, Luhr M, Hijlkema K-J, et al. Chloroquine inhibits autophagic flux by decreasing autophagosome-lysosome fusion. Autophagy. 2018;14(8):1435-55.

37. Konstantinou EK, Notomi S, Kosmidou C, Brodowska K, Al-Moujahed A, Nicolaou F, et al. Verteporfin-induced formation of protein cross-linked oligomers and high molecular weight complexes is mediated by light and leads to cell toxicity. Sci Rep. 21 Apr 2017;7:46581.

38. Grune T, Catalgol B, Licht A, Ermak G, Pickering AM, Ngo JK, et al. HSP70 mediates dissociation and reassociation of the 26S proteasome during adaptation to oxidative stress. Free Radic Biol Med. 1 Oct 2011;51(7):1355-64.

39. Riz I, Hawley TS, Marsal JW, Hawley RG. Noncanonical SQSTM1/p62-Nrf2 pathway activation mediates proteasome inhibitor resistance in multiple myeloma cells via redox, metabolic and translational reprogramming. Oncotarget. 11 Oct 2016;7(41):66360-85.

40. Adamik J, Silbermann R, Marino S, Sun Q, Anderson JL, Zhou D, et al. XRK3F2 Inhibition of p62-ZZ Domain Signaling Rescues Myeloma-Induced GFI1-Driven Epigenetic Repression of the Runx2 Gene in Pre-osteoblasts to Overcome Differentiation Suppression. Front Endocrinol (Lausanne). 2018;9:344.

41. Marino S, Petrusca DN, Silberman R, Toscani D, Anderson JL, Giuliani N, et al. Inhibition of p62-ZZ Domain-Mediated Signaling Overcomes Bortezomib Resistance in Multiple Myeloma Cells Independent of Their p53 Status. Blood. 7 Dec 2017;130(Supplement 1):4421-4421.

42. Silbermann R, Zhou D, Teramachi J, Xie X-Q, Roodman GD, Kurihara N. The p62-ZZ Domain Inhibitor XRK3F2 Alters Myeloma-Induced Suppression of Osteoblast Differentiation and Is Highly Cytotoxic to Myeloma Cells in Combination with Bortezomib. Blood. 6 Dec 2014;124(21):2083-2083.

43. Yong K, Gonzalez-McQuire S, Szabo Z, Schoen P, Hajek R. The start of a new wave: Developments in proteasome inhibition in multiple myeloma. Eur J Haematol. 30 Mar 2018;

44. Azkargorta M, Escobes I, Elortza F, Matthiesen R, Rodríguez MS. TUBEs-Mass Spectrometry for Identification and Analysis of the Ubiquitin-Proteome. Methods Mol Biol. 2016;1449:177-92.

45. Carvalho AS, Ribeiro H, Voabil P, Penque D, Jensen ON, Molina H, et al. Global mass spectrometry and transcriptomics array based drug profiling provides novel insight into glucosamine induced endoplasmic reticulum stress. Mol Cell Proteomics. Dec 2014;13(12):3294-307.

46. Cox J, Mann M. MaxQuant enables high peptide identification rates, individualized p.p.b.-range mass accuracies and proteome-wide protein quantification. Nat Biotechnol. Dec 2008;26(12):1367-72.

47. Bunkenborg J, García GE, Paz MIP, Andersen JS, Molina H. The minotaur proteome: avoiding cross-species identifications deriving from bovine serum in cell culture models. Proteomics. Aug 2010;10(16):3040-4.

48. Matthiesen R, Prieto G, Amorim A, Aloria K, Fullaondo A, Carvalho AS, et al. SIR: Deterministic protein inference from peptides assigned to MS data. J Proteomics. 16 July 2012;75(13):4176-83.

49. GO.db [Internet]. Bioconductor. 2018 [cité 29 oct 2018]. Disponible sur: http://bioconductor.org/packages/GO.db/

50. VennDiagram: Generate High-Resolution Venn and Euler Plots version 1.6.20 from CRAN [Internet]. 2018 [cité 29 Oct 2018]. Disponible sur: https://rdrr.io/cran/VennDiagram/

51. Chen H, Boutros PC. VennDiagram: a package for the generation of highly-customizable Venn and Euler diagrams in R. BMC Bioinformatics. 26 Jan 2011;12:35.

52. Elsasser S, Schmidt M, Finley D. Characterization of the proteasome using native gel electrophoresis. Methods Enzymol. 2005;398:353-63.

53. Body S, Esteve-Arenys A, Recasens-Zorzo C, Troussard X, Roué G, Sola B. A mouse model of disseminated mantle cell lymphoma highlights a lack of activity of estrogen receptor β agonists toward tumor burden. Leuk Lymphoma. July 2018;59(7):1726-9.

54. Esteve-Arenys A, Valero JG, Chamorro-Jorganes A, Gonzalez D, Rodriguez V, Dlouhy I, et al. The BET bromodomain inhibitor CPI203 overcomes resistance to ABT-199 (venetoclax) by downregulation of BFL-1/A1 in in vitro and in vivo models of MYC+/BCL2+ double hit lymphoma. Oncogene. Apr 2018;37(14):1830-44.